CP-47631
Revision 2

Model Package Report: Central Plateau Groundwater Model

Version 6.3.3

Prepared for the U.S. Department of Energy
Assistant Secretary for Environmental Management

Contractor for the U.S. Department of Energy
under Contract DE-AC06-08RL14788

P.O. Box 1600
Richland, Washington 99352

CP-47631
Revision 2

Model Package Report: Central Plateau Groundwater Model

Version 6.3.3

Document Type: ENV   Program/Project: EP&SP

T. M. Clemo
INTERA, Inc.

Date Published
July 2015

Prepared for the U.S. Department of Energy
Assistant Secretary for Environmental Management

Contractor for the U.S. Department of Energy
under Contract DE-AC06-08RL14788

P.O. Box 1600
Richland, Washington 99352

APPROVED
By Janis D. Aardal at 3:33 pm, Jul 16, 2015

Release Approval   Date

Model Package Report

Central Plateau Groundwater Model

Version 6.3.3

May 2014

Prepared for:

Central Plateau Groundwater OU RI/FS Projects

Prepared by:

T. M. Clemo
(INTERA, Inc.)

This page intentionally left blank.

Executive Summary

This model package report documents the groundwater flow component of the Central Plateau Groundwater Model (CPGW Model), a groundwater flow and contaminant fate-and-transport simulation model used for CH2M HILL Plateau Remediation Company work in support of remedial activities at the Hanford Site, Washington. The objective of this model package report is to describe the modeling objectives; conceptualization; model implementation; sensitivity, calibration, and uncertainty analyses; configuration control; and limitations of the groundwater flow component of the CPGW Model.

This report documents the principal elements development of the flow component of the numerical model itself, not a specific calculation made using the model. The report focuses on the spatial discretization of the model, parameterization, and the time discretization during the calibration period—with the goal of providing a technical basis for the use of the model (1) to assist with understanding and/or reconstructing past conditions at the site, and (2) making predictions of possible future conditions. The use of the CPGW Model to perform specific calculations, including application-specific boundary conditions, characterization of current contamination conditions and contaminant transport predictions will be described for each use of the model in separate environmental calculation files.

The CPGW Model provides the computational framework to simulate the fate and transport of contaminants in groundwater associated with the 200-PO-1, 200-UP-1, 200-BP-5, and 200-ZP-1 Groundwater Operable Units (OU) of the Central Plateau region of the U.S. Department of Energy's Hanford Site. In addition, this model covers for adjacent areas and facilities, such as the State-Approved Land Disposal Site (SALDS) facility. Intended and anticipated uses of the model include:

- Calculating water levels, hydraulic gradients, and groundwater flows throughout the model domain, encompassing the 200 West and 200 East Areas, for use in subsequent calculations of the fate and transport of contaminants of concern
- Estimation of future groundwater concentrations of contaminants of concern to support risk screening within and possibly downgradient of each OU

- Estimation of future groundwater concentrations of contaminants of concern to support evaluation of remedial alternatives
- Estimation of the efficacy of selected remedial alternatives and optimization of final remedial design
- Calculation of likely influent concentrations to remedies that extract contaminated water for treatment aboveground, enabling the design and cost of treatment systems

The overall objective of the modeling effort is to provide a basis for making an informed remedial action decisions based on description of current and expected future contaminant concentrations in groundwater at decision points within the OU boundaries. The objective for the model development phase of the effort is to create a common modeling platform that can be used for investigations in each of the Groundwater OUs that exist in the Central Plateau region.

The model domain, representing the suprabasalt aquifers of the Central Plateau, has been divided into six hydrostratigraphic units (HSU) with properties established primarily through model calibration. The properties of these units are treated as constant throughout the units. The boundaries between units are established from ongoing efforts to refine borehole log information and for the basalt surface, which forms the lower boundary of the model, seismic surveys. A large number of historic water level measurements, going back to 1944, have been used in calibration of the HSU properties and other important model parameters.

The CPGW Model calibration placed emphasis on matching water level data from the 1940s and early 1950s to estimate hydraulic properties using flow conditions relatively unperturbed by site operations and matching water level data from the first decade of the 21st century to establish current flow conditions that become initial conditions for predictive simulations using the CPGW Model. The model reproduces measured water levels well throughout this period; however, there is room for improvement in several areas. In a large portion of the model domain, measurements during and shortly after the operational period (1950 to 1995) are thought to be influenced by perching of water discharged to the surface and, hence, not appropriate for direct use in the calibration without explicit consideration of this physical phenomenon in the CPGW Model.

The calibration results indicate that the version of the latest calibration of the CPGW Model described in this document (Version 3.3; updated without recalibration in this revision to Version 6.3.3) provides improved correspondence between modeled outputs and historic measurements compared to the outputs of earlier versions. Version 3.4 incorporated a few minor refinements to resolve some structural issues in preparation for application of the CPGW Model to prepare for simulation needs of the 200-BP-5 Operable Unit Remedial Investigation. Version 3.4 also retained the calibration developed for Version 3.3.

The major sources of uncertainty arise from heterogeneity of the HSUs, uncertainty in the boundaries between HSUs, uncertainty in the elevation in the basalt surface, and fluxes into the central plateau from ephemeral streams.

The calibration results and uncertainty analysis also suggest that improved correspondence between simulated water levels and hydraulic gradients, and those measured at the Hanford Site, could be achieved with further development of the model. Some of these are improved representation of the height across a basalt ridge between the 200 East Area and the northern boundary of the model, refinement of the representation of heterogeneity of hydraulic conductivity particularly the Hanford formation, incorporation of new geologic information for the emplacement of the 200-ZP-1 pump-and-treat wells, and automated calibration.

This page intentionally left blank.

Contents

Appendix

Figures

Tables

Terms

CHPRC	CH2M HILL Plateau Remediation Company
CPGW Model	Central Plateau Groundwater Model
CRBG	Columbia River Basalt Group
DOE	U.S. Department of Energy
EMMA	Environmental Model Management Archive (a model configuration management system)
FEPs	features, events, and processes
FY	fiscal year
GHB	general head boundary (MODFLOW term for mixed boundary condition)
HEIS	Hanford Environmental Information System (environmental database)
HFEPs	Hanford features, events, and processes
HISI	Hanford Information System Inventory (software database)
HSU	hydrostratigraphic unit
HWIS	Hanford Well Information System (well database)
IDMS	Integrated Document Management System
MODFLOW	MODular groundwater FLOW code (software code)
MT3DMS	Modular 3-Dimensional Multiple Species transport code (software code)
OU	Operable Unit
PNNL	Pacific Northwest National Laboratory
RD/RAWP	remedial design/remedial action work plan
RI/FS	remedial investigation/feasibility study
RMS	root mean square (error)
ROD	Record of Decision
SALDS	State-Approved Land Disposal Site
STOMP	Subsurface Transport Over Multiple Phases (software code)

This page intentionally left blank.

1 Introduction

A groundwater model has been developed for the Central Plateau region of the U.S. Department of Energy's (DOE) Hanford Site. The Central Plateau is an informal geographic designation given to the broad central portion of the Hanford Site that encompasses 200 West and 200 East Areas. This groundwater model primarily provides the computational basis for simulation of the fate and transport of contaminants in groundwater within the near-field portion of the affected aquifer associated with the 200-PO-1, 200-UP-1, 200-BP-5, and 200-ZP-1 Groundwater Operable Units (OU) of the Central Plateau region. In addition, this model covers for adjacent areas and facilities, such as the State-Approved Land Disposal Site (SALDS) facility.

The overall objective of the modeling effort is to provide a basis for making an informed remedial action decisions based on description of current and expected future contaminant concentrations in groundwater at decision points within the OU boundaries. The objective for the model development phase of the effort is to create a common modeling platform that can be used for investigations in each of the groundwater OUs that exist in the Central Plateau region.

This document is limited to the development of the groundwater flow component of the model for the Central Plateau. Measurements made during the recent past, since 1944, are used to guide the development of the model. The period encompassed by these past measurements is the simulation period for the model development described in this document. The model assessed through simulation past fluid flow conditions has been and will be used to provide the basis for predictions for the Central Plateau, with appropriate changes to represent future boundary conditions. Problem-specific boundary conditions and characterization of current contamination conditions needed for transport predictions of contamination will be described for each use of the model in separate environmental calculation files.

Modeling is an iterative process and modifications to the Central Plateau Groundwater Model (CPGW Model) will occur continually, in response to new knowledge and information, and in response to new needs, possibly with each use of the model. A version number will identify the evolution of the CPGW Model to delineate the changes made to the model over time. This model package report is intended to be a living report. The revisions of this model package report will keep pace with the developments in the CPGW Model and align to versions of that model. The evolution of the flow model will made more transparent by separating the CPGW Model descriptions as contained in this document from descriptions of specific applications of the model that are documented separately in environmental calculation files.

1.1 Modeling Need

Anticipated and intended uses of the model are to meet the following needs:

- Calculating water levels, hydraulic gradients, and groundwater flows throughout the model domain, encompassing the 200 West and 200 East Areas, for use in subsequent calculations of the fate and transport of contaminants of concern
- Estimation of future groundwater concentrations of contaminants of concern to support risk screening within and possibly downgradient of each OU
- Estimation of future groundwater concentrations of contaminants of concern to support evaluation of remedial alternatives

- Estimation of the efficacy of selected remedial alternatives and optimization of final remedial design
- Calculation of likely influent concentrations to remedies that extract contaminated water for treatment aboveground
- Enabling the design and costing of treatment systems

1.2 Background

A groundwater flow and advective-dispersive transport model was originally developed to perform contaminant fate and transport simulations in support of the 200-ZP-1 Groundwater OU Feasibility Study, Proposed Plan, and Final Record of Decision (ROD) (*Feasibility Study for the 200-ZP-1 Operable Unit* [DOE/RL-2007-28]). This study used analytical and superposition techniques, rather than a numerical model. In anticipation of the need for more rigorous analyses of groundwater flow and contaminant transport, this superposition model was replaced during fiscal year (FY) 2008 with a numerical groundwater flow and contaminant transport model. The model was developed to provide calculations in support of the post-ROD remedy design, focusing on the remedial design/remedial action work plan (RD/RAWP) for 200-ZP-1 (*200 West Area Pre-Conceptual Design for Final Extraction/Injection Well Network: Modeling Analyses* [DOE/RL-2008-56]; *Description of Modeling Analyses in Support of the 200-ZP-1 Remedial Design/Remedial Action* [DOE/RL-2009-38]; *200 West Area 200-ZP-1 Pump-and-Treat Remedial Design/Remedial Action Work Plan* [DOE/RL-2008-78, Draft A]).

The model developed in support of post-ROD activities at the 200-ZP-1 Groundwater OU was constructed with a geographic extent—or domain—that covers most of the area commonly known as the Hanford Central Plateau, encompassing four groundwater OUs that are located in the Central Plateau area: 200-PO-1, 200-BP-5, 200-UP-1, and 200-ZP-1. This model was constructed using the software MODular groundwater FLOW code (MODFLOW) to simulate flow and Modular 3-Dimensional Multiple Species transport code (MT3DMS) to simulate contaminant transport. For clarity in this report, the model developed for the 200-ZP-1 Groundwater OU analyses is referred to as the 200-ZP-1 Model.

During FY 2009, it was decided to accept the general premise (i.e., conceptual basis, computational grid, and discretization) of the 200-ZP-1 Model as a basis for a model to be used throughout the Central Plateau in support of decision making at the encompassed OUs. Because the development of the 200-ZP-1 Model had focused on features, events, and processes (FEPs) associated with the 200-ZP-1 OU, further development of the model was required to make it a suitable tool for use at the other OUs. To distinguish the current version of this model from the precursor 200-ZP-1 Model, the current model is referred to in this report as the CPGW Model. The CPGW Model has replaced the 200-ZP-1 Model in all groundwater simulations for the four groundwater OUs encompassed by the CPGW Model, including any calculations made for the 200-ZP-1 OU. Section 7.1 provides a version history outlining the development of the CPGW Model.

Briefly, the ZP-1 Model (Version 1) was modified extensively in the 200-PO-1 and 200-BP-5 portions of the Central Plateau for use in these OUs. The biggest change was the subdivision of the Hanford unit (as represented in the ZP-1 Model) into the Cold Creek and Hanford units to create Version 2 of the CPGW Model. This version was used for the 200-PO-1 remedial investigation (RI) and initial simulations for the 200-UP-1 OU RI/feasibility study (FS). For Version 3, the number of layers used in the model was increased from five to seven. Extensive refinement of the geology in the 200-BP-5 OU was also implemented. Version 3 was used for the 200-UP-1 OU RI/FS. Version 3.3 has further refinement of the model layering (still seven layers) and improved calibration in the 200-BP-5 region. This version was used for the 200-BP-5 RI. Some minor maintenance issues were resolved to create Version 3.4. The name of the current version, Version 6.3.3, reflects the use of Build 0006 of the CHPRC MODFLOW code, version 3 of the model grid, and version 3 of the boundary conditions as well as an improving nomenclature to identify the models used for analysis. More detail of the version history is provided in Section 7.

1.3 Model Domain

Figure 1-1 shows the location of the Hanford Site. The Central Plateau is south of Gable Butte and Gable Mountain, and includes the 200 West and 200 East Areas depicted in the figure just above the words Central Plateau. Figure 1-2 shows these features and domain of model simulation. To the north, south, and west, the domain is constricted by (depicted as grey colored) basalt subcrops. These subcrops are assumed to constitute impermeable boundaries to flow. There are two gaps in the basalt subcrops along the northern boundary. In these two regions, the water table is above the basalt surface. The westernmost region is referred to as the Western Gap and the eastern region is referred to as the Gable Gap. The water table is also above the basalt surface along the eastern boundary and the easternmost part of the southern boundary. The light brown regions in Figure 1-2 are outside the active portion of the model.

Cold Creek (located in the slot along the western boundary) and Dry Creek (the gap in the basalt subcrops in the southwest corner of the domain) are sources of inflow to the Central Plateau. The model domain includes four groundwater OUs in the Central Plateau area: 200-PO-1, 200-BP-5, 200-UP-1, and 200-ZP-1. Figure 1-2 outlines these four groundwater OUs in red.

The model domain has the following lateral extent and boundaries: extent north to south is 13.4 km (8.3 mi) and extent east to west is 25.6 km (15.9 mi). The lower left corner of the model domain is located at easting 555,650 m, and northing 129,850 m in the Washington State Coordinate System (NAD_1983_StatePlane_Washington_South_FIPS_4602).

The bedrock of the domain is composed of basalts that are assumed to form an impermeable lower boundary. The top of the model is the land surface; however, geologic variations are usually only represented to the maximum measured water table. The water table was higher during the operational period of the Hanford Site than it is currently. Hence, the geologic media extent vertically includes sediments that are presently above the water table to permit historical modeling of water flow.

1.4 Document Organization

The organization of this model package report follows guidance set forth in CHPRC-00189, Appendix G, *Quality Assurance Project Plan for Modeling*. Chapter 2 sets forth the objectives that the CPGW Model is constructed to meet. Chapter 3 describes the conceptualization of the system to be simulated with a numerical model, including identification of the relevant FEPs. Chapter 4 describes the implementation of the conceptual model as a numerical computer simulation model. Chapter 5 provides an overview of the sensitivity and describes sources of uncertainty for the predictions made with this model. There is some intentional redundancy in Chapters 3 to 5 to allow the report to be used as a reference document as well as a descriptive document. Chapter 6 enumerates the limitations of this model that result from the conceptualization, selection, and exclusion of relevant FEPs, assumptions, and numerical implementation. Chapter 7 describes how this model is uniquely identified, tracked, and preserved as a configuration management item. Chapter 8 lists recommended improvements to the model that could be made for future versions. Chapter 9 provides references cited in this model package report.

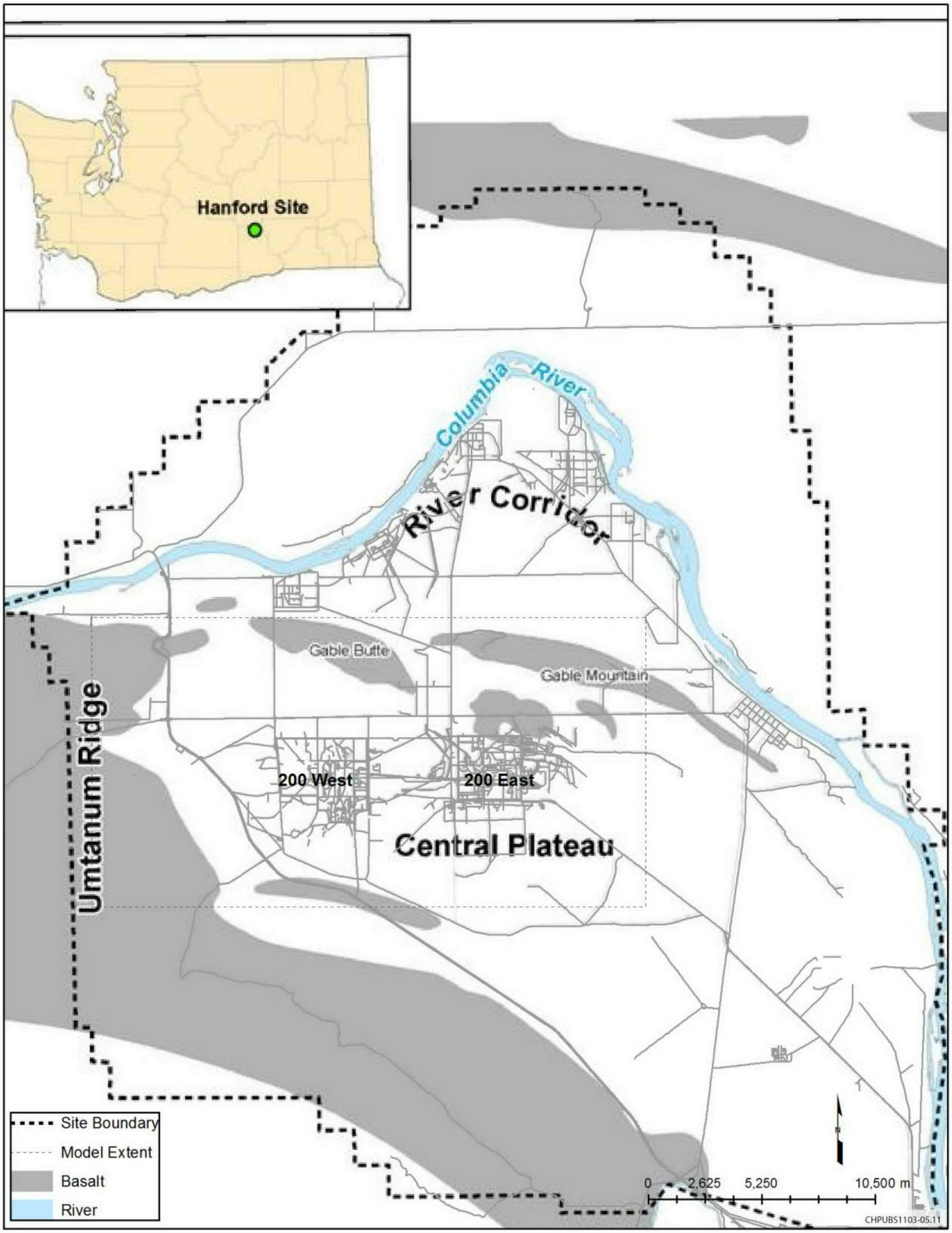

Figure 1-1. Location of Central Plateau

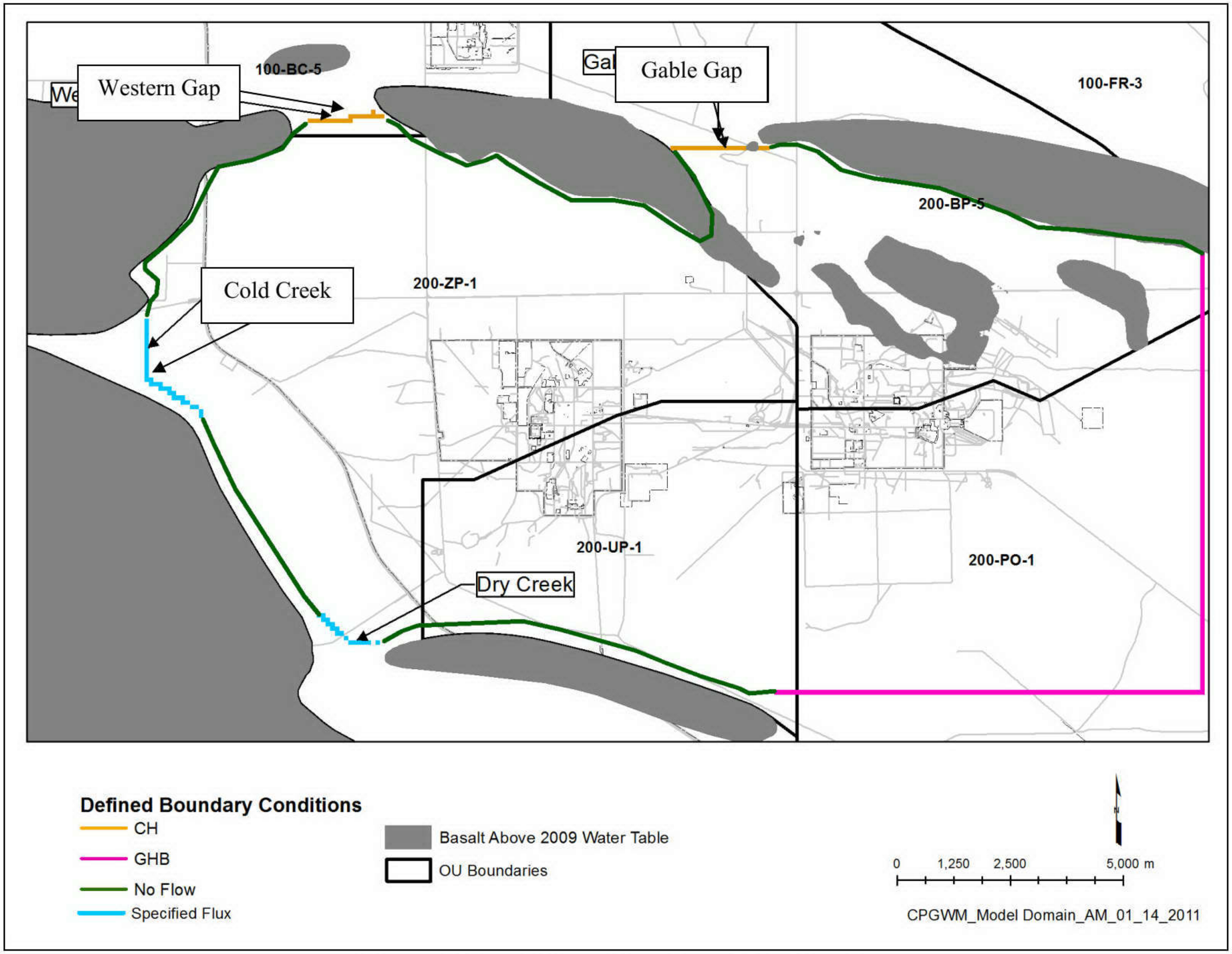

Figure 1-2. Central Plateau Groundwater Model Domain

This page intentionally left blank.

2 Model Objectives

The overall objectives of the modeling effort is to provide a basis for making informed remedial action decisions based on descriptions of current and expected future groundwater contaminant concentrations at decision points within the OU boundaries. The objective for the model development phase of the effort is to create a common modeling platform that can be used for investigations in each of the groundwater OUs that exist in the Central Plateau region.

This document is limited to the development of the flow model for the Central Plateau. Problem-specific boundary conditions, characterization of current contamination conditions, and transport predictions of contamination will be described for each use of the model in separate environmental calculation files.

Section 1.1 specifies anticipated uses of the model. Although the model is developed for the primary purposes listed, it may be suitable for other applications throughout the Central Plateau in support of other decisions and analyses.

This page intentionally left blank.

3 Model Conceptualization

The conceptual model for the CPGW Model considers saturated porous media flow through the unconfined flow system occurs within fluvial, lacustrine, and glaciofluvial sediments that overlay the Columbia River Basalts within the Pasco Basin (Figure 3-1). This uppermost, saturated zone is termed the unconfined aquifer system, although locally confined conditions may exist in certain areas. The local unconfined aquifer system provides a pathway for transport of contaminants released from past, present, and future site activities. Water enters the system through vertical recharge and recharge from upland areas to the west and southwest of the domain, and exits through the Western Gap, Gable Gap, and east and southeast boundaries, and then primarily discharges to the Columbia River.

3.1 Geologic Overview

This section provides an overview of the geology and hydrogeology of the Central Plateau for readers unfamiliar with the Central Plateau. The description presented here is synopsis of the regional geology discussion presented in PNNL-17913, *Hydrogeology of the Hanford Site Central Plateau – A Status Report for the 200 West Area*. More detailed descriptions of the hydrogeology of the Central Plateau can also be found in PNNL-12261, *Revised Hydrogeology for the Suprabasalt Aquifer System, 200-East Area and Vicinity*; PNNL-13858, *Revised Hydrogeology for the Suprabasalt Aquifer System, 200-West Area and Vicinity*; and references therein.

The CPGW Model simulates flow in the saturated portion of sedimentary deposits that have formed locally over the Columbia River Basalt Group (CRBG), a series of flood-basalts that formed over a period of 17 to 6 million years ago in north-central and northwest Oregon, eastern Washington, and western Idaho. Regional subsidence and uplift of the Pasco Basin has led to depositional and erosive periods with depositional features also influenced by local deformation of the basalt. Major flooding events, most dramatically of the Missoula floods, caused deep erosion and deposition during the last ice age.

3.1.1 Ringold Units

The oldest depositional sequence is the Ringold Formation deposited between 10.5 and 3.4 million years ago. BHI-00184, *Miocene- to Pliocene-Aged Suprabasalt Sediments of the Hanford Site, South-Central Washington*, divided the Ringold Formation into three informal members: Wooded Island, Taylor Flat, and Savage Island members (Figure 3-1). BHI-00184 subdivided the Wooded Island member into five subunits, A through E. The Ringold Formation that underlies the Central Plateau mostly belongs to the Wooded Island member along with remnants of the of the Taylor Flat member. For the CPGW Model, these units have been grouped into the following:

- Ringold A (also known as unit 9 in PNNL-12261)
- Ringold mud (also referred to as Ringold lower mud) composed of units B, C, and D (units 8, 7, and 6 in PNNL-12261)
- Ringold E composed of subunit E and the Taylor Flat member (units 5 and 4 in PNNL-12261)

Ringold unit A is composed of extensive gravel with interbedded sand. It was deposited in a braided plain of a meandering Columbia River that exited the Pasco Basin through the present Yakima River gap along the southeast end of the Rattlesnake Mountain anticline ("Paleodrainage of the Columbia River on the Columbia Plateau of Washington State - A Summary" [Fecht et al, 1987]). About 6.7 million years ago, the river outlet was captured through the present Wallula Gap. The main river channel was still through the Central Plateau region but the depositional environment became a much lower energy sandy alluvial system with a period of lacustrine and overbank deposits of the Ringold mud.

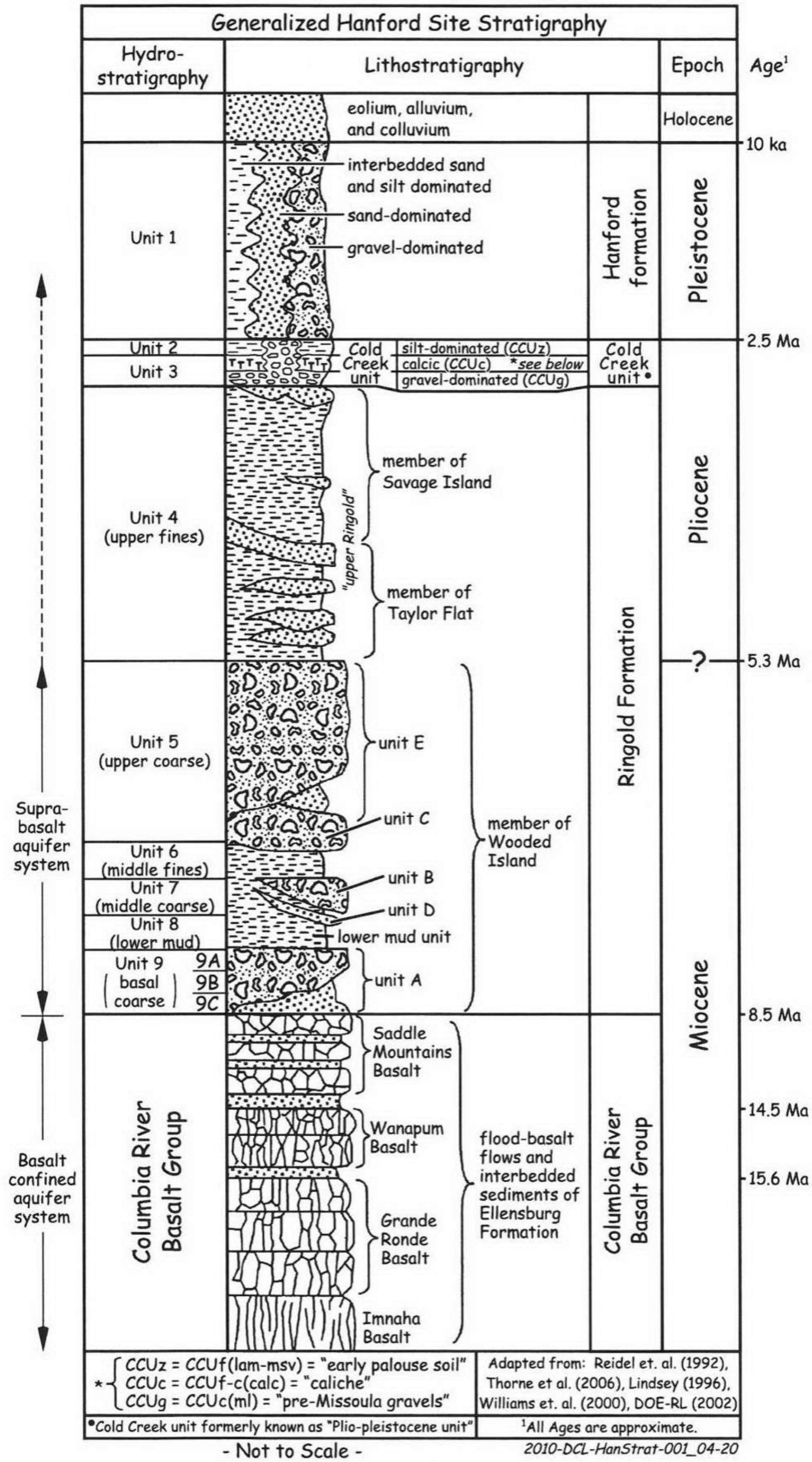

Source: PNNL-14898

Figure 3-1. Generic Stratigraphic Column for the Central Plateau

The Ringold mud was subsequently covered by the extensive sequence of mostly alluvial gravels and sand of the Ringold E subunit. Locally, Ringold unit E also contains fine–grained lenses that may have low permeability. About 5 million years ago, the depositional environment produced more than 90 m of sandy Taylor Flat deposits followed by lacustrine deposits of the Savage Island member from 4.8 to 3.4 million years ago.

Regional uplift starting 3.4 million years ago led to extensive erosion removing an estimated 100 m of deposits from the Hanford Site. The Savage Island member has been completely removed from the Central Plateau region and the Taylor Flat member has been removed over much of it. The erosion was deeper in the eastern portion of the central plateau where the main river channel passed through the gap between Gable Mountain and Gable Butte.

3.1.2 Cold Creek Unit

Following the erosional period was a relatively quiescent period. Alluvial gravel, sand, and silt deposits developed along the main stream channel south of the Gable Gap often referred to as the pre-Missoula gravels (c(ml) in Figure 3-2). Along Cold Creek and Dry Creek, deep drainage channel cuts were filled with alluvium. To the north of the Cold Creek paleochannel (Figure 3-2), overbank deposits form a soil that was calcified by the development of caliche within the soil. Later, less calcified overbank deposits continued to form top of this calcariferous layer. To the south of the Cold Creek paleochannel, coarser grained colluvium from Rattlesnake Mountain accumulated.

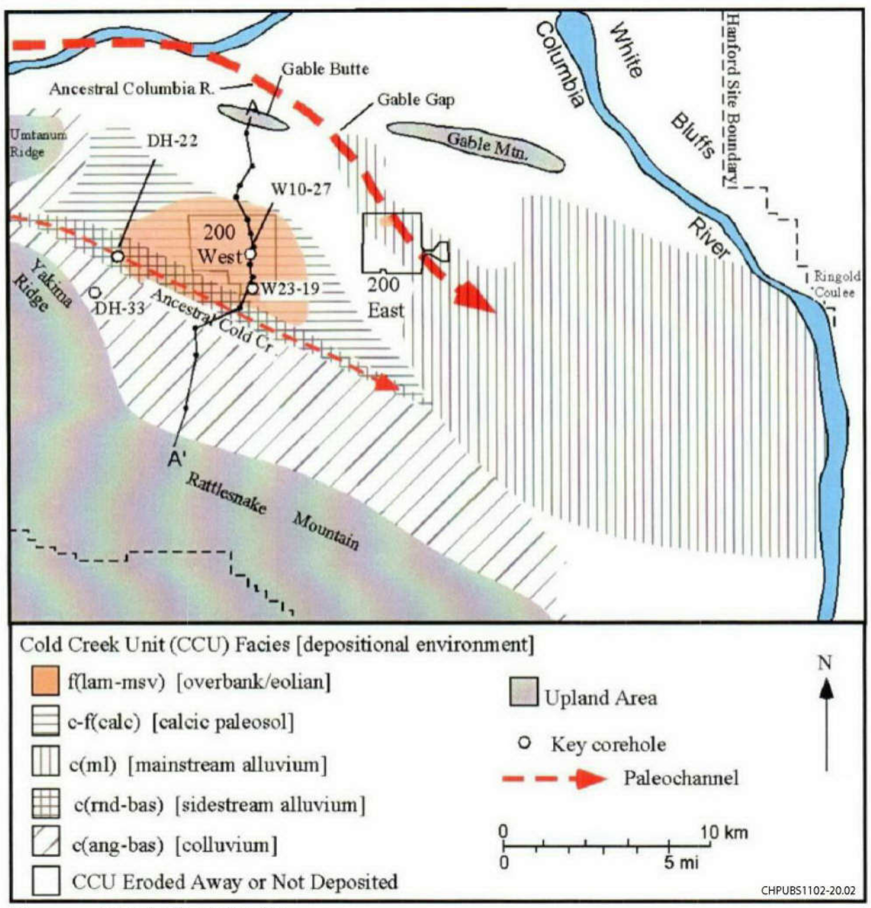

Source: DOE-RL-2002-39

Figure 3-2. Distribution of Cold Creek Facies across the Central Plateau

Only the pre-Missoula (c(ml)) facies of the Cold Creek unit is represented explicitly in the CPGW Model. Except for a very small segments of the Cold Creek channel fill, the western portion of the Cold Creek unit lays above the historically high water level. Despite being located within the vadose zone (and thus not explicitly simulated in the CPGW Model), the Cold Creek unit had a large influence on aquifer recharge and groundwater dynamics during the operational period of the Hanford Site. Significant perching of water disposed near the surface delayed and laterally offset the arrival of this water at the aquifer. Section 4.5.3 discusses perching.

3.1.3 Hanford Formation

The cataclysmic outburst Missoula floods caused repeated large erosional and depositional events, which have significantly shaped the Central Plateau geology that is seen today. Some of these floods may have been the largest ever identified in the history of the world (*The World's Largest Floods, Past and Present – Their Causes and Magnitudes* [O'Conner and Costa, 2004]). The many large floods left a series of overprinted features including scour channels in the basalt, deep erosion of the Cold Creek and Ringold units, highly conductive channel fill deposits extending from the Gable Gap southeast to the Columbia River, and relatively lower energy deposits across the western portion of the Central Plateau. Figure 3-3, from DOE/RL-2002-39, *Standard Stratigraphic Nomenclature for Post-Ringold Formation Sediments Within the Central Pasco Basin*, depicts the inferred pathways of these floods and shows the distributions of the major facies groups. The regions of sand-dominated and interbedded sand and silt facies shown in the figure are all above the historic high water level and hence not represented in the CPGW Model. As would be expected of deposits formed from multiple erosive/depositional flood events, there are large vertical and horizontal variations within the gravel dominated facies ranging from fine sand to open framework deposits, described as boulders in some drillers logs.

3.1.4 Cross Sections

Figure 3-4 displays the lines of three east-west cross sections that are presented in Figure 3-5, Figure 3-6, and Figure 3-7, and two north-south cross sections that are presented in Figure 3-8 and Figure 3-9. In these cross sections, the Taylor Flat member of the Ringold Formation is identified as a separate unit instead of being combined into the Ringold unit E, as is done in the model.

3.1.5 Hydrologic Characterization of Hydrostratigraphy

For use in the CPGW Model, the following six hydrostratigraphic units (HSUs) have been defined:

1. Ringold A
2. Ringold mud
3. Ringold E
4. Cold Creek
5. Hanford coarse-grained
6. Hanford fine-grained

Except for some very small regions, the Cold Creek unit represents only the pre-Missoula gravels of the Cold Creek unit. The Hanford fine-grained HSU represents Hanford deposits near the western gap in the northwest corner of the model domain. The adjective "fine-grained" used here reflects the unit's lower representative hydraulic in the model; it is not directly based on a facies distinction. This section presents a review of property estimates of the different units. These estimates are drawn from compilations of aquifer testing interpretations and on parameter estimates used in previous modeling exercises.

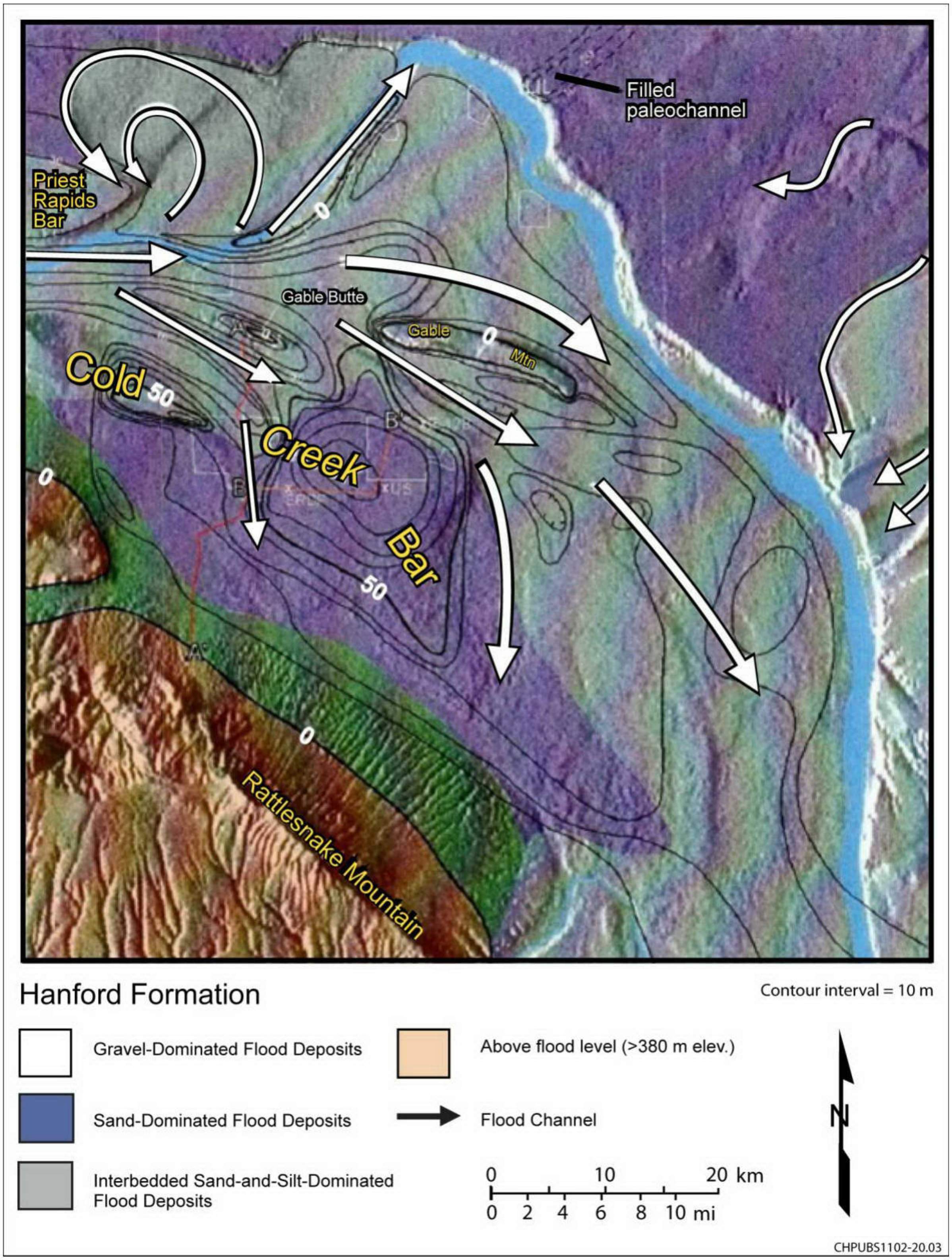

Source: DOE/RL-2002-39

Figure 3-3. Inferred Flood Routes and Associated Hanford Formation Deposit Facies

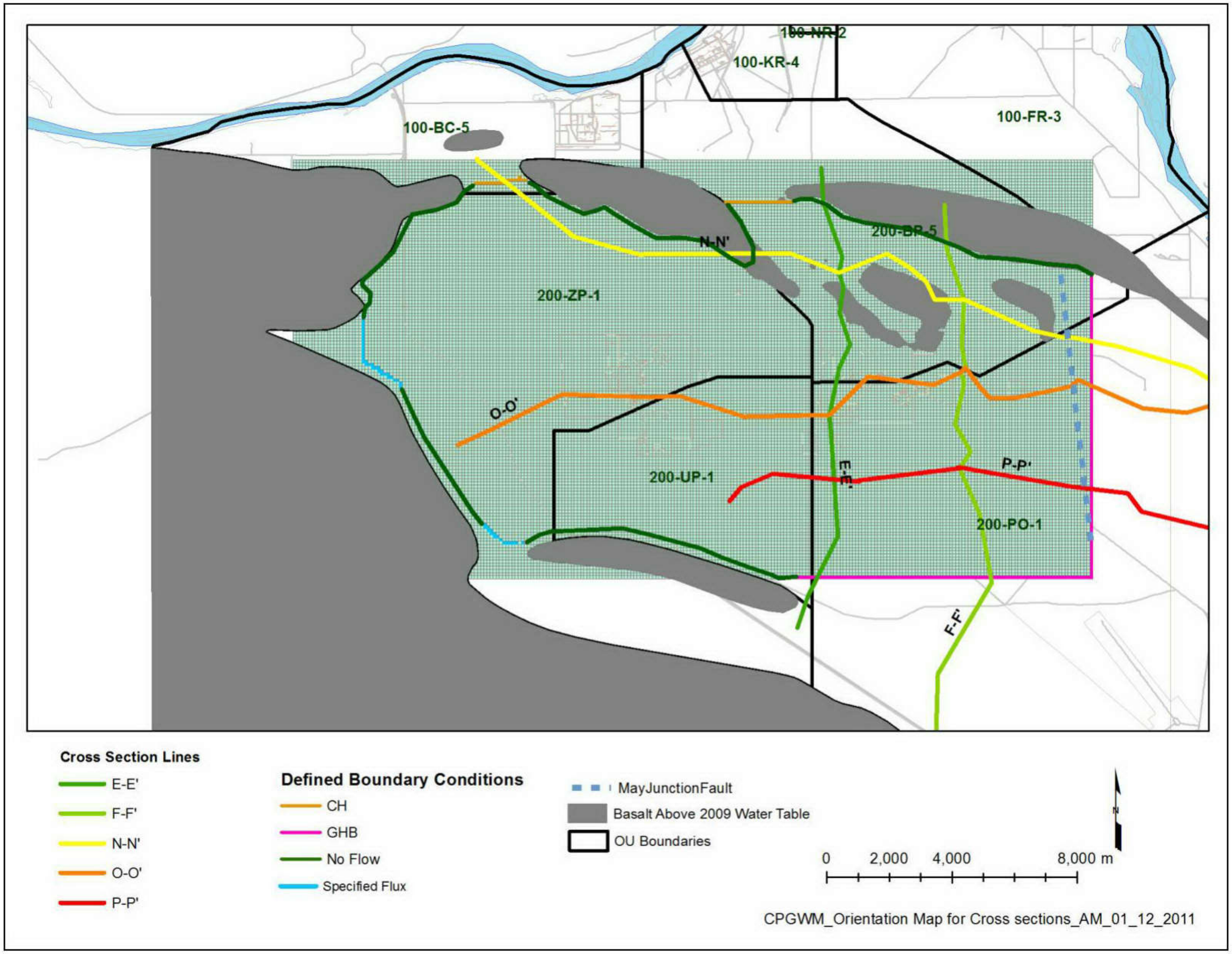

Figure 3-4. Orientation Map for Cross Sections

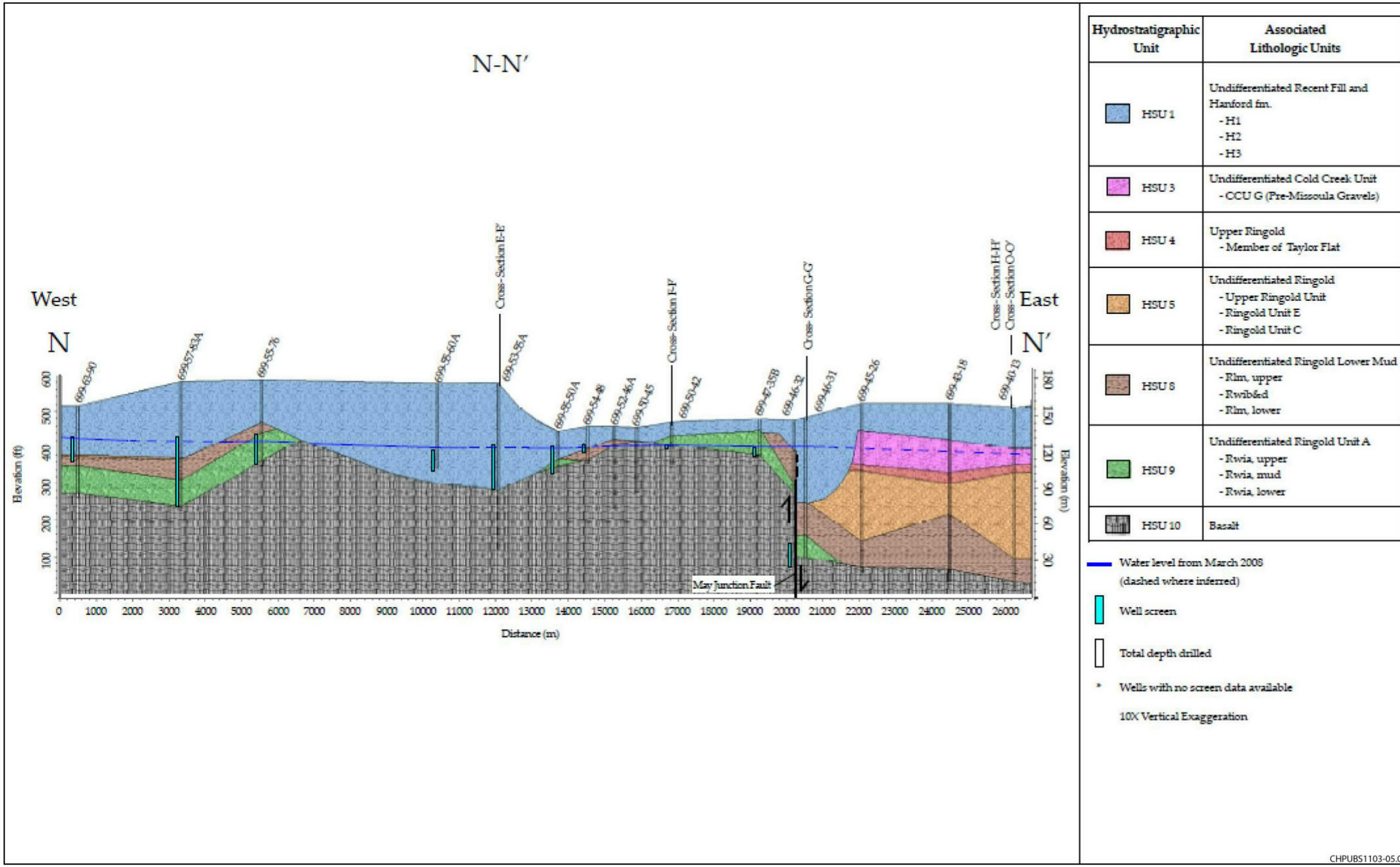

Figure 3-5. Cross Section N-N'

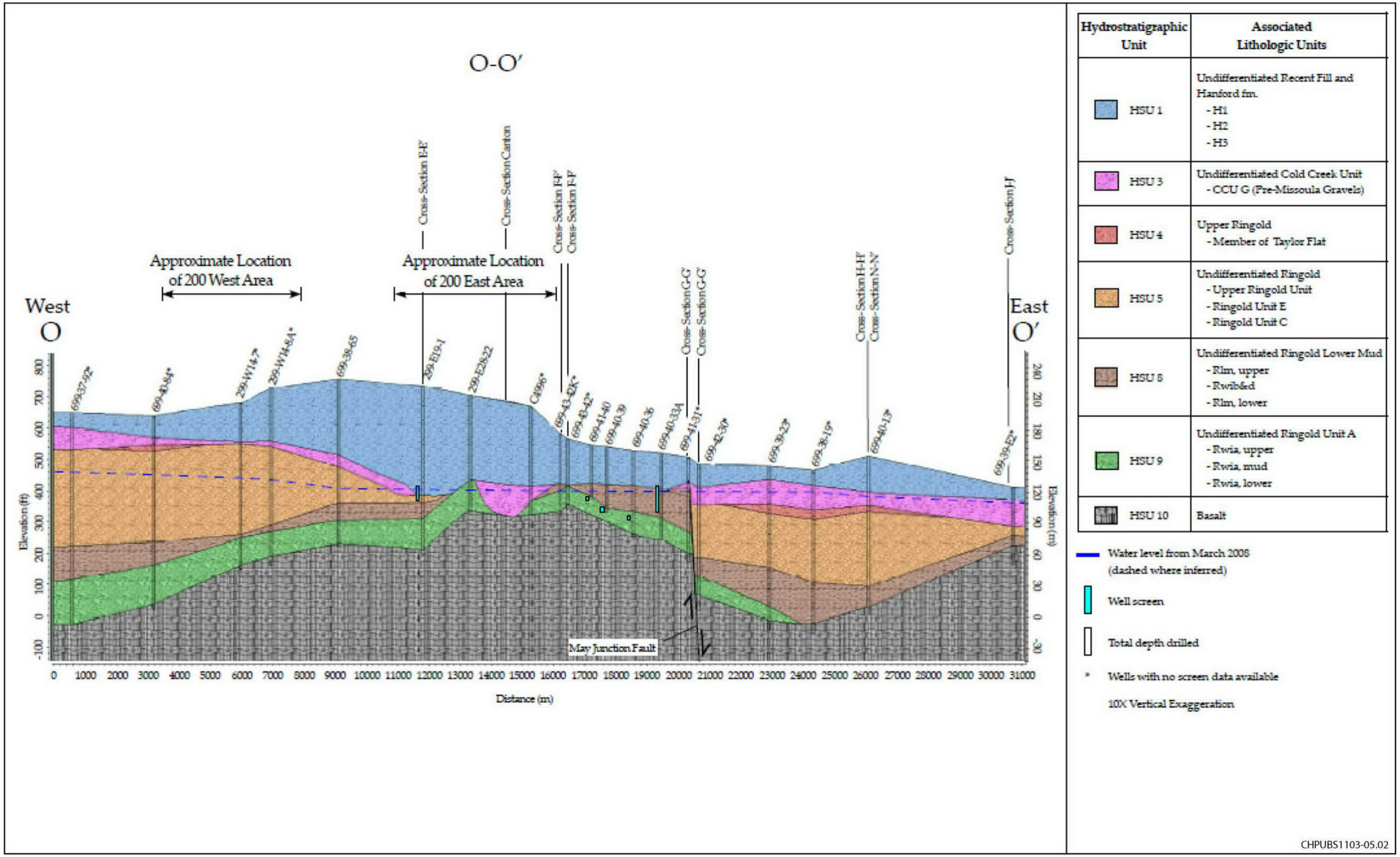

Figure 3-6. Cross Section O-O'

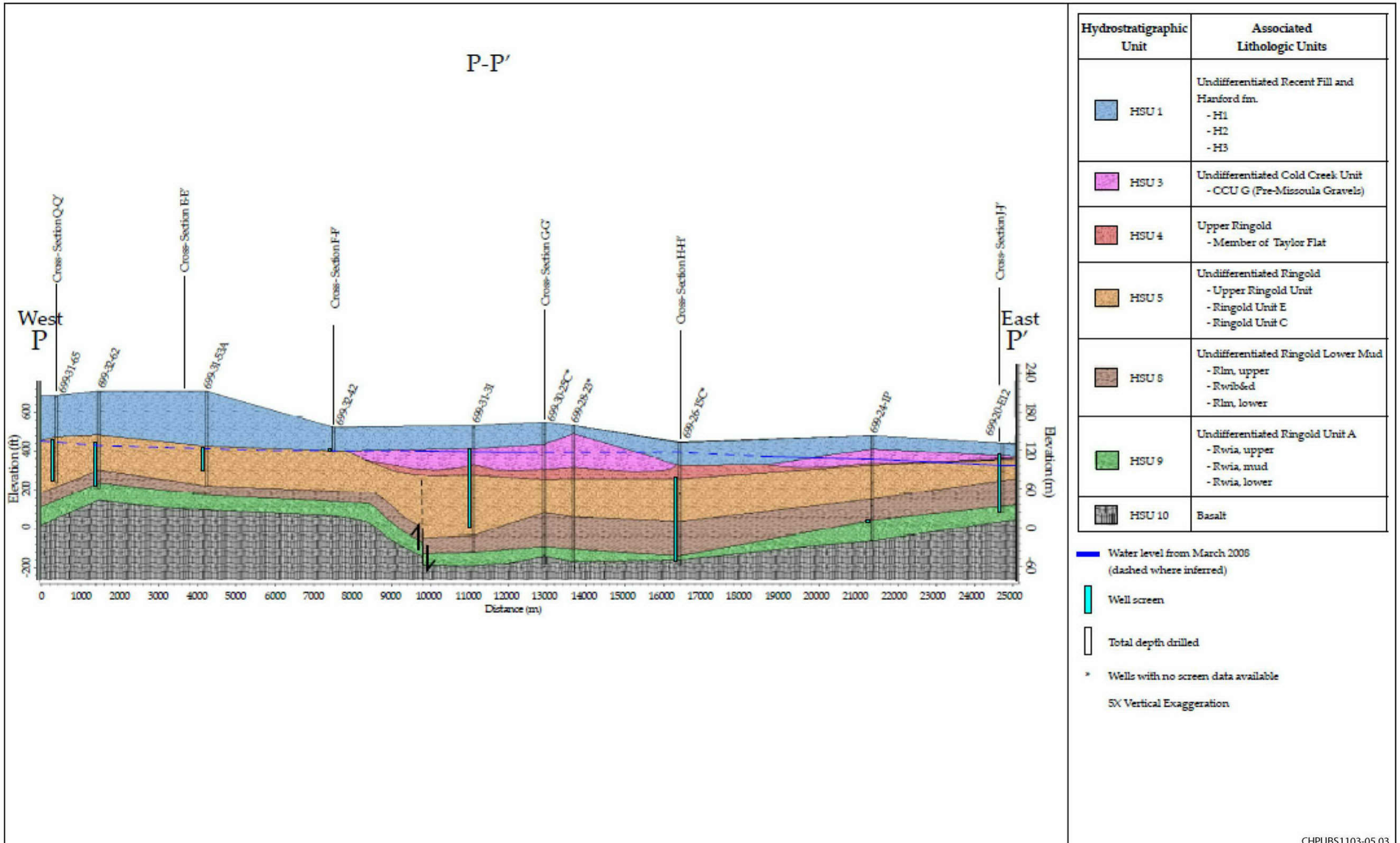

Figure 3-7. Cross Section P-P’

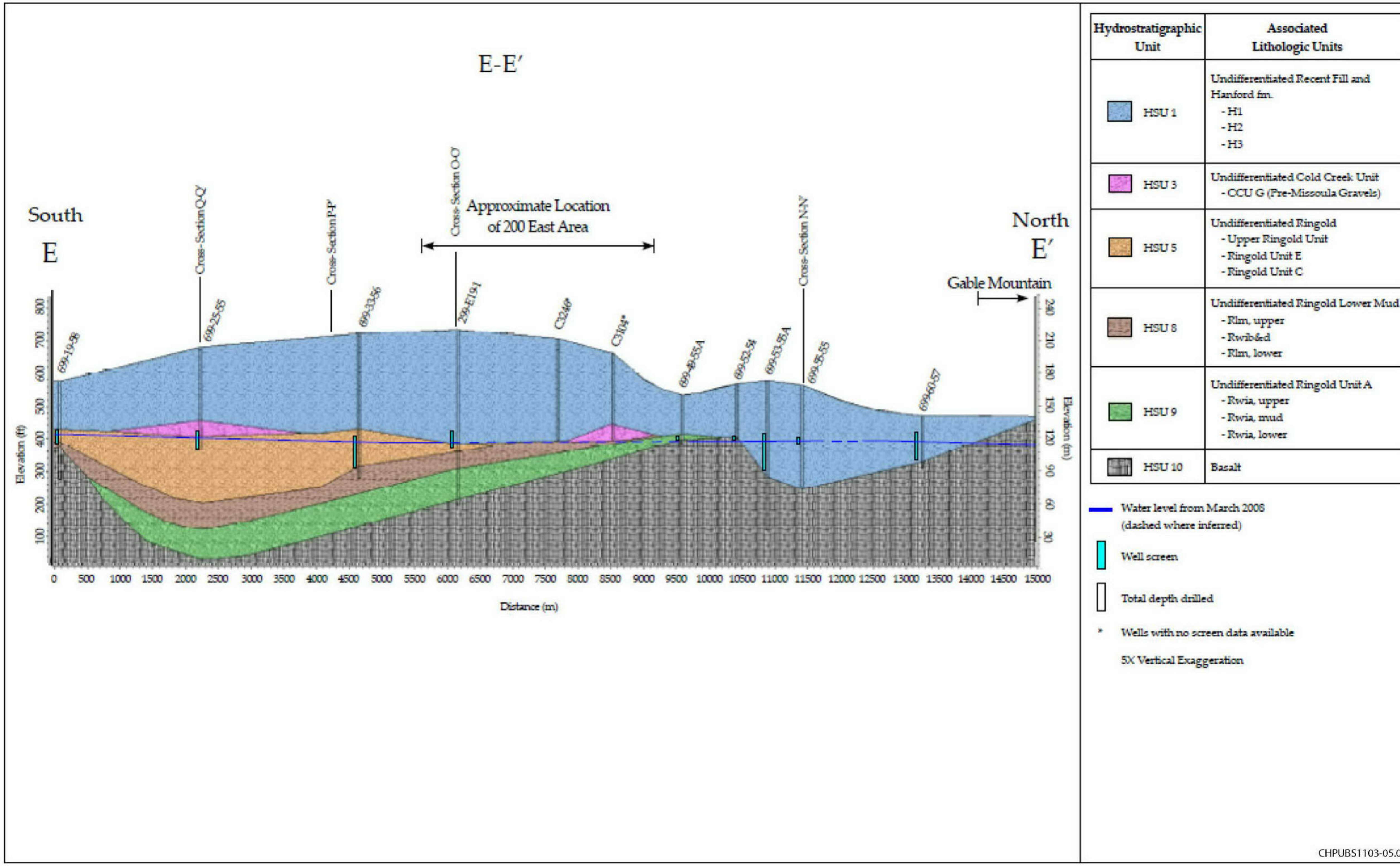

Figure 3-8. Cross Section E-E'

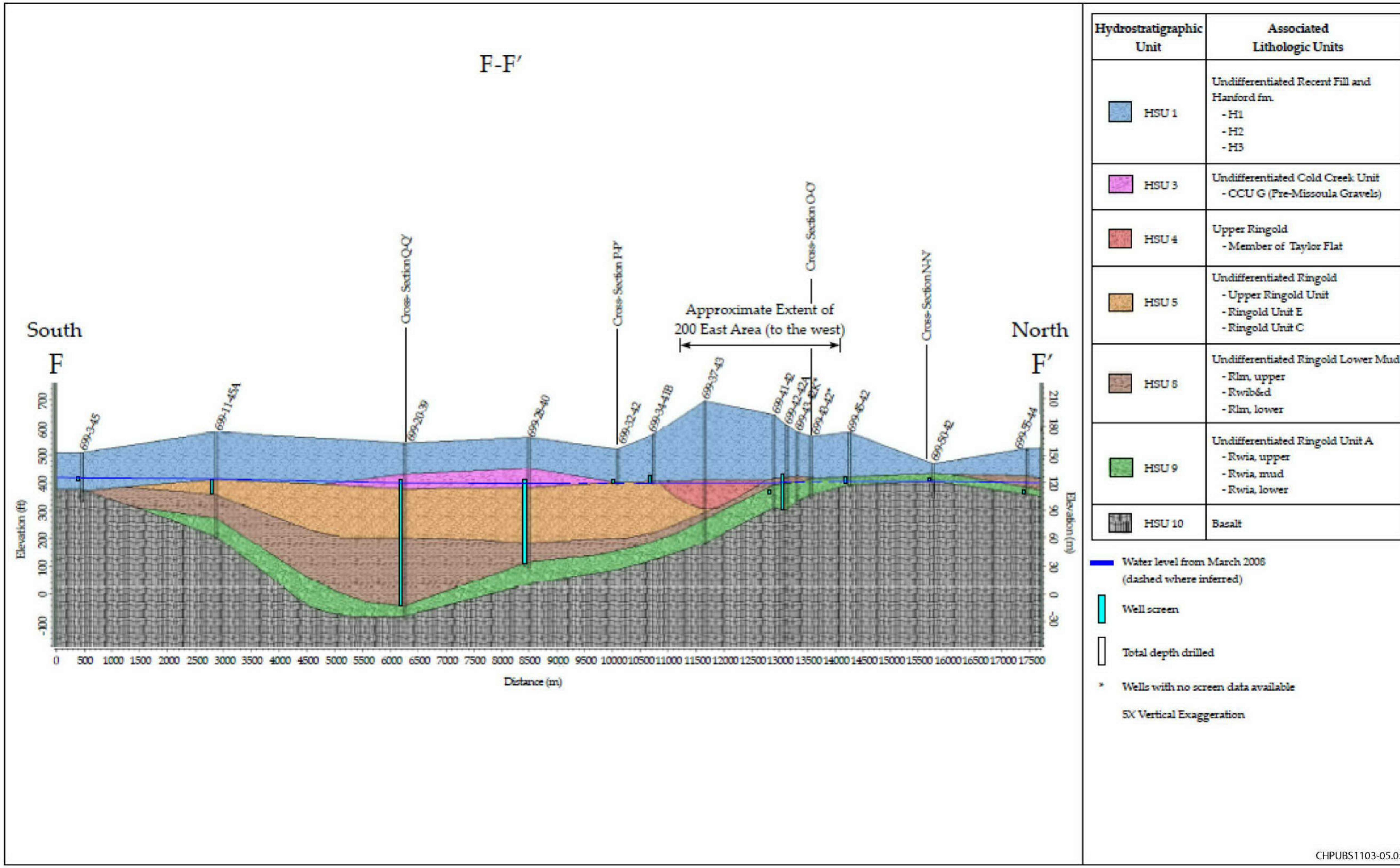

Figure 3-9. Cross Section F-F’

This page intentionally left blank.

Aquifer test data have been organized into a database that is accessible using the Hanford Environmental Information System (HEIS). PNNL-14058, *Prototype Database and User's Guide of the Saturated Zone Hydraulic Properties for the Hanford Site*, describes the original database.

A commonly referenced synopsis of hydraulic properties is provided in PNL-10886, *Development of a Three Dimensional Groundwater Model of the Hanford Site Unconfined Aquifer System: FY 1995 Status Report.* PNNL-13641, *Uncertainty Analysis Framework – Hanford Site-Wide Groundwater Flow and Transport Model*, presents another data review. These two sources have synthesized interpretations of experimental data. Table 3-1 presents ranges of hydraulic conductivity interpretations.

Table 3-1. Review of Hydrostratigraphic Unit Horizontal Hydraulic Conductivity

Unit	PNL-10886 Experimental Data (m/day)	PNNL-13641 Experimental Data (m/day)	PNNL-14398 Calibration (m/day)	PNNL-14753 Calibration (m/day)
Hanford	1 – 10,000	10 – >3,500	4,400 – 37,000	6 – 20,000
Cold Creek			32	1.8 – 5,700
Ringold E	0.1 – 200	0.1 – 560	3 – 10	0.24 – 2,562
Ringold mud	0.03 - <0.06 (unit 6)	0.002 - 0.03 (unit 6)	0.0002	0.00001 – 101
Ringold A	0.1 – 200	8	1 – 2.5	0.0005 – 4.2

Sources:

PNL-10886, 1995, *Development of a Three-Dimensional Ground-Water Model of the Hanford Site Unconfined Aquifer System: FY 1995 Status Report*, Pacific Northwest National Laboratory, Richland, Washington.

PNNL 13641, 2001, *Uncertainty Analysis Framework – Hanford Site Wide Groundwater Flow and Transport Model*, Pacific Northwest National Laboratory, Richland, Washington.

PNNL-14398, 2003, *Transient Inverse Calibration of the Site-Wide Groundwater Flow Model (ACM-2): FY 2003 Progress Report*, Pacific Northwest National Laboratory, Richland, Washington.

PNNL-14753, 2006, *Groundwater Data Package for Hanford Assessments*, Rev. 1, Pacific Northwest National Laboratory, Richland, Washington.

Another source of hydraulic parameter information is past model calibrations. Pacific Northwest National Laboratory (PNNL) developed a series of groundwater flow models. Results from two past model calibrations are included in Table 3-1. These results are taken from PNNL-14398, *Transient Inverse Calibration of the Site-Wide Groundwater Flow Model (ACM-2): FY 2003 Progress Report*, and PNNL-14753, *Groundwater Data Package for Hanford Assessments*.

In both PNL-10886 and PNNL-13641, it is acknowledged that some Hanford formation deposits are essentially too permeable to test and could have hydraulic conductivity as large as 1,000,000 m/day. In PNL-10886, Ringold A, Ringold unit 7, and Ringold E are treated together. The Ringold A value in PNNL-13641 is from a single test. Caution is advised in using the hydraulic values listed in Table 3-1 to evaluate the hydraulic conductivity values used in the CPGW Model. Aquifer tests interrogate properties on a scale of meters to hundreds of meters. A single model cell in the CPGW Model is 100 by 100 m. Even the largest scale tests of the aquifer are small compared to the scale of HSUs.

The hydraulic conductivity values from previous calibrations are more closely aligned with values expected for the CPGW Model, but here too they are not directly comparable. The models used for PNNL-14398 and PNNL-14753, extended to and beyond the Columbia River, hence covering a larger domain, and also have a more variable distribution of the material properties. For PNNL-14398, the Hanford formation was divided into five zones. The range presented in Table 3-1 represents the two zones that correspond to large fractions of the Hanford formation of the CPGW Model. Ringold unit E was also divided into five zones with only two zones coinciding with Ringold unit E of CPGW Model. The value for Ringold mud only represents unit 8 of PNNL-14398 and does not include the more permeable unit 7. The range of 1.0 to 2.5 m/day for Ringold unit A was taken from Figure 4.5 of PNNL-14398 using the color scale of the figure as a guide.

For the model described in PNNL-14753, the hydraulic conductivity values for each unit were distributions of parameter values. The creation of the spatial variation for the different units is based on inverse estimates of transmissivity, which were then converted to hydraulic conductivity as described in PNL-10886. The distribution of conductivity was then modified by a constant factor using parameter estimation as described in PNNL-14753.

An updated review of Ringold E properties was conducted for the development of the 200-ZP-1 Model (DOE/RL-2007-28). Figure 3-10 presents a distribution of experimentally based hydraulic conductivity estimates. The data summarized in Figure 3-10 contain data from slug tests and sediment sample analysis whereas the data summarized in Table 3-1 are limited to pump test analysis.

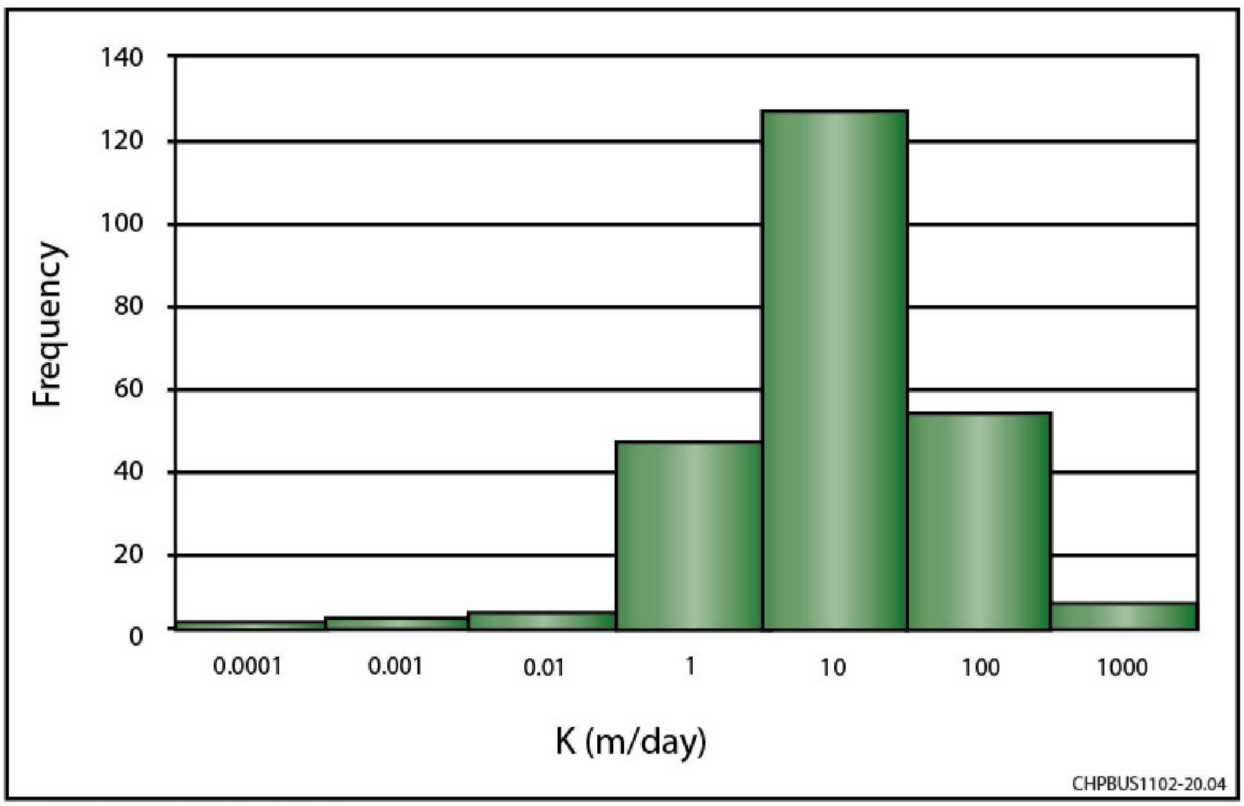

Source: DOE/RL-2007-28

Figure 3-10. Hydraulic Conductivity Distribution Ringold E

Vertical anisotropy has been estimated for pumping tests in Ringold E and for at least one test in the Hanford formation. Ringold E values range from 0.01 to 0.1 (PNL-10886) and 0.015 to 0.5 (DOE/RL-2007-28) for post–2000 testing. A Hanford formation estimate is 0.1 (HEIS Hydraulic properties database). Previous calibrations, prior to development of the CPGW Model, have found the calibration relatively insensitive to vertical anisotropy. This is largely because of the large horizontal scale of most modeling analyses—and lateral extent of the simulated HSUs—versus the relatively small vertical extent of the modeling analyses, and of the simulated HSUs. In addition, most wells are screened across the water table. There are few instances of multiple zones of measurement with depth. Therefore, anisotropy ratios obtained from (1) large-scale, site-specific pumping tests such as those recently conducted in the 200-ZP-1 OU, and from (2) literature values for equivalent or similar aquifer materials, are considered the most reliable source for this value. A value of 0.1 was assumed for all layers in the prior three-dimensional PNNL models (PNNL-14398 and PNNL-14753).

Specific yield has been estimated from tests of the Hanford formation and Ringold Formation as presented in Table 3-2. Ringold A and E are jointly described in PNL-10886. These models encompass a larger domain than the CPGW Model. They had the same water level measurements, over a larger domain, that we have available. They showed limited sensitivity to specific yield. Only the specific yield of the Ringold unit E was modified in the calibration described in PNNL-14753. Specific yield was not estimated for the model described in PNNL-14398.

Table 3-2. Review of Hydrostratigraphic Unit Specific Yield

Unit	PNL-10886 Experimental Data (dimensionless)	PNNL-13641 Experimental Data (dimensionless)	PNNL-14398 Assumed (dimensionless)	PNNL-14753 Assumed (dimensionless)
Hanford	0.1 - 0.3	0.2 - 0.37	0.25	0.1
Cold Creek			0.1	0.1
Ringold E	0.05 - 0.2	0.05 - 0.37	0.1	0.11
Ringold mud				0.1
Ringold A	0.05 - 0.2	0.15		0.1

Sources:

PNL-10886, 1995, *Development of a Three-Dimensional Ground-Water Model of the Hanford Site Unconfined Aquifer System: FY 1995 Status Report*, Pacific Northwest National Laboratory, Richland, Washington.

PNNL-13641, 2001, *Uncertainty Analysis Framework – Hanford Site Wide Groundwater Flow and Transport Model*, Pacific Northwest National Laboratory, Richland, Washington.

PNNL-14398, 2003, *Transient Inverse Calibration of the Site-Wide Groundwater Flow Model (ACM-2): FY 2003 Progress Report*, Pacific Northwest National Laboratory, Richland, Washington.

PNNL-14753, 2006, *Groundwater Data Package for Hanford Assessments*, Rev. 1, Pacific Northwest National Laboratory, Richland, Washington.

3.2 Modeling Related Features, Events, and Processes

This section summarizes the relevant FEPs to be included and excluded from the CPGW Model. The list of exclusions is not exhaustive, but is intended to be extensive enough to support the identification of model limitations addressed in Chapter 6.

The most comprehensive application of the FEPs methodology at the Hanford Site to date is presented in BHI-01573, *The Groundwater/Vadose Zone Integration Project: The Application of Feature, Event, and Process Methodology at the Hanford Site*, and discussed in Last et al (2004). The Hanford features, events, and processes (HFEPs) identified in BHI-01573 are identified here as included or excluded. Additional FEPs not listed in the HFEPs that are considered are added to the list. Table 3-3 lists HFEPs identified in BHI-01573. Table 3-3 lists a HFEP number, if identified in BHI-01573, and a name for the FEP. A column labeled included indicates whether the FEP is included in the historic period flow model (flow) described in this report, used for predictive model flow and transport, or has not yet been not included in either phase (no) either. In the final column labeled “Relevant to CPGW Model,” “yes” identifies FEPs that are relevant to flow and transport in the CPGW Model domain and “no” if they have no relevancy. Many HFEPs that could affect flow in the Central Plateau are listed as not relevant on the assumption of geologic stability for the period to be simulated with this model or because they were rated low or moderate priority in the HFEP evaluation for the groundwater technical element in BHI-01573.

Table 3-3. Hanford Features, Events, and Processes

HFEP Number	Name	Included	Relevant to CPGW Model
2.2.07.30	Groundwater flow (in geosphere)	Flow	Yes
3.2.07.35	Groundwater discharge to surface. Groundwater and associated contaminants (either solutes for suspended particulates) may eventually discharge to the Columbia River, to seeps near the river, to springs, or to wells.	Fate and transport	Yes
2.2.07.51	Far-field transport: hydrodynamic dispersion	Fate and transport	Yes
2.2.04.01	Faulting (large scale, in geosphere). Hydraulic influence of May Junction Fault	Flow	Yes
1.4.04.00.04	Future liquid waste disposal	Fate and transport	Yes
1.4.04.00.17	Water resource exploration	No	Yes
1.1.11.00.02	Post closure monitoring	No	Yes
2.3.11.13	Groundwater discharge. The Columbia River is the principal discharge area for the unconfined aquifer system. In this model, the discharge to the Columbia River is not directly modeled because the model domain does not extend to the river, but it is implicitly included with mixed type boundary conditions that represent the discharge to the river.	Fate and transport	Yes
2.3.11.14	Groundwater recharge. Recharge issues related to groundwater flow and contaminant transport within the context of a conceptual model of the natural system on a large scale. Recharge refers to input of water to the groundwater flow system. Recharge of the uppermost unconfined aquifer takes place from infiltration of precipitation, particularly in elevated regions along the western boundary of the Hanford Site, from infiltration of imported water disposed to waste sites, leaked from distribution systems, and applied for irrigation, and from upward leakage from the deeper confined aquifer system. These are all included except for upward leakage from the deeper confined aquifer system, which is excluded from the model at present.	Flow	Yes
	Basalt surface. Section 3.2.4 discusses the assumption that the basalt surface is an impermeable lower boundary.	Flow	Yes
	Groundwater remedial actions (pump-and-treat systems)	Flow	Yes

Table 3-3. Hanford Features, Events, and Processes

HFEP Number	Name	Included	Relevant to CPGW Model
	Spatial variability. Hydraulic property variation by HSU with differential vertical and horizontal hydraulic conductivity.	Flow	Yes
1.2.02.01.00	Fractures in basalt	No	Yes
1.2.02.02.00	Faulting (movement along existing faults)	No	No
1.2.03.01.00	Seismic activity	No	No
1.2.04.01.00	Magmatic activity affects hydrothermal conditions	No	No
1.2.04.02.00	Magmatic activity affects hydrothermal conditions	No	No
1.4.04.02.00	Abandoned and undetected boreholes	No	No
3.2.07.01.00	Isotopic dilution	No	No
1.2.10.01.00	Hydrological response to seismic activity	No	No
1.2.01.01.01	Folding, uplift, or subsidence lowers facility with respect to the current water table	No	No
1.2.02.01.01	Changes in hydraulic properties of sediments (due to compaction)	No	No
1.2.04.01.01	Volcanism	No	No
1.4.04.02.01	Exploratory borehole creates flow pathway	No	No
1.2.10.01.01	Fault movement pumps fluid from saturated to unsaturated zone (seismic pumping)	No	No
1.2.01.01.02	Tectonic changes to local geothermal flux causes convective flow in saturated zone and elevates water table	No	No
3.2.07.01.02	Natural radionuclides/elements (in host rock disturbed zone)	No	No
1.2.10.01.02	Fault creep causes short term fluctuations of the water table	No	No
1.4.04.02.03	Waste-induced borehole flow (in waste and engineered barrier system)	No	No
1.2.10.01.03	New faulting breaches flow barrier controlling large hydraulic gradient to the north	No	No
1.2.01.01.04	Uplift or subsidence changes drainage at site, increasing infiltration	No	No
1.2.02.02.04	Movements along small-scale faults	No	No
1.2.04.02.04	Igneous activity causes extreme changes in rock geochemical properties	No	No
1.4.04.01.05	Drilling fluid flow	No	No
1.4.04.02.05	Natural borehole fluid flow	No	No
1.2.01.01.06	Effect of plate movements	No	No

Table 3-3. Hanford Features, Events, and Processes

HFEP Number	Name	Included	Relevant to CPGW Model
1.2.01.01.09	Regional vertical movements	No	No
1.4.04.00.01	Geothermal (drilling associated with exploitation of geothermal sources)	No	No
1.4.04.00.02	Other resources (drilling to explore for other resources)	No	No
1.4.04.00.03	Enhanced oil and gas recovery	No	No
1.4.04.00.05	Hydrocarbon storage	No	No
1.4.04.00.06	Exploratory drilling for hydrocarbons	No	No
1.4.04.00.07	Blowouts	No	No
1.4.04.00.24	Oil and gas extraction	No	No
1.4.04.00.25	Liquid waste disposal from oil and gas production	No	No
1.4.04.00.26	Enhanced oil and gas production	No	No
1.1.11.00.01	Monitoring. Boreholes used to monitor performance could provide pathways for contaminant transport between different hydrogeological formations.	No	No
1.2.10.01.10	Fault establishes pathway through the saturated zone	No	No
1.2.01.01.12	Regional horizontal movements	No	No
	Vadose zone flow. This model is restricted to the fully saturated unconfined aquifer and, hence, vadose zone flow and transport is not included directly. However, the inclusion of the attenuating impact of the presence of the vadose zone is indirectly incorporated through the use of vadose zone simulated artificial recharge.	No	Yes
	Perching of artificial recharge, discussed in Section 3.2.2.	No	Yes
	Climate change. This model is restricted to recharge conditions that reflect current climate and does not incorporate climate change effects.	No	Yes
	Dam failure. Potential contaminant transport due to flooding of the site caused by upstream dam failure is not considered in the analysis.	No	Yes

3.2.1 FEP Discussion: Anthropogenic Recharge

Wastewater discharges associated with activities at the Hanford Site were significant sources of water to the subsurface, at times exceeding tens of millions of cubic meters per year (Figure 3-11). Some of the largest sources of process-related water to the subsurface included T-Swamp, U Pond (216-U-10), 216-U-14 Trench, B Pond (216-B-3), 200 Area Treated Effluent Disposal Facility, and Gable Mountain Pond. These large releases exerted significant control on the rates and directions of groundwater flow, as well as contaminant migration and continue to exert some effect as the water table recovers to pre-development conditions. Detailed descriptions of various sources of recharge are provided in several publications, including PNL-6403, *Recharge at the Hanford Site: Status Report*, and PNL-10285, *Estimated Recharge Rates at the Hanford Site*. Both anthropogenic and natural sources of water must traverse a thick, unsaturated (vadose) zone to reach, and ultimately recharge, the unconfined aquifer beneath.

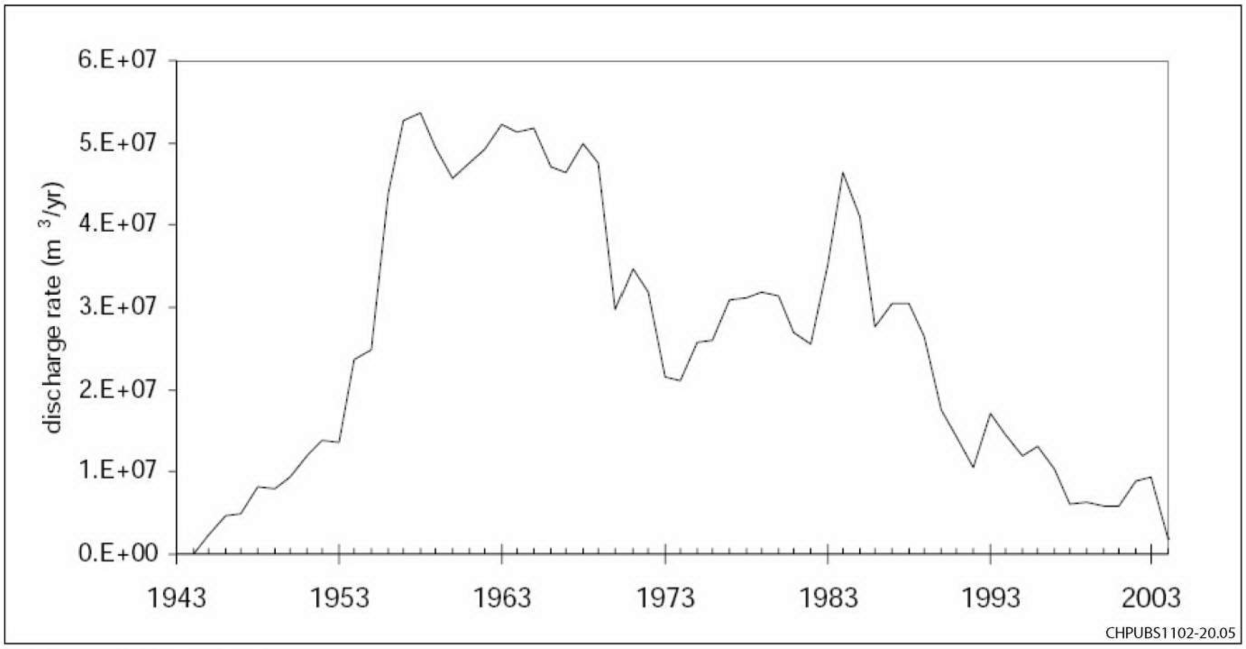

Source: PNNL-14753

Figure 3-11. Historic Anthropogenic Recharge (1944 to 2005)

Arrival of surface discharges at the water table where they provide recharge to the aquifer is attenuated and delayed by the unsaturated zone. A vadose zone transmission of liquid discharges was simulated for each discharge site as a part of the PNNL's model development (PNNL-14753, and *Vadose Zone-Attenuated Artificial Recharge for Input to a Ground Water Model* [Nichols et al, 2007]). Figure 3-12 presents the effects of simulated vadose zone attenuation and delay for the sum of all liquid discharge sites at the Hanford Site. The grey line in this figure is the discharge rate to the surface; the green line is the arrival of water flux at the water table. The discharge rates are plotted as m^3/yr over the length year for surface discharges and length of each calculation time step for the water table arrival. The results of these calculations were used as specify artificial recharge for the CPGW Model in the historic period with the water table arrival averaged over each year. Due to time constraints, surface discharges after 2009 have been applied directly to the water table rather than applied through the vadose zone simulation.

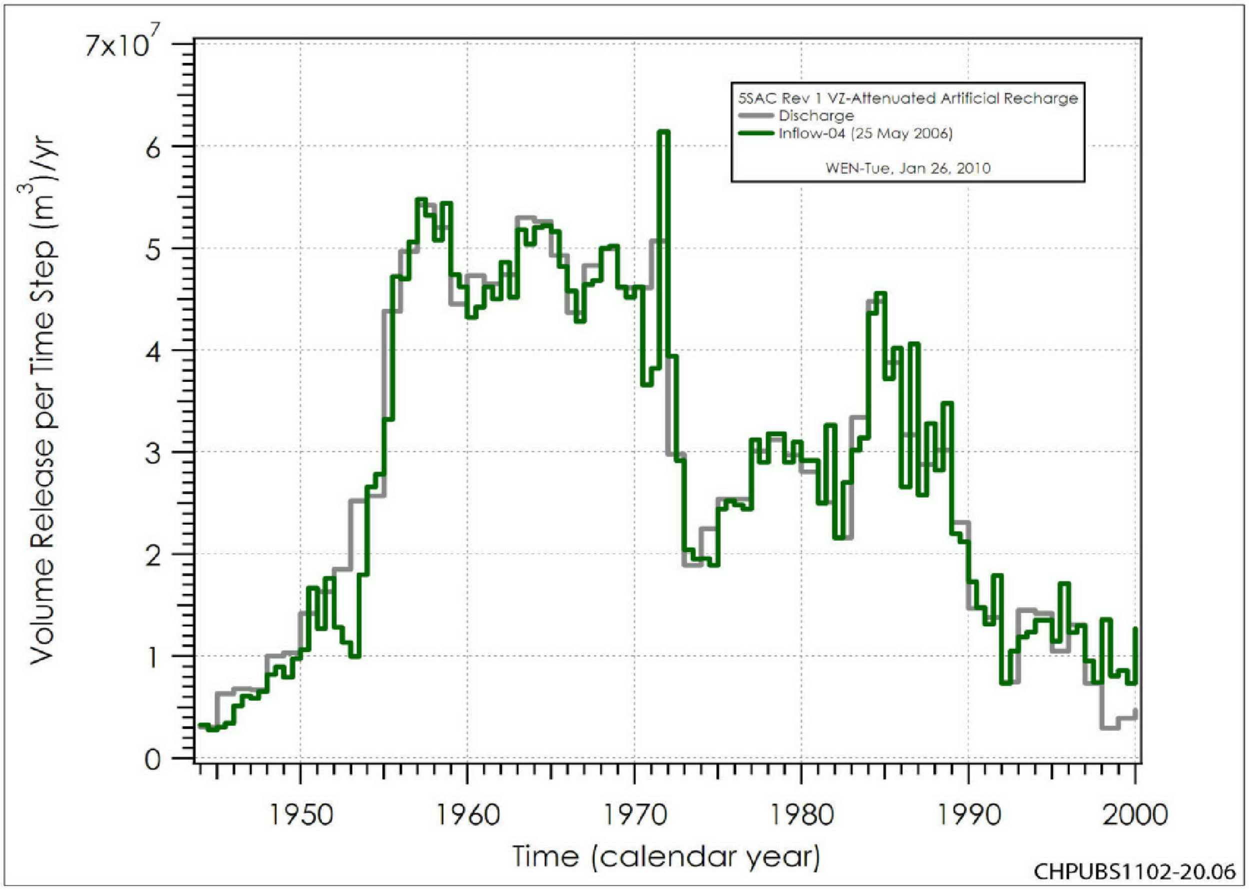

Figure 3-12. Liquid Disposals at Surface and Vadose Zone Simulated Artificial Recharge for the Sum of All Hanford Site Liquid Discharges (1944 to 2000)

3.2.2 FEP Discussion: Perching of Anthropogenic Recharge

There is evidence indicating that perching has occurred influencing flow in the saturated aquifer. Perching is not included in the CPGW Model as a simulated process. Instead, the historical water table measurements that were taken when perching may have influenced anthropogenic recharge have not been directly included in the model hydraulic properties calibration. Section 4.5.3 provides details of how this was accomplished. Locally, the impact can be large. Figure 3-13 compares simulated water level response to measured response in well 299-W19-1. The magnitude of the misfit is larger than any other calibration well in the model. Other wells near well 299-W19-1 also indicate large misfits, but these are less than indicated in Figure 3-13. The misfit shown in Figure 3-13 may be due to both the delay in water reaching the water table and lateral migration of water due to perching. A number of investigations have revealed large perched water bodies in the 200 West Area where well 299-W19-1 is located, summarized here:

1. In 1948, the Office of the Atomic Energy Commission discovered perched conditions in 2 of the 25 wells drilled during the investigation. In one well (identified today as well 699-45-69A), 1.6 to 3 m of water was found at an elevation of approximately 169 m, which was approximately 43.6 m above the water table. 169 m is very close to the top of the Cold Creek unit in this area (Figure 3-14), but the drillers log does not indicate a change in geologic unit at this elevation. This well is more than 2 km west of T-Swamp, the largest known wastewater discharge location at the time. Perched water was also found in well 699-35-70, located 2 km or more south of T-Swamp. This

perched zone was thinner and lower (137 m elevation) than that found in well 699-45-69A. The perched zone is well below the top of Ringold unit E.

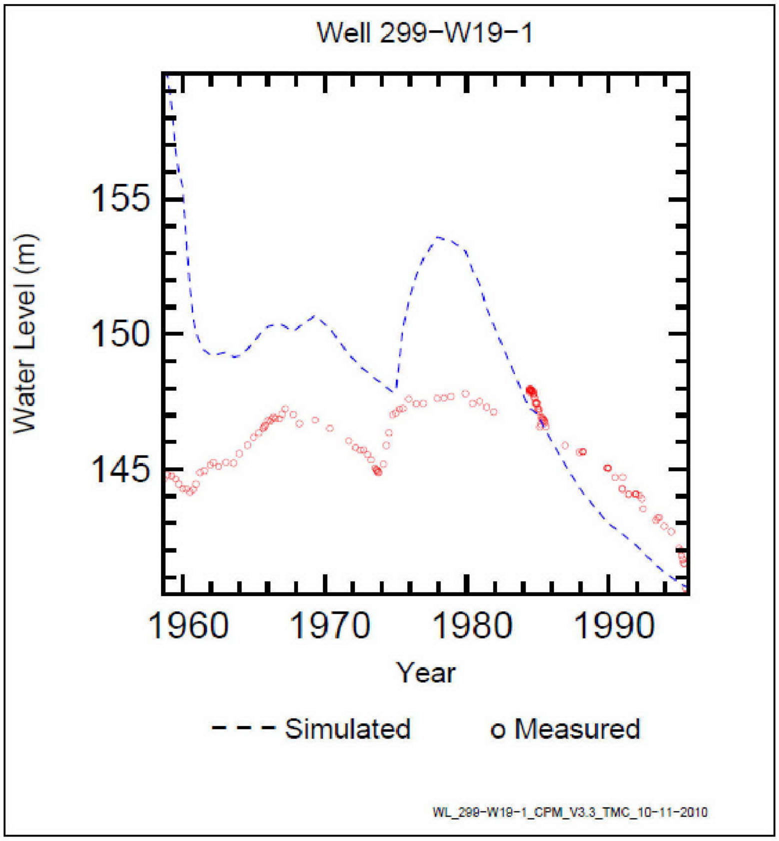

Figure 3-13. Example of Possible Perching Influence

2. Well 699-35-78 was drilled in 1950. The following description is based on the drillers log available on the HEIS. A saturated layer of water at an elevation of 128 m was found. Below an elevation of 127 m, the well was dry again. It was cased and remained dry over a weekend until an elevation of 121.5 m was reached. The well then filled overnight to 128 m. The rapid rise suggests that once the 121.5 m elevation was reached, the well was in hydraulic contact with the same body of water found at 128 m. A 128 m water table elevation is consistent with other wells in the area. It is inferred that near the well, water was perched on a low conductivity lens of Ringold unit E at 128 m, but that away from the well, it was part of the saturated aquifer at nearly the same elevation. Alternately, the lens is saturated but has so little conductivity that only a non-measurable amount of water entered the well over the weekend.

3. A 1994 investigation of perching below the 216-U-14 Ditch identified perched conditions in wells 299-W19-91, 299-W19-92, 299-W19-93, 299-W18-250, 299-W18-251, and 299-W23-27, but not in well 299-W23-22 (*Groundwater Impact Assessment Report for the 216-U-14 Ditch* [WHC-EP-0698-FP]). Perching was considered to be of limited extent beyond the ditch. The top of the perched zone in wells 299-W19-91, 299-W19-92, and 299-W19-93 varied between 190 and 169 m elevation from 1990 through 1994. The perched zone was presumed to extend downward to the top of the Cold Creek unit, which is at an elevation of approximately 165 m at this location.

4. Two dimensional simulations of a perched water table under a generic 200 West Area waste site that incorporated the dip of the Cold Creek unit calculated that 99 percent of the water would exit the down dip side of the simulation rather than directly below the discharge location (*Effects of Varying Recharge on Radionuclide Flux Rates to the Water Table at the Low-Level Solid Waste Burial Site* [WHC-SA-0699-FP]).

5. Mounding evaluations in the unconfined aquifer, in response to discharges at the SALDS facility (Figure 3-14), suggest that the mounding is centered on an area laterally displaced from the SALDS effluent infiltration gallery. This lateral displacement arises from the movement of the discharge water along the Cold Creek unit (*Results of Tritium Tracking and Groundwater Monitoring at the Hanford Site 200 Area State-Approved Land Disposal Site Fiscal Year 2009* [SGW-42604]).

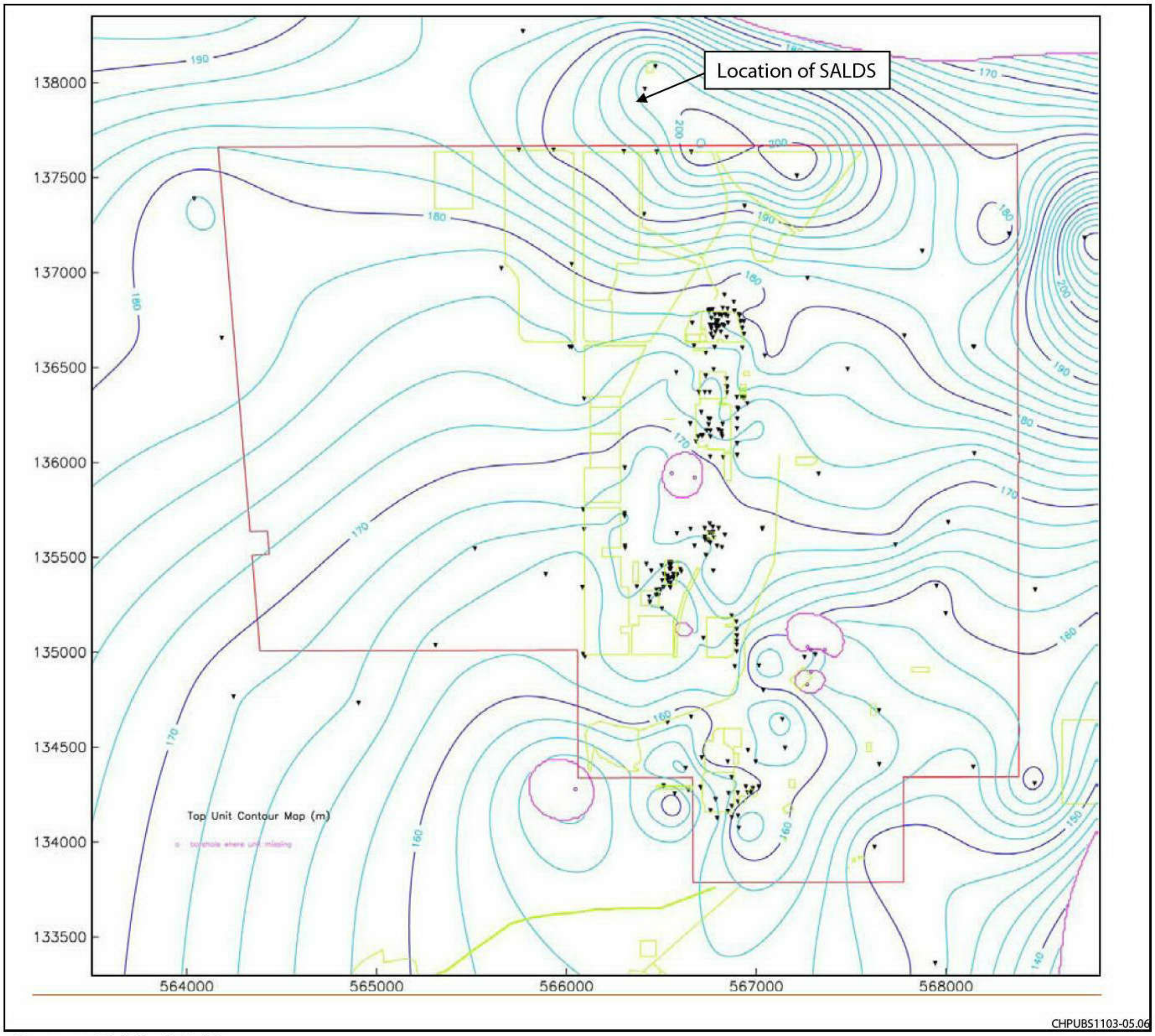

Source: PNNL-17913

Figure 3-14. Top of Carbonate Facies of Cold Creek Unit

These five investigations suggest that perched water has occurred during the Hanford Site operational period and that these areas of perching may have stored substantial volumes of water. In addition, there may have been lateral migration of water infiltrating through the vadose zone en-route to the water table of the unconfined aquifer. The perching appears to have developed above the calcified Cold Creek unit, and on low conductivity lenses of Ringold unit E.

3.2.3 FEP Discussion: Natural Recharge

Natural recharge includes both percolation of net precipitation to the water table and mountain-front recharge arising from infiltration of snowmelt, agricultural return-flows from irrigation, and run-off from elevated areas. The major sources of mountain-front recharge to the CPGW Model are the ephemeral Cold Creek and Dry Creek streams. Rates of net recharge from aerial precipitation were acquired from PNNL-14753. Recharge associated with stream flows are a significant contributor to groundwater recharge upgradient of the Central Plateau (PNNL-17841, *Compendium of Data for the Hanford Site [Fiscal Years 2004 to 2008] Applicable to Estimation of Recharge Rates*). Since the amount of recharge that occurs through the Cold Creek and Dry Creek streams is uncertain, they have been included in the model and varied as calibration parameters. The small amounts of recharge from runoff of Gable Mountain, Gable Butte, the basalt subcrop along the southern boundary of the model, and other small slopes toward the model domain have been neglected.

Natural recharge from precipitation at the Hanford Site is highly variable both spatially and temporally, ranging from near-zero to more than 100 mm/yr depending on climate, vegetation, and soil texture ("Variations in Recharge at the Hanford Site" [Gee et al., 1992] and PNL-10285). Vegetative areas and fine-textured soil like silt loams tend to have lower recharge rates, while areas with little vegetation and coarse-textured soil, such as dune sands, tend to have higher recharge rates. PNL-10285 developed estimates of natural recharge for 1992 conditions using a step-by-step procedure. First, distributions of soil and vegetation types were mapped. Then, a recharge rate was assigned to each combination of soil/vegetation type based on data from lysimeters, tracer studies, neutron probe measurements, and computer modeling. The data used for these estimates derive from a number of sources, such as distribution of recharge estimated using the 1992 climate, a 1966 soil map (*Soil Survey Hanford Project in Benton County, Washington* [BNWL-243]), and 1979 vegetation/land-use patterns. Estimated recharge rates for 1992 ranged from 2.6 to 127 mm/yr, and the total volume of natural recharge from precipitation over the Hanford Site was estimated to be 2.35×10^4 m^3/d. This value is of the same order of magnitude as the artificial recharge to the 200 Area waste disposal facilities during 1992 and approximately one-sixth of peak discharges to these facilities during the 1960s (PNNL-14753). The 1992 estimates were used in the calibration of the 2005 model (PNNL-14753). A constant scale factor adjustment of 1.2 was determined through calibration of the model.

The 1992 estimate from PNL-10285 is used for each year without modification in the CPGW Model. Figure 3-15 presents the recharge data taken that is used in the CPGW Model (taken from PNNL-14753). The white lines to the left of the figure are Cold Creek and Dry Creek fluxes and are beyond the color scale of the plot. The small blue area near the Gable Gap is West Lake, a small pond where the water table is above land surface. The B Pond pit just east of the 200 East Area is also a region of large estimated recharge.

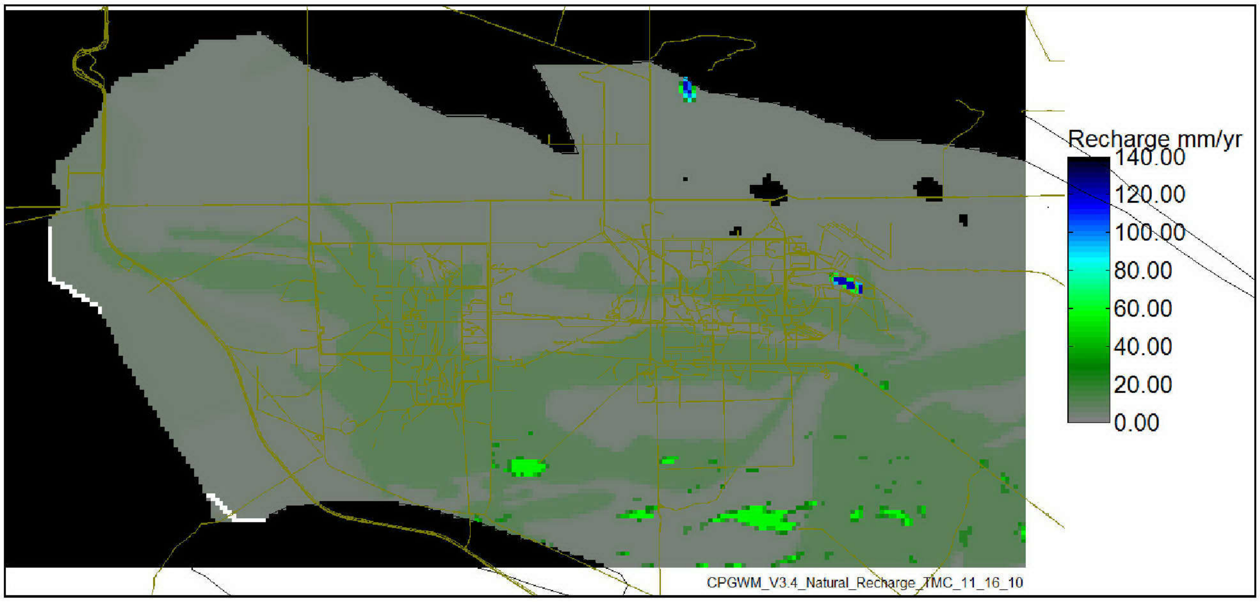

Figure 3-15. Natural Recharge Fluxes Used in the Central Plateau Groundwater Model

Four investigations of ephemeral stream fluxes entering the Central Plateau, as listed in Table 3-4, are reported in BHI-00608, *Hanford Sitewide Groundwater Flow and Transport Model Calibration Report.* Table 3-4 list fluxes for Cold Creek, Dry Creek, and a combination of the two based on these studies. In addition, there are estimates from model calibrations. In three cases, the fluxes were model calibration parameters. In one case, the fluxes were calculated from the calibrated model. These estimates are not entirely consistent. This is in part because the definition of Dry Creek varies. For most studies, Dry Creek refers to the upland area to the west of the CPGW Model Dry Creek boundary condition. However, Dry Creek continues to flow east, south of the southern boundary of the CPGW Model. Whether the upland flow enters the CPGW Model at the location corresponding to the Dry Creek boundary condition or stays south of the model domain is uncertain. In PNNL-11801, *Three-Dimensional Analysis of Future Groundwater Flow Conditions and Contaminant Plume Transport in the Hanford Site Unconfined Aquifer System: FY 1996 and 1997 Status Report*, and PNNL-13447, *Transient Inverse Calibration of Hanford Site-Wide Groundwater Model to Hanford Operational Impact – 1943 to 1996*, most of the Dry Creek flux was assumed to be diverted north in the subsurface to the location corresponding to the CPGW Model boundary condition location for Dry Creek. However, in PNNL-14753, model calibration indicated the entire flow moves east, below the CPGW Model boundary, with no northward flow diversion.

Table 3-4. Estimates of Stream Recharge Fluxes

Cold Creek (m^3/day)	Dry Creek (m^3/day)	Combined (m^3/day)	Research	Notes
1,728	1,231	3,305	Newcomb et al (1972)	After 1954
19,872	9,504	29,376	Livesay (1986)	Too Large?
5,184			RHO-ST-42	
		19,872	Bennet (1992)	Post 1969
8,130	15,700	23,830	PNNL-14398	Preliminary estimates

Table 3-4. Estimates of Stream Recharge Fluxes

Cold Creek (m^3/day)	Dry Creek (m^3/day)	Combined (m^3/day)	Research	Notes
8,812	1,209	10,021	PNL-7144	Model Calibration
10,368	44,068	54,436	BHI-00608	Model Calibration
6,010	1,207	7,217	PNNL-11801	Calculation
5,722	0	6,953	PNNL-14753	Model Calibration Dry Creek too small to estimate

Sources:

Bennet, G.B., 1992, "Draft Report – Ground-Water Aspects of the Macroengineering Approach at the Hanford Reservation," (letter to Heather Duncan of A.J. Kerny, Inc.).

BHI-00608, 1997, *Hanford Sitewide Groundwater Flow and Transport Model Calibration Report*, Rev. 0, Bechtel Hanford, Inc., Richland, Washington.

Livesay, D.M., 1986, *The Hydrology of the Upper Wanapum Basalt, Upper Cold Creek Valley, Washington*, M.S. Thesis, Department of Geologic Engineering, Washington State University, Pullman, Washington.

Newcomb, R.C., J.R. Frank, and F.J. Frank, 1972, *Geology and Groundwater Characteristics of the Hanford Formation of the Hanford Reservation of the U.S. Atomic Energy Commission, Washington*, Professional Paper 717, U.S. Geological Survey, Washington, D.C.

PNL-7144, 1990, *An Initial Inverse Calibration of the Ground-Water Flow Model for the Hanford Unconfined Aquifer*, Pacific Northwest Laboratory, Richland, Washington.

PNNL-11801, 1997, *Three Dimensional Analysis of Future Groundwater Flow Conditions and Contaminant Plume Transport in the Hanford Site Unconfined Aquifer System: FY 1996 and 1997 Status Report*, Pacific Northwest National Laboratory, Richland, Washington.

PNNL-14398, 2003, *Transient Inverse Calibration of the Site-Wide Groundwater Flow Model (ACM-2): FY 2003 Progress Report*, Pacific Northwest National Laboratory, Richland, Washington.

PNNL-14753, 2006, *Groundwater Data Package for Hanford Assessments*, Rev. 1, Pacific Northwest National Laboratory, Richland, Washington.

Newcomb et al (1972) estimated fluxes after 1954, when agricultural use of the upland area of the Cold Creek drainage had been prohibited. That injunction was lifted in 1969. Newcomb et al. also estimated a flux of 347 m^3/day from the unconfined aquifer through the "Cold Creek Barrier" (which may be the Cold Creek fault feature). This amount is included in the "Combined" column of Table 3-4.

Livesay's *The Hydrology of the Upper Wanapum Basalt, Upper Cold Creek Valley, Washington* (1986) estimates were developed using a regression analysis of stream flow data from watersheds that had perennial base flow. Livesay (1986) pointed out that the method may overestimate the estimates for Cold Creek and Dry Creek.

Estimates for Cold Creek (*Hydrology of the Separations Area* [RHO-ST-42]) using Darcy's law ($Q = WBKi$)—assuming a hydraulic conductivity, K, of 12.2 m/day; hydraulic gradient, I, of 0.002; thickness, B, of 61 m; and length, W, of 3,048 m—were 5,184 m^3/day. This estimate is after the resumption of agricultural use in 1969. Bennet,1992, *Draft Report – Ground-Water Aspects of the Macroengineering Approach at the Hanford Reservation*, used a water balance to estimate the combined recharge from Cold Creek and Dry Creek to be 19,872 m^3/day. In summary, these four calculation based estimates have an order of magnitude variation.

PNNL-14398 reports another investigation of Cold Creek (8,130 m^3/day) and Dry Creek (15,700 m^3/day) watersheds using stream flows. The estimates are reported as preliminary as of 2003. A final report detailing this study has not been located at the time of preparation of this report.

Numerical modeling based estimates for Cold Creek vary by less than a factor of two. As indicated in the previous paragraphs, there is disagreement in the numerical studies about if Dry Creek enters the CPGW Model domain or not.

3.2.4 FEP Discussion: Basalt Surface Fluxes

The Hanford Site is located within the CRBG province, which comprises hundreds of stacked basalt flows throughout southern/eastern Washington, northeastern Oregon, and western Idaho. Results of studies completed at the Hanford Site specifically, and throughout the CRBG province generally, indicate that the basalt flows can be categorized broadly as a sequence of dense, low-permeability flow interiors. These are separated by more permeable interflow zones, which comprise the base of an overlying flow and the top of the underlying flow, with occasional intermediate clastic sediments. In some locations throughout the CRBG province, these interflow zones are substantial enough to comprise aquifers.

As described earlier, the CPGW Model is constructed on the assumption that the basalts form an impermeable base to the unconfined aquifer. However, evidence exists showing the unconfined aquifer overlies and is connected with interflow zones. There may be upward and/or downward flow between the unconfined clastic sediments and the basalt interflow. This process is not included in the current version of the CPGW Model. The process was investigated as a part of an alternate conceptual model investigation (*Transient Inverse Calibration of Site-Wide Groundwater Model to Hanford Operational Impacts from 1943 to 1996—Alternative Conceptual Model Considering Interaction with Uppermost Basalt Confined Aquifer* [PNNL-13623], and PNNL-13641). The distributed flux through basalt was estimated using a three-dimensional inverse calibration (PNNL-13623). Implementation of basalt leakage was accomplished by adding:

- Head dependent spatially distributed leakage through the basalt confining layer
- Increased leakage at an erosional window near Gable Mountain/Gable Butte
- Increased leakage at a smaller erosional feature near B Pond
- Increased leakage along two fault zones

Figure 3-16 shows the distribution of basalt surfaces for members of the Ellensburg Formation (Figure 3-1) that have been exposed due to erosion of the upper portion of the basalt. The erosion also exposed the Rattlesnake interbed, a permeable sedimentary confined aquifer, below the topmost Elephant Mountain Member that forms the basalt surface below most of the Central Plateau. Basalt flow tops between members can also host permeable aquifers. The model described in PNNL-13623 included the roughly circular central core of the erosional window as a special surface flux feature. Thinning of the Elephant Mountain Member was simulated near B Pond. The larger contact with the Rattlesnake interbed north of B Pond was apparently not recognized at the time.

Figure 3-17 shows the location of four fault zones on the Hanford Site. The simulation described in PNNL-13623 included the two thrust fault zones. These faults are locations of discontinuity in the basalt. Hydraulically, they may be locations of concentrated flux through the basalt-sedimentary aquifer interface. The two normal faults were not expected to be major contributors of flux. The Gable Mountain Fault is outside the domain of the CPGW Model.

Figure 3-18 presents the estimated distributed flux across the basalt surface and erosional window for 1996. Close inspection reveals much larger fluxes adjacent to the Columbia River, outside the CPGW

Model domain. It also reveals both upward and downward flux in the Central Plateau region of the figure. Figure 3-19 presents the estimates for cumulative upward, downward, and net distributed flux as a function of time. Figure 3-20 allows comparisons of the significance of each feature investigated. It reveals that the distributed fluxes dominate the net fluxes. In addition, that the erosional window and Yakima Ridge Fault are relatively minor contributors. Estimated flux of the Gable Mountain Fault is large, but this is outside the CPGW Model domain. Within the Central Plateau region, the estimated basalt surface fluxes are small relative to an average 180,000 m^3/day anthropogenic recharge for 1980 (refer to Figure 3-11). Fluxes through the basalt surfaces were not included in subsequent versions of PNNL's site-wide groundwater model. Because of the thinness of the aquifer, fluxes to and from the basalt surface have a very similar impact on simulated water levels as changes in natural recharge rates. For these later models, it was concluded that neglecting basalt surface flux in these later models was compensated by the increased estimated precipitation recharge of 26,000 m^3/day (found in the calibration described in PNNL-14753) over cumulative reported recharge determined by PNL-10285 (PNNL-14753, p. 5.8). Again, most of this additional flux is outside the CPGW Model domain.

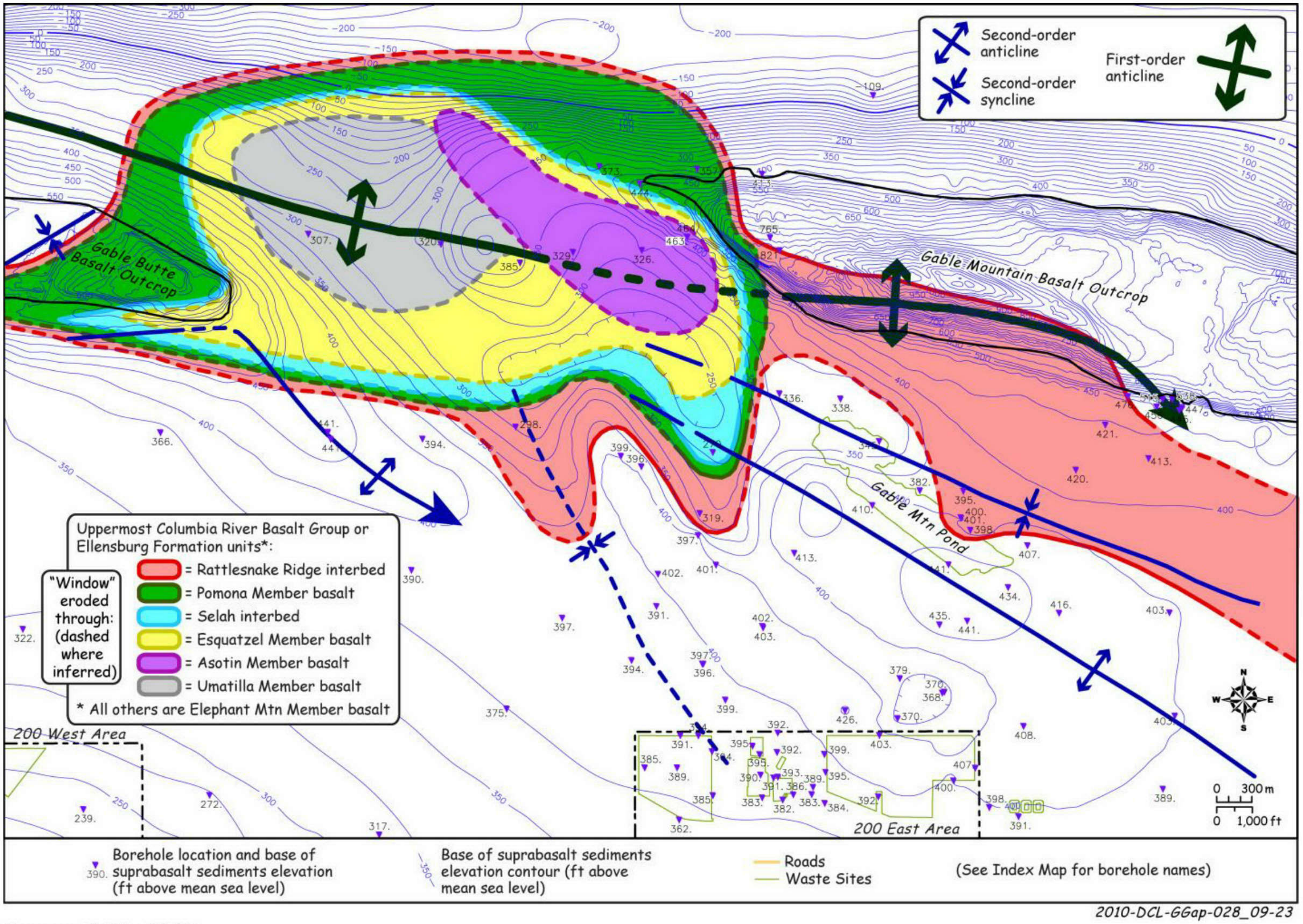

Source: PNNL-19702

Figure 3-16. Map of Upper Confined Basalt Aquifer (Pink) Contact with Unconfined Aquifer of the Central Plateau Groundwater Model

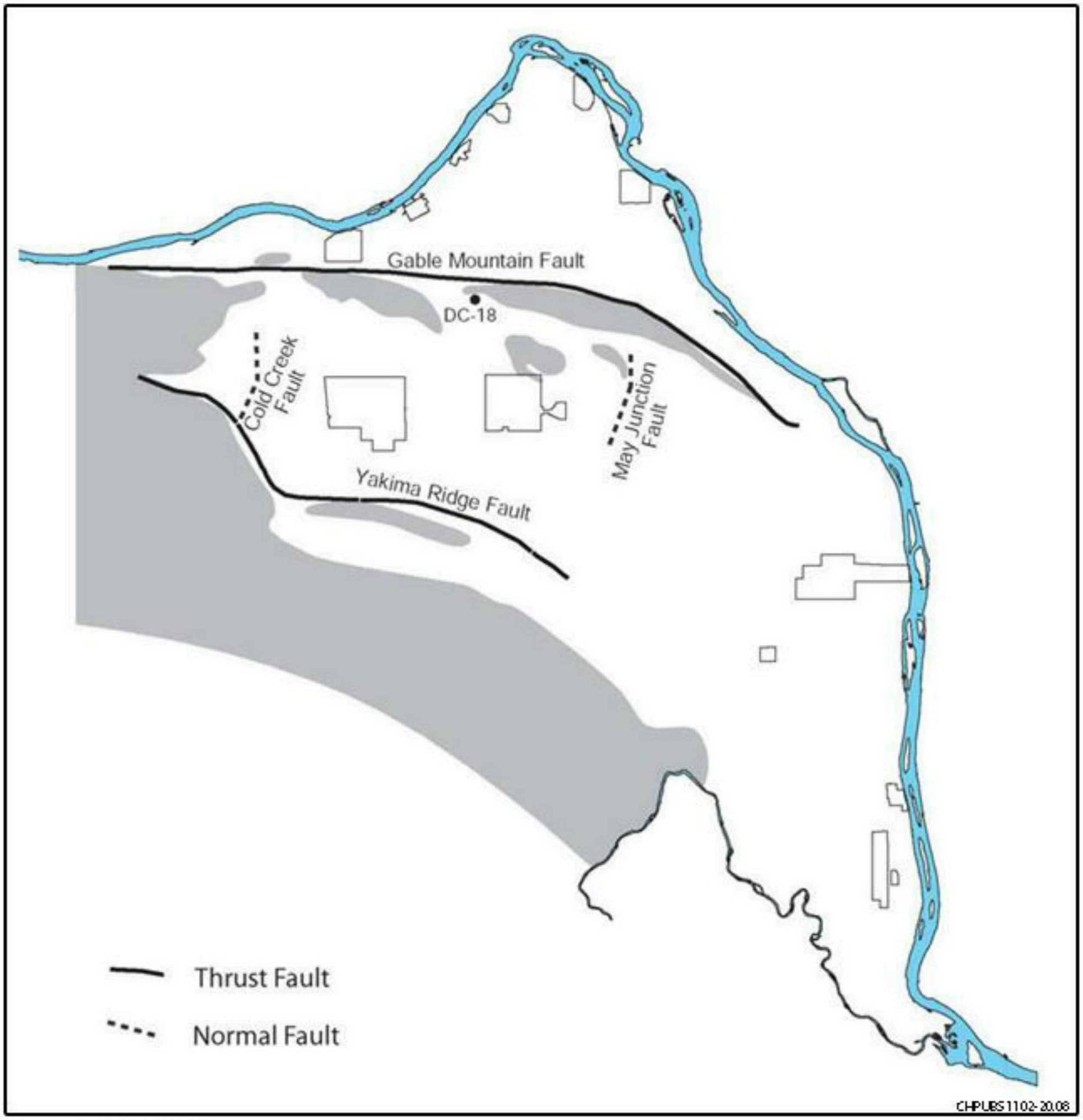

Source: PNNL-13623

Figure 3-17. Location of Thrust and Normal Faults on the Hanford Site

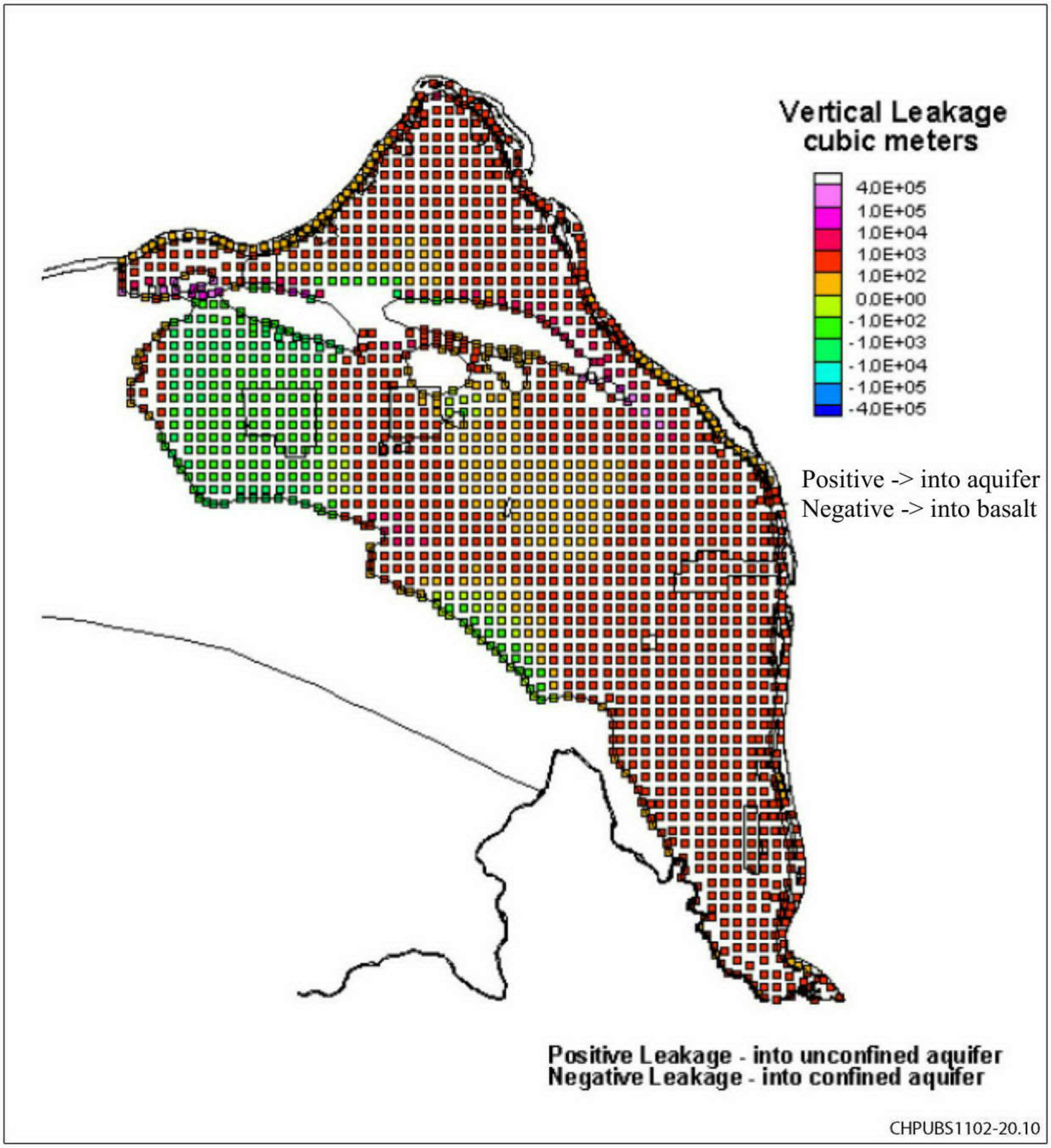

Source: PNNL-13623

Figure 3-18. Estimated Flux across Upper Basalt Surface for 1996

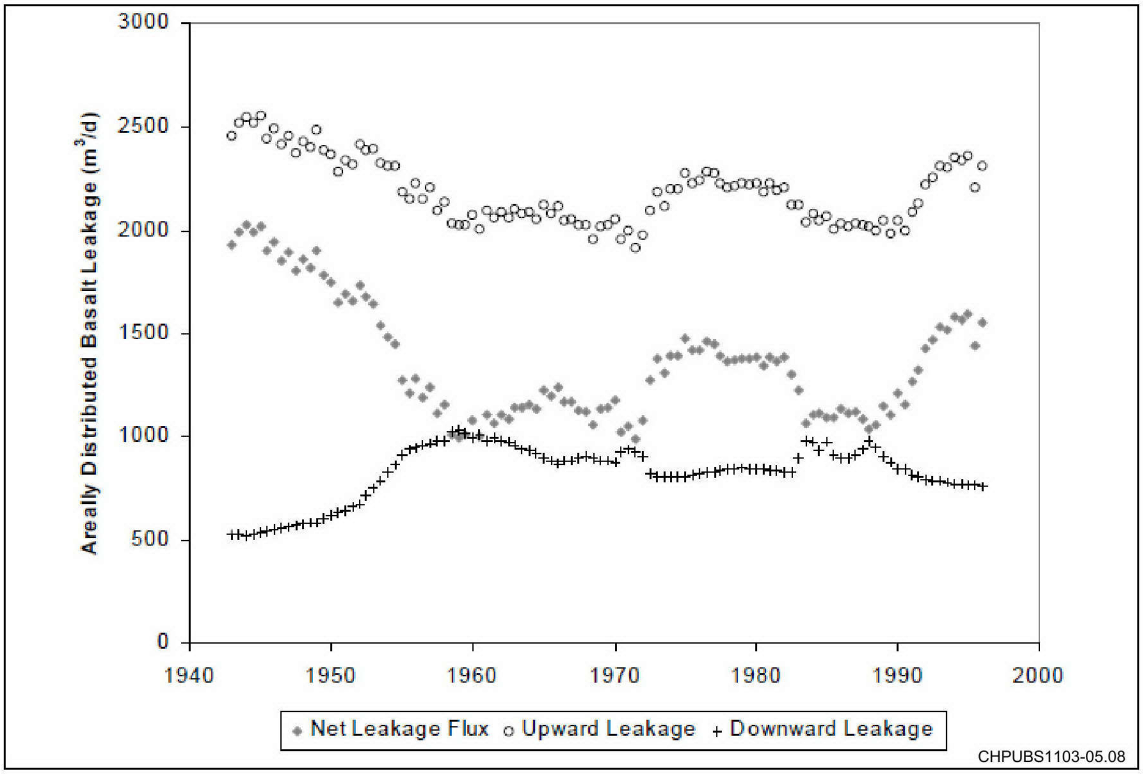

Source: PNNL-13623

Figure 3-19. Temporally Varying Estimated Flux across Upper Basalt Surface

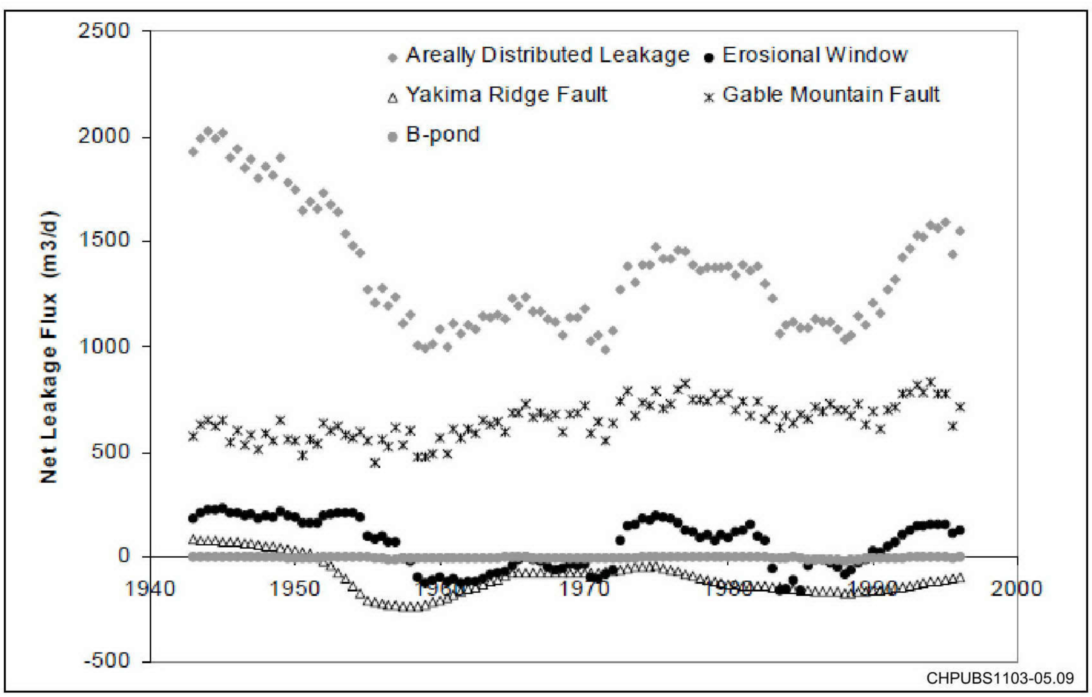

Source: PNNL-13623

Figure 3-20. Relative Contribution of Each Basalt Leakage Feature to Net Leakage

3.2.5 FEP Discussion: Basalt Ridge Flow Barrier

Figure 3-21 presents a map of basalt above the present water table along with deformational controls of basalt elevation in this region between Gable Gap and 200 East Area. Figure 3-21 suggests the presence of three paleochannel related lows in the basalt surface. Because of a limited number of wells in the area, uncertainty exists on the configuration of the paleochannels and top of basalt. The middle channel crossing the northeast corner of the 200 East Area is thought to be currently above the water table (*Hydrogeologic Model for the Gable Gap Area, Hanford Site* [PNNL-19702]). Water levels have dropped an average rate of about 0.14 m/y in the northern portion of the 200 East Area since the cessation of most surface water disposal (*Data Package for Past and Current Groundwater Flow and Contamination Beneath Single-Shell Tank Waste Management Areas* [PNNL-15837]).

If the water table drops far enough, as seems likely, the ridge of high basalt northeast of the 200 East Area will form a flow barrier between the 200 East Area and the Gable Gap effectively stopping the current flow direction northward from the Central Plateau. The timing of closure will affect contaminant transport. However, there could be channels across the basalt divide that are incised deeper into the basalt than is currently represented in the model, resulting in localized conduits for the preferential flow of groundwater. The Grand Coulee channeled scabland is an example of features that may exist in and south of the Gable Gap. The scabland is about 150 km north of the Hanford Site. Figure 3-22 depicts the Lower Grand Coulee channeled scabland carved out by the Missoula floods. The figure shows multiple meter variations in surface elevation over distances that are small compared to the well spacing used to control the surface of the basalt in the Gable Gap area of the CPGW Model. Being upstream of the Hanford Site, the erosional forces were larger at Grand Coulee, so the scale of erosional features is larger, but similar to what would be expected in 200-BP-5. Figure 3-22 conveys the concept that if the 200-BP-5 basalt is similar to the Grand Coulee scablands, it is impossible to estimate basalt surface elevations at the scale of the model cells within a meter from our limited borehole contact information with high confidence.

The basalt saddle to the northwest of the 200 East Area has a minimum elevation of 121.6 m in the model. Historic water level measurements may indicate that this level is too high in the model compared to the actual geography. Figure 3-23 presents water level measurements from 1948 to 1960 for five wells that straddle the basalt ridge saddle. The figure also shows Columbia River discharge measurements over the period. Figure 3-24 shows the locations of these wells. Wells 699-60-60 and 699-55-50A are north of the saddle. The plots indicate that these wells have an annual cycle that lags roughly 4 to 6 months behind the river. Starting in 1950, these wells indicate a steady rise in water level, possibly from discharges at B Pond or possibly due to discharges near the 100-BC Reactors or 100-K Reactor. Well 699-47-60, south of the saddle, indicates a hydraulic connection with the wells north of the saddle below elevation 121.6 m. The well was not installed in time for earlier water level measurements.

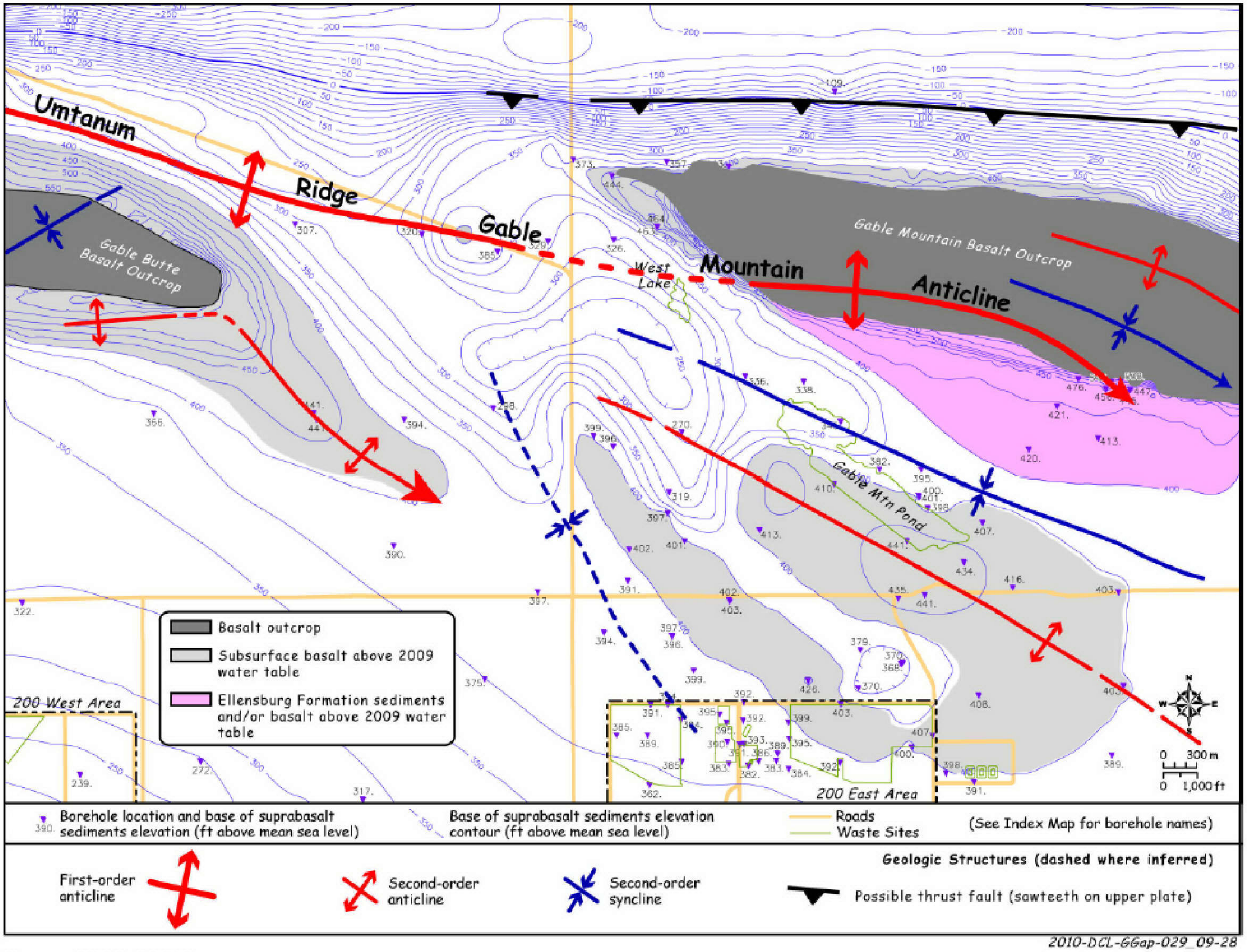

Source: PNNL-19702

Figure 3-21. Basalt Deformation and Surface Expression in the Gable Gap and 200 East Area

Source: PNNL-19702
Note: View looking north; blue block arrows show general movement of floodwaters, which scoured and overtopped the crest of the basalt ridge along left side of image.

Figure 3-22. Example of Highly Irregular Topography Eroded by Ice Age Floods, Lower Grand Coulee, Channeled Scabland

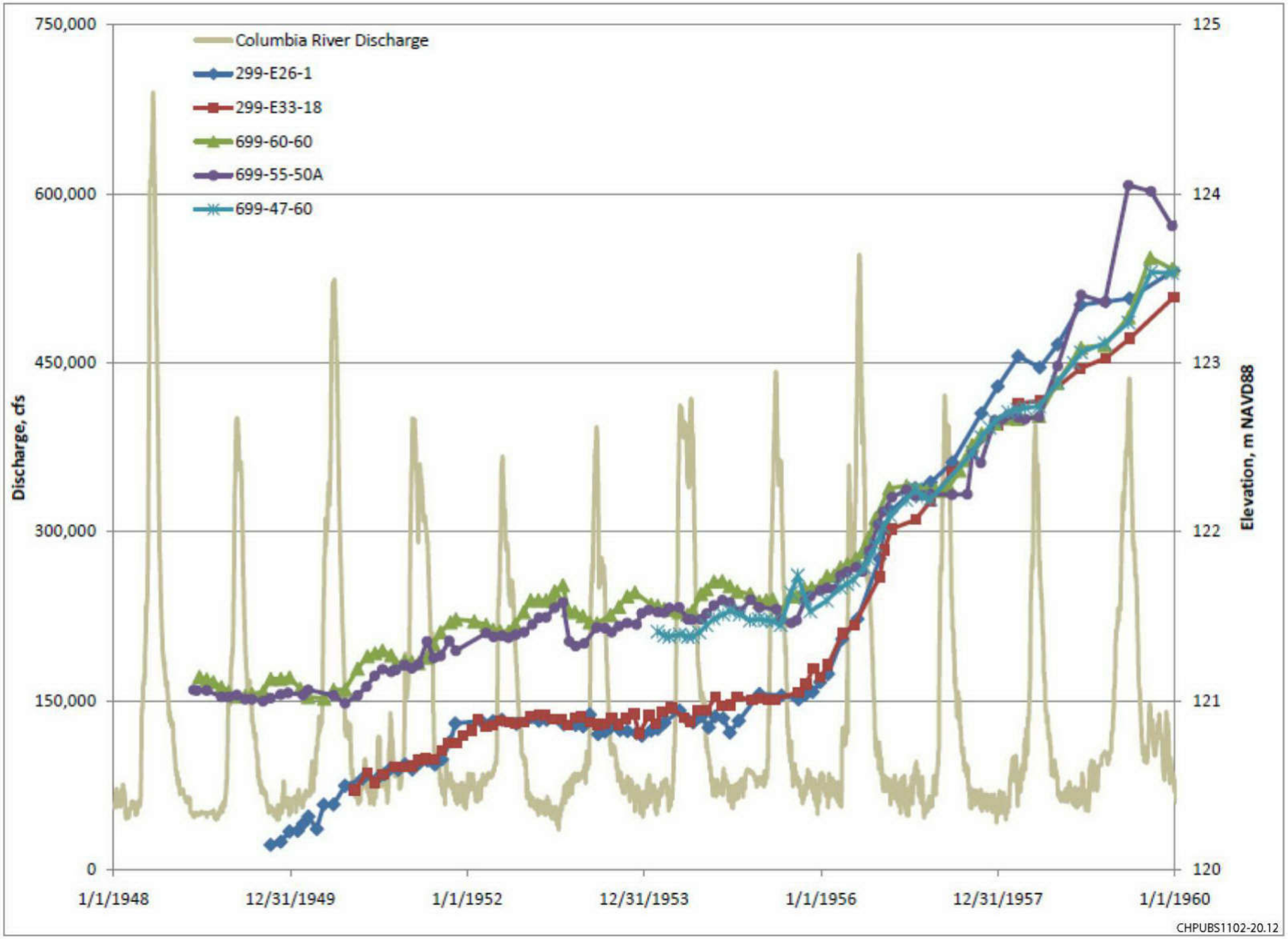

Figure 3-23. Historic Water Level Measurements near the Basalt Ridge Saddle

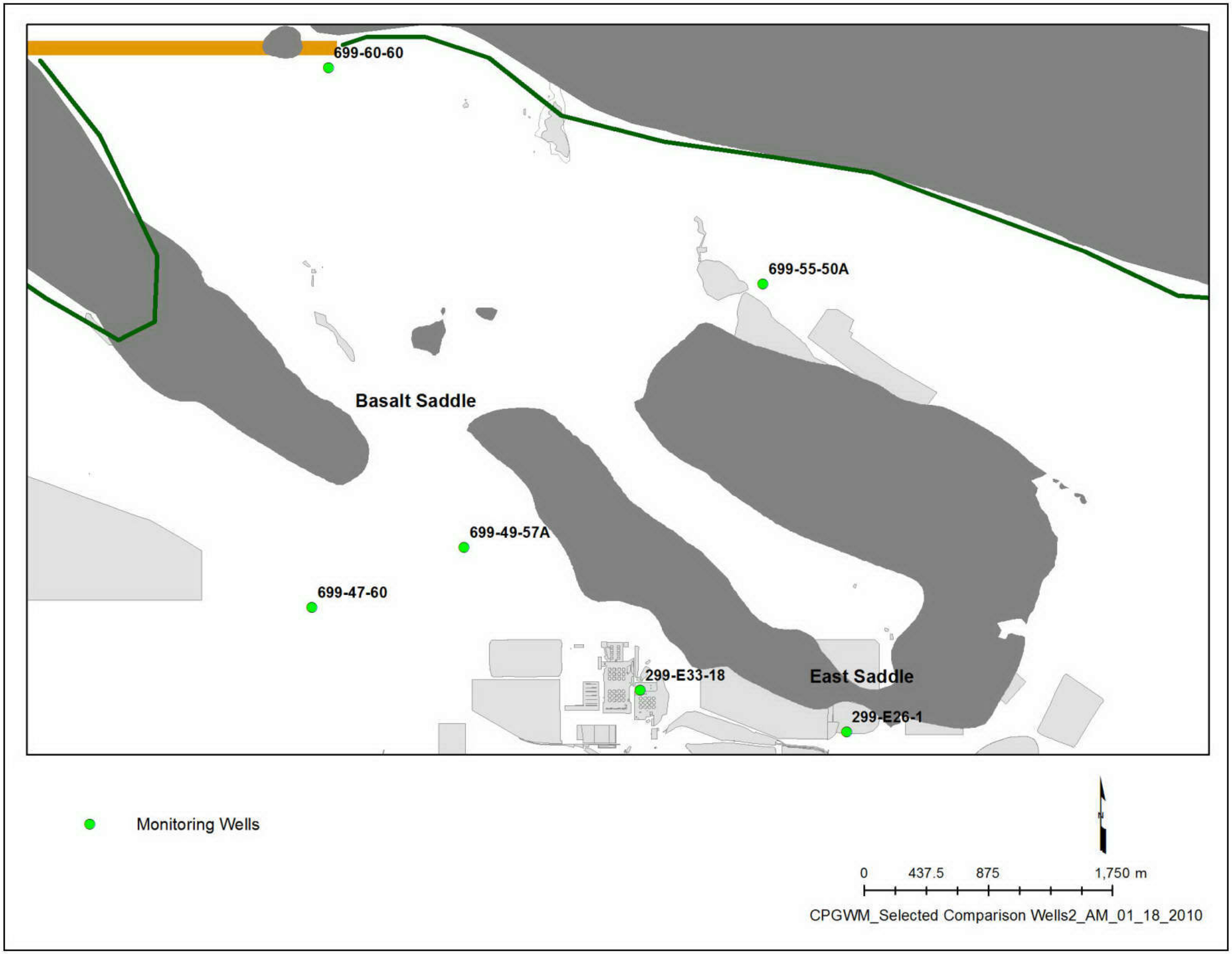

Figure 3-24. Locations of Wells Referred to in Figure 3-23

4 Model Implementation

The approach to the near-field groundwater flow and contaminant fate and transport modeling utilizes a mathematical hydrogeological construct to represent the physical conditions within the aquifer of the OU. This construct is developed using a modified versions of the acquired computer software called MODFLOW and MT3DMS (Section 4.1, Software). This report specifies the data files that were used in the development of the model. These data files are accessible through the Environmental Model Management Archive (EMMA), as required by the CH2M HILL Plateau Remediation Company (CHPRC) Quality Assurance Project Plan for Modeling (*CH2M HILL Plateau Remediation Company Quality Assurance Project Plan* [CHPRC-00189, Appendix K]). This report is limited to the development of the flow model capability using MODFLOW. The application of the flow model in combination with transport simulations using MT3DMS will be documented in application specific environmental calculation files.

Figure 1-2 depicts the domain of model simulation. Basalt subcrops above the water table of the aquifer constrict the domain to the north, south, and west. These subcrops are assumed impermeable barriers to flow. There are two gaps in the basalt subcrops along the northern boundary. In these two regions, the water table is above the basalt surface. The westernmost region is referred to as the Western Gap and the eastern region is referred to as the Gable Gap. Along the eastern boundary and the easternmost part of the southern boundary, the water table is also above the basalt surface. In general, water has flowed out of all of these boundaries during the operational period of the Hanford Site. Cold Creek (located in the slot along the western boundary) and Dry Creek (the gap in the basalt subcrops in the southwest corner of the domain) are sources of inflow to the Central Plateau. Recharge from precipitation and a net upward flux through the basalt basement also provide additional sources of inflow. Artificial recharge from the disposal of facility effluents to surface ponds, cribs, and shallow wells represented a very large source of inflow to the domain during the operational period of the site.

The basic methodology for the development of the CPGW Model is as follows:

1. Develop an understanding of the simulation/calculation needs across the Central Plateau.
2. Define lateral and vertical extents (i.e., the domain) over which calculations of groundwater flow and subsequent contaminant transport are needed.
3. Construct a representative flow model of the Central Plateau using the MODFLOW code using site-specific descriptions of the local physical and hydrogeologic conditions.
4. Verify the representativeness of the model by comparing the construct to available geologic descriptions, well logs, cross sections, and other appropriate sources of information.
5. Define appropriate boundary conditions. Uncertain boundary conditions may be estimated through model calibration.
6. Calibrate the hydraulic performance of the model by comparing the simulated groundwater head at selected locations to actual measurements at wells, and comparing the simulated resultant groundwater gradient to the observed gradient in nearby wells. This calibration was implemented for the period from 1944 to 2008. The comparison has been extended to 2014 in revision 2. Quantitative comparisons to historic contaminant plume movement are not part of the historic flow model calibration.

7. Iteratively update the structure, boundary conditions, and parameterization (calibration) of the CPGW Model as more information and knowledge becomes available, new data are acquired, and new interpretations of these data provide for improvements to the model.

4.1 Software

MODFLOW (USGS, 2000) was selected for implementation of the CPGW Model because it fulfills the following specifications:

- It is one of the more versatile and widely used software packages for models of this type.
- It is freely available and distributed with the source code.
- It is fully documented and has been verified in applications similar to those at the Hanford Site.
- There is wide expertise in its use.
- It is capable of directly simulating the principal FEPs that are relevant to the Central Plateau simulation requirements.
- For those FEPs that it does not directly simulate, the needs can be met through links to other codes, such as linking to Subsurface Transport Over Multiple Phases (STOMP) for vadose calculations as described in the FEP section on recharge.

Use of MODFLOW is in keeping with DOE direction for simulation of groundwater at the Hanford Site (*Hanford Groundwater Modeling Integration* [Klein, 2006]). All software for implementation of this model was used in accordance with PRC-PRO-IRM-309, *Controlled Software Management*.

The software used to implement this model, and to perform calculations, was approved under the requirements of, and use was compliant with, PRC-PRO-IRM-309. This software is managed under the following software quality assurance documents consistent with PRC-PRO-IRM-309 requirements:

- CHPRC-00257, *MODFLOW and Related Codes Functional Requirements Document*
- CHPRC-00258, *MODFLOW and Related Codes Software Management Plan*
- CHPRC-00259, *MODFLOW and Related Codes Software Test Plan*
- CHPRC-00260, *MODFLOW and Related Codes Acceptance Test Report*
- CHPRC-00261, *MODFLOW and Related Codes Requirements Traceability Matrix*

CHPRC-00259 distinguishes between safety software and support software based on whether the software managed calculates reportable results or provides run support, visualization, or other similar functions.

4.1.1 MODFLOW Controlled Calculation Software

The following describes the MODFLOW Controlled Calculation software.

- Software Title: MODFLOW-2000 (*MODFLOW-2000, the U.S. Geological Survey Modular Ground-water Model - User Guide to Modularization Concepts and the Ground-Water Flow* [Open File Report 00-92])—solves transient groundwater flow equations using the finite difference discretization technique.
- Software Version: MODFLOW-2000 modified by S.S. Papandopalous and Associates for minimum saturated thickness and to use the ORTHOMIN Solver—approved as CHPRC Build 0003 using

executable mf2k-mst-0006dp.x (for Linux®) or mf2k-mst-0006dp.exe (for Windows®), both compiled to default double precision for real variables.

- Hanford Information System Inventory (HISI) Identification Number: 2517 (Safety Software S3, graded Level C).

4.1.2 MODFLOW Support Software

Support software is used that has been identified in CHPRC-00258, or is scheduled by the software owner to be included as support software in the next revision to that document. Software with a trademark designation is commercial software. Software listed without a trademark has been developed internally.

- **allocateQ_MNW2:** creates the MODFLOW MNW2 formatted input files for both historic and predictive simulations. WEL or MNW are available as alternative formats
- **headtarg_d:** Retrieves and interpolates simulated heads allowing for dry model cells. It is used for model calibration. Performs linear interpolation between model nodes to the coordinates of the monitoring location, and includes options to "hunt" down through dry layers for the water table.
- **calcgradients:** Calculates simulated gradient directions and magnitudes from calculated head values.
- **Read-lst-budget:** Creates a file "prefix"-budget.out that can be brought into a spreadsheet to tabulate and plot (1) the volumetric budget terms (IN and OUT), and (2) the mass balance error of the MODFLOW simulation, as reported by MODFLOW at the end of each interval specific in the output control (OC) file.
- **Starthead _multi_option_lahey:** Created the initial head conditions for the predictive flow calculations by taking the last time step head result from historic run heads output.
- **makeghb4:** Calculated the general head boundary (GHB) input file for MODFLOW using the procedure described in Section 4.4.1.
- **makerecharge3:** Creates the MODFLOW RCH input files for both the historic and predictive model simulations, specifying recharge values from natural, artificial, and overland flow data sets.
- **create_CHD_V6:** Creates MODFLOW CHD input files for both the historic and predictive model simulations, specifying time variant head along the Gable Gap and Western Gap boundaries.
- **CP_ModelStrat-Version3**: Translates interpolated HSU surfaces into model layer elevations and assigns HSU zone identification to the individual layer cells. The process is described in Section 4.2.6.
- **Surfer™:** (*Surfer® Getting Started Guide: Contouring and 3D Surface Mapping for Scientists and Engineers* [Golden Software, 2009].) Interpolated well contact information to create HSU surface data arrays as described in Section 4.2.4 and Section 4.2.5.
- **Groundwater Vistas™:** (*Guide to Using Groundwater Vistas* [Rumbaugh and Rumbaugh, 2007].) Translated well pumping data from spreadsheet HistroricWells.csv to WEL file. It also provided graphical tools used for model quality assurance.

™ Surfer is a trademark of Golden Software, Golden, Colorado.

™ Groundwater Vistas is a trademark of Environmental Simulations Incorporated, Reinholds, Pennsylvania.

- **ArcGIS™:** (*The ESRI Guide to GIS Analysis, Volume 1: Geographic Patterns and Relationships* [Mitchell, 1999].) Provided visualization tool for assessing validity of interpolated HSU surfaces and HSU extents. Used to locate control points visually to constrain the HSU surfaces as explained in Section 4.2.1.
- **PEST™:** (*User's Manual for PEST Version 11* [Doherty, 2007].) Used for automated calibration and run coordination.
- **LEAPFROG Hydro™:** (Version 1.2.0.62.) Used for creating three-dimensional plume volumes and initial concentrations for the CPGW Model. The software uses radial basis functions to interpolate continuous 3-D concentration distributions of X, Y, Z, and concentration data.

4.1.3 Software Installation and Checkout

Safety Software (CHPRC Build 0006 of MODFLOW-2000) is checked out in accordance with procedures specified in CHPRC-00258. Executable files are obtained from the CHPRC software owner who maintains the configuration-managed copies in MKS Integrity™, installation tests identified in CHPRC-00259 are performed and successful installation confirmed, and software installation and checkout forms are required and must be approved for installations used to perform model runs. Approved users are registered in HISI for safety software.

4.1.4 Statement of Valid Software Application

Use of the software previously identified must be consistent with intended use for CHPRC as identified in CHPRC-00257 and be a valid use of this software for the problem addressed in this application. The software must be used within its limitations as identified in CHPRC-00257.

4.2 Spatial Discretization (Model Grid)

Details of the discretization of the model domain are provided in the subsections that follow.

4.2.1 Introduction

This section on model discretization describes development of the geometric structure of the model. The section includes both definition of the geometry of the model boundaries and the representation of HSUs within the model domain. The HSUs are identified by their close relationship to geologic units; however, they are not directly comparable.

Hydrostratigraphic units are represented as homogeneous, (i.e., constant properties). They approximate the hydraulic character of geologic features that may have significant variation on the scale of tens of meters to several kilometers. Changing the hydrostratigraphic definition at some locations in the model has been demonstrated to improve the performance of the model with respect to model calibration. This report provides examples.

Correctly characterizing the thickness of the unconfined aquifer is an important task for developing the CPGW Model. The first element in this task is to create the most accurate representation of the base of the model domain, the basalt surface. This is especially true in the region of the 200-BP-5 OU where the aquifer is thin and the basalt surface complex. As described in Section 4.2.4, point borehole contact information obtained directly from wells has been supplemented with basalt surface information from the

---

™ ArcGIS is a trademark of ESRI, Redlands, California.

™ PEST is a trademark of Watermark Numerical Computing, Brisbane, Australia.

™ LEAPFROG Hydro is a trademark of ARANZ Geo Limited, Christchurch, New Zealand.

™ MKS Integrity is a trademark of MKS, Incorporated.

PNNL-14753 hydrology database; hand drawn contours in the 200-BP-5 region developed by CHPRC (Personal Communication [Narbutovskih, 2008]); and recent basalt elevation estimates derived from seismic investigations. The geologic units and, hence, HSUs are not continuous over the Central Plateau. While contact data from borehole logs are numerous, they are still sparse with respect to the 100 m scale of individual grid blocks. Two sets of information were derived from the contact information. One of these sets is surfaces defining the vertical extent of individual HSUs obtained by kriging-based interpolation. Only data from boreholes where the unit was identified were used in the kriging interpolation. Therefore, kriging establishes elevation information even in locations where the unit is known not to exist.

The other set of information is a simple binary representation of where a unit exists in the stratigraphic column and where it does not exist. The algorithm used to define the extent of existence determines the closest set of data to a grid location and uses the data from that location to assign existence. This simple algorithm does not use soft information that is available from geologic understanding of the depositional environment of the Central Plateau. Where it was obvious by inspection that the algorithm was flawed, control points were added to constrain the algorithm. Control points were also added where calibration of the model suggested flaws in the unit extent determination. Section 4.2.5 describes the development of the HSU surfaces and the extent grids.

The surfaces and extent grids of each HSU is consistent at borehole locations but may not be consistent away from the boreholes. The interpolated surfaces are independent of each other and may cross far from boreholes. Because of the extent information, the number and type of unit represented at a grid location varies. A numerical algorithm has been developed to resolve conflicts and accommodate the changing extents. The algorithm assigns HSUs and thicknesses to model cells. A development priority was to avoid numerical problems introduced by thin layers and to maintain lateral continuity of hydrologic properties within layers. Section 4.2.5.1 provides details of this step of the model development process.

4.2.2 Grid Design

The model domain has the following spatial extent and boundaries:

Horizontal extent: rectangular region.

- 13.4 km north-south
- 25.6 km east-west
- The lower left corner of the model domain is located at: easting 555650 m, and northing 129850 m in the Washington State Coordinate System: NAD_1983_StatePlane_Washington_South_FIPS_4602

Vertical extent: the basalt that is assumed to constitute an impermeable lower boundary defines the base of the domain. The top of the aquifer model is the land surface; however, since the CPGW Model only simulates saturated groundwater flow, geologic differentiation was implemented only below the highest water table. The water table is not static and was higher during the operational period of the Hanford Site than it is now. The geologic media represented in the model includes sediments that are presently above the water table to permit simulation of historic water flow.

The model domain is discretized into a finite difference grid:

- Uniform grid of square cells in the horizontal (plan view) of 100 m square uniform cells.

- The seven vertical layers vary in thickness so that any one model cell only represents a single HSU. To the degree possible with a 100 m horizontal discretization, the best estimate elevations of the tops and bottoms of the HSUs are preserved by the variations in layer thickness.
- An HSU is not equivalent to a model layer; rather, each HSU defined in Table 4-1 may occur in one or more model layers and each model layer contains multiple HSUs.

Table 4-1. Hydrostratigraphic Units in the Central Plateau Groundwater Model

CPGW Model HSU Number	Description	PNNL-14753 Unit Number	Notes
1	Hanford formation coarse grained unit	Unit 1	Dominated by gravel and sand within the aquifer
2	Hanford formation fine grained unit	Unit 1	Dominated by sand and silt
3	Eastern portion of the Cold Creek unit	Unit 3	Dominated by gravelly sand, also called the Pre-Missoula gravel
4	Ringold Formation unit E	Combination of Ringold units 4 and 5	Composed primarily of fluvial gravel that grades upward into interbedded fluvial sand and silt of the Ringold unit 4 (BHI-00184)
5	Ringold Formation lower mud unit	Combination of Ringold units 6, 7, and 8 (B, C, and D units)	Composed of a thick sequence of fluvial overbank, paleosol, and lacustrine silts and clay with minor sand and gravel (PNNL-13858)
6	Ringold Formation unit A	Unit 9	Composed primarily of fluvial gravel (PNNL-13858)

Sources:

BHI-00184, 1995, *Miocene- to Pliocene Aged Suprabasalt Sediments of the Hanford Site, South Central Washington*, Rev. 0, Bechtel Hanford, Inc., Richland, Washington.

PNNL-13858, 2002, *Revised Hydrogeology for the Suprabasalt Aquifer System, 200 West Area and Vicinity, Hanford Site, Washington*, Pacific Northwest National Laboratory, Richland, Washington.

PNNL-14753, 2006, *Groundwater Data Package for Hanford Assessments*, Rev. 1, Pacific Northwest National Laboratory, Richland, Washington.

Note:

HSU = hydrostratigraphic unit (An HSU is not equivalent to a model layer; rather each HSU defined in this table may occur in one or more model layers and each model layer contains multiple HSUs.)

Prior to Version 3, five vertical layers were used (ECF-HANFORD-10-259). The increase in number of layers allowed finer discretization where transport was expected to occur. It also allowed the freedom to assign layers to cells that were needed for historic calibration so that they were completely above the water table in the predictive model simulations when the water table is well below its maximum height. A new algorithm was developed to assign layers that did not take into account the previous layering.

4.2.3 Discretization of the Unconfined Aquifer into Hydrostratigraphic Units

The interior of the model domain is divided into six HSUs. The division presented in Table 4-1 is strongly influenced by the hydrostratigraphy descriptions presented in PNNL-14753 (Table 4-1). Sections 4.2.4

and 4.2.5 describe the development of the surface for each HSU along with the development of the bedrock surface (top of basalt) that defines the bottom of the model.

4.2.4 Development of Top of Basalt Surface (Bottom of the Model)

The top of basalt defines the lower boundary of the CPGW Model. This boundary was defined as follows:

- The top of basalt (bedrock) elevation was taken from Figure 5.13 of PNNL-14753 by digitizing the contours as shown in Figure 4-1. This approach was taken because more detail is shown in the figure than is obtained when directly interpolating the top of basalt data in the data table of geologic units. However, the top of basalt was modified on the basis of various additional data sources:
  - In the area of Gable Gap, the elevation was modified based on top-of-basalt contours shown in Figure 4-2 (Personal Communication [Narbutovskih, 2008]).
  - The new top-of-basalt contours were digitized from Figure 4-2 and replaced the existing top of basalt elevation. The new boring data were used directly as data points and supplemented the top of basalt data set for interpolation. The top of basalt was incorporated into the model by kriging the top of basalt data set onto the model grid.
  - Recent boring locations compiled and provided by Freestone Environmental Services, Inc. were added as additional data points (*200-1PO-1 Groundwater Operable Unit Remedial Investigation Report-Geologic Cross Sections*: Near_Field_Geo_Elevations_7_16_ 09.mdb [ECF-200PO1-09-2074]).
  - New seismic data were added to the data set (File "200E_Seismic_Basalt_June2009.xls:" SGW-39675, *Reflection Seismic Survey Report*), which contained seismic data from 2008, BWIP FY 79_03 and BWIP FY80_12).
  - Kriging was used to interpolate the data from these three sources onto the model grid.
- Additional changes were made to the basalt surface elevation for Version 3.3 of the CPGW Model. These were as follows:
  - Removed existing seismic data used in the CPGW Model Versions 1 and 2, and substituted a subset of most recent seismic data and control points as directed by Michael Thompson, author of SGW-39675 (200-BP-5_BasaltData_MDT2010.xls).
  - Updated existing well control in the 200-BP-5 Groundwater OU area with Freestone Environmental Services, Inc. dataset (*200-BP-5 Hydrostratigraphic Database Development*; BP5_HSU_12_15_09.mdb [ECF-200BP5-10-00344]) consistent with December 3, 2009 PNNL contacts database (Geologic Contact Depths_2009_12_03.xls [PNNL, 2009]) for which a "Best Estimate" was designated.
  - Added additional control points to adjust the basalt surface where basalt data were deemed insufficient and where the reinterpreted surface was considered erroneous.

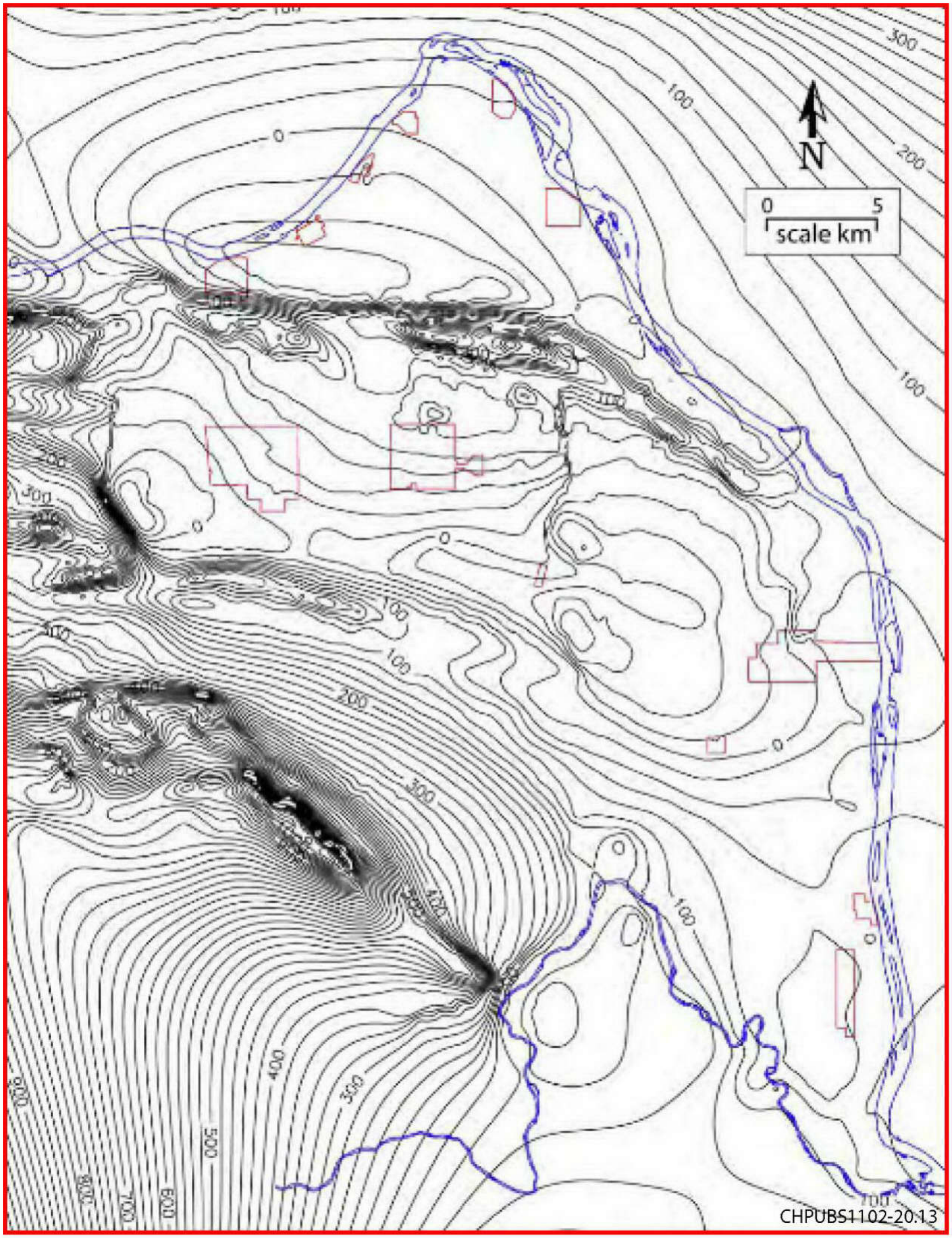

Source: PNNL 14753; Regional Scale
Note: Elevations are in meters above sea level.

Figure 4-1. Top of Basalt

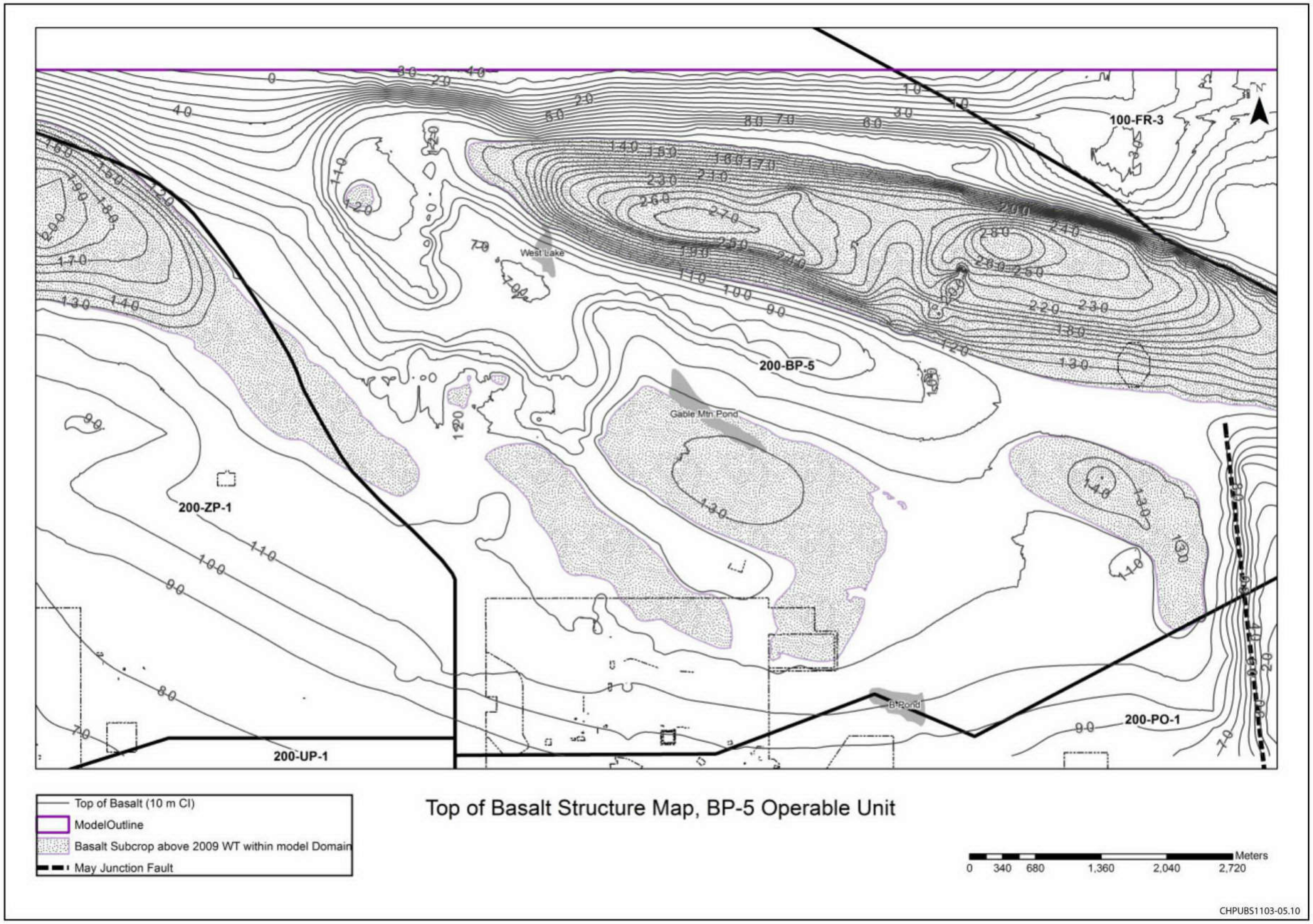

Source: Narbutovskih, 2008

Figure 4-2. Top of Basalt in the Area of Gable Gap

The file TOB072109.xls contains all final elevation point data for the top of basalt. Columns A, B, and C of the first sheet of the Microsoft Excel® file contain Easting, Northing, and the elevation data in meters, respectively. The elevation data are interpolated on to the model grid using the software Surfer™. The following options were selected to interpolate elevation data using kriging.

- X: Column A Easting (m)
- Y: Column B Northing (m)
- Z: Column C Elevation (m)
- Gridding Method Kriging
- Output Grid File TOB_rev1b_m.grd
- X Direction Minimum 555700
- X Direction Maximum 581200
- X Direction Spacing 100
- Y Direction Minimum 129900
- Y Direction Maximum 143200
- Y Direction Spacing 100

Figure 4-3 displays the final estimated basalt surface in TOB_rev1b_m.grd that was used to define the bottom of the model domain. The contoured surface is truncated at the edges of the grey no-flow regions of the model. Near the eastern edge of the figure, a red dashed line indicates the position of the control points introduced to enable the May Junction Fault to be adequately incorporated into the kriging procedure.

4.2.5 Development of Hydrostratigraphic Unit Surfaces

HSU geometry was defined by interpolating the bottom elevations of the units as determined from the borehole logs and according to the fixed stratigraphic order of the HSUs. No deformation has changed the relative vertical positions of the HSUs. These interpolated elevations do not directly reflect information of where units are present or missing in the borehole data. To bring information of unit presence to the layering algorithm (described in the next section), unit extent files were created to define whether a unit exists, a value of 1 or, if does not exist, a value of 0, in the stratigraphic column as the third definition of HSU geometry.

Freestone Environmental Services, Inc. provided borehole data for the entire model domain in the form of a geodatabase (Near_Field_Geo_Elevations_7_16_09.mdb). See ECF-200PO1-09-2074 for details on the synthesis of these data. Unit top and bottom elevations provided in the geodatabase include the following:

- Unit 1 (Hanford formation) (at this point both the Hanford fine-grained unit and the coarse-grained unit are treated as unit 1)
- Unit 3 (Cold Creek unit)
- Unit 5 (Ringold Formation, units E and C)
- Unit 8 (Ringold Formation lower mud, with units 6 and 7 lumped within)
- Unit 9 (Ringold Formation unit A)
- Unit 10 (Basalt): for this, only the top elevation was included

™ Surfer is a trademark of Golden Software, Golden, Colorado.

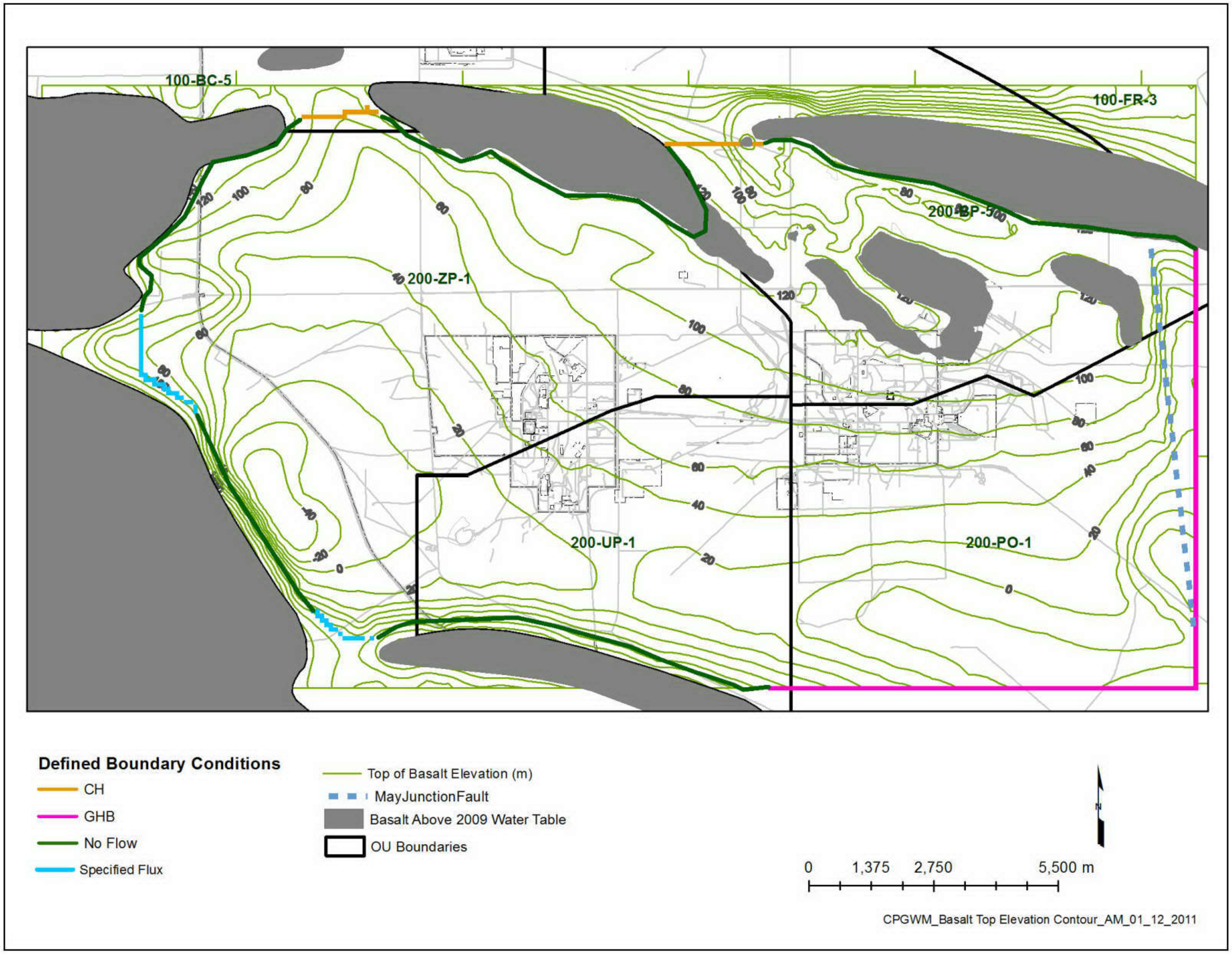

Figure 4-3. Top of Basalt Surface Used for Bottom of Model Domain

This dataset was supplemented with data used in the development of the HSUs for the 200-ZP-1 model as described in DOE/RL-2008-56 and extracted from PNNL-14753, (geo_Thorne_2006_working_copy.xls). Unit elevations were calculated by subtracting the depth to the HSU as recorded in the well logs from ground surface elevation where it was known; otherwise, top of well casing was used. Where the top of the well casing is used as the reference elevation, this generally resulted in a 1.0 m higher shift than the actual elevation obtained when the ground surface was used.

In preparing the HSU mapping, 18 “control points” (i.e., point locations with values assigned that are based upon independent information about the unit geometry) were added to the Cold Creek gravels dataset to either offset artifacts created by unit extent interpolations or to supplement surface interpolations where limited well data were not producing the perceived surface. In addition, five wells (299-W10-113, 699-43-89, 699-39-79, 699-48-77 d, and 699-26-51) were deleted from the unit 5 (Ringold Formation, units E and C) dataset due to questionable bottom picks. Twelve control points were added to the Hanford unit dataset to supplement surface interpolations where limited well data were not producing the perceived surface. Four well picks were determined to be inaccurate with respect to the elevation of bottom of Hanford formation, because the bottom of the wells had apparently not intercepted the bottom of the Hanford formation. The contact was adjusted to 117 m at the location of these wells. These wells are 699-32-42, 699-33-42, 699-34-41B, and 699-25-31.

4.2.5.1 Version 3 Hydrostratigraphic Unit Elevation Refinements

A total of 56 wells in the 200-BP-5 Groundwater OU area have undergone elevation adjustments after receiving the HSU database from Freestone Environmental Services, Inc. Most of these involve the bottom elevation of the Hanford formation. A number of issues led to the reevaluation of HSU elevations in the 200-BP-5 Groundwater OU area including:

- Discrepancies in the PNNL tops database (PNNL, 2009) identified by inspection and review of specific well logs by a geologist.
- Discrepancies in entries in the database compiled by Freestone Environmental Services, Inc., identified by comparison to the PNNL tops database (PNNL, 2009).
- Gaps of missing elevations between units identified by inspection.
- Errors/reinterpretation based on review of well logs.

The Hanford formation bottom elevations were lowered to the top of basalt for 49 wells located in the paleochannel area extending from 200 East and through the Gable Gap (between Gable Mountain and Gable Butte). This modification was justified based on the review of well logs that reported the Cold Creek unit beneath the Hanford formation in 200-BP-5 Groundwater OU area to be of large grain size, indicating that it may behave hydraulically much like the Hanford formation. Furthermore, a subset of wells had information gaps where no units were specified below the Hanford formation, and the gap between the bottom of the Hanford unit and the basalt surface needed to be filled for developing a three-dimensional model.

Additionally, two wells had elevation gaps filled, one in the Cold Creek unit and one in the Ringold Formation unit E. An elevation gap exists, for example, when the top of Ringold unit E does not coincide with the bottom of the Cold Creek unit. Review during model calibration phase identified three additional wells that could have errors in locating the unit contacts. The well logs were checked and it was confirmed that the Hanford formation could drop below the water table. Lastly, two additional wells were removed from the dataset due to unreasonably low placement of the bottom of the Hanford formation (below sea level). Refer to Table 4-2 for a listing of all wells and associated changes.

Table 4-2. Modified Hydrostratigraphic Unit Bottom Contact Elevations

Name	X	Y	Unit	Original Elevation (m)	Adjusted Elevation (m)	Change in Model (m)
299-E27-22	575185.12	136685.33	Unit 1 Hanford	123.11	110.92	-12.19
299-E27-9	574917.62	137040.91	Unit 1 Hanford	117.56	117.62	0.06
299-E33-11	573901.31	137635.81	Unit 1 Hanford	120.63	120.47	-0.15
299-E33-12	573780.56	137632.23	Unit 1 Hanford	116.53	119.58	3.05
299-E33-13	573706.50	137584.39	Unit 1 Hanford	120.78	120.17	-0.61
299-E33-15	573810.31	137540.70	Unit 1 Hanford	118.91	118.76	-0.15
299-E33-16	573791.69	137465.30	Unit 1 Hanford	133.98	119.81	-14.17
299-E33-17	573878.50	137467.19	Unit 1 Hanford	131.80	119.15	-12.65
299-E33-18	573779.19	137386.06	Unit 1 Hanford	133.06	116.21	-16.86
299-E33-2	573617.00	137641.27	Unit 1 Hanford	121.40	120.94	-0.46
299-E33-20	573847.62	137397.91	Unit 1 Hanford	132.87	118.54	-14.33
299-E33-205	573633.37	137406.22	Unit 1 Hanford	132.98	118.96	-14.02
299-E33-24	573493.56	137578.53	Unit 1 Hanford	119.27	120.19	0.91
299-E33-25	573365.25	137681.62	Unit 1 Hanford	119.21	120.73	1.52
299-E33-3	573633.12	137666.03	Unit 1 Hanford	120.55	120.85	0.30
299-E33-30	572923.81	137467.78	Unit 1 Hanford	117.84	118.45	0.61
299-E33-31	573525.00	137491.44	Unit 1 Hanford	136.16	119.46	-16.70
299-E33-32	573524.81	137354.02	Unit 1 Hanford	132.97	119.25	-13.72
299-E33-33	574080.12	137301.94	Unit 1 Hanford	132.20	118.49	-13.72
299-E33-334	573514.69	137256.37	Unit 1 Hanford	135.62	117.94	-17.68
299-E33-335	573568.44	137222.23	Unit 1 Hanford	134.53	117.92	-16.61
299-E33-337	573821.81	137193.87	Unit 1 Hanford	136.46	116.34	-20.12
299-E33-338	573912.06	137238.23	Unit 1 Hanford	135.34	117.66	-17.68
299-E33-339	573716.87	137221.52	Unit 1 Hanford	134.33	117.26	-17.07
299-E33-340	573779.62	137763.84	Unit 1 Hanford	124.33	119.42	-4.91
299-E33-341	573565.19	137652.50	Unit 1 Hanford	134.26	120.39	-13.87
299-E33-342	573625.69	137579.95	Unit 1 Hanford	136.22	120.24	-15.97
299-E33-343	573744.00	137382.25	Unit 1 Hanford	134.48	119.57	-14.90
299-E33-345	573780.87	137388.23	Unit 1 Hanford	132.95	119.76	-13.20

Table 4-2. Modified Hydrostratigraphic Unit Bottom Contact Elevations

Name	X	Y	Unit	Original Elevation (m)	Adjusted Elevation (m)	Change in Model (m)
299-E33-37	574091.50	137185.42	Unit 1 Hanford	139.75	117.50	-22.25
299-E33-4	573616.75	137693.11	Unit 1 Hanford	121.82	121.21	-0.61

Final HSU point data for top elevations, bottom elevations, and thicknesses are available in the Excel file CentralPlateauGeologySep 2009.xls. This spreadsheet was generated from the geologic data provided by Freestone Environmental Services, Inc. combined with data from PNNL-14753. The PNNL-14753 data was used only to fill in missing data points from Freestone Environmental Services, Inc. (approximately 45 well points on the outskirts of the model domain). Data from the CentralPlateauGeologySep2009.xls spreadsheet were interpolated onto the model grid. Interpolation settings described in Step 3 for Top of Basalt interpolation were used to create top elevation, bottom elevation, thickness grid files, and unit extents' grid files using appropriate data from the two spreadsheets listed. Table 4-3 lists the tabs and columns used from the unit *.xls files, respective output grid files used by program CP_ModelStrat_version3, and, in the last column, the gridding method adopted. Figure 4-4 through Figure 4-7 display the resulting bottom elevation information used to define the HSU surfaces for the Hanford units, the Cold Creek/Pre-Missoula Gravel unit, Ringold unit E, and the Ringold mud unit. The top of basalt was used to define the bottom of Ringold unit A.

Table 4-3. File Structure of Hydrostratigraphic Unit Surface Interpretation

Tab in File CentralPlateauGeology Sep2009.xls	Column Selected for "Z:" in Surfer™ Interpolation	Output Grid File	Interpolation Method Table Head Style
Unit 1	G (Bot_m)	bot_1_m.grd	Kriging (filtered data, Z < -1000)
Unit 1	I (Present _1)	unit_1_extent.grd	Nearest Neighbor
Unit 3	G (Bot_m)	bot_3_m.grd	Kriging (filtered data, Z < -1000)
Unit 3	I (Present _1)	unit_3_extent.grd	Nearest Neighbor
Unit 5	I (Bot7(m))	bot_5_m.grd	Kriging
Unit 5	M (Present =1)	unit_5_extent.grd	Nearest Neighbor
Unit 8	I (Bot8(m))	bot_8_m.grd	Kriging
Unit 8	M (Present =1)	unit_8_extent.grd	Nearest Neighbor
Unit 9	M (Present =1)	unit_9_extent.grd	Nearest Neighbor

However, surfaces are portrayed in the figures throughout the domain. The western half of Figure 4-5 represents an extrapolation of the Cold Creek gravels into this part of the model domain. It does not represent the lower surface of the western portion of the Cold Creek unit that is above the maximum water table elevation.

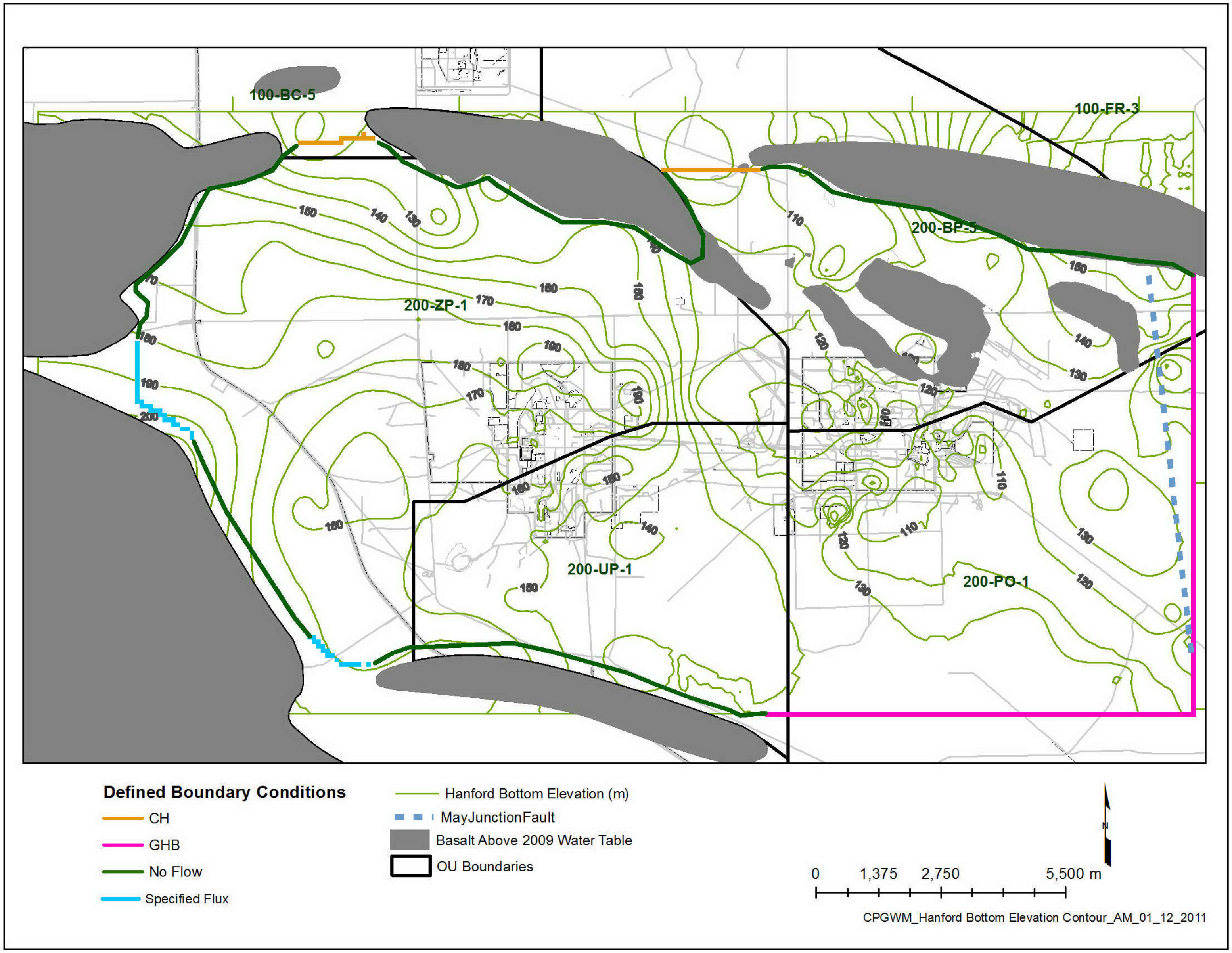

Figure 4-4. Bottom Elevation of the Hanford Formation (HSU 1 and 2)

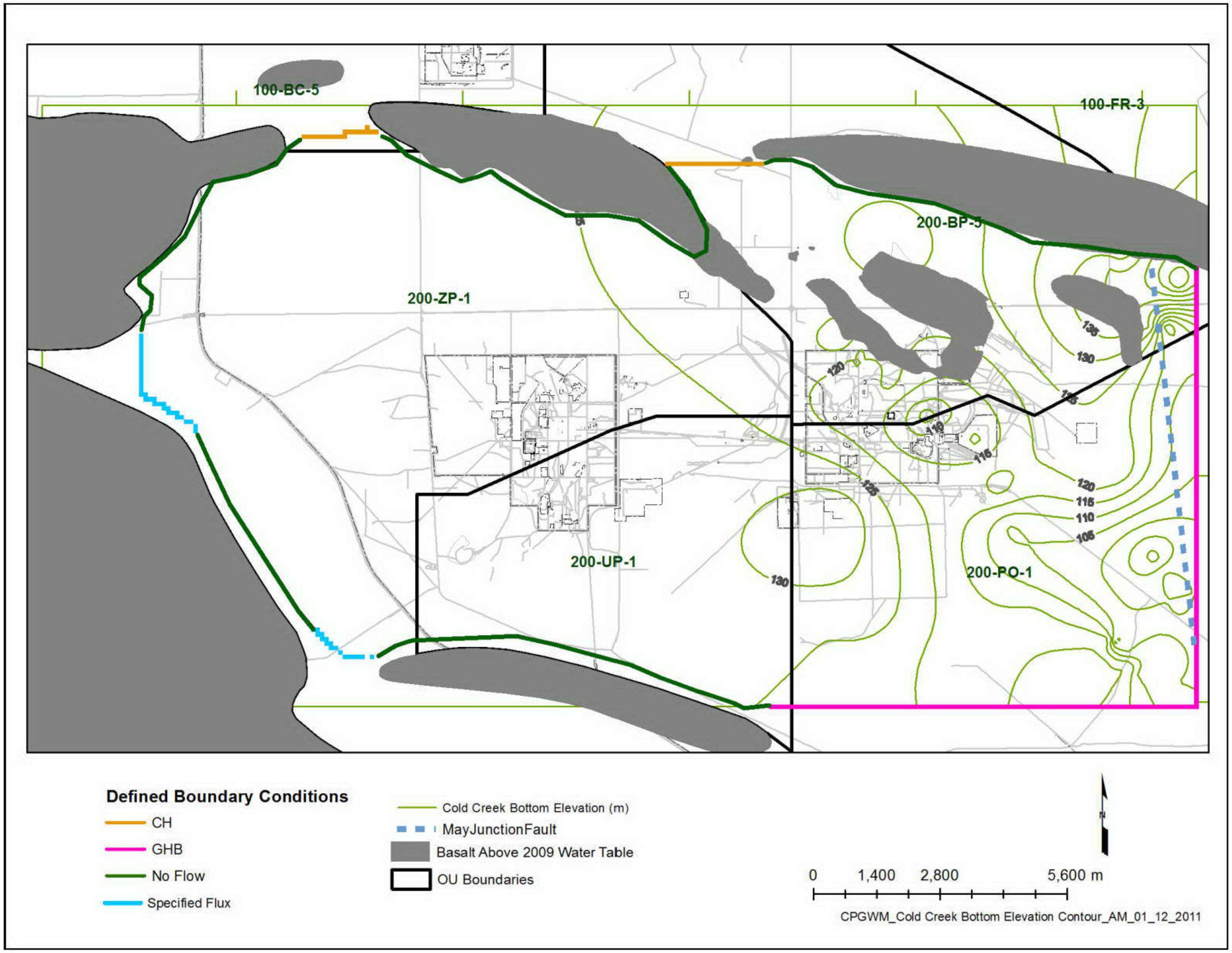

Figure 4-5. Bottom Elevation of the Cold Creek (Pre-Missoula Gravel) Unit (HSU 3)

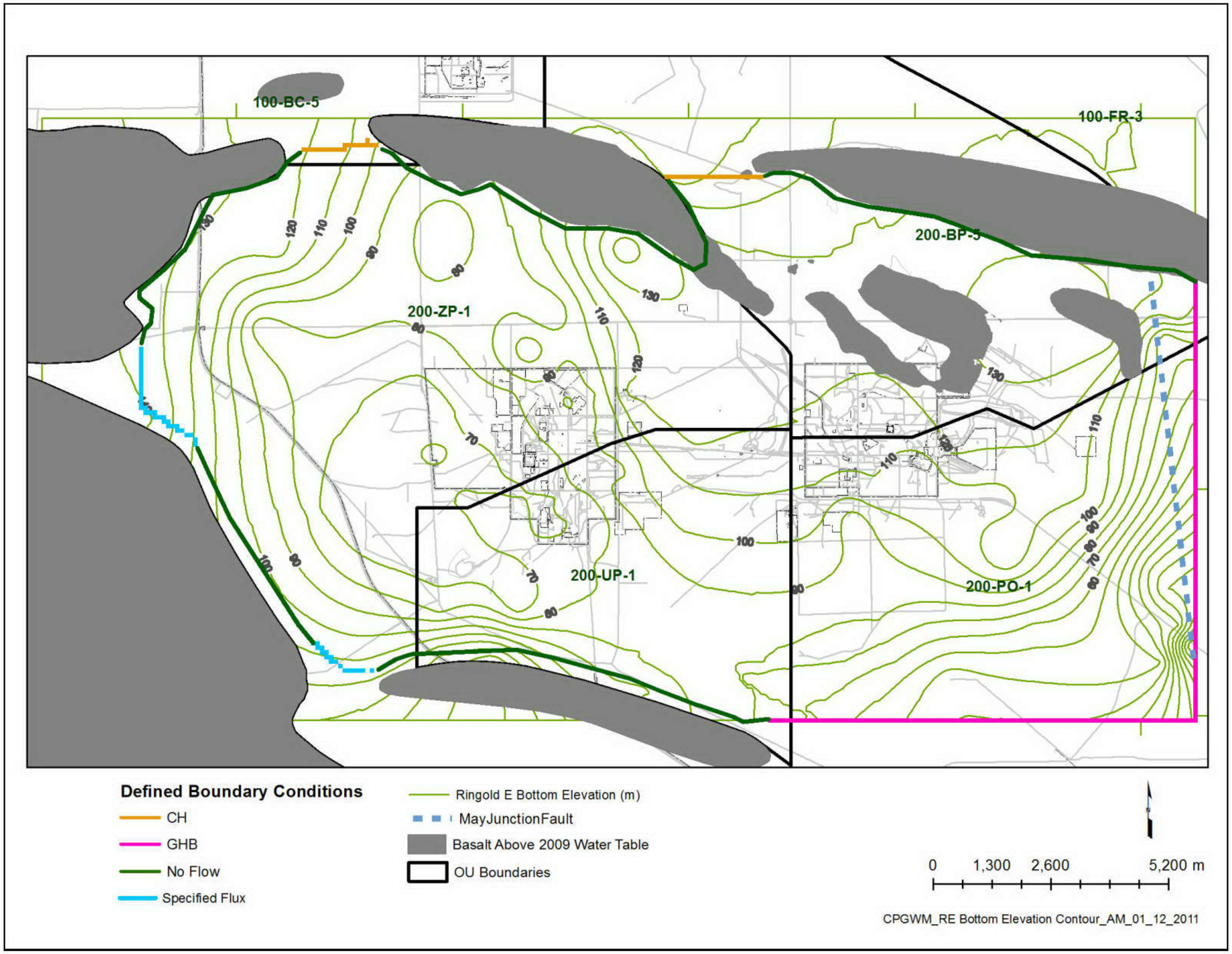

Figure 4-6. Bottom Elevation of Ringold Unit E (HSU 5)

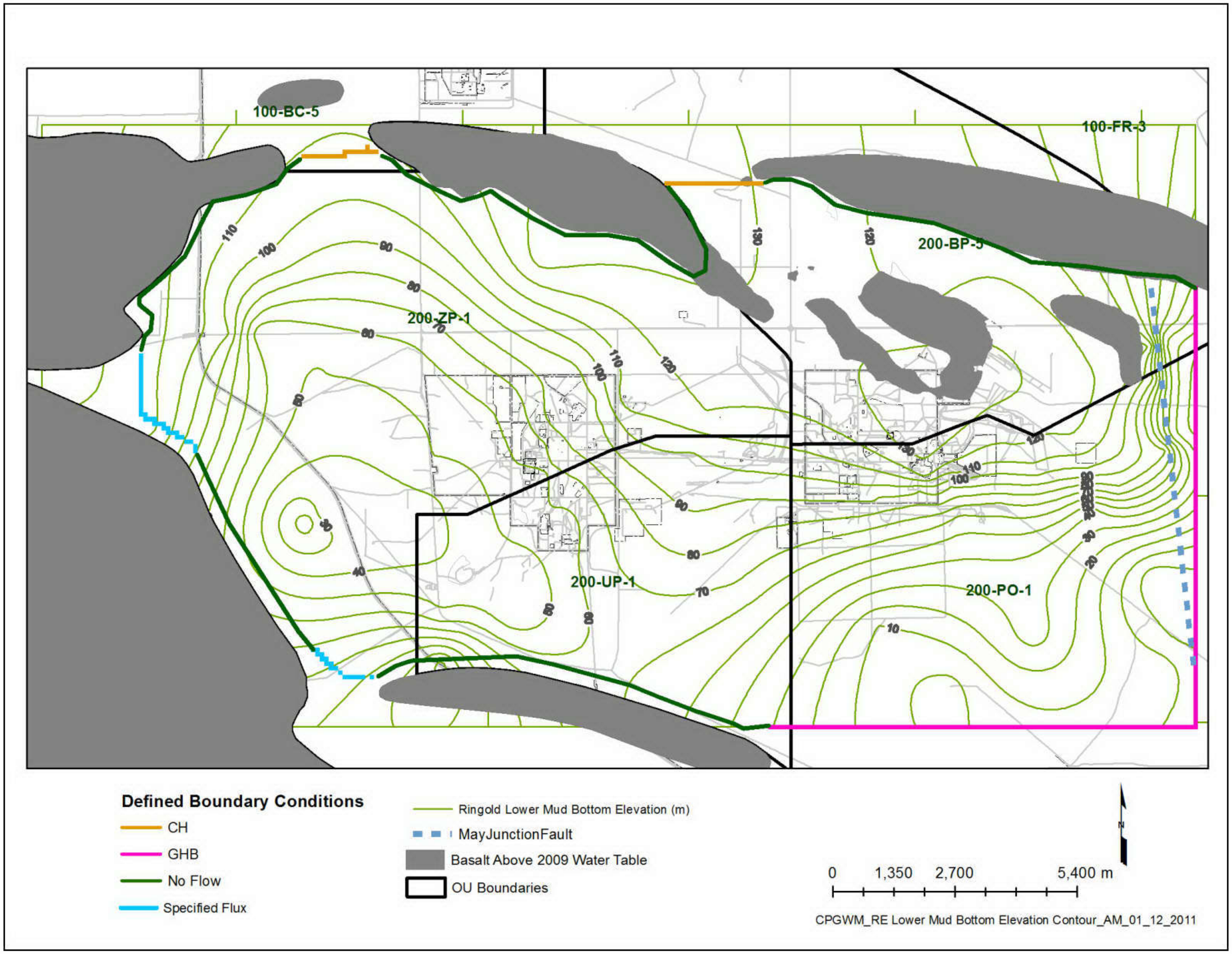

Figure 4-7. Bottom Elevation of the Ringold Mud Unit (HSU 8)

4.2.5.2 Version 3.4 HSU Elevation Refinements

In preparation for modeling work to support the 200-BP-5 OU RI/FS, a change was manually introduced in CPGW Model Version 3.4 to the HSU assignment in Layer 6, as illustrated in Figure 4-8. This change is implemented through a modification to the discretization file (.DIS), and was applied to both the historic and predictive models.

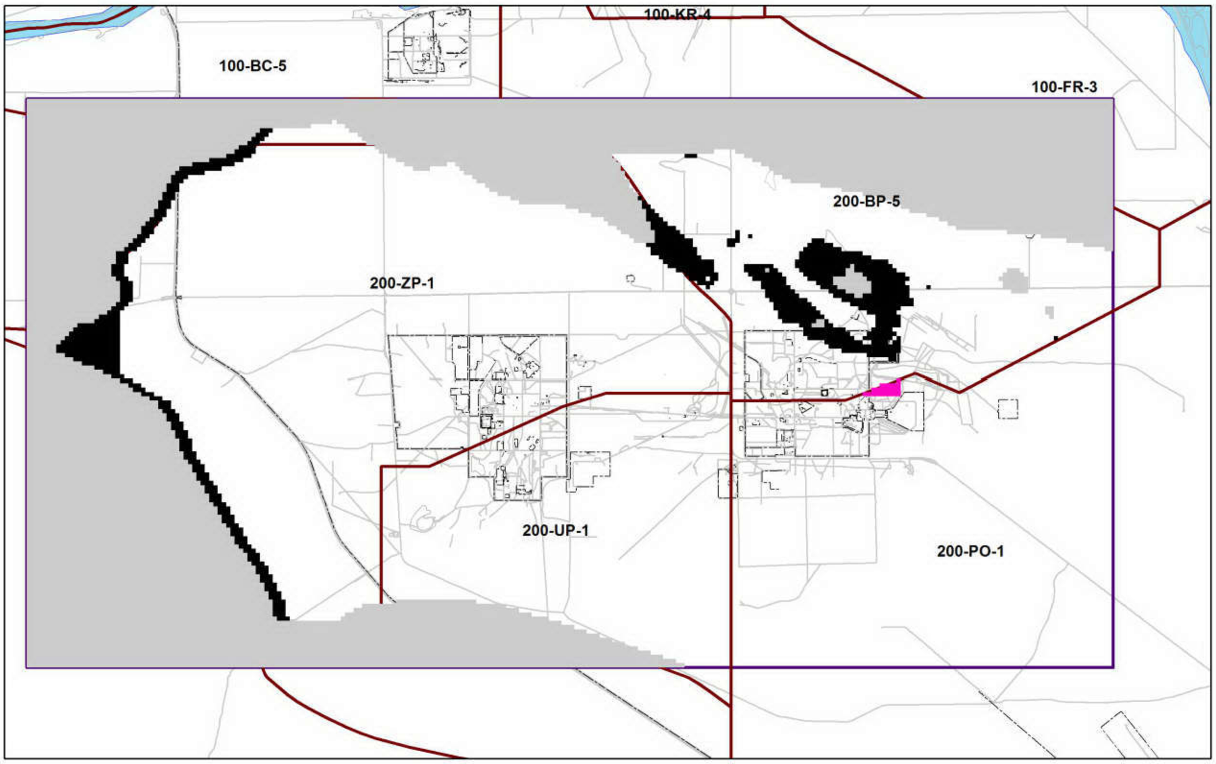

Figure 4-8. Differences in Bottom Elevations of Layer 6 between Versions 3.3 and 3.4 (pink cells denote locations that differ)

4.2.5.3 Vertical Extent of Geologic Resolution

Mapping of measured groundwater levels was used to establish the upper surface of the saturated domain, and from this upper surface, to define the thicknesses (tops and bottoms) of the saturated HSUs. The water level was only used to define the maximum saturated zone. Above the maximum saturated zone, there is no need to represent changes in the hydrostratigraphy, so the exact water level used is not vital unless it is in error by many meters, which is unlikely given the known variation in water levels and locations of conditioning data.

Wells within the model domain that are included in the HEIS database are listed in LongTermWellsforCalibrationQry_working_copy.xls. On the third sheet of the spreadsheet ("LongTermWellsforCalibrationQry"), column J, are water level data in feet. Under column O are notes with respect to corrections to high and/or low water levels. This was done by examining the hydrographs in the file 200-ZP-1Hydrographs_edit.xls. Erroneous data were removed from the dataset for wells used in the interpolation. An example of this type of error is illustrated for well 699-19-88 in the file 200-ZP-1Hydrographs_edit.xls. Interpolation of column J (the maximum water level data), using Surfer with kriging, and a linear drift, and subsequent conversion of all dimension units to meters, resulted in the surfer grid file max_WL_m.grd except in the immediate vicinity of B Pond. Near B Pond, the maximum water table elevation was increased by approximately 5 m to accommodate the historic rise in water table at B Pond that was not sufficiently reflected in the interpolated map. This rise in water levels saturated a portion of the Hanford formation that lies on the Ringold A and lower mud units.

4.2.6 Model Layer Elevations

Model layer elevations were generated using a Fortran program named CP_ModelStrat-Version3. The program translates the interpolated surfaces generated in the steps above into top and bottom elevations for the layers used in Central Plateau MODFLOW model. The following section presents an outline of the procedure used in the program. In the next few paragraphs, a point refers to a single set of row and column coordinates (i.e., a single model row-column location that possesses bottom elevations for the seven model layers). The CP_ModelStrat-Version3 program evolved as the generated model elevations were evaluated.

In addition to the grids of Table 4-3, the top of basalt (TOB_rev2b_m.grd) was used to define the bottom of the model grid and the maximum historic water level (max_WL_m.grd) was used to define the top of the model. An interpolated surface of the water table measured in year 2009 (File WT09asc.grd) was used to guide the internal separation of the HSUs into seven layers. To reduce problems with layers becoming unsaturated during the predictive simulations, the top of a layer was set 0.4 m above the water table in the western portion of the domain and 0.1 m above the water table in the eastern portion of the domain. Using the water table as a guide also allows for increasing the vertical resolution of the grid structure for contaminant transport simulation using MT3DMS.

The procedure used in CP_ModelStrat_Version3 resolves conflicts arising from the fact that the HSU bottom surfaces are created independently. Where there is well control, HSU boundary surfaces have a defined relation to each other. Away from the well control, the interpolated surfaces may cross over each other causing an inconsistency in the representation of the HSU domains.

Conflicts in the representation of units in the model are resolved in a top down approach. This is motivated by the assumption that upper units tend to be more permeable and that their proper representation is more important. The upper surface of lower units is assumed to be defined by the bottom of the unit above. If the bottom surface of an upper unit is below that of a lower unit, then the lower unit is assumed to be missing at the point. An exception to this rule is that the basalt surface is always used to define the lower surface of the aquifer. If the surface data indicate an HSU is completely below the basalt surface at a point, then the unit is assumed not to be present at that point, overriding the information in the extend grid for that HSU.

The interpolation algorithm defines surfaces over the entire domain—even where well control data indicate that a unit is not present (i.e., extrapolation). The nearest neighbor algorithm defines the unit presence/absence, and effectively maps the boundary of the unit extents has halfway between wells that indicate the unit is present and those wells that indicate the unit is not present. The unit extents grids report local existence as defined by the nearest neighbor algorithm and indicate to the layering algorithm where units exist and where they do not.

The program CP_ModelStrat-Version3 operates in a globally naive fashion. Only the surface data for a particular point were used to define the layering for that point. This procedure can introduce layer discontinuities into the model where a layer does not share a physical interface with the same layer in an adjacent cell. In the finite difference formulation implemented in MODFLOW, layers are assumed to be continuous from cell to cell. Therefore, in some cases, the representation of connections in the model between adjacent cells does not accurately reflect actual (or likely) physical relationships and transitions between units. In some circumstances, the continuity of layers that are too thin to have overlapping continuity at the scale of 100 m wide cells provides a better representation than a strict interpretation of the discretized geometry. An important example of this is the continuity of the lower mud that is always represented in layer six when indicated as present by the Ringold mud extent grid. In other circumstances, noncontinuous layers may be a poor representation of the geometry.

Figure 4-9 through Figure 4-13 show where units are not represented in the stratigraphic column for a particular model cell and whether the extent file, unit surface conflicts, or minimum thickness is the reason why it is not represented. Where multiple reasons occur for excluding a unit, only one is depicted. Therefore, a unit might that excluded by both the extent file and a surface conflict will show only the surface conflict. The light green areas are where the unit is represented in at least one layer of the model.

In development of the seven-layer CPGW Model, a number of minor issues were identified for which reconciliation was deemed desirable to improve the flow model in 200-BP-5 Groundwater OU. Modifications were made to reduce the number of discontinuities at grid-block cell interfaces where changes in basalt surface elevation is a significant fraction of the saturated thickness of the aquifer or where changes in the makeup of the stratigraphic column was causing lateral discontinuity in the neighboring cells of the same layer. These potential problems arise predominantly in the thin aquifer of the 200-BP-5 Groundwater OU and not in other portions of the CPGW Model, such as the area that is encompassed by the 200-ZP-1 OU. The continuity problems were identified and addressed on a case-by-case basis by modifying the logic of the layering code rather than by hand manipulation of the layers produced by the code. This makes future modification of the geologic stratigraphy easier, more repeatable and transparent and, hence, more efficient to implement than would be the case if hand manipulation of the layers were performed for each change. It is, however, not completely comprehensive since now not all discontinuities have been eliminated using the stratigraphy program. A by-product of these changes is a larger number of non-active no-flow cells that are set below the basalt surface and fewer cells that are always dry in the simulation (desirable from a computational standpoint). In Version 3.3, there is a much greater tendency for the cells of layer 2 to include the water table rather than to be dry because of using the modified layering logic than when the prior algorithm was used for Version 3.

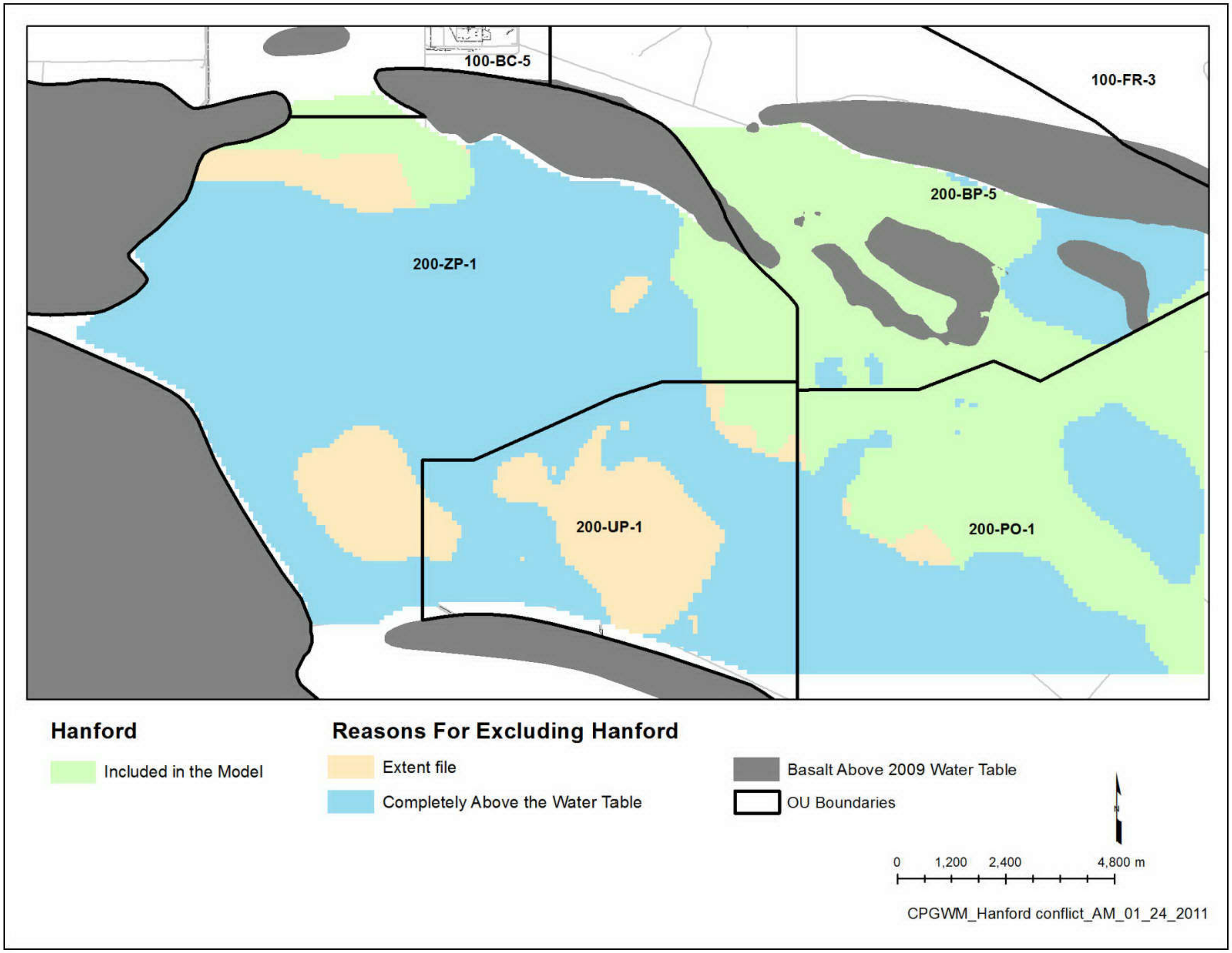

Figure 4-9. Unit Extent Information for the Hanford Units (HSU 1 and 2)

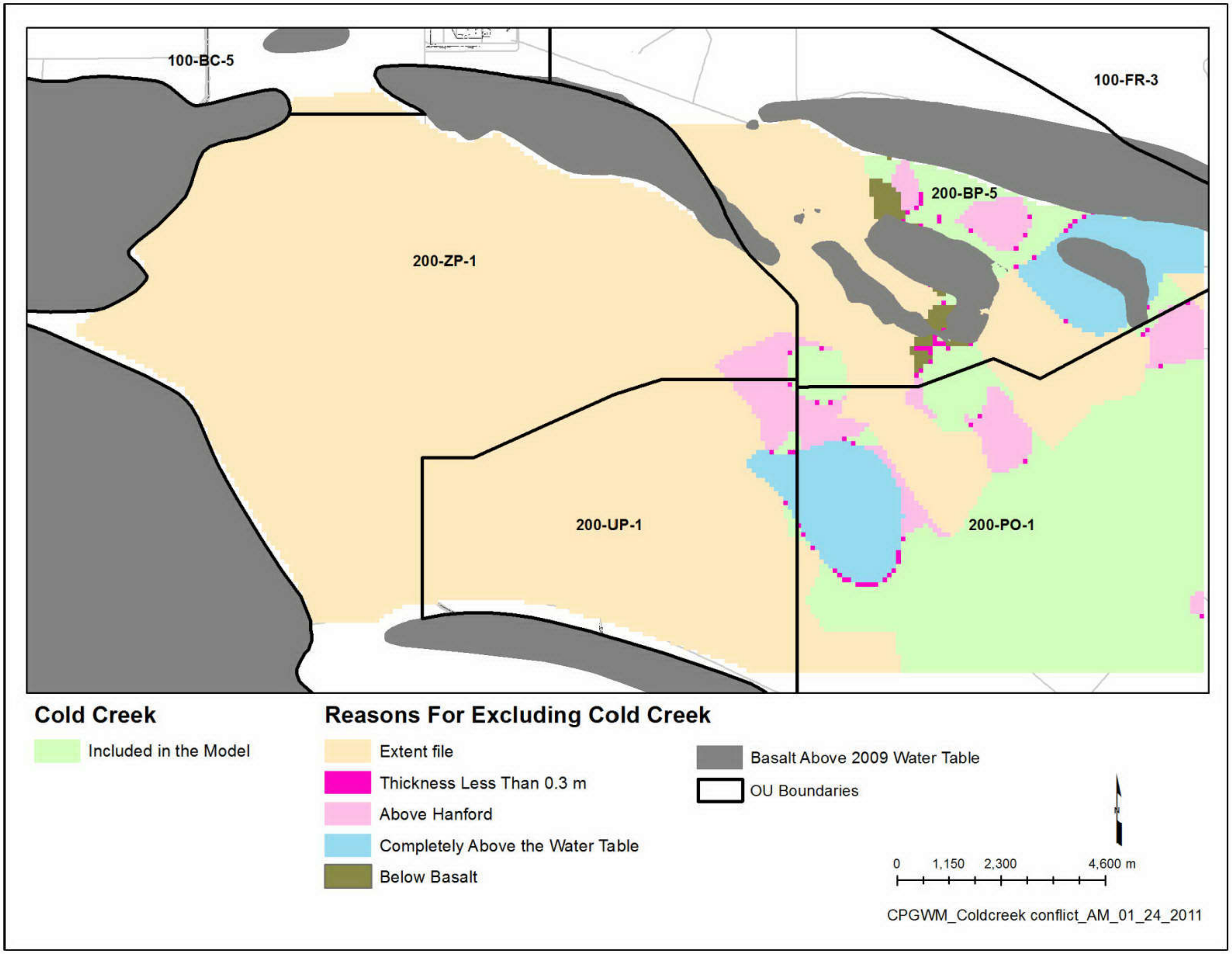

Figure 4-10. Unit Extent Information for the Cold Creek Unit (HSU 3)

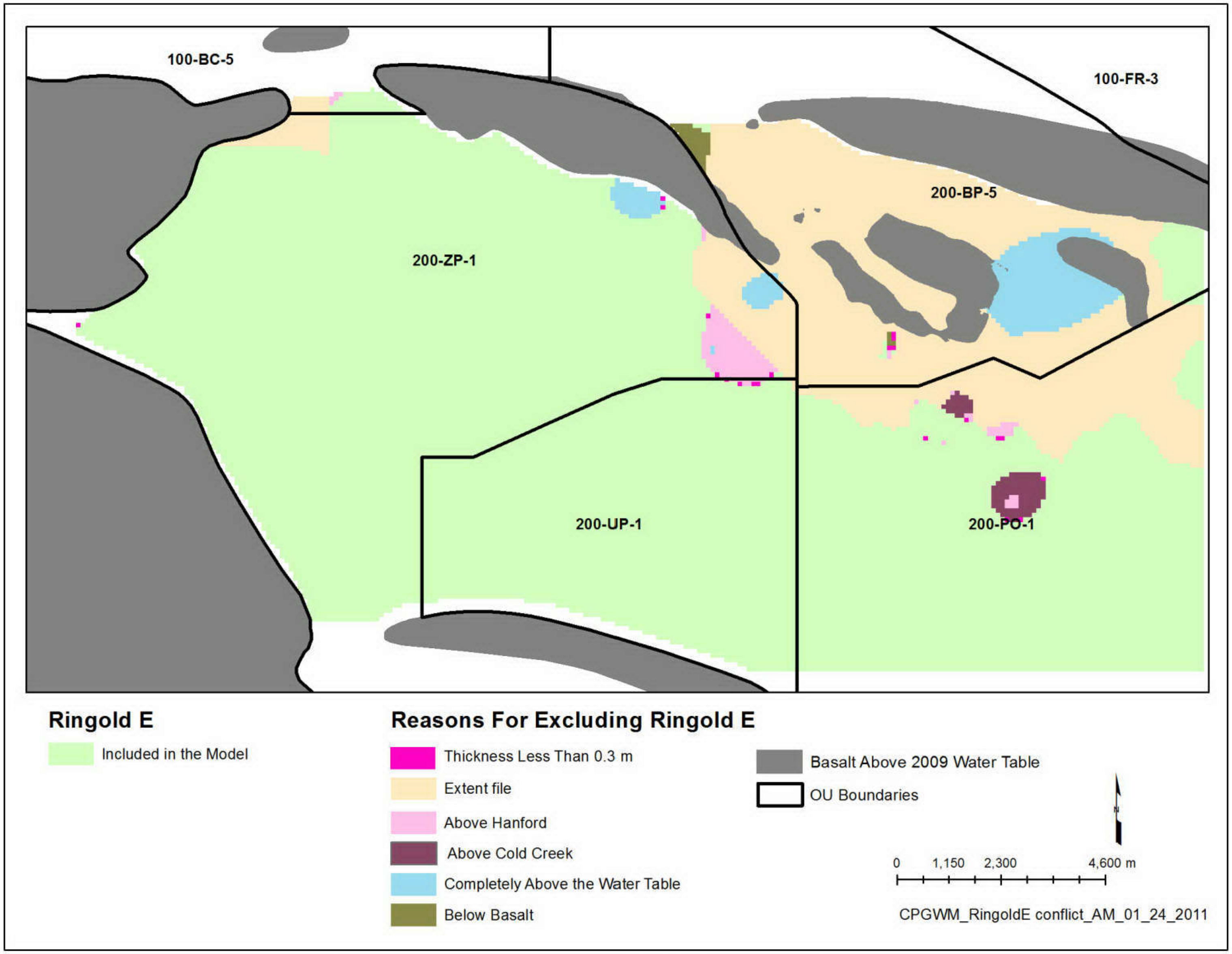

Figure 4-11. Unit Extent Information for Ringold Unit E (HSU 5)

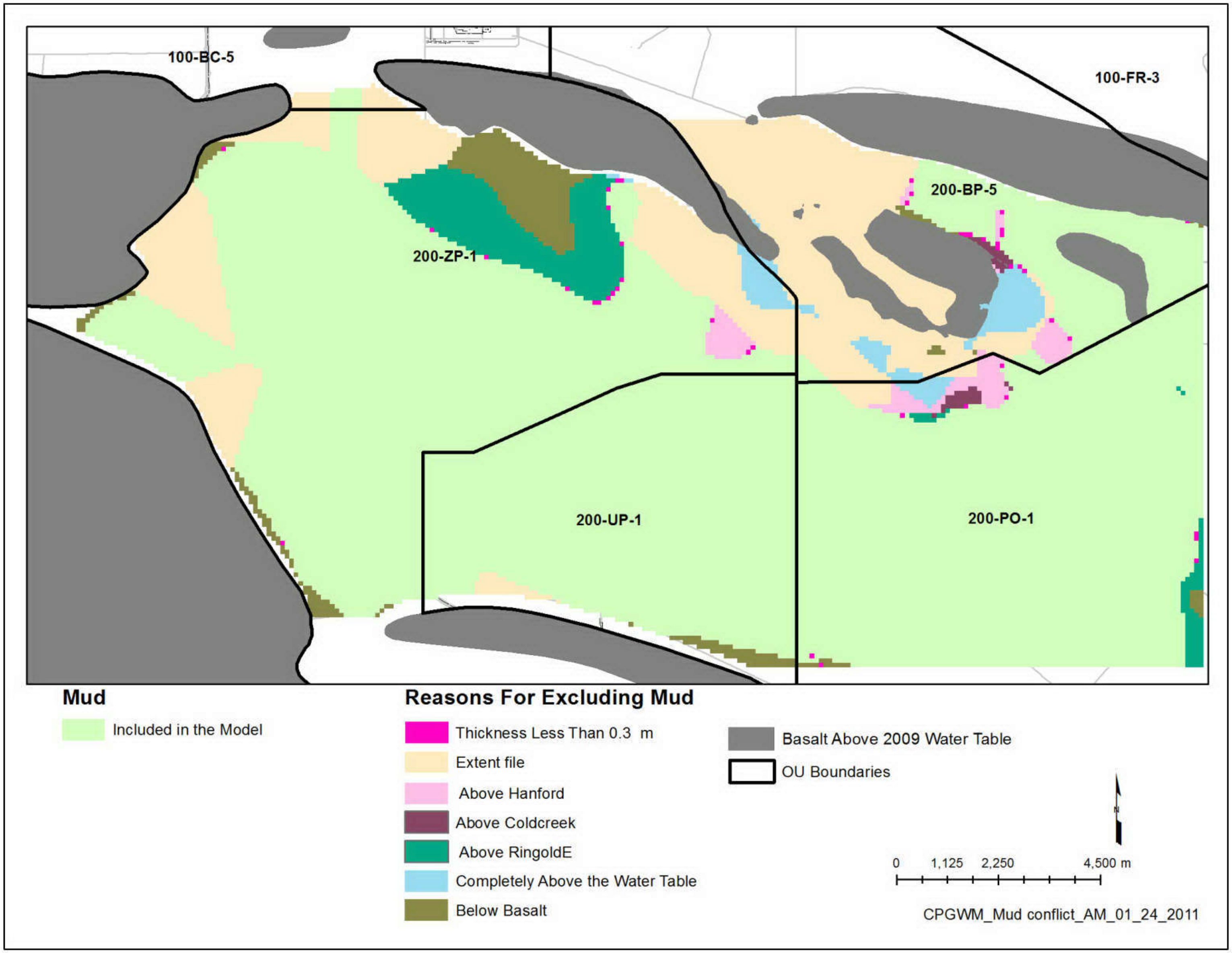

Figure 4-12. Unit Extent Information for the Ringold Lower Mud Unit (HSU 8)

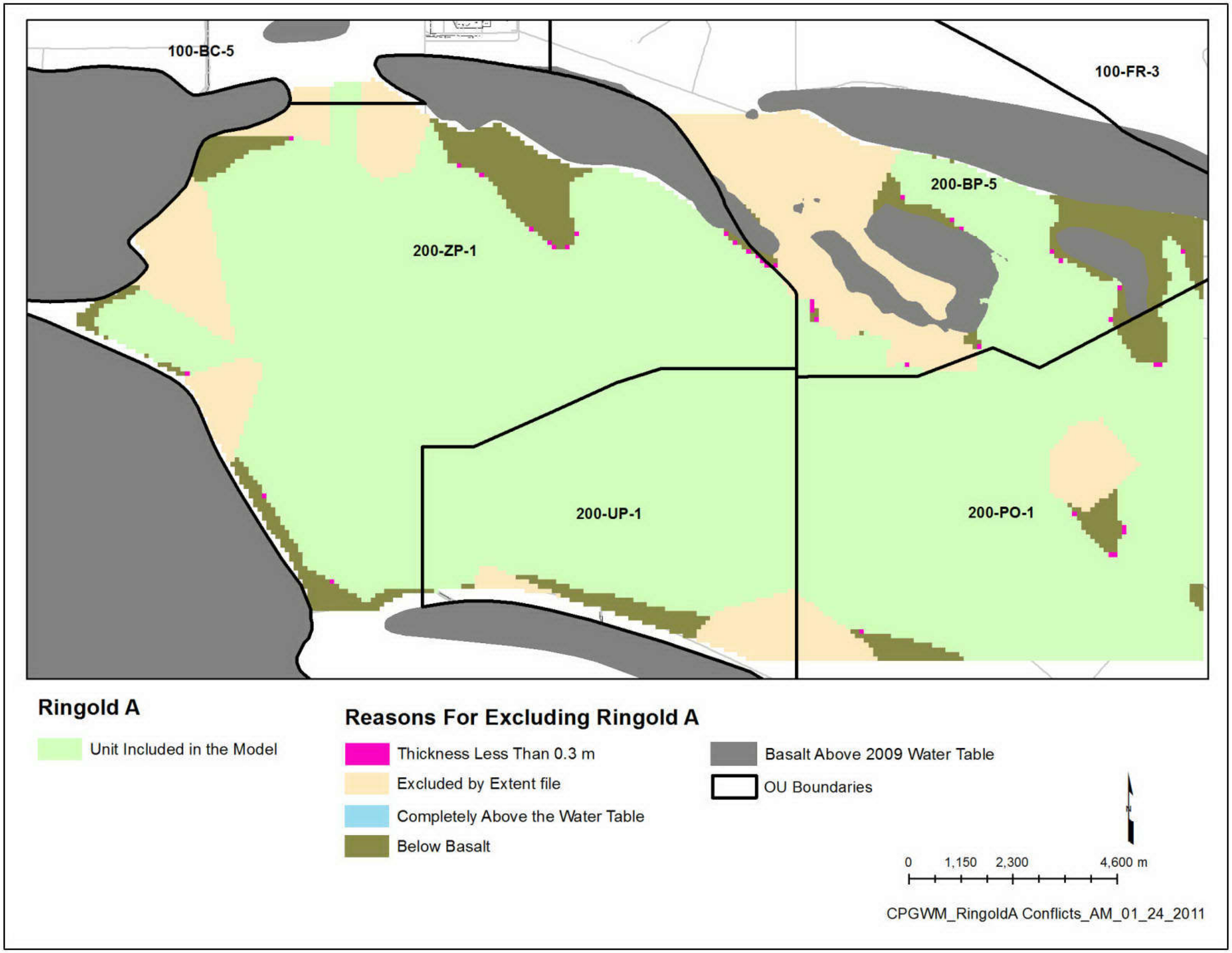

Figure 4-13. Unit Extent Information for Ringold Unit A (HSU 9)

Figure 4-15 through Figure 4-20 illustrate the representation of the six HSUs in each of the seven model layers, respectively. These can be compared to the cross sections in Figure 3-5 through Figure 3-9. The figures display hydraulic conductivities for each HSU. These are the hydraulic conductivity values determined by the calibration of the Version 3.3 model (presented later in this report; Section 4.5.5.3, Table 4-9). A zone ID is used to identify the HSU Conductivity, as follows:

1. Coarse-grained Hanford
2. Fine-grained Hanford
3. Cold Creek
4. Ringold E
5. Ringold mud
6. Ringold A

The inactive portion of the model domain is shown in black. Outlines of major facilities are shown for orientation. Green lines show groundwater OU boundaries. Note that Layer 1 (Figure 4-1) is above the current water table.

4.2.6.1 Version 3.4 Refinements to HSU Zonation

The zonation of model layers 6 and 7 was modified in Version 3.4 in preparation for modeling work focused on the 200-BP-5 OU. The extent of the change is shown in pink color for model layer 6 in Figure 4-21 and for model layer 7 in Figure 4-22. The extent shown was assigned to the Ringold A ($K_{s,x}$ = 4.8 m/d) in Versions 3 and 3.3; in Version 3.4 this extent is reassigned to the Ringold Mud ($K_{s,x}$ = 0.008 m/d). This change is implemented through modification of the zone file (.ZONE).

4.3 Simulation Period

Simulation of the historic period for the purpose of calibration is performed in two parts: a pre-operational stress period is simulated to achieve steady-state conditions taken to represent the initial condition of the unconfined aquifer in 1944, the year when Hanford Site operations commenced; the second period is from 1944 through 2013, simulated in one-year increments. . (Version 6.3.3 switches to monthly stress periods after 2007.) The second period encompasses both the operational period (1944 through 1988) of the Hanford Site and the environmental restoration mission (1989 to present). Historic well records are available for use in model calibration after 1948. Table 4-4 summarizes the temporal discretization of the Version 6.3.3 historic model. The 274-year (100,000 days) period of stress period 1 provides a robustly long time to adjust the steady-state conditions to changed parameter values.

With respect to the 1944 to 2013 historic simulation period, the following details apply:

- Recharge fluxes are averaged over one-year periods: this time discretization leads to time-averaging of quarterly based data and to outputs that represent the effects of this annual time-averaging.
    - An exception is discharges at the SALDS facility where discharges are averaged monthly after 2007.
- Specified head boundary conditions are either constant through the entire simulation period or vary linearly from the beginning of one year to the beginning of the next until 2008 when they are linearly interpolated from representative well data.
- Time units for the simulation are days.

Table 4-4. Temporal Discretization of the Central Plateau Groundwater Model

Model	Stress Period(s)	Duration	Description
Historic	1	Approx. 274 years	The initial transient stress period is specified prior to the calibration period to establish an initial pre-development groundwater condition.
Historic	2 to 65	64 years	The 64 transient annual stress periods span the calibration period from 1944 through 2007.
Historic	66 to 137	6 years	The 72 transient monthly stress periods span the calibration period from 2008 through 2013.

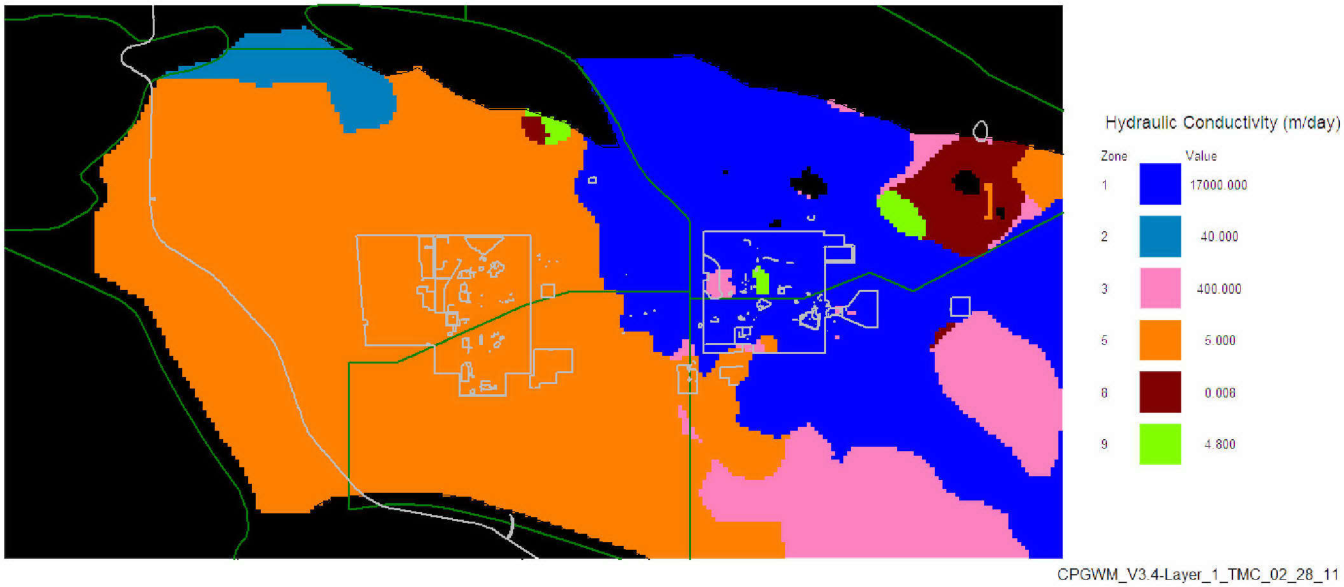

Figure 4-14. Hydrostratigraphic Units of Model Layer 1 above Current Water Table

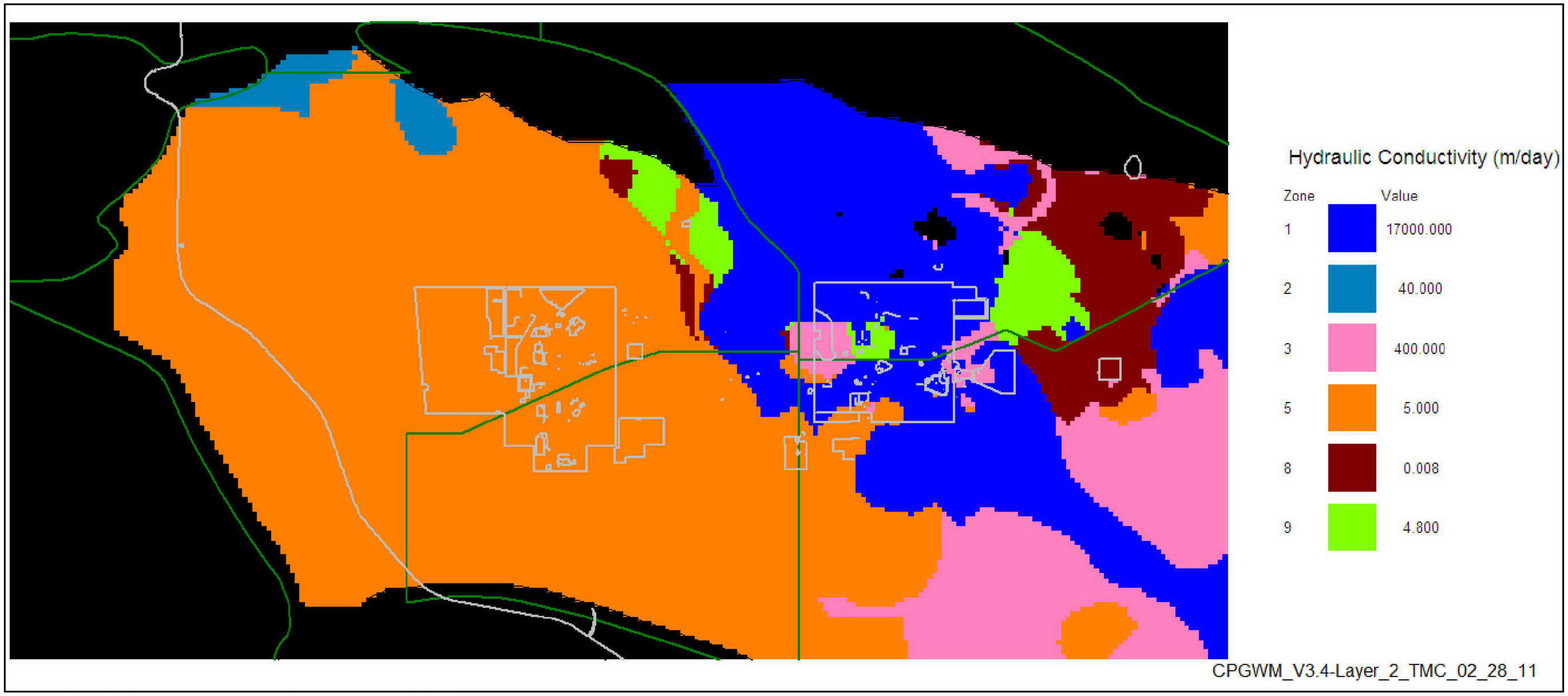

Note: Current Water Table is mostly in Layer 2.

Figure 4-15. Hydrostratigraphic Units of Model Layer 2

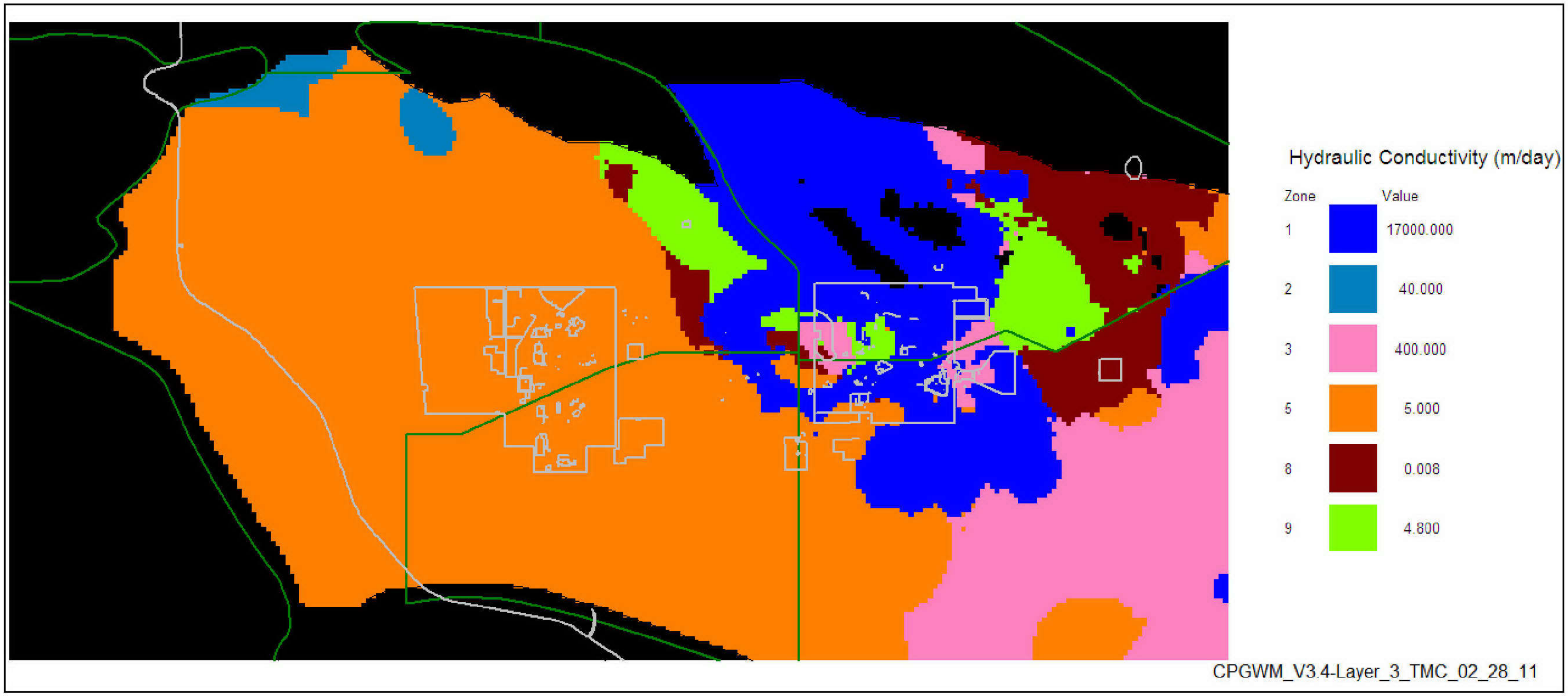

Figure 4-16. Hydrostratigraphic Units of Model Layer 3

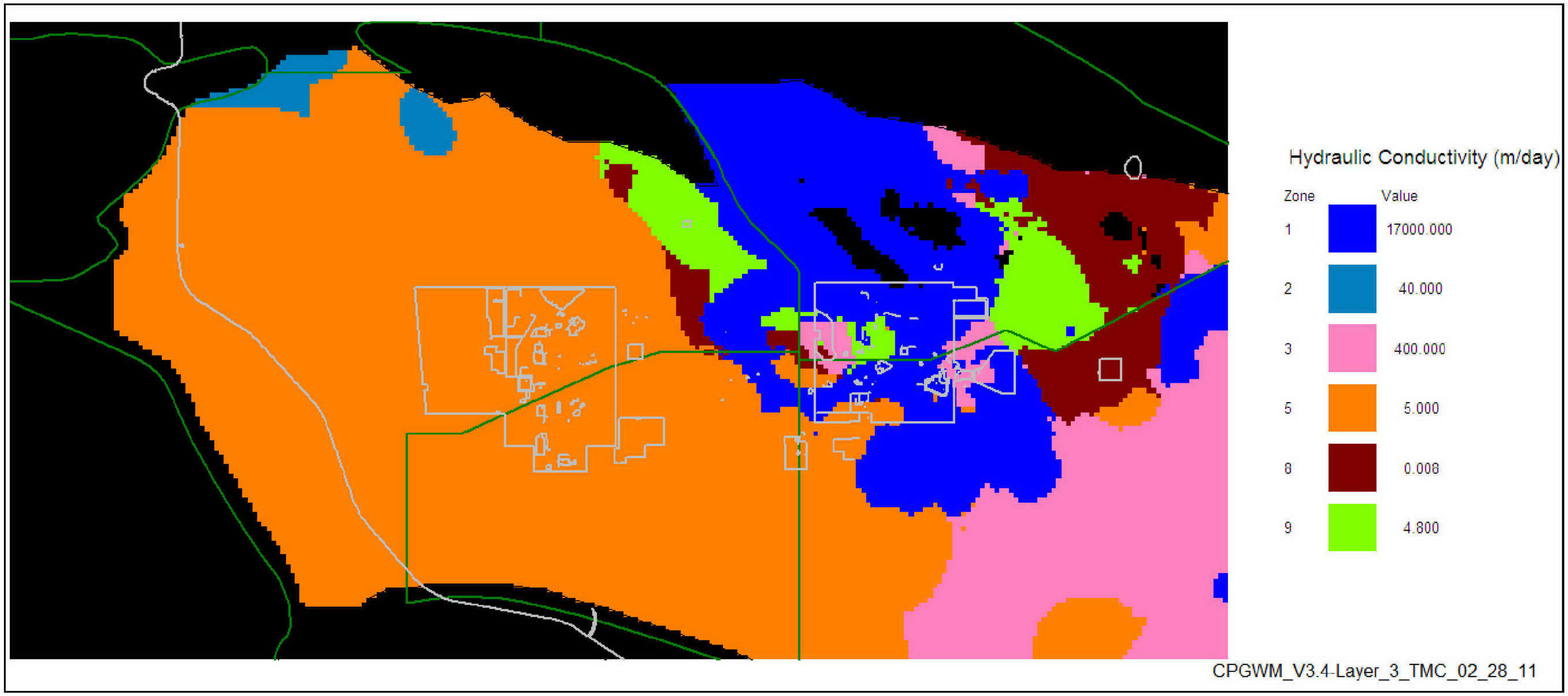

Figure 4-17. Hydrostratigraphic Units of Model Layer 4

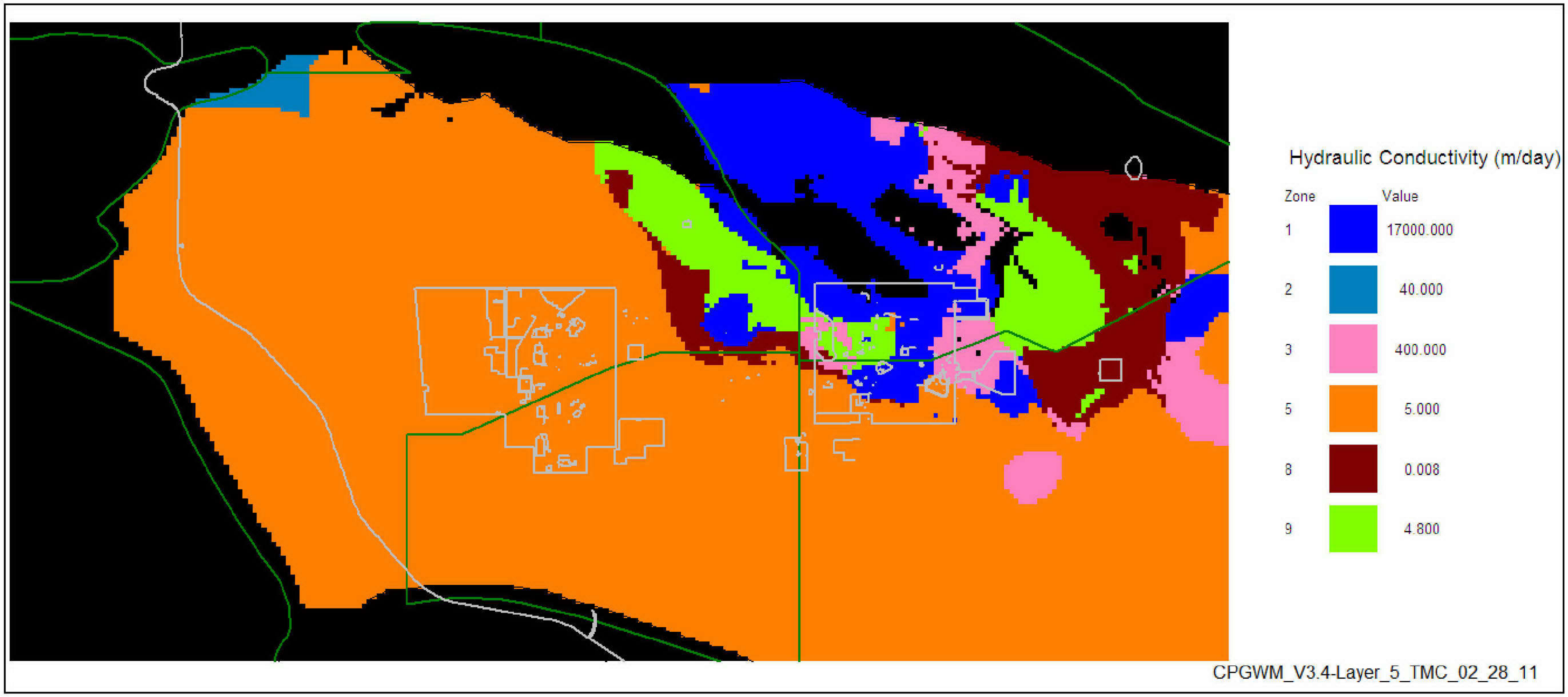

Figure 4-18. Hydrostratigraphic Units of Model Layer 5

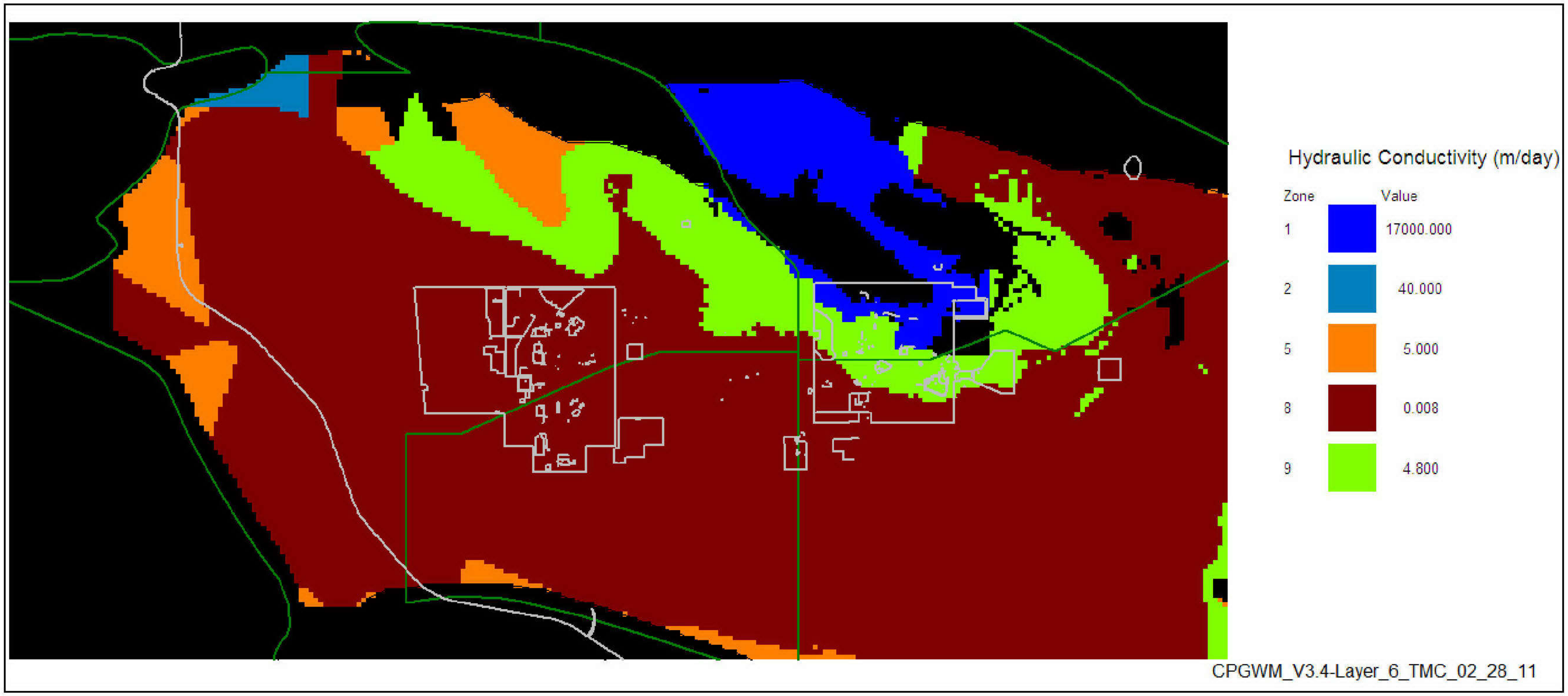

Figure 4-19. Hydrostratigraphic Units of Model Layer 6

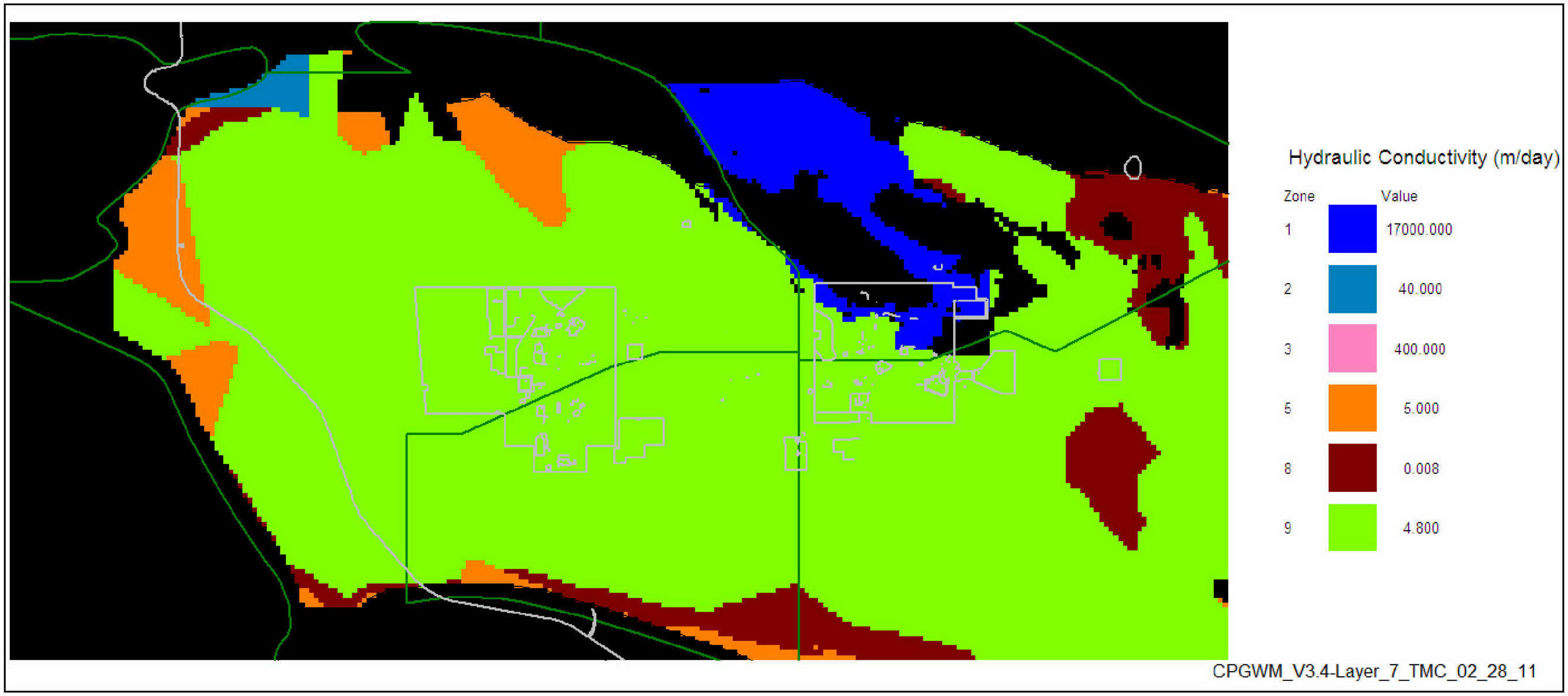

Figure 4-20. Hydrostratigraphic Units of Model Layer 7

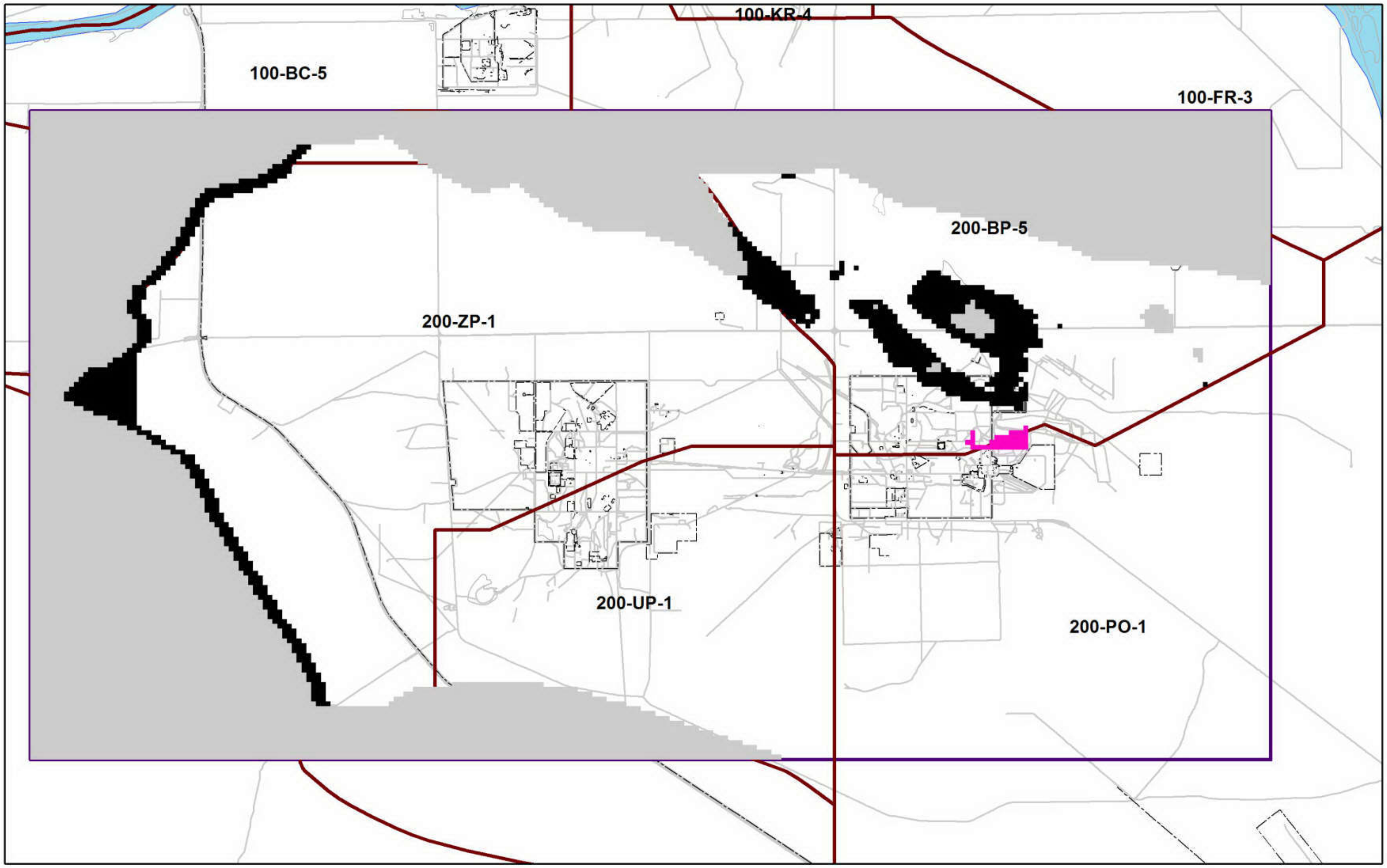

Figure 4-21. Extent of Zone (HSU) Reassignments in Model Layer 6 for Version 3.4 (extent shown in pink color was reassigned from Ringold A to Ringold Mud unit)

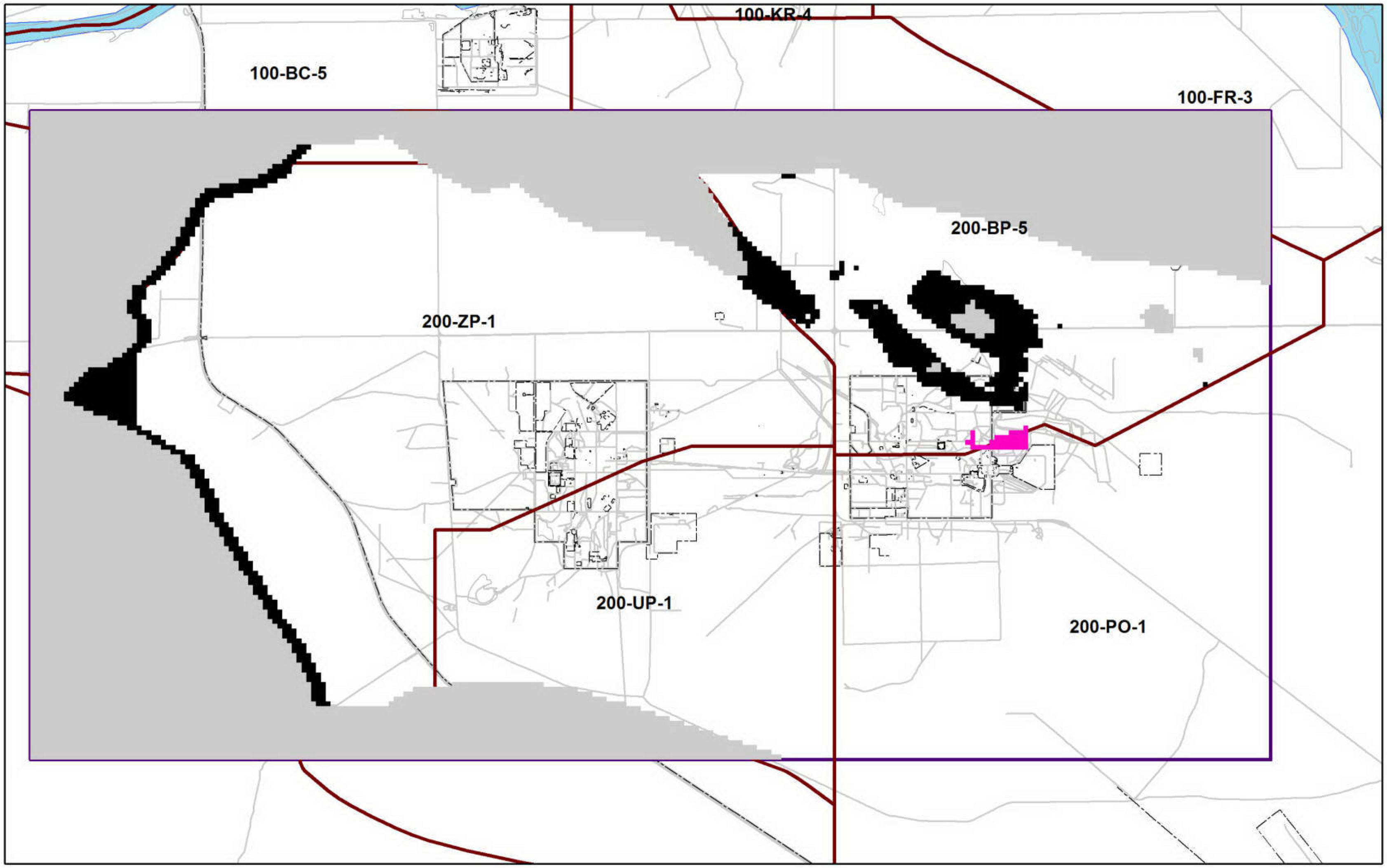

Figure 4-22. Extent of Zone (HSU) Reassignments in Model Layer 7 for Version 3.4 (extent shown in pink color was reassigned from Ringold A to Ringold Mud unit)

4.4 Parameterization

The basalt top elevation defines the bottom and most of the lateral boundaries of the model domain, depicted as the grey regions in Figure 4-23. Two gaps where the water table is above the top of Gable Ridge/Mountain feature are treated as specified head boundaries, as shown as blue lines in Figure 4-23. The parameterization of lateral boundaries is as follows:

- The western gap water level was assigned using water level data from well 699-63-90 acquired from HEIS. The water level is held constant based upon little yearly average variation during the calibration period (1944 to 2008). A value of 122.69 m was calculated as the average over this time interval. The data from well 699-63-90 is plotted along with the constant head value of 122.69 m in Figure 4-24.
- Water level data from well 699-60-60 acquired from HEIS was used to set the head for the Gable Gap boundary. Figure 4-25 presents the well 699-60-60 water level measurement data. . The period from 1944-1948 is an estimate based on calibration. Its starts at 120.6 m in 1944 and increases linearly to 121.14, the 1948 measurement. Both data for the western gap and the Gable Gap are incorporated into input file CHD.dat. Program CP_ModelStrat-Version3 uses CHD.dat to assign the specified head values to each cell of the boundary and stores the resulting data in file CHD_historic.in. CHD_historic.in is used by program create_CHD_V6 to create the MODFLOW.chd input file

The eastern boundary is treated as a mixed (Cauchy) boundary condition (MODFLOW general GHB), as depicted with a vertical pink line in Figure 4-23. The horizontal pink line is a GHB for the southern boundary. The GHB was constructed in several steps that have evolved during model development resulting in a highly adjustable, but complex method of formulating the boundary condition. These steps are described in the sections that follow.

4.4.1 General Head Boundary

Development of the GHB has been a complicated process with numerous revisions of the process. The general outline of the approach is as follows:

- The Columbia River is the basic water table reference (h_r).
- A hydraulic distance to the river is calculated following the water table gradient to define a path from a model cell to the river.
- The hydraulic conductivity along the path is defined as the hydraulic conductivity of the path.
- The conductance (C) to the river is calculated using the hydraulic conductivity, the cell's saturated cross-sectional area, and the path length.
- The boundary condition for the cell is $q_{bc}=C*(h-h_r)$, where q_{bc} is the water flux out of the cell and h is the hydraulic head in the cell.

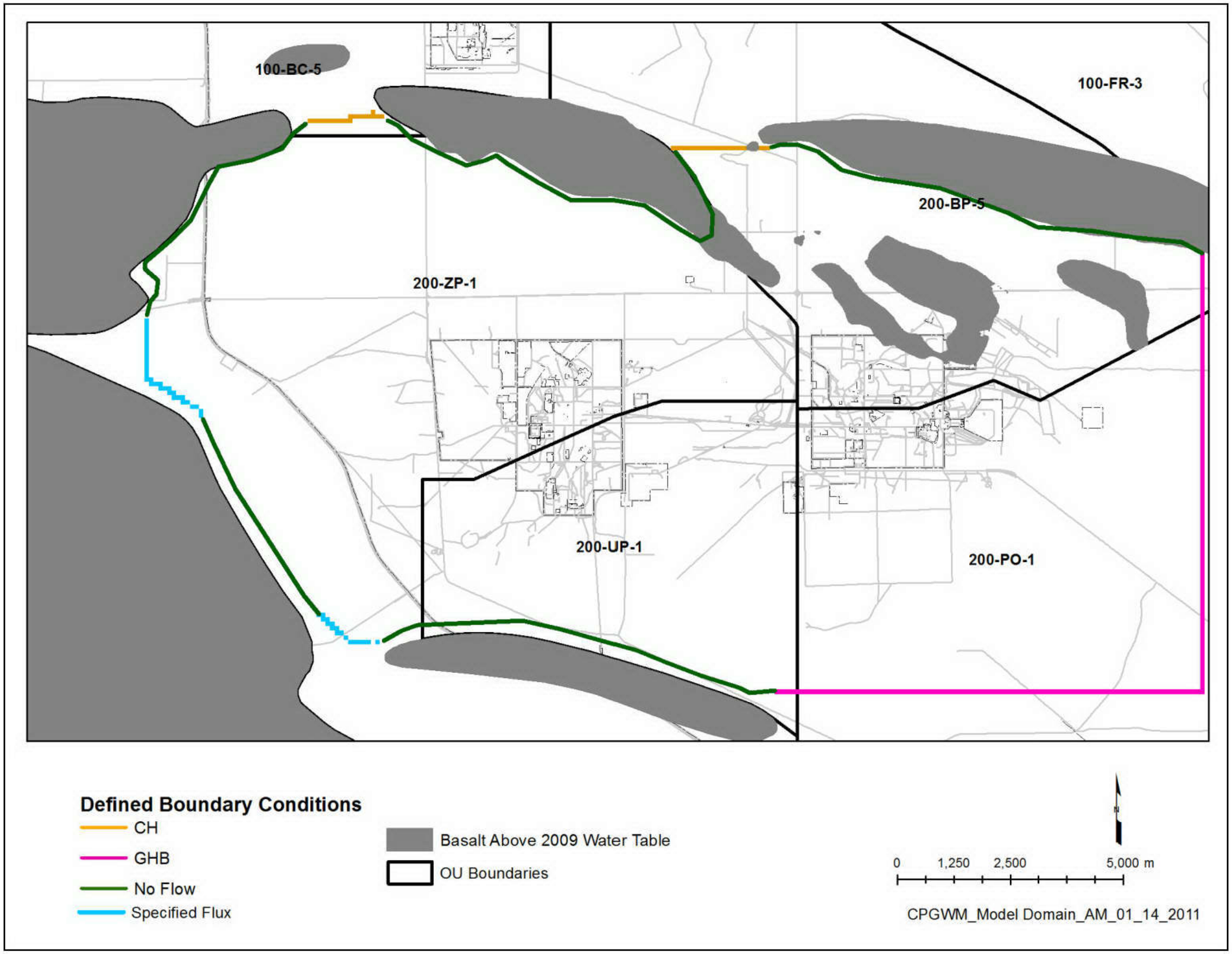

Figure 4-23. Flow Model Lateral Boundary Conditions

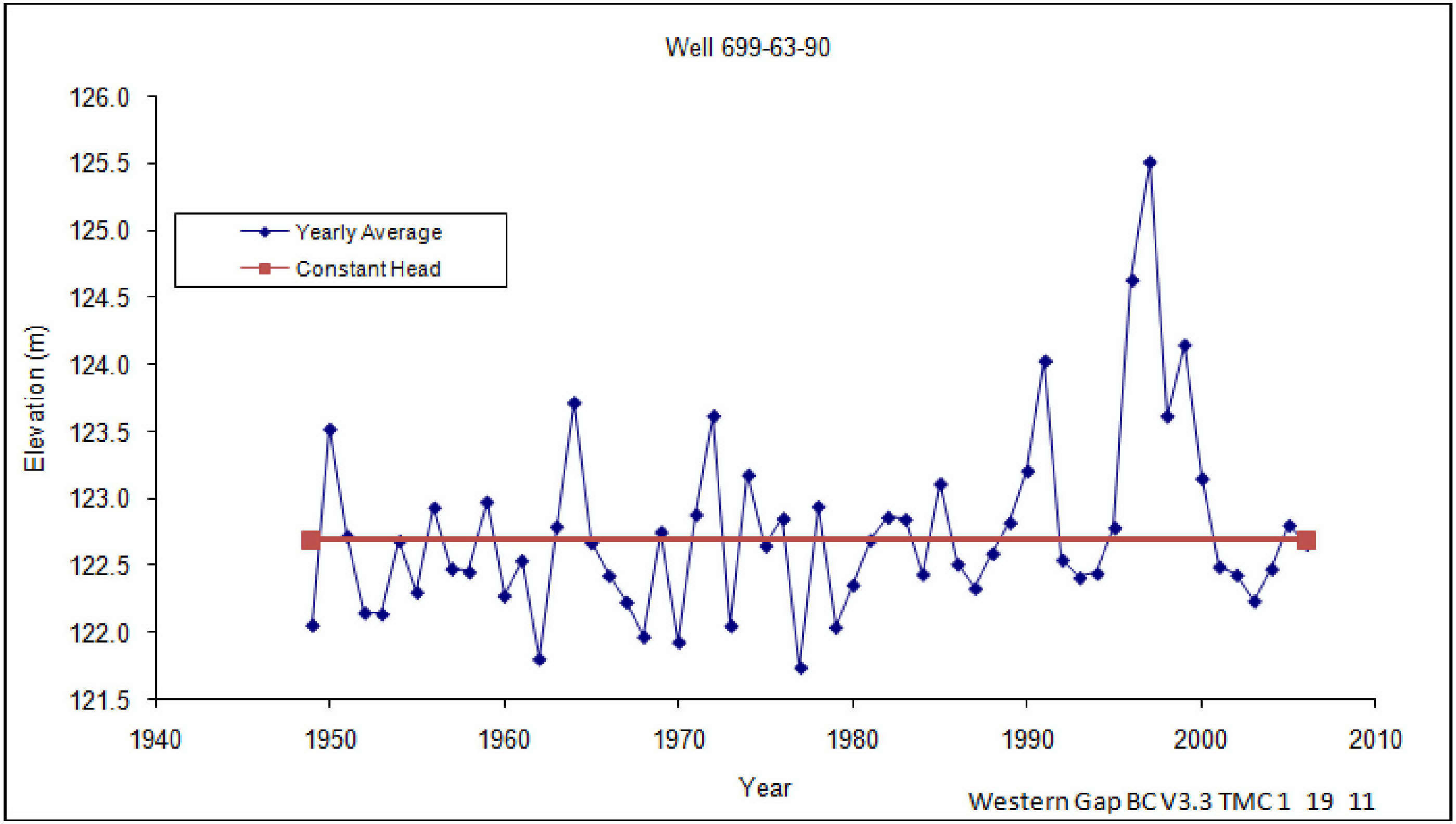

Figure 4-24. Historic Water Levels for Well 699-63-90

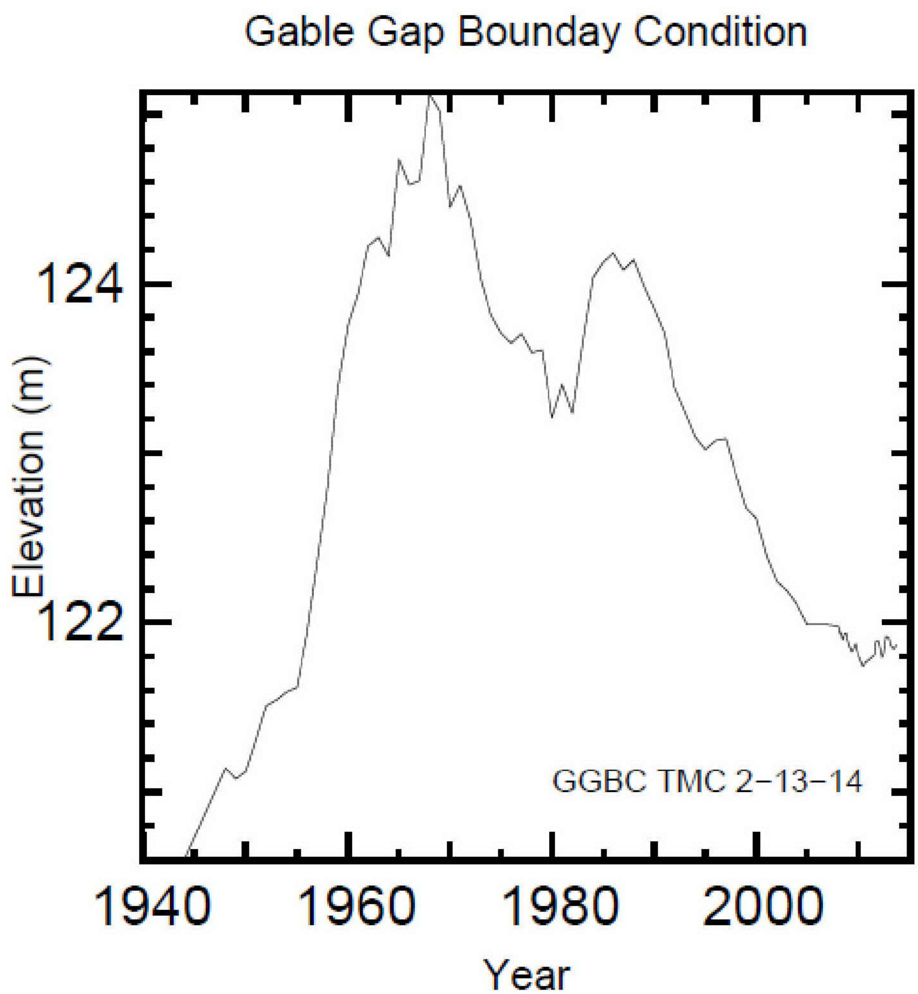

Note: Period prior to 1948 estimated through calibration.

Figure 4-25. Historic Water Levels for Well 699-60-60

To calculate the path length, a continuous water level surface was constructed for 2007. This was prepared using a shape file (*.shp) of the 2007 measured water level contours (*Hanford Site Groundwater Monitoring for Fiscal Year 2007* [DOE/RL-2008-01]) and using the "Topo to Raster" function in ArcMAP Spatial Analyst to provide a continuous and smoothly varying surface. Particle tracking utilizing the Runge-Kutta method was undertaken using this water level surface from every GHB cell, until the particle discharges at the Columbia River. The distance traveled by each particle was recorded to determine a distance for the path from each cell to the river.

A Fortran program (makeghb4) calculates the conductance of each GHB cell according to the following equation:

$$C = B \times DX \times HHK/D$$

where:

B = saturated cell thickness

DX = cell column or row dimension

HHK = hydraulic conductivity of the cell within the corresponding formation

D = the distance to the discharge point along the particle path

The saturated thicknesses of GHB cells were determined for each stress period from a previous simulation run that was calibrated to provide close agreement with historic water level measurements observed for well 699-24-33, which is the closest well to the boundary in the high conductivity channel that has a long record of water level measurements. This introduces an iterative process into the GHB definition.

Calibration multipliers were applied to the Hanford, Cold Creek, and Ringold units. Where a cell represents the Ringold lower mud, a zero value was used for the conductance. The GHB along the eastern boundary was divided into three segments, where separate additional calibration factors were used to adjust the average conductance term along the segment:

- The northern segment extends from Washington State Northing coordinates (581250, 143250) to (581250, 133250) (Model rows 1-90). The reference head for the Columbia River is taken as 111.0 m.
- The central segment extends from Washington State Northing coordinates (582250, 133150) to (581250, 130250) (Model rows 91-110). The reference head for the Columbia River is taken as 110.0 m.
- The southern segment extends from Washington State Northing coordinates (582150, 131250) to (581250, 129850) (Model rows 111-134). The reference head for the Columbia River is taken as 110.0 m.

The resultant conductance term for the GHB has the form:

$$Conductance = mu \times fs \times C$$

where:

mu	=	the calibration multiplier for a unit
fs	=	the calibration factor for a segment,
conductance C	=	defined in the previous equation

Section 4.5 presents the final calibration multipliers and factors.

The southeastern boundary of the model is treated as impermeable along the Rattlesnake Ridge subcrop and a mixed boundary condition towards the east. The no-flow segment (green line) extends from the Rattlesnake Ridge sub-crop to Washington State Easting coordinates (571750, 129850) (model column 161) reflecting the extension of the subcrop to the east below the model. A horizontal pink line in Figure 4-23 shows the GHB.

The southern GHB is a superposition of two source influences. This approach was taken so that, over time, the boundary condition led to patterns of groundwater flow in the southern and eastern part of the model domain that reflected patterns in historic water level maps. For the first source influence, the calculation described for the eastern boundary was applied. The calibration factors applied to the southern boundary differed from those applied to the eastern boundary.

For the second source, the influence of inflows from the Dry Creek Valley, located south of the model active domain, is calculated using the conductance formulation, with the distance D determined as the linear distance from the cell center to the X-ordinate of the 132 m contour on the 2007 annual water level map (DOE/RL-2008-1). The location of this 132 m contour is reasonably constant over time in previously presented water level maps. An additional multiplier (F_s) was introduced to vary the contribution of the two sources. The multiplier, South GHB scale factor, reduces the conductance term for the Dry Creek compared to the conductance term for the Columbia River. The flux boundary condition for the southern boundary is $q_{bc}=F_s*q_{DC}+q_{CR}$, where *DC* refers to Dry Creek as a source and *CR* refers to the Columbia River as a source.

These GHBs are defined based on uniform elevations for relatively long stretches of the Columbia River Hanford Reach. However, a possible improvement to the definition of these GHBs would be to define them based on a river stage that varies along the length of the corresponding stretch of the Hanford Reach. Chapter 8 lists this possible improvement.

4.4.1.1 Version 3.4 Generalized Head Boundary Refinements

The river conductance for the marked portion of the GHB boundary in Figure 4-26 was refined in Version 3.4. This refinement was applied only to the predictive model (not the historic model).

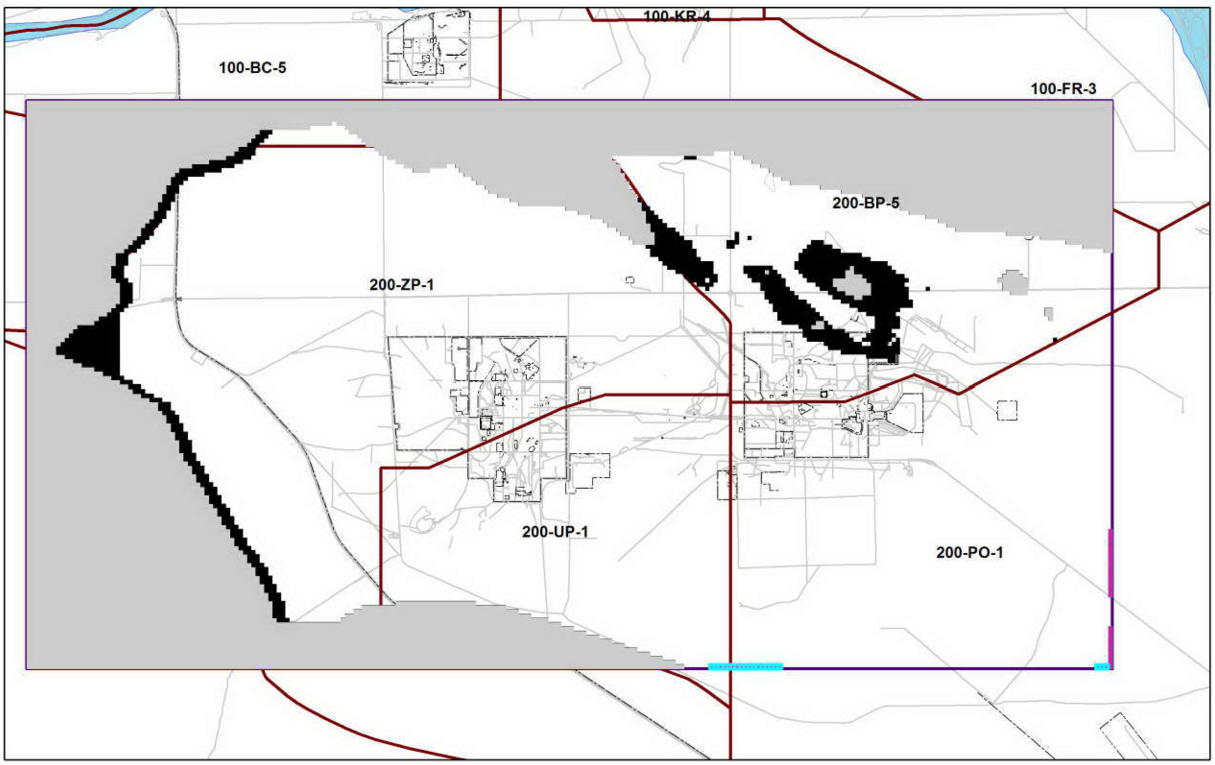

Figure 4-26. Segments of the Generalized Head Boundary Refined in Version 3.4 (river conductance changed for the boundary segments shown in cyan)

4.4.2 Recharge

Recharge at the water table in the historic model comprises the following contributions:

- Deep percolation of precipitation that is not evaporated/transpired and is not retained in storage in the vadose zone.
- Historic wastewater discharges.

- Mountain-front recharge arising from infiltration of snowmelt and runoff from elevated areas to the ephemeral Cold Creek and Dry Creek streambeds.

Net recharge from aerial precipitation rates were acquired as an electronic ASCII grid file (n_rech.dat) from PNNL-14753.

Artificial recharge values from the vadose zone to the aquifer previously calculated using STOMP in the System Assessment Capability, Rev. 1, framework based on historic liquid discharge records and are documented in an application log; this input is summarized in electronic model data transmittal EMDT-BC-0002, *Vadose Zone Attenuated Recharge from Inflow-04 Assessment* (archived in EMMA).[1]

Recharge associated with stream flows are a significant contributor to groundwater recharge upgradient of the Central Plateau (PNNL-17841).

The transient recharge arrays provided as model input combine the various recharge sources are calculated using program MakeRecharge3. This program reads input file MakeRecharge2Historic.in that provides the following information:

- Name of the MODFLOW discretization ("DIS") file.
- Name of the MODFLOW Basic Package ("BAS") file.
- Model origin coordinate offset and model grid rotation
    - 555650
    - 129850
    - 0
- The name of a file that lists the locations of polygons encompassing model cells within which feature-specific recharge loading rates should be applied (this file is currently named "PondRechargeInflow04.dat").
- The name of the output MODFLOW recharge ("RCH") file to be created by program MakeRecharge3.
- PrecipitationRechargeSGM2.asc contains the spatially varying array of recharge rates from net precipitation.
- The name of the ASCII file that contains the recharge rates within the ephemeral stream features is StreamRecharge32.dat.
- SALDS_MonthlyDischarges_V6.dat contains post 2007 recharge rates for the SALDS facility on a monthly basis.
- 1670.215 establishes the date of the year when model starts. It synchronizes the model with its long initial period to establish steady state conditions with the dates used in PondRechargeInflow04.dat.

Figure 3-15 displays natural recharge used in the model. The white stripes are where the Cold Creek and Dry Creek fluxes are applied. These are offset from the edge of the model to prevent recharge from being

---

[1] EMDT-BC-0002, 2009, *Vadose Zone Attenuated Recharge from Inflow-04 Assessment*, Rev. 0, Electronic Modeling Data Transmittal – Boundary Condition (Artificial Recharge). This is an internal data tracking number used to document receipt and review of information incorporated into models by CHPRC.

directly applied to the low conductivity Ringold mud. The grey area has a value of 2 mm/yr recharge from infiltration. The large light green areas are about 8 mm/yr and the smaller dark green areas reach 55 mm/yr. The two pond locations in the northeastern part of the model domain have a maximum value of 122 mm/yr.

4.4.3 Pumping Rates

Version 6.3.3 includes historic pumping rates obtained from the annual summary reports for the 200-ZP-1 and 200-UP-1 OU's as documented in EMDT-ST-0004 Rev.0. The physical specifications for the relevant wells are contained in file wellinfo.txt. Pumping rates for each stress period are listed in file PumpingRatesfor2013update.txt. The program reads instruction file allocateQWell.in that provides the following information:

- Number of wells in the wellinfo file and the pumping rate file.
- makeghb4_dummy.nam; pseudo MODFLOW name file that provides the names of MODFLOW input files that are used to locate the wells within the model grid and to establish the hydraulic conductivity of model cells hosting wells.
- Name of the heads files used to define the water table used to set the top of the screen interval for wells screened above the water table.
- Model origin coordinate offset and model grid rotation
    - 555650
    - 129850
    - 0
- Name of the wellinfo file i.e. wellinfo.txt
- Name of the pumping rate file i.e. PumpingRatesfor2013update.txt
- Name of the "WEL" output file
- Name of the "MNW" output file
- Name of the "MNW2" output file
- Name of the well stratigraphy output file i.e. strat.txt. This file can be used to verify the code's correct interpretation of model geometry and water level interpretation.
- Start time. This defines to relative correspondence of the model time to the pump rate time. Negative values indicate units of model stress periods. Positive values indicate units of days.
- MNWFLAG Set to 0 for .WEL, 1 for .MNW, 2 for .MNW2, and 3 for both .WEL and .MNW2 2
- IWL2CB Sets the unit number for cell-by-cell flow term output. This unit should correspond to the .CBB file specified in the MODFLOW name file. Zero indicates no cell-by-cell flow term output and a negative sign indicates output of additional flow information to the CBB file.
- IADJUSTBOT Set to 1 if the bottoms of well screens are to be tested and adjusted to be at or above the top of the basalt.

4.5 Calibration

Measured water level data from 1944 through 2008 are used as the qualitative measure of model accuracy. Our goal has been to apply automated calibration to the large set of historic water level data using the PEST parameter estimation software (Doherty, 2007) to optimize the estimate of the model parameter values. Due to the slow approach to convergence, it became apparent that automated parameter estimation alone would not result in an adequately calibrated model rapidly enough to meet required short-term predictive objectives. Nonetheless, automated calibration provides valuable information on the response of the model outputs to parameter changes, and can help to identify quickly structural weaknesses in a model. As a result, the calibration described here used a combination of automated and manual manipulation of the parameters. Many of the computational difficulties have been overcome through modifications to the MODFLOW code (CHPRC-00260), which should make the automated calibration much faster and more practical.

The calibration of the CPGW Model is an ongoing process that has improved with each successive version. As new geologic information and other data are incorporated into each new version, the calibration must be undertaken again and results in newly calibrated input parameters. The calibrated model for Version 3.3 provides a closer match to historic water levels than was achieved for Versions 2 and 3. The Version 3.3 match in the 200 West Area was only slightly improved over Version 3, but the match for well data in the 200 East Area was greatly improved, especially for initial conditions and for 2008. This reflects the subjective weight given to hydraulic head data in the early and late times of the 1944 to 2011 historic simulation period. Early times are less perturbed by the large operational discharges to the surface, and late times are more representative of the conditions for which the predictive model (beyond 2010) will simulate.

4.5.1 Compilation and Disposition of Hydraulic Head Data

The locations of all 420 wells available for calibration and meeting the criteria described in the following list are shown in Figure 4-27 for the 200 West Area vicinity and in Figure 4-28 for the 200 East Area vicinity. Not all the wells are labeled in the figure to preserve legibility of the figure. The period of water level measurements in these wells varies from 1944 to 2008 to just a couple of years. Appendix A presents comparisons of measured and simulated water levels to these measurements. A representative subset of the calibrations wells used to present the calibration results, presented in Figure 4-29.

Historical well water level data were downloaded from the 2008 annual groundwater monitoring report (DOE/RL-2008-66, *Hanford Site Groundwater Monitoring for Fiscal Year 2008*). The text file Hist_WL was converted in to a *.dbf table, which was imported to ArcMap®. The *.dbf table was summarized in ArcGIS® by well name and then joined to the imwelwel.shp file last updated on February 3, 2009. This shape file was generated from the Hanford Well Information System (HWIS) database to represent all of the wells historically used for producing groundwater levels. Attributes from this shape file were then used to refine the calibration well list. The set of wells contained within this shape file was further refined based upon the following criteria:

- Well location within the model domain
- Horizontal coordinate system and coordinates known
- Vertical datum known
- Screened interval known (note: data were supplemented from HEIS for this purpose)
- Greater than or equal to 5-year period of record
- Well ground surface or brass plate elevation known or able to be calculated within tolerances

All wells that did not meet the above criteria were removed from the dataset. The resultant well shapefile, ModelCalibrationWells_pt.shp, the well screen data table, ModelCalibrationWells.dbf, and the water level table, ModelCalibrationWaterLevels.dbf, were merged into one geodatabase called CPModelCalibrationWells.mdb with feature class CalibrationWells (same as ModelCalibrationWells_pt.shp), tables ScreenData, and WaterLevels, respectively.

Thirty-two calibration wells from the 200-ZP-1 Model were added to the database as a separate feature class and were subject to the above criteria. Five new wells were added to the database to fill in well location gaps in the model. Screen data for these five wells were manually retrieved from well completion and construction summary reports from the Integrated Document Management System (IDMS) database.

Five wells were determined to be measuring perched water levels. Two of these wells and their measurements were removed completely from the dataset while the other three were kept in the dataset, but the water level measurements that reflected perched water levels were removed from the dataset. Well 699-55-89 water level measurements were corrected between the period of February 17, 1949 and December 1, 1984. A value of 3.967 m was subtracted from these measurements due to a re-survey of the well in 1984.

4.5.2 Review and Disposition of Well Screen Data

Screened interval information of the wells was not part of the original (Hist_WL) water level dataset. The following steps were taken to compile a sufficient tabulation of well screen data:

- The available screen information was supplemented by the dataset based contained within the file (WellInfoforModelArea.xls). The source for this file is the HEIS database. The query that retrieved these data was the same query used to retrieve the original 969 wells from the 2008 groundwater monitoring report (DOE/RL-2008-66).
- This table was joined to the water level dataset that had been refined to the wells only in the model area.
- Depths to water were then converted to elevations (in meters) by subtracting the depth to water from the Disc_Z field (brass plate/ground surface reference elevation). To supplement missing Disc_Z values, well casing "stick up" measurements provided by CHPRC (Personal Communication [Webber, 2009]) were used.
- Well screen information compiled in support of the precursor 200-ZP-1 Model was added to this database: this screen information was sourced from IDMS well construction and completion summary reports.
- Screen bottom elevations were updated with the elevations of the bottom of the well where that elevation was greater than the original screen bottom elevation. This update resulted from some screens extending below a "cement plug."

Finally, some of the wells that were updated to match the bottom of the wells were reverted to the original well depth reflective of the period the wells were functioning as water level monitoring wells. These wells had experienced a collapse, and the current depth to bottom was not reflective of the depth when the well was actually used for monitoring. The information for making this change was obtained from HWIS.

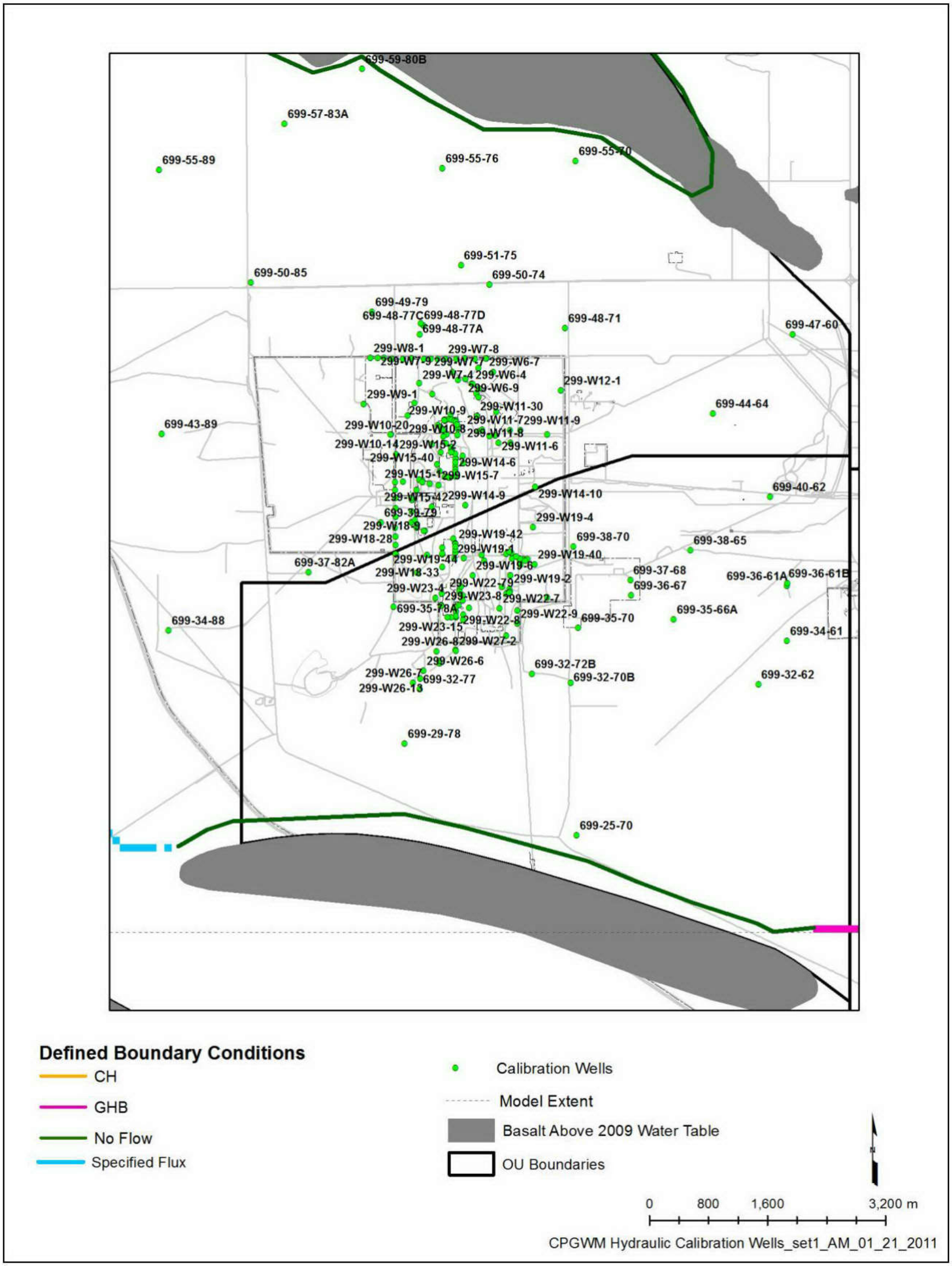

Figure 4-27. Calibration Wells in the 200 West Area Vicinity

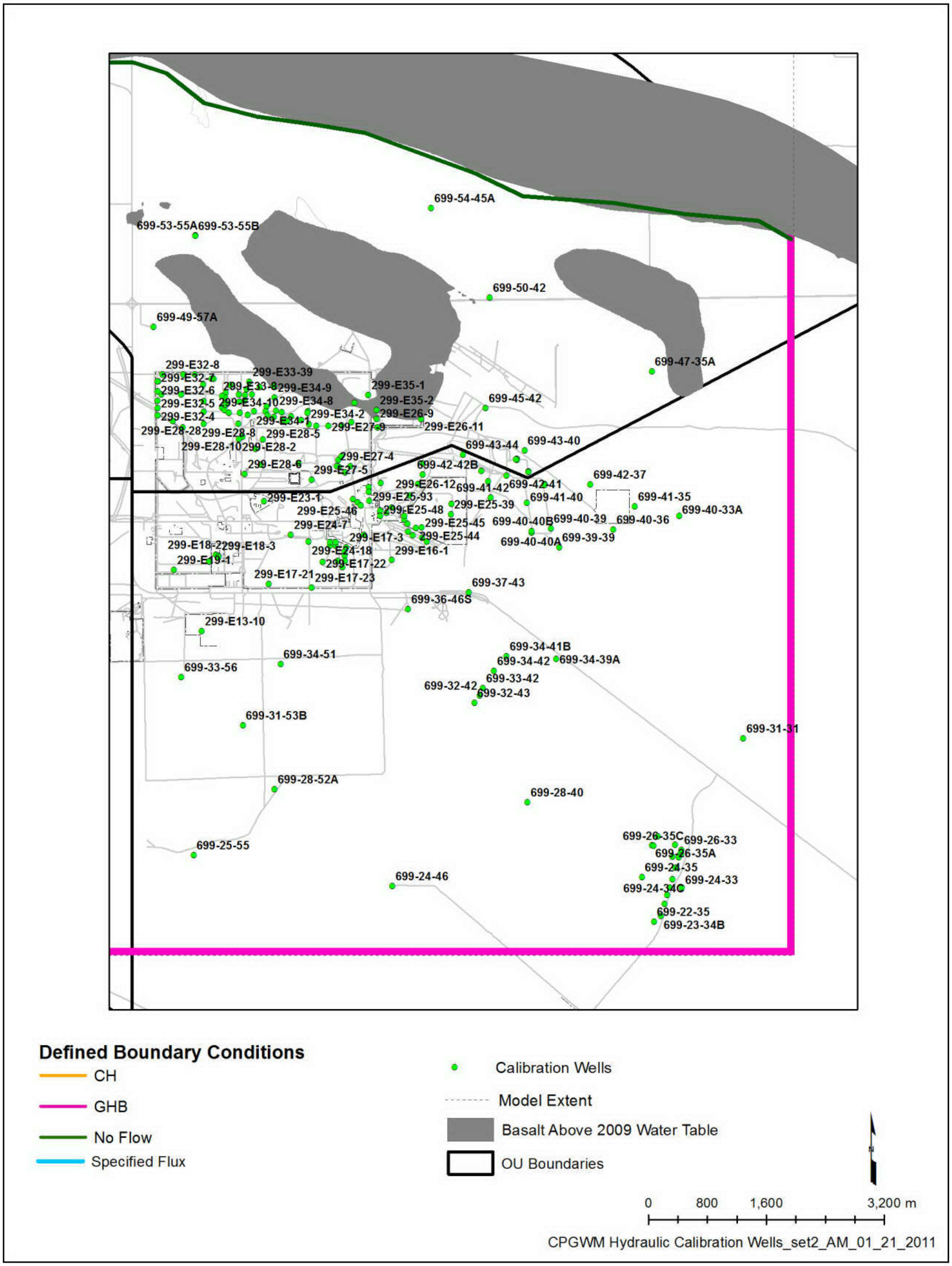

Figure 4-28. Calibration Wells in the 200 East Area Vicinity

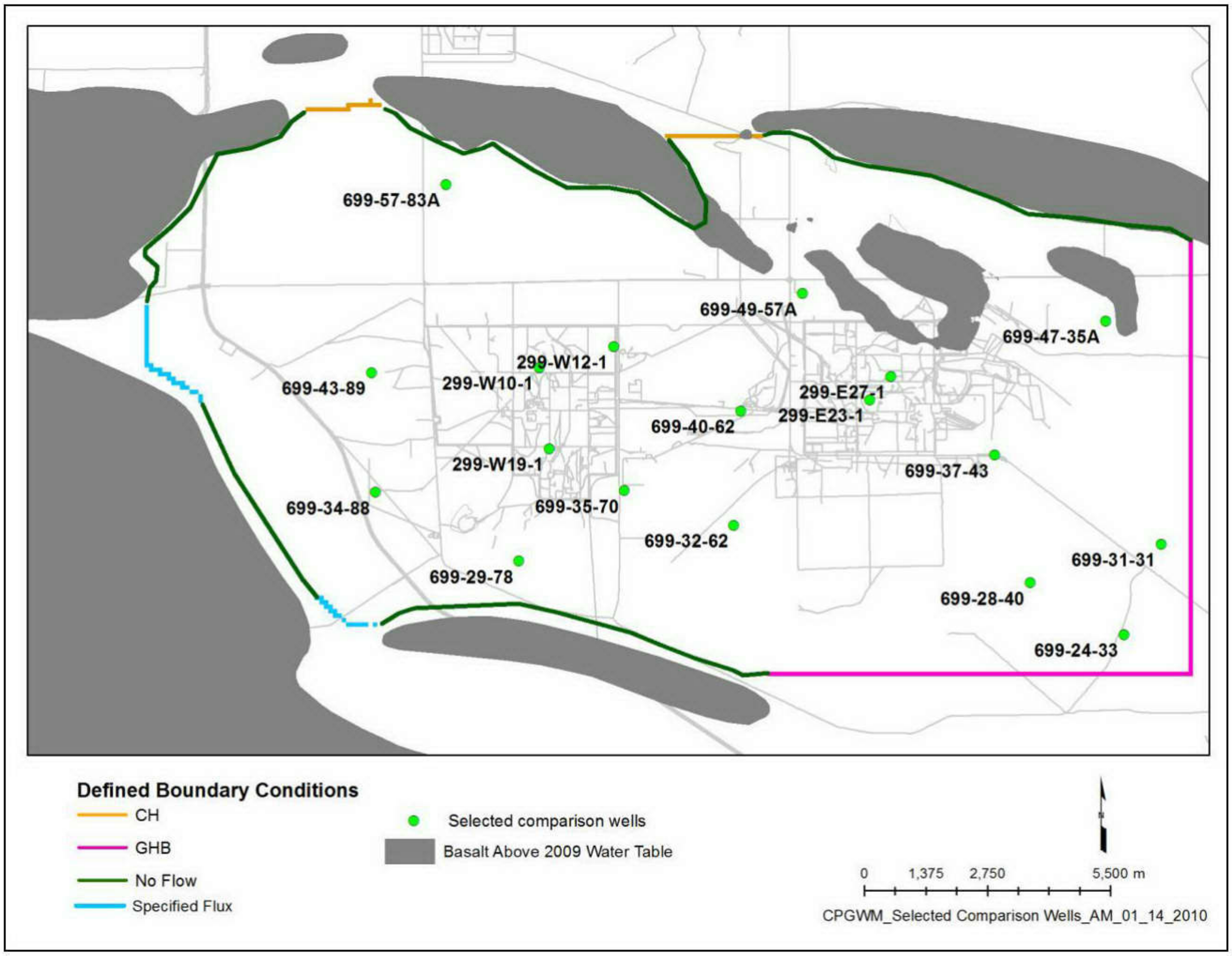

Figure 4-29. Wells Selected for Hydrograph Comparisons

4.5.3 Weighting of Water Level Data

Model calibration proceeds by estimating parameter values that improve the "fit" of the model outputs to historic measurements. When using automated parameter estimation techniques, a weight can be assigned to each measurement that reflects the (relative) accuracy, or reliability, of that measurement. If a high weight is used, this suggests that there is a high degree of confidence in that measurement, and that the model should be expected to reproduce (fit) that observation closely. Use of a low weight suggests that there is a low degree of confidence in that measurement, and that the model should not necessarily be expected to reproduce that observation closely. Low weights can also be used when it is acknowledged that a model does not simulate a particular feature, event, or process. As a result, it should not be expected to reproduce measurements that result from that feature, event, or process. Reproducing a measurement that it is not reasonable to reproduce can introduce errors in other aspects of the model.

In addition, weighting is used to scale observation data with different units. A mixture of water level measurements, gradient magnitude, and gradient direction were used in the calibration. Scale factors were introduced to normalize the expected error of the three different measurement types: water level, gradient magnitude, and gradient azimuth. Scale factors of 20,000 and 0.1 were applied to the gradient magnitude and gradient direction respectively. The scale factors are applied to the square of the data misfit. Scaling of the measurements to reduce the influence of clustering (e.g., high concentrations of wells in 200 West and 200 East Areas) has not yet been attempted.

Weighting was also used to increase the importance of closely fitting the data in certain regions. To reflect the importance of obtaining close fits near the specified head boundaries of the two northern gaps, the weighting was increased near these boundaries. Specifically, wells 699-53-55A, 699-53-55B, 699-55-89, and 699-57-83A were given a weight of 10. Additionally, due to the importance of closely matching the water level of well 699-49057A (the closest well to the basalt saddle; Section 3.2.5), its water level measurements were assigned a weight of 10.

The weighting of one well, 699-55-70, was modified by assigning a zero weight during the automated portion for Version 3 calibration to remove the influence of large residuals. This well is located close to the south side of the Gable Butte subcrop. The well is fairly isolated by Gable Butte and low conductivity sediments. It is a situation where local heterogeneity is very important to the well response. Therefore, reducing large residuals at this well by adjusting constant HSU properties would likely result in a poorer model for simulating contaminant transport than a better model. It is far from the contaminated regions of the Central Plateau, so a good representation of local heterogeneity near well 699-55-70 is relatively unimportant.

Perching of significant amounts of water, disposed near land surface, on fine grained material above the water table has been identified as a process that is not simulated by the CPGW Model (Section 3.2.2). A time variable weighting scheme was adopted to reduce the impact of perching on the calibration. This weighting was used explicitly for the automated calibration and subjectively in the manual calibration that established the final parameter values for Versions 3 and 3.3 listed in Table **4-5**. The variable weighting was set to accomplish two objectives. The first objective was to rely on early measurements in the 1944 to 1989 site operational period as indications of pre-perturbed conditions. The second objective was to match 2009 water level measurements, as these are the initial conditions for the predictive simulations. None of the water level measurements are completely free of operational perturbations to the water table. To reduce the impact of perching on the calibration, only water level measurements from 1948 to 1953 and after 2000 were given non-zero weights west of a north-south oriented dividing line approximated 1 km west of the eastern boundary of the 200 West Area. If a well had records for 1948 to 1949, then the periods from 1950 to 1953 were also given a zero weight. The period 1948 to 1953 was given a weight of 100 for each measurement. The period 2000 to 2008 was given a weight of 1. Other periods were given a weight of zero in the west and 1 in the east. It was assumed that perching was not a significant factor in the eastern portion of the model even though perch zones have been identified in this region. East of the dividing line, a weighting of 1 was applied for all measurements between 1953 and 2000 as well.

Wells 699-59-80B and 699-54-45A were given zero weights for all periods because it was evident that the wells were not responding as unconfined aquifer conditions. Despite the use of these variable weights during the calibration, the entire water level records (hydrographs) were reviewed qualitatively throughout the calibration, to evaluate the “fit” of the model to the water level record visually, focusing on the periods for which non-zero weights were used.

Table 4-5. Weighting of Water Level Data

Wells	1948 to 1949	1950 to 1953	1954 to 1999	2000 to 2010
699-24-33, 699-25-55, 699-35-51, and 699-36-61A	100	1	1	1
699-53-55A, 699-53-55B, and 699-49-57A	NA	NA	10	10
699-25-70, 699-39-79, and 699-49-79	100	0	0	1
699-55-89	100	0	0	10
699-57-83A	NA	NA	0	10
699-43-89	NA	100	0	1
699-55-70, 699-59-80B and 699-54-45A	0	0	0	0
699-34-88	NA	10	0	1
All other water levels west of division line	1	1	0	1
All other water levels east of division line	1	1	1	1
Gradient magnitude west of division line	20,000	0	0	20,000
Gradient magnitude east of division line	20,000	20,000	20,000	20,000
Gradient azimuth west of division line	0.1	0	0	0.1
Gradient azimuth east of division line	0.1	0.1	0.1	0.1

NA = not available

4.5.4 Hydraulic Gradients

Calculation of hydraulic gradients between monitor wells was introduced during the original 200-ZP-1 Model development and calibration. Gradients were introduced in areas where large water level changes have occurred over time; it is possible to achieve visually (and statistically) good correspondence between model outputs and measured water levels although the simulated gradients and, hence, flow directions can differ markedly from actual gradients and flow directions as reflected in the measured water level data. This is readily apparent if a gradient is calculated using water levels obtained at three wells that form a triangle. If the simulated water level at only one well differs from the measured water level at that same location, then the gradient calculated using the model outputs can be of a different magnitude and, perhaps more importantly, different direction than the measured gradient. This has great import since one of the intended uses of this model is to predict the fate and transport of contaminants in groundwater.

Starting with the calibration of the Version 3 model, a subset of gradients was formally built into the automated calibration. Gradients are constructed from the measurement data of three wells, a triplet, that are used to define a hydraulic gradient plane. Figure 4-30 presents the locations of the gradients used for calibration. Table 4-6 lists the well triplets used to define the gradients. Figure 4-31 presents the direction and magnitude of the gradient for triplet set 1. Inclusion of Figure 4-31 is for introducing the concept of gradient calculations. Discussion of the interesting features seen in the figure is postponed until the next section on calibration where this figure is presented again. The direction is plotted in terms of azimuth (degrees clockwise from north). An azimuth of 90 degrees is due east. A measured gradient can only be calculated when all three wells have measurements during a given year. Temporal offsets between the three measurements introduced a form of noise into the data. Section 4.5.5.3 presents the gradient plots from the Version 3.3 calibration.

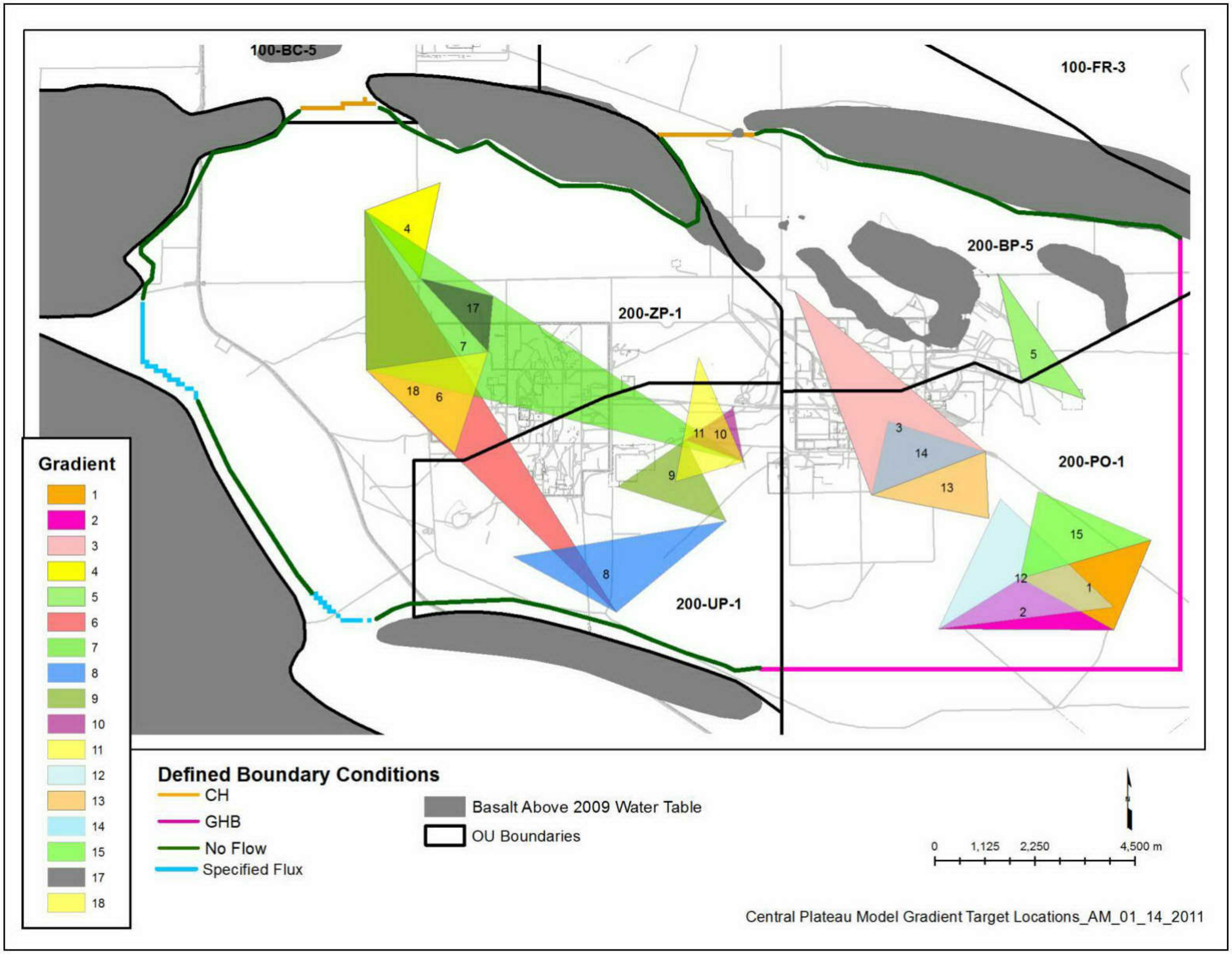

Figure 4-30. Locations of Gradient Calculations

Table 4-6. Well Triplets Used to Define Gradients

Gradient Number	Well 1	Well 2	Well 3
1	699-28-40	699-31-31	699-24-33
2	699-28-40	699-24-46	699-24-33
3	699-49-57A	699-37-43	699-34-51
4	699-57-83A	699-50-85	699-55-89
5	699-50-42	699-42-40A	699-41-35
6	699-43-89	699-25-70	699-55-89
7	699-43-89	699-36-61A	699-55-89
8	699-29-78	699-32-62	699-25-70
9	699-32-62	699-38-65	699-35-70
10	699-38-65	699-40-62	699-36-61A
11	699-36-61A	699-35-66A	699-44-64
12	699-34-66	699-34-42	699-26-33
13	699-32-43	699-37-43	699-34-51
14	699-E24-18	699-37-43	699-34-51
15	699-31-31	699-28-40	699-34-39A
17	299-W9-1	699-49-79	699-50-85
18	299-W9-1	699-37-82A	699-43-89

The well triplets used in the gradient calculations all have long water level measurement records. Gradients 3, 6, and 7 are intended to capture regional head variations. The other gradients are smaller in scale. Gradients 8, 9, 10, and 11 are useful for appraising representation of flow in the 200-UP-1 OU. Gradients 1, 2, 12, 13, 14, and 15 cover the high conductivity channel and the southern ones are useful in appraising the GHB conditions. Gradients 4, 17, and 18 provide additional information about the 200-ZP-1 OU. Gradient 5 provides some information about the northeast corner of the model. Smaller scale gradient calculations have been avoided because these can be strongly influenced by local variations in hydraulic properties.

4.5.5 Calibration

Calibration of the CPGW Model is an evolving process that entails more than manipulating parameter values. Modifications to the interpreted HSU geometry and the method of assigning the GHB conditions are also part of the calibration process. As model development has progressed, features introduced in earlier calibrations have been subsequently retained. To provide a complete and coherent description of these changes, the relevant aspects of each episode of model calibration are presented separately. The following subsections present the complete evolution of the model development. The description of the Version 3.3 calibration continues in Section 4.5.5.3.

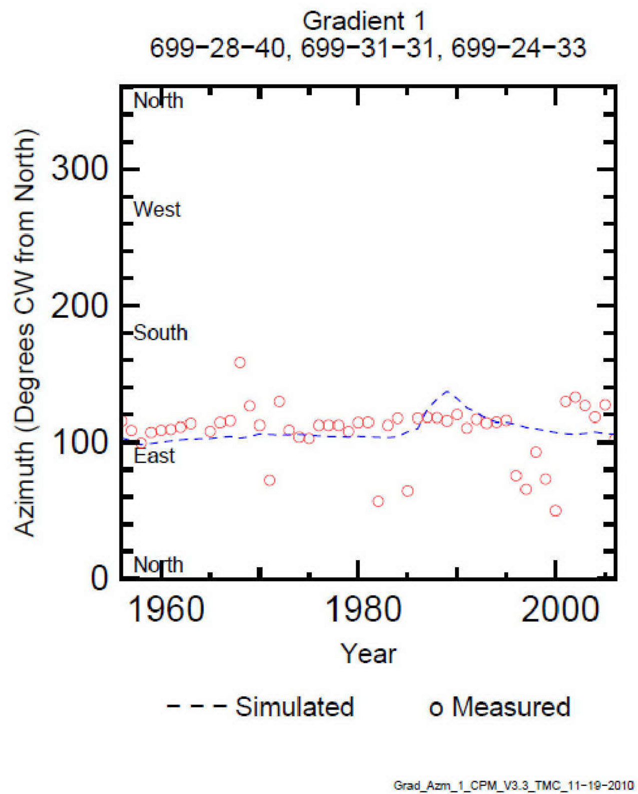

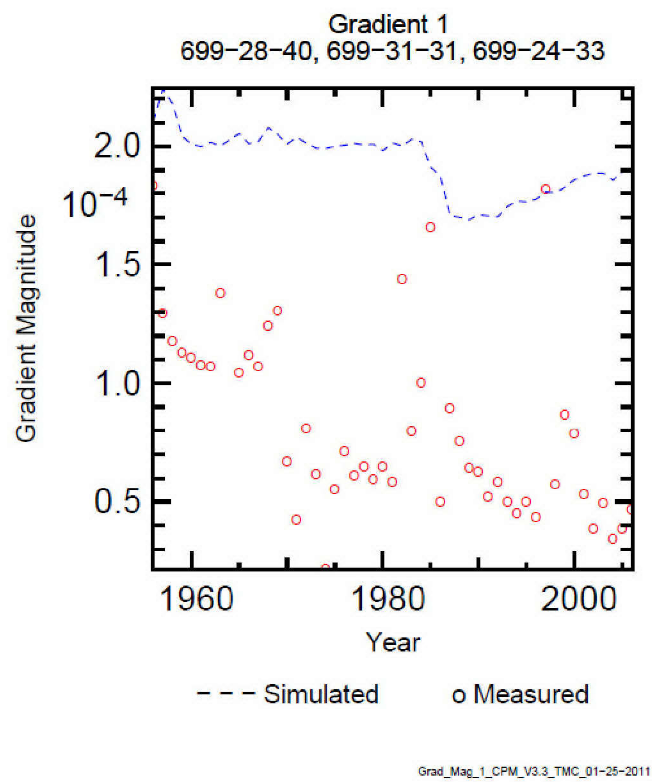

Figure 4-31. Gradient for Well Triplet 1 (699-28-40, 699-31-31, 699-24-33)

4.5.5.1 Version 2 Calibration

Automated calibration proved relatively ineffective for estimating parameters of the Version 2 CPGW Model. During the calibration of model Version 2 that was conducted for simulation of the 200-PO-1 OU, the calibration focused on the incised channel of Hanford formation into the Cold Creek unit (southeast corner of Figure 4-14) as the key region that needed to have an improved geologic description. Attempts to match the head difference between wells in the 200 East Area and wells in the southeast corner of the model by adjusting hydraulic conductivity of the Hanford formation and Cold Creek unit resulted in extremely large values for both and hydraulic control that would be inconsistent with historic plume configurations. This motivated reexamination of the well logs used to define the boundary between the Hanford formation and the Cold Creek unit. The re-examination of the wells indicated that, in much of the 200 East Area, the Cold Creek unit was as coarse-grained as most of the Hanford formation was. Therefore, re-designating some of the Cold Creek unit as the hydrostratigraphic equivalent to the Hanford formation, as indicated by the calibration, was supported by the well logs.

Once the HSU geometry definition, which was consistent with the high conductance channel indicated by the plume maps and which allowed simulation of hydraulic gradients in this channel, was developed, the GHB condition multipliers and factors were adjusted to cause flow directions in the southeast corner to be consistent with the plume contour data. The GHB factors were also adjusted to maintain agreement of the hydrograph for well 699-24-33 in 1976, the middle of a long period of relatively constant water level in the well. Figure 4-29 provides the location of well 699-24-33 and the three other wells mentioned in this section. The GHB condition for the northern segment of the eastern boundary was adjusted to maintain a small flux across the boundary in agreement with apparent contaminant movement indicated by the contaminant plume contours.

Effective hydraulic conductivity estimates for the Hanford formation and Cold Creek unit were obtained by forcing a match to the hydrograph for well 299-E23-1 (Figure 4-32), which is representative of the 200 East Area, with simulated hydraulic heads in 1975. During this period, simulated hydraulic heads are insensitive to specific yield and storage parameters. The GHB multipliers and factors were simultaneously adjusted to maintain the fit to well 699-24-33. Well 699-28-40 was also used to establish agreement of simulated hydraulic gradient in the channel with calculated gradients from the hydrographs in 1976.

Well 299-W12-1 (Figure 4-32) was used as representative of the 200 West Area. The head variation between well 299-W12-1 and well 299-E23-1 is primarily dependent on the effective hydraulic conductivity of the Ringold A and Ringold E HSUs. Again, 1976 was chosen for the match point because of the relatively constant water levels for a few years. Additional hydrograph plots from the Version 2 calibration can be found in ECF-200PO1-10-0259, *Central Plateau MODFLOW Model - Version 2 Calculation Brief.*

Table 4-7 presents a synopsis of the calibrated input parameters used in the CPGW Model Version 2. Figure 4-34, Figure 4-34, and Figure 4-35 provide an overview of calibration success. Figure 4-33 presents the probability distribution of misfits to measured hydrograph data. None of the calibrations discussed in this report use these misfits as a basis for the calibration. Water level measurements from 1944 to 1953 and 2000 to 2009 were used for creating the distribution shown (Section 4.5.3 provides the rationale). This figure is intended to provide information for comparison of successive calibrations. Figure 4-34 shows the cumulative probability. Figure 4-35 presents a cross-plot of simulated values as a function of measured values. The cross-plot reveals that larger measured values (the western region) tend to have simulated too large values and that the fit tends to be poorer for larger measured values.

Table 4-7. Central Plateau Groundwater Model Version 2 Calibration Results

Parameter	Value	Units
Coarse Grained Hanford Hydraulic Conductivity	8,500 (Horizontal) 850 (Vertical)	m/day
Fine Grained Hanford Hydraulic Conductivity	NA NA	m/day
Cold Creek Hydraulic Conductivity	100 (Horizontal) 10 (Vertical)	m/day
Ringold E Hydraulic Conductivity	5 (Horizontal) 0.5 (Vertical)	m /day
Ringold A Hydraulic Conductivity	3.5 (Horizontal) 0.35 (Vertical)	m/day
Ringold Mud Hydraulic Conductivity	0.3 (Horizontal) 0.03 (Vertical)	m/day
Hanford and Cold Creek Specific Yield - SY1	0.15	m/m
Ringold E, mud and Ringold A Specific Yield - SY2	0.18	m/m
Hanford and Cold Creek Specific Storage - SS1	0.00001	1/m
Ringold E, mud and Ringold A Specific Storage - SS2	0.00001	1/m
Cold Creek Flow	5,722	m^3/day
Dry Creek Flow	1,231	m^3/day
East GHB Hanford Multiplier	0.1	Unitless
East GHB Cold Creek Multiplier	0.1	Unitless
East GHB Ringold E and A Multiplier	0.1	Unitless
South GHB Hanford formation Multiplier	0.1	Unitless
South GHB Cold Creek unit Multiplier	0.1	Unitless
South GHB Ringold units E and A Multiplier	0.1	Unitless
South GHB Scale Factor	0.3	Unitless
East GHB North Factor	1	Unitless
East GHB Central Factor	NA	Unitless
East GHB South Factor	0.5	Unitless
Division between North East and Central East	Row 90	Unitless
Division between Central East and South East	NA	Unitless

NA = not applicable

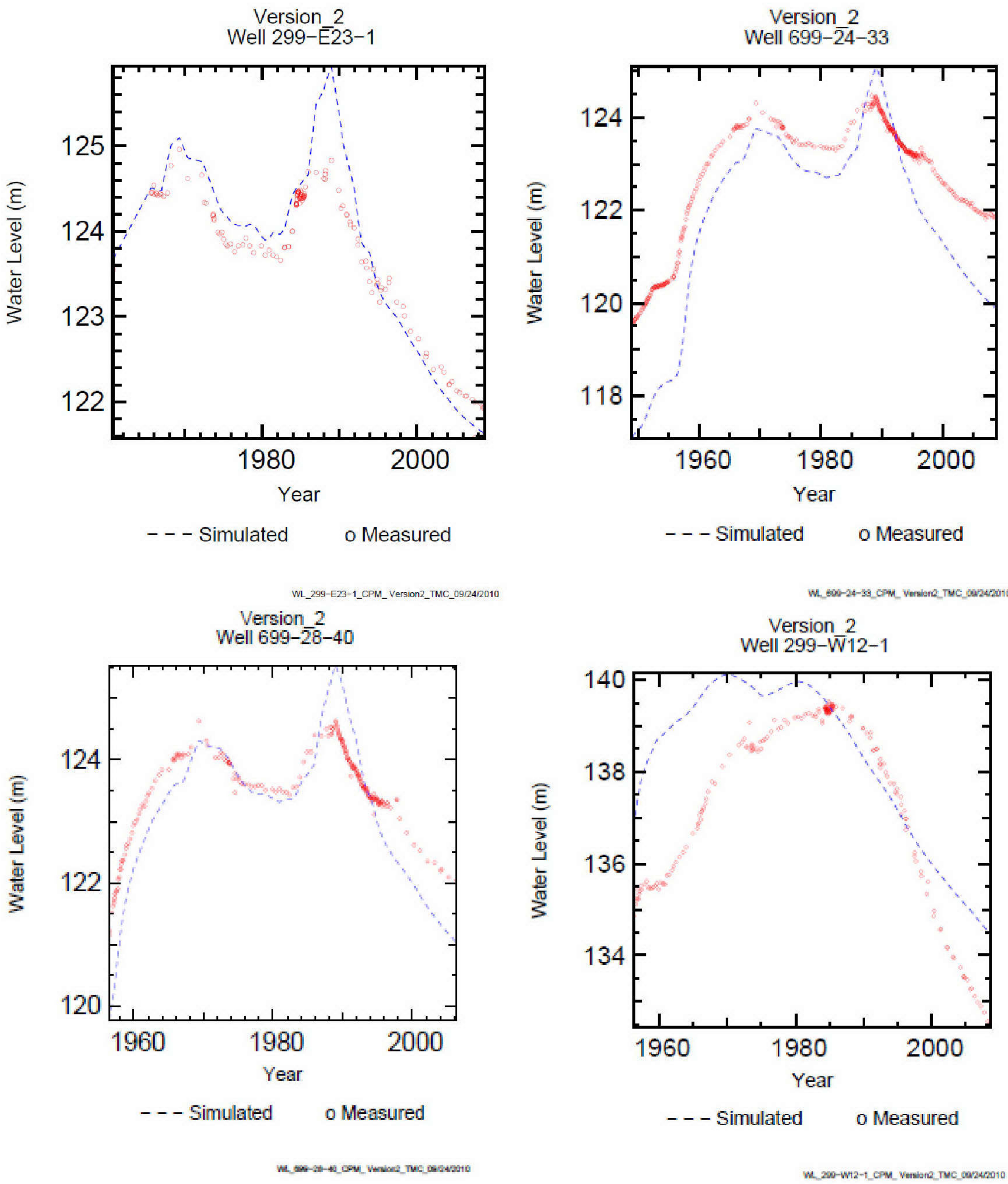

Figure 4-32. Measured and Simulated Hydrographs for Version 2 Calibration

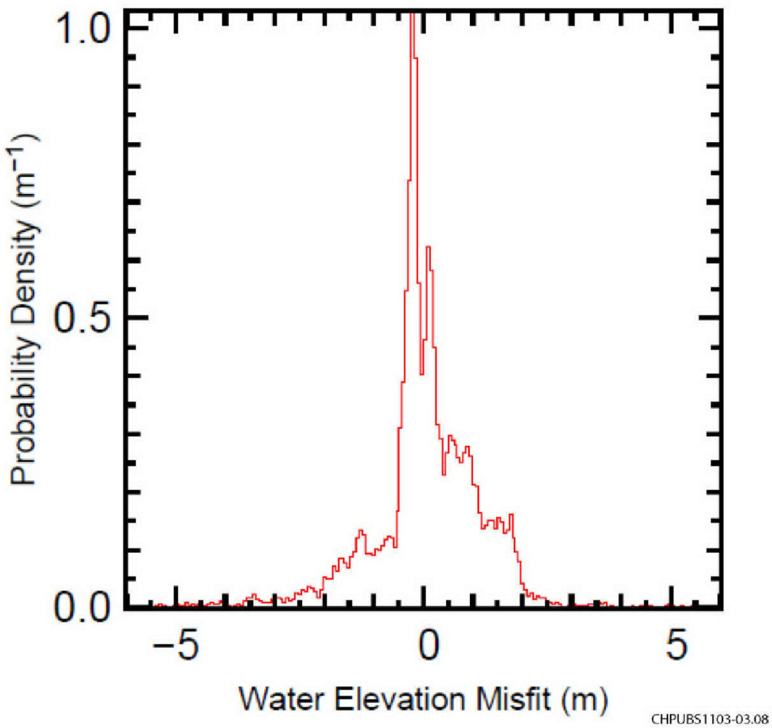

Figure 4-33. Version 2 Calibration Misfit Probability Density (1948 to 1953 and 2000 to 2009)

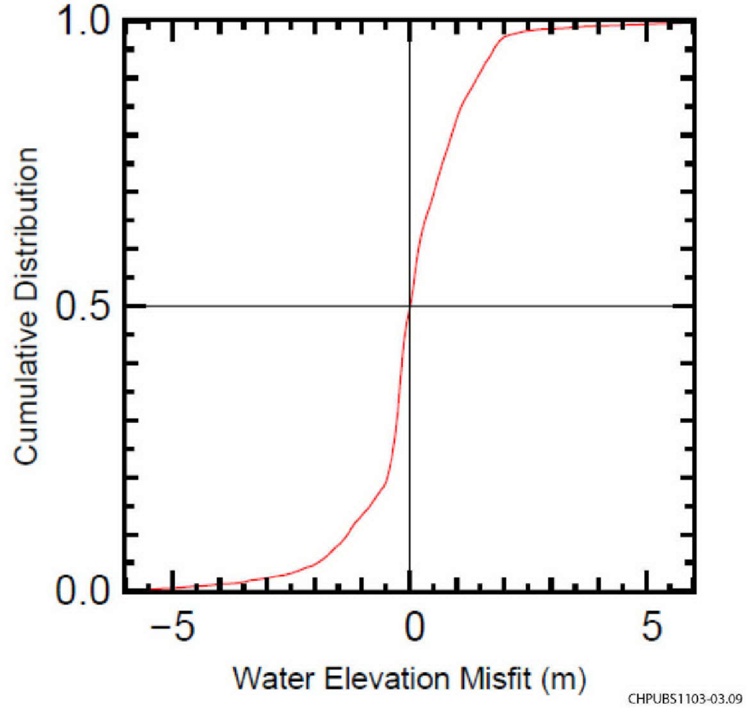

Figure 4-34. Version 2 Calibration Misfit Cumulative Probability (1948 to 1953 and 2000 to 2009)

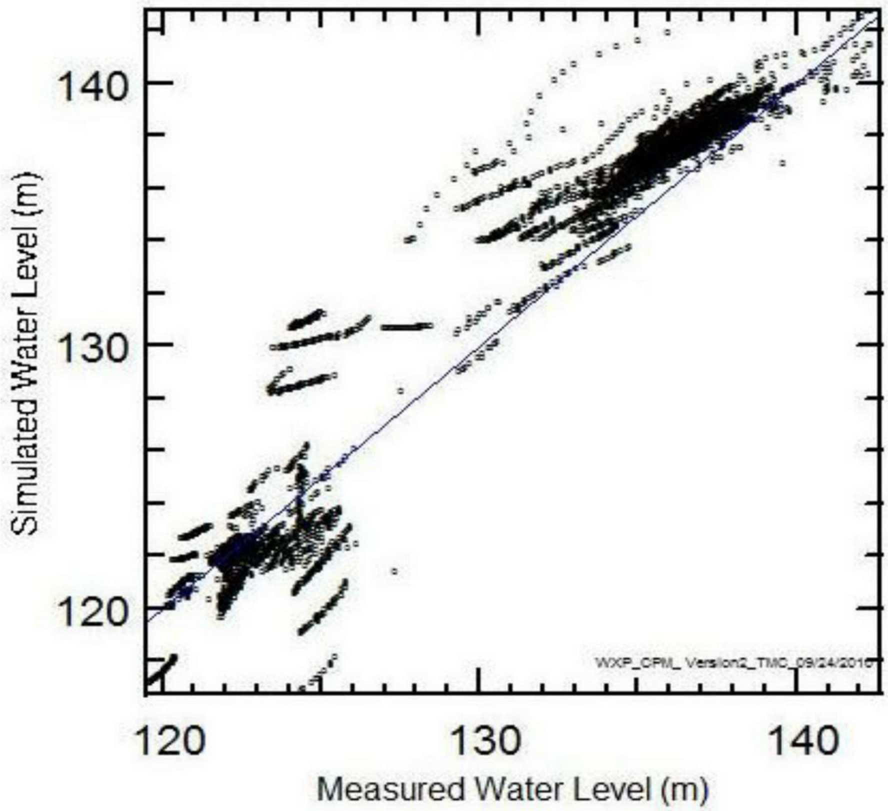

Figure 4-35. Version 2 Water Level Cross-Plot (1948 to 1953 and 2000 to 2009)

4.5.5.2 Version 3 Calibration

The calibration conducted for Version 3 of the CPGW Model was conducted prior to use for the RI/FS for the 200-UP-1 Groundwater OU. The resulting calibration improved the performance of the model in the 200-UP-1 and 200-ZP-1 OUs significantly at a cost of decreased ability to match 1940s data and, presumably, long-term predictions in the 200-PO-1 OU. Prior to this effort, changes were made to the discretization of the model. The vertical discretization was increased from five layers to seven and the basalt and HSU information and was updated and improved. Improved performance of the model, in terms of calibration fits, was noticeable from these improvements. The correspondence improvement between the model simulated water levels and measured water levels was marked in some locations (Figure 4-37), although large improvements tended to be restricted to reasonably small regions of the model domain. Table 4-8 presents a synopsis of the calibrated input parameters used in the CPGW Model Version 3.

The identification of historic perching in the 200-ZP-1 and 200-UP-1 OUs as a major issue for calibration was identified between the Version 2 and the Version 3 calibrations. The weighting of water level measurements described earlier was introduced for the Version 3 calibration, as was the use of gradient calculations. Automated calibration proved useful in identifying important parameters and indicating combinations of changes that would improve the calibration. However, progress of the automated calibration was deemed too slow to meet the time constraints. The calibration was completed by manual manipulation of the parameters, using the intermediate results provided by the automated calibration as a starting point.

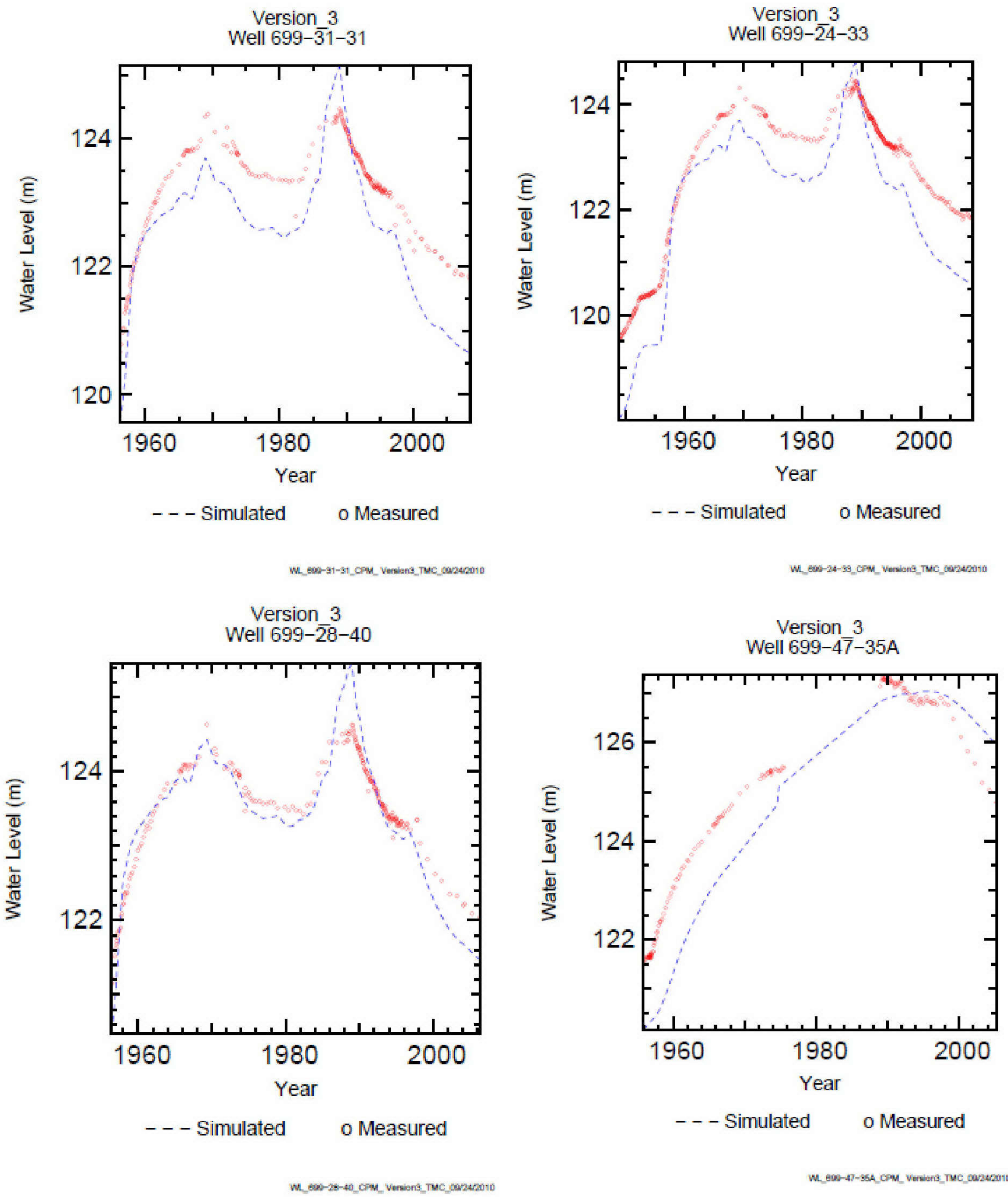

Figure 4-36. Measure and Simulated Hydrographs for Version 3 Calibration

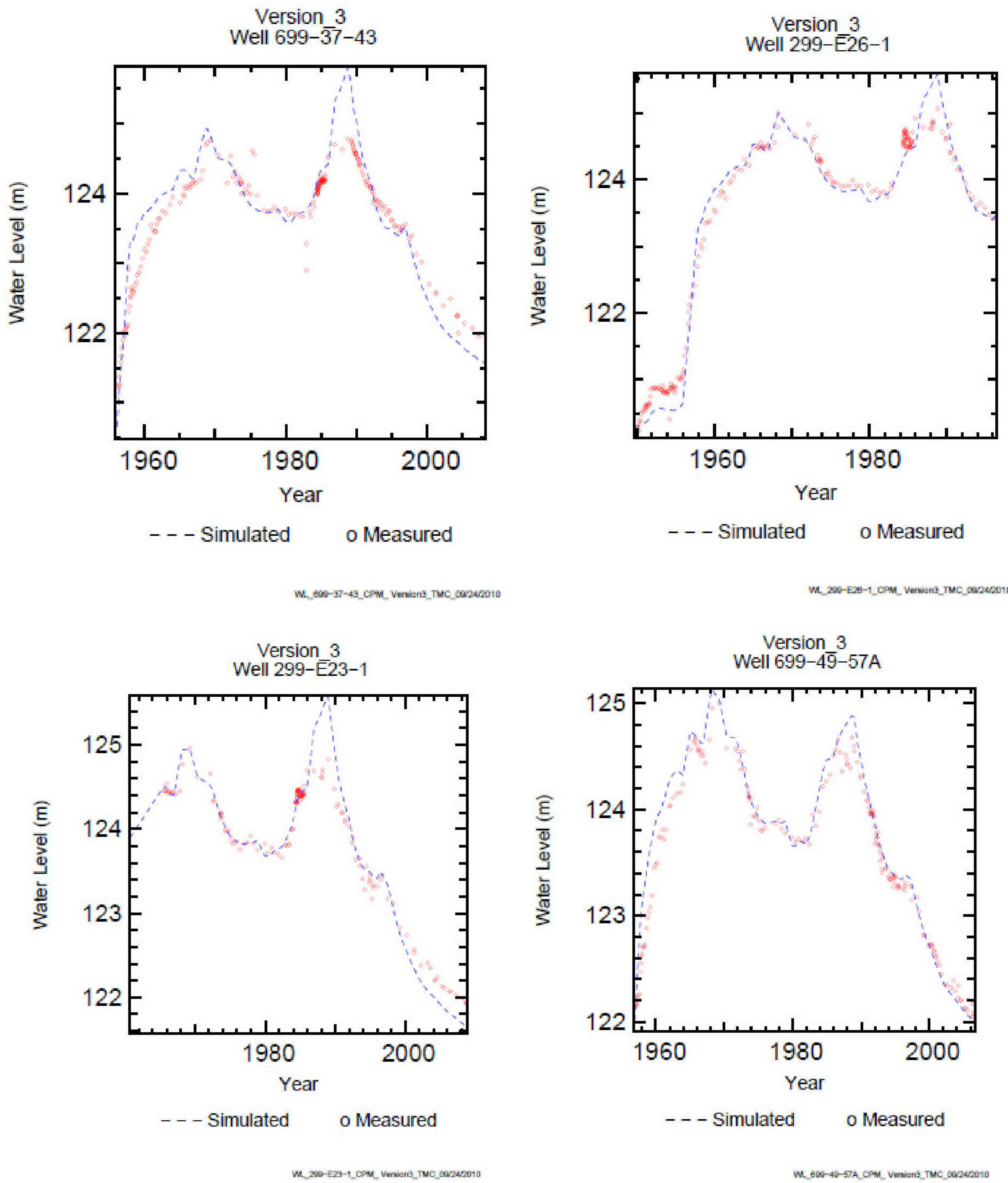

Figure 4-36 (Cont'd). Measure and Simulated Hydrographs for Version 3 Calibration

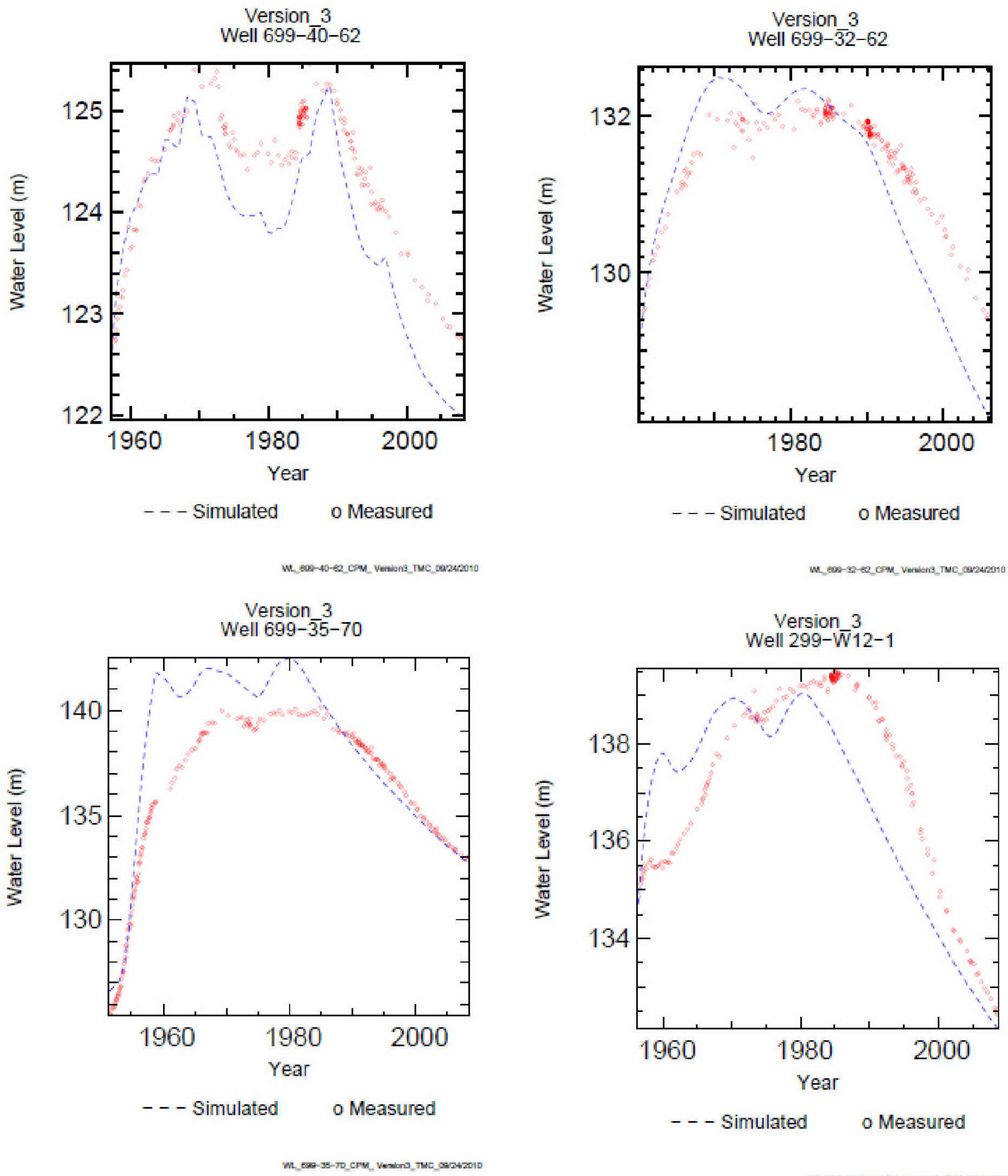

Figure 4-36 (Cont'd). Measure and Simulated Hydrographs for Version 3 Calibration

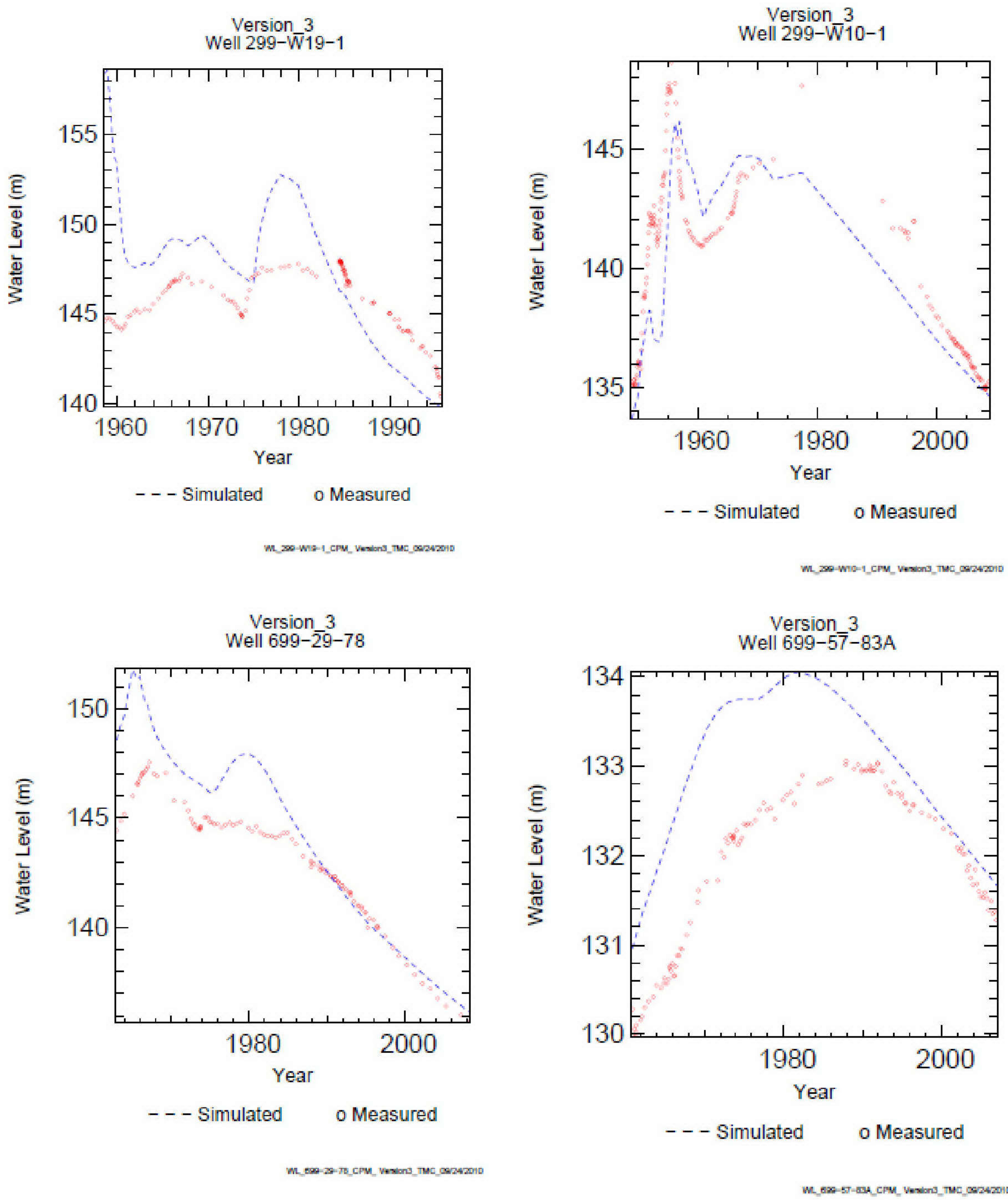

Figure 4-36 (Cont'd). Measure and Simulated Hydrographs for Version 3 Calibration

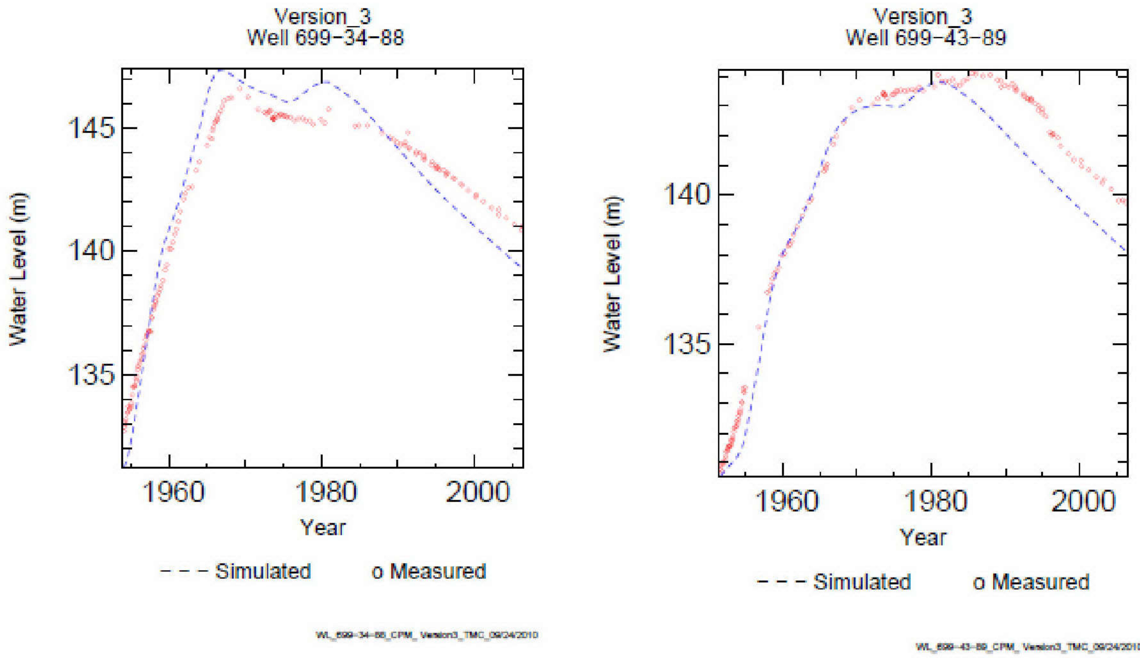

Figure 4-36 (Cont'd). Measure and Simulated Hydrographs for Version 3 Calibration

Table 4-8. Central Plateau Groundwater Model Version 3 Calibration Results

Parameter	Value	Units	Version 2
Coarse Grained Hanford Hydraulic Conductivity	10,000 (Horizontal) 1,000 (Vertical)	m/day	8,500 850
Fine Grained Hanford Hydraulic Conductivity	100 (Horizontal) 10 (Vertical)	m/day	NA
Cold Creek Hydraulic Conductivity	106 (Horizontal) 10.6 (Vertical)	m/day	100 10
Ringold E Hydraulic Conductivity	5 (Horizontal) 0.5 (Vertical)	m /day	5 0.5
Ringold A Hydraulic Conductivity	4.8 (Horizontal) 0.48 (Vertical)	m/day	3.5 0.35
Ringold Mud Hydraulic Conductivity	0.008 (Horizontal) 0.0008 (Vertical)	m/day	0.3 0.03
Hanford and Cold Creek Specific Yield - SY1	0.1	m/m	0.15
Ringold E, mud and Ringold A - SY2	0.0905	m/m	0.18
Hanford and Cold Creek Specific Storage - SS1	0.00001	1/m	0.00001
Ringold E, mud and Ringold A - SS2	0.00001	1/m	0.00001
Cold Creek Flow	2,500	m^3/day	5,722
Dry Creek Flow	700	m^3/day	1,231
East GHB Hanford Multiplier	0.25	Unitless	0.1
East GHB Cold Creek Multiplier	0.06	Unitless	0.1
East GHB Ringold E and A Multiplier	0.06	Unitless	0.1
South GHB Hanford formation Multiplier	0.25	Unitless	0.1
South GHB Cold Creek unit Multiplier	0.06	Unitless	0.1
South GHB Ringold units E and A Multiplier	0.05	Unitless	0.1
South GHB Scale Factor	0.1	Unitless	0.3
East GHB North Factor	0.035	Unitless	1.0
East GHB Central Factor	0.28	Unitless	NA
East GHB South Factor	0.38	Unitless	0.5
Division between North East and Central East	Row 90	Unitless	Row 90
Division between Central East and South East	Row 120	Unitless	NA

NA = not applicable

Comparing the summary statistics of the Version 3 calibration (Figure 4-37, Figure 4-38, and Figure 4-39) to the summary statistics of Version 2 (Figure 4-33, Figure 4-34, and Figure 4-35) indicates the improvement of the calibration over the entire domain. The mean error was reduced from 0.5 m to 0.3 m and the root mean square (RMS) error was reduced from 1.5 to 0.8 m. In Version 2, roughly 50 percent of the fits were within a meter and 90 percent were within 2 m. The Version 3 calibration brought about 85 percent of the fits within a meter and 95 percent within 2 m.

4.5.5.3 Version 3.3 Calibration

The calibration conducted for Version 3.3 of the CPGW Model was conducted prior to the RI for the 200-BP-5 Groundwater OU. The resulting calibration returned performance in the 200-PO-1 Groundwater OU to pre-Version 3 levels without significant loss of 200-UP-1 and 200-ZP-1 performance. In the 200 East Area, and northwest of the 200 East Area, matches to water levels in the post-2000 period tend to be within tens of centimeters (Figure 4-40) and are generally within the apparent variation in the data. However, hydraulic performance directly east and northeast of the 200 East Area, a region dominated by the Ringold lower mud HSU, is quite poor.

Since the grid and parameter set has not changed from Version 3.3, the comparisons of this section serve for Version 6.3.3 as well as Version 3.3. The performance of the Version 6.3,3 has been verified by comparing the simulated output to the calibration data set. Prior to 2007, the only noticeable differences between Version 6.3.3 and Version 3.3 occur between 1948 and 1960 where there is relatively unimportant improvement. Performance of Version 6.3.3 after 1990 is presented in Section 4.5.5.5

A key aspect of the RI investigation for 200-BP-5 has been the flow regime in the region between the Gable Gap and the 200 East Area. The basalt surface forms a ridge just north of well 699-49-57A, which trends southwest (Section 3.2.5). There is some uncertainty whether and when this ridge will entirely close off the hydraulic connection between the 200 East Area and the Gable Gap. In the model, the low point on this ridge has an elevation of 121.6 m above sea level. While the water level is far enough above the elevation of the low point, there should be enough transmissivity across the ridge to maintain flow northward toward the Gable Gap. As the water level approaches the elevation of the low point, the transmissivity will become much less, reducing northward flow across the ridge. If the water level drops below the low point, then flow across the ridge will be closed off and the flow north of the ridge will be independent of water levels south of the ridge. A successful effort was made to reproduce historic heads in the 200 East Area very accurately (well 699-47-57A in Figure 4-40). Thus, the remaining source of uncertainty about whether and when the flow across the ridge will stop is the elevation of the low point.

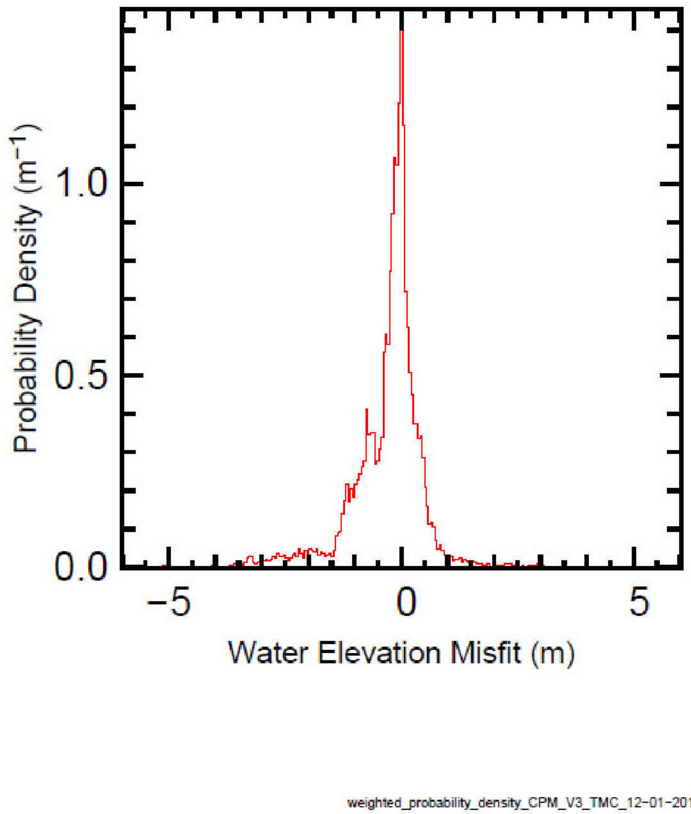

Figure 4-37. Version 3 Calibration Misfit Probability Density (1948 to 1953 and 2000 to 2009)

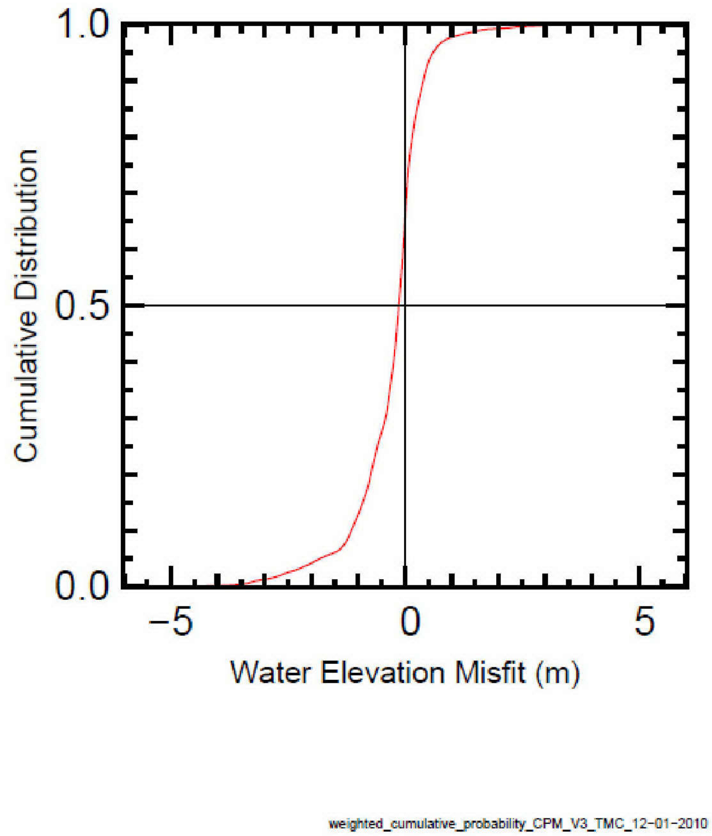

Figure 4-38. Version 3 Calibration Misfit Cumulative Probability (1948 to 1953 and 2000 to 2009)

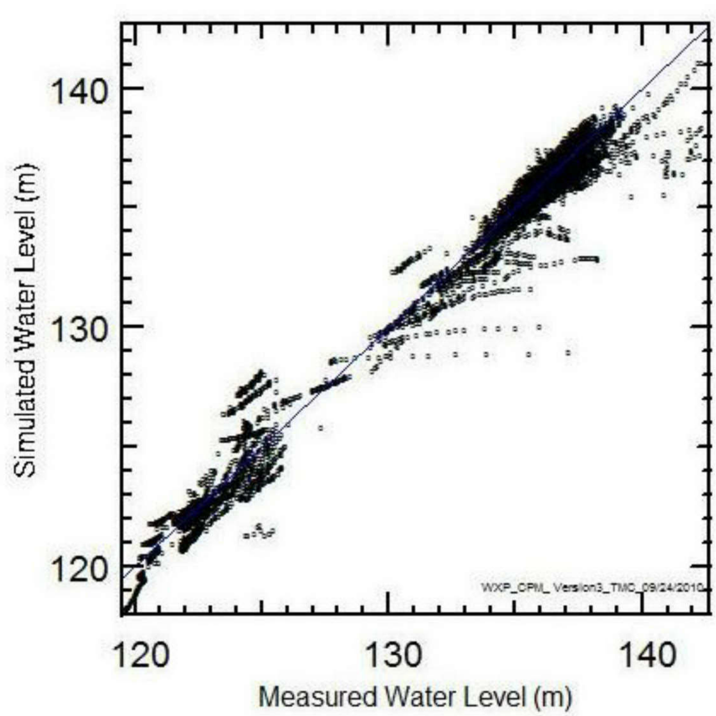

Figure 4-39. Version 3 Water Level Cross-Plot (1948 to 1953 and 2000 to 2009)

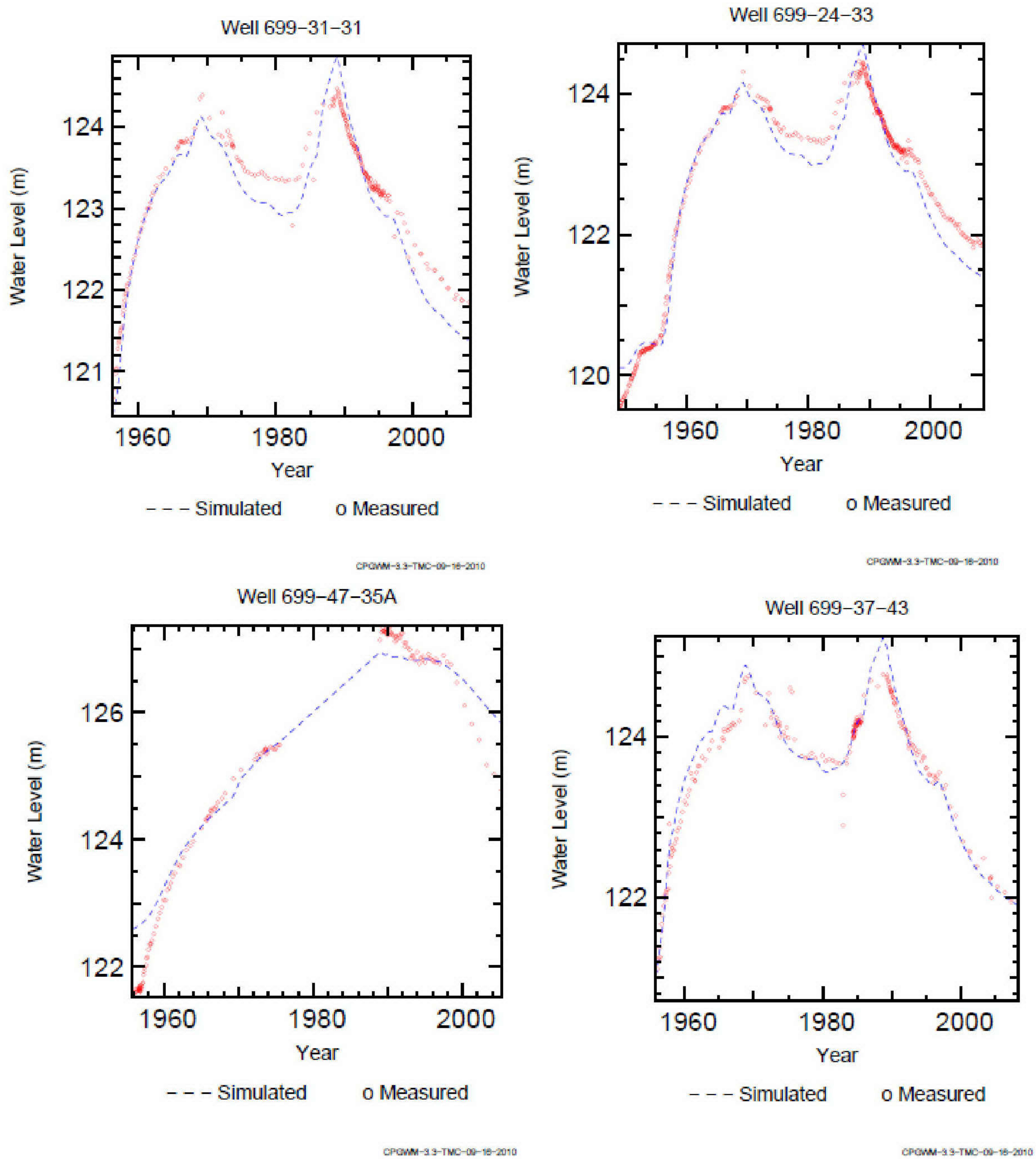

Figure 4-40. Selected Measured and Simulated Hydrographs Version 3.3 Calibration

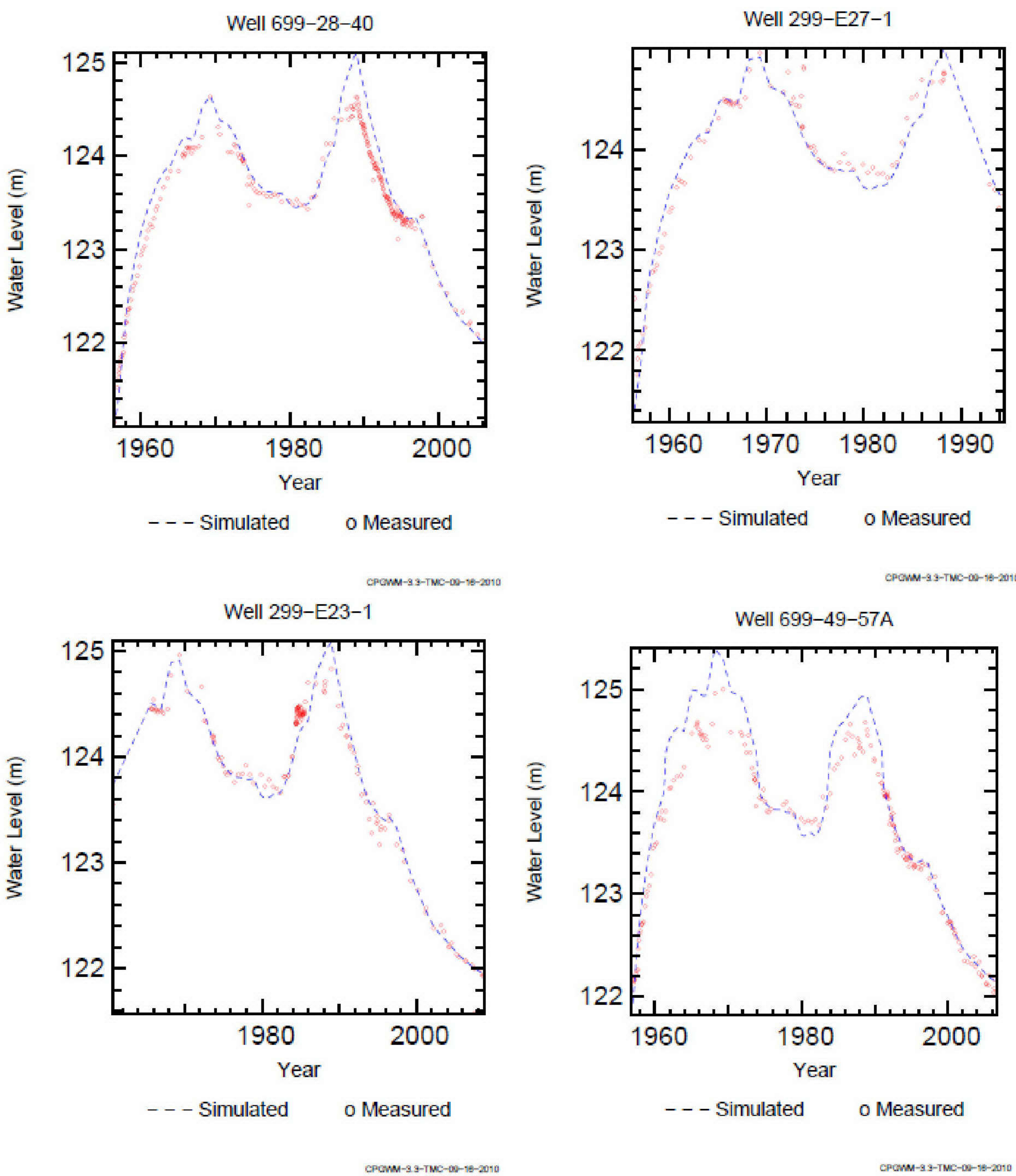

Figure 4-40 (Cont'd). Selected Measured and Simulated Hydrographs Version 3.3 Calibration

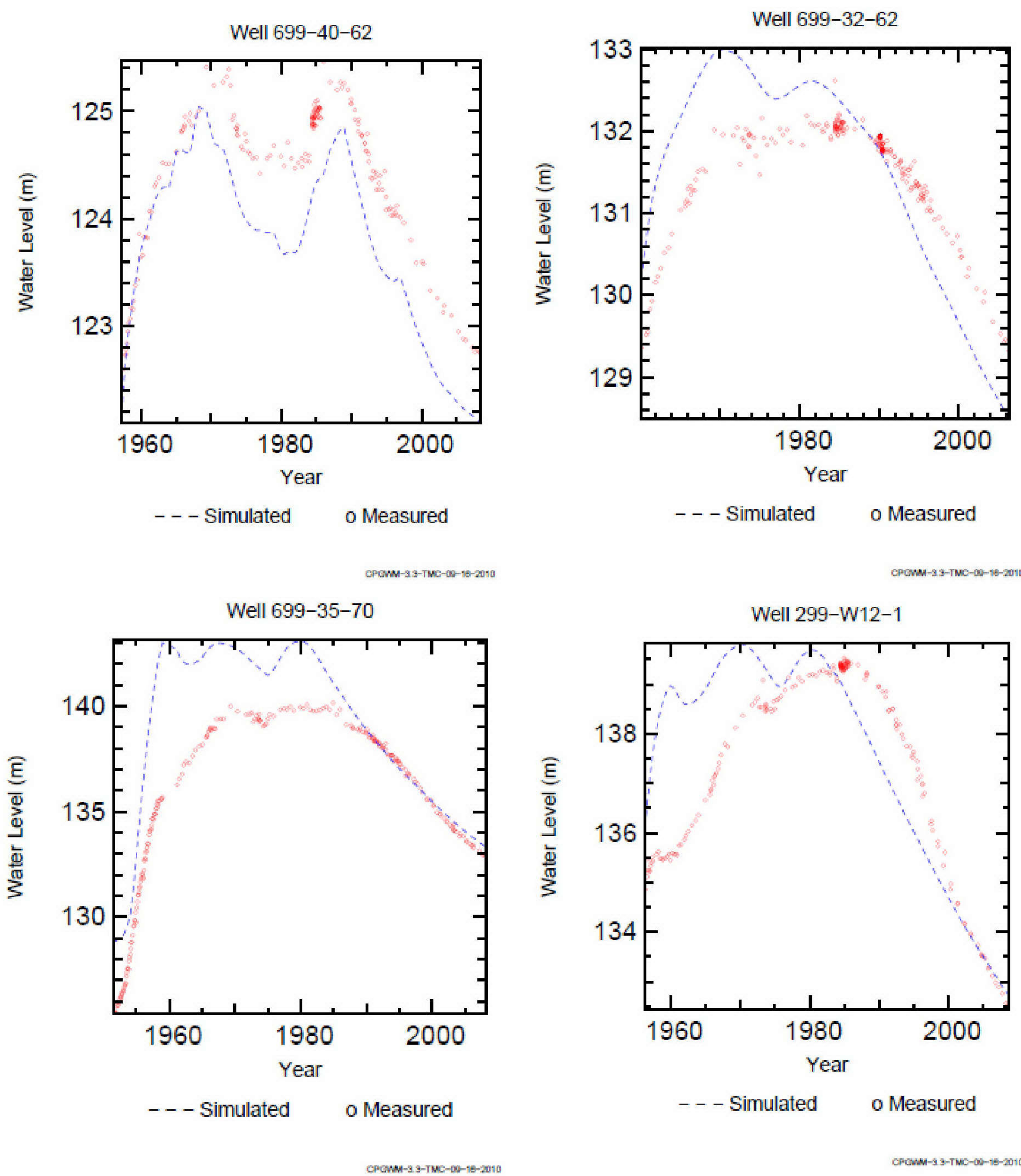

Figure 4-40 (Cont'd). Selected Measured and Simulated Hydrographs Version 3.3 Calibration

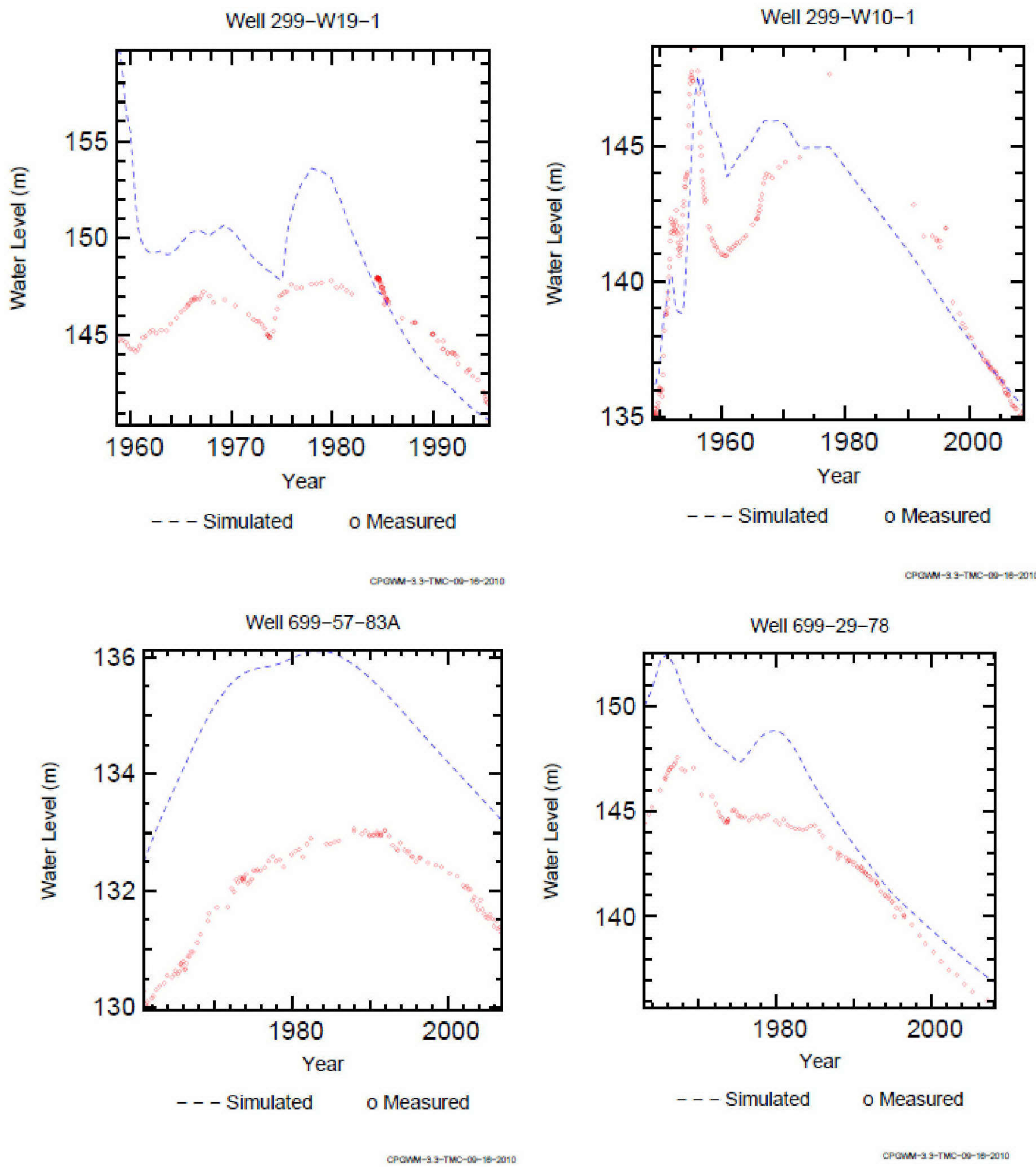

Figure 4-40 (Cont'd). Selected Measured and Simulated Hydrographs Version 3.3 Calibration

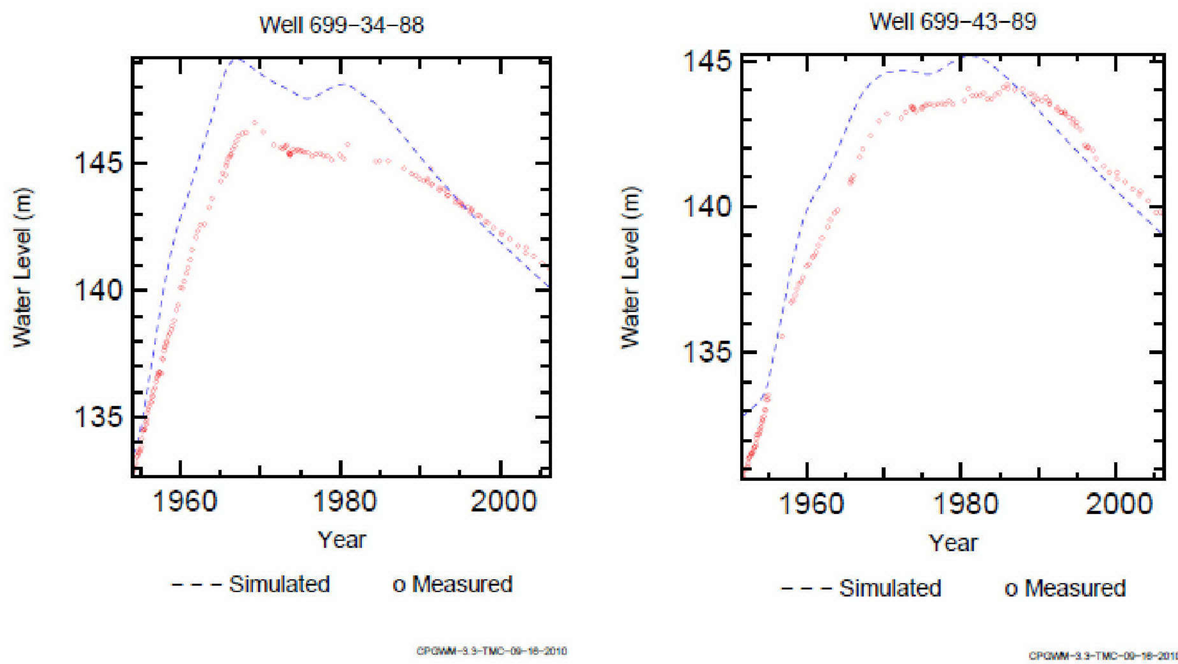

Figure 4-40 (Cont'd). Selected Measured and Simulated Hydrographs Version 3.3 Calibration

Table 4-9 presents a synopsis of the calibrated input parameters used in the CPGW Model Version 3.3. Figure 4-29 identifies the well locations. Hydrographs are presented east-to-west. In general, the fits in the 200 East Area are very good. Nearer to the southeast boundary, the fit is very good until the water level declines of the late 1990s and beyond. Fits just west of the Hanford channels can be quite poor (well 699-40-62 and well 699-32-62). More refinement of the extent of the HSU may improve the model here. It is believed that the delay and lateral transport of fluid due to perching is an important factor contribution to poor matches near the 200 West Area. The fact that the CPGW Model, which simulates saturated groundwater flow, does not represent this feature of the recharge process can be considered a source of structural weakness in the mode; however, the significance of this structural weakness is not altogether clear since it depends on the intended use of the model. Regardless, as described earlier in the discussion of observation weights for model calibration, it would be an error to force the model to reproduce the hydrographs here accurately without introducing a perching sub model. The fits in the northwest portion of the model domain are amenable to improvement with further effort.

Table 4-9. Central Plateau Groundwater Model Calibration Results

Parameter	Units	CPGW Model Version		
		2.0	3.0	3.3*
Coarse Grained Hanford Hydraulic Conductivity	m/day (horizontal)	8,500	10,000	17,000
	m/day (vertical)	850	1,000	1,200
Fine Grained Hanford Hydraulic Conductivity	m/day (horizontal)	NA	100.0	40
	m/day (vertical)	NA	10.0	5

Table 4-9. Central Plateau Groundwater Model Calibration Results

Parameter	Units	CPGW Model Version		
		2.0	3.0	3.3*
Cold Creek Hydraulic Conductivity	m/day (horizontal)	100	106	400
	m/day (vertical)	10	10.6	20
Ringold E Hydraulic Conductivity	m/day (horizontal)	5	5	5
	m/day (vertical)	0.5	0.5	0.5
Ringold A Hydraulic Conductivity	m/day (horizontal)	3.5	4.8	4.8
	m/day (vertical)	0.35	0.48	0.48
Ringold Mud Hydraulic Conductivity	m/day (horizontal)	0.3	0.008	0.008
	m/day (vertical)	0.03	0.0008	0.0008
Hanford and Cold Creek Specific Yield - SY1	m/m	0.15	0.1	0.2
Ringold E, mud and Ringold A - SY2	m/m	0.18	0.0905	0.0905
Hanford and Cold Creek Specific Storage -SS1	1/m	0.00001	0.00001	0.00001
Ringold E, mud and Ringold A - SS2	1/m	0.00001	0.00001	0.00001
Cold Creek Flow	m^3/day	5,722	2,500	2,500
Dry Creek Flow	m^3/day	1,231	700	700
East GHB Hanford Multiplier	Unitless	0.1	0.25	0.25
East GHB Cold Creek Multiplier	Unitless	0.1	0.06	0.06
East GHB Ringold E and A Multiplier	Unitless	0.1	0.06	0.06
South GHB Hanford formation Multiplier	Unitless	0.1	0.25	0.3
South GHB Cold Creek unit Multiplier	Unitless	0.1	0.06	0.3
South GHB Ringold E and A units Multiplier	Unitless	0.1	0.05	0.3
South GHB Scale Factor	Unitless	0.3	0.1	1
East GHB North Factor	Unitless	1	0.035	0.03
East GHB Central Factor	Unitless	NA	0.28	0.2
East GHB South Factor	Unitless	0.5	0.38	0.14
Division between North East and Central East	Unitless	Row 90	Row 90	Row 90
Division between Central East and South East	Unitless	NA	Row 120	Row 110

NA = not applicable

* Version 3.4 retains the calibration developed for Version 3.3, with minor refinements to HSU assignments and boundary conditions noted in Sections 4.2.5.2, 4.2.6.1, and 4.4.1.1.

Figure 4-41 compares the water table map for Year 2009 to the simulated heads generated for the model time step close to Year 2009. See DOE/RL-2010-11, *Hanford Site Groundwater Monitoring and Performance Report for 2009*, for details of the water table construction. Simulated contours were calculated using Groundwater Vistas™. Note that DOE/RL-2010-11 is also the source of the water level measurements used for calibration. The simulated results are extracted from Layer 2 in the model (most likely location of the water table). There is a general agreement with the shape of the water table in most of the model. The brown areas in the figure obscure contour lines where the water table resides in the Ringold mud unit. Simulated heads can be high in these areas due to simulated recharge into a very low conductivity unit.

Simulated gradients are compared to those calculated from water table measurements in Figure 4-42. Figure 4-42 presents the gradient comparison for the Version 3.3 calibration (for the gradients areas shown in Figure 4-30). In general, larger gradients are simulated better than smaller gradients, both in terms of magnitude and direction. In the 200 East Area, the gradients are small with considerable noise in the measured values. Gradients dominated by the existence of the Hanford formation are often only matched within a factor of two. Near the high conductivity channel, the simulated gradient is too small by a factor of two or more (Gradients 13 and 14; Figure 4-30). Further north, the gradient tends to be too large by a factor of two (Gradients 1, 12, and 15; Figure 4-30), indicating that the simulation could be improved by subdividing the Hanford coarse-grained HSU into multiple zones.

™ Groundwater Vistas is a trademark of Environmental Simulations Incorporated, Reinholds, Pennsylvania.

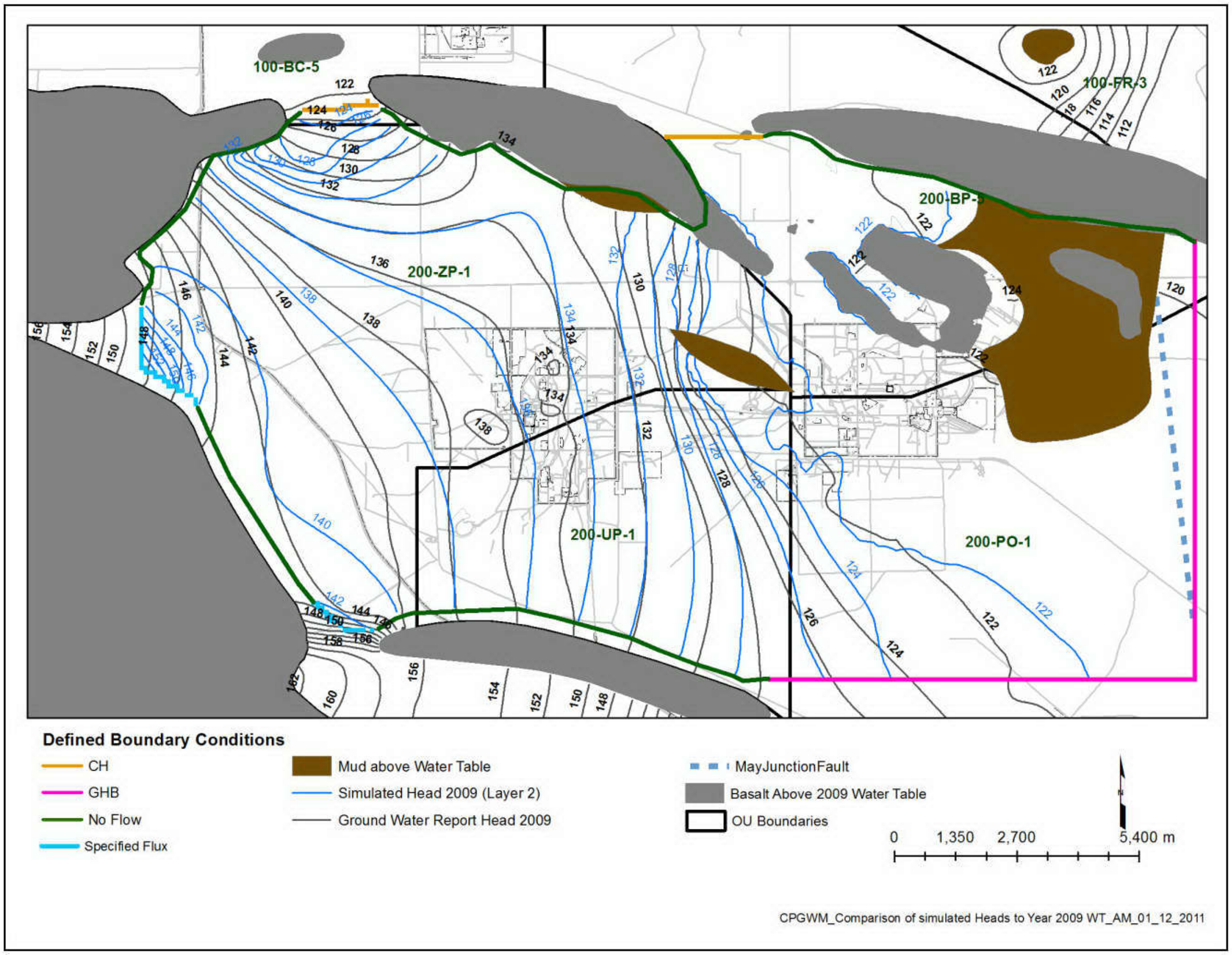

Figure 4-41. Comparison of Version 3.3 Simulated Heads to the Year 2009 Water Table Map

Figure 4-43, Figure 4-44, and Figure 4-45 present calibration statistics for the Version 3.3 calibration. These statistics demonstrate the improvement over previous calibrations. The misfit of water levels as depicted in the probability density plots is more concentrated on small residuals than earlier calibrations: since the peak is nearly centered on zero, this suggests that the mean value of the residuals is close to zero. However, because of the focus on the 200 East Area in recent calibrations, there has been a tendency for development of some high simulated values in the 200 West Area after 2000 creating a positive skew in the distribution of the misfit density functions. This skew should be addressed in the subsequent calibrations by focusing efforts in the 200 West Area.

The mean error was reduced by an order of magnitude from 0.31 to 0.03 m, but the RMS error increased from 0.77 to 0.86 m. In Version 3, roughly 85 percent of the fits were within a meter and 95 percent were within 2 m. The Version 3.3 calibration brought about 86 percent of the fits within a meter and 94 percent within 2 m.

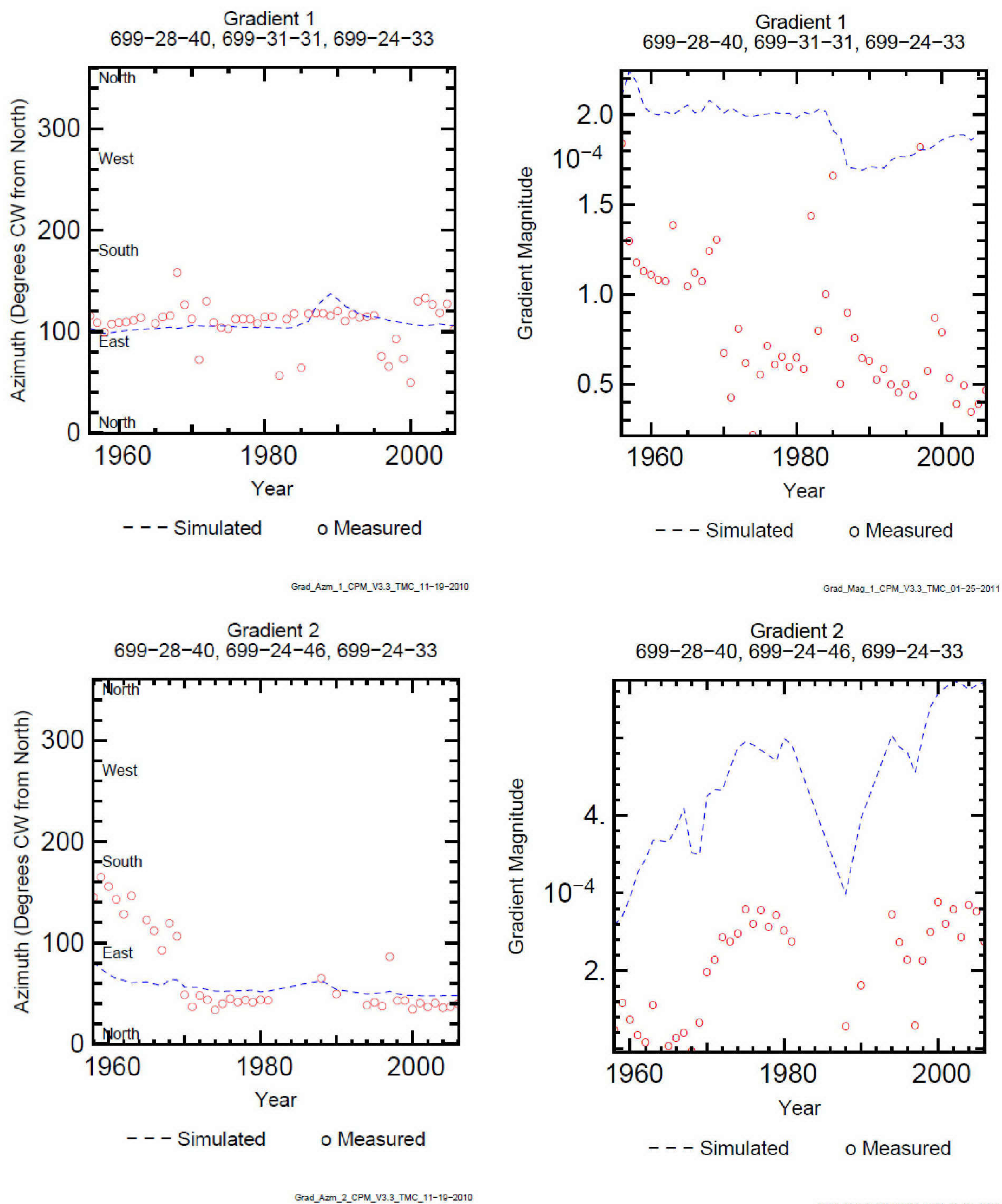

Figure 4-42. Gradient Comparison for Version 3.3 Calibration

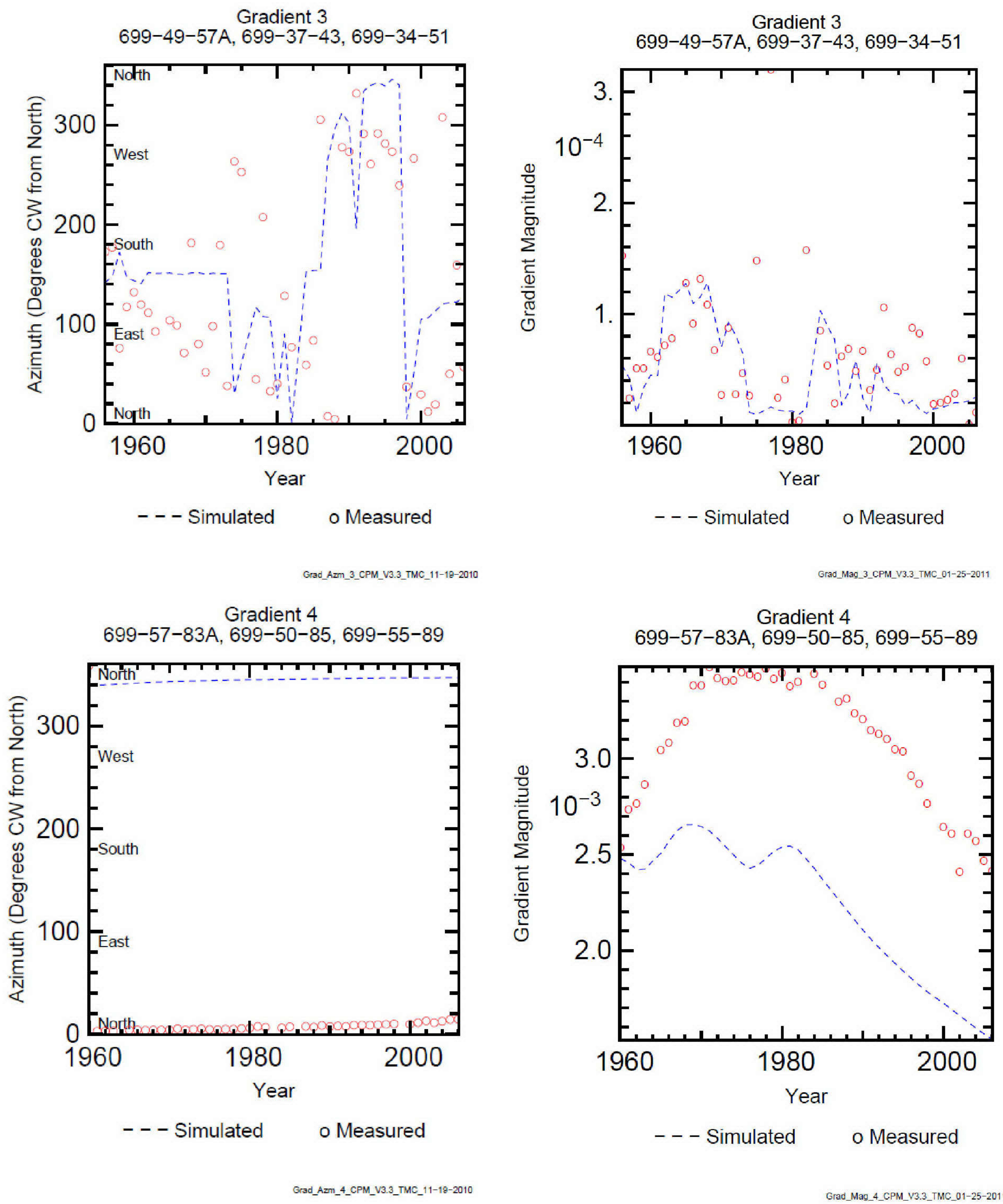

Figure 4-42 (Cont'd). Gradient Comparison for Version 3.3 Calibration

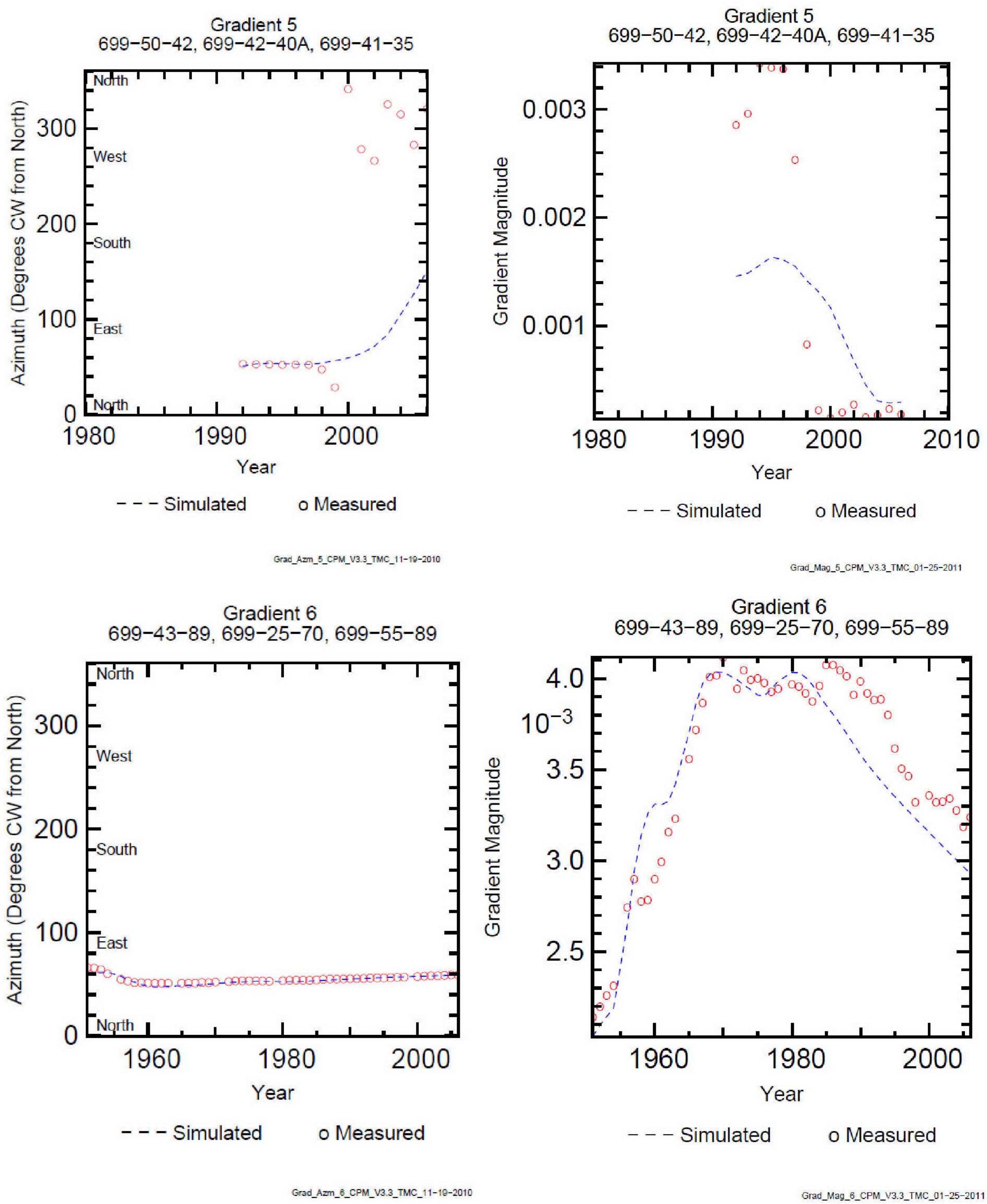

Figure 4-42 (Cont'd). Gradient Comparison for Version 3.3 Calibration

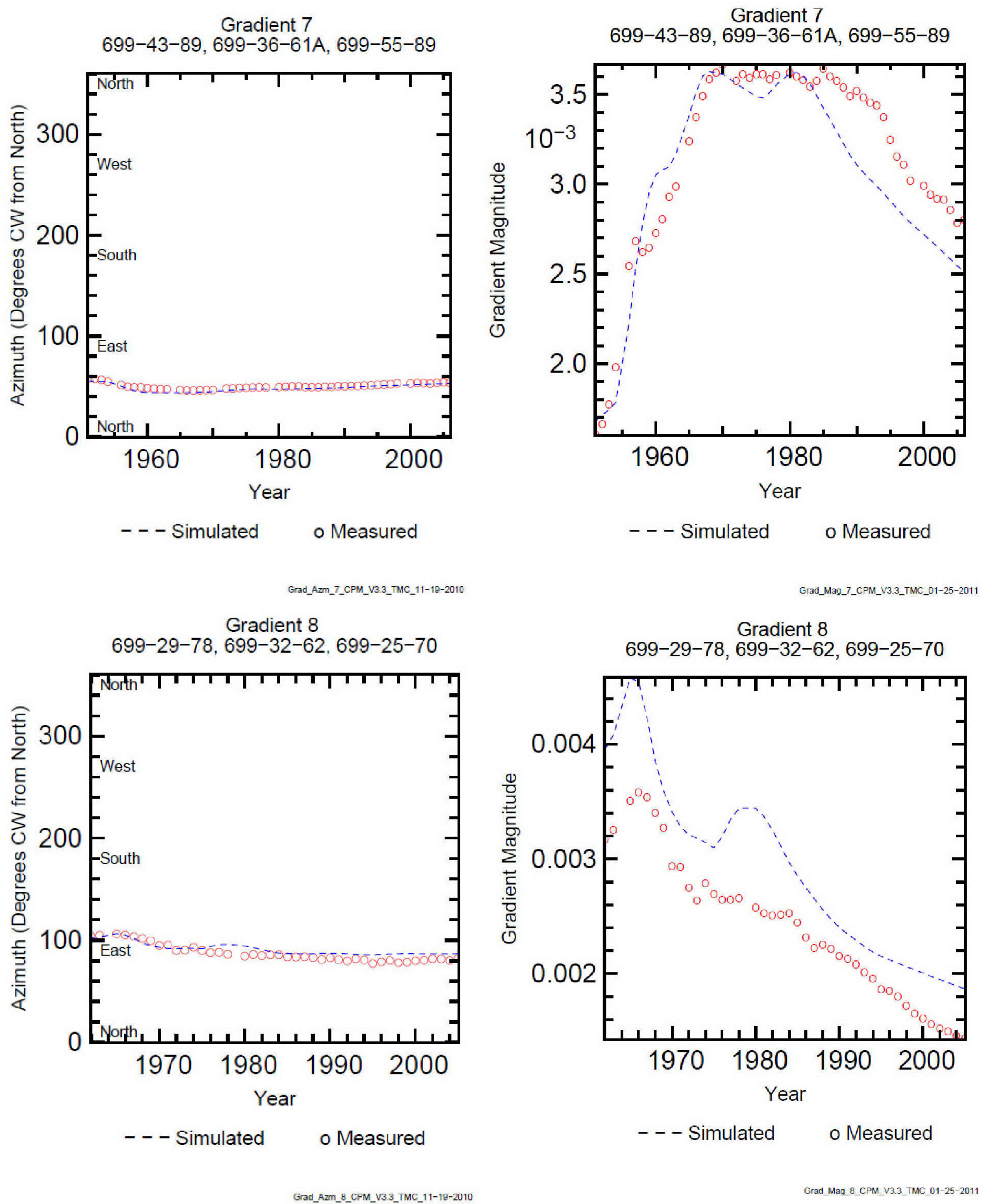

Figure 4-42 (Cont'd). Gradient Comparison for Version 3.3 Calibration

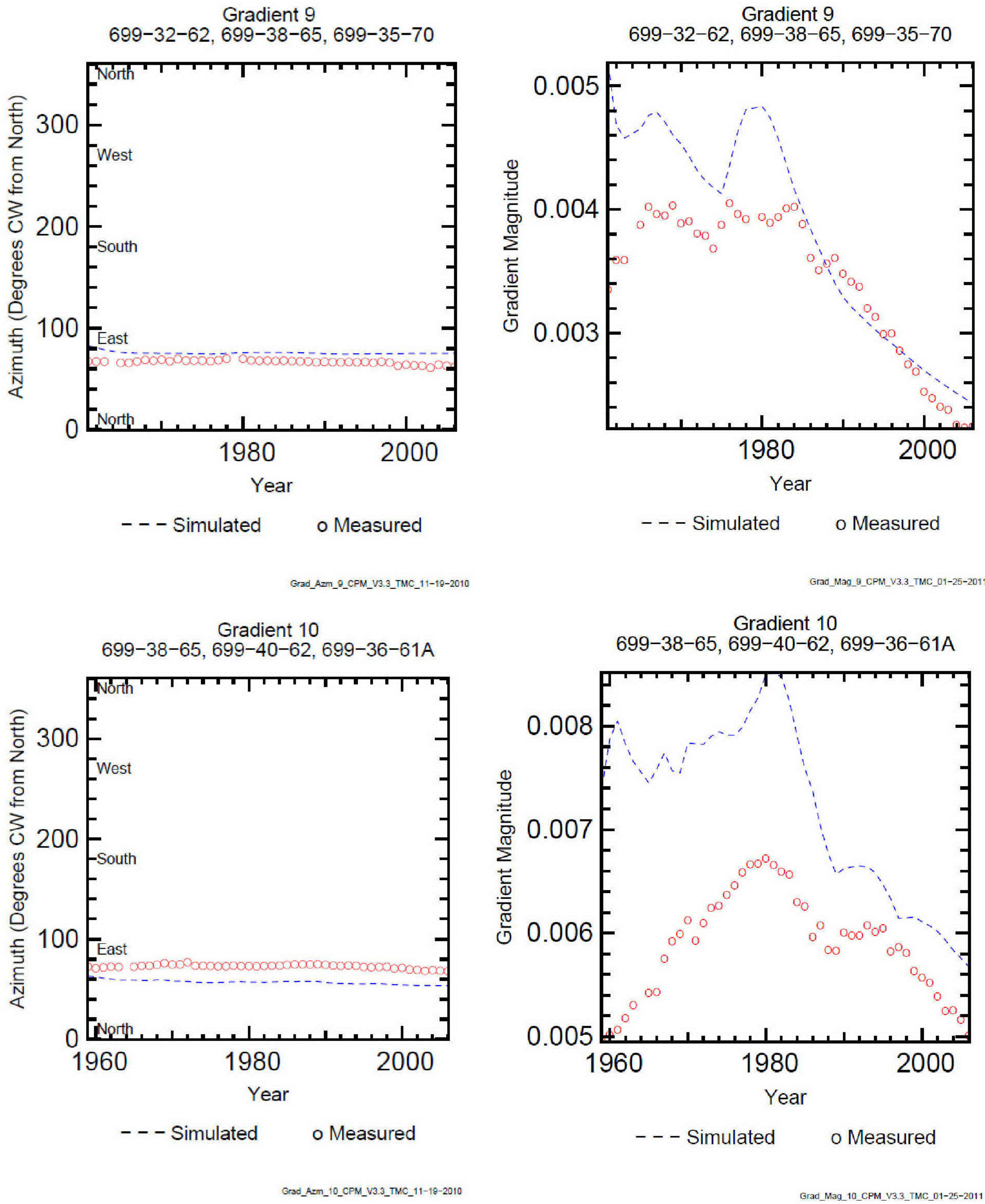

Figure 4-42 (Cont'd). Gradient Comparison for Version 3.3 Calibration

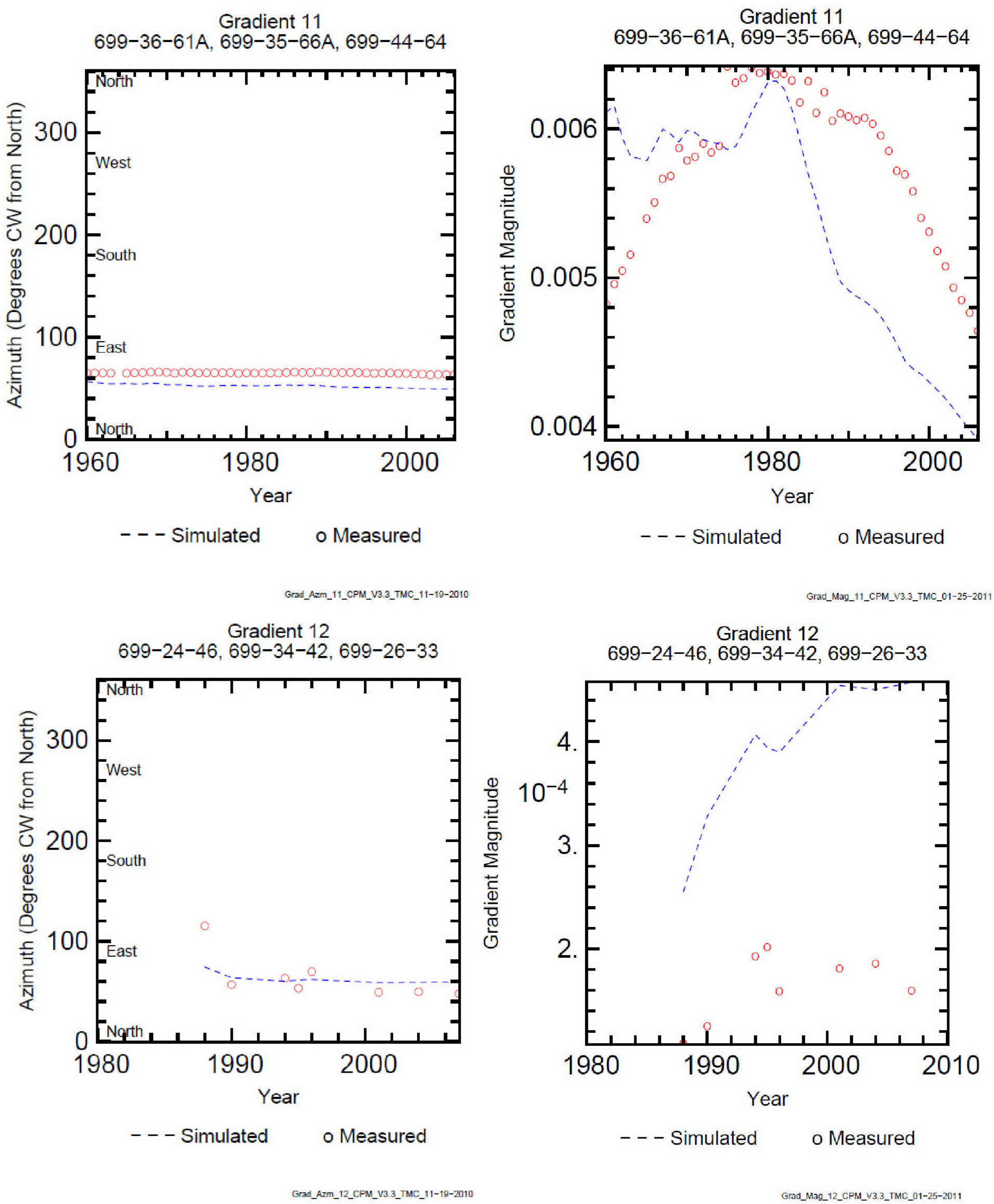

Figure 4-42 (Cont'd). Gradient Comparison for Version 3.3 Calibration

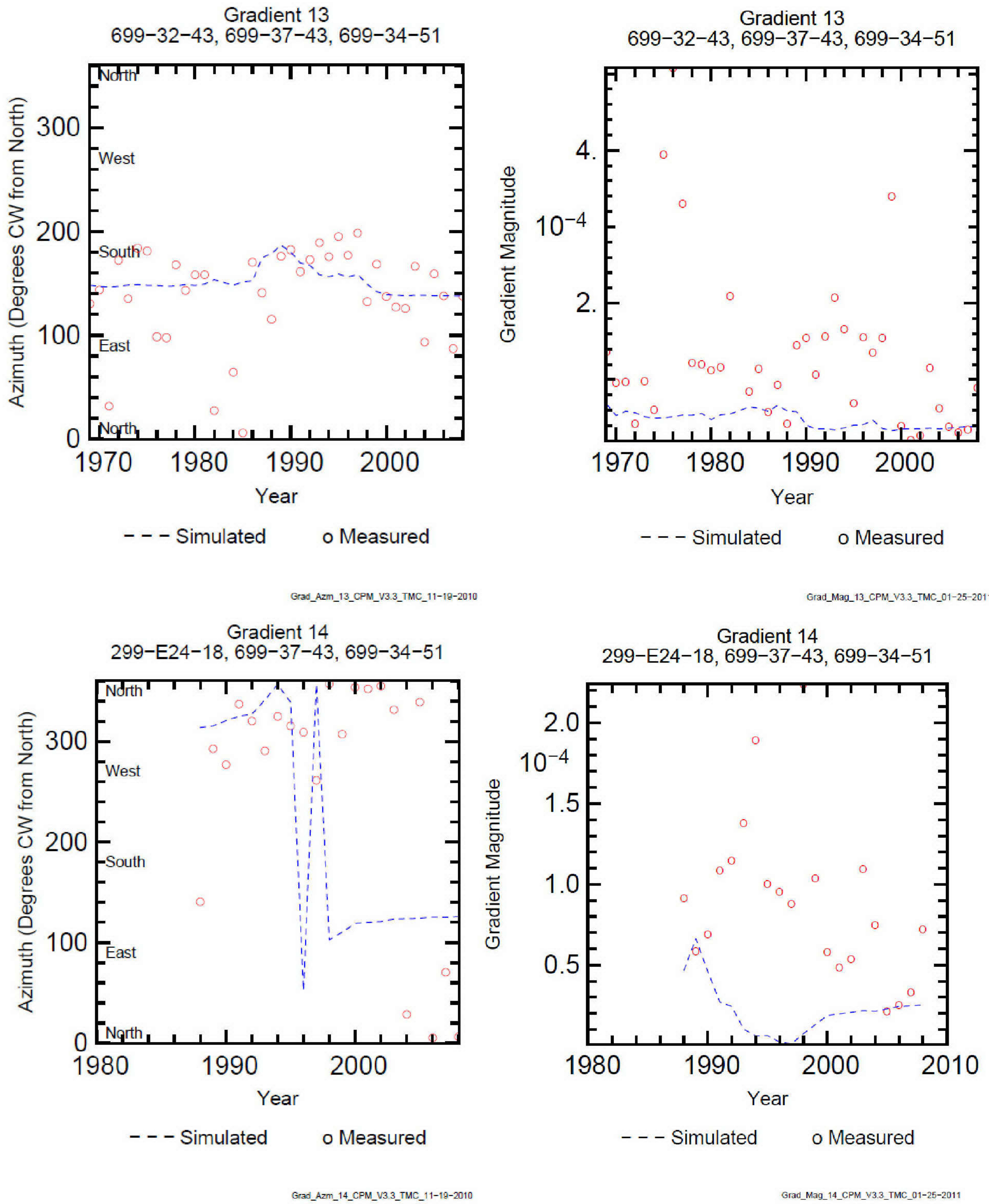

Figure 4-42 (Cont'd). Gradient Comparison for Version 3.3 Calibration

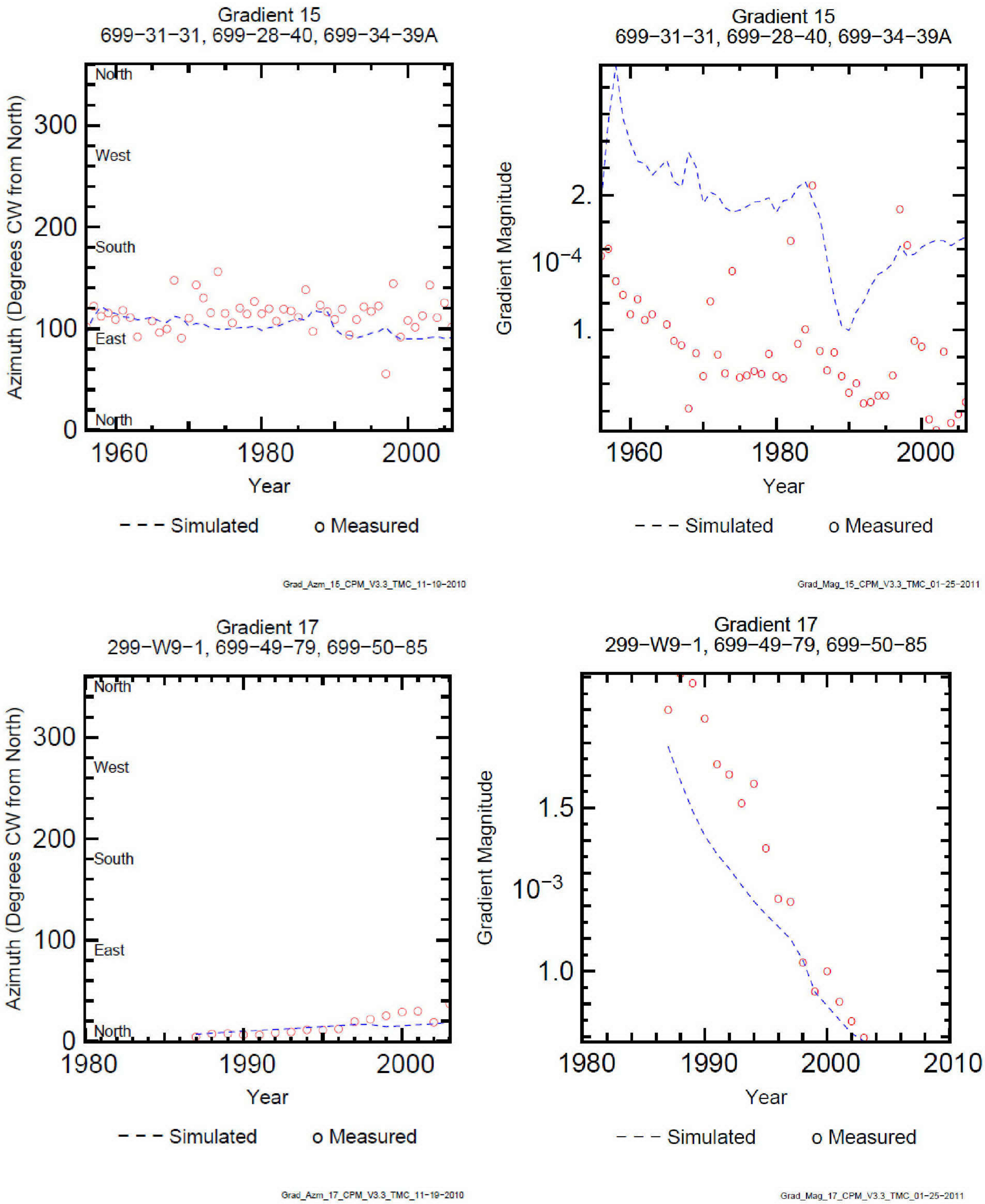

Figure 4-42 (Cont'd). Gradient Comparison for Version 3.3 Calibration

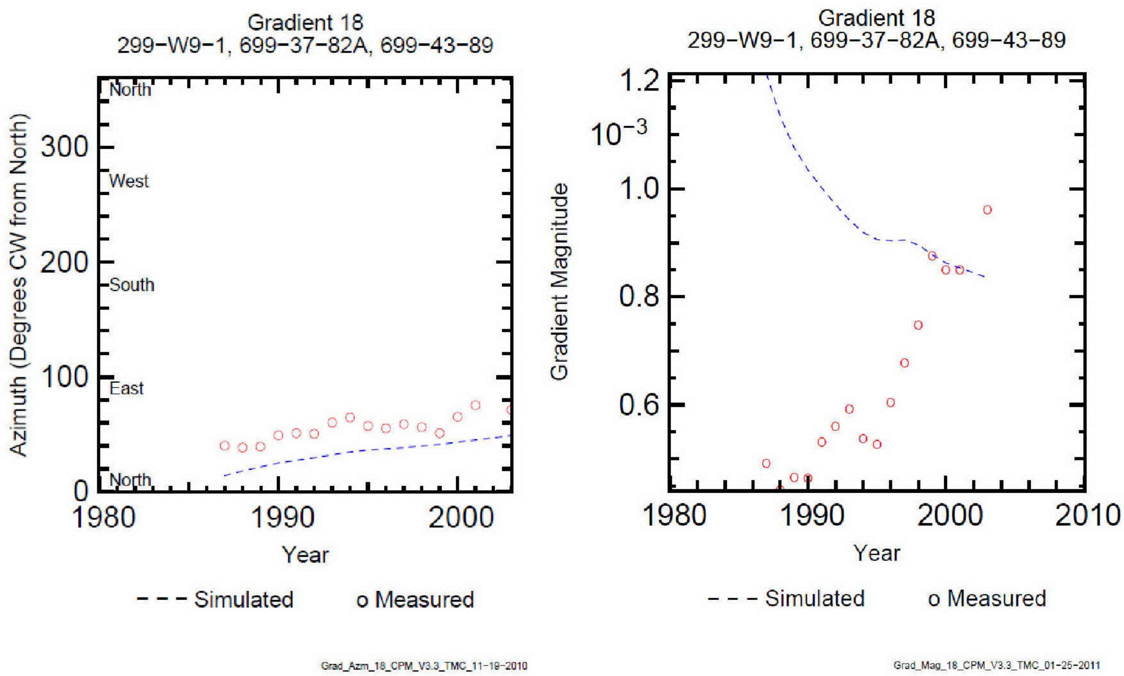

Figure 4-42 (Cont'd). Gradient Comparison for Version 3.3 Calibration

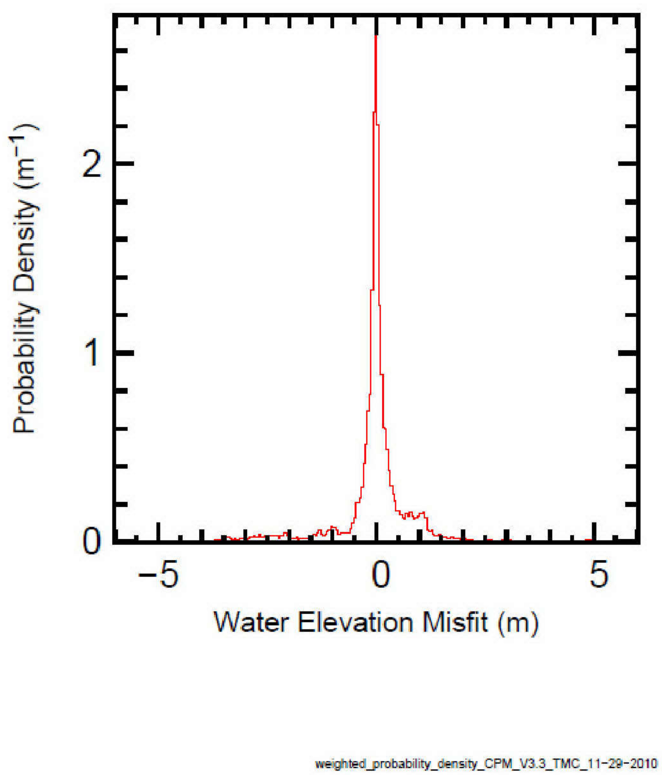

Figure 4-43. Version 3.3 Calibration Misfit Probability Density (1948 to 1953 and 2000 to 2009)

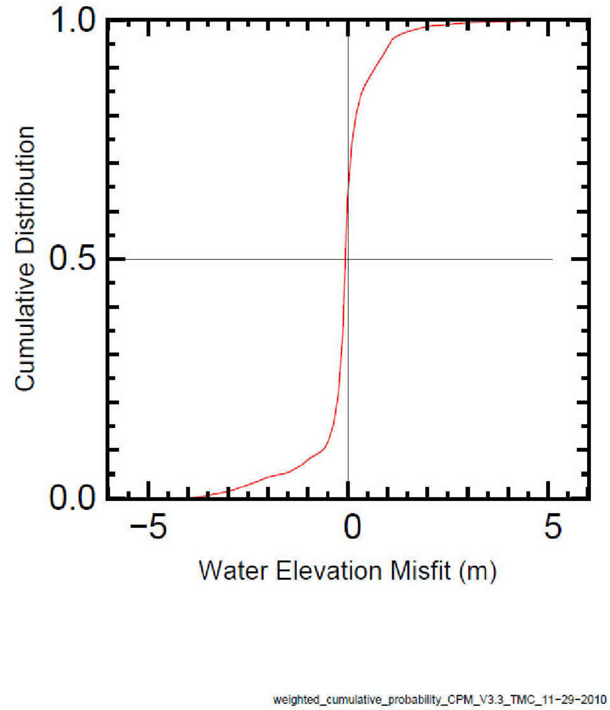

Figure 4-44. Version 3.3 Calibration Misfit Cumulative Probability (1948 to 1953 and 2000 to 2009)

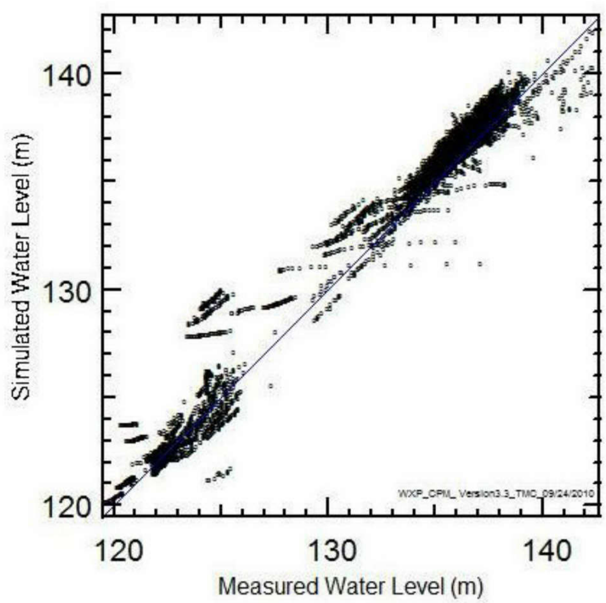

Figure 4-45. Version 3.3 Water Level Cross-Plot (1948 to 1953 and 2000 to 2009)

4.5.5.4 Version 3.4 Calibration (Retains Version 3.3 Calibration)

Version 3.4 was not recalibrated; it retains the calibration developed for Version 3.3 with minor refinements to HSU elevations noted in Section 4.2.5.2, to HSU assignments in model layers 6 and 7 noted in Section 4.2.6.1, and to the generalized head boundary condition for the predictive period as noted in Section 4.4.1.1.

4.5.5.5 Statistical Comparison of Successive Calibrations

Figure 4-46 and **Error! Reference source not found.** along with Table 4-10, present a comparison of calibration statistics for each successive calibration of the CPWG Model. Each set of statistics uses the same measurement data. Only data from 1944 to 1953 and 2000 to 2009 are used to generate the statistics to reduce the influence of perching on the results. These statistics demonstrate the continual improvement of the calibrations. The misfit of water levels is much more peaked in each successive calibration. The side lobes have become much smaller. In the summary statistics presented in Table 4-10, improvement is most evident in the average error that has been reduced by over an order of magnitude.

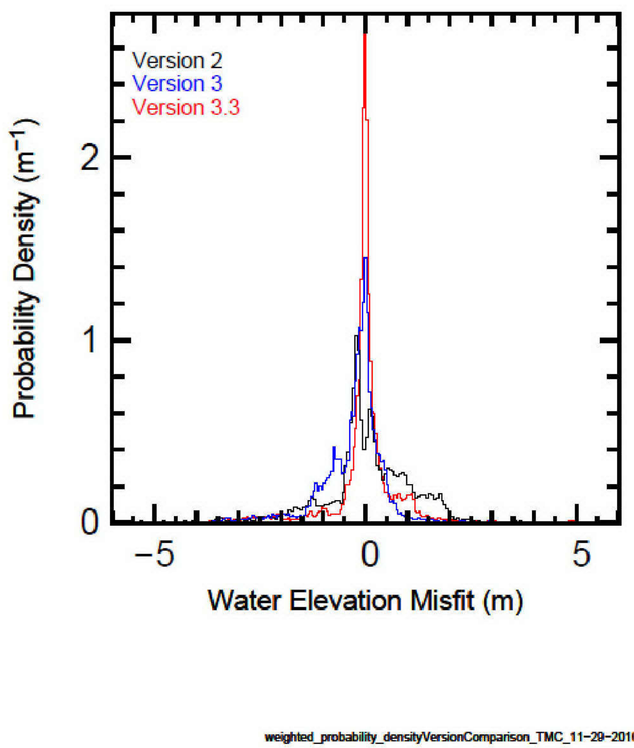

Figure 4-46. Comparison of Calibration Misfit Probability Densities (1948 to 1953 and 2000 to 2009)

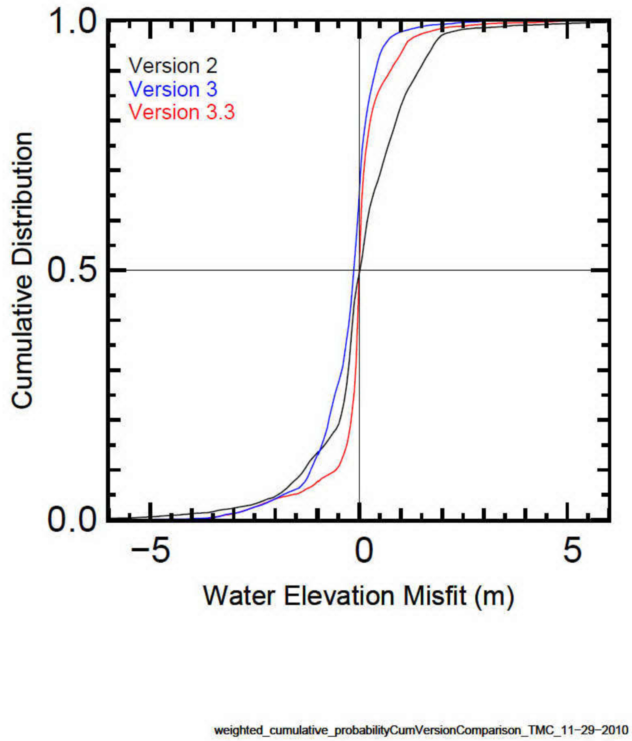

Figure 4-47. Comparison of Calibration Cumulative Distributions (1948 to 1953 and 2000 to 2009)

Table 4-10. Calibration Statistics Comparison

Statistic	Version 2	Version 3	Version 3.3*
Average Error	0.54	0.31	0.03
RMS Error	1.52	0.77	0.86
Maximum Error	7.7	-8.2	-5.9
Average Positive Error	1.53	0.48	0.38
Average Negative Error	-0.56	-0.54	-0.57

* Version 3.4 retains the calibration developed for Version 3.3, with minor refinements to HSU assignments and boundary conditions noted in Sections 4.2.5.2, 4.2.6.1, and 4.4.1.1.

4.5.5.6 Version 6.3.3 extension to 2014

Below are plots of the standard set of calibration well hydrographs from 1990 to December 31 2013. Three wells from the standard set have been replaced since they were not sampled from 2009 to 2014. Well 299-E27-1 replaces Well 299-E33-14, Well 699-35-70 replaces Well 19-4, and Well 299-W19-1 replaces Well 299-W18-30. The hydrographs of Section 4.5.5.3 serve to represent the performance of Version 6.3.3 prior to 1990.

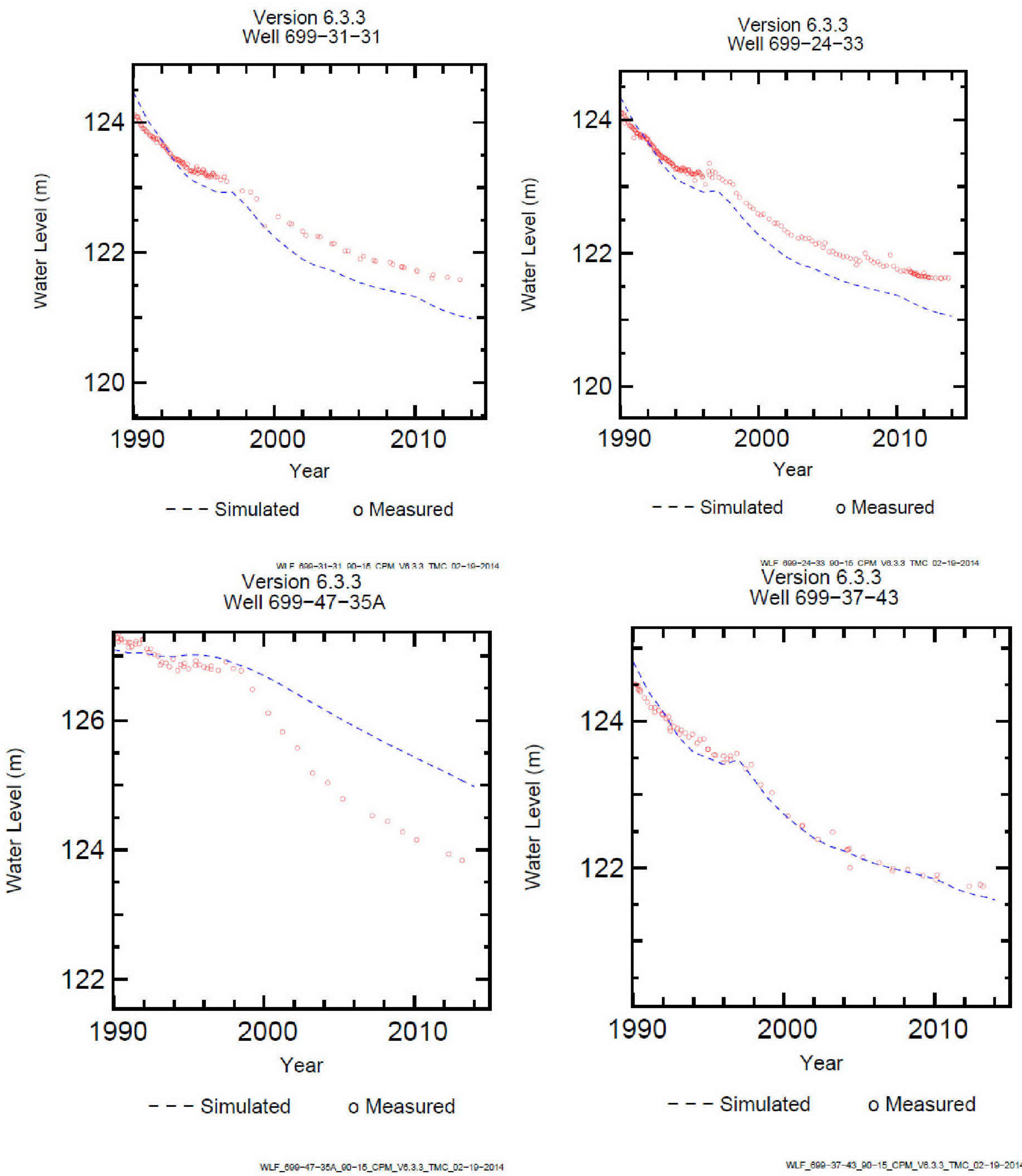

Figure 4-48. Version 6.3.3 Hydrographs (1990-2014)

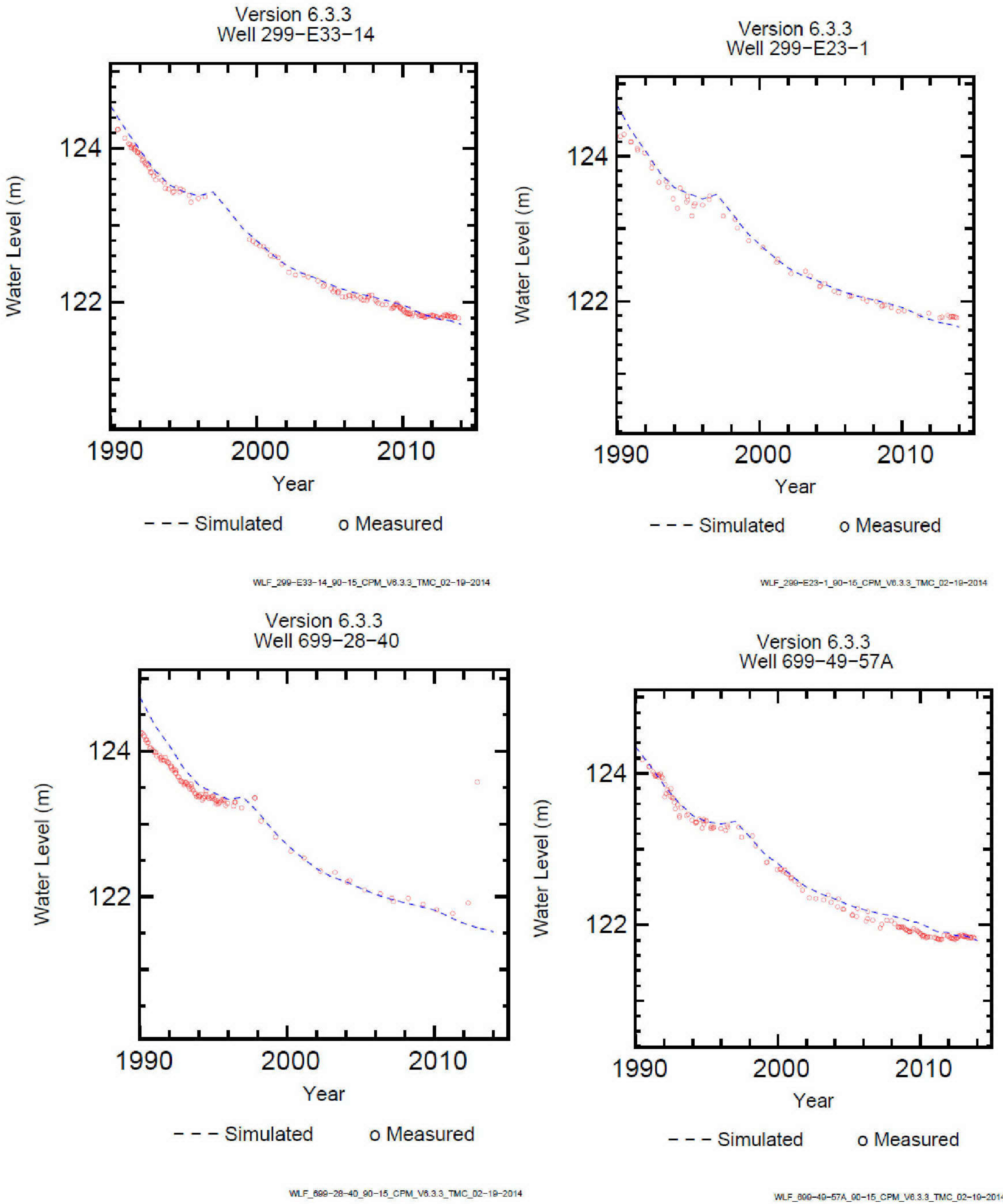

Figure 4-48 (Cont.) Version 6.3.3 Hydrographs (1990-2014)

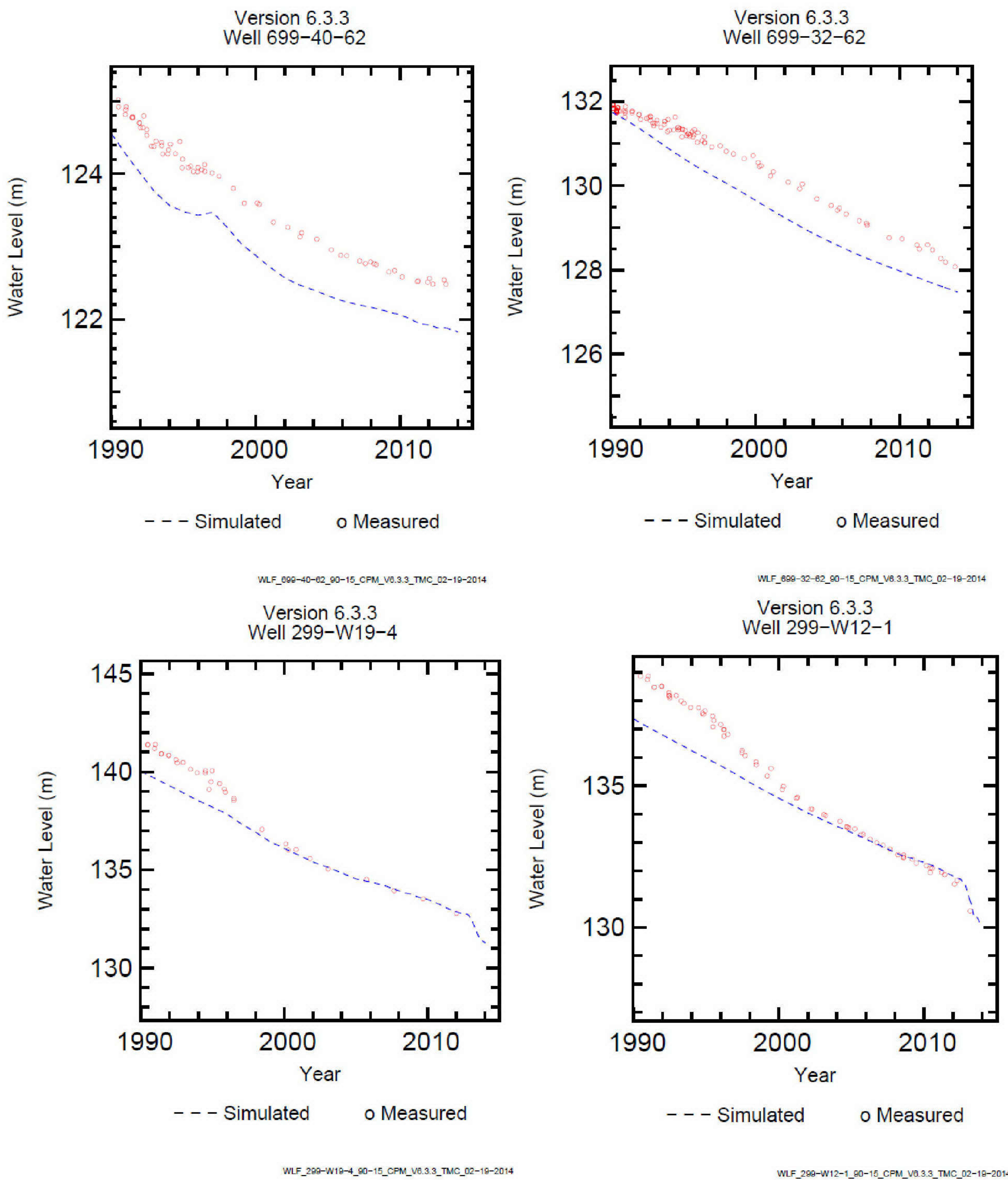

Figure 4-48 (Cont.) Version 6.3.3 Hydrographs (1990-2014)

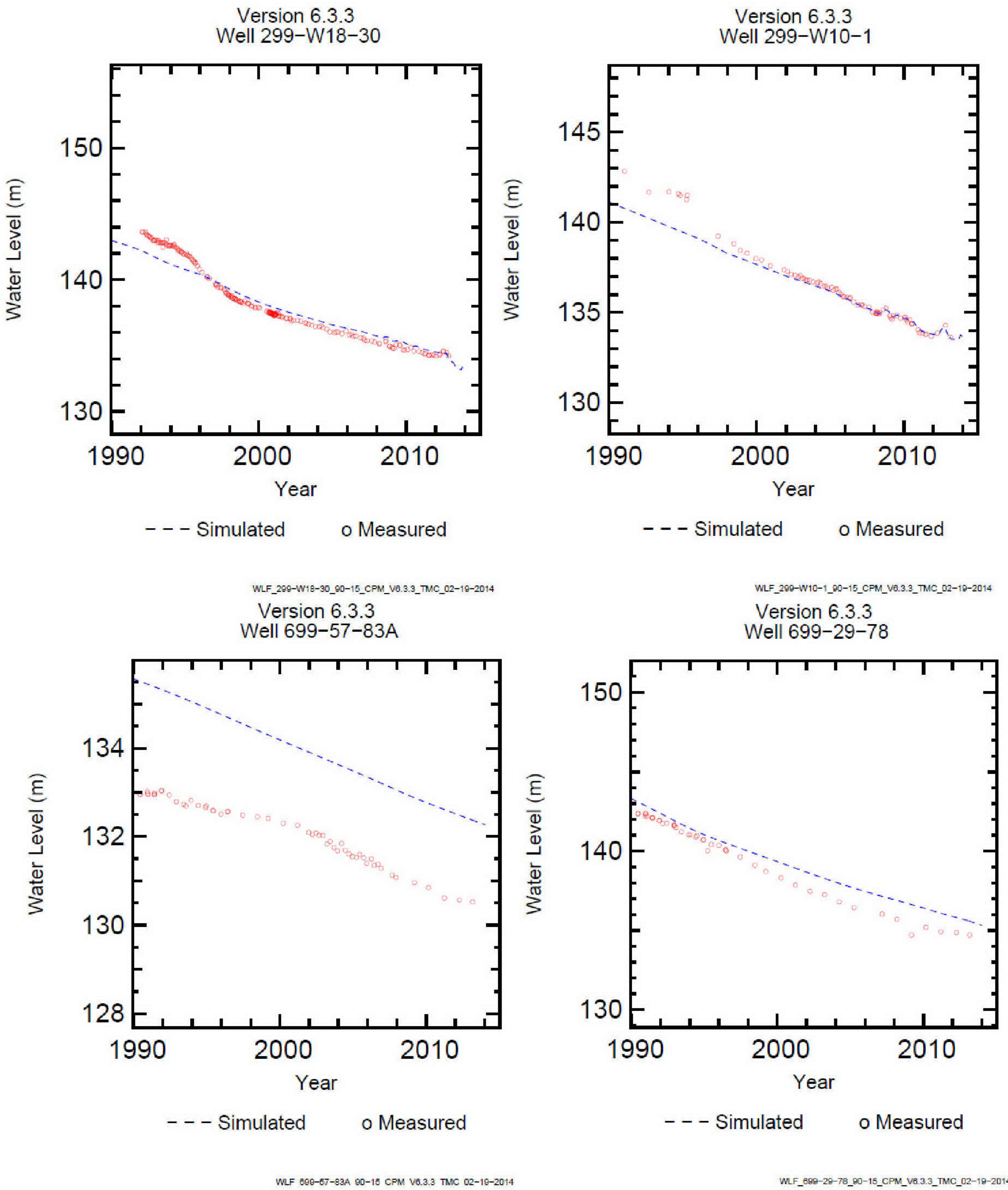

Figure 4-48 **(Cont.) Version 6.3.3 Hydrographs (1990-2014)**

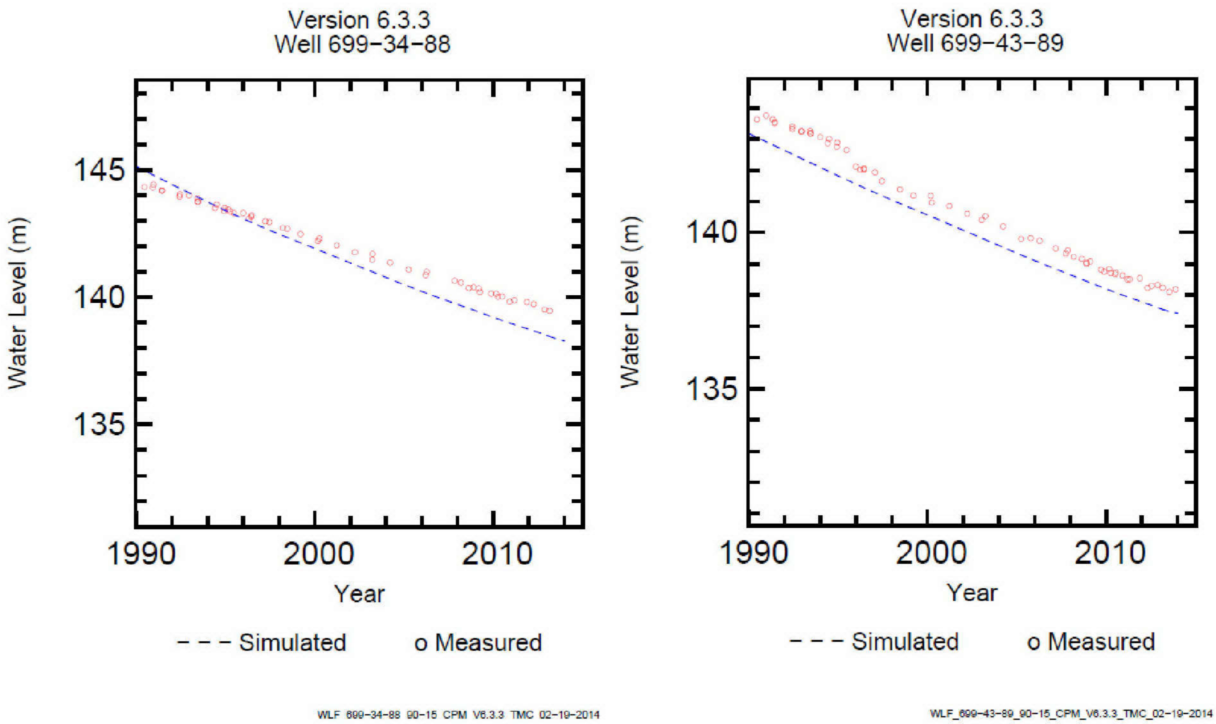

Figure 4-48 **(Cont.) Version 6.3.3 Hydrographs (1990-2014)**

5 Model Sensitivity and Uncertainty Analyses

This chapter provides a discussion on the topics of model sensitivity and uncertainty analyses. Since detailed, quantitative, and formal sensitivity and uncertainty analyses have not been completed using the CPGW Model to date, this chapter focuses on qualitative aspects of sensitivity and uncertainty analyses, and on qualitative findings in this regard to date.

5.1 Introduction

Sensitivity and uncertainty analyses are related aspects of model analysis that seek to identify the elements that have a significant effect on the outputs produced by the model, and how these outputs may vary as a result of changes in these model inputs. To the extent that an output of a model is sensitive to an element of the model about which there is imperfect knowledge (such as a parameter value, or a boundary condition), the outputs of the model are "uncertain" and hence are prone to error. Sensitivity and/or uncertainty analyses can be undertaken in a variety of ways, from qualitative assessment of model outputs throughout the model development process (what you see here), to formal quantitative analyses that propagate lack of knowledge about elements of the model (such as potential error in parameters) to potential error in model outputs.

There is a distinction between intrinsic *variability* and true *uncertainty* when considered within the decision-making context. *Variability* refers to real and potentially identifiable variation. An example would be the property of aquifer heterogeneity, which may have a true distribution (population of values) but for which this true distribution cannot be known. The existence of variability implies that a single model or model output does not encompass the range of possibilities, and may not therefore be optimal under all conditions. Variability that exists below the scale that it is represented in the model becomes an approximation with an error that cannot be fully defined. The impact of unrepresented variability may change when differing model outputs are considered. We use calibration to find a representative approximate value. It does not necessarily follow, however, that parameter input values that provide the best match to historic water levels are the best for approximating transport.

Uncertainty stems from a lack of precise knowledge as to what the truth is, qualitatively or quantitatively. From a modeling standpoint, when making predictions using a model, uncertainty may on some occasions result from the existence of variability below the scale of the model resolution while, on other occasions, it may arise from incomplete information about what the model is representing.

5.2 Sensitivity Analysis

No rigorous, formal sensitivity analysis has been completed for the CPGW Model (although such an effort is planned; see Chapter 8 of this report). However, throughout the development of the model, and progression from the 200-ZP-1 Model through CPGW Model Versions 1, 2, and 3.3, two types of sensitivity analysis have been conducted:

- Qualitative analysis of model outputs as the model has been developed, revised and calibrated
- Quantitative "local" sensitivity calculations that are an intrinsic part of automated model calibration techniques

As a result, while no rigorous formal sensitivity analyses have been completed to date, a great deal has been learned about the sensitivity of model outputs to many elements of the CPGW Model construction and parameterization that has guided the development from the initial construction of the model and provided bases for much of the discussion presented in this report.

5.3 Uncertainty Analysis

No attempt has yet been made to quantify uncertainty in the flow simulations formally beyond limited qualitative assessments undertaken throughout the model development process in a manner similar to the continual qualitative evaluation of sensitivities. As a result, what follows is a qualitative discussion of sources of uncertainty and their implications to predictive transport modeling.

5.3.1 Conceptual Model Uncertainty—Scale of Heterogeneity Represented by HSUs

It is often argued that conceptual model uncertainty is usually the dominant form of uncertainty in a modeling exercise (Konikow, 1986; Konikow and Bredehoft, 1992; National Research Council, 2000; Oreskes and Belitz, 2001; and *A Comprehensive Strategy of Hydrologic Modeling and Uncertainty Analysis for Nuclear Facilities and Sites* [NUREG/CR-6805]). This is likely true for the CPGW Model as well. An important source of conceptual uncertainty is the treatment of a geologically related HSU as a region of constant hydraulic properties, when it is acknowledged that a geologically contemporaneous HSU more likely than not exhibits considerable intrinsic variability in its hydrologic (water transmitting) characteristics. The fluvial environments that lead to deposition of most of the aquifer are associated with heterogeneous structures, especially for the Hanford and Cold Creek units. Local variations in properties can cause local regions of relatively large flow rates and, hence, faster transport of contaminants. These can be significant as evidenced by the experience obtained from calibrating the model. During the calibration of Version 2, the Cold Creek unit near the 200 East Area was found to be more permeable than a representative value would allow. The hydrologic unit definition of this portion of the Cold Creek unit was changed to the Hanford formation to provide a more accurate reflection of the very permeable coarse grain nature of this portion of the Cold Creek unit. This region was identified because it was very important to the flow calibration. Probably other smaller regions had less impact on the hydraulic calibration but still could have a strong but more localized influence on transport.

Fluid flow and hence transport is extremely sensitive to the interpretation of geology in the entire eastern portion of the model. This region is complex geologically and there is not a one-to-one correspondence between geologic formation and proper hydraulic representation. Strict reliance on geologic characterization was found to be incorrect. There may more variation of hydraulic conductivity within the Hanford formation and within the Cold Creek unit than there is between representative values for these HSUs. To create a model that matched historic head data, interpretation of some drilling logs had to be re-examined, and many of the logs that were re-examined could be, and needed to be, interpreted differently than had been done previously. The interpreted distribution of hydrostratigraphy was influenced by historic contaminant plume interpretations that indicate the presence of a large conductive channel from just south of the 200 East Area to the southeast corner of the CPGW Model domain. The hydraulic head data strongly correlate with this interpretation. There are, however, little geologic data from well log interpretation to corroborate this interpretation.

While there is enough evidence to support a highly conductive channel, there is insufficient evidence to define its shape and size accurately. The uncertainty implies that there is insufficient evidence to provide good constraint of the velocity of groundwater flow in the channel. Potentially, examination of historic plume movement could help constrain flow velocities in the channel, but this has not been done. A corollary to the importance and uncertainty of the channel geometry is the impact of the channel on model calibration. Because of the importance of the channel on the water levels throughout the model domain, the inferred hydraulic conductivity for the channel region dominates the calibrated hydraulic conductivity value of the Hanford formation. The calibrated value is applied to the entire Hanford formation. The calibrated value is larger than most, if not all, values estimated from pumping tests. However, it is questionable whether the pump tests could have estimated such a large value

(PNL-10886, p. 2.18). Further, it is suggested in this report that the model could be improved if the Hanford formation HSU were subdivided further.

The location and extent of an HSU is based on interpolation of sparse data. In areas where an HSU may have been eroded, or is pinching out, not knowing the exact extent of the HSU can lead to uncertainty in flow and transport predictions. This could lead to assumption of spatially invariant hydraulic properties of the HSUs.

5.3.2 Flow through the Gable Gap

A question that the CPGW Modeling should help to evaluate is the likelihood and potential magnitude of future groundwater flow and contaminant transport through the Gable Gap. Currently, there is northward flow out of the Central Plateau. Four significant sources of uncertainty influence the flow through the gap. The most dramatic of these is the influence of the elevation of the basalt saddle northwest of the 200 East Area (Section 3.2.5). At some time it is likely, but not certain, that flow across the saddle will stop, effectively closing the area to the north of the CPGW Model domain (comprising the 100 Area OUs) off from flow from the 200 West and 200 East Areas. As the water table near the saddle drops, the saddle will have diminishing transmissivity leading to less flow across the gap. As this occurs, the divide between flow that goes through the gap and flows southeast out the high conductivity channel will shift northward. Uncertainty in the representation of flow through the gap may be a contributor to a poor representation of flow in the northeast corner of the 200 East Area.

The second is the uncertainty of how much flow is entering the model domain from the western streams, from surface infiltration, and through leakage upward from the basalt. Of these, flux from the western streams dominates. The stream values were obtained from calibration of groundwater flow in the CPGW Model, but these are not tightly constrained by the calibration. The third source of uncertainty is non-equilibrium storage in the aquifer. The Central Plateau is presently not in equilibrium with respect to inflow and outflow. The Central Plateau unconfined aquifer still exhibits more outflow than inflow because of the remaining fraction of the tremendous buildup of stored water in the aquifer during the operational period of the Hanford Site. The aquifer is still attenuating this buildup that ended after the termination of production activities at the Hanford Site in 1989. The calibration is such that uncertainty in these two influences do not lead to uncertainty in the current predictions of water levels but may affect flux rates. The uncertainty in future impacts of these factors may influence predictions of both head and flux rates.

The fourth major source of uncertainty that affects fluxes and transport velocities near and through the Gable Gap are the local variations of hydraulic conductivity of the Hanford formation. The basis for this uncertainty has been discussed in the previous subsection. The impact on flow across the gap is that the hydraulic conductivity parameter of the Hanford formation is not influenced strongly by the actual formation hydraulic conductivity in this region and, hence, may not be a good representation.

5.3.3 Parameter Uncertainty

The discussion that follows is based upon qualitative assessments and observations made throughout the development of the CPGW Model. They do not reflect the results of quantitative sensitivity or uncertainty analyses.

Aspects of the conceptualization of HSUs as homogeneous features with effective single valued properties for predictive modeling purposes have been discussed previously. The present discussion focuses on the selection of the effective values. The hydraulic parameters are specific storage, hydraulic conductivity, and specific yield.

- The value of specific storage was set to a conceptually appropriate value that lies within the range of literature values for similar geologic media. Specific storage cannot be usefully constrained by calibration of the model because the impact of specific storage on water level predictions is negligible.
- Hydraulic conductivity and specific yield values were established through calibration.
  - **Hanford coarse-grained unit.** All of the wells in the 200 East Area and as well as wells in the highly conductive channel in the southeastern region of the model, such as well 699-24-33, are very sensitive to the hydraulic conductivity of the coarse-grained unit of the Hanford formation. This well was selected because of the perceived importance of the Hanford units in defining the conductive channel extending from the 200 East Area to the southeast corner of the model. The sensitivity ensured that only a narrow range of effective hydraulic conductivity would result in a good match. However, because the fluid flux going through the channel is uncertain and the size of the channel is uncertain, the representativeness of the effective parameter for the hydraulic conductivity of the Hanford coarse-grained unit is also uncertain.

    Specific yield has been set to an appropriate value that was not well constrained by the calibration.
  - **Hanford fine-grained unit.** Water levels in the northeast corner of the model are sensitive to the Hanford fine-grained unit. However, establishing the effective hydraulic conductivity value of the Hanford fine-grained unit was not a high priority in the calibration.
  - **Cold Creek.** Only gradients 1, 2, and 15 had sensitivity to the Cold Creek hydraulic conductivity that was noticeable in the manual calibration. Therefore, the local characteristics of the southeast corner of the model dominates the Cold Creek hydraulic conductivity estimate. Here, the GHB parameters are also important, increasing the uncertainty in the calibrated value of the Cold Creek hydraulic conductivity.

    Specific yield has been set to an appropriate value that was not well constrained by the calibration.
  - **Ringold E.** The hydraulic conductivity and specific yield of Ringold E HSU along with the Cold Creek and Dry Creek fluxes were found to be correlated during the flow model calibration. We chose to fix Ringold E hydraulic conductivity at 5 m/day because of 2009 pumping test results in the 200-ZP-1 OU. This then constrained the values of the stream fluxes and the specific yield.

    The Ringold E and the Ringold mud hydraulic conductivity are important to transport in the CPGW Model, but the correlation of the Ringold E conductivity with both the specific yield and the stream fluxes leads to a complex relationship that is not fully understood at this point. Potentially, the stream fluxes could be larger than currently represented.
  - **Ringold mud unit.** The Ringold mud has been set to an appropriate value that was not well constrained by the calibration.
  - **Ringold A.** The Ringold A HSU is also not well constrained. A value slightly lower than that used for the Ringold E HSU was adopted based Ringold A being older and of similar composition to Ringold E.

6 Model Limitations

The CPGW Model is limited in intent and purpose to the simulation of saturated flow in the unconsolidated aquifer above the underlying basalts. As a result, the model is suitable for calculating water levels, hydraulic gradients, and groundwater flow directions and rates throughout the Central Plateau. Predictions made with the CPGW Model will be most reliable in those areas that with a high density of water level data that were incorporated in the model calibration, and for those areas where model outputs correspond closely with the measured data. Conversely, model predictions will be less reliable in those areas where fewer water level data are available, as well as in those areas where model predictions do not closely correspond to measured data. Finally, it is expected that the results of groundwater flow simulations completed using the CPGW Model will be used to evaluate the fate and transport of contaminants using advection-only (particle-tracking) and advective-dispersive-reactive transport as embodied in the MT3DMS simulation code. For all of these intended applications of the CPGW Model, the following limitations apply:

- The flow model is regional in nature. Hydraulic property variation is generally recognized at the scale of HSUs (km to 10s of km horizontally). At the scale of the HSUs down to the model grid scale (100 m), the eastern portion of the model is geologically more complex than the western portion of the model. Especially in the eastern portion of the model domain, these limitations of the scale at which variation is represented limits the scale that simulated results should be considered reliable as evidenced by two observations:
  - Model calibrations indicate that there are some regions of kilometer scale, such as the northeast corner of the model domain, where flow is not well represented.
  - Review of flow simulations in the 200 East Area, at less than a kilometer scale, have revealed very poor agreement with interpreted flow directions.
- The model grid represents the aquifer with cells of dimension 100 by 100 m. It is expected that the model is most suitable for making predictions of heads, hydraulic gradients, and groundwater flow rates over areas that comprise many model cells, and that predictions of these quantities on scales smaller than 100 m are not reliable except in circumstances of uniform hydraulic gradients.
- Fluid flow and transport in the vadose zone above the aquifer are not explicitly simulated.
- The application of recharge derived from deep percolation of precipitation at the land surface implicitly represents the effects of vadose zone migration and storage. The rates used represent a best practice combination of empirical data and model simulations of vadose zone migration characteristics at the Hanford Site, to arrive at a fractional rate of meteoric water that constitutes recharge to the unconfined aquifer.
- Attenuation of facility discharges to the ground surface, cribs, trenches, shallow wells, ponds, ditches, and other infiltration areas is indirectly accounted for using STOMP simulations of the discharge sites following the methodology of Nichols et al (2007). The predicted attenuation (delay of recharge arrival and reduction in peak volume) of discharge to the surface at the water table is included as data input for the CPGW Model. This methodology does provide a dramatic improvement compared to ignoring the presence of the considerable vadose zone when incorporating artificial discharges, but it nevertheless has several limitations at present:
  - The vadose zone for each liquid discharge site is simulated as a quasi-two-dimensional cross section model using local hydraulic stratigraphy, scaling the horizontal dimension to

achieve unit gradient conditions in the lowest conductivity layer during the highest artificial discharge period. Further, some calibration was applied for certain sites where more detailed three-dimensional modeling studies were available.

  - This approach achieves rapid simulation times and a generally representative treatment of vadose zone attenuation of liquid discharges, but is not entirely adequate where perching of water on fine-grained layers and subsequent lateral redistribution of moisture in the vadose zone occurs.
  - Perching is believed to have been a significant vadose zone process in the 200 West Area (200-ZP-1 and 200-UP-1 Groundwater OUs) and is suspected to be the reason for the inability of the calibration to date to match measured water levels in these locales.

- It is assumed that the large discharges to the surface that occurred in the historic period will not occur in the future. Therefore, perching is not considered a significant process in predictive simulations of future flow and transport.
- Fluid flow through the basalt bedrock is assumed negligible, and as a result, is not explicitly simulated. If there are sources and/or sinks of water associated with the basalt bedrock, then the model is limited with respect to the exclusion of this FEPs item (Section 3.2.4).
- The calibration used weighting that emphasized early and late hydraulic head data to ensure a better match for those periods considered closest to the conditions of the future predictive simulation period (where the unconfined aquifer is not strongly influenced by high operational liquid discharges). The model is, therefore, limited in its ability to match hydraulic heads during the peak of the historic operational period.
- There remain considerable areas with limited well control in the Central Plateau; consequently, the assignment of HSUs is subject to continued refinement, as more information is made available for such areas.

7 Model Configuration Management

The model described in this model package report is uniquely designated as the CPGW Model Version 6.3.3. . Revision 0 of this model package report describes the Central Plateau Groundwater Model Version 3.3. The full model history is provided in Section 7.1, below.

Version numbering for this model has followed the following convention;

- The first decimal is matched to the build number of the MODFLOW and Related Codes software the model is implemented with; e.g., Version 2 of this model uses Build 0002 of the CHPRC MODFLOW and related codes software.
- The second decimal place denotes sequential revisions of the model grid(The use of grid here refers to both the grid structure and parameter values); thus Version 3.1 designates using Build 0003 of the MODFLOW and related codes software to simulate grid 1.
- The third decimal refers to the boundary conditions used.

Variant versions that do not involve recalibration, such as may occur for special handling of initial conditions, certain sensitivity analyses, and similar special applications are denoted using the fourth decimal place (e.g., 6.3.3.1).Individual simulations (applications) are also configuration controlled following the guidance provided in Appendix G of CHPRC-00189.

As required by Appendix G of CHPRC-00189, all inputs and outputs for the development of the baseline CPGW Model Version 6.3.3 were committed to EMMA to maintain and preserve this configuration-managed model. Basis information (that information collected to form the basis for model input parameterization) is also stored in the EMMA for traceability purposes.

The software used to implement this model, CHPRC Build 6 of MODFLOW-2000, is configuration managed as discussed in Section 4.1. This configuration-managed version was committed to the Hanford Site MKS Integrity™ configuration management system as required by CHPRC-00258.

7.1 Model Version History

The CPGW Model is not a single-time-use tool, but represents the product of ongoing development and continued improvement.

The CPGW Model was developed based on a groundwater model that was constructed supporting decision making at the 200-ZP-1 OU. This was in anticipation of the need for analyses of groundwater flow and contaminant transport in support of 200-ZP-1 post-ROD remedy design, focusing on the RD/RAWP (DOE/RL-2008-56; DOE/RL-2009-38; DOE/RL-2008-78, Draft A). This model was constructed using MODFLOW to simulate flow, and MT3DMS to simulate contaminant transport. For clarity in this report, the model developed for the 200-ZP-1 Groundwater OU analyses was referred to as the 200-ZP-1 Model. The 200-ZP-1 Model was primarily used to develop an extraction/injection well field suitable for containing and recovering contaminants in the 200-ZP-1 OU.

During FY 2009, the general premise (i.e., conceptual basis, computational grid, and discretization) of the 200-ZP-1 Model was adopted as a basis for the CPGW Model. The CPGW Model therefore replaced the 200-ZP-1 Model: all groundwater simulations for the four groundwater OUs encompassed by the CPGW Model are undertaken using the CPGW Model, including any calculations made for the 200-ZP-1 OU.

7.1.1 Version 1.0

Version 1.0 of the CPGW Model is undocumented, since it represented an initial development effort that began as a modification of the 200-ZP-1 Model and commenced with refinements focused in the 200 East Area of the Central Plateau that would ultimately lead to a tool suitable for supporting decisions throughout the Central Plateau. The same lateral extent (model domain) as the 200-ZP-1 Model was retained; however, several other FEPs were refined. This developmental version of the CPGW Model was not used to support any decision basis.

7.1.2 Version 2.0

Version 2.0 of the CPGW Model was originally developed to perform contaminant fate and transport to support the 200-PO-1 Remedial Investigation. The HSU definitions were refined in this version of the model, particularly in the eastern portion of the domain, using newer data. The May Junction Fault feature was incorporated into the model. Boundary conditions were refined in an effort to improve predictive value in the 200-PO-1 portion of the model domain. The transformation of the ZP Model into the CPGW Model Version 2 is described in ECF-200PO1-10-0259, *Central Plateau MODFLOW Model – Version 2 Calculation Brief*. This model was manually calibrated to data from a limited number of wells.

7.1.3 Version 3.0

Version 3.0 of the CPGW Model was created through continued improvements to the model to perform fate and transport calculations to support the 200-UP-1 RI/FS. Improvements included use of a new version of MODFLOW-2000 with the inclusion of the ORTHOMIN solver that reduced calculation time and use of depth-discrete initial contaminant concentrations. The CPGW Model Version 3.0 is described in ECF-Hanford-10-0371, *Central Plateau Version 3 MODFLOW Model*.

7.1.3.1 Version 3.1

Version 3.1 was a development effort that was never used for decision-making and was set aside following adoption of Version 3.3.

7.1.3.2 Version 3.2

Version 3.2 was also a development effort that was not used for decision-making and was set aside following adoption of Version 3.3.

7.1.3.3 Version 3.3

The new basalt surface was especially important because of the critical importance of the elevation of the Gable Gap as a control feature of the unconfined aquifer; accurate vertical location of this subsurface feature and tight tolerance on the predicted hydraulic head in this area is crucial to providing an effective predictive model for the 200-BP-5 Groundwater OU.

Version 3.3 of the CPGW Model is implemented using the same version of MODFLOW-2000-SSPA software but includes additional improvements, as follows:

- New basalt surface interpretation to support predictive runs in the 200-BP-5 Groundwater OU portion of the model domain
- Limited refinement of HSUs in the 200-BP-5 Groundwater OU area
- Inclusion of depth-discrete initial contaminant concentration plumes in the 200-BP-5 Groundwater OU area, and recalibration with this new information

7.1.3.4 Version 3.4

Version 3.4 of the CPGW Model is designated as an incremental maintenance update that incorporated minor refinements to resolve issues encountered while evaluating the model for application to simulation needs for the 200-BP-4 OU RI/FS. These refinements did not introduce significant differences to the model; hence, the calibration developed for Version 3.3 was retained in Version 3.4. The refinements involved the HSU assignments and elevations in a small area north of 200 East Area (Sections 4.2.5.2 and 4.2.6.1) and adjustment to the river conductance term in a portion of the generalized head boundary (Section 4.4.1.1).

7.1.4 Version 6.3.3

Version 6.3.3 of the CPGW Model was is an extension of Version 3.3 for Build 6 of CHPRC MODFLOW. No changes were needed to apply build 6. Part of this extension is an update of the simulation period to 2014, which entailed extending the temporal boundary conditions (Sections 4.4, 4.4.2, and 4.4.3). To accommodate recent pumping in the 200-west region, the simulation time periods were changed from yearly to monthly after 2007 (Section 4.3). The last 3 in 6.3.3 was introduced to refer to this change in boundary conditions.

7.2 Model Application History

Table 7-1 lists application environmental calculation documents for the application of these versions of the CPGW Model. Note that this listing includes only general applications at the scale of the CPGW Model; derivative sub-models (e.g., a study that evaluated the interim remedial action pump-and-treat system at the S-SX Waste Management Area using a telescopic mesh refinement model derived from the CPGW Model) are not listed in Table 7-1.

Table 7-1. Applications of the Central Plateau Groundwater Model

CPGW Model Version	Application
Version 2.0	ECF-200PO1-09-2352 Rev. 0, *Remedial Investigation Report - Near-Field Groundwater Fate & Transport Modeling*
	ECF-200PO1-09-2352 Rev. 1, *Remedial Investigation Report - Near-Field Groundwater Fate & Transport Modeling*
Version 3.0	ECF-200UP1-10-0357 Rev. 0, *Evaluation of Water and Contaminant Mass Capture Performance of Containment Alternatives for the 200-UP-1 Operable Unit*
	ECF-200UP1-10-0373 Rev. 0, *200-UP-1 Remedial Investigation Report; Groundwater Contaminant Fate and Transport Model*
	ECF-200UP1-10-0373 Rev. 1, *200-UP-1 Remedial Investigation Report; Groundwater Contaminant Fate and Transport Model*
	ECF-200UP1-10-0374 Rev. 0, *Development and Evaluation of Remedial Alternatives for Iodine, Uranium, and Nitrate Plumes in the 200-UP-1 Operable Unit Using Central Plateau Groundwater Model Version 3*
Version 3.3	ECF-200UP1-10-0374 Rev. 1, *Development and Evaluation of Remedial Alternatives for Iodine, Uranium, and Nitrate Plumes in the 200-UP-1 Operable Unit Using Central Plateau Groundwater Model Version 3*

Version 3.4	ECF-200UP1-10-0374 Rev. 2, *Development and Evaluation of Pumping Scenarios for Iodine, Uranium, Nitrate, Technetium-99, Tritium, and Chromium Plumes in the 200-UP-1 Operable Unit Using Central Plateau Groundwater Model, Version 3*.
Version 6.3.3	ECF-200UP1-14-0031, *Optimization Of 200-Up-1 Uranium Pump-And-Treat Well Locations With Resultant Contaminant Effluent Concentrations*. ECF-200UP1-14-0032, *Local-Scale Simulation Of Uranium Plume Capture At The 200-Up-1 Uranium Pump-And-Treat Well Locations*.

8 Model Enhancement Recommendations

Recommendations for future development of the CPGWM are under evaluation as part of a larger strategy for Hanford Site model maintenance.

9 References

Bennet, G.B., 1992, "Draft Report – Ground-Water Aspects of the Macroengineering Approach at the Hanford Reservation," (letter to Heather Duncan of A.J. Kerny, Inc.).

BHI-00184, 1995, *Miocene- to Pliocene-Aged Suprabasalt Sediments of the Hanford Site, South-Central Washington*, Rev. 00, Bechtel Hanford, Inc., Richland, Washington.

BHI-00608, 1997, *Hanford Sitewide Groundwater Flow and Transport Model Calibration Report* Rev. 0, Bechtel Hanford, Inc., Richland, Washington. Available at: http://www5.hanford.gov/arpir/?content=findpage&AKey=D197189692.

BHI-01573, 2001, *The Groundwater/Vadose Zone Integration Project: the Application of Features, Events, and Process Methodology at the Hanford Site*, Rev. 0, Bechtel Hanford, Inc., Richland, Washington.

BNWL-243, 1966, *Soil Survey Hanford Project in Benton County Washington*, Battelle Pacific Northwest Laboratory, Richland, Washington. Available at: http://www5.hanford.gov/arpir/?content=findpage&AKey=D196018787.

CHPRC-00189, 2013, *CH2M HILL Plateau Remediation Company Environmental Quality Assurance Program Plan*, Rev. 10, CH2M HILL Plateau Remediation Company, Richland, Washington. (Includes Appendix G, *Quality Assurance Project Plan for Modeling*.)

CHPRC-00257, 2010, *MODFLOW and Related Codes Functional Requirements Document*, Rev. 1, CH2M HILL Plateau Remediation Company, Richland, Washington.

CHPRC-00258, 2010, *MODFLOW and Related Codes Software Management Plan*, Rev. 2, CH2M HILL Plateau Remediation Company, Richland, Washington. Available at: http://pdw.hanford.gov/arpir/index.cfm/viewDoc?accession=0911120137.

CHPRC-00259, 2012, *MODFLOW and Related Codes Software Test Plan*, Rev. 2, CH2M HILL Plateau Remediation Company, Richland, Washington.

CHPRC-00260, 2012, *MODFLOW and Related Codes Requirements Traceability Matrix*, Rev. 5, CH2M HILL Plateau Remediation Company, Richland, Washington.

CHPRC-00261, 2012, *MODFLOW and Related Codes Acceptance Test Report*, Rev. 5, CH2M HILL Plateau Remediation Company, Richland, Washington.

DOE/RL-2002-39, 2002, *Standardized Stratigraphic Nomenclature for Post-Ringold-Formation Sediments Within the Central Pasco Basin*, Rev. 0, U.S. Department of Energy, Richland Operations Office, Richland, Washington.

DOE/RL-2007-28, 2008, *Feasibility Study Report for the 200-ZP-1 Groundwater Operable Unit*, Rev. 0, U.S. Department of Energy, Richland Operations Office, Richland, Washington. Available at: http://www5.hanford.gov/arpir/?content=findpage&AKey=0808050315. http://www5.hanford.gov/arpir/?content=findpage&AKey=00098828.

DOE/RL-2008-01, 2008, *Hanford Site Groundwater Monitoring for Fiscal Year 2007*, Rev. 0, U.S. Department of Energy, Richland Operations Office, Richland, Washington. Available at: http://www5.hanford.gov/arpir/?content=findpage&AKey=00098824.

DOE/RL-2008-56, 2008, *200-West Area Pre-Conceptual Design for Final Extraction/Injection Well Network: Modeling Analyses*, Rev. 0, U.S. Department of Energy, Richland Operations Office, Richland, Washington.

DOE/RL-2008-66, 2009, *Hanford Site Groundwater Monitoring for Fiscal Year 2008*, Rev. 0, U.S. Department of Energy, Richland Operations Office, Richland, Washington. Available at: http://www2.hanford.gov/arpir/?content=findpage&AKey=0905131281. http://www2.hanford.gov/arpir/?content=findpage&AKey=0905131282.

DOE/RL-2008-78, 2009, *200 West Area 200-ZP-1 Pump-and-Treat Remedial Design/Remedial Action Work Plan*, Draft A, U.S. Department of Energy, Richland Operations Office, Richland, Washington. Available at: http://www2.hanford.gov/arpir/?content=findpage&AKey=0904130567.

DOE/RL-2009-38, 2009, *Description of Modeling Analyses in Support of the 200-ZP-1 Remedial Design/ Remedial Action Work Plan*, Rev. 0, U.S. Department of Energy, Richland Operations Office, Richland, Washington. Available at: http://www5.hanford.gov/arpir/?content=findpage&AKey=0095363.

DOE/RL-2010-11, 2010, *Hanford Site Groundwater Monitoring and Performance Report for 2009: Volumes 1 & 2*, Rev. 1, U.S. Department of Energy, Richland Operations Office, Richland, Washington. Available at: http://www5.hanford.gov/arpir/?content=findpage&AKey=0084237.

Doherty, J., 2007, *User's Manual for PEST Version 11*, Watermark Numerical Computing, Brisbane, Australia.

ECF-200BP5-10-00344, 2010, *Geologic Data Package: 200-BP-5 Hydrostratigraphic Database Development*, Rev. 0, CH2M HILL Plateau Remediation Company, Richland, Washington.

ECF-HANFORD-10-0371, 2010, *Central Plateau Version 3 MODFLOW Model*, Rev. 0, CH2M HILL Plateau Remediation Company, Richland, Washington. Available at: http://www5.hanford.gov/arpir/?content=findpage&AKey=0084305.

ECF-200PO1-09-2352, 2010, *200-PO-1 Remedial Investigation Report – Near-Field Groundwater Contaminant Fate and Transport Modeling*, Rev. 0, CH2M HILL Plateau Remediation Company, Richland, Washington. Available at: http://www5.hanford.gov/arpir/?content=findpage&AKey=0084348.

ECF-200PO1-10-0259, 2010, *Central Plateau MODFLOW Model Development*, Rev. 0, CH2M HILL Plateau Remediation Company, Richland, Washington. Available at: http://www5.hanford.gov/arpir/?content=findpage&AKey=0084344.

ECF-200PO1-09-2074, 2010, *200-PO-1 Groundwater Operable Unit Remedial Investigation Report-Geologic Cross Sections*, Rev. 0, CH2M HILL Plateau Remediation Company, Richland, Washington. Available at: http://www5.hanford.gov/arpir/?content=findpage&AKey=0084350.

ECF-200UP1-10-0357, *Evaluation of Water and Contaminant Mass Capture Performance of Containment Alternatives for the 200-UP-1 Operable Units*, Rev. 0, CH2M HILL Plateau Remediation Company, Richland, Washington.

ECF-200UP1-10-0373, 2010, *200-UP-1 Remedial Investigation Report; Groundwater Contaminant Fate and Transport Model*, Rev. 0, CH2M HILL Plateau Remediation Company, Richland, Washington. Available at: http://www5.hanford.gov/arpir/?content=findpage&AKey=0084304.

ECF-200UP1-10-0373, 2012, *200-UP-1 Remedial Investigation Report; Groundwater Contaminant Fate and Transport Model*, Rev. 1, CH2M HILL Plateau Remediation Company, Richland, Washington.

ECF-200UP1-10-0374, 2010, *Development and Evaluation of Remedial Alternatives for Iodine, Uranium, and Nitrate Plumes in the 200-UP-1 Operable Unit Using Central Plateau Groundwater Model Version 3*, Rev. 0, CH2M HILL Plateau Remediation Company, Richland, Washington.

ECF-200UP1-10-0374, 2010, *Development and Evaluation of Remedial Alternatives for Iodine, Uranium, and Nitrate Plumes in the 200-UP-1 Operable Unit Using Central Plateau Groundwater Model Version 3*, Rev. 1, CH2M HILL Plateau Remediation Company, Richland, Washington. Available at: http://www5.hanford.gov/arpir/?content=findpage&AKey=0084253.

ECF-200UP1-10-0374, 2010, *Development and Evaluation of Remedial Alternatives for Iodine, Uranium, and Nitrate Plumes in the 200-UP-1 Operable Unit Using Central Plateau Groundwater Model Version 3*, Rev. 2, CH2M HILL Plateau Remediation Company, Richland, Washington.

Fecht, K.R., S.P. Reidel, and A.M. Tallman, 1987, "Paleodrainage of the Columbia River on the Columbia Plateau of Washington State - A Summary," In *Selected Papers on the Geology of Washington*, Bulletin 77:219-248, Washington Department of Natural Resources, Olympia, Washington.

Gee, G.W., M.J. Fayer, M.L. Rockhold, and M.D. Campbell, 1992, "Variations in Recharge at the Hanford Site," *Northwest Science* 66:237-250. Available at: http://www.vetmed.wsu.edu/org_nws/NWSci%20journal%20articles/1992%20files/Issue%204/v66%20p237%20Gee%20et%20al.PDF.

Golden Software, 2009, *Surfer® Getting Started Guide: Contouring and 3D Surface Mapping for Scientists and Engineers*, Golden Software, Inc., Golden Colorado. Available at: http://www.goldensoftware.com/Surfer9Guide.pdf.

Klein, K.A., 2006, "Hanford Groundwater Modeling Integration," (Memo: RE Contract No. DE-AC06-96RL13200R to G. Gallagher), U.S. Department of Energy, Richland Operations Office, Richland, Washington.

Konikow, L.F., 1986, "Predictive Accuracy of a Ground-Water Model - Lessons from a Postaudit," *Groundwater* 24(2):173-185.

Konikow, L.F and Bredehoeft, J.D., 1992, "Ground-water Models Cannot be Validated," *Advances in Water Resources* 15:75-83.

Last, G.V., V.J. Rohay, F.J. Schelling, A.L. Bunn, M.A. Delamare, R.L. Dirkes, R.D. Hildebrand, J.G. Morse, B.A. Napier, R.G. Riley, L. Soler, and P.D. Thorne, 2004, "A Comprehensive and Systematic Approach to Developing and Documenting Conceptual Models of Contaminant Release and Migration at the Hanford Site," *Journal of Stochastic Environmental Research and Risk Assessment* 18(2):109-116.

Livesay, D.M., 1986, *The Hydrology of the Upper Wanapum Basalt, Upper Cold Creek Valley, Washington*, M.S. Thesis, Department of Geologic Engineerinng, Washington State University, Pullman, Washington.

Mitchell, A., 1999, "The ESRI Guide to GIS Analysis, Volume 1: Geographic Patterns and Relationships," ESRI Press, Redlands, California.

Narbutovskih, S., 2008, (Personal Communication), Fluor Hanford Inc., Richland, Washington.

National Research Council, 2000, *Research Needs in Subsurface Science*, National Academy Press, Washington, D.C.

Nichols, W.E., S.K. Wurstner and P.W. Eslinger, 2007, "Vadose Zone-Attenuated Artificial Recharge for Input to a Ground Water Model," *Ground Water* 45(4): 491-498.

Newcomb, R.C., J.R. Frank, and F.J. Frank, 1972, *Geology and Groundwater Characteristics of the Hanford Formation of the Hanford Reservation of the U. S. Atomic Energy Commission, Washington*, Professional Paper 717, U.S. Geological Survey, Washington, D.C.

NUREG/CR-6805, 2003, *A Comprehensive Strategy of Hydrogeologic Modeling and Uncertainty Analysis for Nuclear Facilities and Sites*, University of Arizona, Tucson, Arizona. Available at: http://www.nrc.gov/reading-rm/doc-collections/nuregs/contract/cr6805/cr6805.pdf.

O'Conner, J.E. and J.E. Costa, 2004, *The World's Largest Floods, Past and Present – Their Causes and Magnitudes*, U.S. Geological Survey, Washington, D.C. Available at: http://pubs.usgs.gov/circ/2004/circ1254/pdf/circ1254.pdf.

Oreskes, N and K. Belitz, 2001, "Philosophical Issues in Model Assessment," In *Model Validation: Perspectives in Hydrological Science*, Anderson and Bates (eds.), p 23-41, John Wily & Sons, Ltd. Available at: http://history.ucsd.edu/_files/faculty/oreskes-naomi/PhilIssuesModelAssessOreskes.pdf.

PNL-6403, 1987, *Recharge at the Hanford Site: Status Report,* Pacific Northwest Laboratory, Richland, Washington. Available at: http://www5.hanford.gov/arpir/?content=findpage&AKey=D196008009.

PNL-7144, 1990, *An Initial Inverse Calibration of the Ground-Water Flow Model for the Hanford Unconfined Aquifer*, Pacific Northwest Laboratory, Richland, Washington. Available at: http://www.osti.gov/energycitations/servlets/purl/6913533-WmNF7M/6913533.pdf.

PNL-10285, 1995, *Estimated Recharge Rates at the Hanford Site*, Pacific Northwest Laboratory, Richland, Washington. Available at: http://www.osti.gov/energycitations/servlets/purl/10122247-XORHkt/webviewable/10122247.pdf.

PNL-10886, 1995, *Development of a Three-Dimensional Ground-Water Model of the Hanford Site Unconfined Aquifer System: FY 1995 Status Report*, Pacific Northwest National Laboratory, Richland, Washington. Available at: http://www.osti.gov/energycitations/servlets/purl/195772-hDCgun/webviewable/195772.pdf.

PNNL, 2009, "Contract 00036402, Release 00051, Task 2, Activity 1: 'Geologic Contact Depths_2009_12_03.xls'," (letter report to CH2M HILL Plateau Remediation Company, from Pacific Northwest National Laboratory) Pacific Northwest National Laboratory, Richland, Washington, December 15.

PNNL-11801, 1997, *Three-Dimensional Analysis of Future Groundwater Flow Conditions and Contaminant Plume Transport in the Hanford Site Unconfined Aquifer System: FY 1996 and 1997 Status Report*, Pacific Northwest National Laboratory, Richland, Washington. Available at: http://www.osti.gov/energycitations/servlets/purl/572724-1bqL0a/webviewable/572724.pdf.

PNNL-12261, 2000, *Revised Hydrogeology for the Suprabasalt Aquifer System, 200-East Area and Vicinity, Hanford Site, Washington*, Pacific Northwest National Laboratory, Richland, Washington. Available at: http://www5.hanford.gov/arpir/?content=findpage&AKey=0906180659.

PNNL-13447, 2001, *Transient Inverse Calibration of Hanford Site-Wide Groundwater Model to Hanford Operational Impact – 1943 to 1996*, Pacific Northwest National Laboratory, Richland, Washington. Available at: http://www.pnl.gov/main/publications/external/technical_reports/PNNL-13447.pdf.

PNNL-13623, 2001, *Transient Inverse Calibration of Site-Wide Groundwater Model to Hanford Operational Impacts from 1943 to 1996—Alternative Conceptual Model Considering Interaction with Uppermost Basalt Confined Aquifer*, Pacific Northwest National Laboratory, Richland, Washington. Available at: http://www.pnl.gov/main/publications/external/technical_reports/pnnl-13623.pdf.

PNNL-13641, 2001, *Uncertainty Analysis Framework – Hanford Site-Wide Groundwater Flow and Transport Model*, Pacific Northwest National Laboratory, Richland, Washington. Available at: http://www.pnl.gov/main/publications/external/technical_reports/pnnl-13641.pdf.

PNNL-13858, 2002, *Revised Hydrogeology for the Suprabasalt Aquifer System, 200-West Area and Vicinity, Hanford Site, Washington*, Pacific Northwest National Laboratory, Richland, Washington. Available at: http://www.pnl.gov/main/publications/external/technical_reports/PNNL-13858.pdf.

PNNL-14058, 2002, *Prototype Database and User's Guide of Saturated Zone Hydraulic Properties for the Hanford Site*, Pacific Northwest National Laboratory, Richland, Washington. Available at: http://www.pnl.gov/main/publications/external/technical_reports/PNNL-14058.pdf.

PNNL-14398, 2003, *Transient Inverse Calibration of the Site-Wide Groundwater Flow Model (ACM-2): FY 2003 Progress Report*, Pacific Northwest National Laboratory, Richland, Washington. Available at: http://www.pnl.gov/main/publications/external/technical_reports/PNNL-14398.pdf.

PNNL-14753, 2006, *Groundwater Data Package for Hanford Assessments*, Rev. 1, Pacific Northwest National Laboratory, Richland, Washington. Available at: http://www.pnl.gov/main/publications/external/technical_reports/PNNL-14753Rev1.pdf.

PNNL-14898, *Results of Groundwater Modeling for Tritium Tracking at the Hanford Site 200 Area State-Approved Land Disposal Site* – 2004, Pacific Northwest Laboratory, Richland, Washington. Available at: http://www.pnl.gov/main/publications/external/technical_reports/PNNL-14898.pdf.

PNNL-15837, 2007, *Data Package for Past and Current Groundwater Flow and Contamination Beneath Single-Shell Tank Waste Management Areas*, Pacific Northwest National Laboratory, Richland, Washington. Available at: http://www5.hanford.gov/arpir/?content=findpage&AKey=0911240061.

PNNL-17841, 2008, *Compendium of Data for the Hanford Site (Fiscal Years 2004 to 2008) Applicable to Estimation of Recharge Rates*, Pacific Northwest National Laboratory, Richland, Washington. Available at: http://www.pnl.gov/main/publications/external/technical_reports/PNNL-17841.pdf.

PNNL-17913, 2009, *Hydrogeology of the Hanford Site Central Plateau – A Status Report for the 200 West Area*, Rev. 1, Pacific Northwest National Laboratory, Richland, Washington. Available at: http://www.pnl.gov/main/publications/external/technical_reports/PNNL-17913rev1.pdf.

PNNL-18732, 2009, *Field Test Report: Preliminary Aquifer Test Characterization Results for Well 299-W15-225: Supporting Phase I of the 200-ZP-1 Groundwater Operable Unit Remedial Design*, Pacific Northwest National Laboratory, Richland, Washington. Availabe at: http://www.pnl.gov/main/publications/external/technical_reports/PNNL-18732.pdf.

PNNL-19702, 2010, *Hydrogeologic Model for the Gable Gap Area, Hanford Site*, Pacific Northwest National Laboratory, Richland, Washington. Available at: www.pnl.gov/main/publications/external/technical_reports/PNNL-19702.pdf.

RHO-ST-42, 1981, *Hydrology of the Separations Area*, Rockwell Hanford Operations, Richland, Washington. Available at: http://www5.hanford.gov/arpir/?content=findpage&AKey=D195065240.

Rumbaugh, J.O. and D.B. Rumbaugh, 2007, *Guide to Using Groundwater Vistas*, Version 5, Environmental Simulations, Inc. Available at: http://www.groundwatermodels.com/Groundwater_Vistas.php.

SGW-39675, 2009, *Reflection Seismic Survey Report, 200 East Area, Hanford Site*, Rev. 0, CH2M HILL Plateau Remediation Company, Richland, Washington. Available at: http://www5.hanford.gov/arpir/?content=findpage&AKey=0084392.

SGW-42604, 2009, *Results of Tritium Tracking and Groundwater Monitoring at the Hanford Site 200 Area State-Approved Land Disposal Site Fiscal Year 2009*, Rev. 0, CH2M HILL Plateau Remediation Company, Richland, Washington.

USGS Open File Report 00-92, 2000, *MODFLOW-2000, the U.S. Geological Survey Modular Ground-water Model -- User Guide to Modularization Concepts and the Ground-Water Flow Process*, U.S. Geological Survey, Denver, Colorado. Available at: http://water.usgs.gov/nrp/gwsoftware/modflow2000/ofr00-92.pdf.

USGS-W-P-7, Interim Report 1, 1949, *Geologic and Hydrologic Features of the Richland Area, Washington, Relevant to Disposal of Waste at the Hanford Operations Office of the Atomic Energy Commission*, U.S. Geological Survey, Portland, Oregon.

Webber, W., 2009, (Personal Communication), CH2M HILL Plateau Remediation Company, Richland, Washington.

WHC-EP-0698, 1994, *Groundwater Impact Assessment Report for the 216-U-14 Ditch*, Rev. 0, Westinghouse Hanford Company, Richland, Washington. Available at: http://www5.hanford.gov/arpir/?content=findpage&AKey=D196093455.

WHC-SA-0699-FP, 1990, *Effects of Varying Recharge on Radionuclide Flux Rates to the Water Table at the Low-Level Solid Waste Burial Site*, Washington Hanford Company, Richland, Washington. Available at: http://www5.hanford.gov/arpir/?content=findpage&AKey=D196000242.

Appendix A

Comparison of Simulated Water Levels Using the Central Plateau Groundwater Model Version 3.3 to Measured Water Levels

This appendix presents a comparison of all simulated water level with measured data from the Version 3.3 calibration. Plots are provided for each well available for calibration. It includes wells that have been removed from the calibration and measurements that are assigned zero weight. The wells are presented in alphanumeric order at four plots per page.

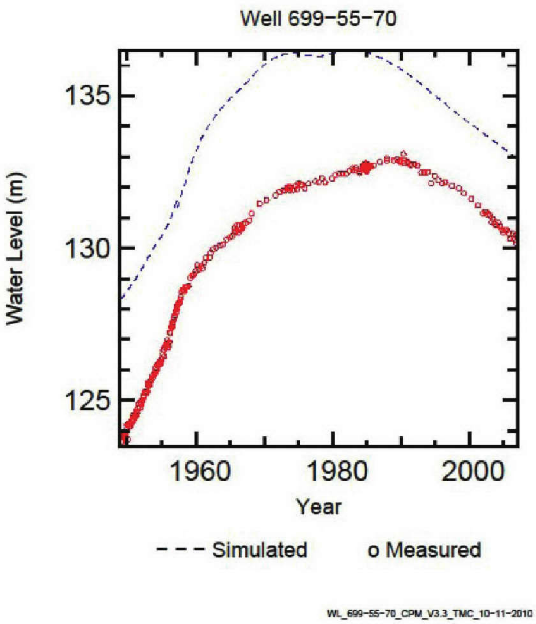
Well 699−55−70
135
130
125
Water Level (m)
1960
1980
2000
Year
− − − Simulated
o Measured
WL_699−55−70_CPM_V3.3_TMC_10−11−2010

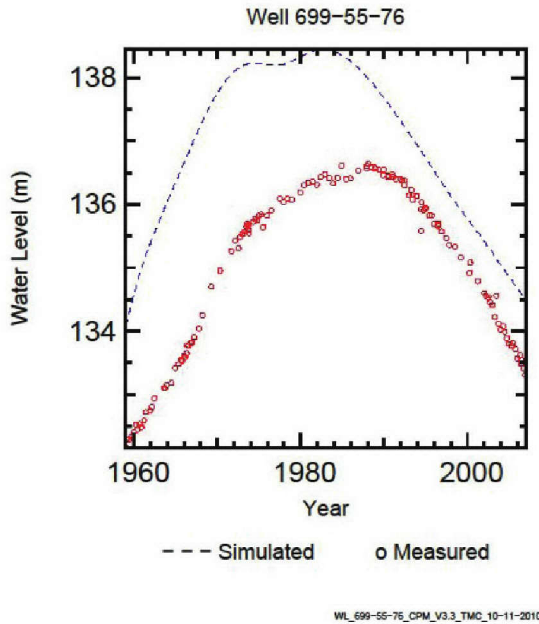
Well 699−55−76
138
136
134
Water Level (m)
1960
1980
2000
Year
− − − Simulated
o Measured
WL_699−55−76_CPM_V3.3_TMC_10−11−2010

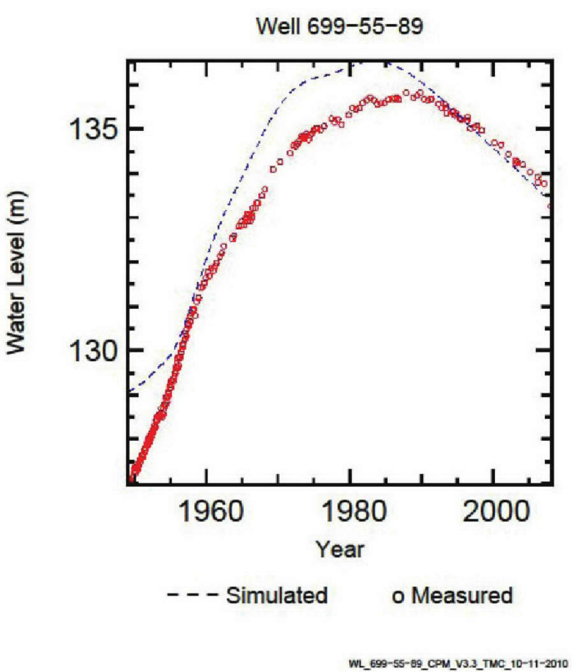
Well 699−55−89
135
130
Water Level (m)
1960
1980
2000
Year
− − − Simulated
o Measured
WL_699−55−89_CPM_V3.3_TMC_10−11−2010

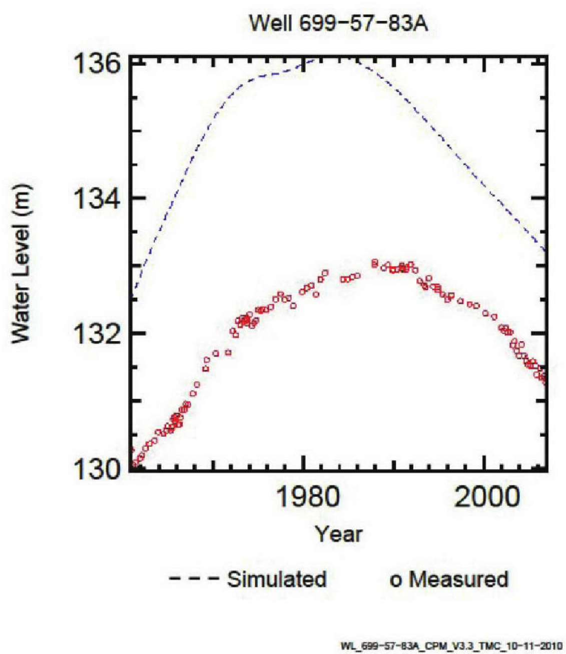
Well 699−57−83A
136
134
132
130
Water Level (m)
1980
2000
Year
− − − Simulated
o Measured
WL_699−57−83A_CPM_V3.3_TMC_10−11−2010

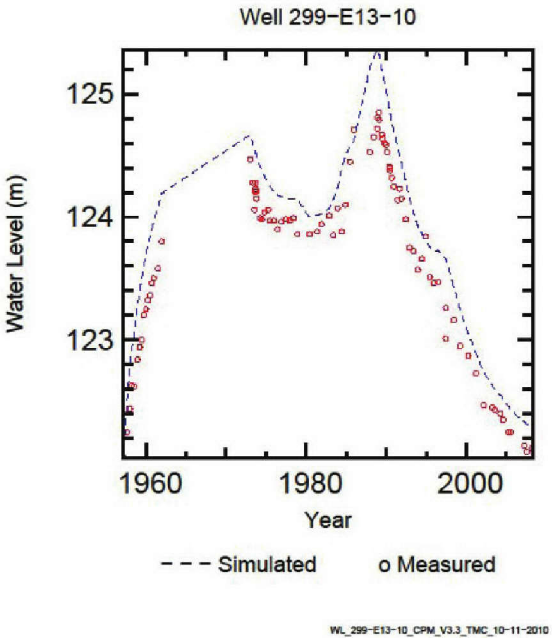
Well 299-E13-10
Water Level (m)
125
124
123
1960
1980
2000
Year
- - - Simulated
o Measured
WL_299-E13-10_CPM_V3.3_TMC_10-11-2010

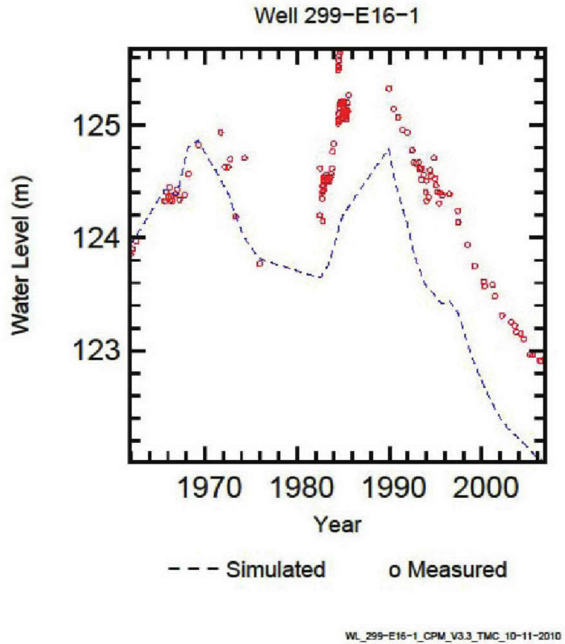
Well 299-E16-1
Water Level (m)
125
124
123
1970
1980
1990
2000
Year
- - - Simulated
o Measured
WL_299-E16-1_CPM_V3.3_TMC_10-11-2010

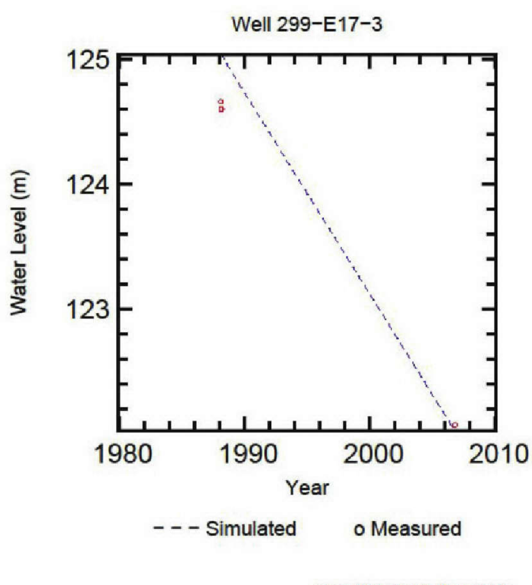
Well 299-E17-3
Water Level (m)
125
124
123
1980
1990
2000
2010
Year
- - - Simulated
o Measured
WL_299-E17-3_CPM_V3.3_TMC_10-11-2010

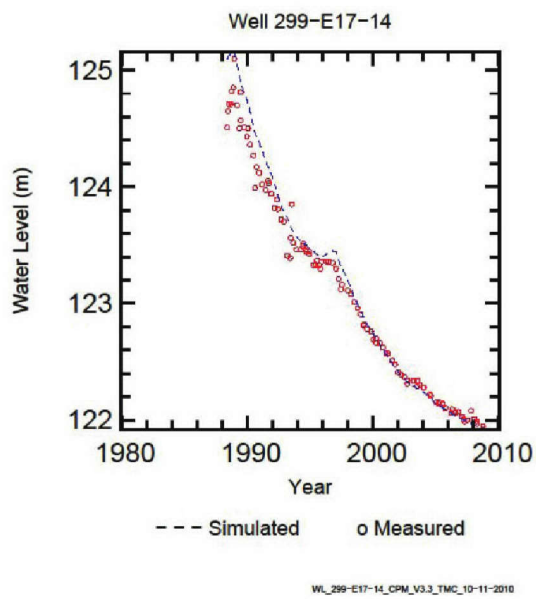
Well 299-E17-14
Water Level (m)
125
124
123
122
1980
1990
2000
2010
Year
- - - Simulated
o Measured
WL_299-E17-14_CPM_V3.3_TMC_10-11-2010

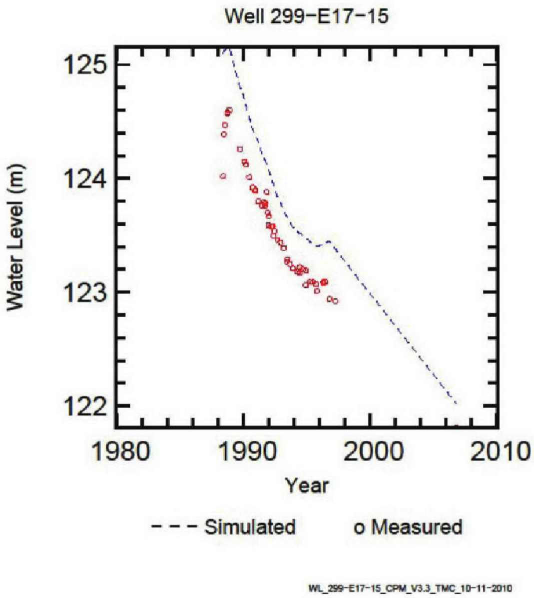
Well 299−E17−15
Water Level (m)
125
124
123
122
1980
1990
2000
2010
Year
Simulated
Measured
WL_299−E17−15_CPM_V3.3_TMC_10−11−2010

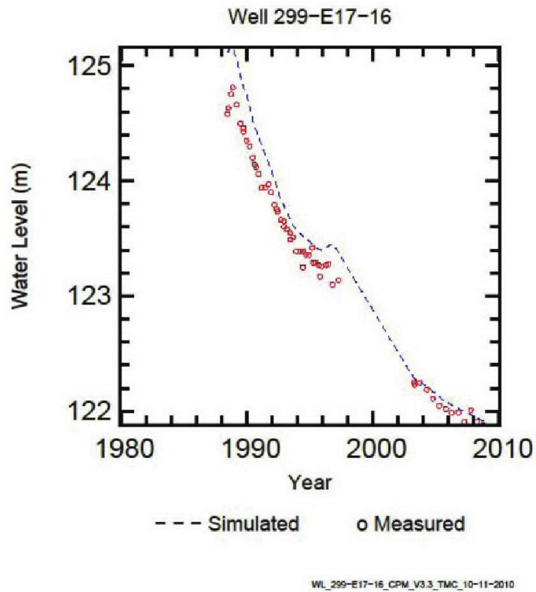
Well 299−E17−16
Water Level (m)
125
124
123
122
1980
1990
2000
2010
Year
Simulated
Measured
WL_299−E17−16_CPM_V3.3_TMC_10−11−2010

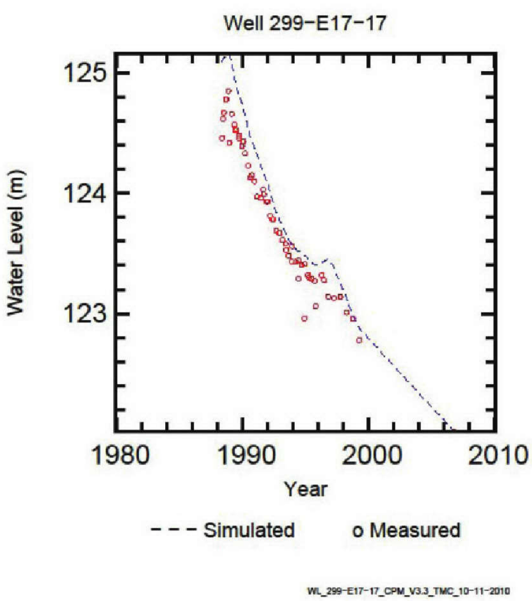
Well 299−E17−17
Water Level (m)
125
124
123
1980
1990
2000
2010
Year
Simulated
Measured
WL_299−E17−17_CPM_V3.3_TMC_10−11−2010

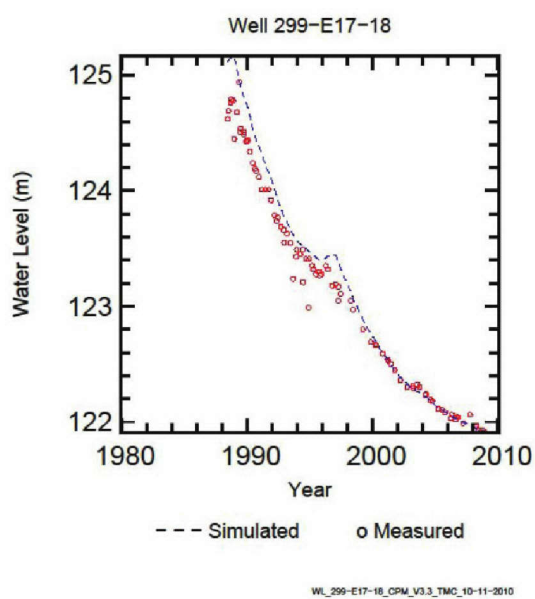
Well 299−E17−18
Water Level (m)
125
124
123
122
1980
1990
2000
2010
Year
Simulated
Measured
WL_299−E17−18_CPM_V3.3_TMC_10−11−2010

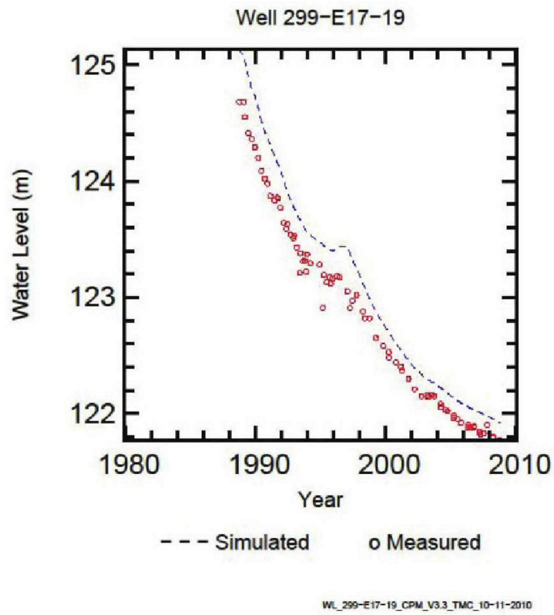
Well 299−E17−19
125
124
123
122
Water Level (m)
1980
1990
2000
2010
Year
- - - Simulated
o Measured
WL_299-E17-19_CPM_V3.3_TMC_10-11-2010

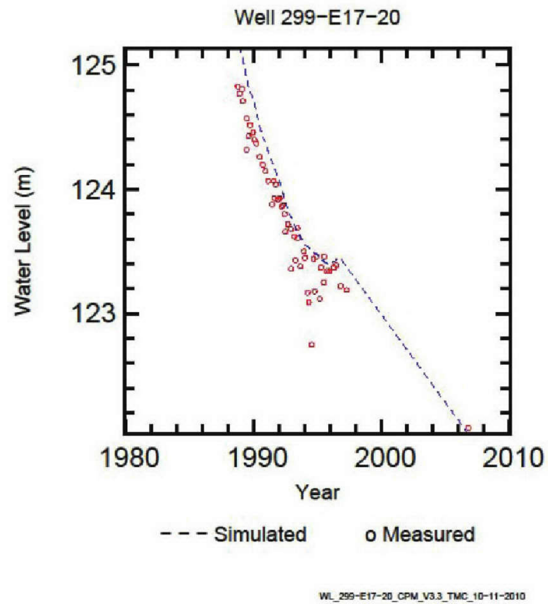
Well 299−E17−20
125
124
123
Water Level (m)
1980
1990
2000
2010
Year
- - - Simulated
o Measured
WL_299-E17-20_CPM_V3.3_TMC_10-11-2010

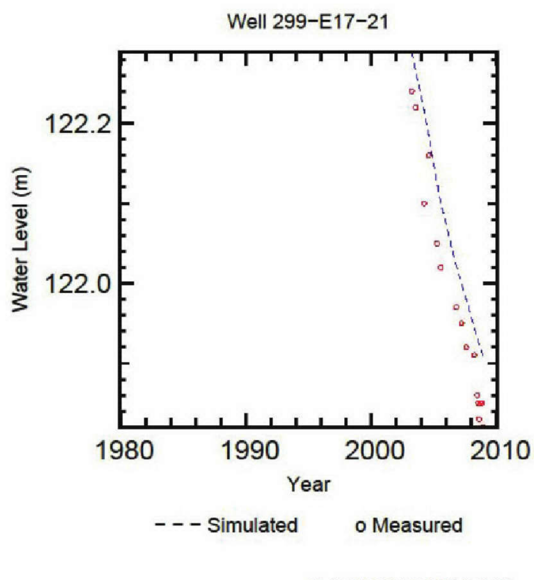
Well 299−E17−21
122.2
122.0
Water Level (m)
1980
1990
2000
2010
Year
- - - Simulated
o Measured
WL_299-E17-21_CPM_V3.3_TMC_10-11-2010

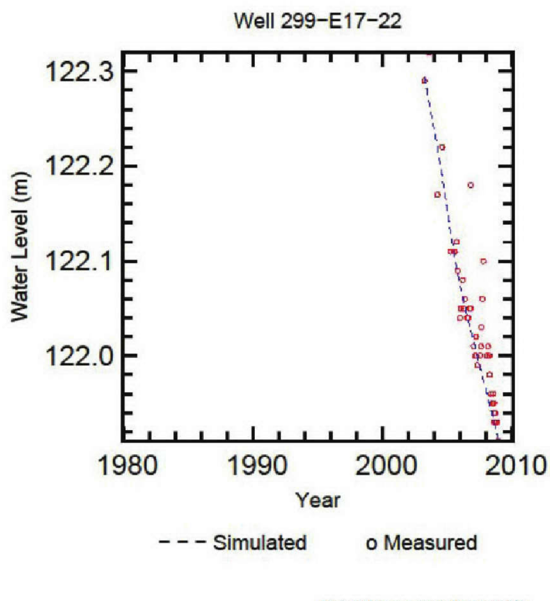
Well 299−E17−22
122.3
122.2
122.1
122.0
Water Level (m)
1980
1990
2000
2010
Year
- - - Simulated
o Measured
WL_299-E17-22_CPM_V3.3_TMC_10-11-2010

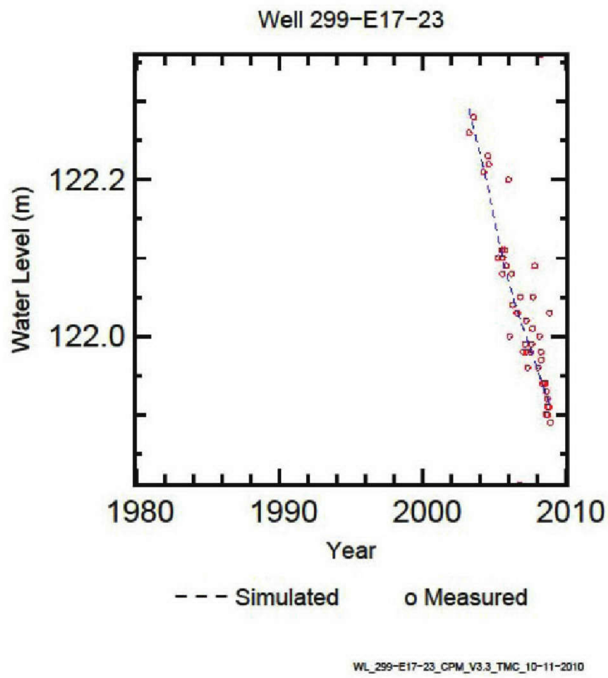
Well 299−E17−23
Water Level (m)
122.2
122.0
1980
1990
2000
2010
Year
- - - Simulated
o Measured
WL_299-E17-23_CPM_V3.3_TMC_10-11-2010

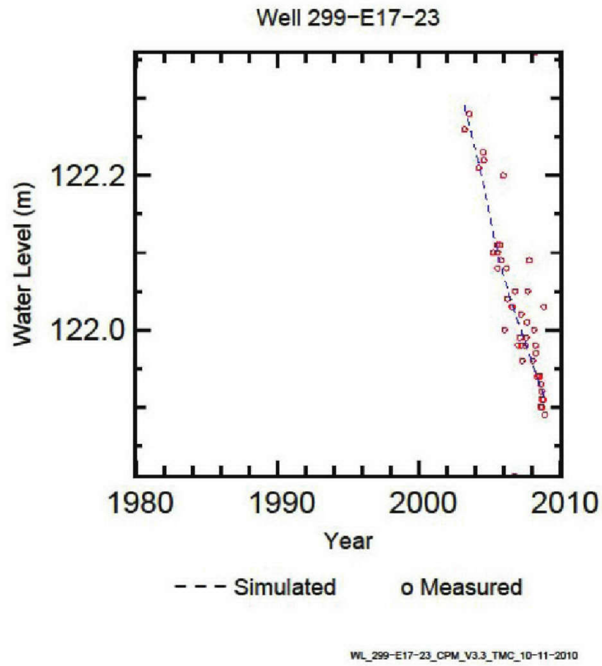
Well 299−E17−23
Water Level (m)
122.2
122.0
1980
1990
2000
2010
Year
- - - Simulated
o Measured
WL_299-E17-23_CPM_V3.3_TMC_10-11-2010

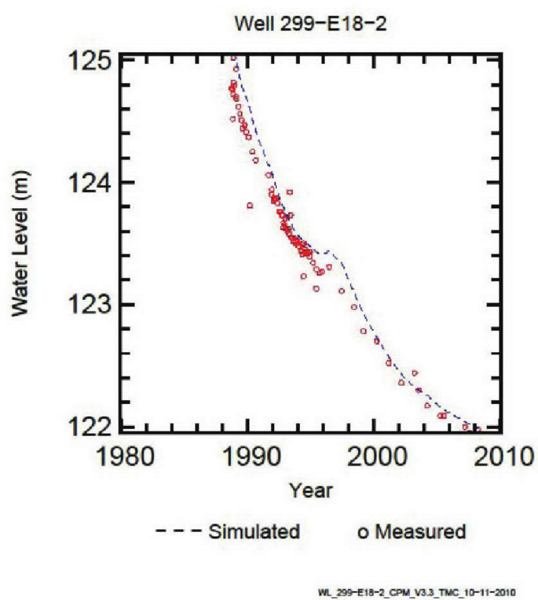
Well 299−E18−2
Water Level (m)
125
124
123
122
1980
1990
2000
2010
Year
- - - Simulated
o Measured
WL_299-E18-2_CPM_V3.3_TMC_10-11-2010

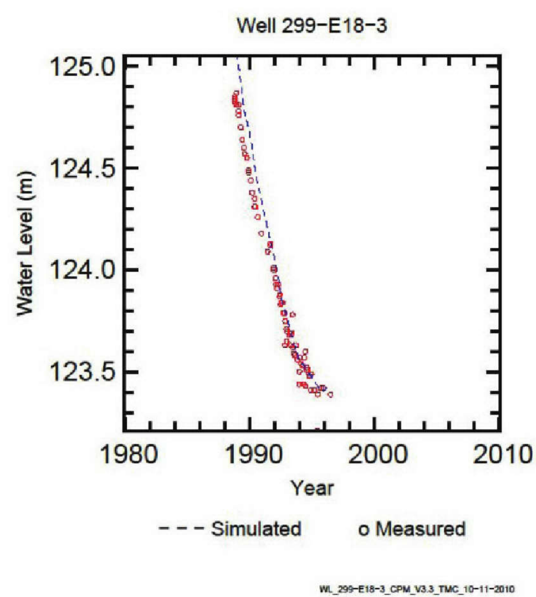
Well 299−E18−3
Water Level (m)
125.0
124.5
124.0
123.5
1980
1990
2000
2010
Year
- - - Simulated
o Measured
WL_299-E18-3_CPM_V3.3_TMC_10-11-2010

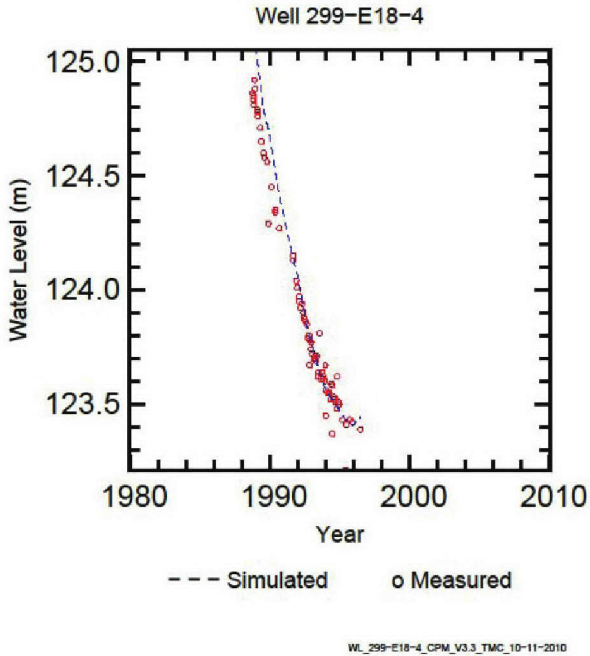
Well 299−E18−4
125.0
124.5
124.0
123.5
Water Level (m)
1980
1990
2000
2010
Year
- - - Simulated
o Measured
WL_299-E18-4_CPM_V3.3_TMC_10-11-2010

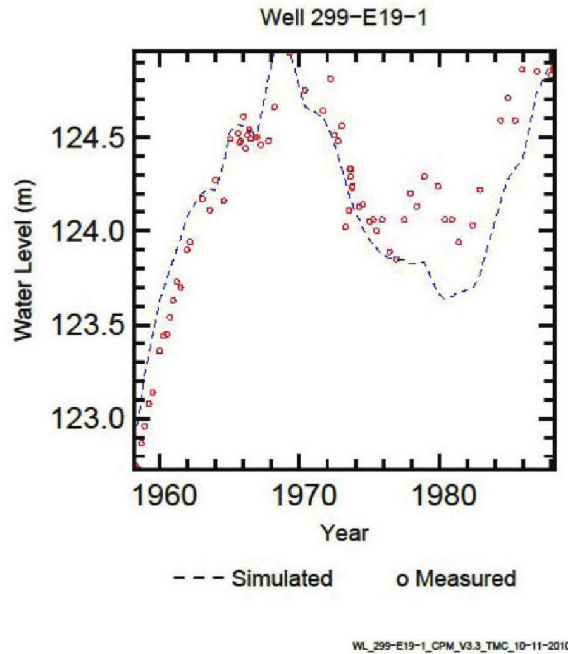
Well 299−E19−1
124.5
124.0
123.5
123.0
Water Level (m)
1960
1970
1980
Year
- - - Simulated
o Measured
WL_299-E19-1_CPM_V3.3_TMC_10-11-2010

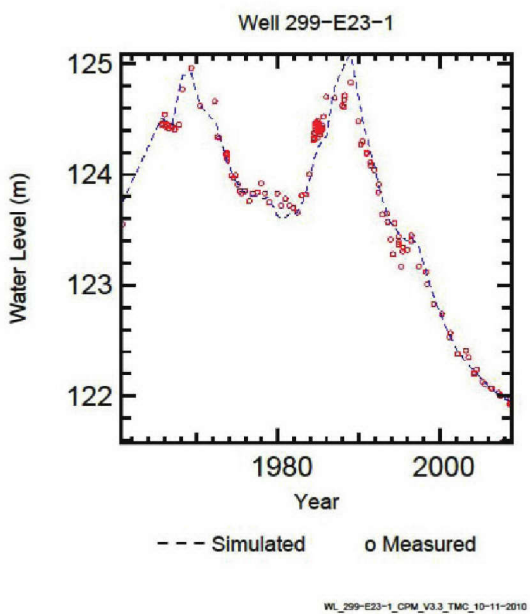
Well 299−E23−1
125
124
123
122
Water Level (m)
1980
2000
Year
- - - Simulated
o Measured
WL_299-E23-1_CPM_V3.3_TMC_10-11-2010

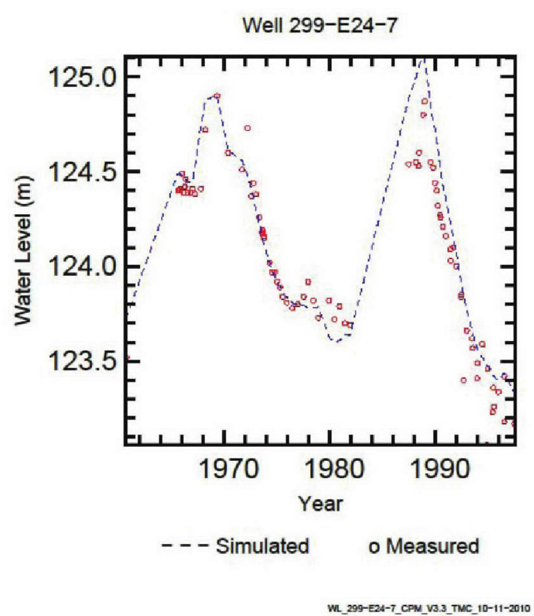
Well 299−E24−7
125.0
124.5
124.0
123.5
Water Level (m)
1970
1980
1990
Year
- - - Simulated
o Measured
WL_299-E24-7_CPM_V3.3_TMC_10-11-2010

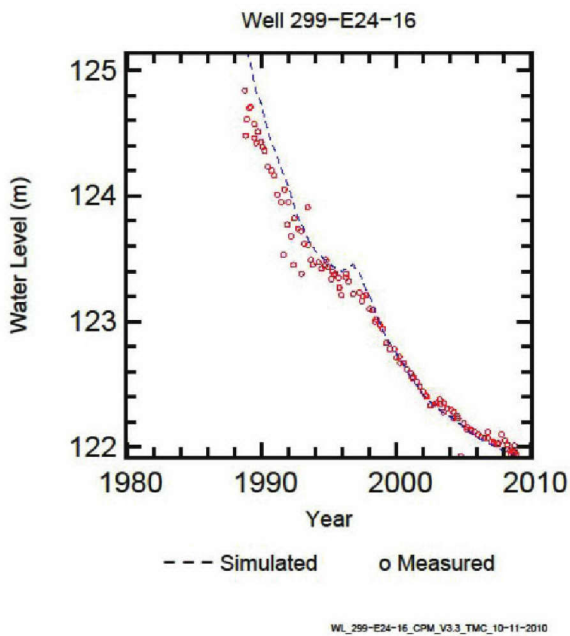
Well 299-E24-16
Water Level (m)
125
124
123
122
1980
1990
2000
2010
Year
Simulated
o Measured
WL_299-E24-16_CPM_V3.3_TMC_10-11-2010

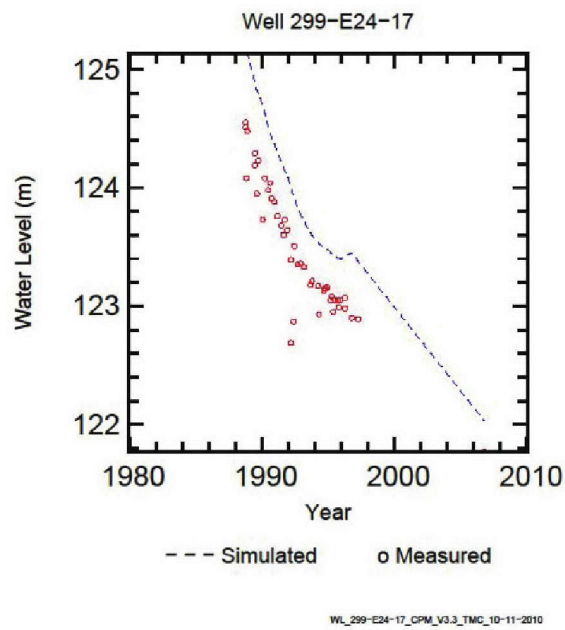
Well 299-E24-17
Water Level (m)
125
124
123
122
1980
1990
2000
2010
Year
Simulated
o Measured
WL_299-E24-17_CPM_V3.3_TMC_10-11-2010

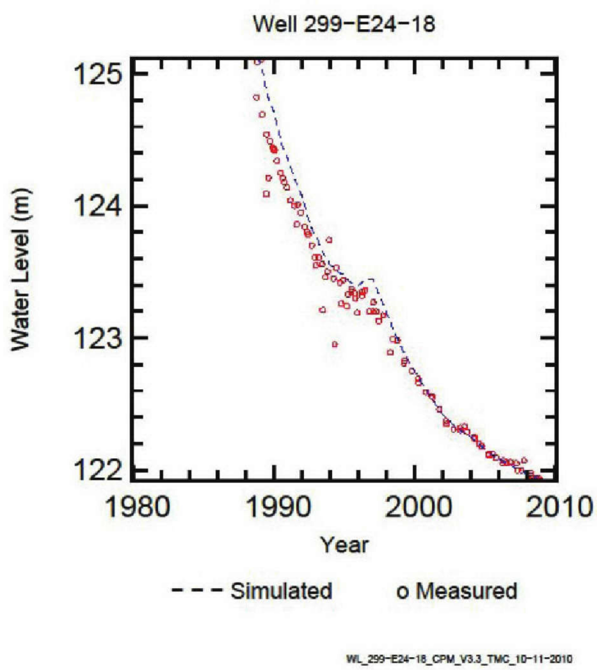
Well 299-E24-18
Water Level (m)
125
124
123
122
1980
1990
2000
2010
Year
Simulated
o Measured
WL_299-E24-18_CPM_V3.3_TMC_10-11-2010

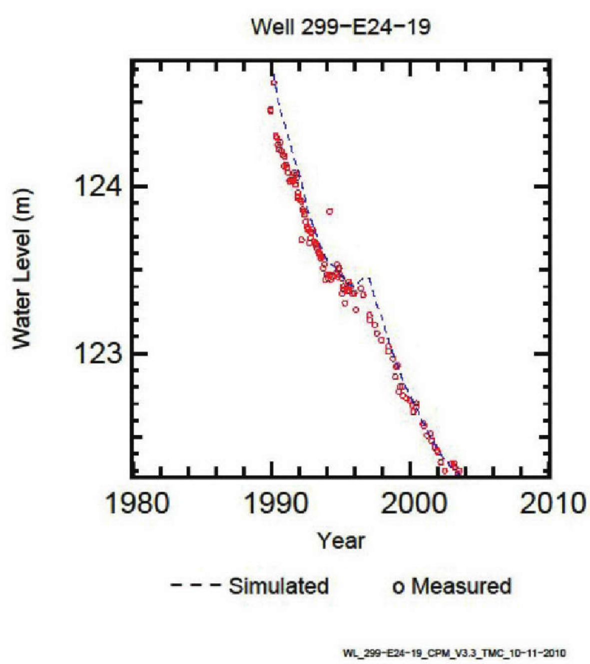
Well 299-E24-19
Water Level (m)
124
123
1980
1990
2000
2010
Year
Simulated
o Measured
WL_299-E24-19_CPM_V3.3_TMC_10-11-2010

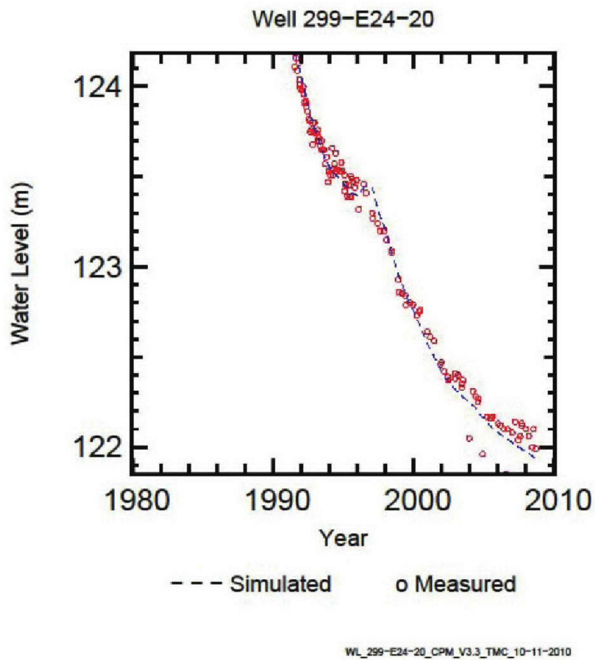
Well 299-E24-20
Water Level (m)
124
123
122
1980
1990
2000
2010
Year
Simulated
o Measured
WL_299-E24-20_CPM_V3.3_TMC_10-11-2010

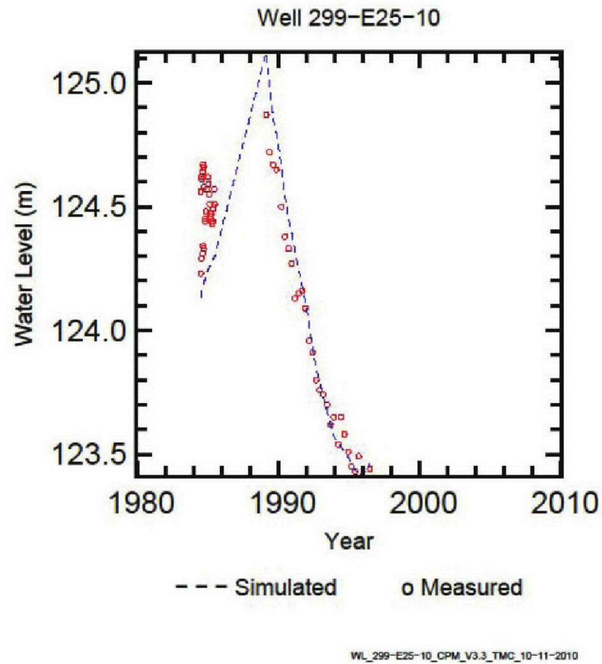
Well 299-E25-10
Water Level (m)
125.0
124.5
124.0
123.5
1980
1990
2000
2010
Year
Simulated
o Measured
WL_299-E25-10_CPM_V3.3_TMC_10-11-2010

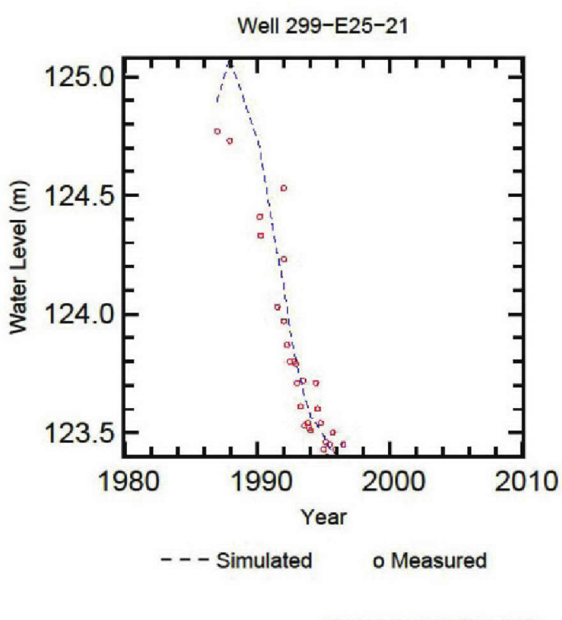
Well 299-E25-21
Water Level (m)
125.0
124.5
124.0
123.5
1980
1990
2000
2010
Year
Simulated
o Measured
WL_299-E25-21_CPM_V3.3_TMC_10-11-2010

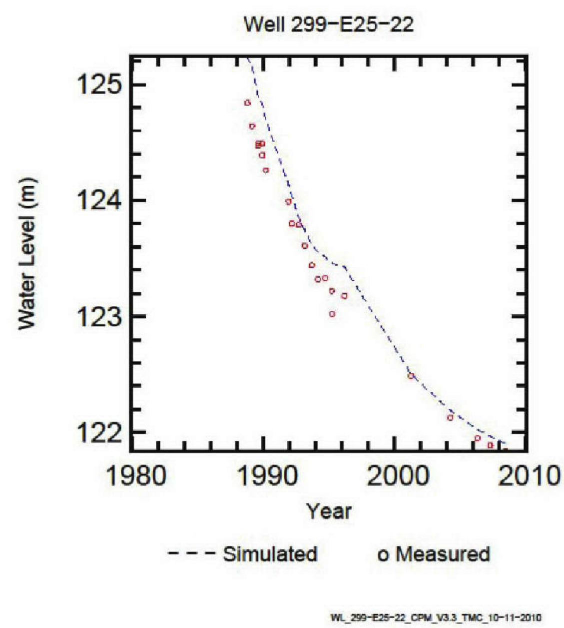
Well 299-E25-22
Water Level (m)
125
124
123
122
1980
1990
2000
2010
Year
Simulated
o Measured
WL_299-E25-22_CPM_V3.3_TMC_10-11-2010

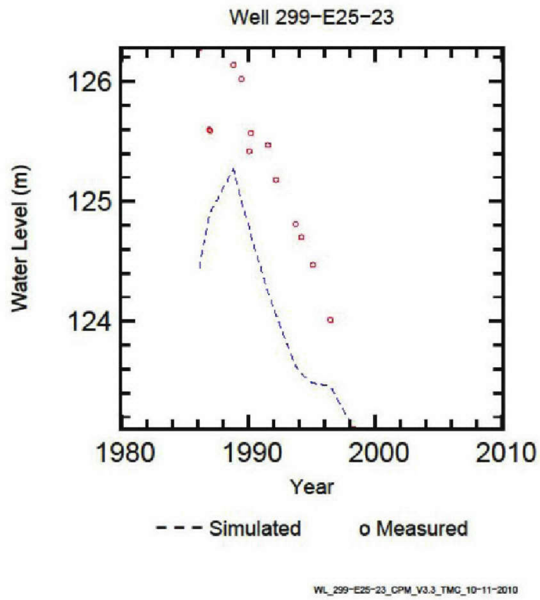
Well 299−E25−23
126
125
124
Water Level (m)
1980
1990
2000
2010
Year
- - - Simulated
o Measured
WL_299-E25-23_CPM_V3.3_TMC_10-11-2010

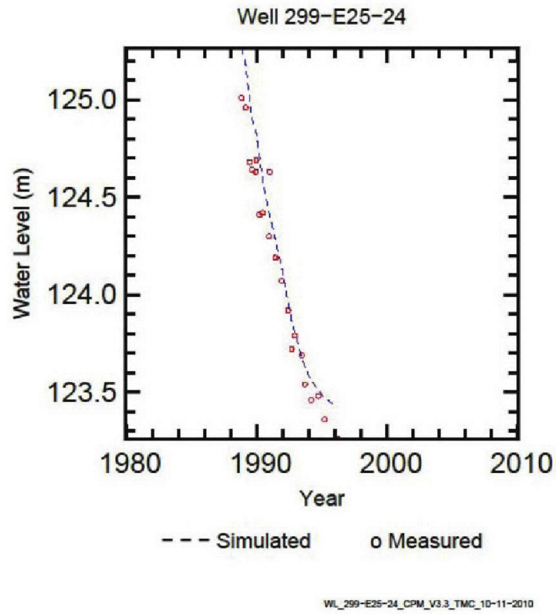
Well 299−E25−24
125.0
124.5
124.0
123.5
Water Level (m)
1980
1990
2000
2010
Year
- - - Simulated
o Measured
WL_299-E25-24_CPM_V3.3_TMC_10-11-2010

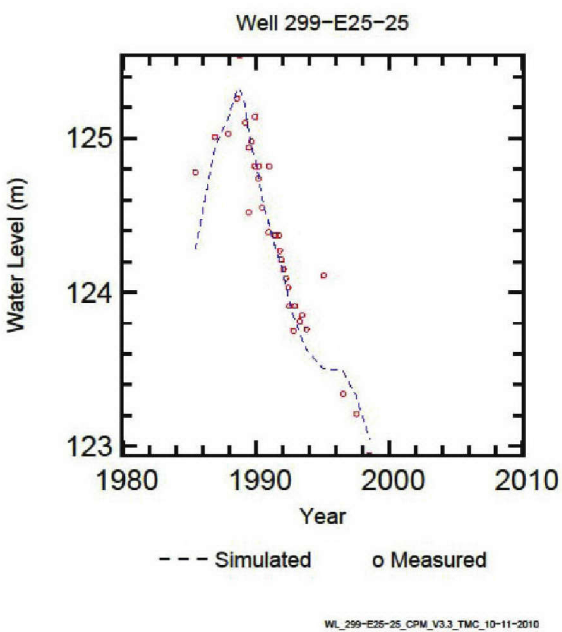
Well 299−E25−25
125
124
123
Water Level (m)
1980
1990
2000
2010
Year
- - - Simulated
o Measured
WL_299-E25-25_CPM_V3.3_TMC_10-11-2010

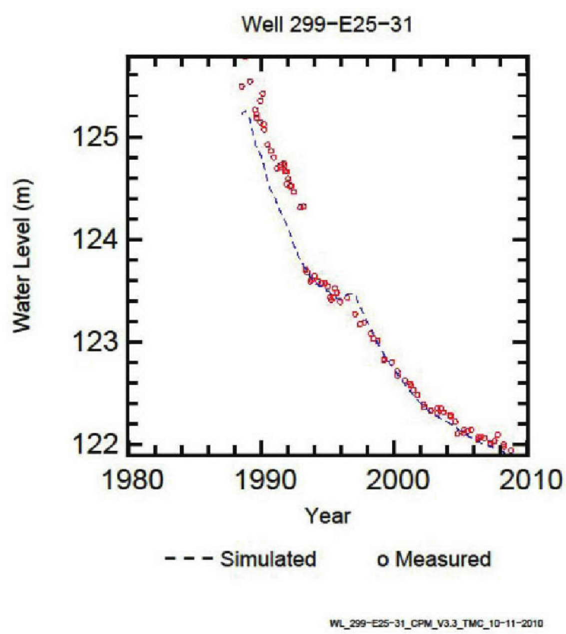
Well 299−E25−31
125
124
123
122
Water Level (m)
1980
1990
2000
2010
Year
- - - Simulated
o Measured
WL_299-E25-31_CPM_V3.3_TMC_10-11-2010

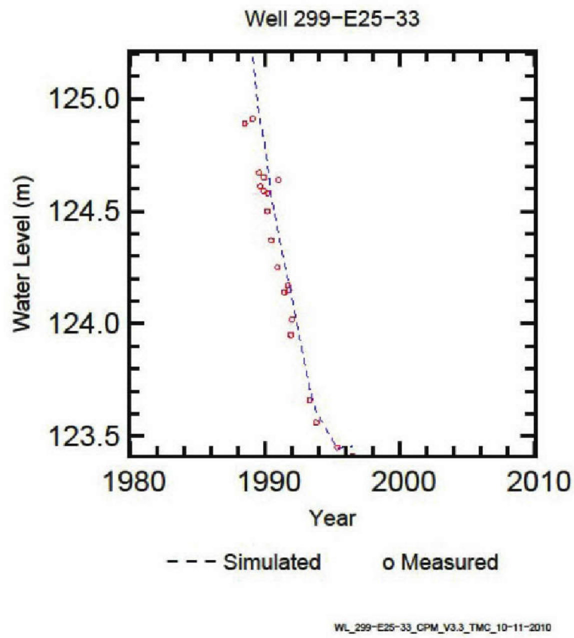
Well 299-E25-33
Water Level (m)
125.0
124.5
124.0
123.5
1980
1990
2000
2010
Year
- - - Simulated
o Measured
WL_299-E25-33_CPM_V3.3_TMC_10-11-2010

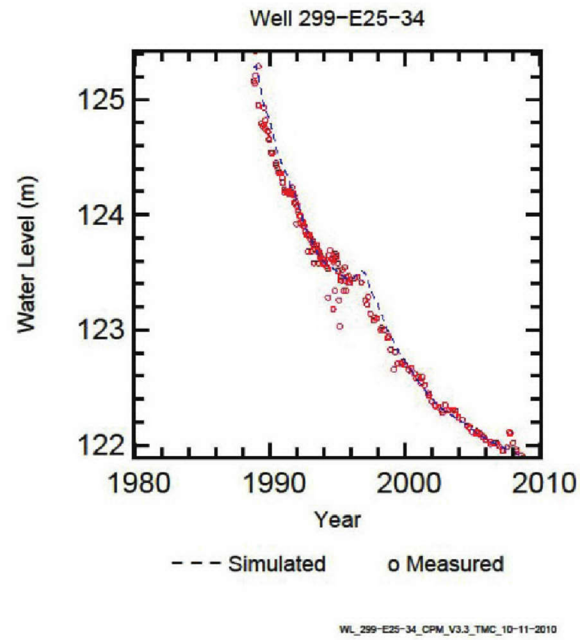
Well 299-E25-34
Water Level (m)
125
124
123
122
1980
1990
2000
2010
Year
- - - Simulated
o Measured
WL_299-E25-34_CPM_V3.3_TMC_10-11-2010

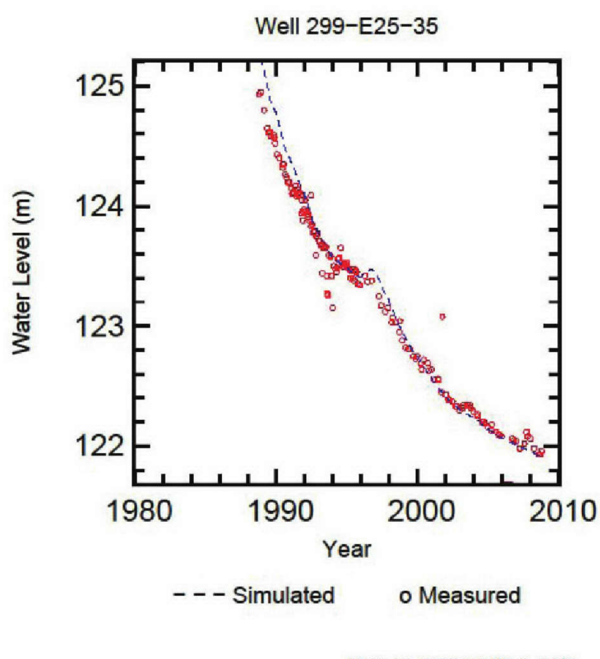
Well 299-E25-35
Water Level (m)
125
124
123
122
1980
1990
2000
2010
Year
- - - Simulated
o Measured
WL_299-E25-35_CPM_V3.3_TMC_10-11-2010

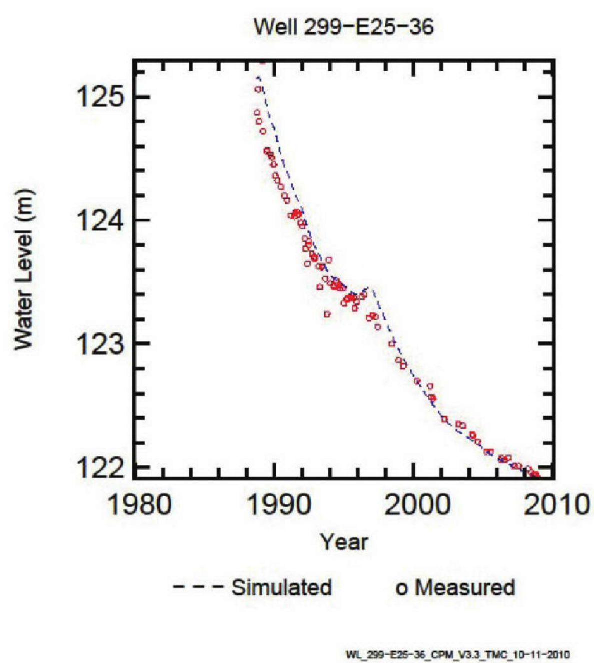
Well 299-E25-36
Water Level (m)
125
124
123
122
1980
1990
2000
2010
Year
- - - Simulated
o Measured
WL_299-E25-36_CPM_V3.3_TMC_10-11-2010

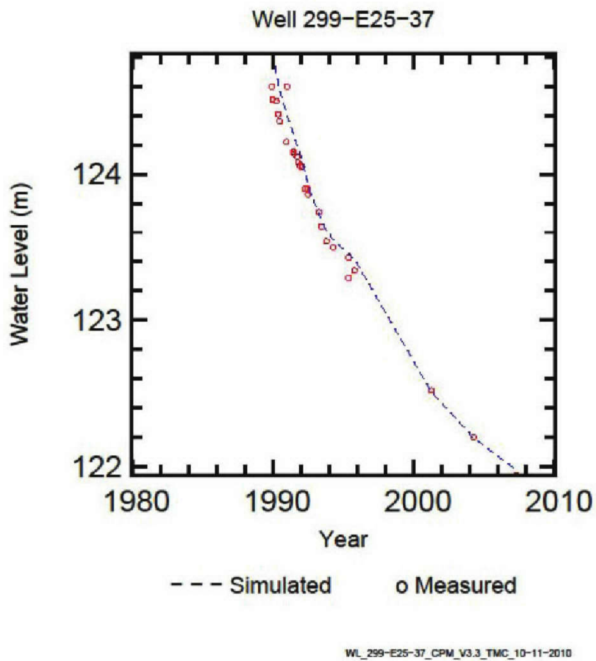
Well 299-E25-37
Water Level (m)
124
123
122
1980
1990
2000
2010
Year
- - - Simulated
o Measured
WL_299-E25-37_CPM_V3.3_TMC_10-11-2010

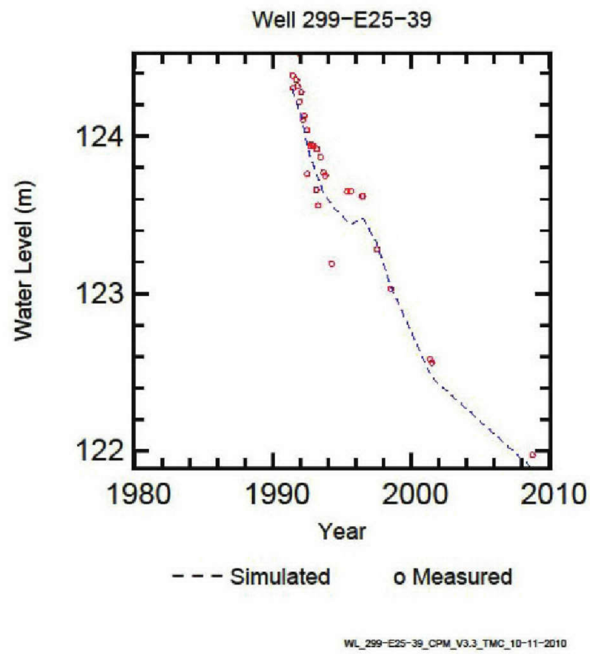
Well 299-E25-39
Water Level (m)
124
123
122
1980
1990
2000
2010
Year
- - - Simulated
o Measured
WL_299-E25-39_CPM_V3.3_TMC_10-11-2010

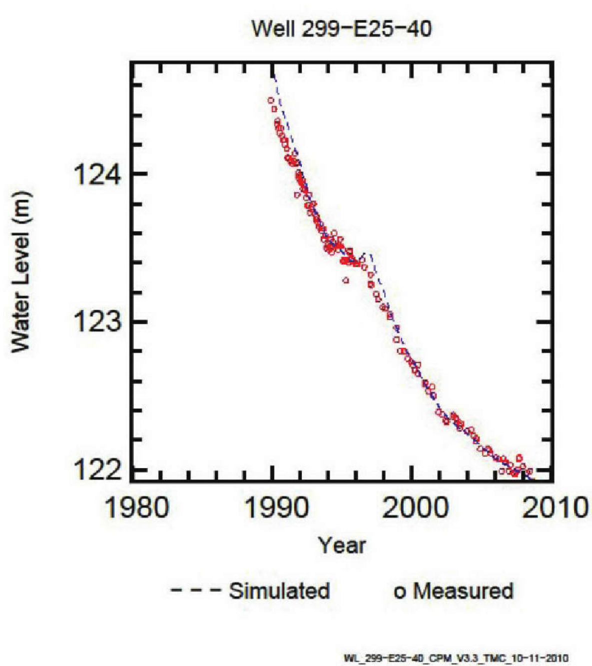
Well 299-E25-40
Water Level (m)
124
123
122
1980
1990
2000
2010
Year
- - - Simulated
o Measured
WL_299-E25-40_CPM_V3.3_TMC_10-11-2010

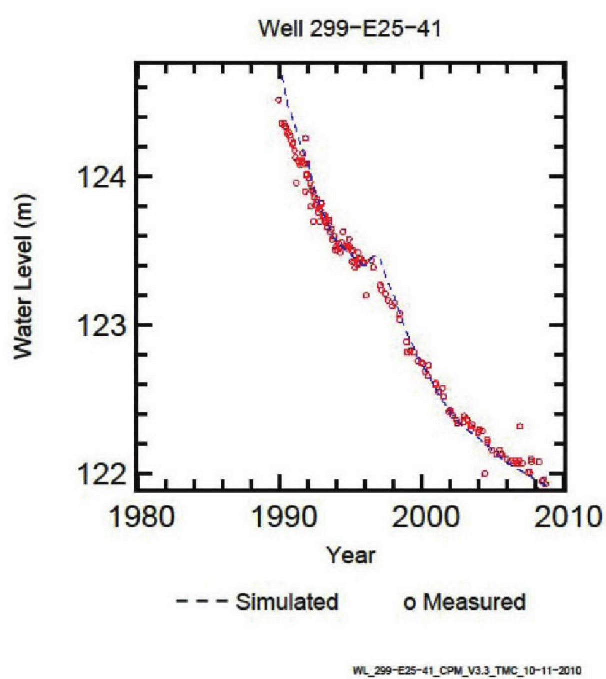
Well 299-E25-41
Water Level (m)
124
123
122
1980
1990
2000
2010
Year
- - - Simulated
o Measured
WL_299-E25-41_CPM_V3.3_TMC_10-11-2010

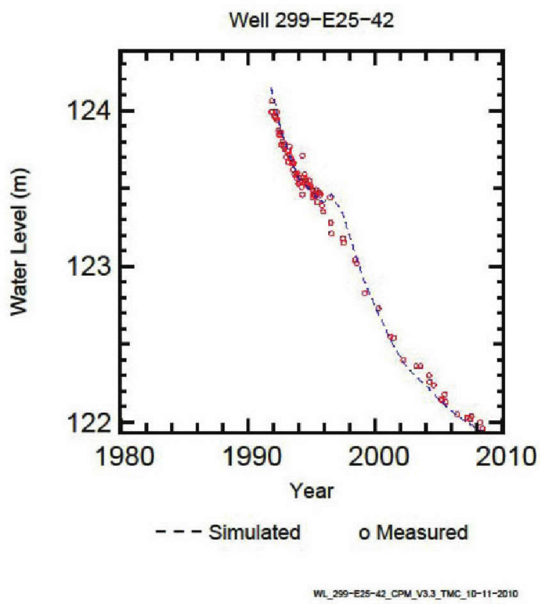
Well 299−E25−42
Water Level (m)
124
123
122
1980
1990
2000
2010
Year
- - - Simulated
o Measured
WL_299-E25-42_CPM_V3.3_TMC_10-11-2010

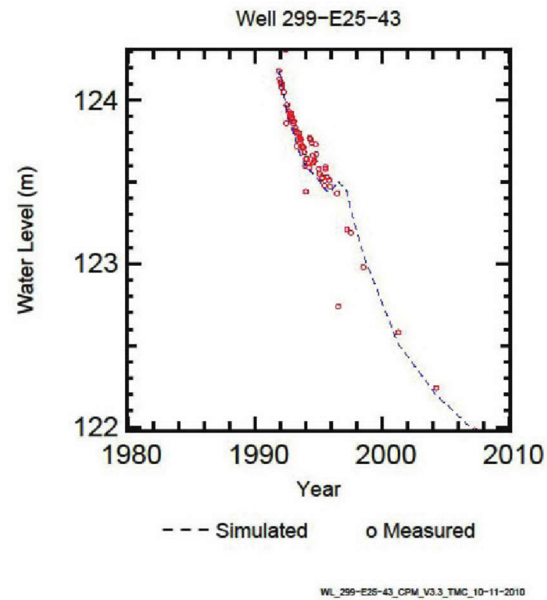
Well 299−E25−43
Water Level (m)
124
123
122
1980
1990
2000
2010
Year
- - - Simulated
o Measured
WL_299-E25-43_CPM_V3.3_TMC_10-11-2010

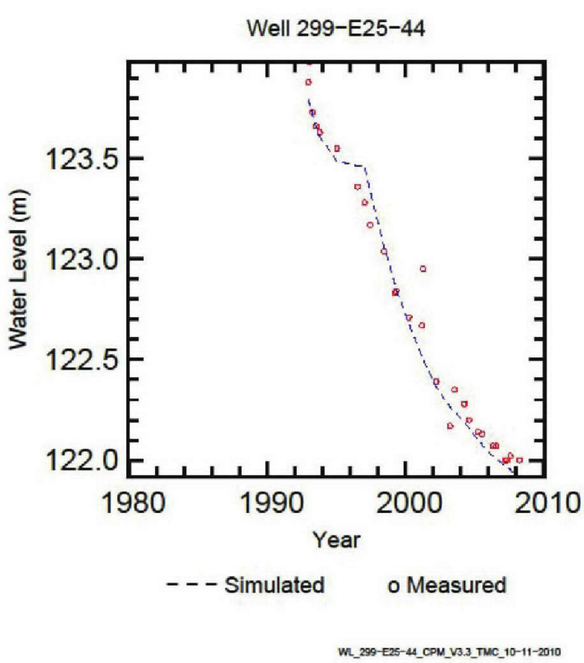
Well 299−E25−44
Water Level (m)
123.5
123.0
122.5
122.0
1980
1990
2000
2010
Year
- - - Simulated
o Measured
WL_299-E25-44_CPM_V3.3_TMC_10-11-2010

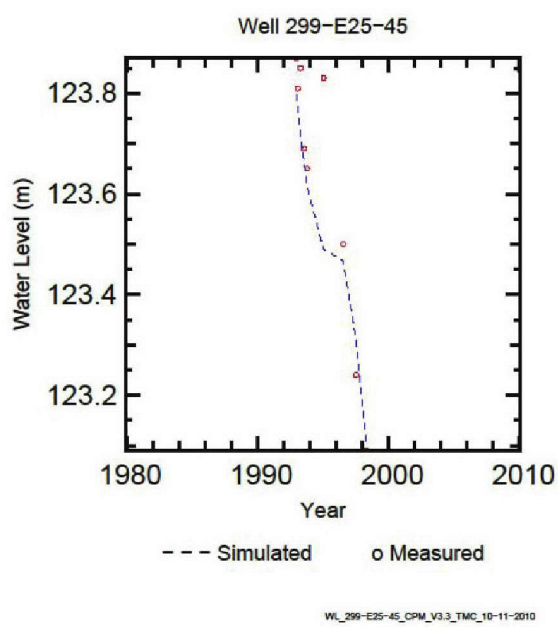
Well 299−E25−45
Water Level (m)
123.8
123.6
123.4
123.2
1980
1990
2000
2010
Year
- - - Simulated
o Measured
WL_299-E25-45_CPM_V3.3_TMC_10-11-2010

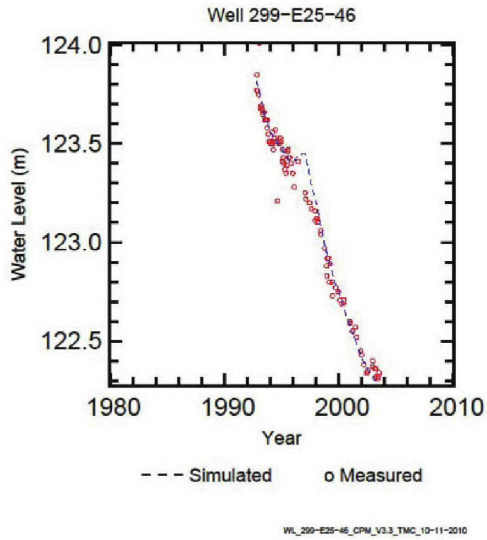
Well 299-E25-46
124.0
123.5
123.0
122.5
Water Level (m)
1980
1990
2000
2010
Year
Simulated
Measured
WL_299-E25-46_CPM_V3.3_TMC_10-11-2010

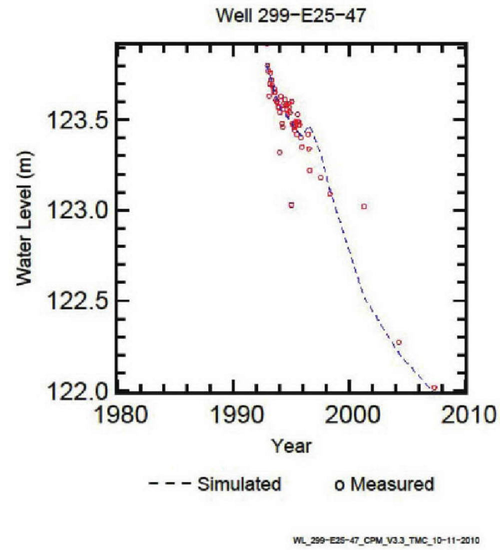
Well 299-E25-47
123.5
123.0
122.5
122.0
Water Level (m)
1980
1990
2000
2010
Year
Simulated
Measured
WL_299-E25-47_CPM_V3.3_TMC_10-11-2010

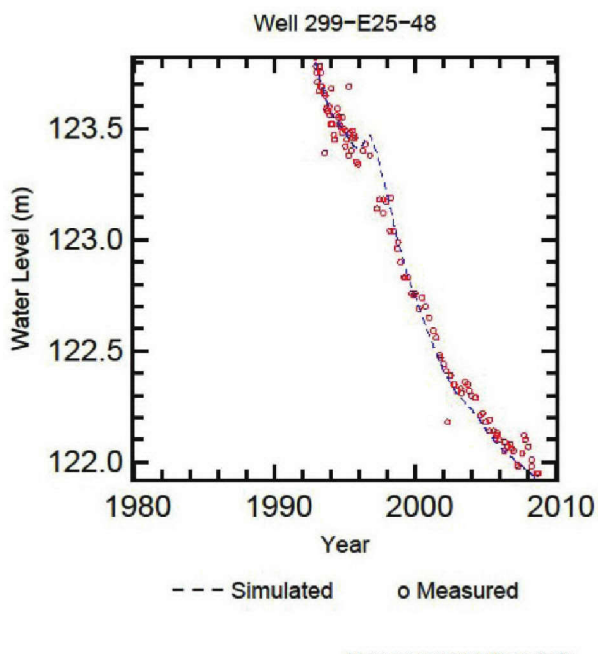
Well 299-E25-48
123.5
123.0
122.5
122.0
Water Level (m)
1980
1990
2000
2010
Year
Simulated
Measured
WL_299-E25-48_CPM_V3.3_TMC_10-11-2010

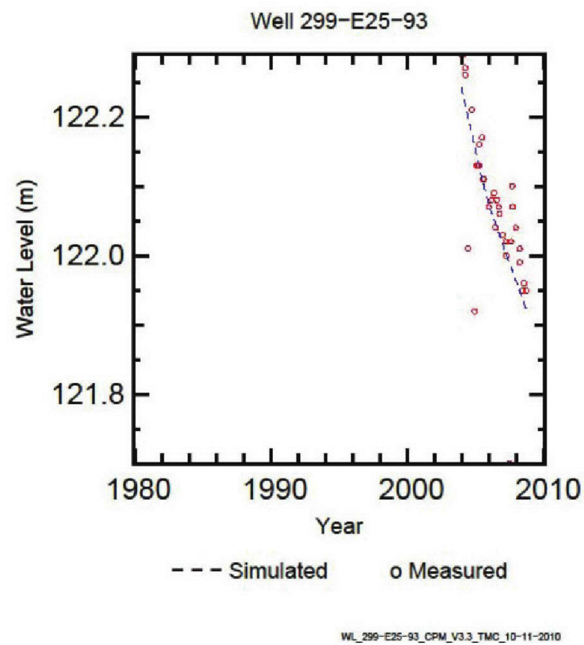
Well 299-E25-93
122.2
122.0
121.8
Water Level (m)
1980
1990
2000
2010
Year
Simulated
Measured
WL_299-E25-93_CPM_V3.3_TMC_10-11-2010

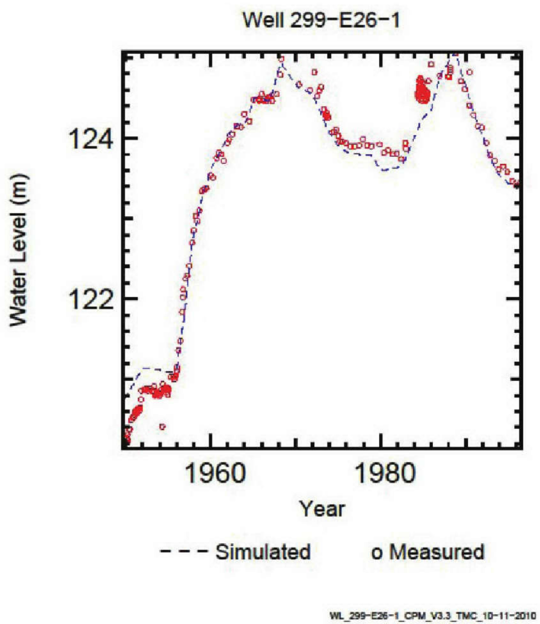
Well 299-E26-1
Water Level (m)
124
122
1960
1980
Year
--- Simulated
o Measured
WL_299-E26-1_CPM_V3.3_TMC_10-11-2010

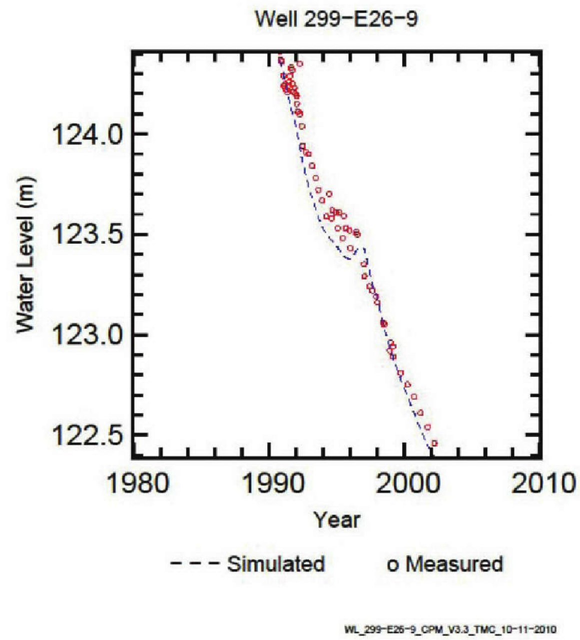
Well 299-E26-9
Water Level (m)
124.0
123.5
123.0
122.5
1980
1990
2000
2010
Year
--- Simulated
o Measured
WL_299-E26-9_CPM_V3.3_TMC_10-11-2010

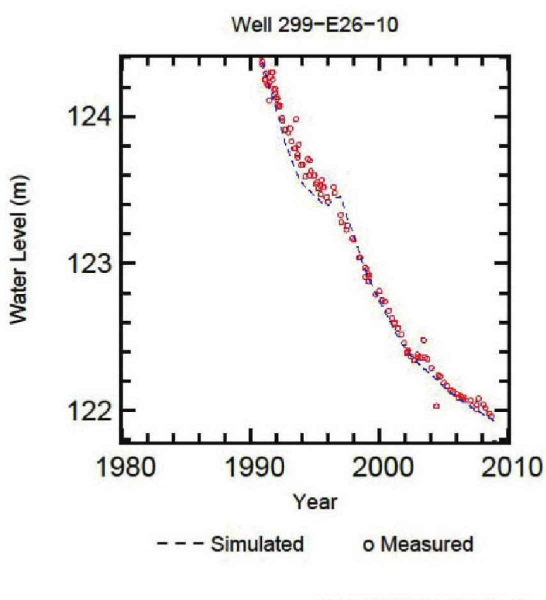
Well 299-E26-10
Water Level (m)
124
123
122
1980
1990
2000
2010
Year
--- Simulated
o Measured
WL_299-E26-10_CPM_V3.3_TMC_10-11-2010

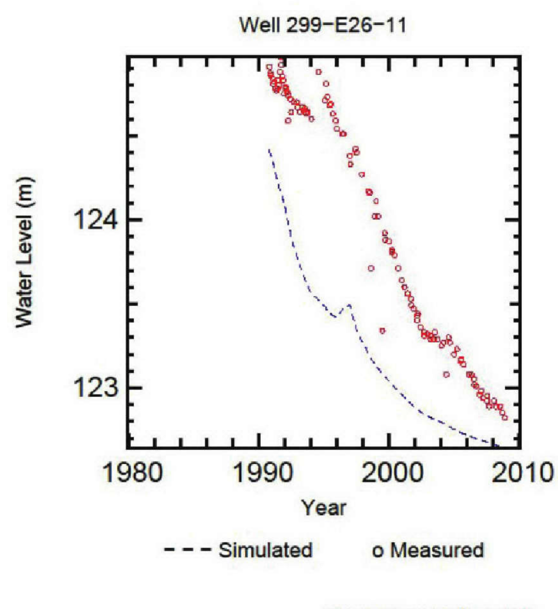
Well 299-E26-11
Water Level (m)
124
123
1980
1990
2000
2010
Year
--- Simulated
o Measured
WL_299-E26-11_CPM_V3.3_TMC_10-11-2010

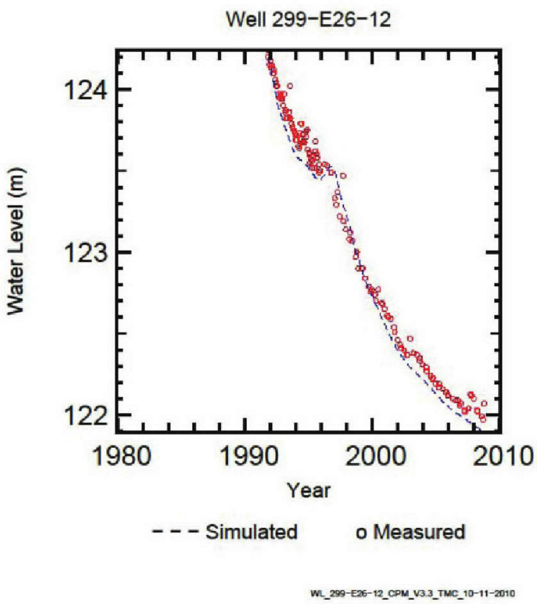
Well 299−E26−12
Water Level (m)
124
123
122
1980
1990
2000
2010
Year
- - - Simulated
o Measured
WL_299-E26-12_CPM_V3.3_TMC_10-11-2010

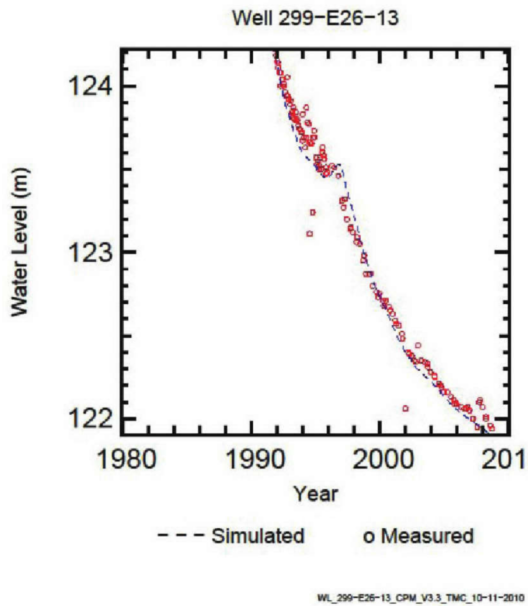
Well 299−E26−13
Water Level (m)
124
123
122
1980
1990
2000
2010
Year
- - - Simulated
o Measured
WL_299-E26-13_CPM_V3.3_TMC_10-11-2010

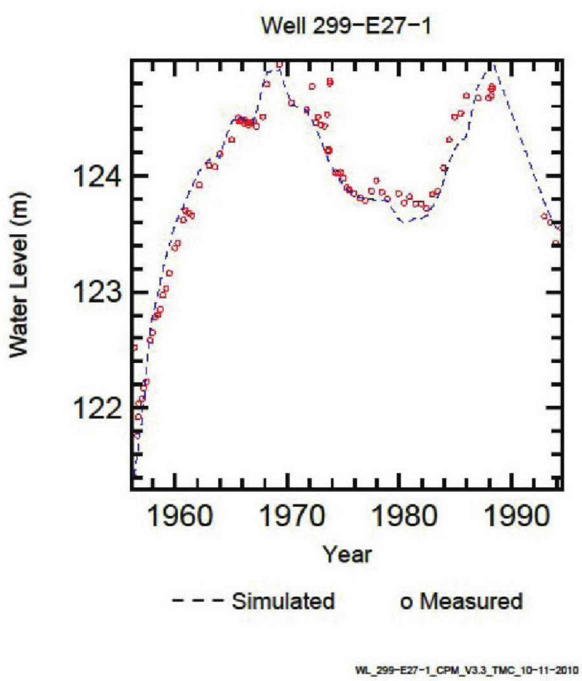
Well 299−E27−1
Water Level (m)
124
123
122
1960
1970
1980
1990
Year
- - - Simulated
o Measured
WL_299-E27-1_CPM_V3.3_TMC_10-11-2010

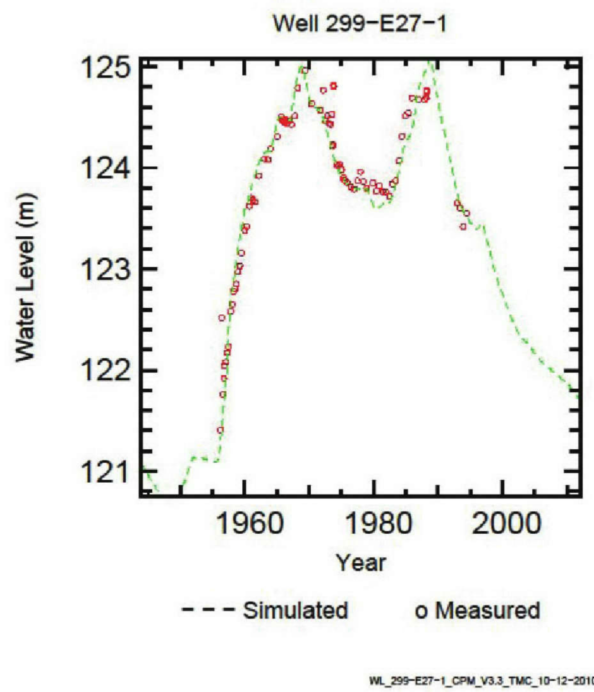
Well 299−E27−1
Water Level (m)
125
124
123
122
121
1960
1980
2000
Year
- - - Simulated
o Measured
WL_299-E27-1_CPM_V3.3_TMC_10-12-2010

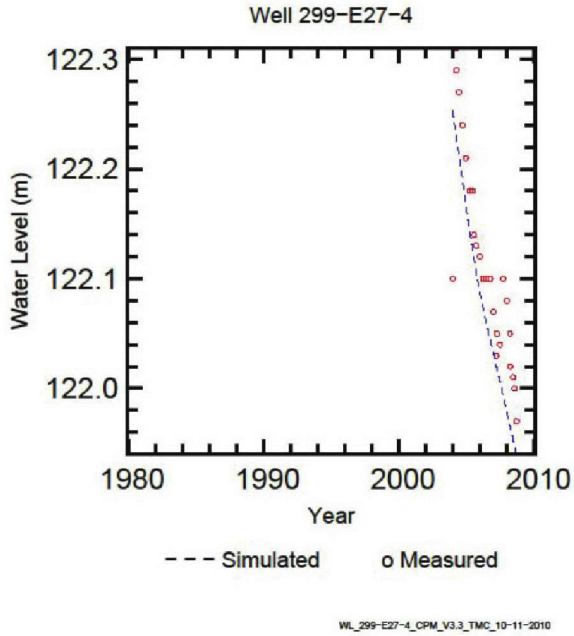
Well 299−E27−4
Water Level (m)
122.3
122.2
122.1
122.0
1980
1990
2000
2010
Year
– – – Simulated
o Measured
WL_299-E27-4_CPM_V3.3_TMC_10-11-2010

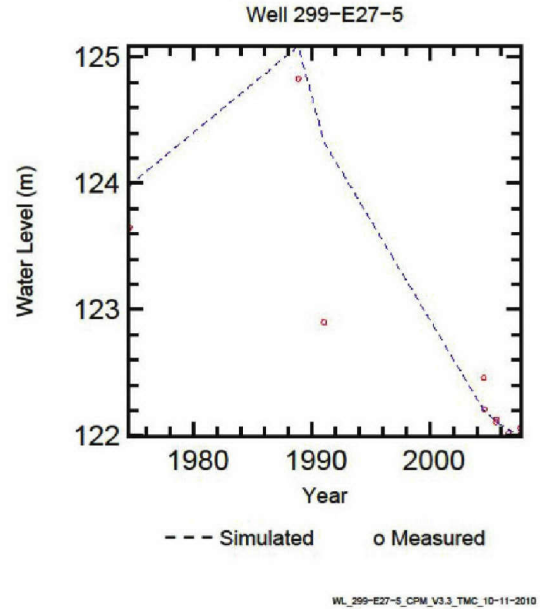
Well 299−E27−5
Water Level (m)
125
124
123
122
1980
1990
2000
Year
– – – Simulated
o Measured
WL_299-E27-5_CPM_V3.3_TMC_10-11-2010

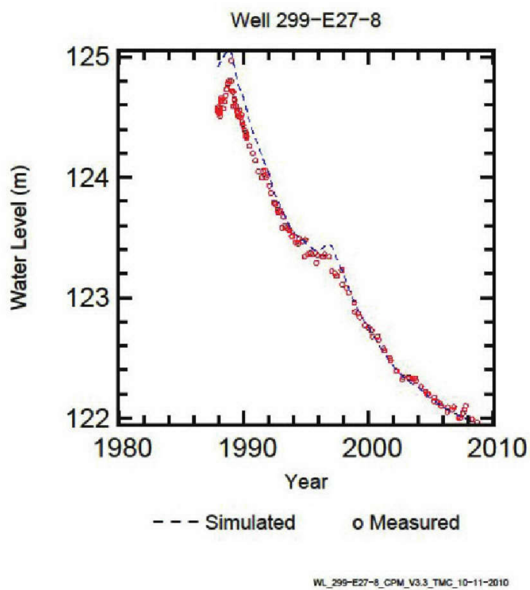
Well 299−E27−8
Water Level (m)
125
124
123
122
1980
1990
2000
2010
Year
– – – Simulated
o Measured
WL_299-E27-8_CPM_V3.3_TMC_10-11-2010

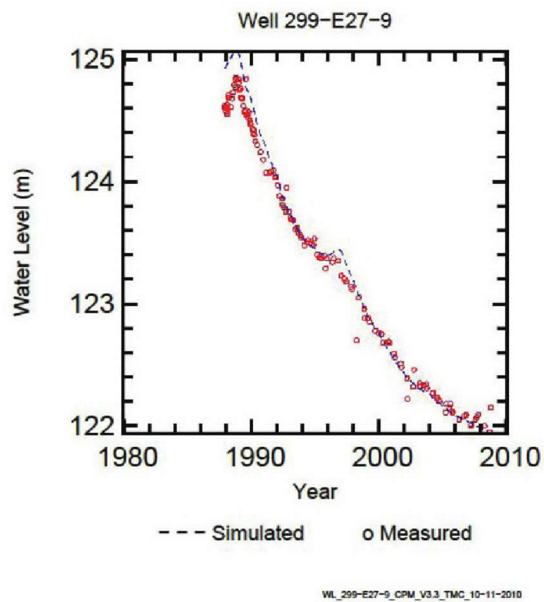
Well 299−E27−9
Water Level (m)
125
124
123
122
1980
1990
2000
2010
Year
– – – Simulated
o Measured
WL_299-E27-9_CPM_V3.3_TMC_10-11-2010

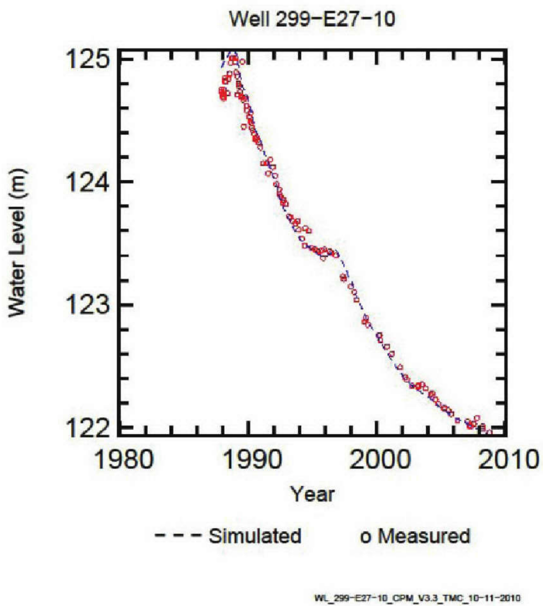
Well 299−E27−10
125
124
123
122
Water Level (m)
1980
1990
2000
2010
Year
− − − Simulated
o Measured
WL_299−E27−10_CPM_V3.3_TMC_10−11−2010

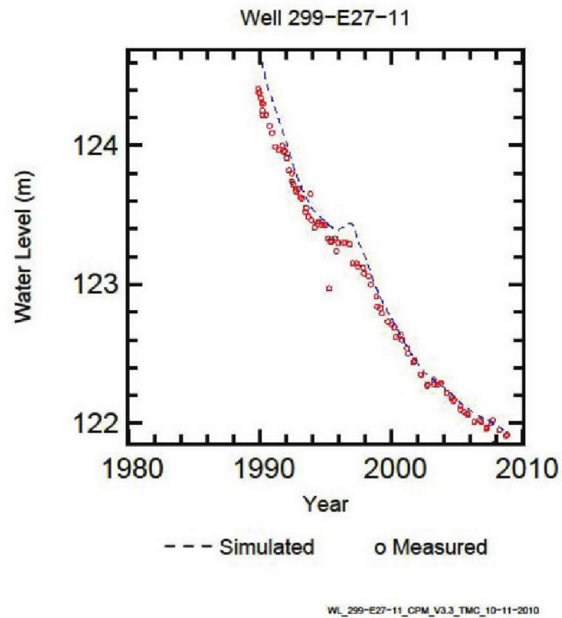
Well 299−E27−11
124
123
122
Water Level (m)
1980
1990
2000
2010
Year
− − − Simulated
o Measured
WL_299−E27−11_CPM_V3.3_TMC_10−11−2010

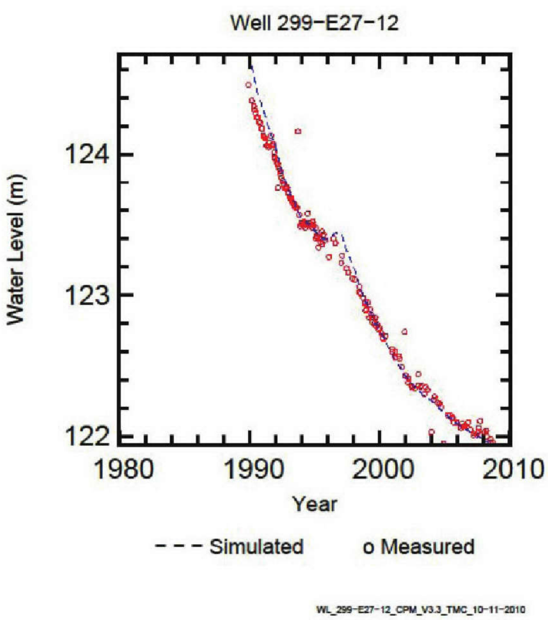
Well 299−E27−12
124
123
122
Water Level (m)
1980
1990
2000
2010
Year
− − − Simulated
o Measured
WL_299−E27−12_CPM_V3.3_TMC_10−11−2010

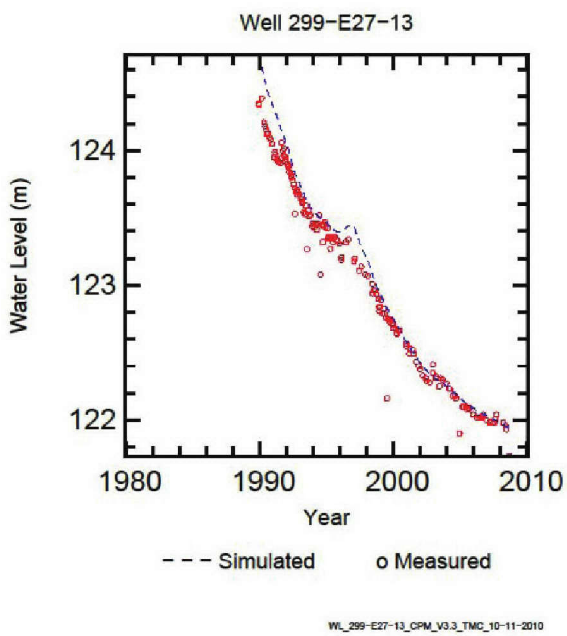
Well 299−E27−13
124
123
122
Water Level (m)
1980
1990
2000
2010
Year
− − − Simulated
o Measured
WL_299−E27−13_CPM_V3.3_TMC_10−11−2010

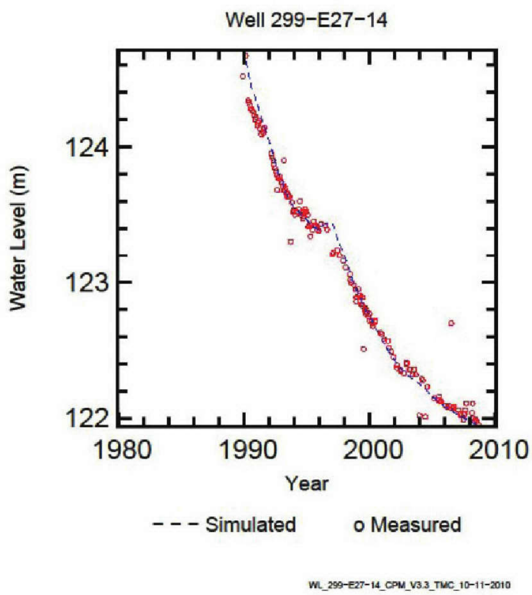
Well 299-E27-14
Water Level (m)
122
123
124
1980
1990
2000
2010
Year
- - - Simulated
o Measured
WL_299-E27-14_CPM_V3.3_TMC_10-11-2010

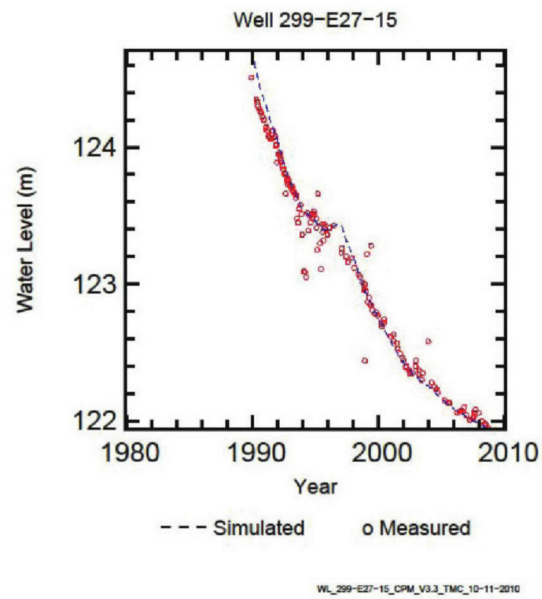
Well 299-E27-15
Water Level (m)
122
123
124
1980
1990
2000
2010
Year
- - - Simulated
o Measured
WL_299-E27-15_CPM_V3.3_TMC_10-11-2010

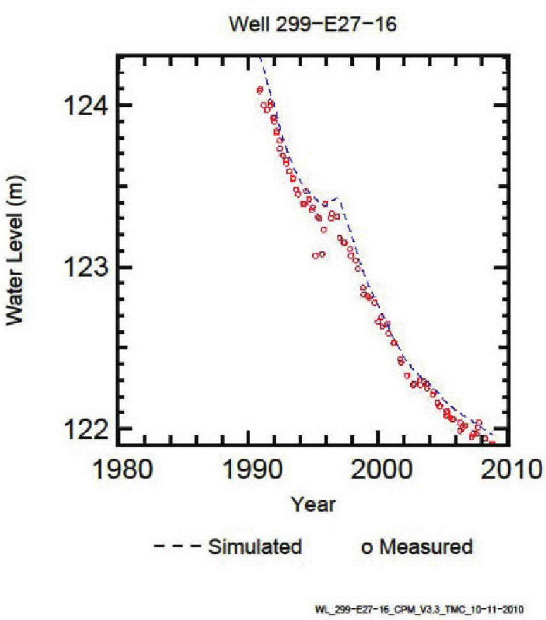
Well 299-E27-16
Water Level (m)
122
123
124
1980
1990
2000
2010
Year
- - - Simulated
o Measured
WL_299-E27-16_CPM_V3.3_TMC_10-11-2010

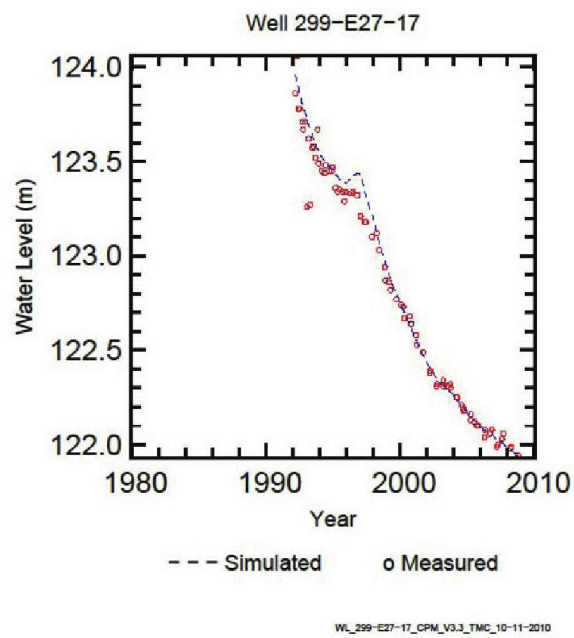
Well 299-E27-17
Water Level (m)
122.0
122.5
123.0
123.5
124.0
1980
1990
2000
2010
Year
- - - Simulated
o Measured
WL_299-E27-17_CPM_V3.3_TMC_10-11-2010

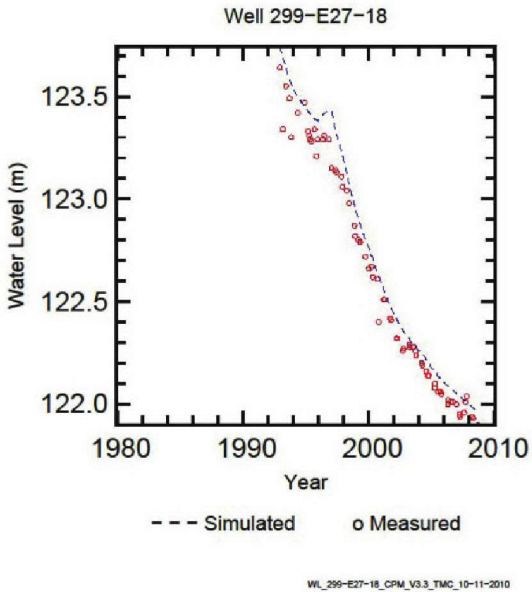
Well 299−E27−18
123.5
123.0
122.5
122.0
Water Level (m)
1980
1990
2000
2010
Year
- - - Simulated
o Measured
WL_299−E27−18_CPM_V3.3_TMC_10−11−2010

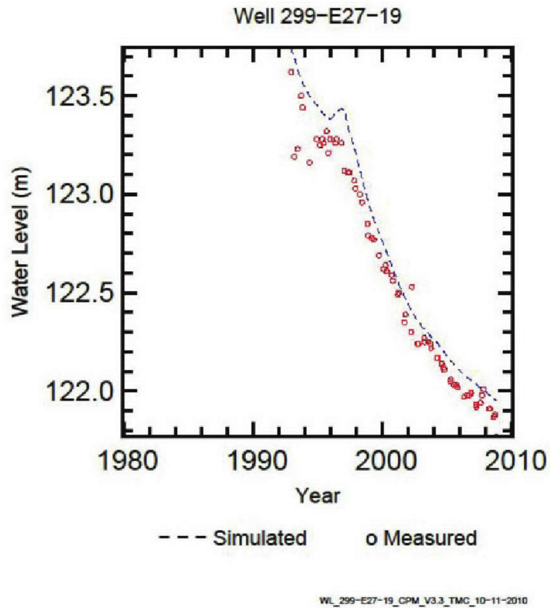
Well 299−E27−19
123.5
123.0
122.5
122.0
Water Level (m)
1980
1990
2000
2010
Year
- - - Simulated
o Measured
WL_299−E27−19_CPM_V3.3_TMC_10−11−2010

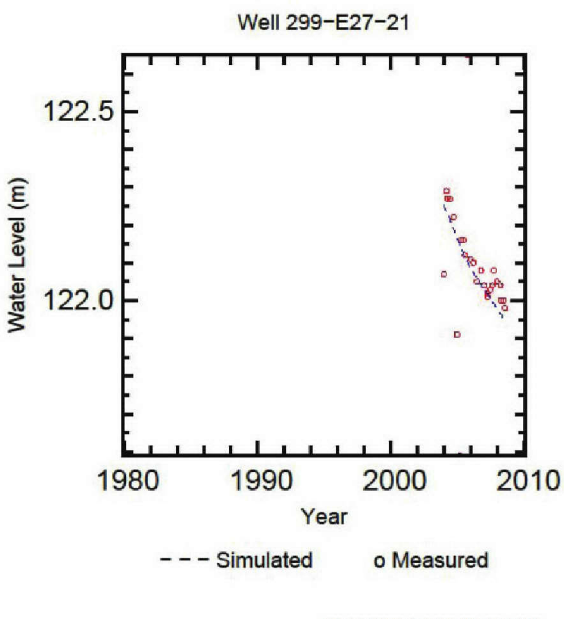
Well 299−E27−21
122.5
122.0
Water Level (m)
1980
1990
2000
2010
Year
- - - Simulated
o Measured
WL_299−E27−21_CPM_V3.3_TMC_10−11−2010

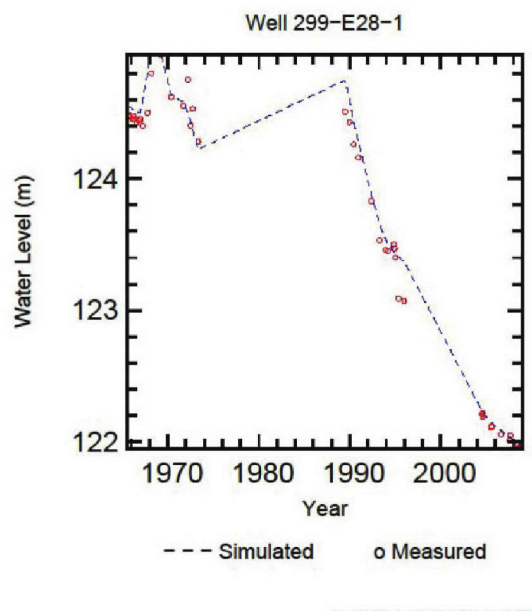
Well 299−E28−1
124
123
122
Water Level (m)
1970
1980
1990
2000
Year
- - - Simulated
o Measured
WL_299−E28−1_CPM_V3.3_TMC_10−11−2010

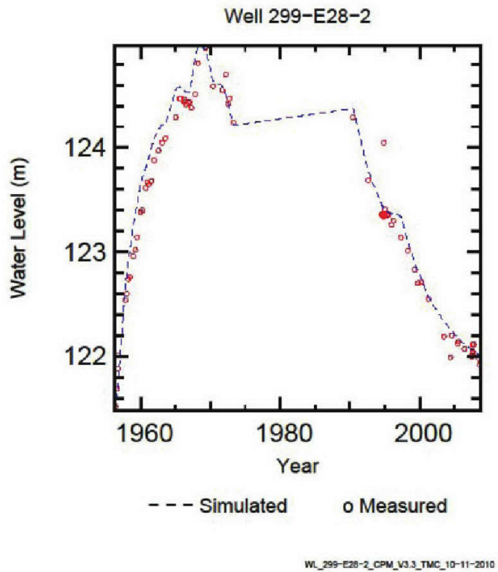
Well 299-E28-2
Water Level (m)
124
123
122
1960
1980
2000
Year
- - - Simulated
o Measured
WL_299-E28-2_CPM_V3.3_TMC_10-11-2010

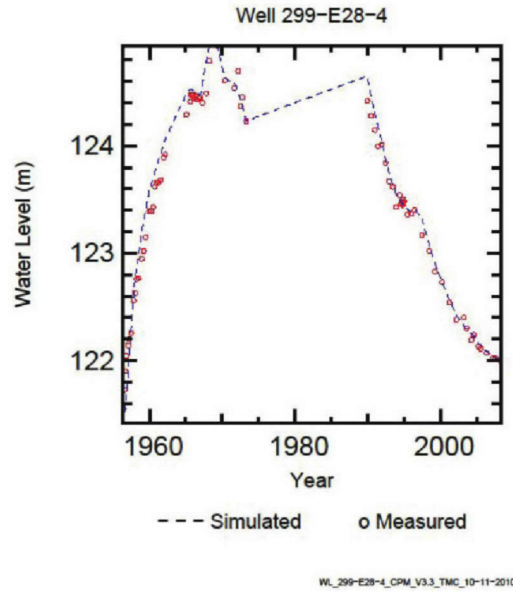
Well 299-E28-4
Water Level (m)
124
123
122
1960
1980
2000
Year
- - - Simulated
o Measured
WL_299-E28-4_CPM_V3.3_TMC_10-11-2010

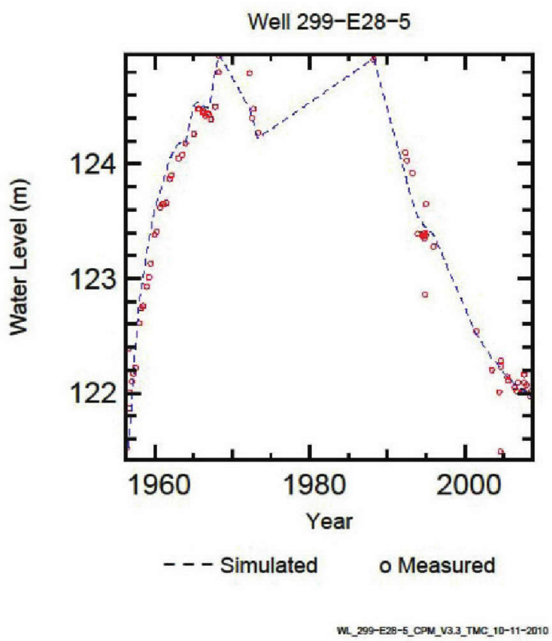
Well 299-E28-5
Water Level (m)
124
123
122
1960
1980
2000
Year
- - - Simulated
o Measured
WL_299-E28-5_CPM_V3.3_TMC_10-11-2010

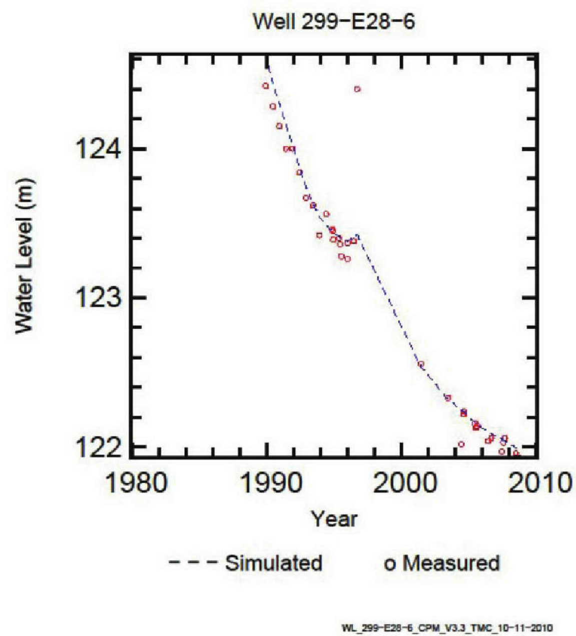
Well 299-E28-6
Water Level (m)
124
123
122
1980
1990
2000
2010
Year
- - - Simulated
o Measured
WL_299-E28-6_CPM_V3.3_TMC_10-11-2010

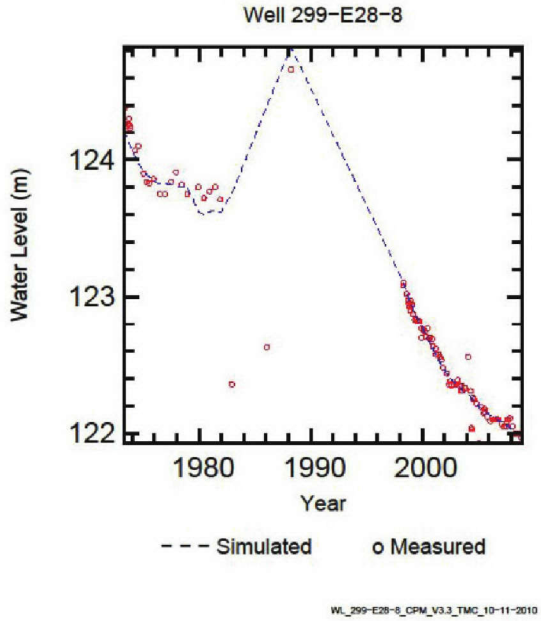
Well 299−E28−8
Water Level (m)
124
123
122
1980
1990
2000
Year
- - - Simulated
o Measured
WL_299-E28-8_CPM_V3.3_TMC_10-11-2010

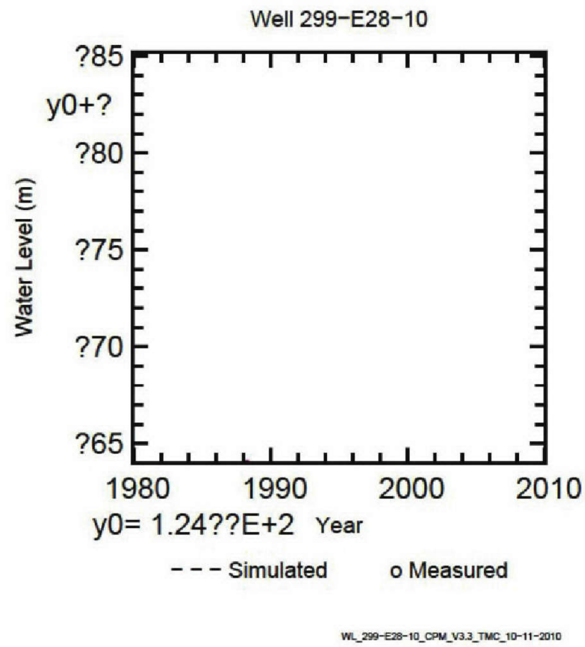
Well 299−E28−10
?85
y0+?
?80
?75
?70
?65
Water Level (m)
1980
1990
2000
2010
y0= 1.24??E+2
Year
- - - Simulated
o Measured
WL_299-E28-10_CPM_V3.3_TMC_10-11-2010

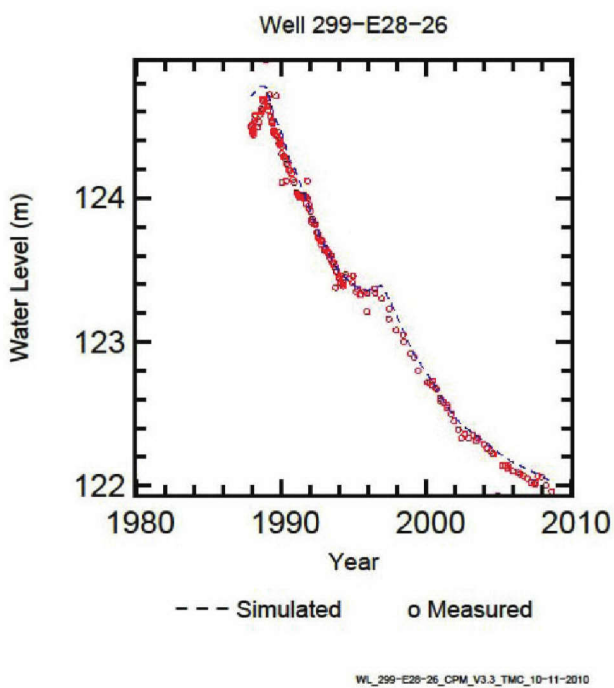
Well 299−E28−26
Water Level (m)
124
123
122
1980
1990
2000
2010
Year
- - - Simulated
o Measured
WL_299-E28-26_CPM_V3.3_TMC_10-11-2010

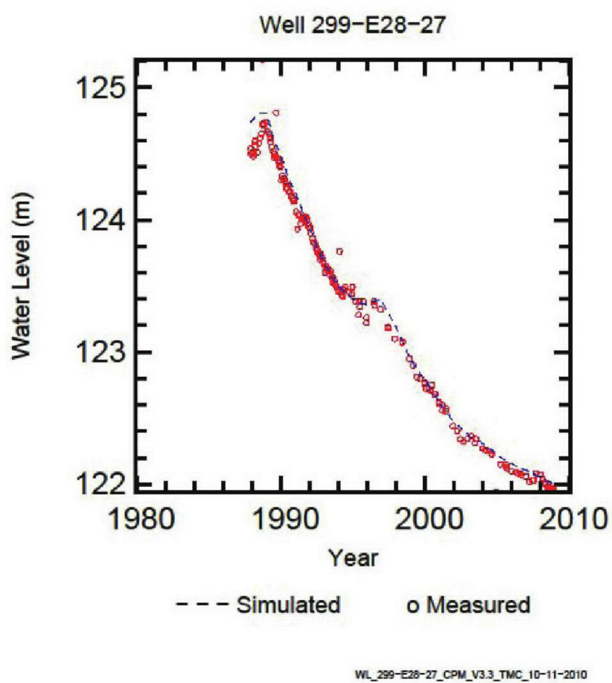
Well 299−E28−27
Water Level (m)
125
124
123
122
1980
1990
2000
2010
Year
- - - Simulated
o Measured
WL_299-E28-27_CPM_V3.3_TMC_10-11-2010

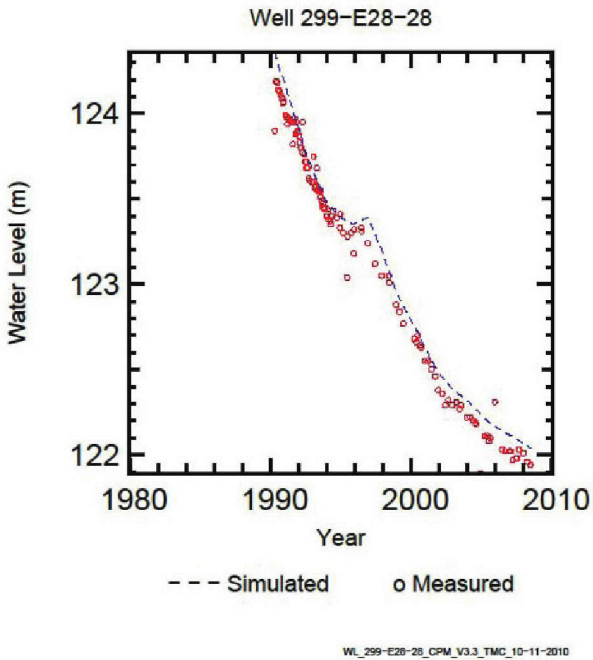
Well 299−E28−28
Water Level (m)
124
123
122
1980
1990
2000
2010
Year
- - - Simulated
o Measured
WL_299-E28-28_CPM_V3.3_TMC_10-11-2010

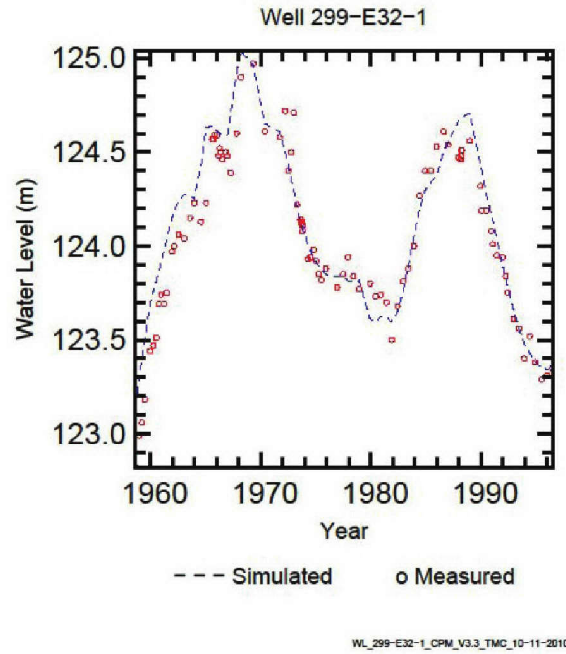
Well 299−E32−1
Water Level (m)
125.0
124.5
124.0
123.5
123.0
1960
1970
1980
1990
Year
- - - Simulated
o Measured
WL_299-E32-1_CPM_V3.3_TMC_10-11-2010

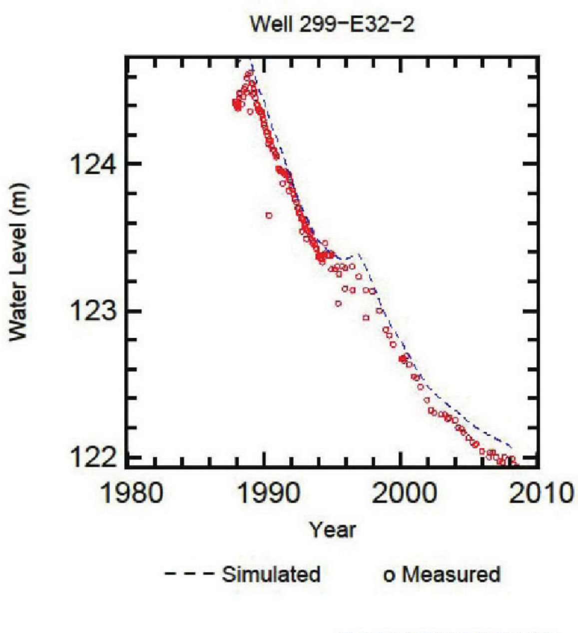
Well 299−E32−2
Water Level (m)
124
123
122
1980
1990
2000
2010
Year
- - - Simulated
o Measured
WL_299-E32-2_CPM_V3.3_TMC_10-11-2010

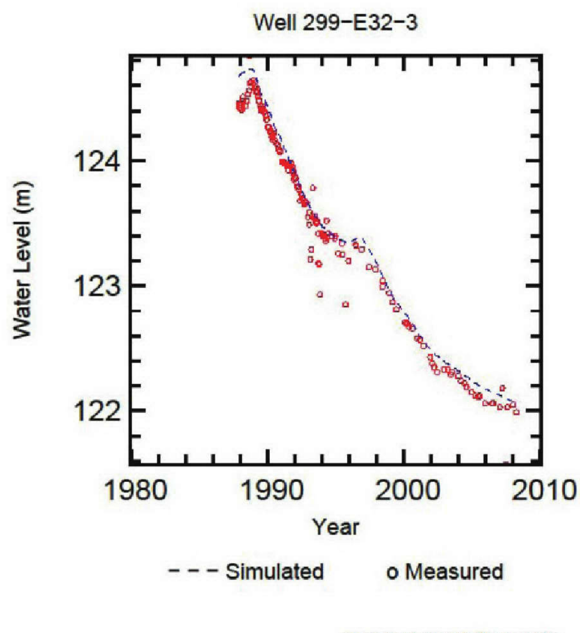
Well 299−E32−3
Water Level (m)
124
123
122
1980
1990
2000
2010
Year
- - - Simulated
o Measured
WL_299-E32-3_CPM_V3.3_TMC_10-11-2010

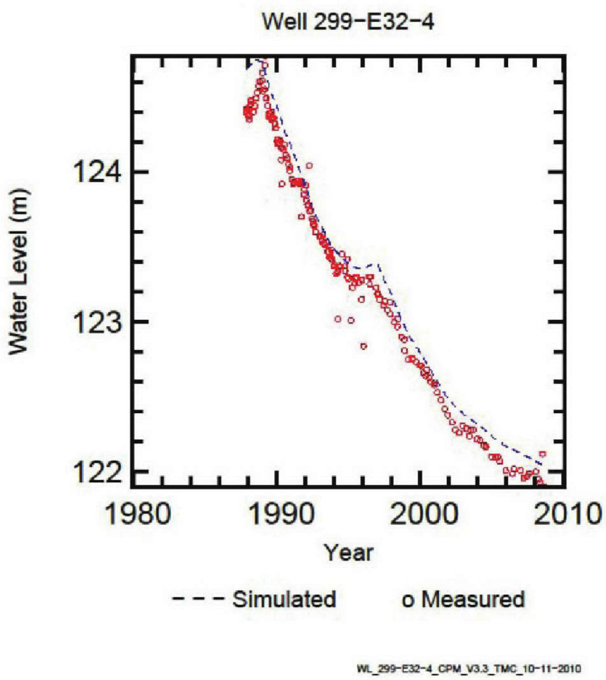
Well 299−E32−4
Water Level (m)
122
123
124
1980
1990
2000
2010
Year
- - - Simulated
o Measured
WL_299-E32-4_CPM_V3.3_TMC_10-11-2010

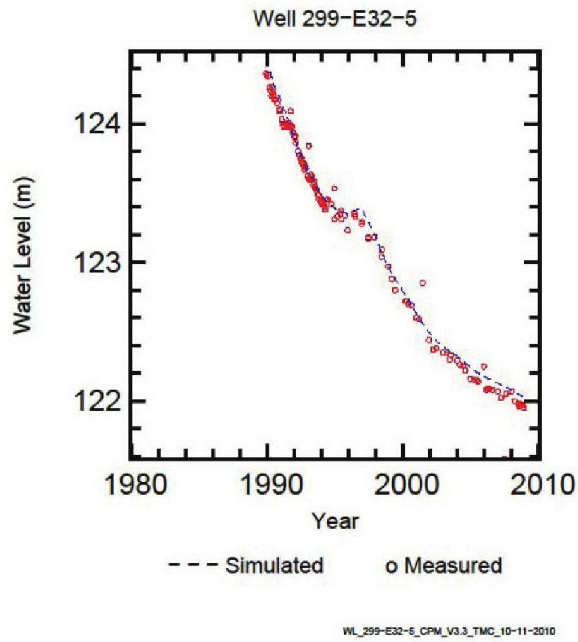
Well 299−E32−5
Water Level (m)
122
123
124
1980
1990
2000
2010
Year
- - - Simulated
o Measured
WL_299-E32-5_CPM_V3.3_TMC_10-11-2010

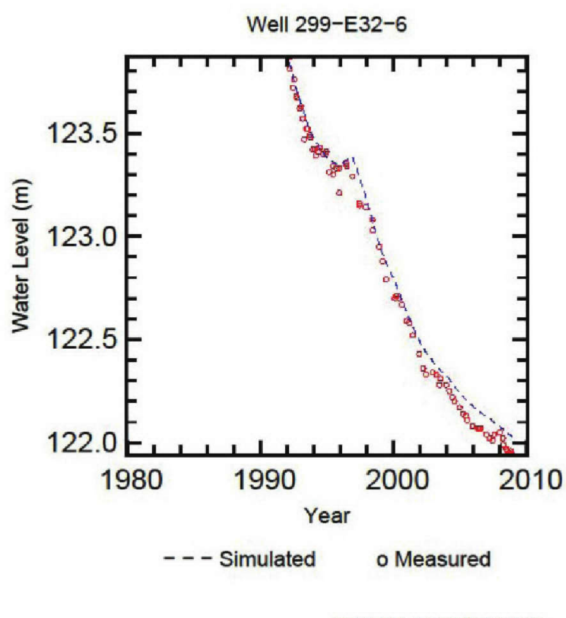
Well 299−E32−6
Water Level (m)
122.0
122.5
123.0
123.5
1980
1990
2000
2010
Year
- - - Simulated
o Measured
WL_299-E32-6_CPM_V3.3_TMC_10-11-2010

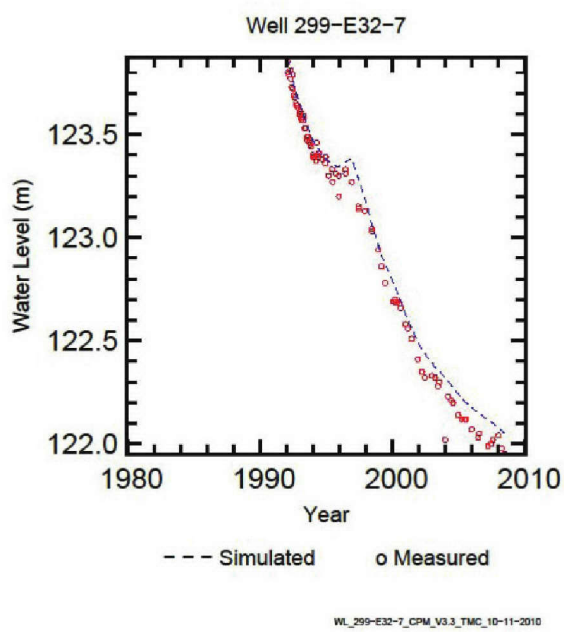
Well 299−E32−7
Water Level (m)
122.0
122.5
123.0
123.5
1980
1990
2000
2010
Year
- - - Simulated
o Measured
WL_299-E32-7_CPM_V3.3_TMC_10-11-2010

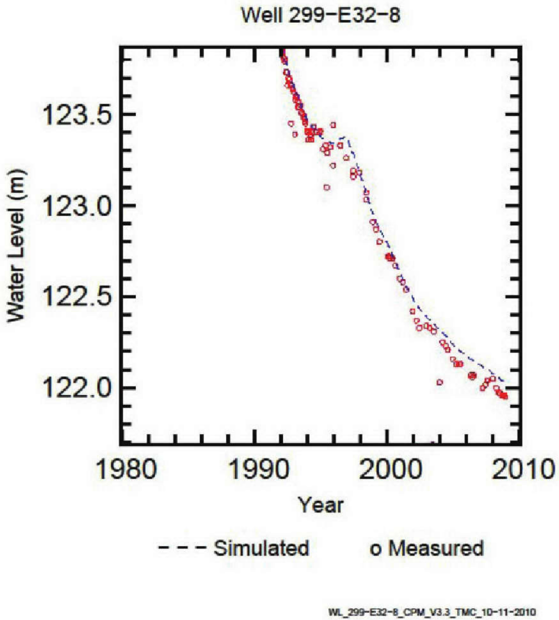
Well 299−E32−8
Water Level (m)
123.5
123.0
122.5
122.0
1980
1990
2000
2010
Year
- - - Simulated
o Measured
WL_299−E32−8_CPM_V3.3_TMC_10−11−2010

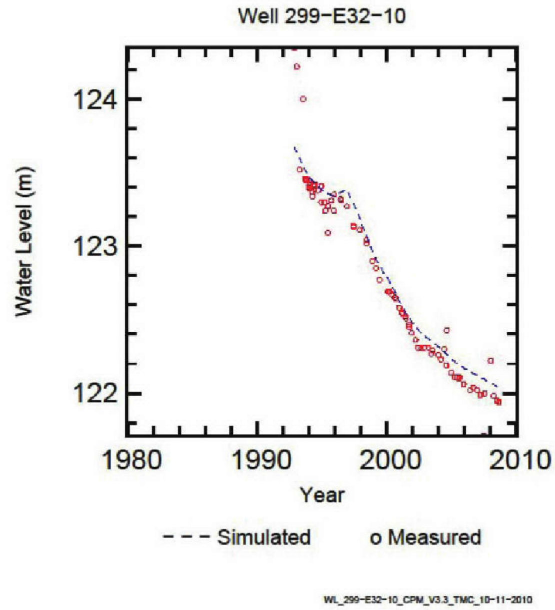
Well 299−E32−10
Water Level (m)
124
123
122
1980
1990
2000
2010
Year
- - - Simulated
o Measured
WL_299−E32−10_CPM_V3.3_TMC_10−11−2010

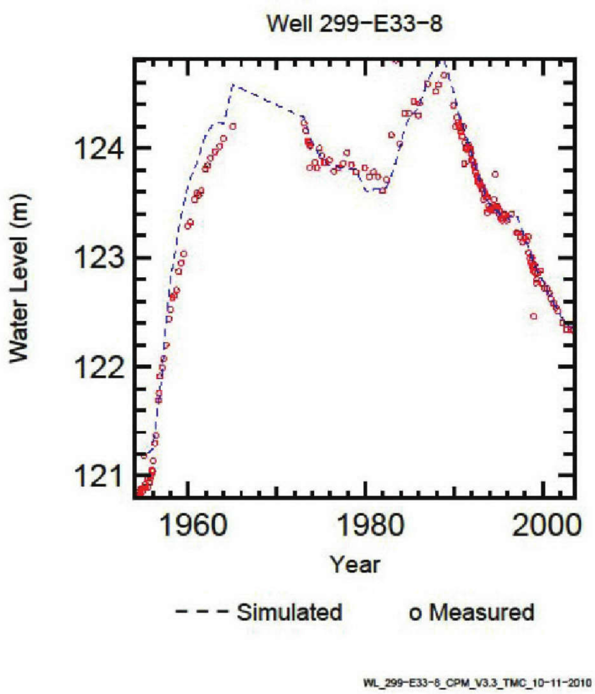
Well 299−E33−8
Water Level (m)
124
123
122
121
1960
1980
2000
Year
- - - Simulated
o Measured
WL_299−E33−8_CPM_V3.3_TMC_10−11−2010

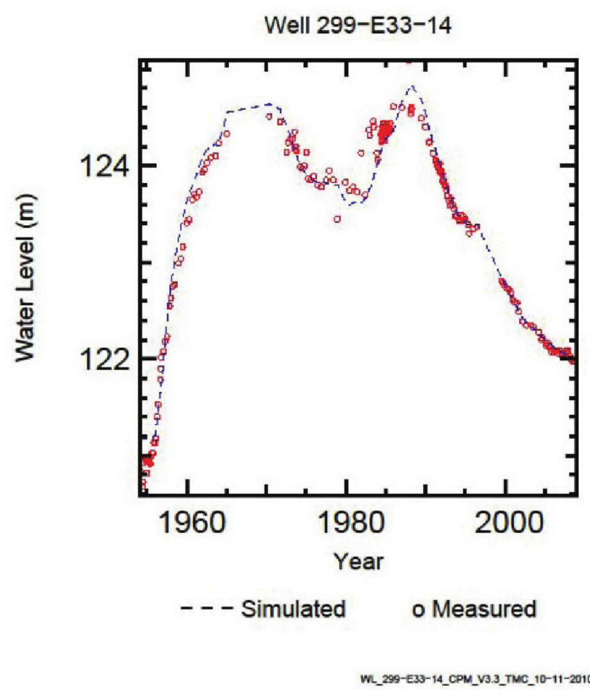
Well 299−E33−14
Water Level (m)
124
122
1960
1980
2000
Year
- - - Simulated
o Measured
WL_299−E33−14_CPM_V3.3_TMC_10−11−2010

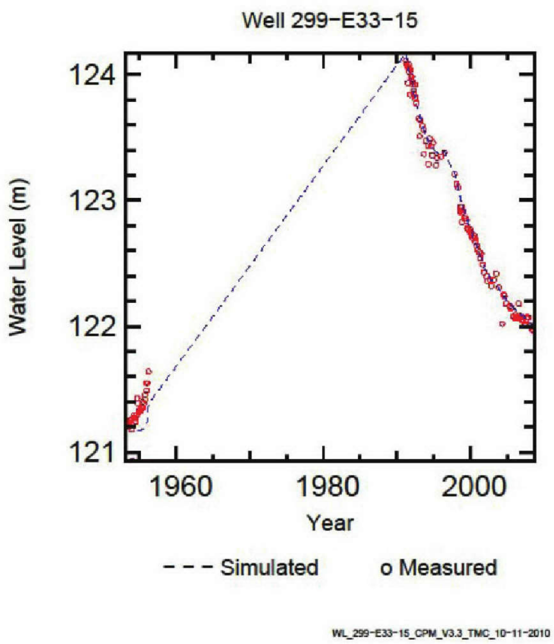
Well 299-E33-15
124
123
122
121
Water Level (m)
1960
1980
2000
Year
- - - Simulated
o Measured
WL_299-E33-15_CPM_V3.3_TMC_10-11-2010

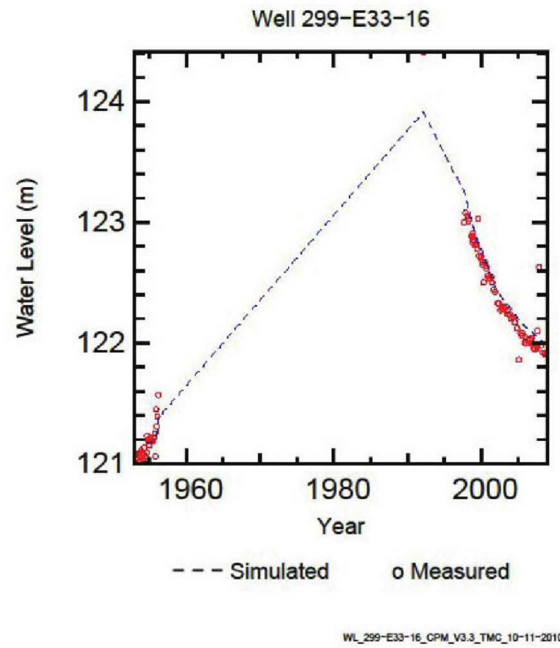
Well 299-E33-16
124
123
122
121
Water Level (m)
1960
1980
2000
Year
- - - Simulated
o Measured
WL_299-E33-16_CPM_V3.3_TMC_10-11-2010

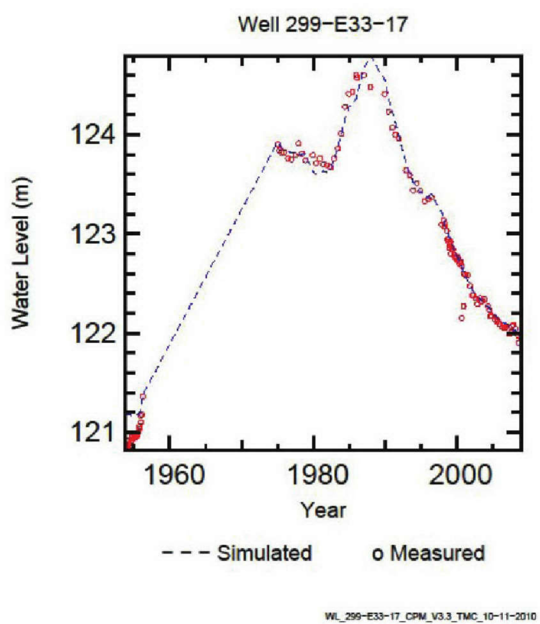
Well 299-E33-17
124
123
122
121
Water Level (m)
1960
1980
2000
Year
- - - Simulated
o Measured
WL_299-E33-17_CPM_V3.3_TMC_10-11-2010

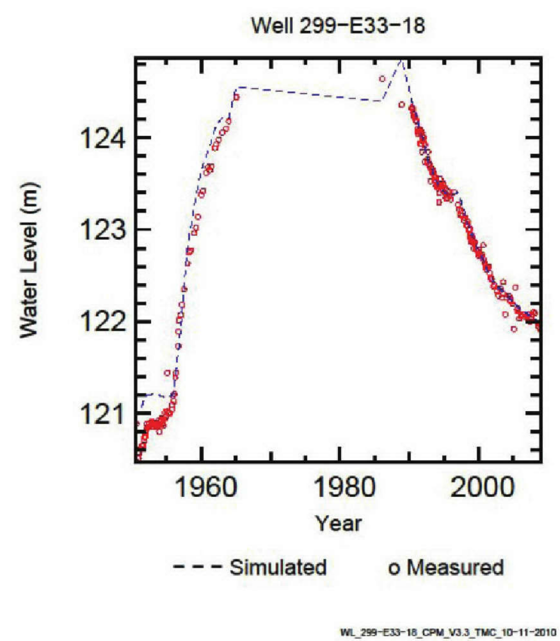
Well 299-E33-18
124
123
122
121
Water Level (m)
1960
1980
2000
Year
- - - Simulated
o Measured
WL_299-E33-18_CPM_V3.3_TMC_10-11-2010

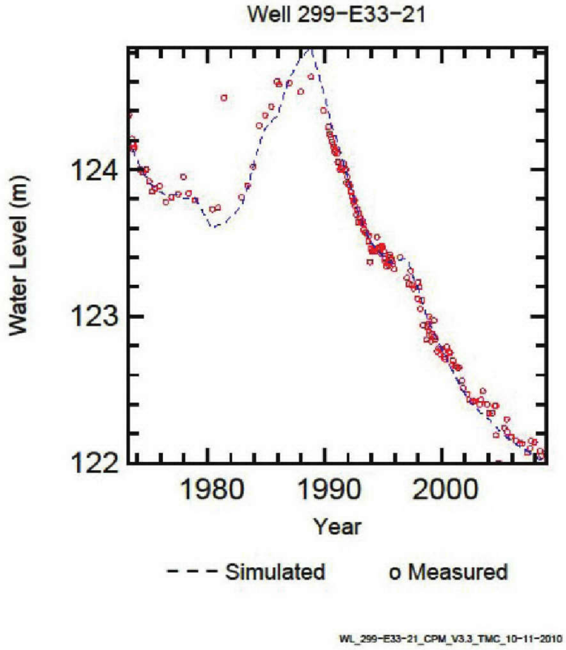
Well 299−E33−21
Water Level (m)
124
123
122
1980
1990
2000
Year
Simulated
o Measured
WL_299-E33-21_CPM_V3.3_TMC_10-11-2010

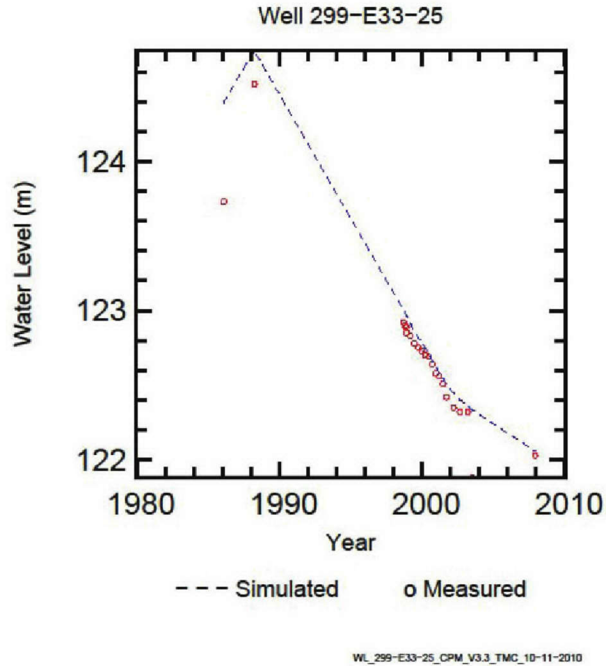
Well 299−E33−25
Water Level (m)
124
123
122
1980
1990
2000
2010
Year
Simulated
o Measured
WL_299-E33-25_CPM_V3.3_TMC_10-11-2010

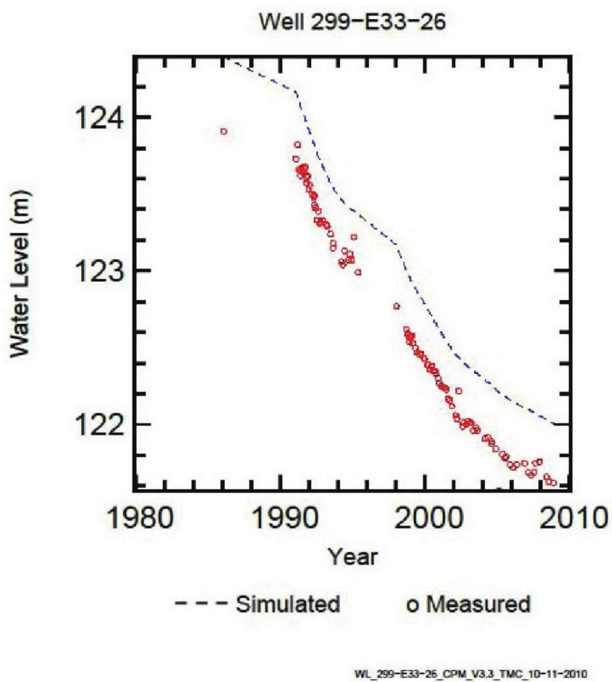
Well 299−E33−26
Water Level (m)
124
123
122
1980
1990
2000
2010
Year
Simulated
o Measured
WL_299-E33-26_CPM_V3.3_TMC_10-11-2010

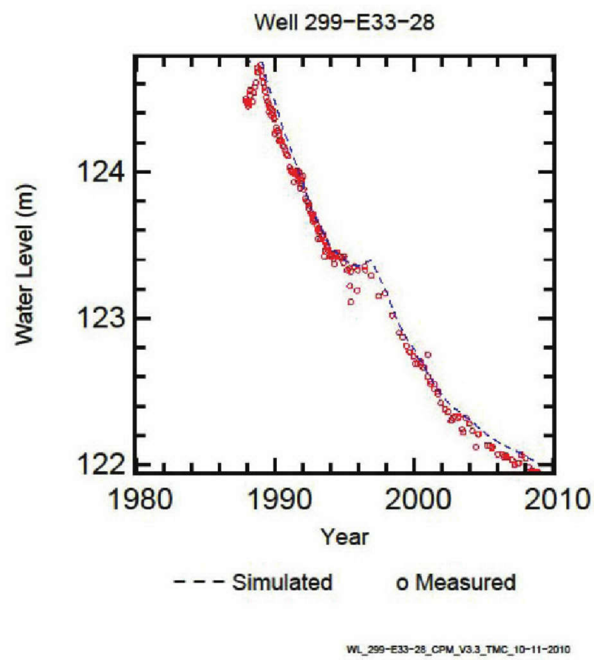
Well 299−E33−28
Water Level (m)
124
123
122
1980
1990
2000
2010
Year
Simulated
o Measured
WL_299-E33-28_CPM_V3.3_TMC_10-11-2010

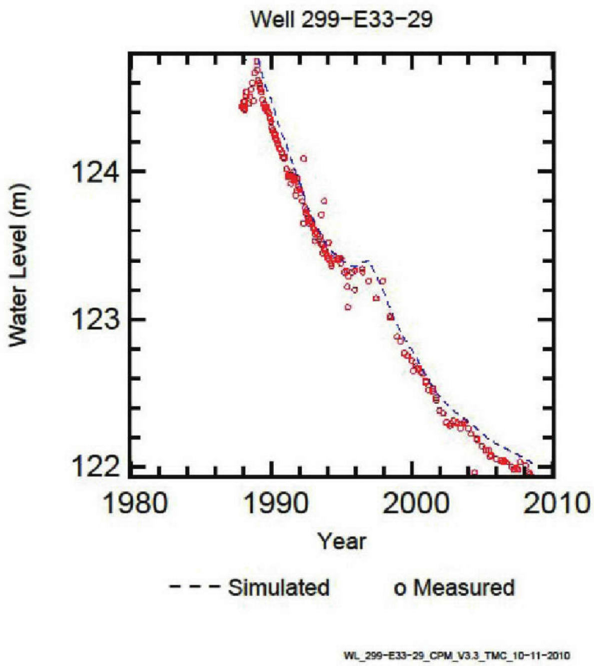
Well 299−E33−29
Water Level (m)
124
123
122
1980
1990
2000
2010
Year
- - - Simulated
o Measured
WL_299-E33-29_CPM_V3.3_TMC_10-11-2010

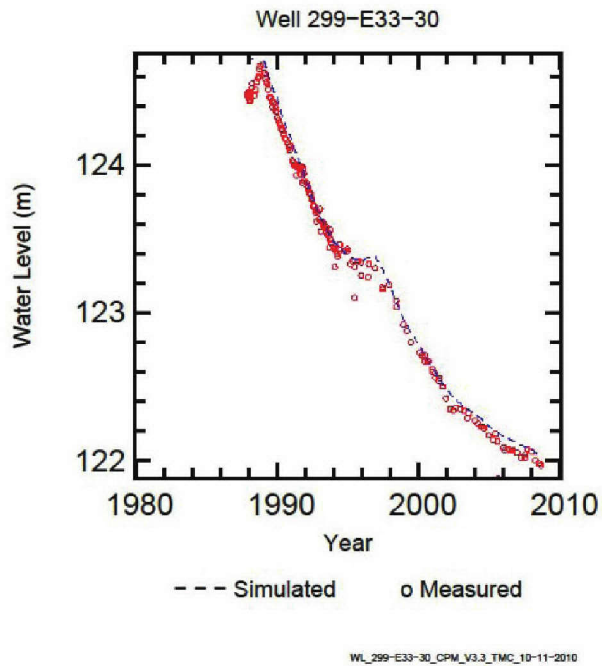
Well 299−E33−30
Water Level (m)
124
123
122
1980
1990
2000
2010
Year
- - - Simulated
o Measured
WL_299-E33-30_CPM_V3.3_TMC_10-11-2010

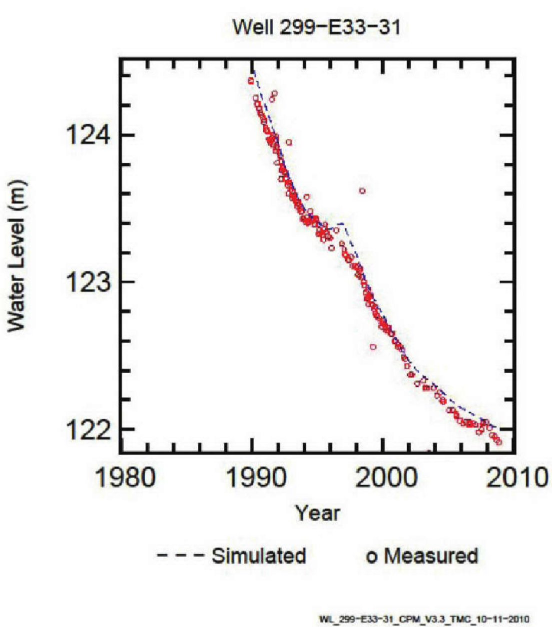
Well 299−E33−31
Water Level (m)
124
123
122
1980
1990
2000
2010
Year
- - - Simulated
o Measured
WL_299-E33-31_CPM_V3.3_TMC_10-11-2010

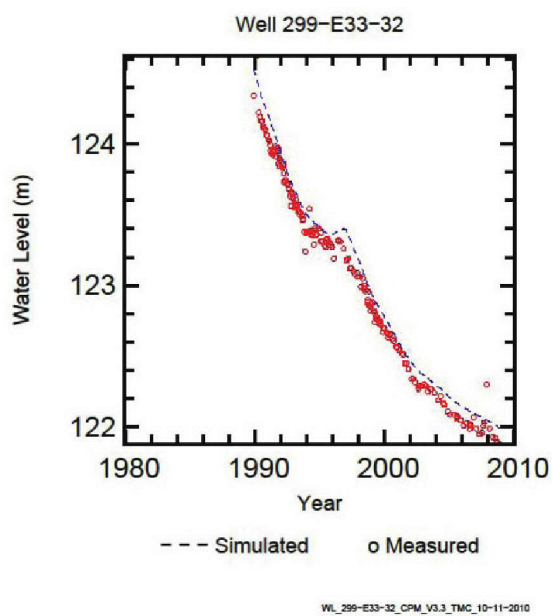
Well 299−E33−32
Water Level (m)
124
123
122
1980
1990
2000
2010
Year
- - - Simulated
o Measured
WL_299-E33-32_CPM_V3.3_TMC_10-11-2010

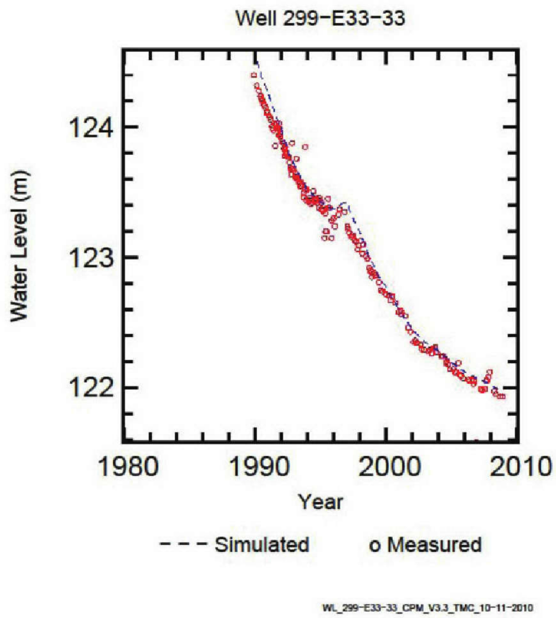
Well 299-E33-33
124
123
122
Water Level (m)
1980
1990
2000
2010
Year
- - - Simulated
o Measured
WL_299-E33-33_CPM_V3.3_TMC_10-11-2010

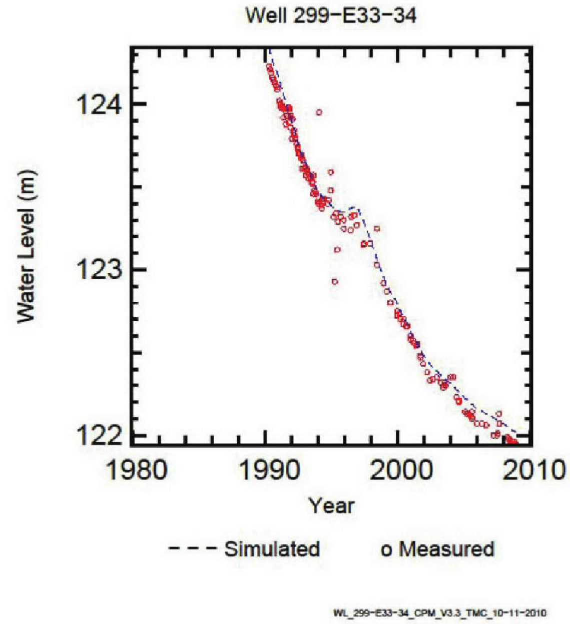
Well 299-E33-34
124
123
122
Water Level (m)
1980
1990
2000
2010
Year
- - - Simulated
o Measured
WL_299-E33-34_CPM_V3.3_TMC_10-11-2010

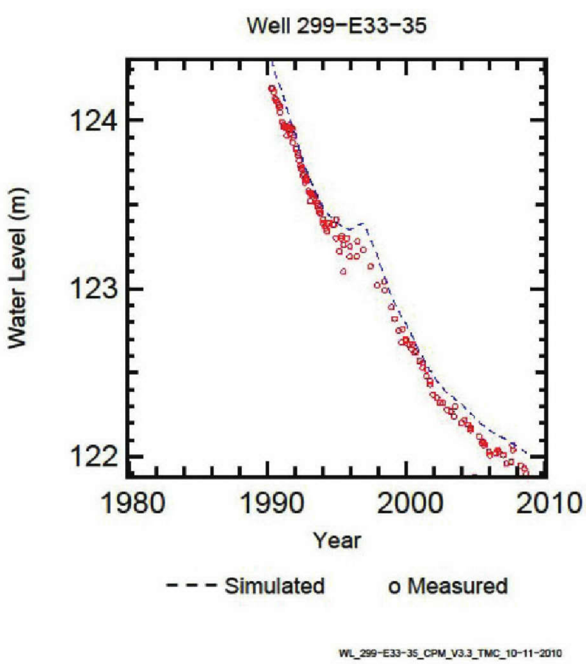
Well 299-E33-35
124
123
122
Water Level (m)
1980
1990
2000
2010
Year
- - - Simulated
o Measured
WL_299-E33-35_CPM_V3.3_TMC_10-11-2010

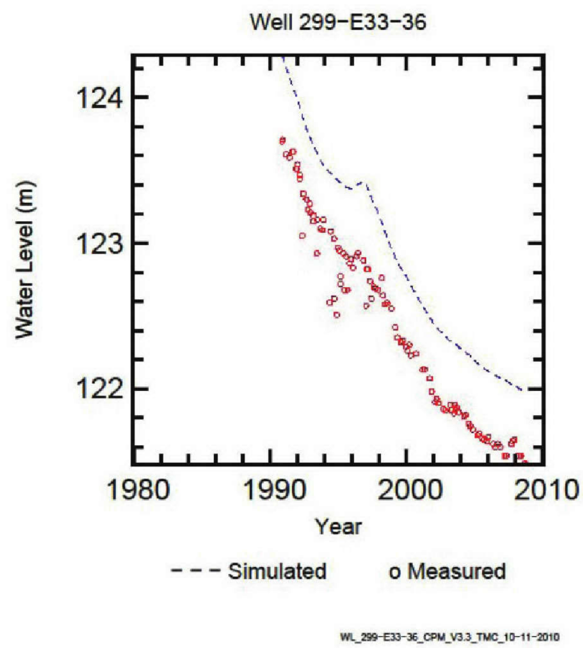
Well 299-E33-36
124
123
122
Water Level (m)
1980
1990
2000
2010
Year
- - - Simulated
o Measured
WL_299-E33-36_CPM_V3.3_TMC_10-11-2010

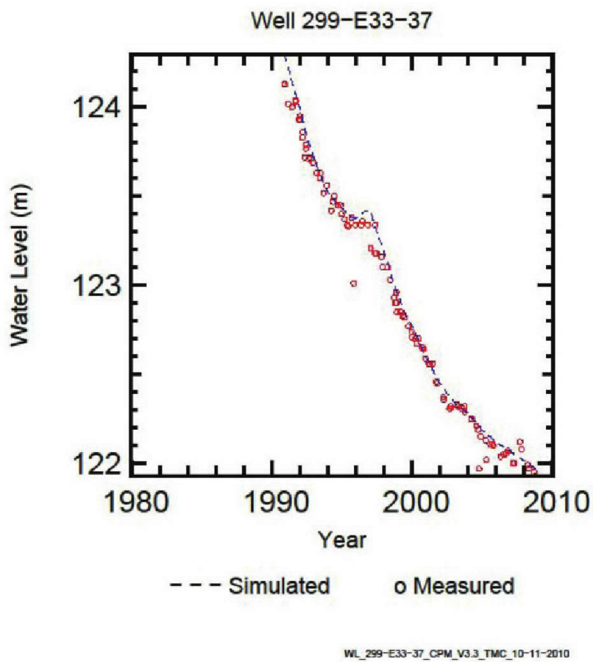
Well 299−E33−37
Water Level (m)
124
123
122
1980
1990
2000
2010
Year
- - - Simulated
o Measured
WL_299-E33-37_CPM_V3.3_TMC_10-11-2010

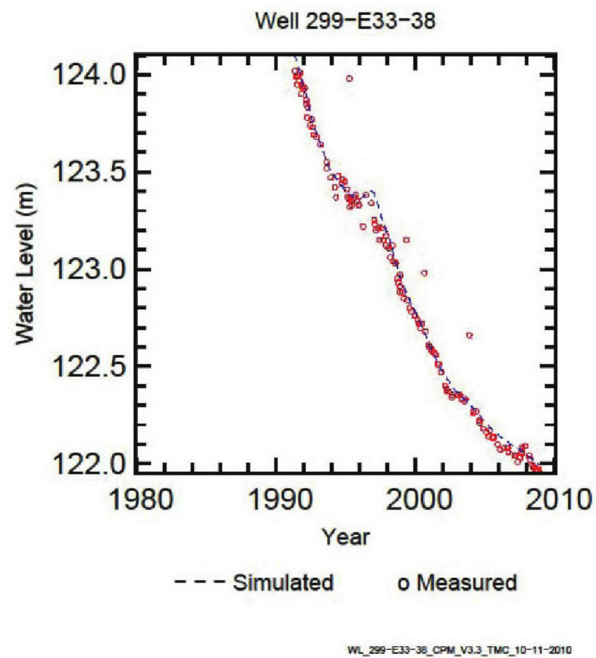
Well 299−E33−38
Water Level (m)
124.0
123.5
123.0
122.5
122.0
1980
1990
2000
2010
Year
- - - Simulated
o Measured
WL_299-E33-38_CPM_V3.3_TMC_10-11-2010

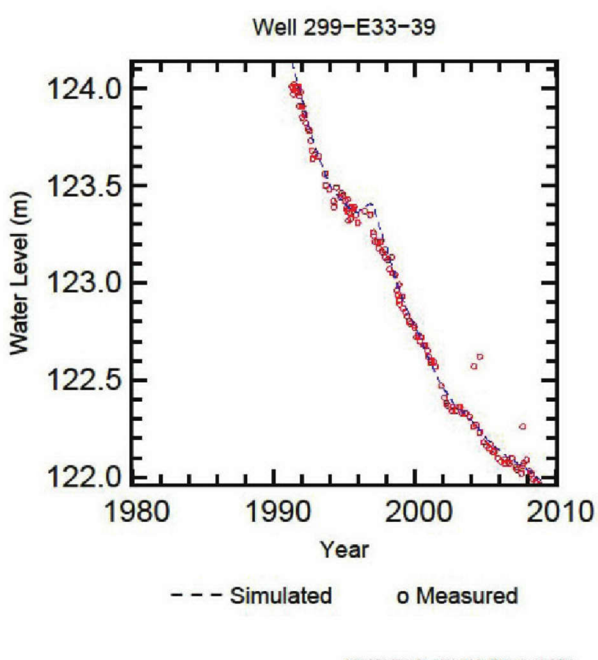
Well 299−E33−39
Water Level (m)
124.0
123.5
123.0
122.5
122.0
1980
1990
2000
2010
Year
- - - Simulated
o Measured
WL_299-E33-39_CPM_V3.3_TMC_10-11-2010

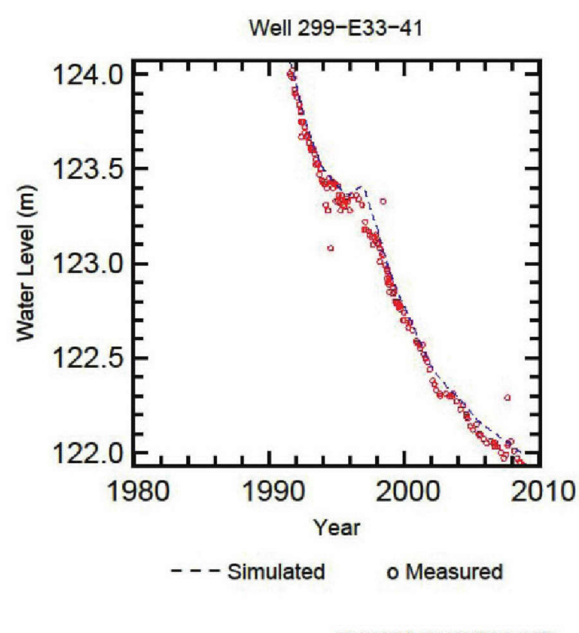
Well 299−E33−41
Water Level (m)
124.0
123.5
123.0
122.5
122.0
1980
1990
2000
2010
Year
- - - Simulated
o Measured
WL_299-E33-41_CPM_V3.3_TMC_10-11-2010

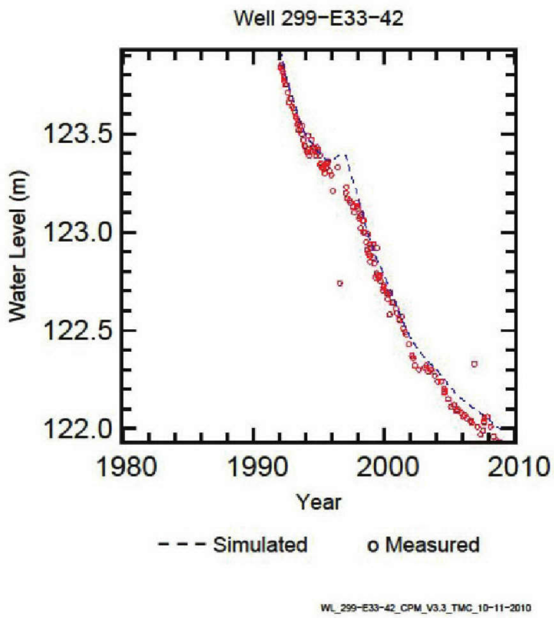
Well 299-E33-42
Water Level (m)
Year
--- Simulated
o Measured
WL_299-E33-42_CPM_V3.3_TMC_10-11-2010

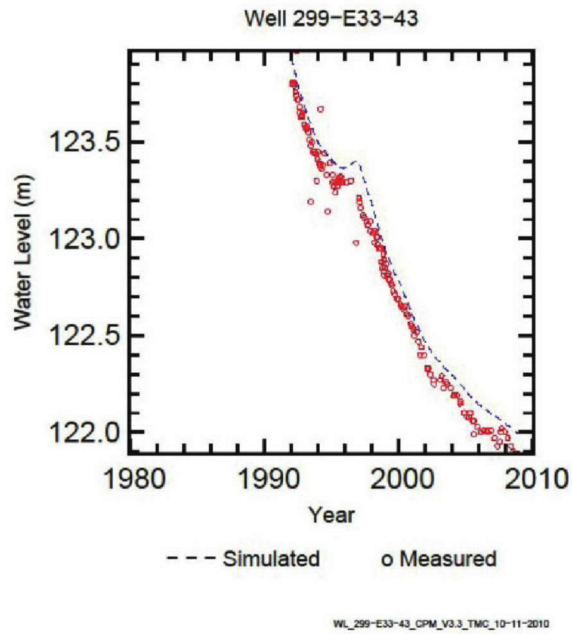
Well 299-E33-43
Water Level (m)
Year
--- Simulated
o Measured
WL_299-E33-43_CPM_V3.3_TMC_10-11-2010

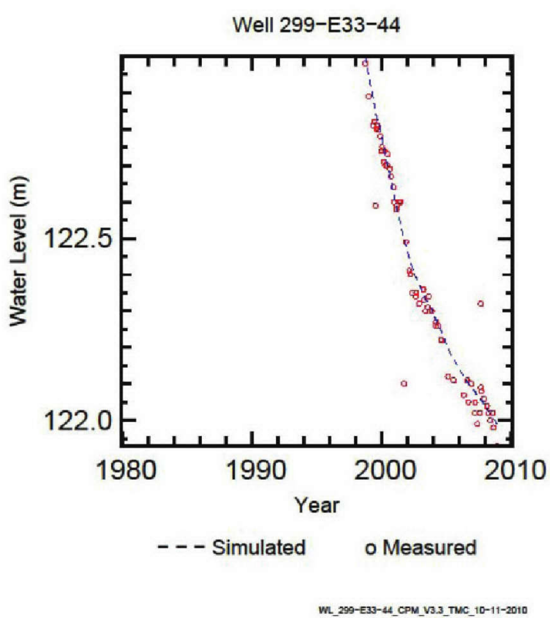
Well 299-E33-44
Water Level (m)
Year
--- Simulated
o Measured
WL_299-E33-44_CPM_V3.3_TMC_10-11-2010

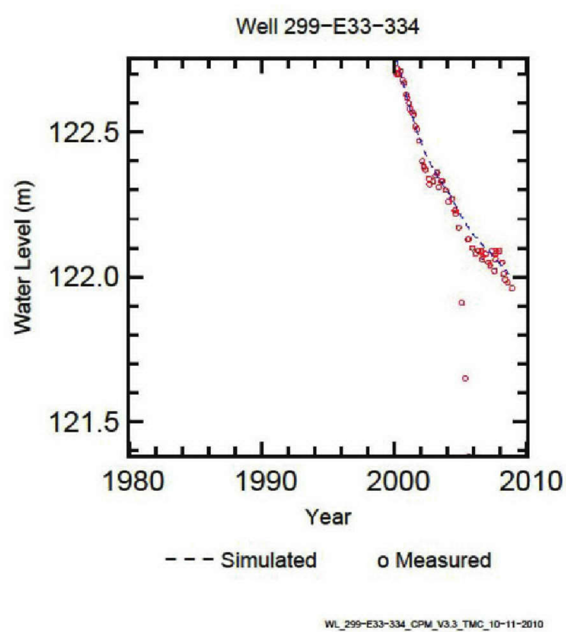
Well 299-E33-334
Water Level (m)
Year
--- Simulated
o Measured
WL_299-E33-334_CPM_V3.3_TMC_10-11-2010

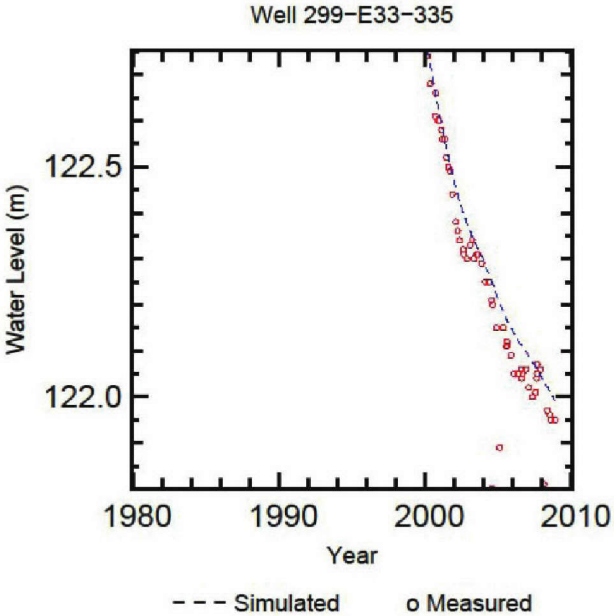

WL_299-E33-335_CPM_V3.3_TMC_10-11-2010

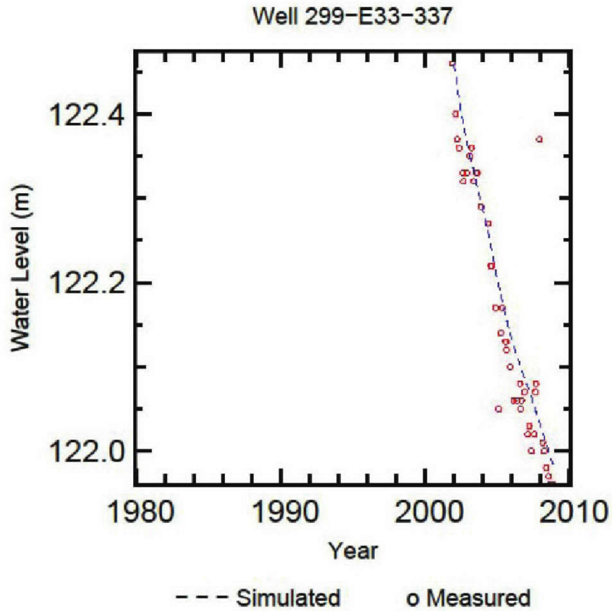

WL_299-E33-337_CPM_V3.3_TMC_10-11-2010

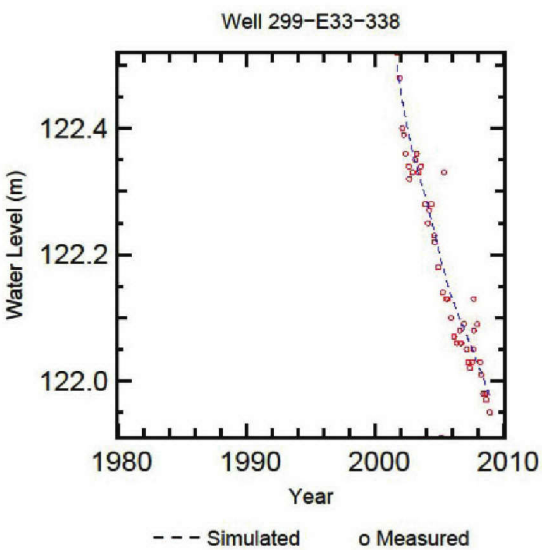

WL_299-E33-338_CPM_V3.3_TMC_10-11-2010

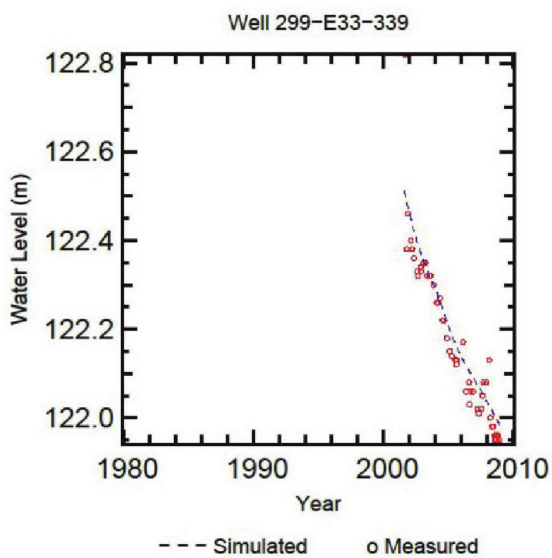

WL_299-E33-339_CPM_V3.3_TMC_10-11-2010

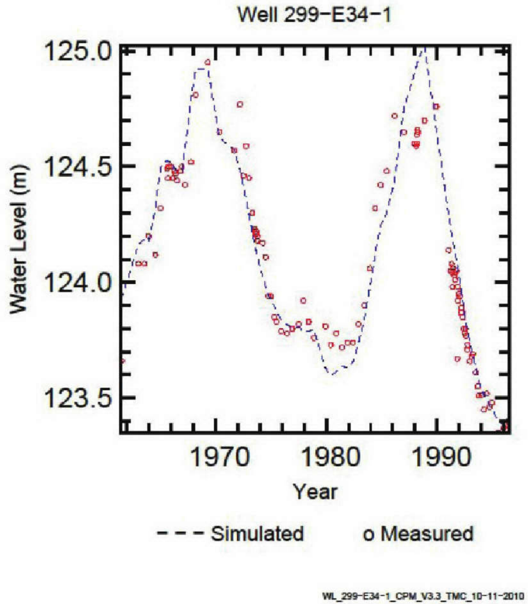
Well 299-E34-1
125.0
124.5
124.0
123.5
1970
1980
1990
Water Level (m)
Year
--- Simulated
o Measured
WL_299-E34-1_CPM_V3.3_TMC_10-11-2010

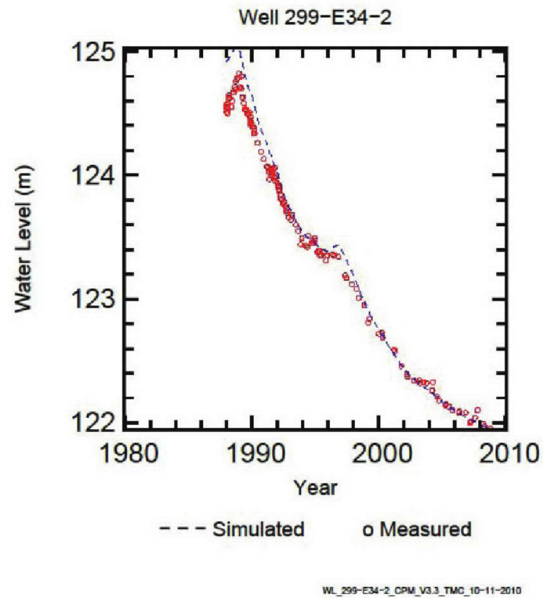
Well 299-E34-2
125
124
123
122
1980
1990
2000
2010
Water Level (m)
Year
--- Simulated
o Measured
WL_299-E34-2_CPM_V3.3_TMC_10-11-2010

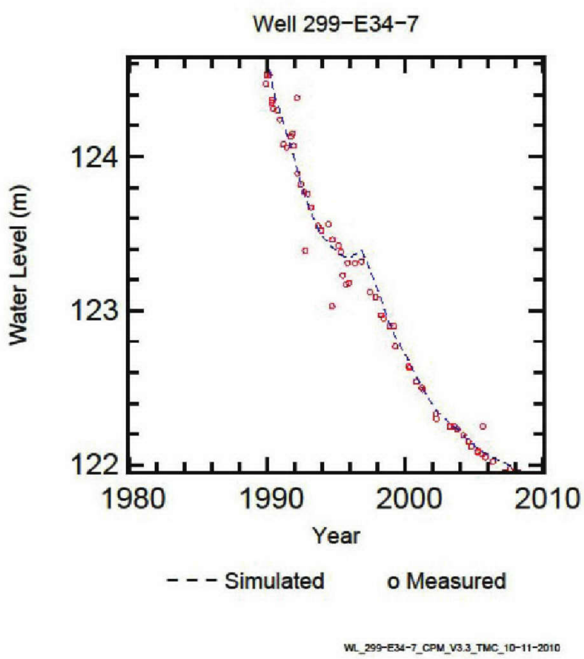
Well 299-E34-7
124
123
122
1980
1990
2000
2010
Water Level (m)
Year
--- Simulated
o Measured
WL_299-E34-7_CPM_V3.3_TMC_10-11-2010

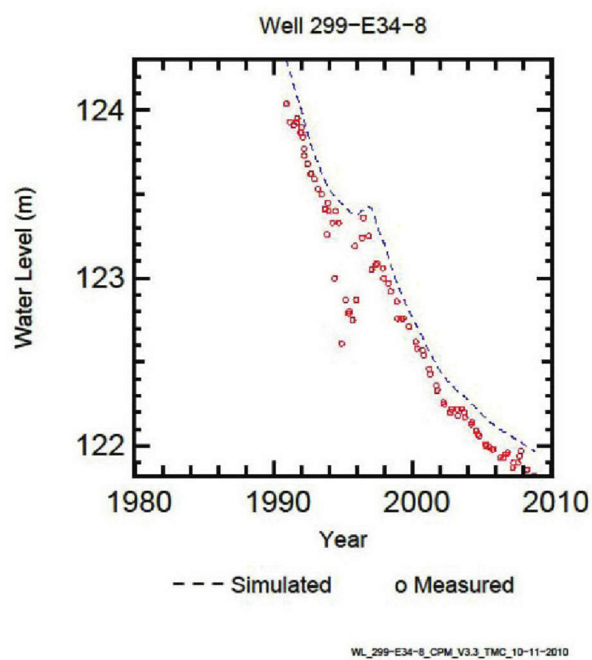
Well 299-E34-8
124
123
122
1980
1990
2000
2010
Water Level (m)
Year
--- Simulated
o Measured
WL_299-E34-8_CPM_V3.3_TMC_10-11-2010

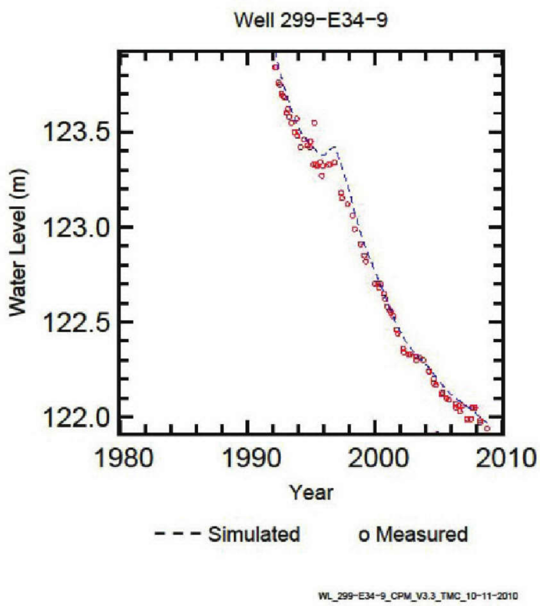
Well 299-E34-9
Water Level (m)
123.5
123.0
122.5
122.0
1980
1990
2000
2010
Year
- - - Simulated
o Measured
WL_299-E34-9_CPM_V3.3_TMC_10-11-2010

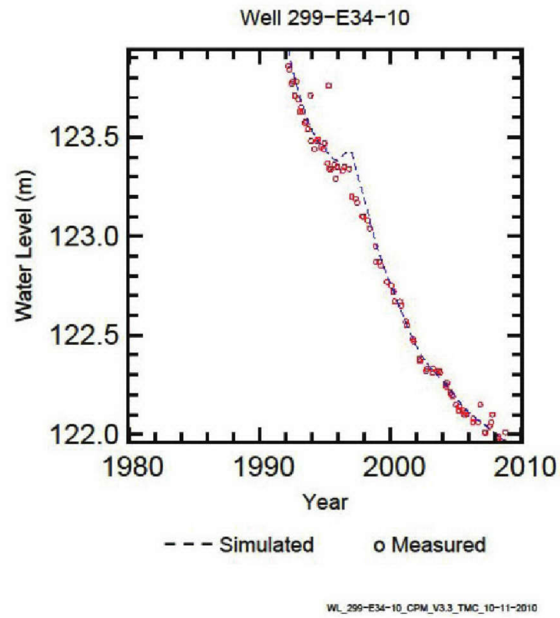
Well 299-E34-10
Water Level (m)
123.5
123.0
122.5
122.0
1980
1990
2000
2010
Year
- - - Simulated
o Measured
WL_299-E34-10_CPM_V3.3_TMC_10-11-2010

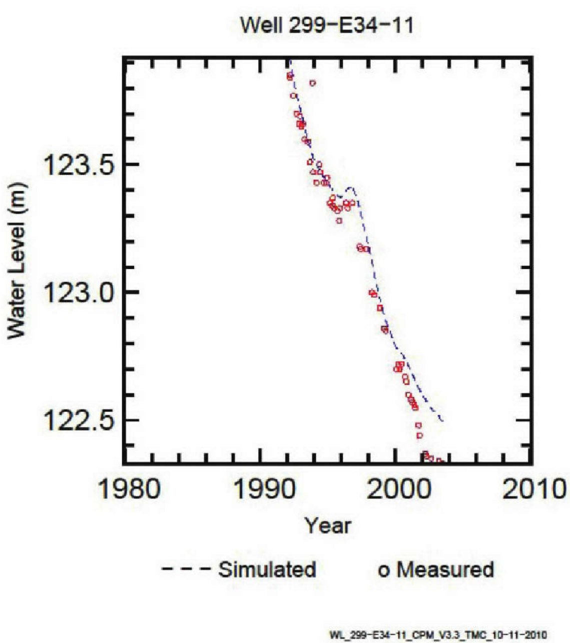
Well 299-E34-11
Water Level (m)
123.5
123.0
122.5
1980
1990
2000
2010
Year
- - - Simulated
o Measured
WL_299-E34-11_CPM_V3.3_TMC_10-11-2010

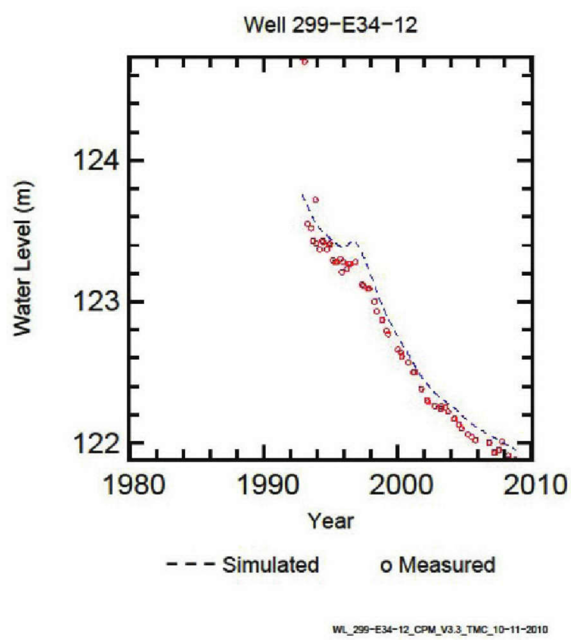
Well 299-E34-12
Water Level (m)
124
123
122
1980
1990
2000
2010
Year
- - - Simulated
o Measured
WL_299-E34-12_CPM_V3.3_TMC_10-11-2010

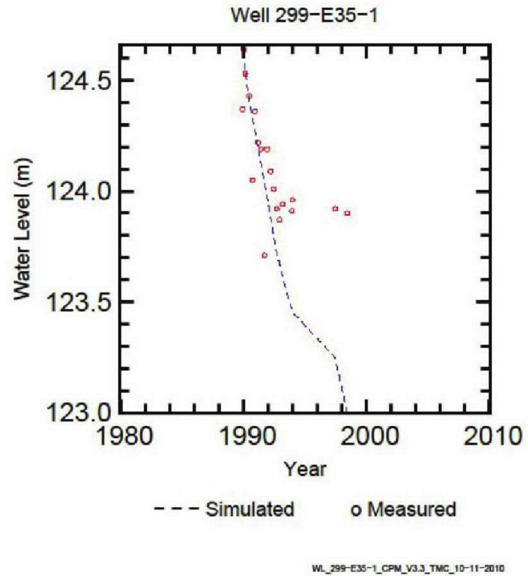
Well 299-E35-1
Water Level (m)
124.5
124.0
123.5
123.0
1980
1990
2000
2010
Year
- - - Simulated
o Measured
WL_299-E35-1_CPM_V3.3_TMC_10-11-2010

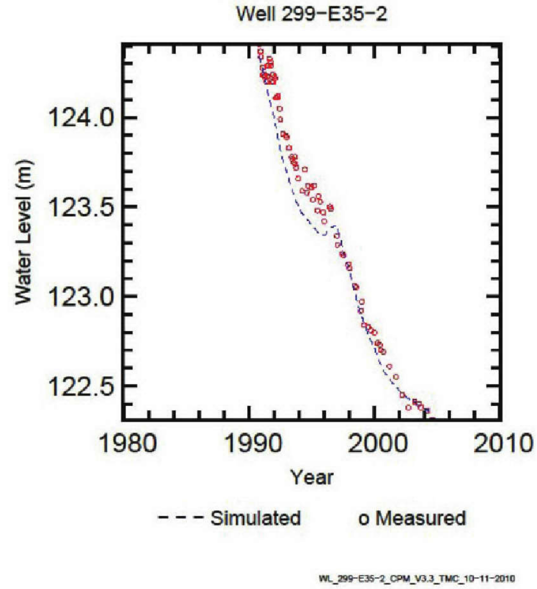
Well 299-E35-2
Water Level (m)
124.0
123.5
123.0
122.5
1980
1990
2000
2010
Year
- - - Simulated
o Measured
WL_299-E35-2_CPM_V3.3_TMC_10-11-2010

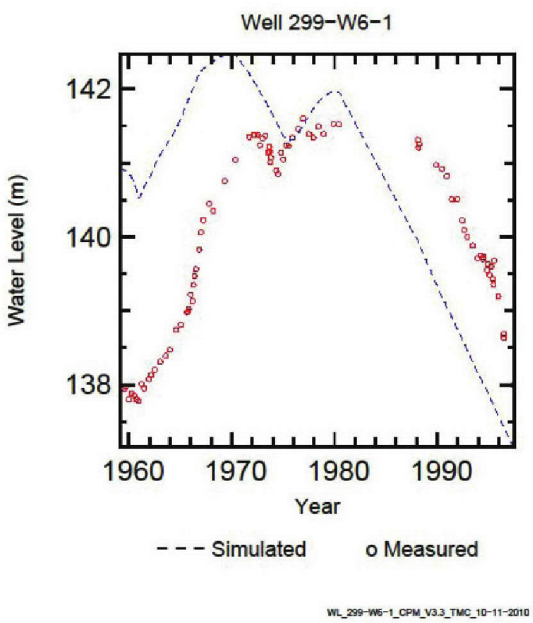
Well 299-W6-1
Water Level (m)
142
140
138
1960
1970
1980
1990
Year
- - - Simulated
o Measured
WL_299-W6-1_CPM_V3.3_TMC_10-11-2010

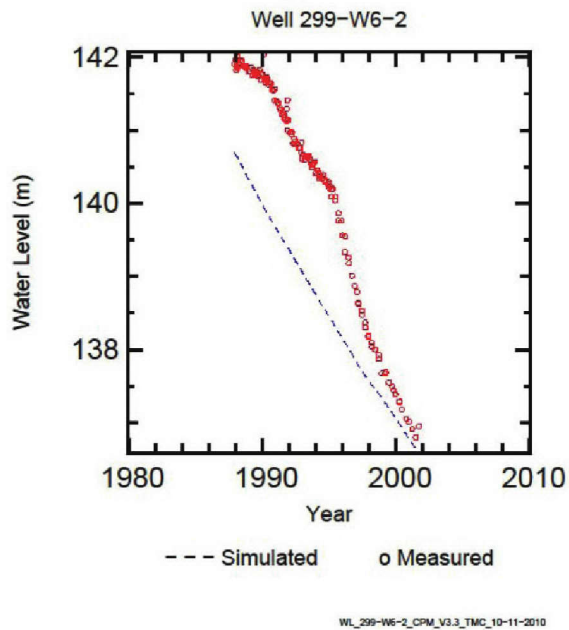
Well 299-W6-2
Water Level (m)
142
140
138
1980
1990
2000
2010
Year
- - - Simulated
o Measured
WL_299-W6-2_CPM_V3.3_TMC_10-11-2010

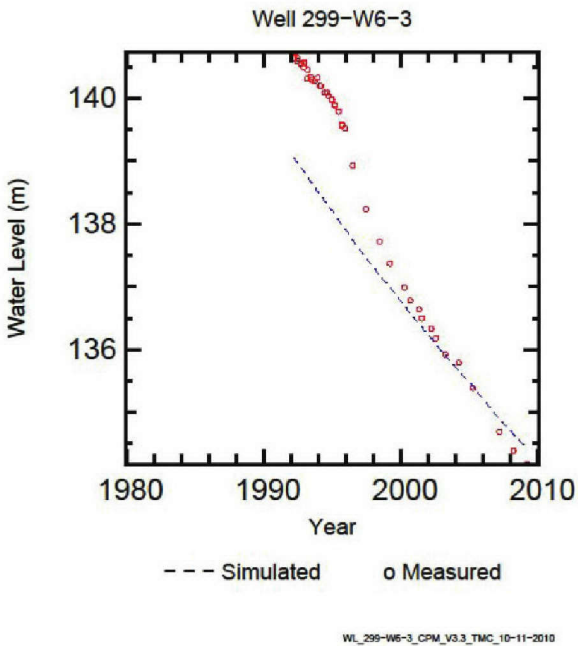
Well 299-W6-3
Water Level (m)
140
138
136
1980
1990
2000
2010
Year
Simulated
Measured
WL_299-W6-3_CPM_V3.3_TMC_10-11-2010

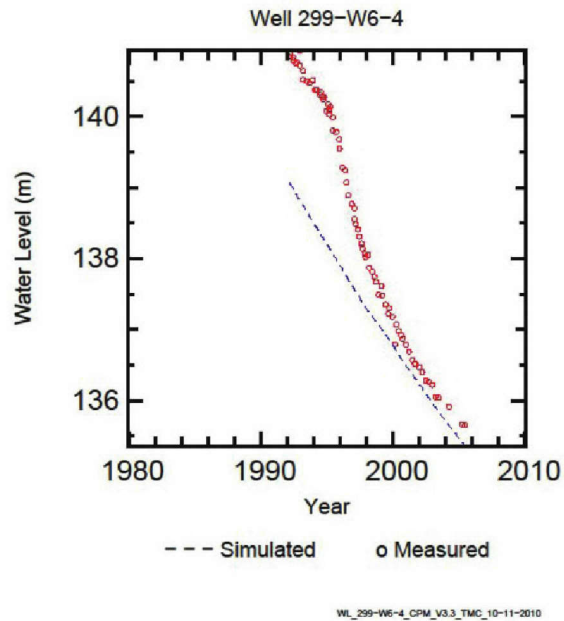
Well 299-W6-4
Water Level (m)
140
138
136
1980
1990
2000
2010
Year
Simulated
Measured
WL_299-W6-4_CPM_V3.3_TMC_10-11-2010

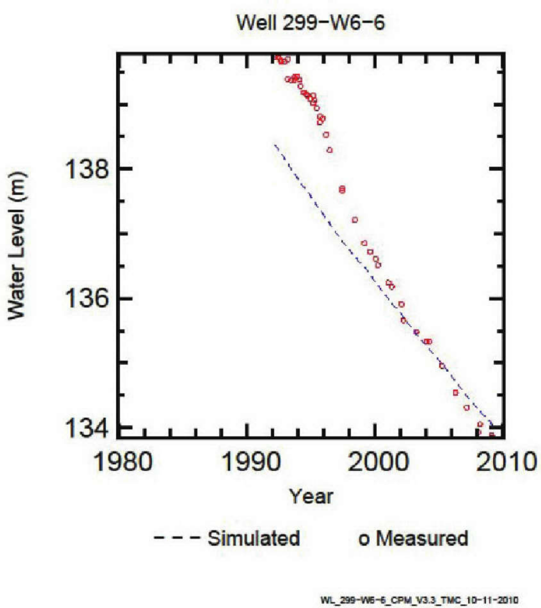
Well 299-W6-6
Water Level (m)
138
136
134
1980
1990
2000
2010
Year
Simulated
Measured
WL_299-W6-6_CPM_V3.3_TMC_10-11-2010

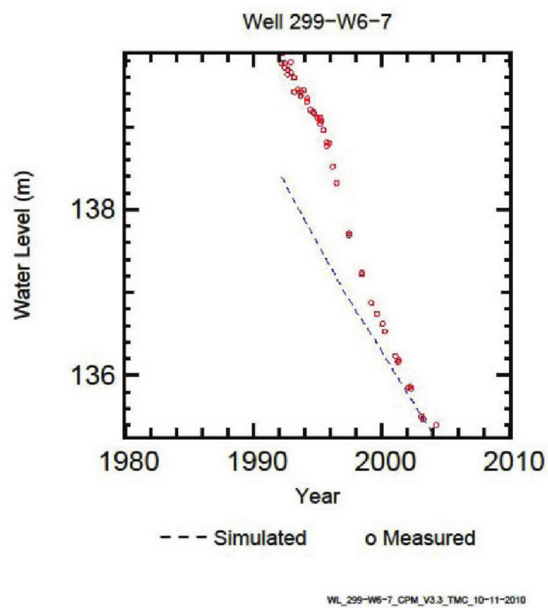
Well 299-W6-7
Water Level (m)
138
136
1980
1990
2000
2010
Year
Simulated
Measured
WL_299-W6-7_CPM_V3.3_TMC_10-11-2010

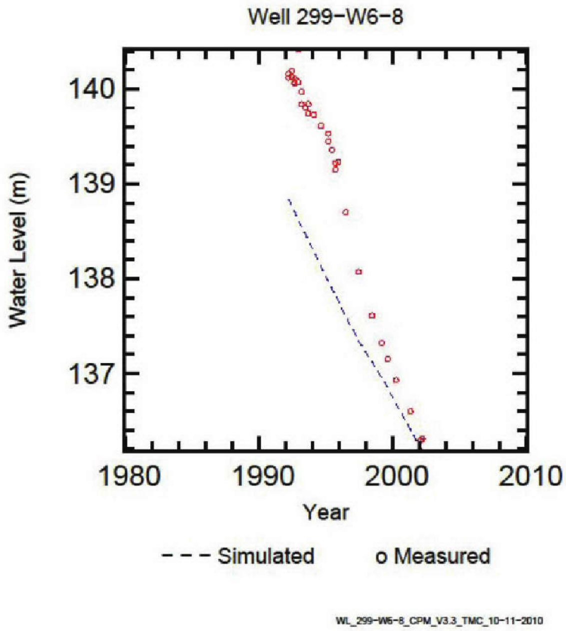
Well 299-W6-8
Water Level (m)
140
139
138
137
1980
1990
2000
2010
Year
- - - Simulated
o Measured
WL_299-W6-8_CPM_V3.3_TMC_10-11-2010

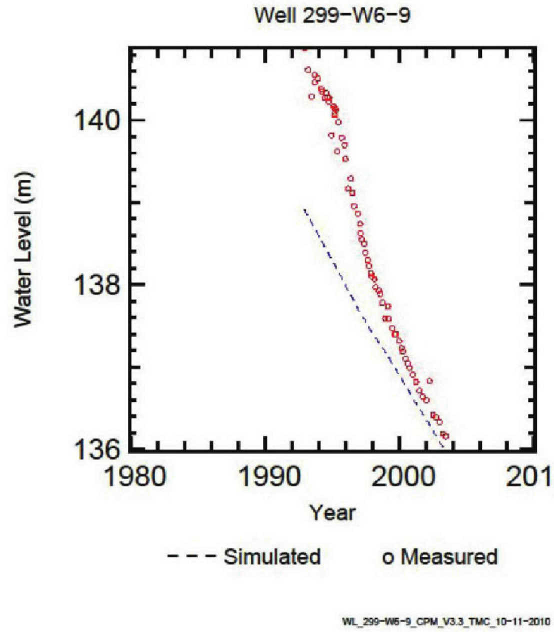
Well 299-W6-9
Water Level (m)
140
138
136
1980
1990
2000
2010
Year
- - - Simulated
o Measured
WL_299-W6-9_CPM_V3.3_TMC_10-11-2010

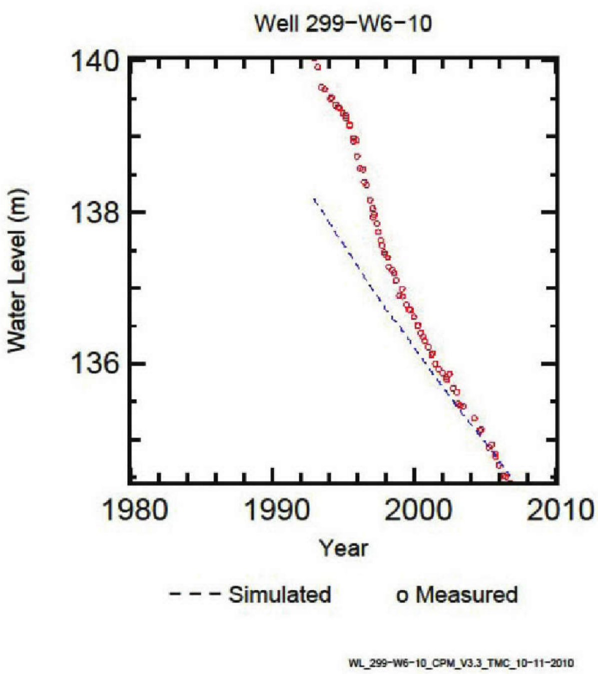
Well 299-W6-10
Water Level (m)
140
138
136
1980
1990
2000
2010
Year
- - - Simulated
o Measured
WL_299-W6-10_CPM_V3.3_TMC_10-11-2010

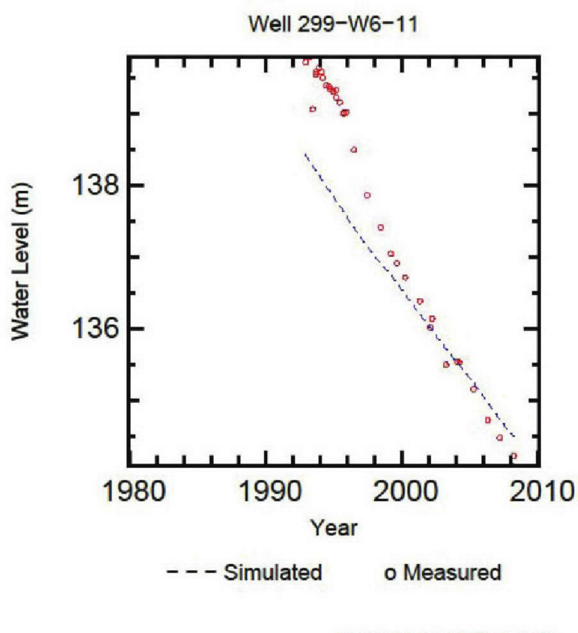
Well 299-W6-11
Water Level (m)
138
136
1980
1990
2000
2010
Year
- - - Simulated
o Measured
WL_299-W6-11_CPM_V3.3_TMC_10-11-2010

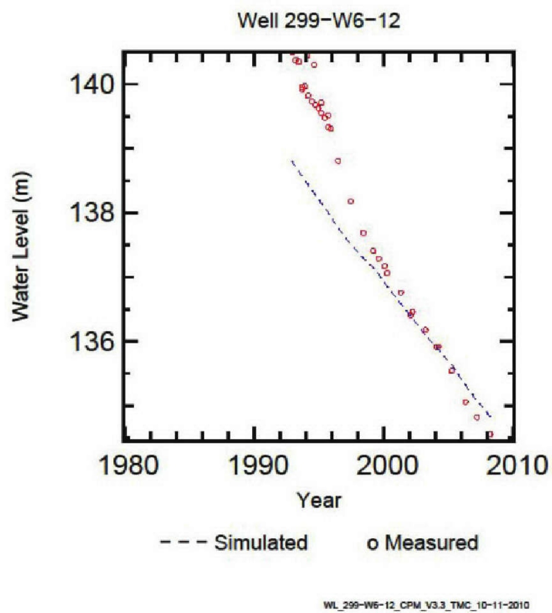
Well 299-W6-12
Water Level (m)
140
138
136
1980
1990
2000
2010
Year
- - - Simulated
o Measured
WL_299-W6-12_CPM_V3.3_TMC_10-11-2010

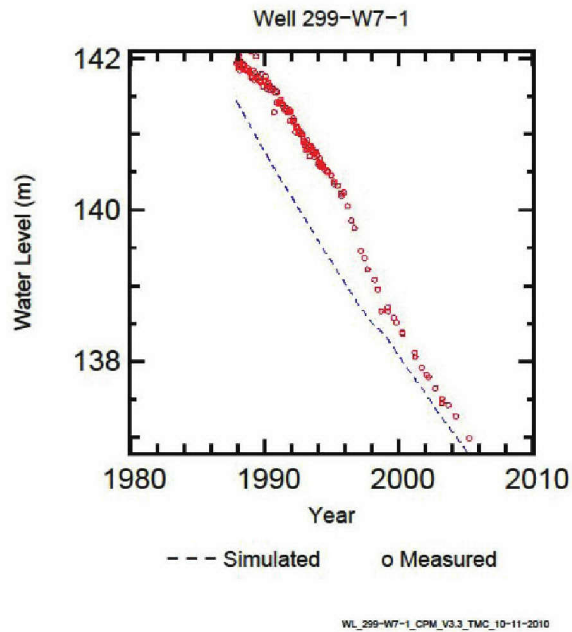
Well 299-W7-1
Water Level (m)
142
140
138
1980
1990
2000
2010
Year
- - - Simulated
o Measured
WL_299-W7-1_CPM_V3.3_TMC_10-11-2010

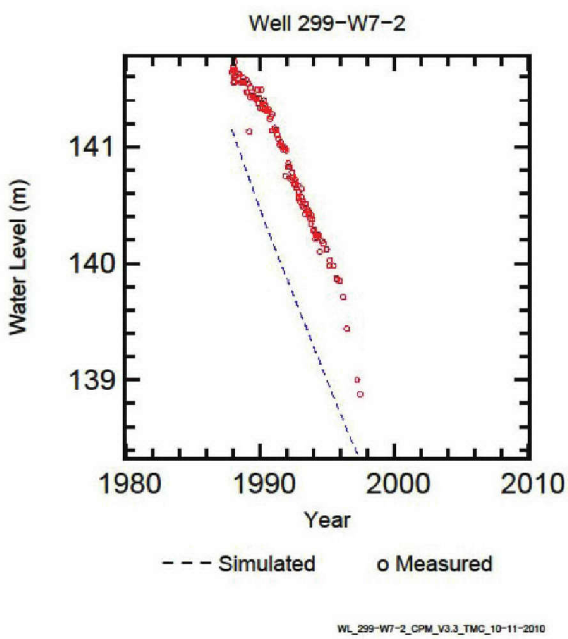
Well 299-W7-2
Water Level (m)
141
140
139
1980
1990
2000
2010
Year
- - - Simulated
o Measured
WL_299-W7-2_CPM_V3.3_TMC_10-11-2010

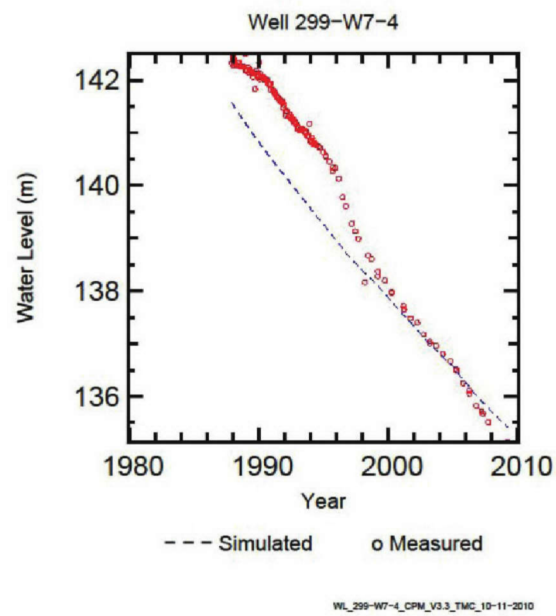
Well 299-W7-4
Water Level (m)
142
140
138
136
1980
1990
2000
2010
Year
- - - Simulated
o Measured
WL_299-W7-4_CPM_V3.3_TMC_10-11-2010

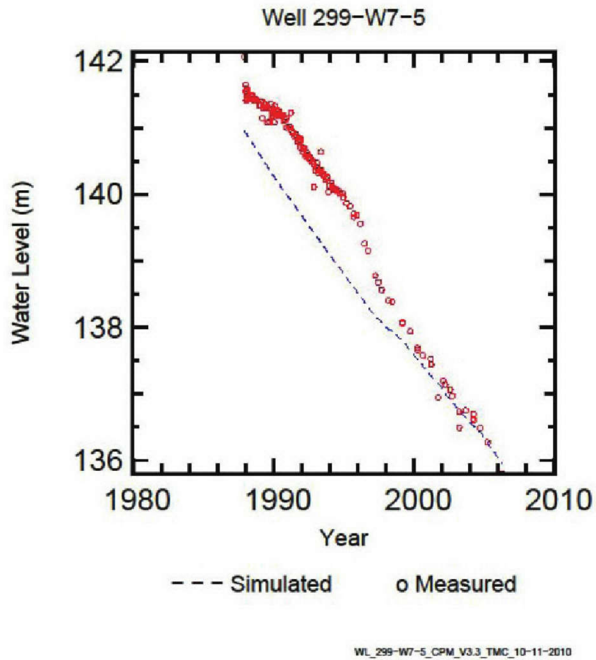
Well 299−W7−5
142
140
138
136
Water Level (m)
1980
1990
2000
2010
Year
- - - Simulated
o Measured
WL_299-W7-5_CPM_V3.3_TMC_10-11-2010

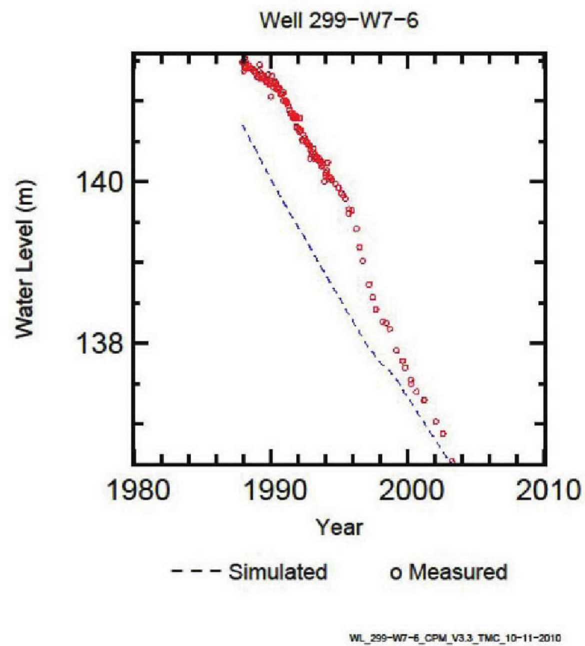
Well 299−W7−6
140
138
Water Level (m)
1980
1990
2000
2010
Year
- - - Simulated
o Measured
WL_299-W7-6_CPM_V3.3_TMC_10-11-2010

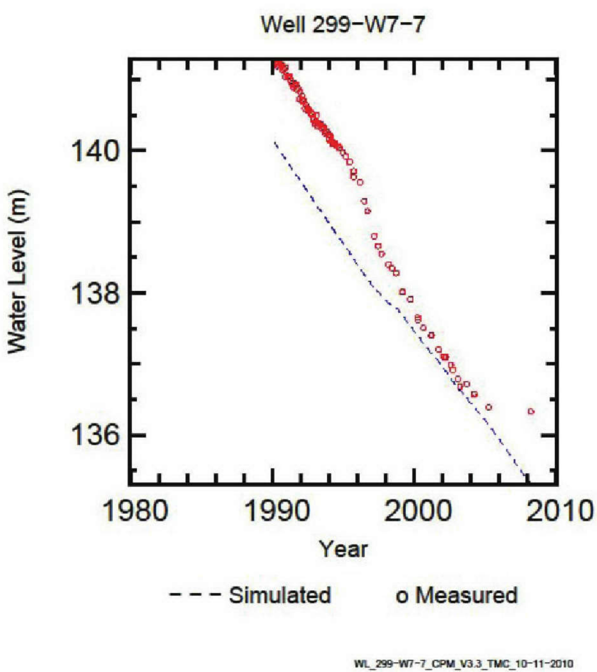
Well 299−W7−7
140
138
136
Water Level (m)
1980
1990
2000
2010
Year
- - - Simulated
o Measured
WL_299-W7-7_CPM_V3.3_TMC_10-11-2010

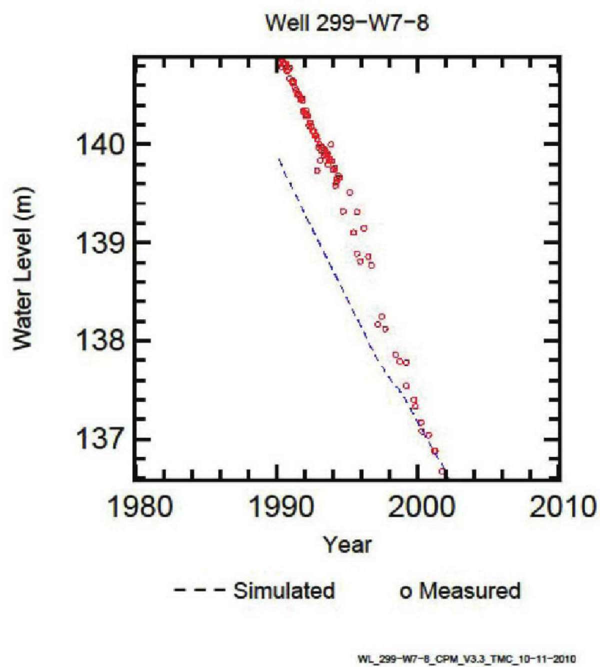
Well 299−W7−8
140
139
138
137
Water Level (m)
1980
1990
2000
2010
Year
- - - Simulated
o Measured
WL_299-W7-8_CPM_V3.3_TMC_10-11-2010

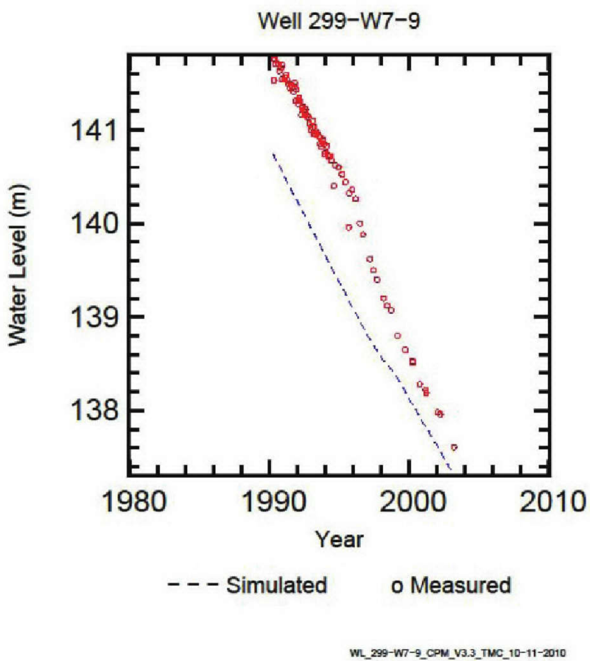
Well 299-W7-9
Water Level (m)
141
140
139
138
1980
1990
2000
2010
Year
Simulated
o Measured
WL_299-W7-9_CPM_V3.3_TMC_10-11-2010

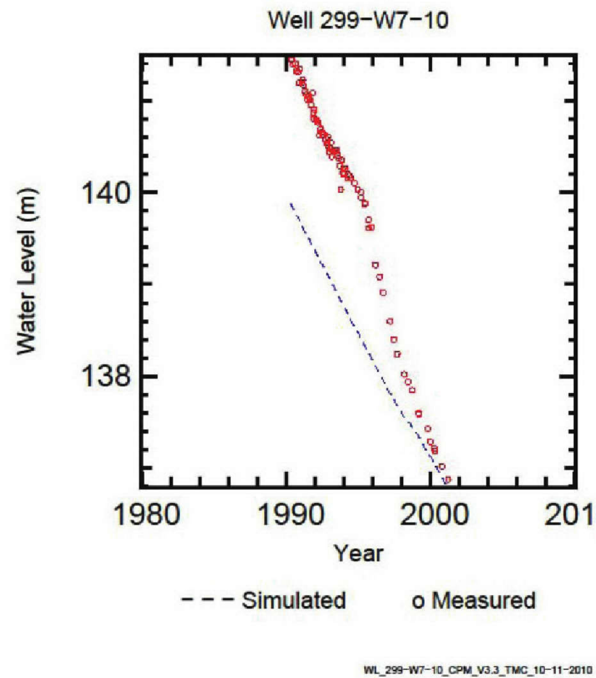
Well 299-W7-10
Water Level (m)
140
138
1980
1990
2000
2010
Year
Simulated
o Measured
WL_299-W7-10_CPM_V3.3_TMC_10-11-2010

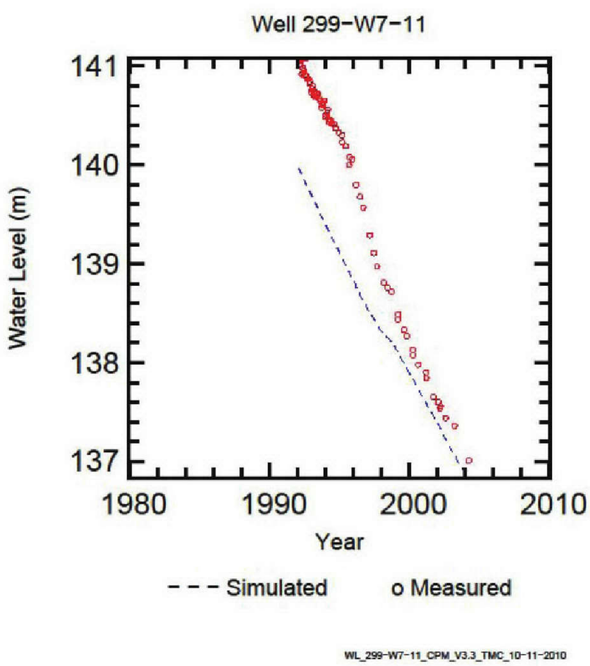
Well 299-W7-11
Water Level (m)
141
140
139
138
137
1980
1990
2000
2010
Year
Simulated
o Measured
WL_299-W7-11_CPM_V3.3_TMC_10-11-2010

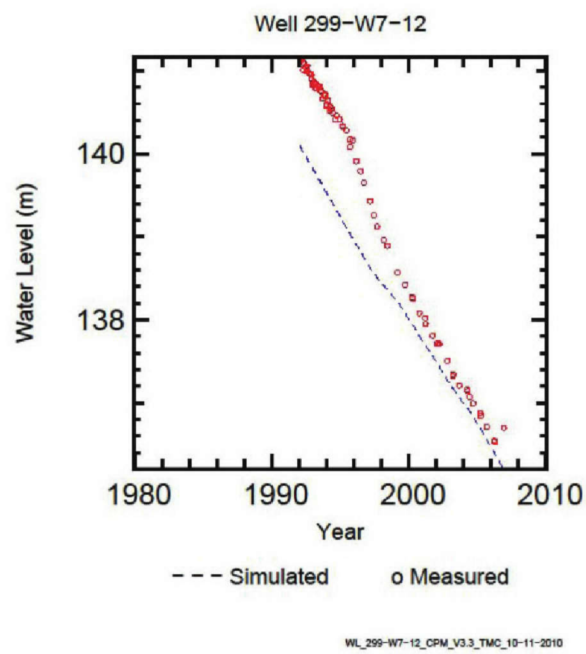
Well 299-W7-12
Water Level (m)
140
138
1980
1990
2000
2010
Year
Simulated
o Measured
WL_299-W7-12_CPM_V3.3_TMC_10-11-2010

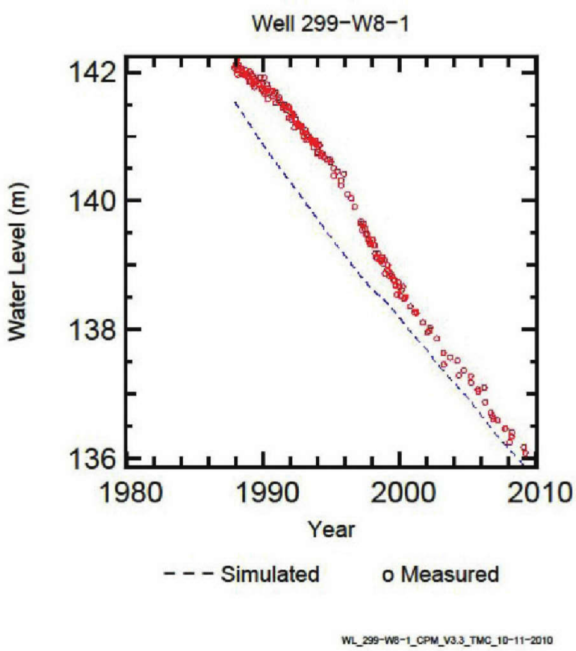
Well 299-W8-1
Water Level (m)
142
140
138
136
1980
1990
2000
2010
Year
- - - Simulated
o Measured
WL_299-W8-1_CPM_V3.3_TMC_10-11-2010

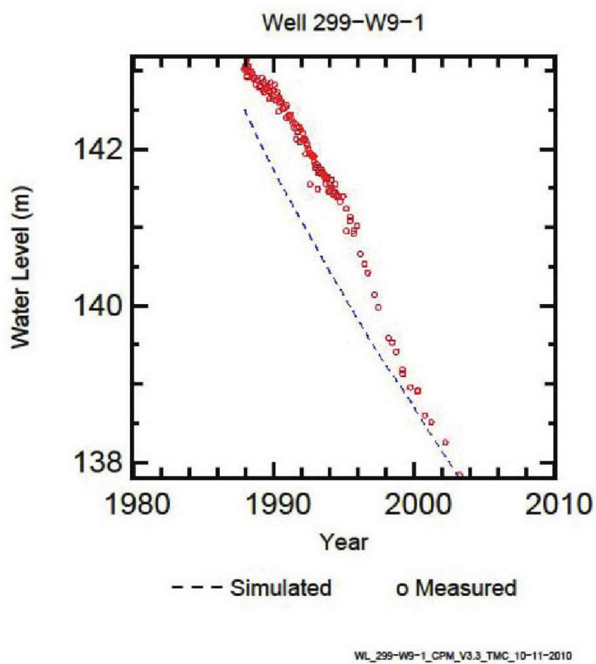
Well 299-W9-1
Water Level (m)
142
140
138
1980
1990
2000
2010
Year
- - - Simulated
o Measured
WL_299-W9-1_CPM_V3.3_TMC_10-11-2010

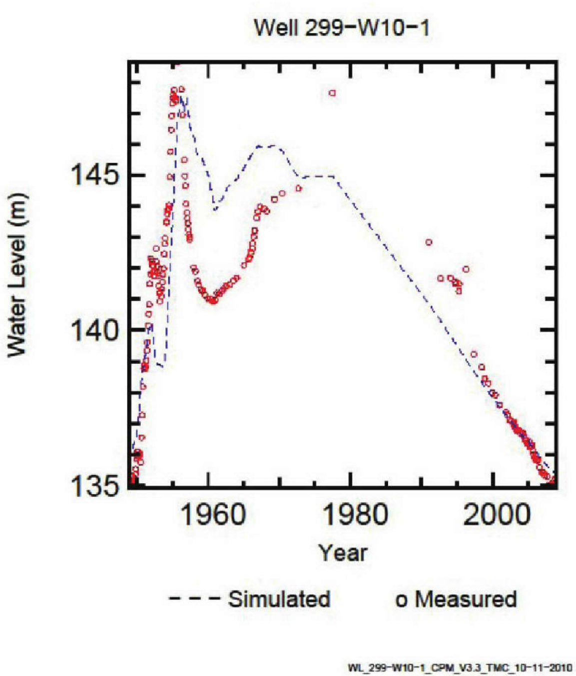
Well 299-W10-1
Water Level (m)
145
140
135
1960
1980
2000
Year
- - - Simulated
o Measured
WL_299-W10-1_CPM_V3.3_TMC_10-11-2010

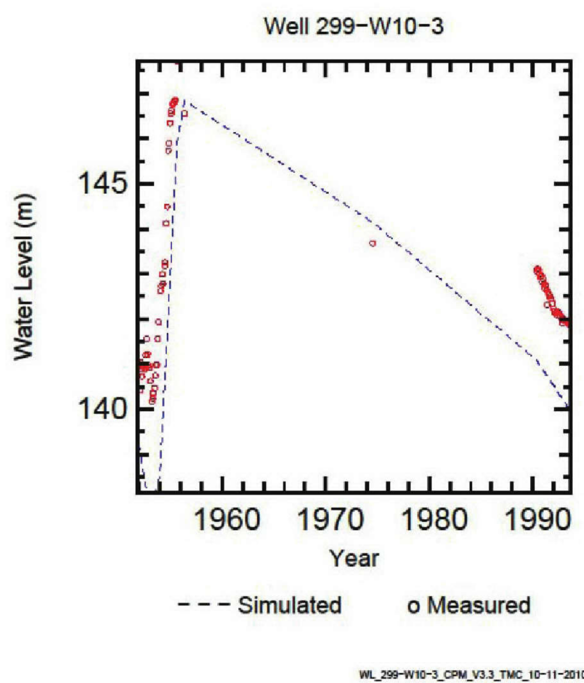
Well 299-W10-3
Water Level (m)
145
140
1960
1970
1980
1990
Year
- - - Simulated
o Measured
WL_299-W10-3_CPM_V3.3_TMC_10-11-2010

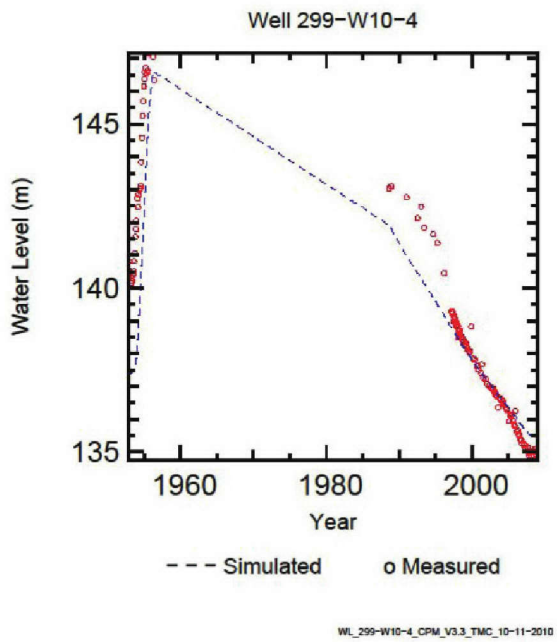
Well 299-W10-4
Water Level (m)
145
140
135
1960
1980
2000
Year
- - - Simulated
o Measured
WL_299-W10-4_CPM_V3.3_TMC_10-11-2010

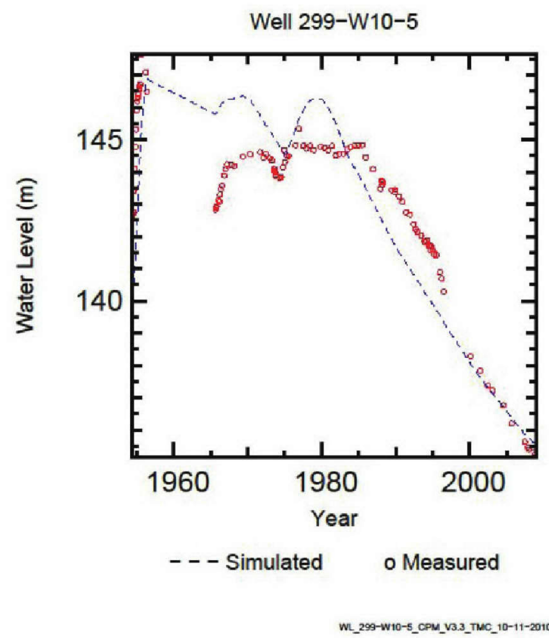
Well 299-W10-5
Water Level (m)
145
140
1960
1980
2000
Year
- - - Simulated
o Measured
WL_299-W10-5_CPM_V3.3_TMC_10-11-2010

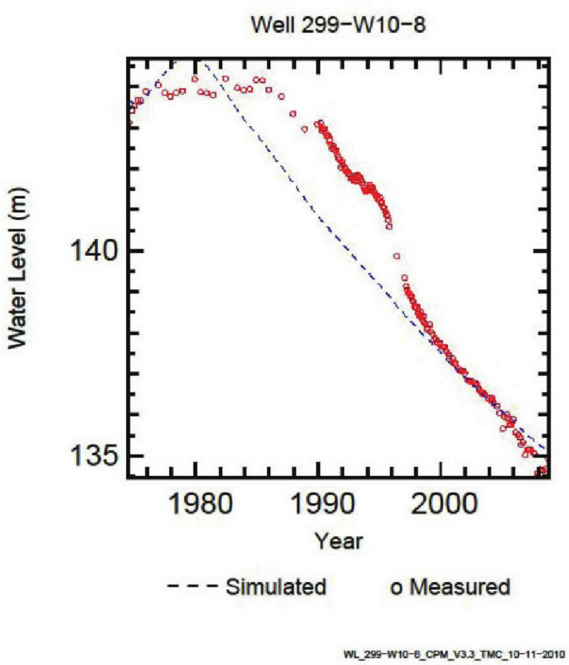
Well 299-W10-8
Water Level (m)
140
135
1980
1990
2000
Year
- - - Simulated
o Measured
WL_299-W10-8_CPM_V3.3_TMC_10-11-2010

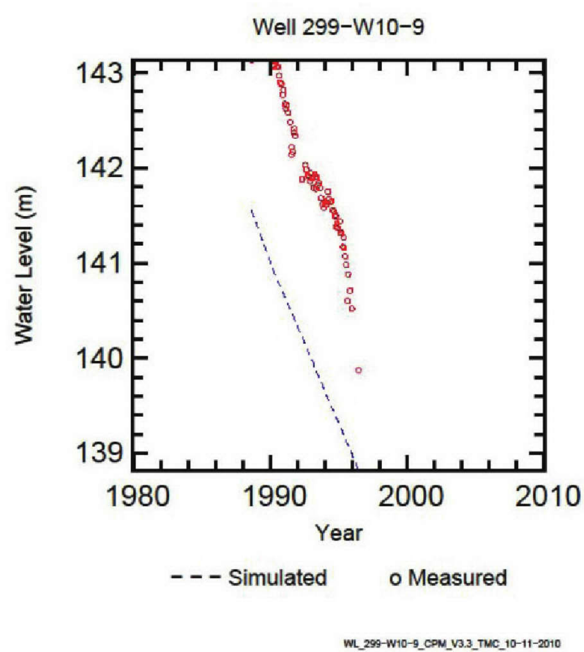
Well 299-W10-9
Water Level (m)
143
142
141
140
139
1980
1990
2000
2010
Year
- - - Simulated
o Measured
WL_299-W10-9_CPM_V3.3_TMC_10-11-2010

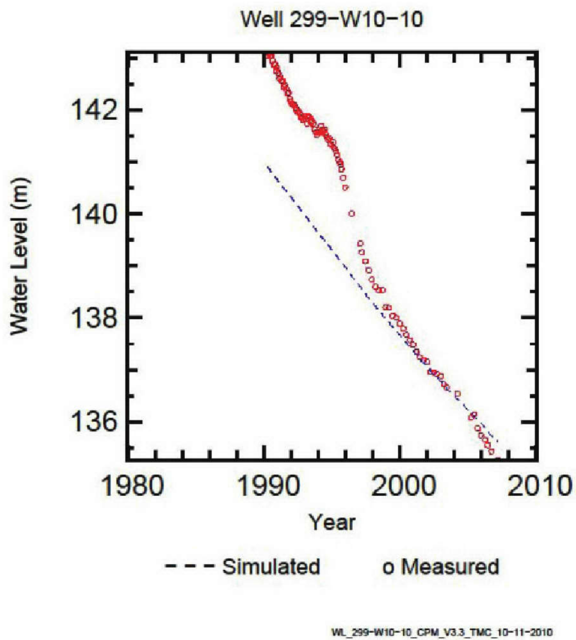
Well 299-W10-10
Water Level (m)
142
140
138
136
1980
1990
2000
2010
Year
Simulated
Measured
WL_299-W10-10_CPM_V3.3_TMC_10-11-2010

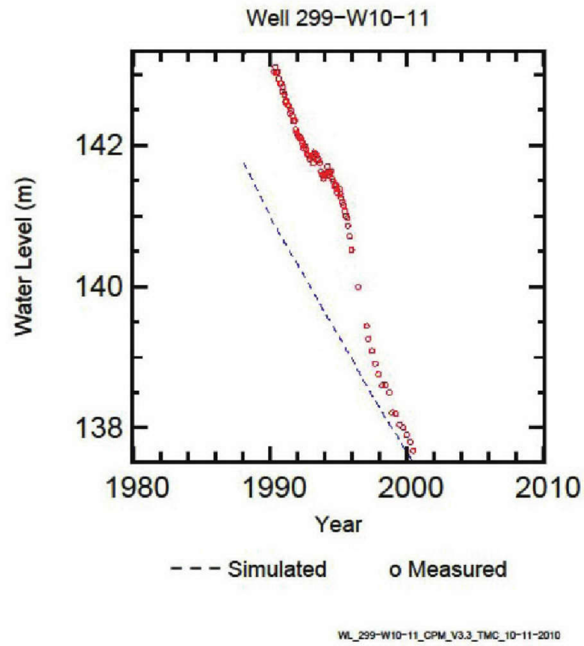
Well 299-W10-11
Water Level (m)
142
140
138
1980
1990
2000
2010
Year
Simulated
Measured
WL_299-W10-11_CPM_V3.3_TMC_10-11-2010

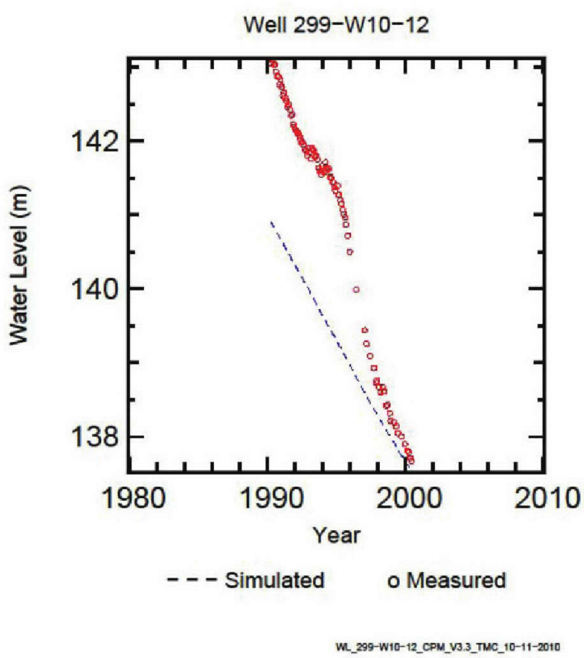
Well 299-W10-12
Water Level (m)
142
140
138
1980
1990
2000
2010
Year
Simulated
Measured
WL_299-W10-12_CPM_V3.3_TMC_10-11-2010

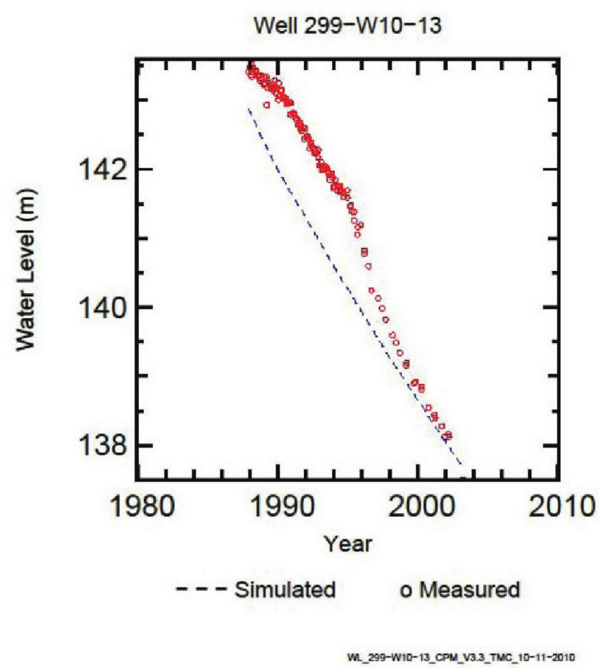
Well 299-W10-13
Water Level (m)
142
140
138
1980
1990
2000
2010
Year
Simulated
Measured
WL_299-W10-13_CPM_V3.3_TMC_10-11-2010

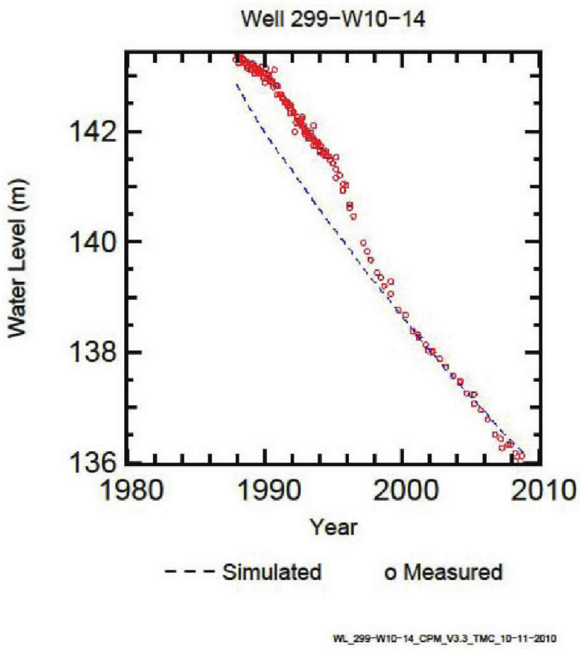
Well 299-W10-14
Water Level (m)
136
138
140
142
1980
1990
2000
2010
Year
Simulated
o Measured
WL_299-W10-14_CPM_V3.3_TMC_10-11-2010

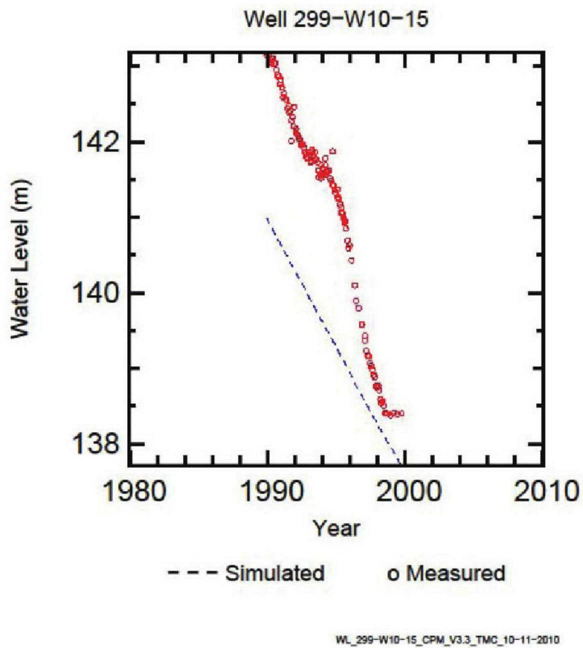
Well 299-W10-15
Water Level (m)
138
140
142
1980
1990
2000
2010
Year
Simulated
o Measured
WL_299-W10-15_CPM_V3.3_TMC_10-11-2010

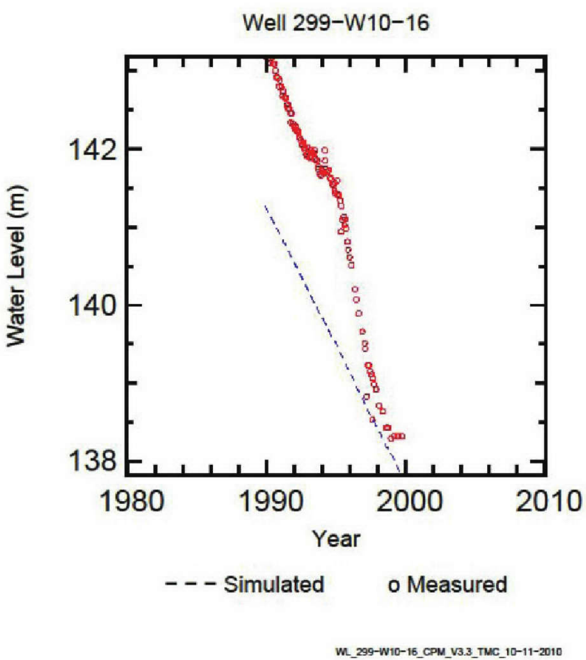
Well 299-W10-16
Water Level (m)
138
140
142
1980
1990
2000
2010
Year
Simulated
o Measured
WL_299-W10-16_CPM_V3.3_TMC_10-11-2010

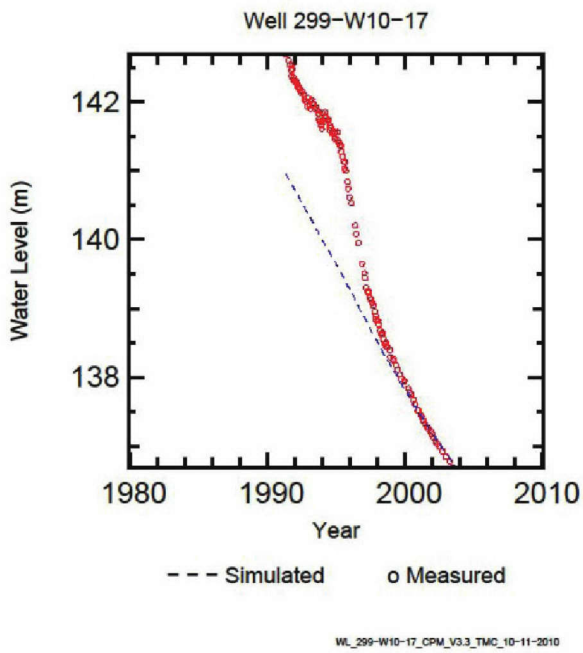
Well 299-W10-17
Water Level (m)
138
140
142
1980
1990
2000
2010
Year
Simulated
o Measured
WL_299-W10-17_CPM_V3.3_TMC_10-11-2010

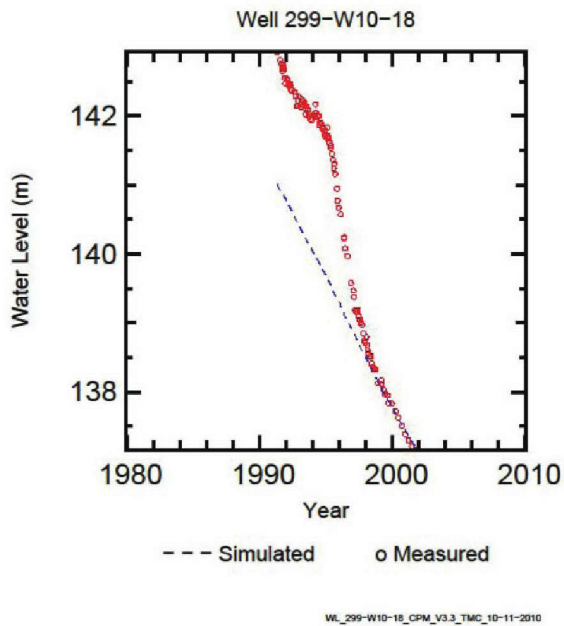
Well 299-W10-18
142
140
138
Water Level (m)
1980
1990
2000
2010
Year
Simulated
Measured
WL_299-W10-18_CPM_V3.3_TMC_10-11-2010

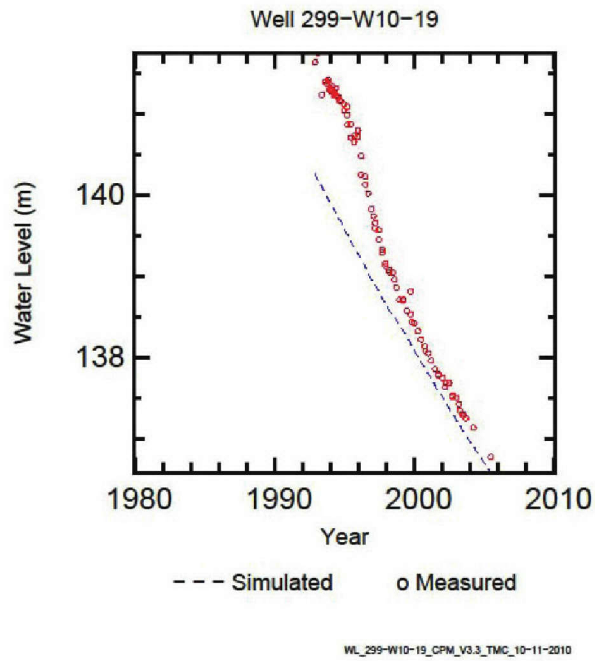
Well 299-W10-19
140
138
Water Level (m)
1980
1990
2000
2010
Year
Simulated
Measured
WL_299-W10-19_CPM_V3.3_TMC_10-11-2010

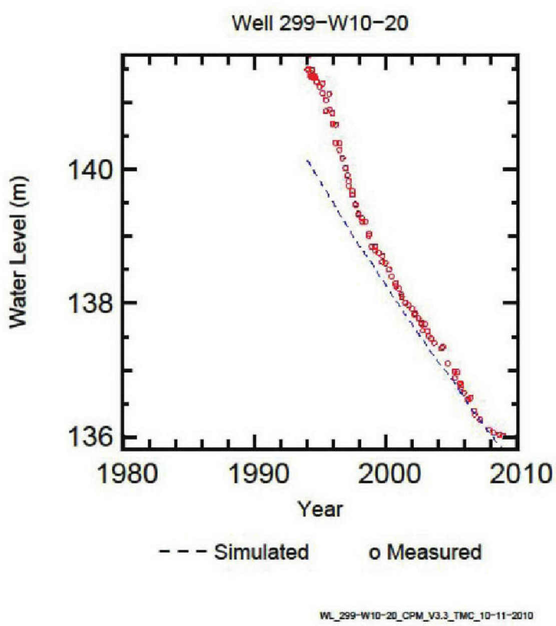
Well 299-W10-20
140
138
136
Water Level (m)
1980
1990
2000
2010
Year
Simulated
Measured
WL_299-W10-20_CPM_V3.3_TMC_10-11-2010

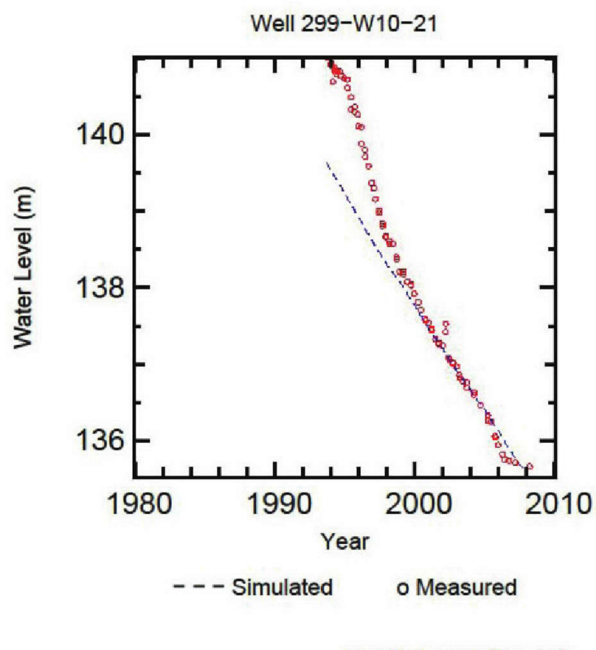
Well 299-W10-21
140
138
136
Water Level (m)
1980
1990
2000
2010
Year
Simulated
Measured
WL_299-W10-21_CPM_V3.3_TMC_10-11-2010

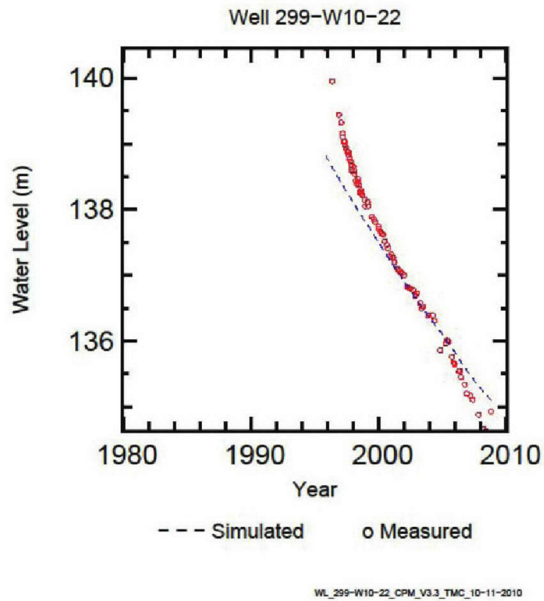
Well 299-W10-22
140
138
136
Water Level (m)
1980
1990
2000
2010
Year
- - - Simulated
o Measured
WL_299-W10-22_CPM_V3.3_TMC_10-11-2010

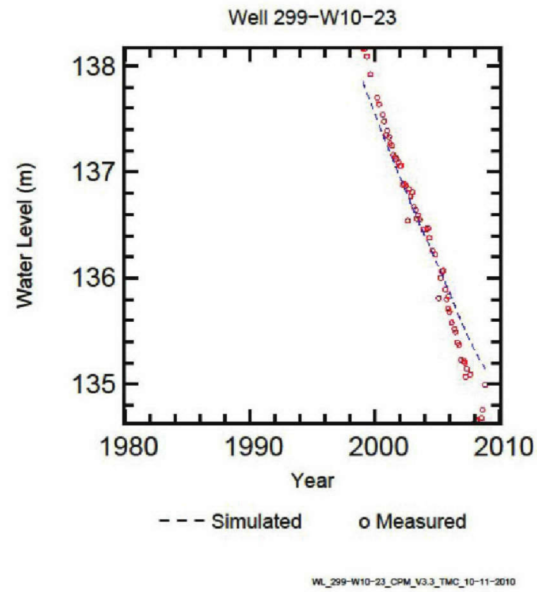
Well 299-W10-23
138
137
136
135
Water Level (m)
1980
1990
2000
2010
Year
- - - Simulated
o Measured
WL_299-W10-23_CPM_V3.3_TMC_10-11-2010

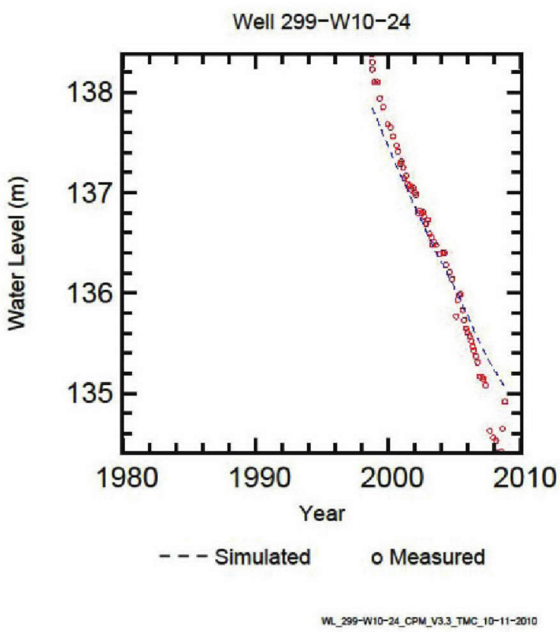
Well 299-W10-24
138
137
136
135
Water Level (m)
1980
1990
2000
2010
Year
- - - Simulated
o Measured
WL_299-W10-24_CPM_V3.3_TMC_10-11-2010

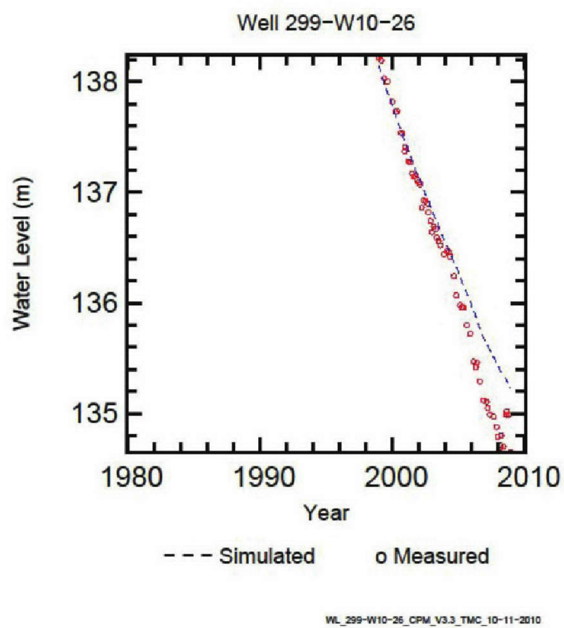
Well 299-W10-26
138
137
136
135
Water Level (m)
1980
1990
2000
2010
Year
- - - Simulated
o Measured
WL_299-W10-26_CPM_V3.3_TMC_10-11-2010

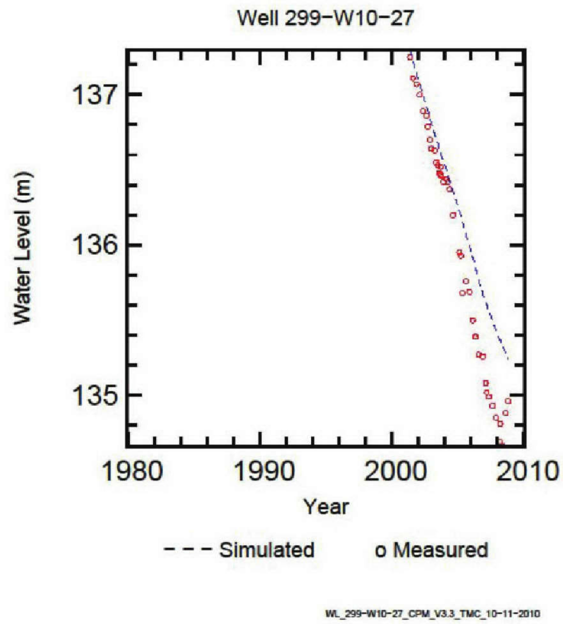
Well 299-W10-27
Water Level (m)
137
136
135
1980
1990
2000
2010
Year
- - - Simulated
o Measured
WL_299-W10-27_CPM_V3.3_TMC_10-11-2010

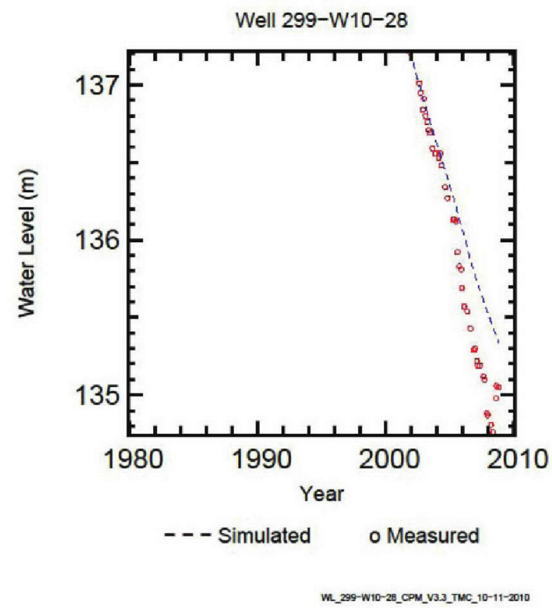
Well 299-W10-28
Water Level (m)
137
136
135
1980
1990
2000
2010
Year
- - - Simulated
o Measured
WL_299-W10-28_CPM_V3.3_TMC_10-11-2010

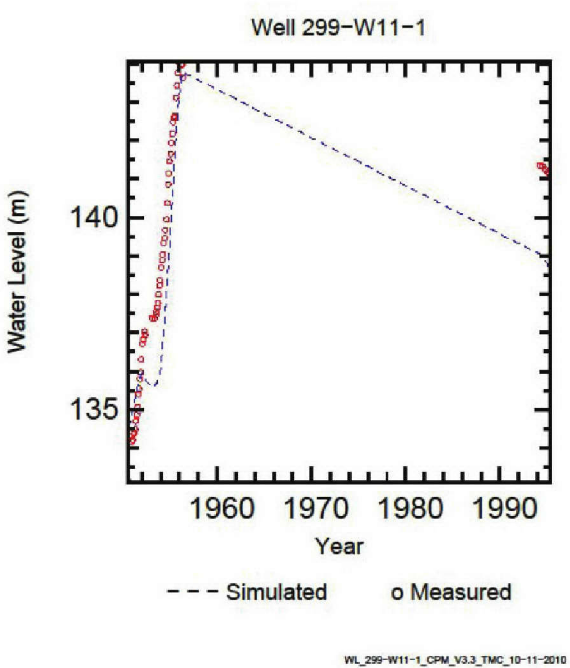
Well 299-W11-1
Water Level (m)
140
135
1960
1970
1980
1990
Year
- - - Simulated
o Measured
WL_299-W11-1_CPM_V3.3_TMC_10-11-2010

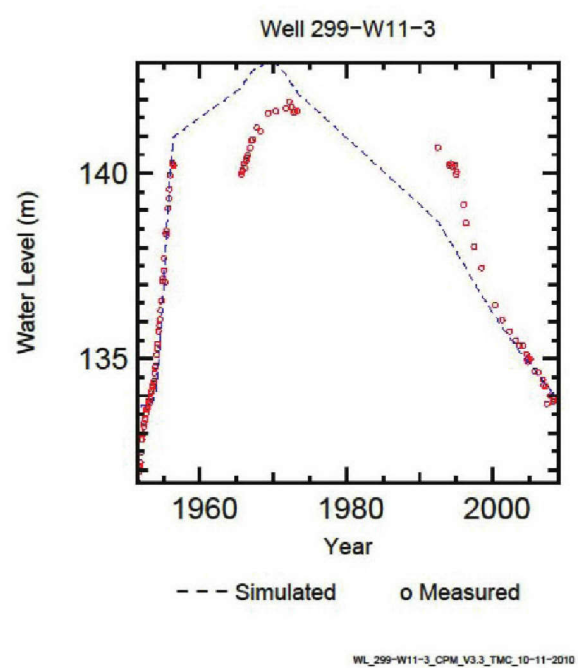
Well 299-W11-3
Water Level (m)
140
135
1960
1980
2000
Year
- - - Simulated
o Measured
WL_299-W11-3_CPM_V3.3_TMC_10-11-2010

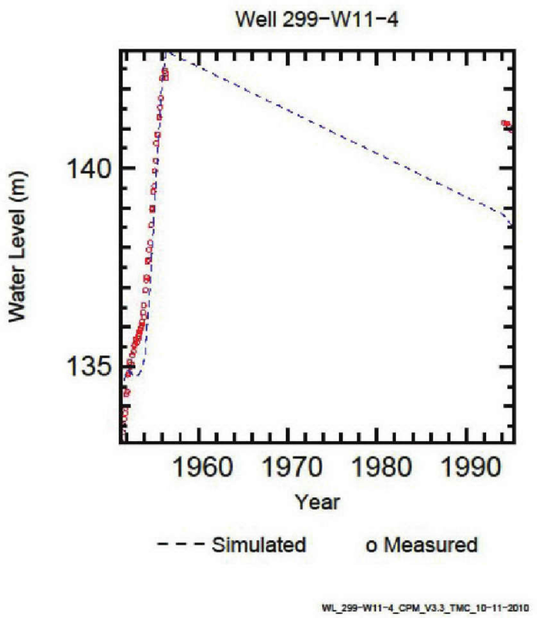
Well 299-W11-4
Water Level (m)
140
135
1960
1970
1980
1990
Year
--- Simulated
o Measured
WL_299-W11-4_CPM_V3.3_TMC_10-11-2010

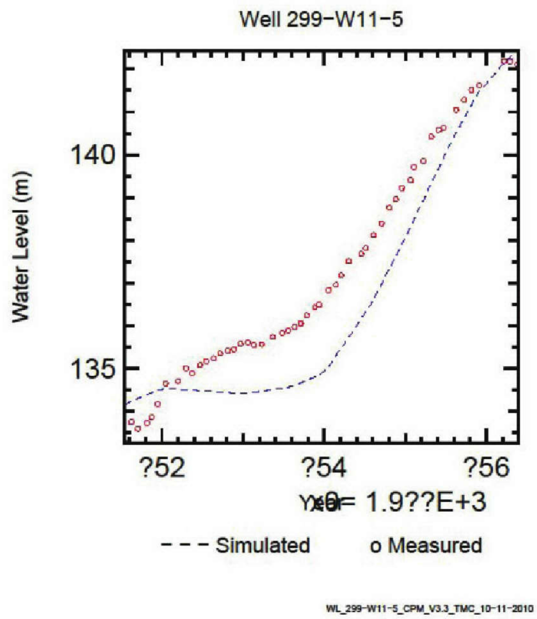
Well 299-W11-5
Water Level (m)
140
135
?52
?54
?56
Year
x0 = 1.9??E+3
--- Simulated
o Measured
WL_299-W11-5_CPM_V3.3_TMC_10-11-2010

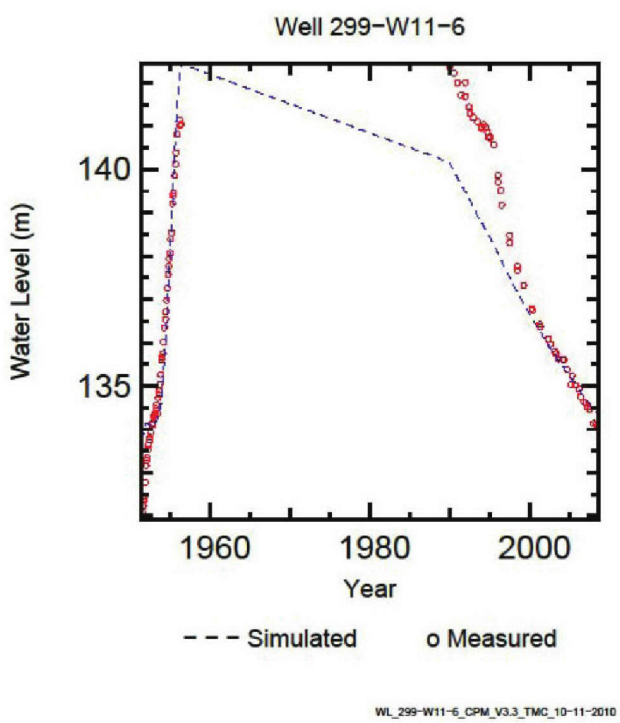
Well 299-W11-6
Water Level (m)
140
135
1960
1980
2000
Year
--- Simulated
o Measured
WL_299-W11-6_CPM_V3.3_TMC_10-11-2010

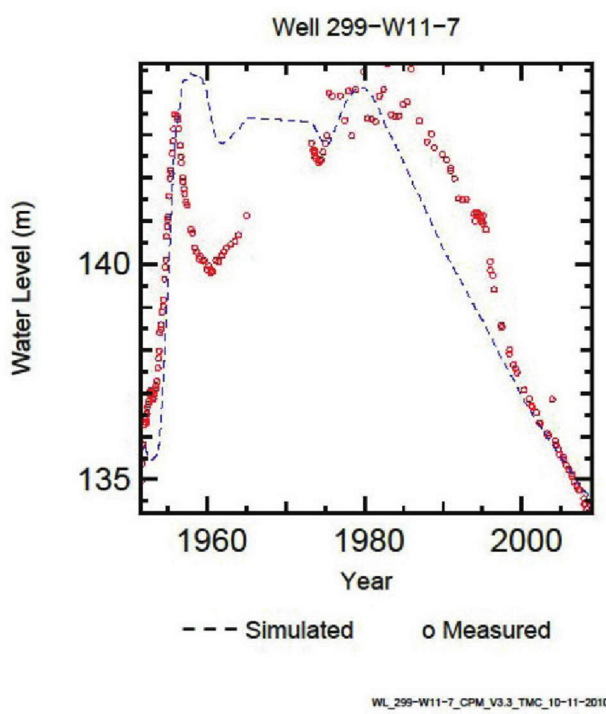
Well 299-W11-7
Water Level (m)
140
135
1960
1980
2000
Year
--- Simulated
o Measured
WL_299-W11-7_CPM_V3.3_TMC_10-11-2010

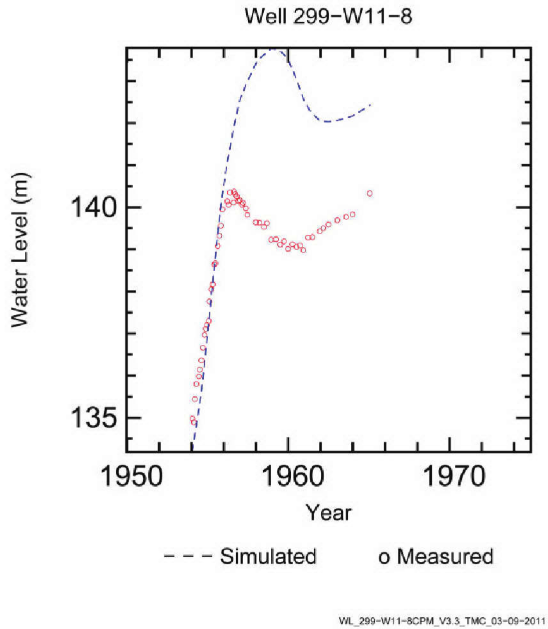
Well 299−W11−8
Water Level (m)
140
135
1950
1960
1970
Year
- - - Simulated
o Measured
WL_299-W11-8CPM_V3.3_TMC_03-09-2011

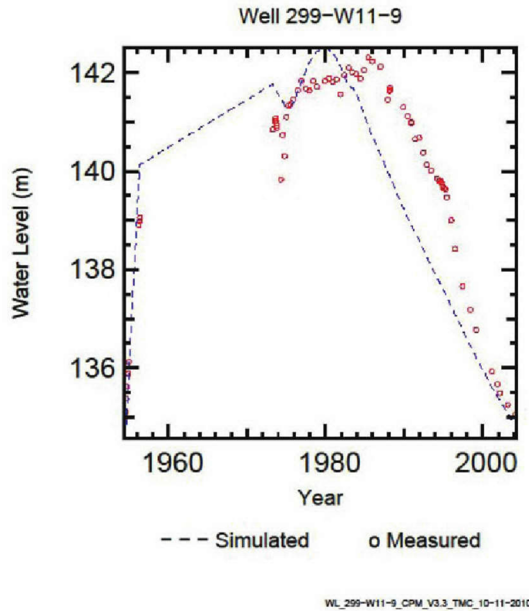
Well 299−W11−9
Water Level (m)
142
140
138
136
1960
1980
2000
Year
- - - Simulated
o Measured
WL_299-W11-9_CPM_V3.3_TMC_10-11-2010

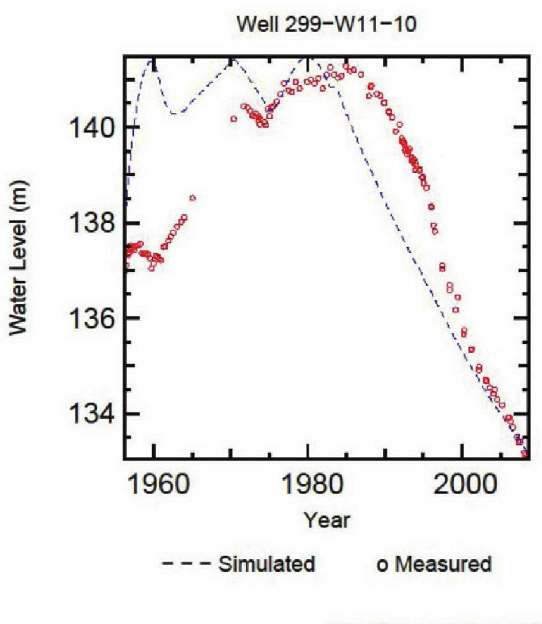
Well 299−W11−10
Water Level (m)
140
138
136
134
1960
1980
2000
Year
- - - Simulated
o Measured
WL_299-W11-10_CPM_V3.3_TMC_10-11-2010

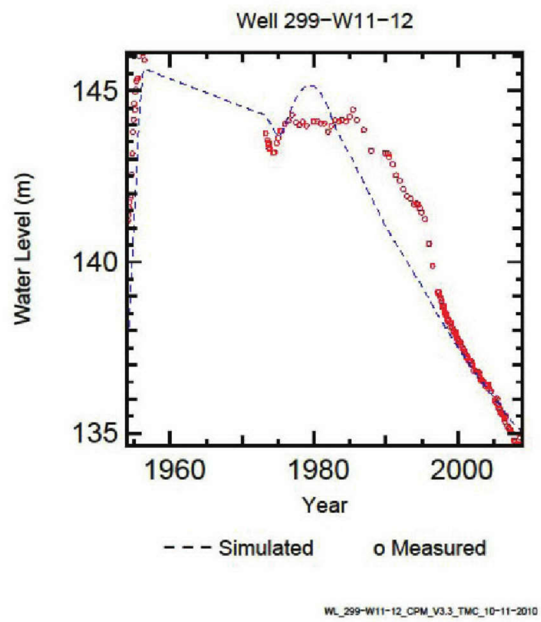
Well 299−W11−12
Water Level (m)
145
140
135
1960
1980
2000
Year
- - - Simulated
o Measured
WL_299-W11-12_CPM_V3.3_TMC_10-11-2010

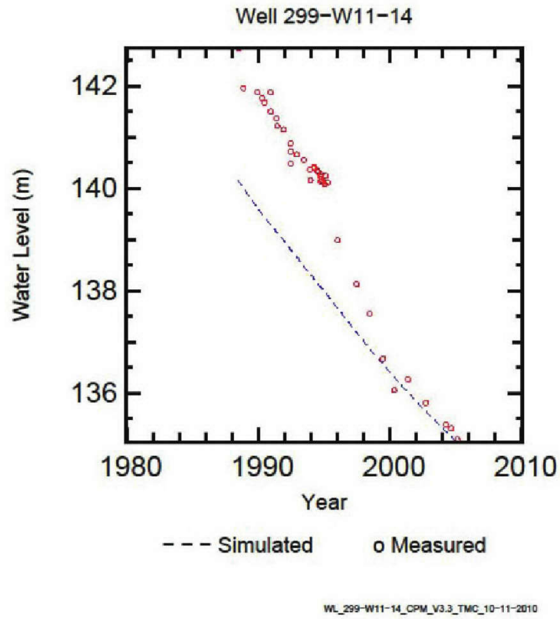
Well 299-W11-14
Water Level (m)
142
140
138
136
1980
1990
2000
2010
Year
- - - Simulated
o Measured
WL_299-W11-14_CPM_V3.3_TMC_10-11-2010

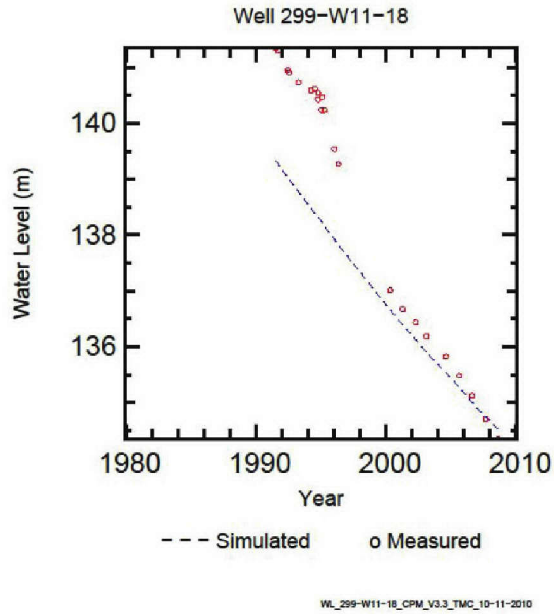
Well 299-W11-18
Water Level (m)
140
138
136
1980
1990
2000
2010
Year
- - - Simulated
o Measured
WL_299-W11-18_CPM_V3.3_TMC_10-11-2010

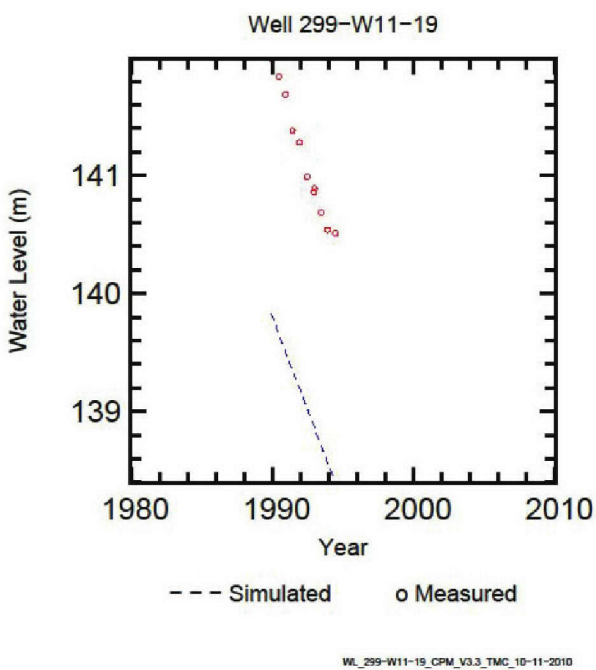
Well 299-W11-19
Water Level (m)
141
140
139
1980
1990
2000
2010
Year
- - - Simulated
o Measured
WL_299-W11-19_CPM_V3.3_TMC_10-11-2010

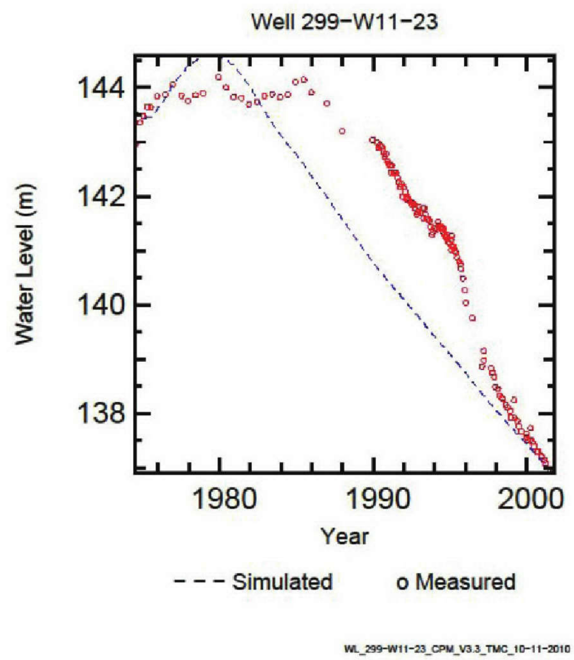
Well 299-W11-23
Water Level (m)
144
142
140
138
1980
1990
2000
Year
- - - Simulated
o Measured
WL_299-W11-23_CPM_V3.3_TMC_10-11-2010

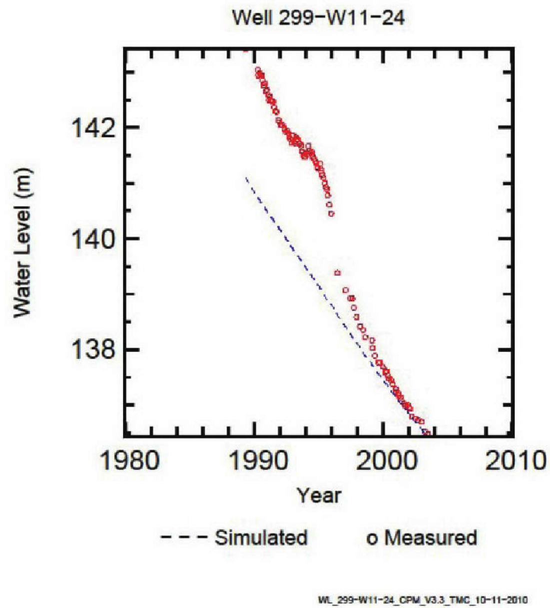
Well 299-W11-24
Water Level (m)
142
140
138
1980
1990
2000
2010
Year
- - - Simulated
o Measured
WL_299-W11-24_CPM_V3.3_TMC_10-11-2010

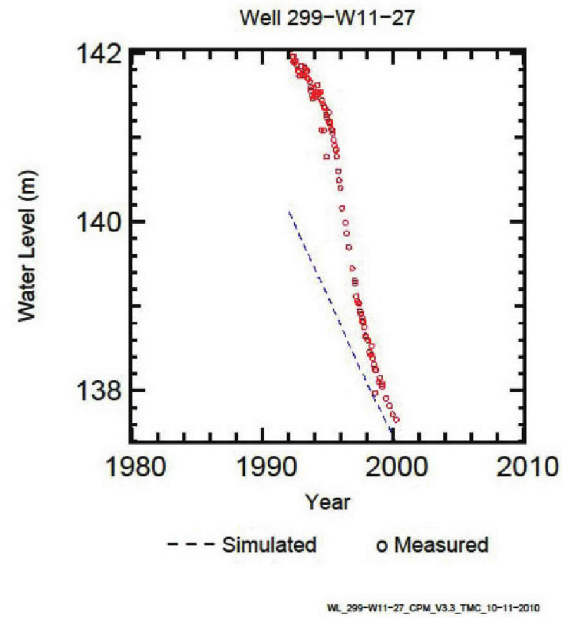
Well 299-W11-27
Water Level (m)
142
140
138
1980
1990
2000
2010
Year
- - - Simulated
o Measured
WL_299-W11-27_CPM_V3.3_TMC_10-11-2010

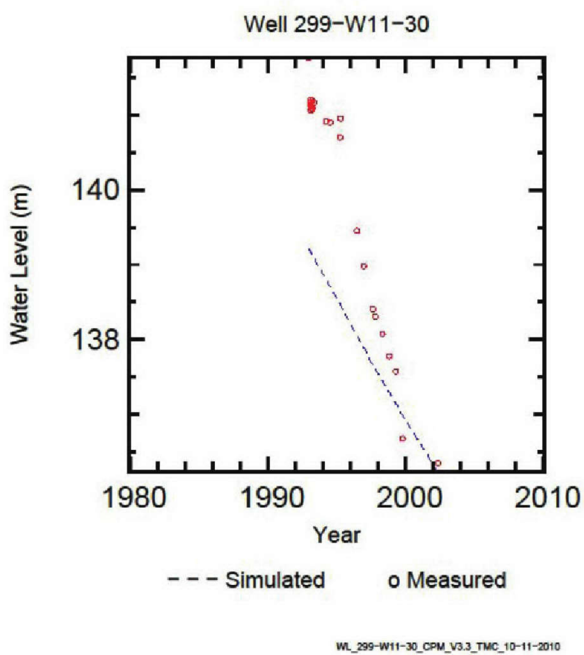
Well 299-W11-30
Water Level (m)
140
138
1980
1990
2000
2010
Year
- - - Simulated
o Measured
WL_299-W11-30_CPM_V3.3_TMC_10-11-2010

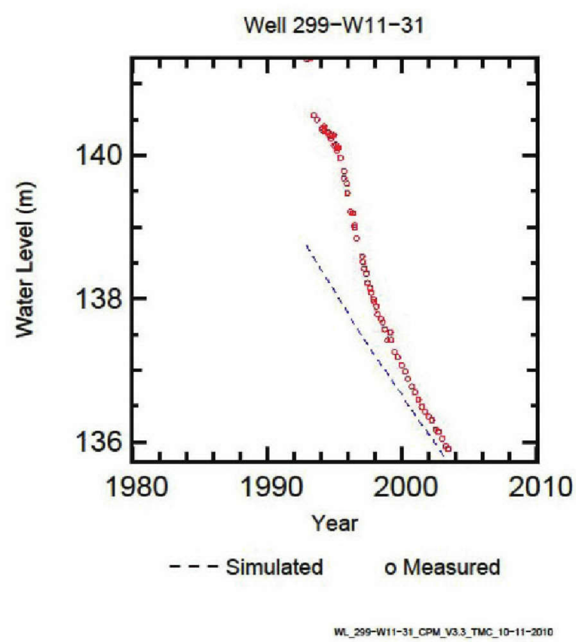
Well 299-W11-31
Water Level (m)
140
138
136
1980
1990
2000
2010
Year
- - - Simulated
o Measured
WL_299-W11-31_CPM_V3.3_TMC_10-11-2010

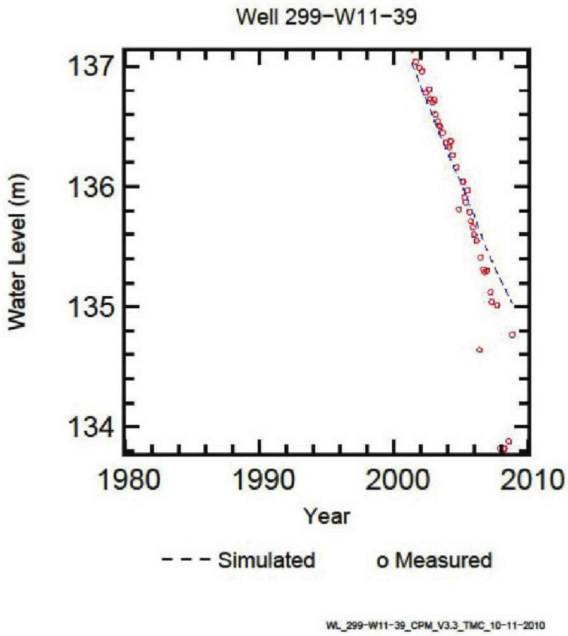
Well 299-W11-39
137
136
135
134
Water Level (m)
1980
1990
2000
2010
Year
- - - Simulated
o Measured
WL_299-W11-39_CPM_V3.3_TMC_10-11-2010

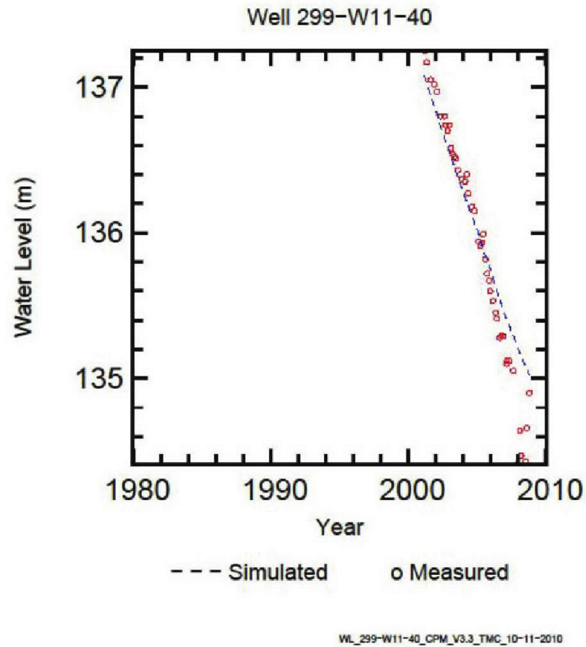
Well 299-W11-40
137
136
135
Water Level (m)
1980
1990
2000
2010
Year
- - - Simulated
o Measured
WL_299-W11-40_CPM_V3.3_TMC_10-11-2010

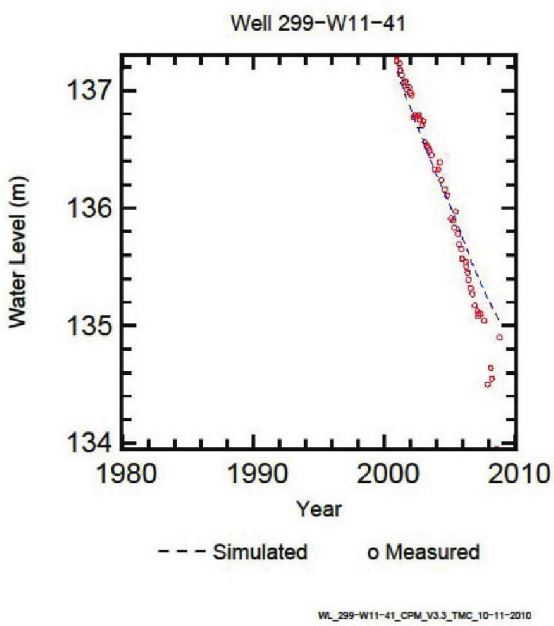
Well 299-W11-41
137
136
135
134
Water Level (m)
1980
1990
2000
2010
Year
- - - Simulated
o Measured
WL_299-W11-41_CPM_V3.3_TMC_10-11-2010

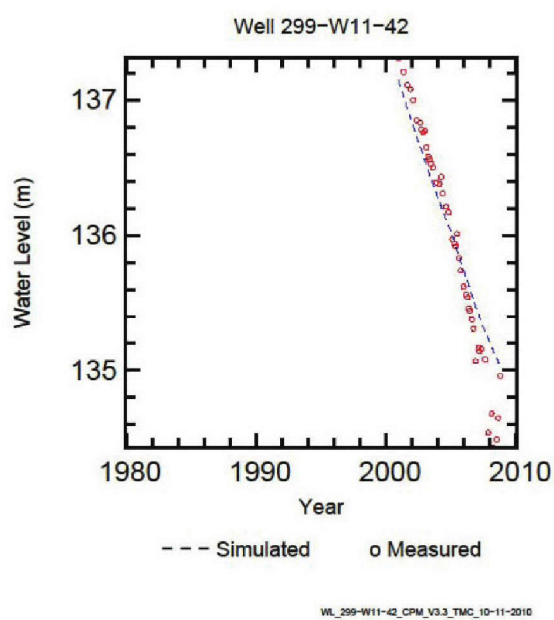
Well 299-W11-42
137
136
135
Water Level (m)
1980
1990
2000
2010
Year
- - - Simulated
o Measured
WL_299-W11-42_CPM_V3.3_TMC_10-11-2010

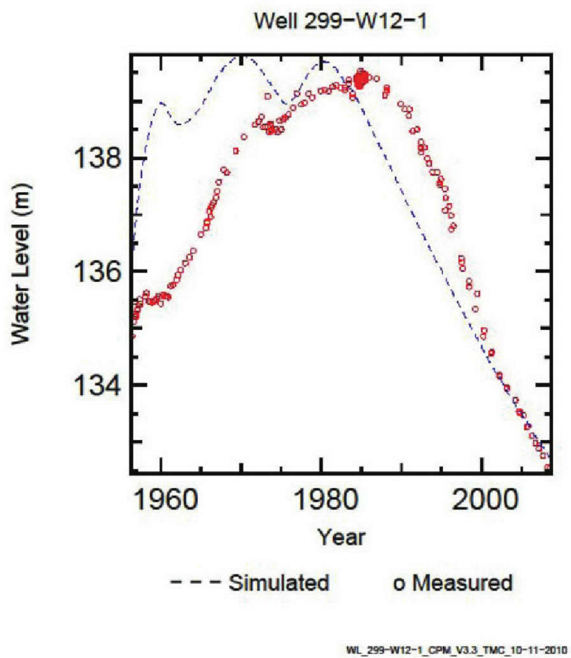
Well 299-W12-1
Water Level (m)
138
136
134
1960
1980
2000
Year
- - - Simulated
o Measured
WL_299-W12-1_CPM_V3.3_TMC_10-11-2010

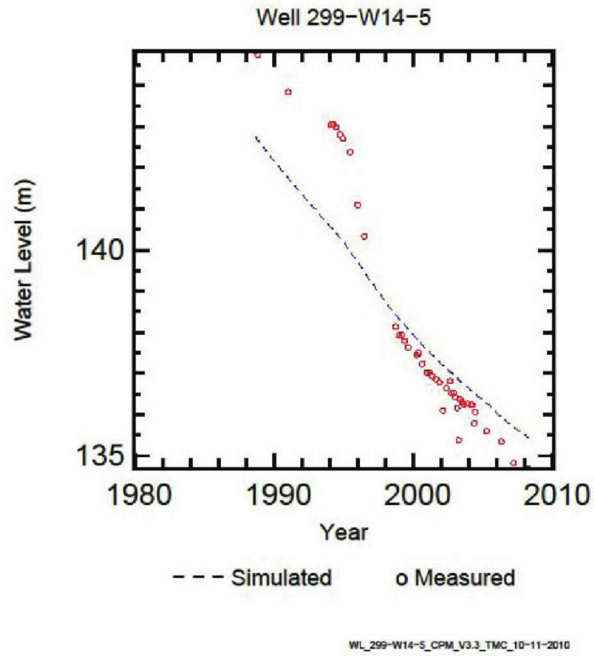
Well 299-W14-5
Water Level (m)
140
135
1980
1990
2000
2010
Year
- - - Simulated
o Measured
WL_299-W14-5_CPM_V3.3_TMC_10-11-2010

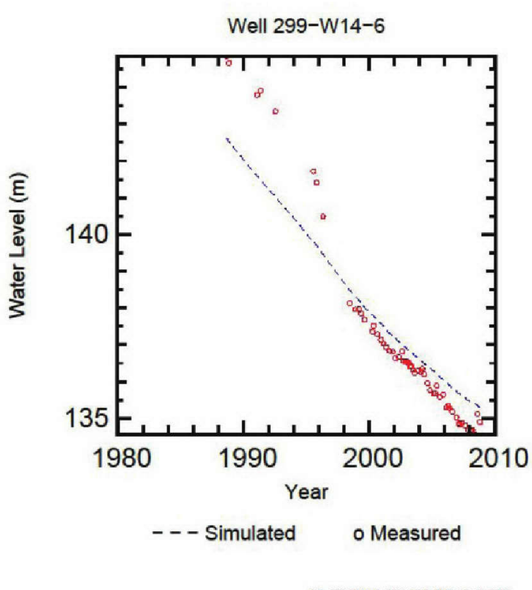
Well 299-W14-6
Water Level (m)
140
135
1980
1990
2000
2010
Year
- - - Simulated
o Measured
WL_299-W14-6_CPM_V3.3_TMC_10-11-2010

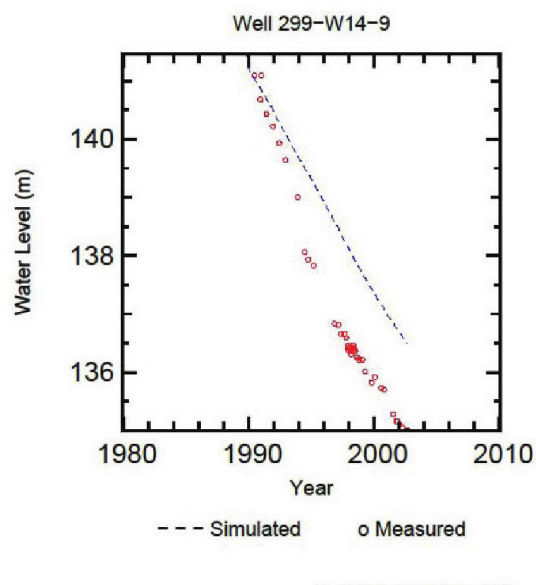
Well 299-W14-9
Water Level (m)
140
138
136
1980
1990
2000
2010
Year
- - - Simulated
o Measured
WL_299-W14-9_CPM_V3.3_TMC_10-11-2010

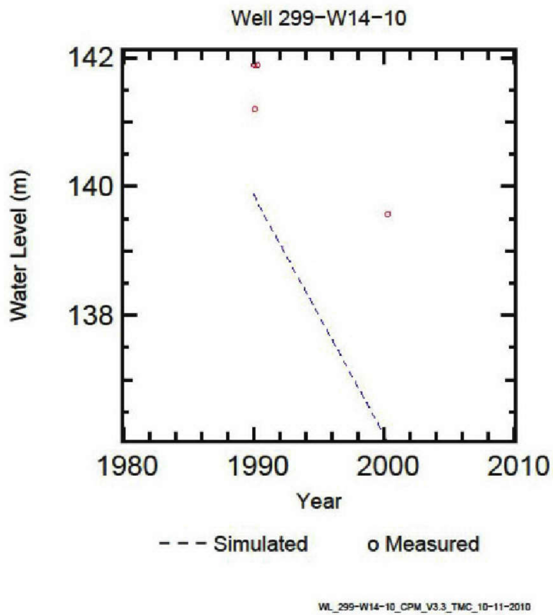
Well 299-W14-10
Water Level (m)
142
140
138
1980
1990
2000
2010
Year
Simulated
o Measured
WL_299-W14-10_CPM_V3.3_TMC_10-11-2010

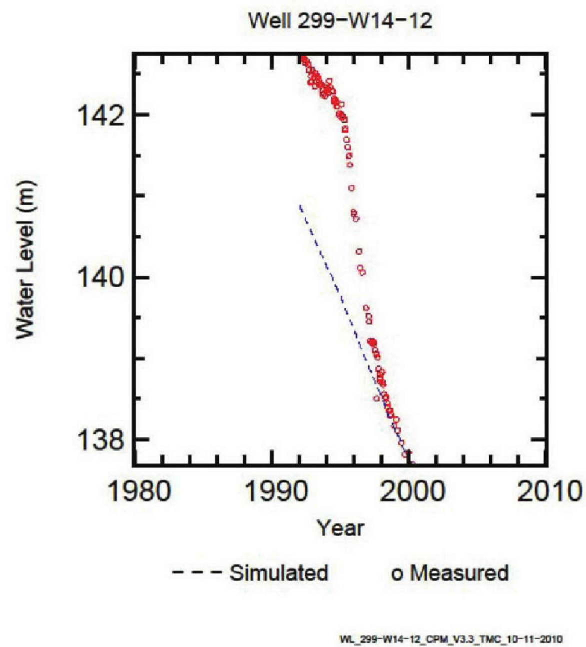
Well 299-W14-12
Water Level (m)
142
140
138
1980
1990
2000
2010
Year
Simulated
o Measured
WL_299-W14-12_CPM_V3.3_TMC_10-11-2010

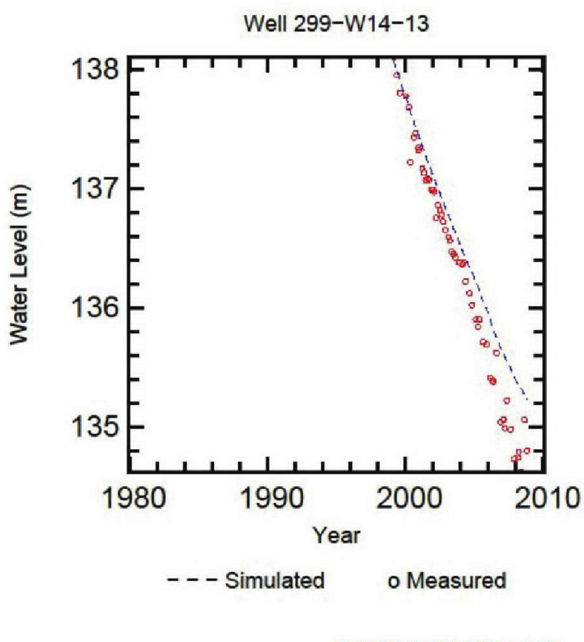
Well 299-W14-13
Water Level (m)
138
137
136
135
1980
1990
2000
2010
Year
Simulated
o Measured
WL_299-W14-13_CPM_V3.3_TMC_10-11-2010

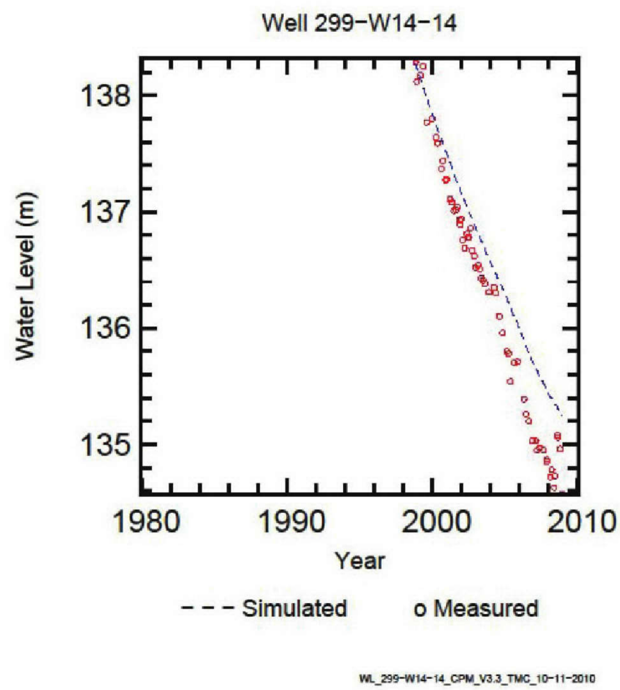
Well 299-W14-14
Water Level (m)
138
137
136
135
1980
1990
2000
2010
Year
Simulated
o Measured
WL_299-W14-14_CPM_V3.3_TMC_10-11-2010

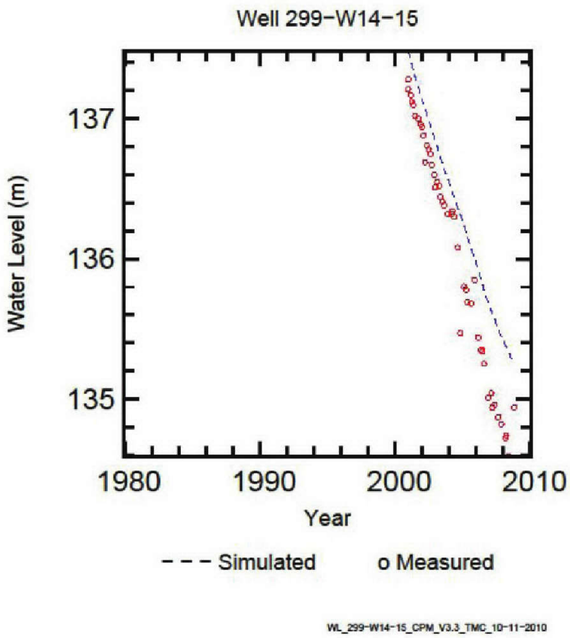
Well 299-W14-15
Water Level (m)
137
136
135
1980
1990
2000
2010
Year
- - - Simulated
o Measured
WL_299-W14-15_CPM_V3.3_TMC_10-11-2010

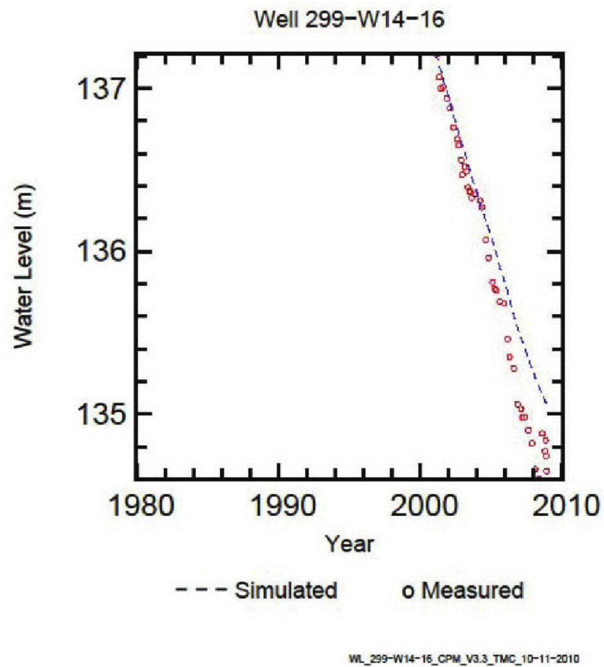
Well 299-W14-16
Water Level (m)
137
136
135
1980
1990
2000
2010
Year
- - - Simulated
o Measured
WL_299-W14-16_CPM_V3.3_TMC_10-11-2010

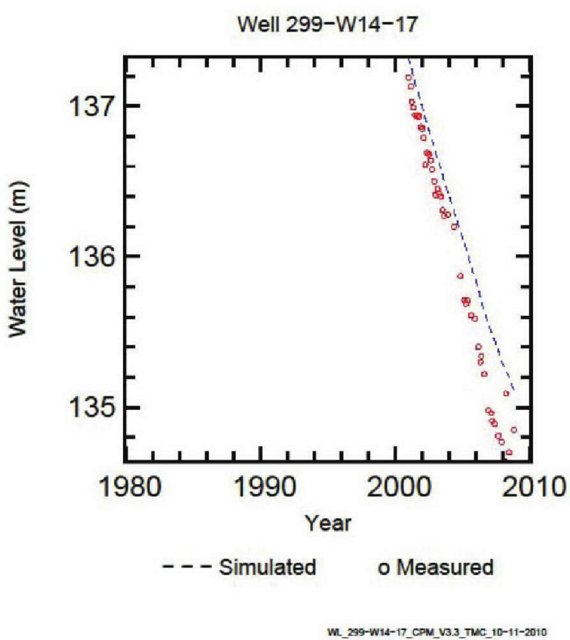
Well 299-W14-17
Water Level (m)
137
136
135
1980
1990
2000
2010
Year
- - - Simulated
o Measured
WL_299-W14-17_CPM_V3.3_TMC_10-11-2010

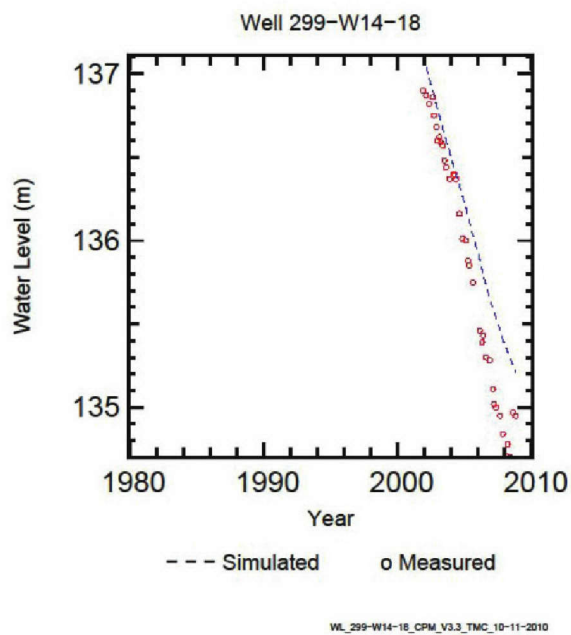
Well 299-W14-18
Water Level (m)
137
136
135
1980
1990
2000
2010
Year
- - - Simulated
o Measured
WL_299-W14-18_CPM_V3.3_TMC_10-11-2010

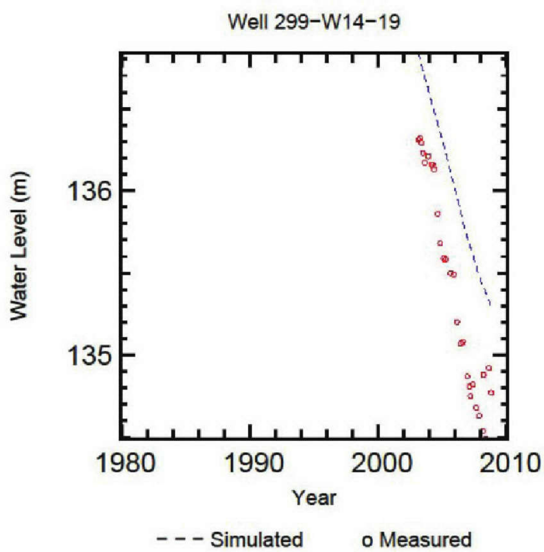

WL_299-W14-19_CPM_V3.3_TMC_10-11-2010

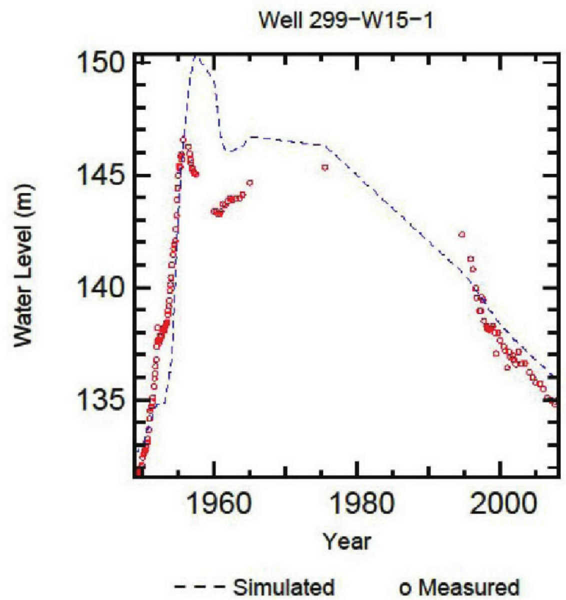

WL_299-W15-1_CPM_V3.3_TMC_10-11-2010

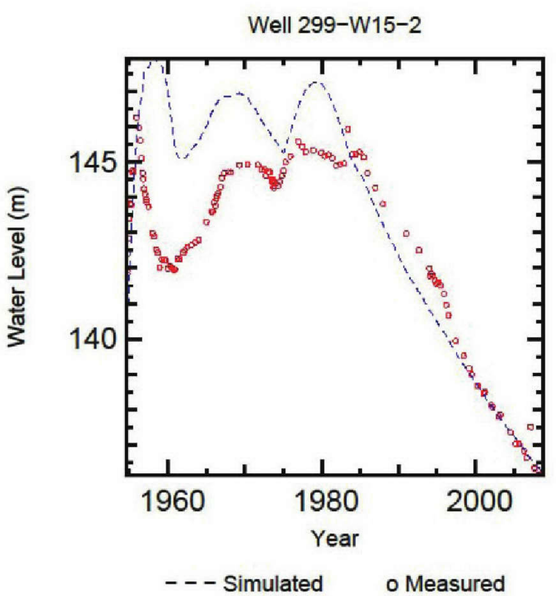

WL_299-W15-2_CPM_V3.3_TMC_10-11-2010

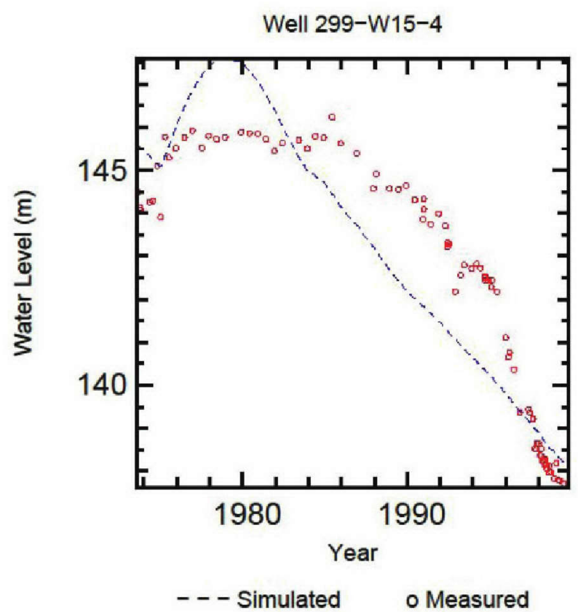

WL_299-W15-4_CPM_V3.3_TMC_10-11-2010

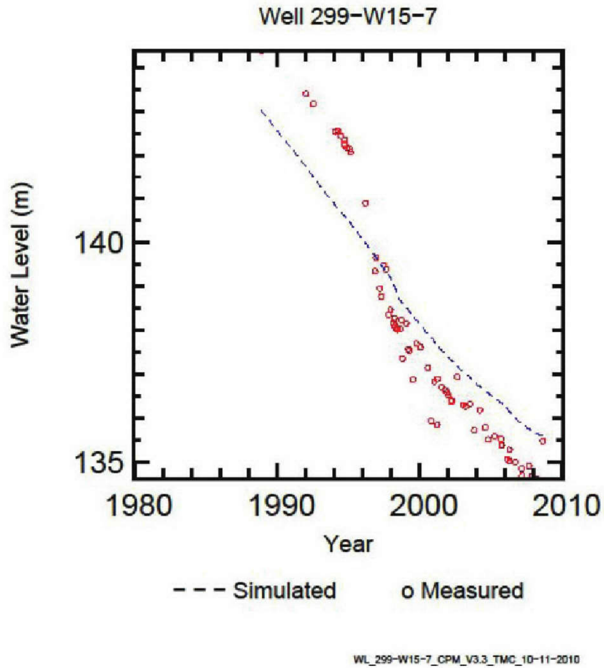

Well 299-W15-7
Water Level (m)
140
135
1980
1990
2000
2010
Year
- - - Simulated
o Measured
WL_299-W15-7_CPM_V3.3_TMC_10-11-2010

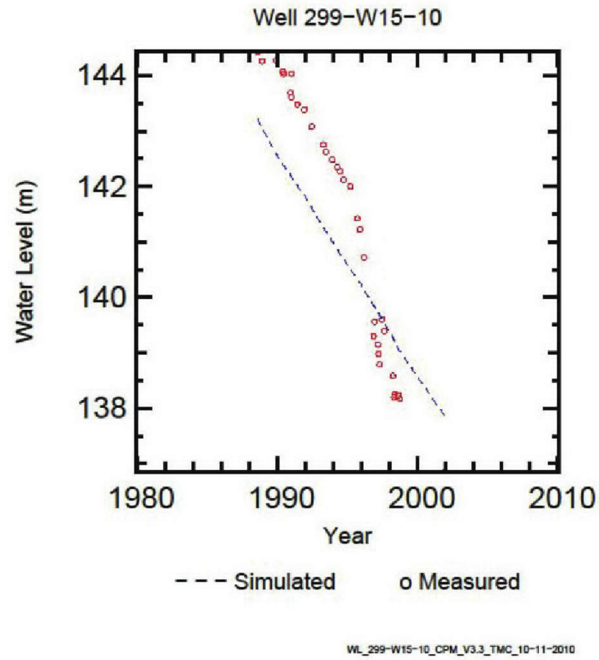

Well 299-W15-10
Water Level (m)
144
142
140
138
1980
1990
2000
2010
Year
- - - Simulated
o Measured
WL_299-W15-10_CPM_V3.3_TMC_10-11-2010

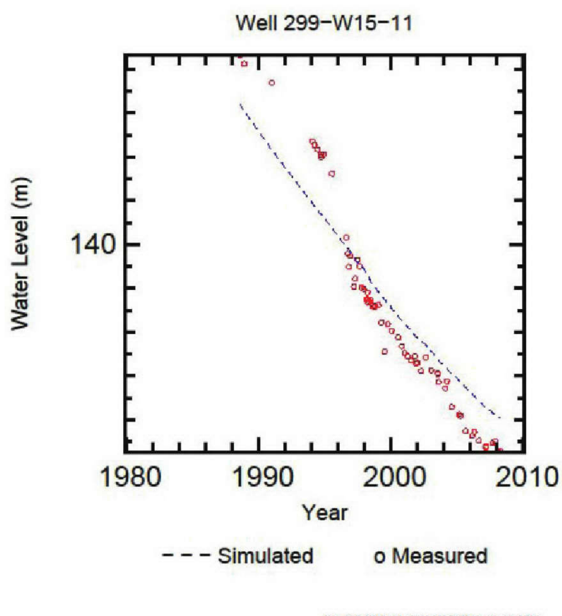

Well 299-W15-11
Water Level (m)
140
1980
1990
2000
2010
Year
- - - Simulated
o Measured
WL_299-W15-11_CPM_V3.3_TMC_10-11-2010

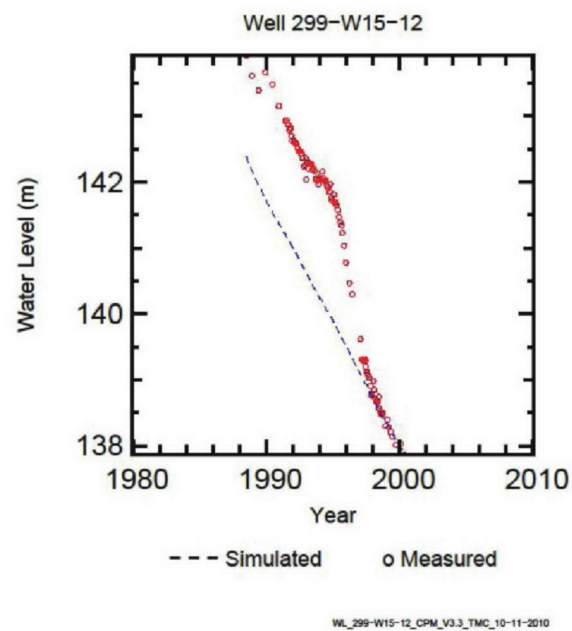

Well 299-W15-12
Water Level (m)
142
140
138
1980
1990
2000
2010
Year
- - - Simulated
o Measured
WL_299-W15-12_CPM_V3.3_TMC_10-11-2010

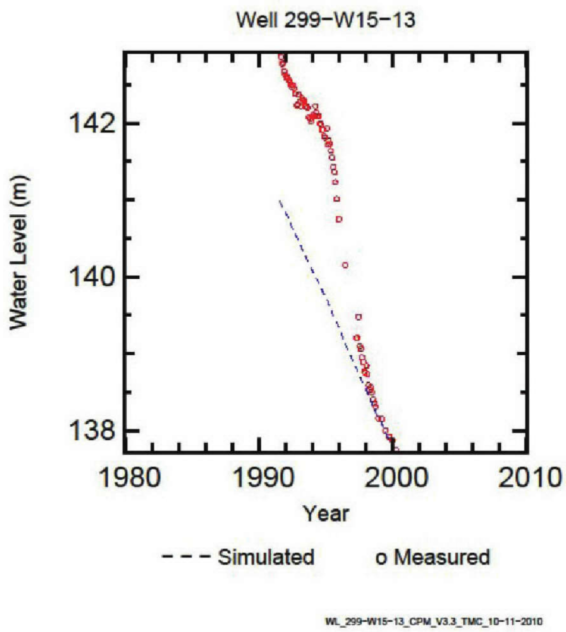
Well 299−W15−13
Water Level (m)
142
140
138
1980
1990
2000
2010
Year
- - - Simulated
o Measured
WL_299-W15-13_CPM_V3.3_TMC_10-11-2010

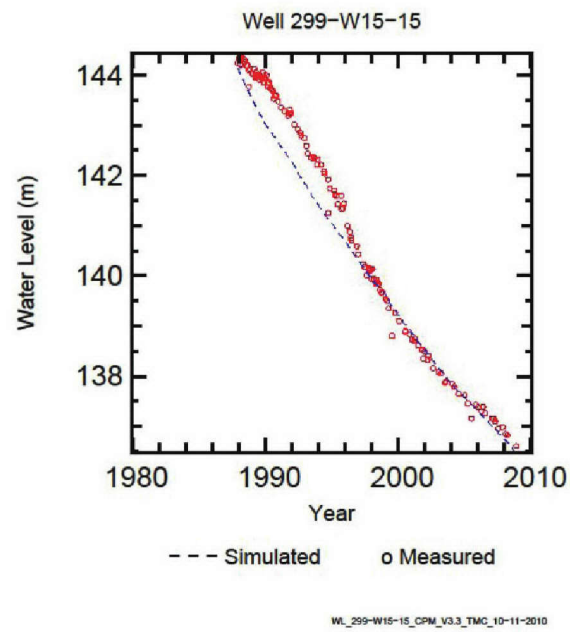
Well 299−W15−15
Water Level (m)
144
142
140
138
1980
1990
2000
2010
Year
- - - Simulated
o Measured
WL_299-W15-15_CPM_V3.3_TMC_10-11-2010

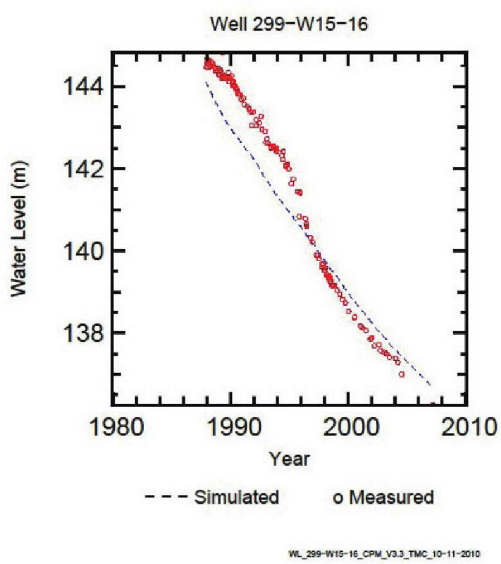
Well 299−W15−16
Water Level (m)
144
142
140
138
1980
1990
2000
2010
Year
- - - Simulated
o Measured
WL_299-W15-16_CPM_V3.3_TMC_10-11-2010

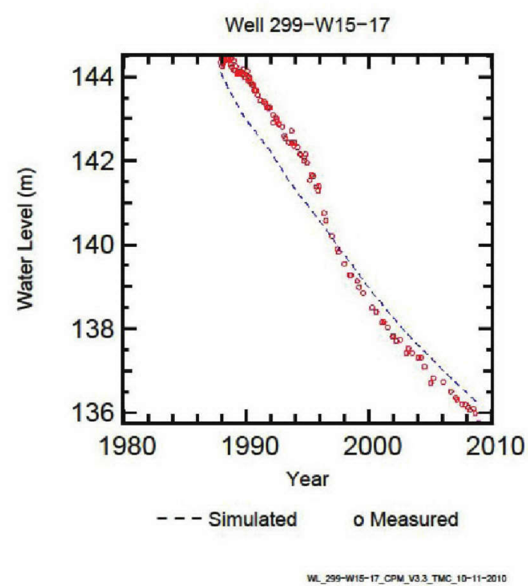
Well 299−W15−17
Water Level (m)
144
142
140
138
136
1980
1990
2000
2010
Year
- - - Simulated
o Measured
WL_299-W15-17_CPM_V3.3_TMC_10-11-2010

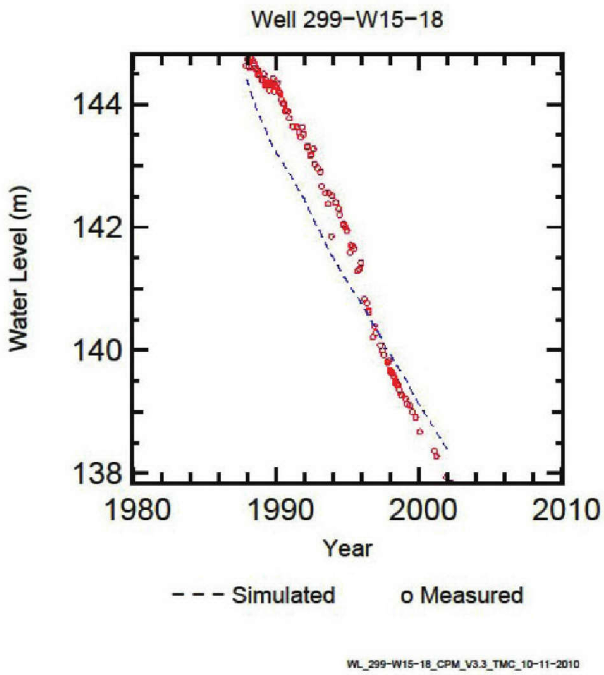
Well 299-W15-18
Water Level (m)
138
140
142
144
1980
1990
2000
2010
Year
- - - Simulated
o Measured
WL_299-W15-18_CPM_V3.3_TMC_10-11-2010

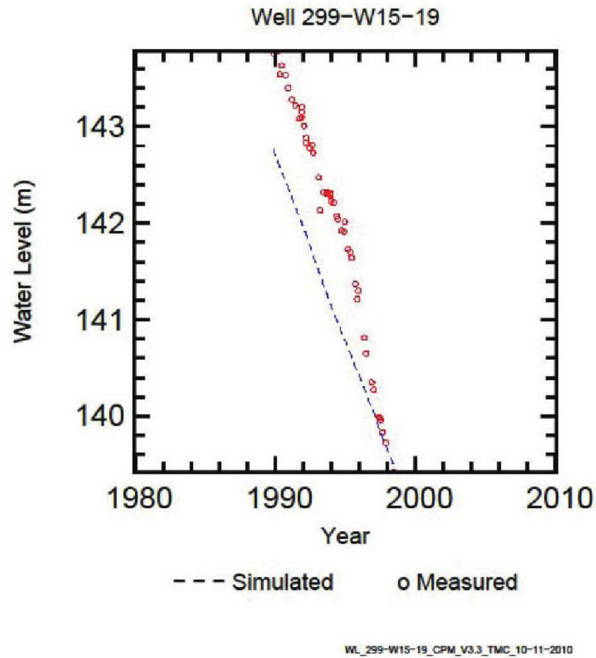
Well 299-W15-19
Water Level (m)
140
141
142
143
1980
1990
2000
2010
Year
- - - Simulated
o Measured
WL_299-W15-19_CPM_V3.3_TMC_10-11-2010

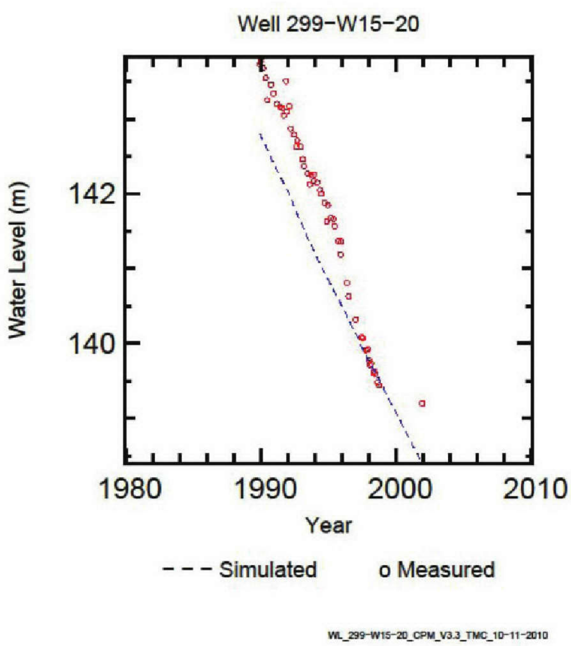
Well 299-W15-20
Water Level (m)
140
142
1980
1990
2000
2010
Year
- - - Simulated
o Measured
WL_299-W15-20_CPM_V3.3_TMC_10-11-2010

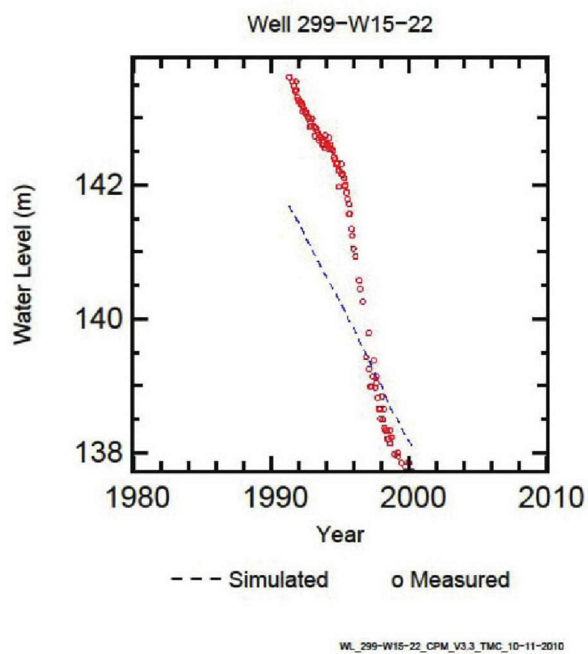
Well 299-W15-22
Water Level (m)
138
140
142
1980
1990
2000
2010
Year
- - - Simulated
o Measured
WL_299-W15-22_CPM_V3.3_TMC_10-11-2010

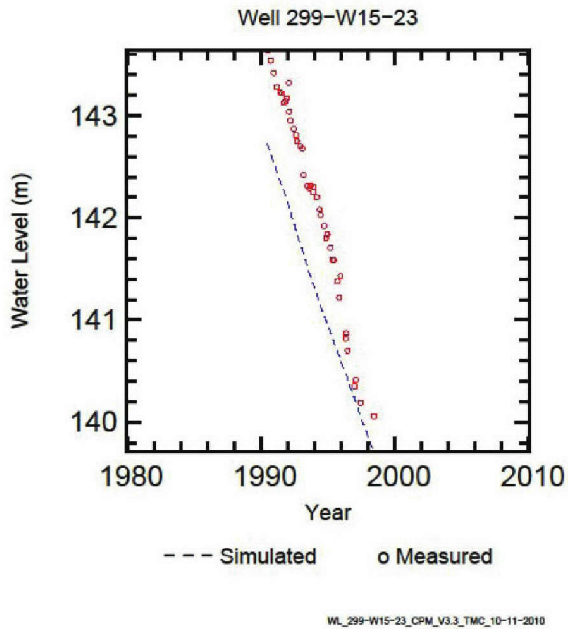
Well 299-W15-23
Water Level (m)
143
142
141
140
1980
1990
2000
2010
Year
Simulated
o Measured
WL_299-W15-23_CPM_V3.3_TMC_10-11-2010

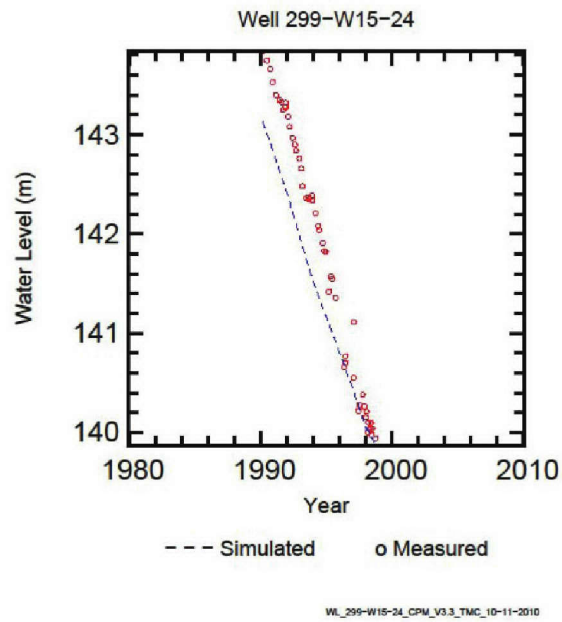
Well 299-W15-24
Water Level (m)
143
142
141
140
1980
1990
2000
2010
Year
Simulated
o Measured
WL_299-W15-24_CPM_V3.3_TMC_10-11-2010

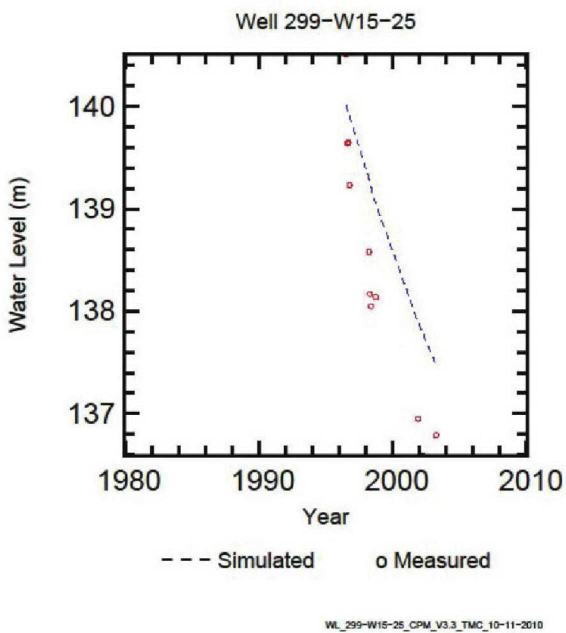
Well 299-W15-25
Water Level (m)
140
139
138
137
1980
1990
2000
2010
Year
Simulated
o Measured
WL_299-W15-25_CPM_V3.3_TMC_10-11-2010

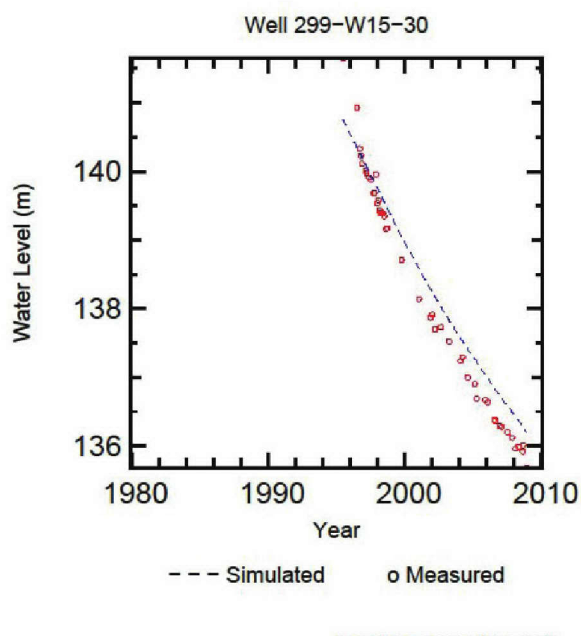
Well 299-W15-30
Water Level (m)
140
138
136
1980
1990
2000
2010
Year
Simulated
o Measured
WL_299-W15-30_CPM_V3.3_TMC_10-11-2010

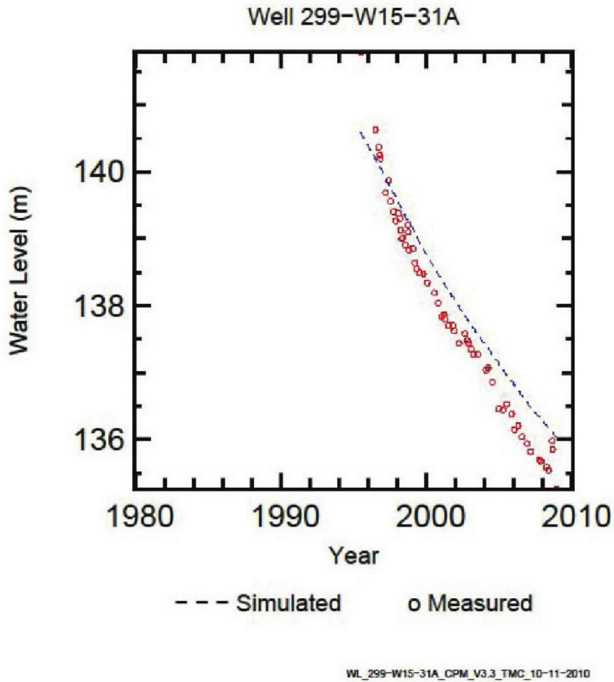
Well 299-W15-31A
Water Level (m)
140
138
136
1980
1990
2000
2010
Year
- - - Simulated
o Measured
WL_299-W15-31A_CPM_V3.3_TMC_10-11-2010

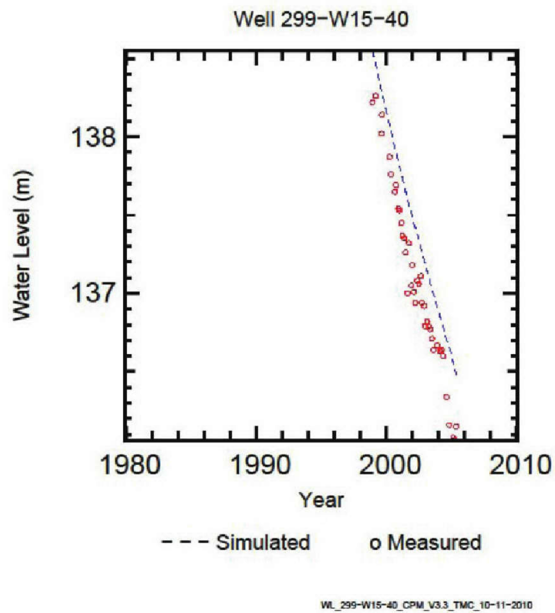
Well 299-W15-40
Water Level (m)
138
137
1980
1990
2000
2010
Year
- - - Simulated
o Measured
WL_299-W15-40_CPM_V3.3_TMC_10-11-2010

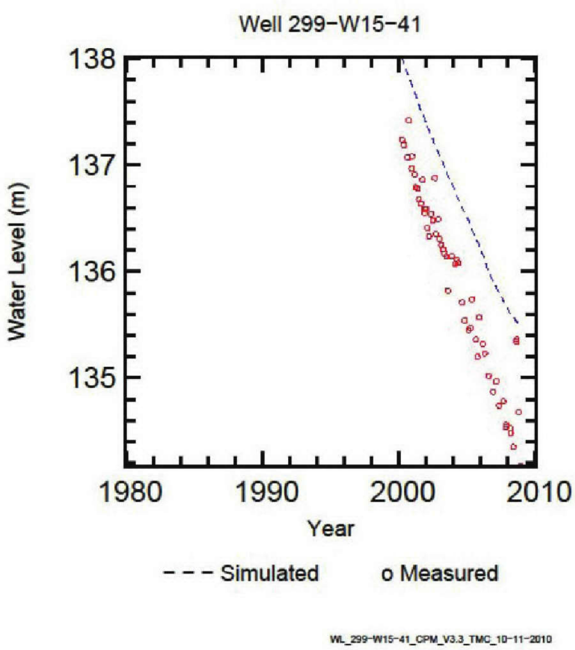
Well 299-W15-41
Water Level (m)
138
137
136
135
1980
1990
2000
2010
Year
- - - Simulated
o Measured
WL_299-W15-41_CPM_V3.3_TMC_10-11-2010

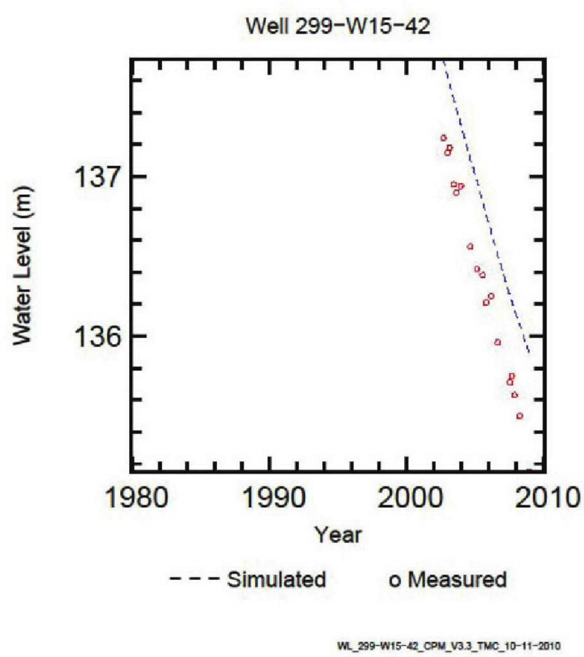
Well 299-W15-42
Water Level (m)
137
136
1980
1990
2000
2010
Year
- - - Simulated
o Measured
WL_299-W15-42_CPM_V3.3_TMC_10-11-2010

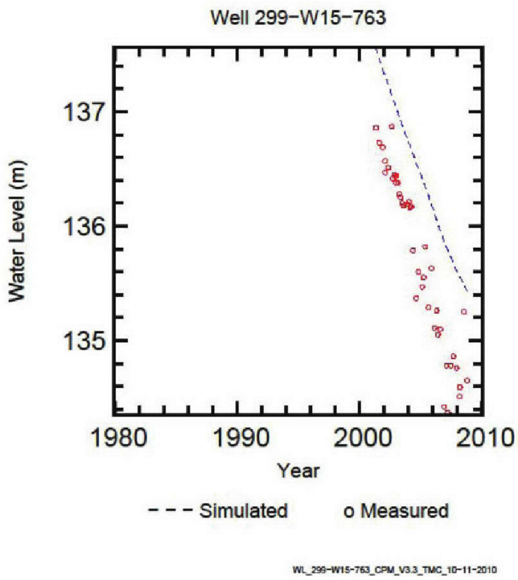
Well 299-W15-763
Water Level (m)
Year
- - - Simulated
o Measured
WL_299-W15-763_CPM_V3.3_TMC_10-11-2010

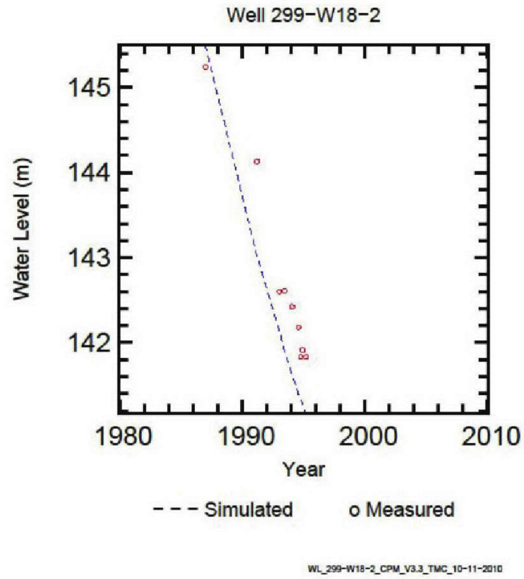
Well 299-W18-2
Water Level (m)
Year
- - - Simulated
o Measured
WL_299-W18-2_CPM_V3.3_TMC_10-11-2010

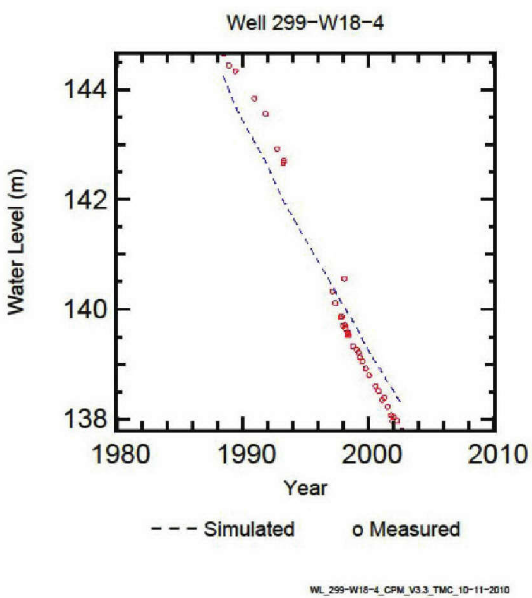
Well 299-W18-4
Water Level (m)
Year
- - - Simulated
o Measured
WL_299-W18-4_CPM_V3.3_TMC_10-11-2010

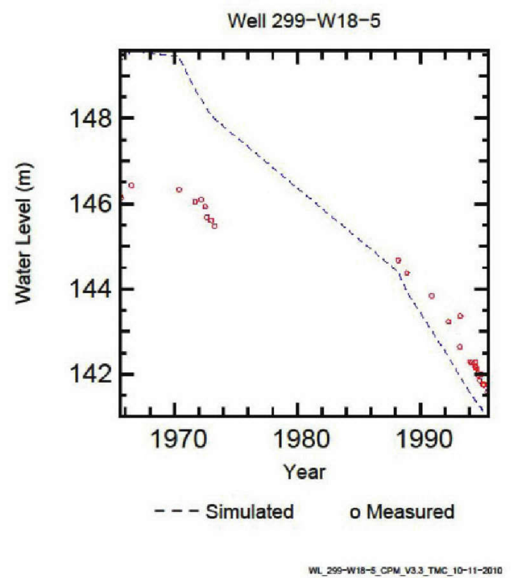
Well 299-W18-5
Water Level (m)
Year
- - - Simulated
o Measured
WL_299-W18-5_CPM_V3.3_TMC_10-11-2010

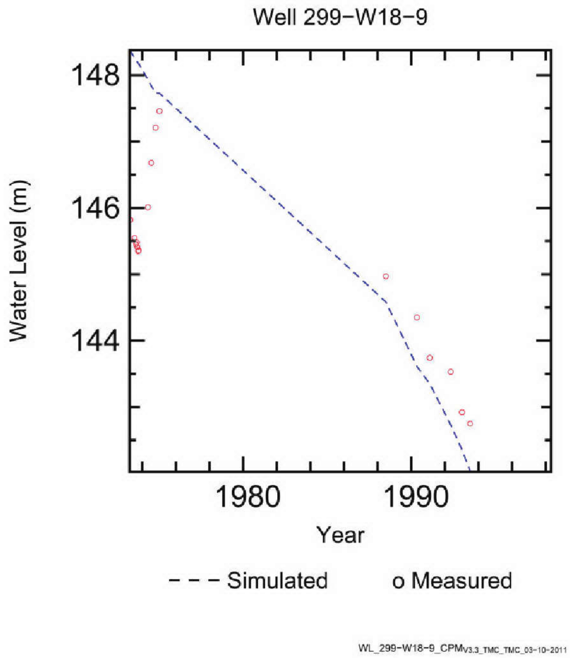
Well 299-W18-9
148
146
144
Water Level (m)
1980
1990
Year
- - - Simulated
o Measured
WL_299-W18-9_CPMv3.3_TMC_TMC_03-10-2011

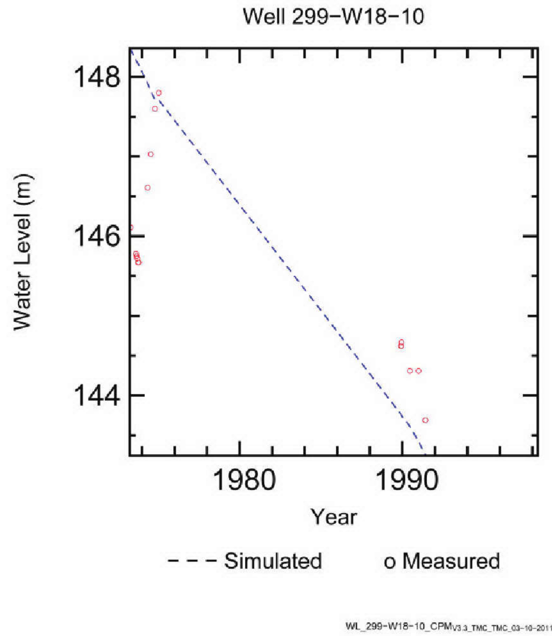
Well 299-W18-10
148
146
144
Water Level (m)
1980
1990
Year
- - - Simulated
o Measured
WL_299-W18-10_CPMv3.3_TMC_TMC_03-10-2011

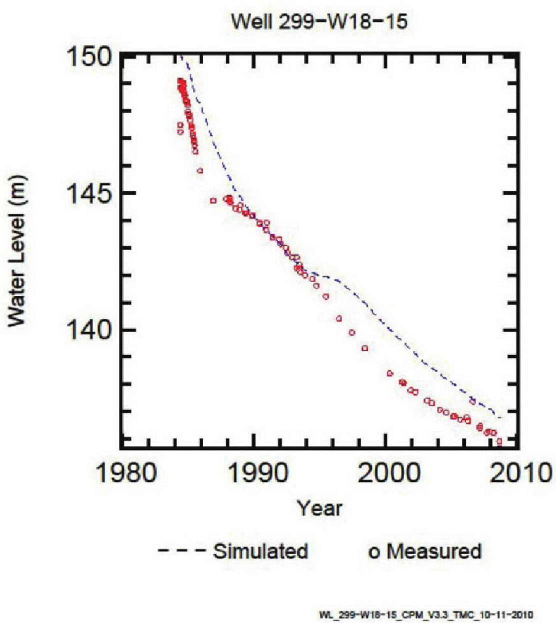
Well 299-W18-15
150
145
140
Water Level (m)
1980
1990
2000
2010
Year
- - - Simulated
o Measured
WL_299-W18-15_CPM_V3.3_TMC_10-11-2010

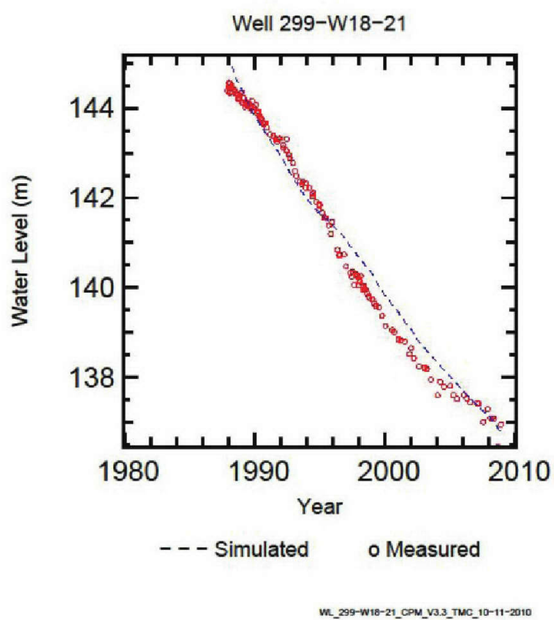
Well 299-W18-21
144
142
140
138
Water Level (m)
1980
1990
2000
2010
Year
- - - Simulated
o Measured
WL_299-W18-21_CPM_V3.3_TMC_10-11-2010

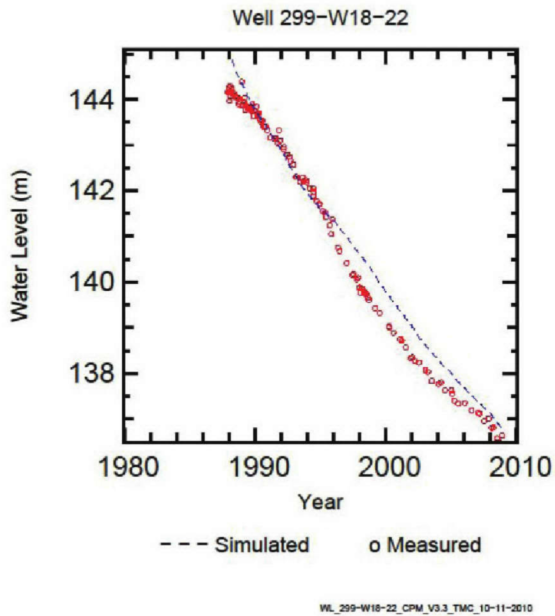
Well 299-W18-22
Water Level (m)
144
142
140
138
1980
1990
2000
2010
Year
- - - Simulated
o Measured
WL_299-W18-22_CPM_V3.3_TMC_10-11-2010

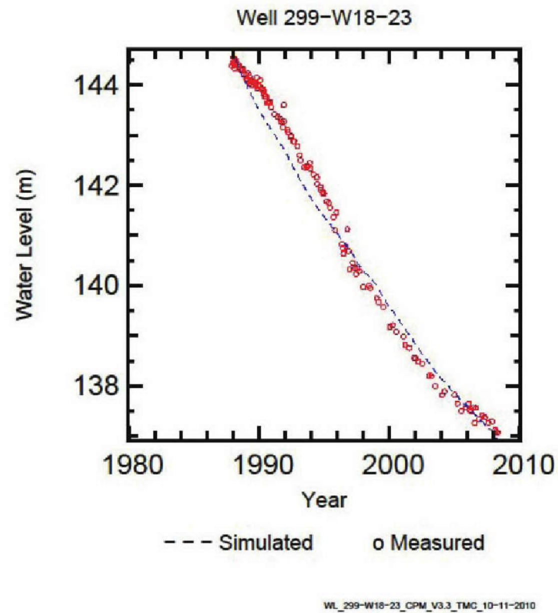
Well 299-W18-23
Water Level (m)
144
142
140
138
1980
1990
2000
2010
Year
- - - Simulated
o Measured
WL_299-W18-23_CPM_V3.3_TMC_10-11-2010

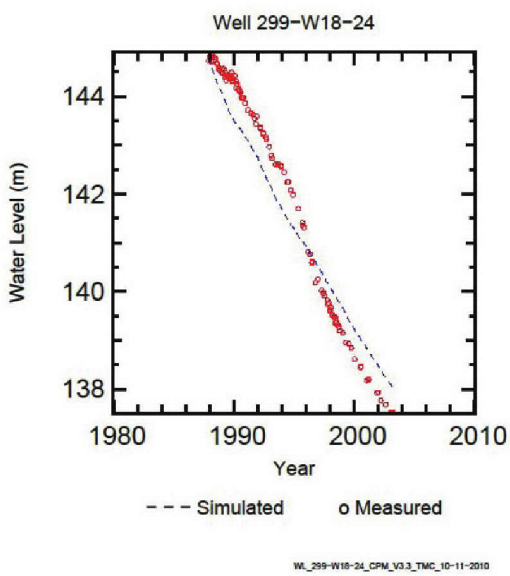
Well 299-W18-24
Water Level (m)
144
142
140
138
1980
1990
2000
2010
Year
- - - Simulated
o Measured
WL_299-W18-24_CPM_V3.3_TMC_10-11-2010

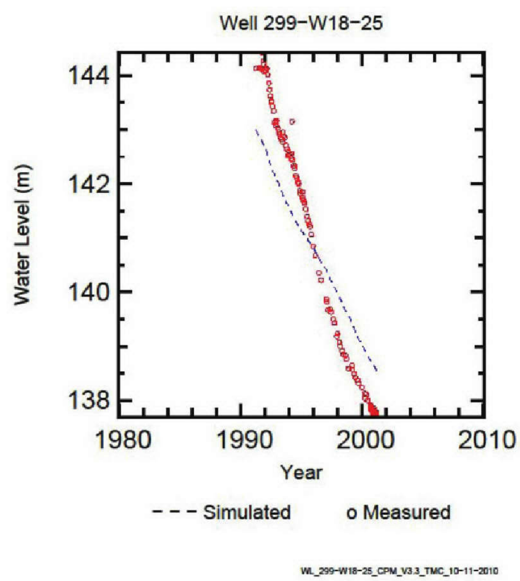
Well 299-W18-25
Water Level (m)
144
142
140
138
1980
1990
2000
2010
Year
- - - Simulated
o Measured
WL_299-W18-25_CPM_V3.3_TMC_10-11-2010

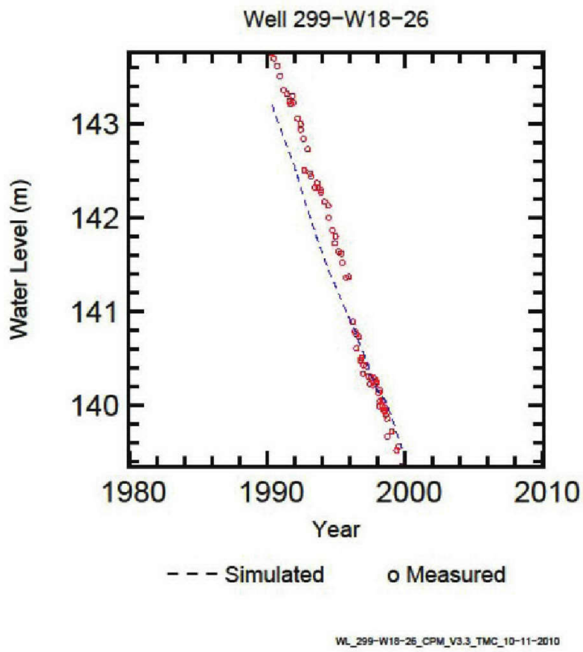
Well 299-W18-26
Water Level (m)
143
142
141
140
1980
1990
2000
2010
Year
- - - Simulated
o Measured
WL_299-W18-26_CPM_V3.3_TMC_10-11-2010

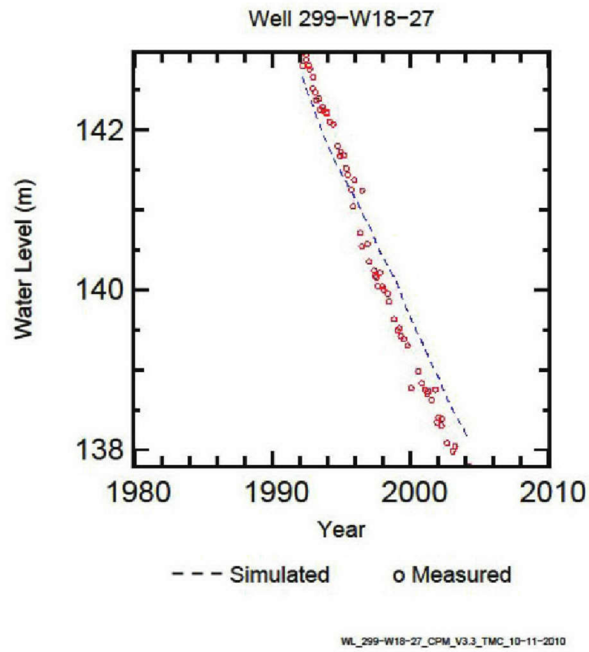
Well 299-W18-27
Water Level (m)
142
140
138
1980
1990
2000
2010
Year
- - - Simulated
o Measured
WL_299-W18-27_CPM_V3.3_TMC_10-11-2010

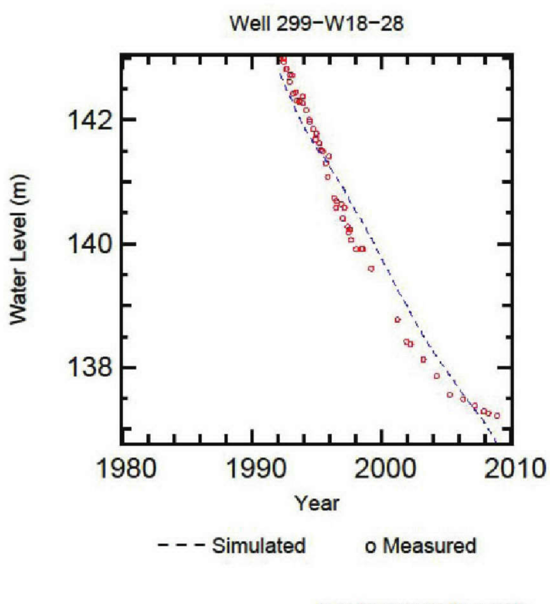
Well 299-W18-28
Water Level (m)
142
140
138
1980
1990
2000
2010
Year
- - - Simulated
o Measured
WL_299-W18-28_CPM_V3.3_TMC_10-11-2010

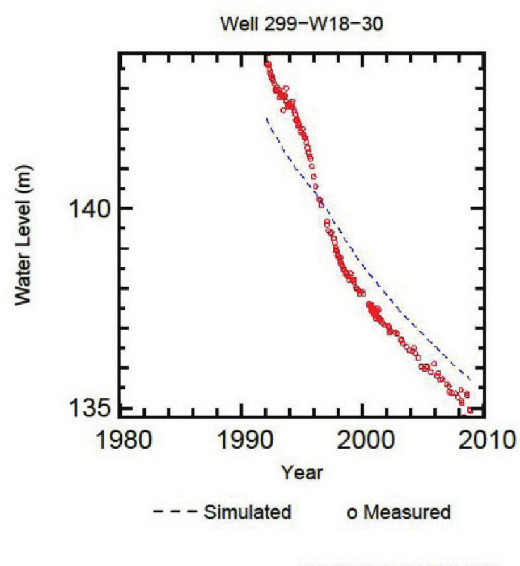
Well 299-W18-30
Water Level (m)
140
135
1980
1990
2000
2010
Year
- - - Simulated
o Measured
WL_299-W18-30_CPM_V3.3_TMC_10-11-2010

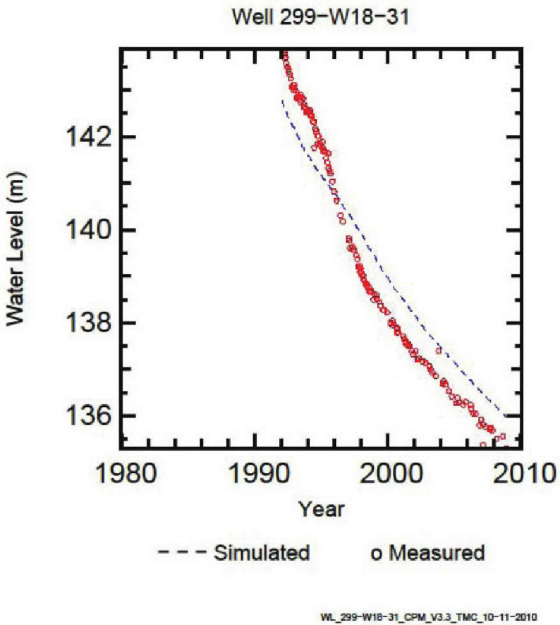
Well 299-W18-31
Water Level (m)
142
140
138
136
1980
1990
2000
2010
Year
- - - Simulated
o Measured
WL_299-W18-31_CPM_V3.3_TMC_10-11-2010

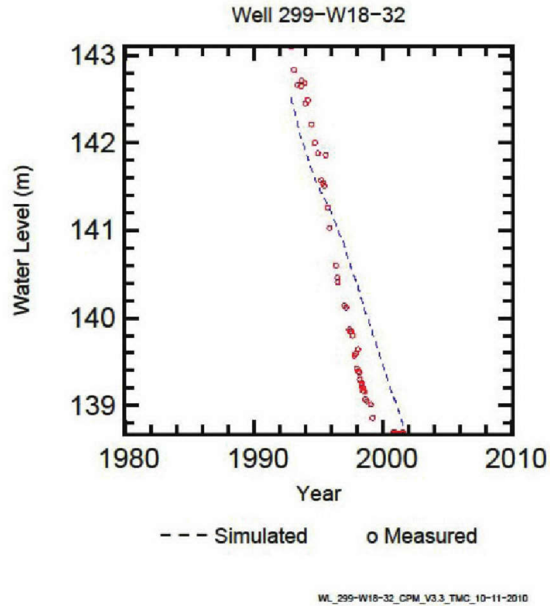
Well 299-W18-32
Water Level (m)
143
142
141
140
139
1980
1990
2000
2010
Year
- - - Simulated
o Measured
WL_299-W18-32_CPM_V3.3_TMC_10-11-2010

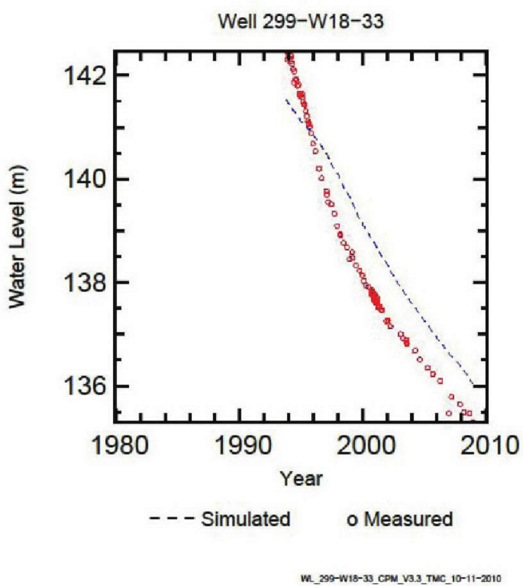
Well 299-W18-33
Water Level (m)
142
140
138
136
1980
1990
2000
2010
Year
- - - Simulated
o Measured
WL_299-W18-33_CPM_V3.3_TMC_10-11-2010

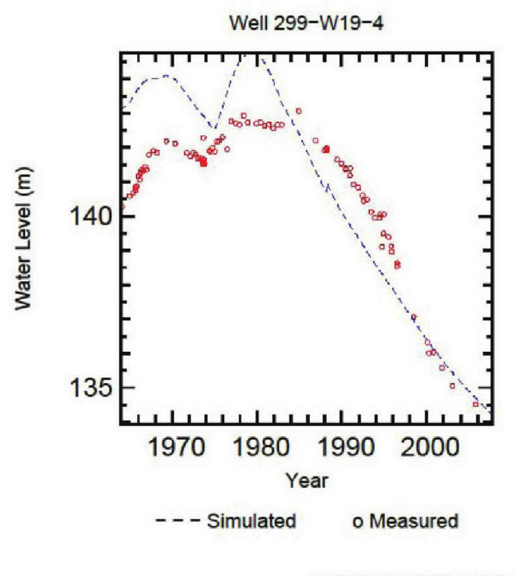
Well 299-W19-4
Water Level (m)
140
135
1970
1980
1990
2000
Year
- - - Simulated
o Measured
WL_299-W19-4_CPM_V3.3_TMC_10-11-2010

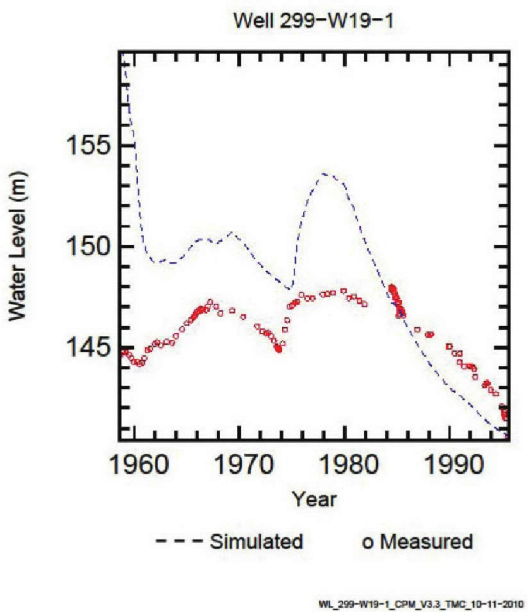
Well 299-W19-1
Water Level (m)
155
150
145
1960
1970
1980
1990
Year
- - - Simulated
o Measured
WL_299-W19-1_CPM_V3.3_TMC_10-11-2010

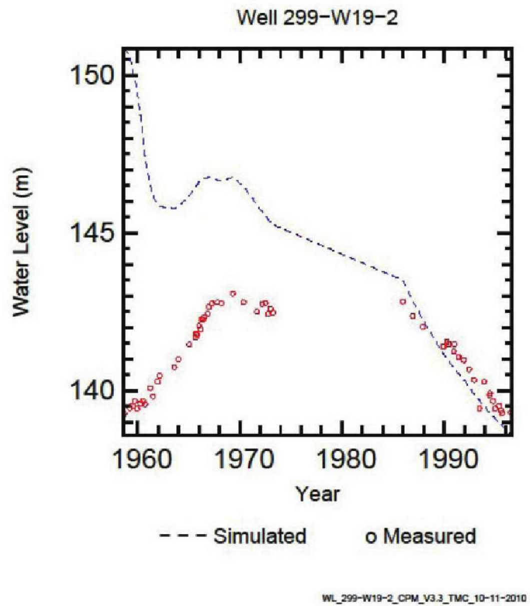
Well 299-W19-2
Water Level (m)
150
145
140
1960
1970
1980
1990
Year
- - - Simulated
o Measured
WL_299-W19-2_CPM_V3.3_TMC_10-11-2010

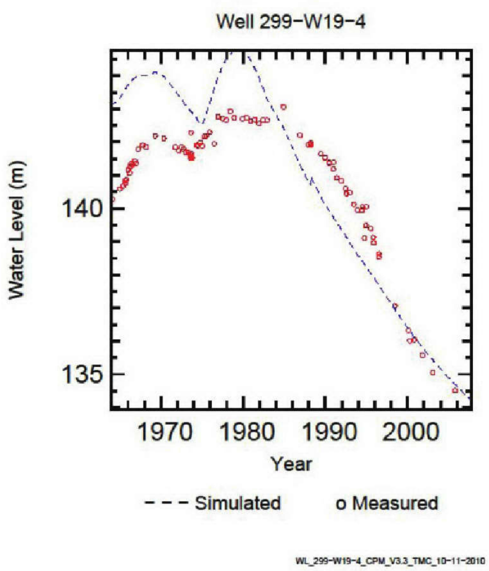
Well 299-W19-4
Water Level (m)
140
135
1970
1980
1990
2000
Year
- - - Simulated
o Measured
WL_299-W19-4_CPM_V3.3_TMC_10-11-2010

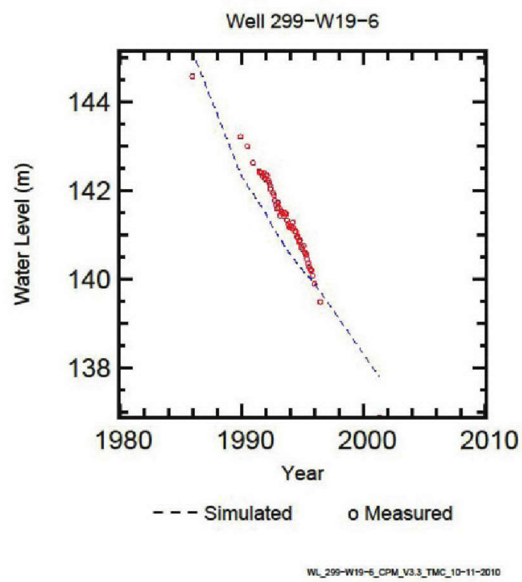
Well 299-W19-6
Water Level (m)
144
142
140
138
1980
1990
2000
2010
Year
- - - Simulated
o Measured
WL_299-W19-6_CPM_V3.3_TMC_10-11-2010

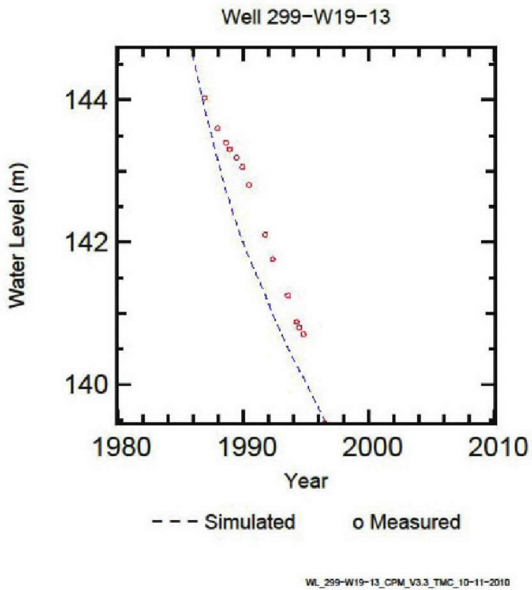
Well 299-W19-13
Water Level (m)
144
142
140
1980
1990
2000
2010
Year
Simulated
Measured
WL_299-W19-13_CPM_V3.3_TMC_10-11-2010

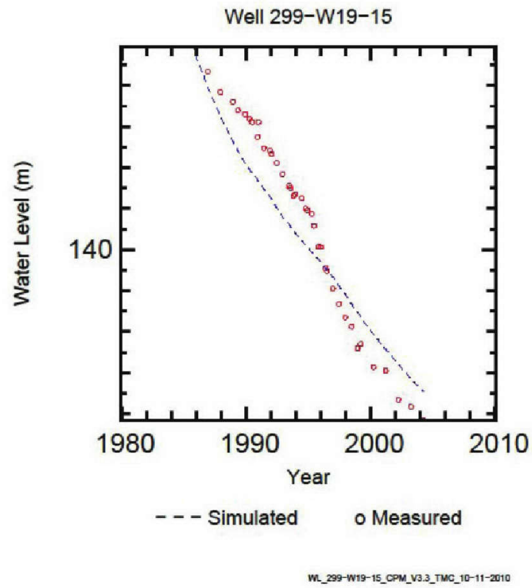
Well 299-W19-15
Water Level (m)
140
1980
1990
2000
2010
Year
Simulated
Measured
WL_299-W19-15_CPM_V3.3_TMC_10-11-2010

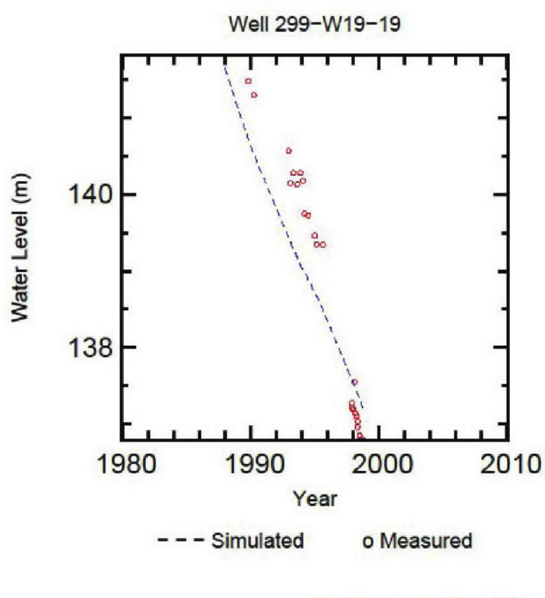
Well 299-W19-19
Water Level (m)
140
138
1980
1990
2000
2010
Year
Simulated
Measured
WL_299-W19-19_CPM_V3.3_TMC_10-11-2010

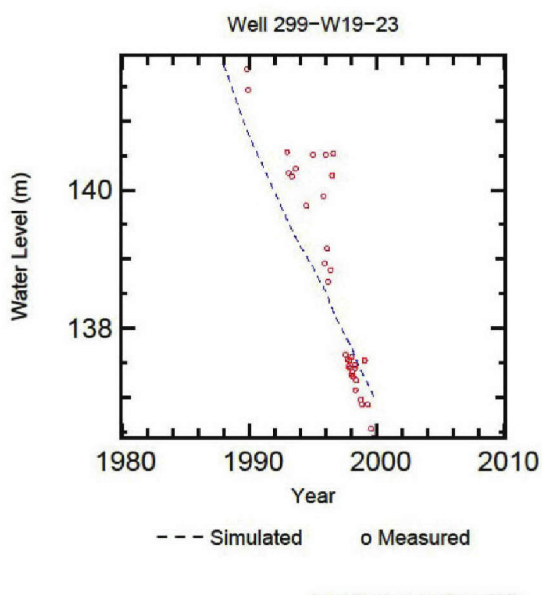
Well 299-W19-23
Water Level (m)
140
138
1980
1990
2000
2010
Year
Simulated
Measured
WL_299-W19-23_CPM_V3.3_TMC_10-11-2010

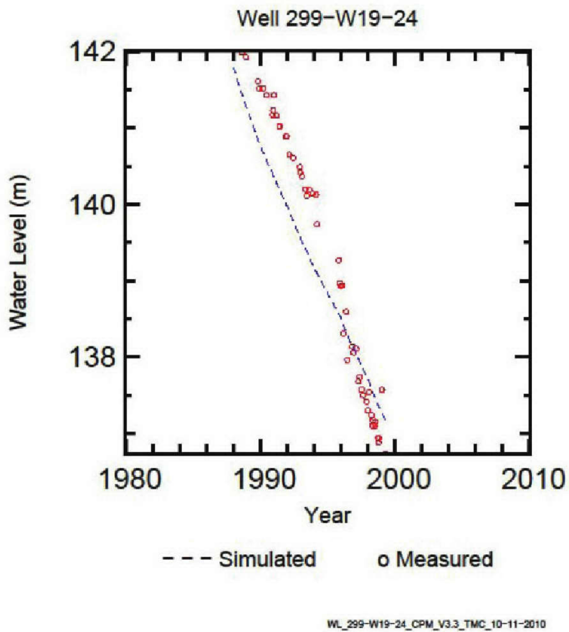
Well 299-W19-24
Water Level (m)
142
140
138
1980
1990
2000
2010
Year
- - - Simulated
o Measured
WL_299-W19-24_CPM_V3.3_TMC_10-11-2010

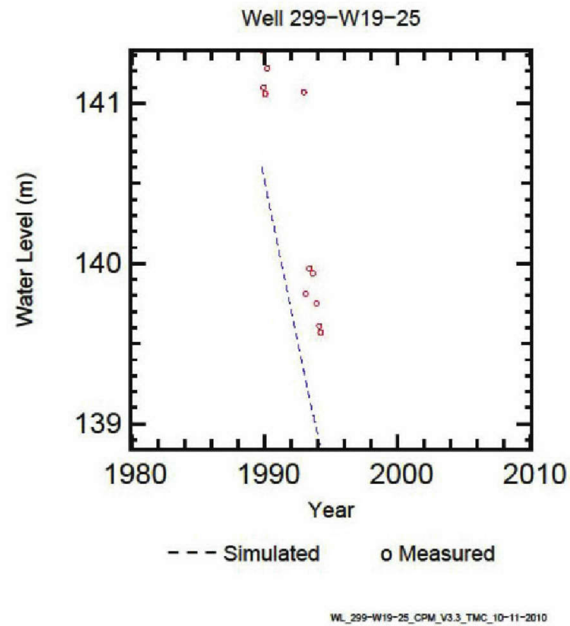
Well 299-W19-25
Water Level (m)
141
140
139
1980
1990
2000
2010
Year
- - - Simulated
o Measured
WL_299-W19-25_CPM_V3.3_TMC_10-11-2010

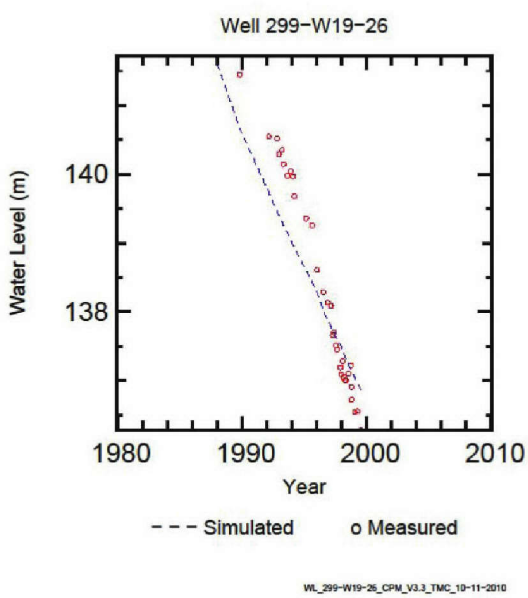
Well 299-W19-26
Water Level (m)
140
138
1980
1990
2000
2010
Year
- - - Simulated
o Measured
WL_299-W19-26_CPM_V3.3_TMC_10-11-2010

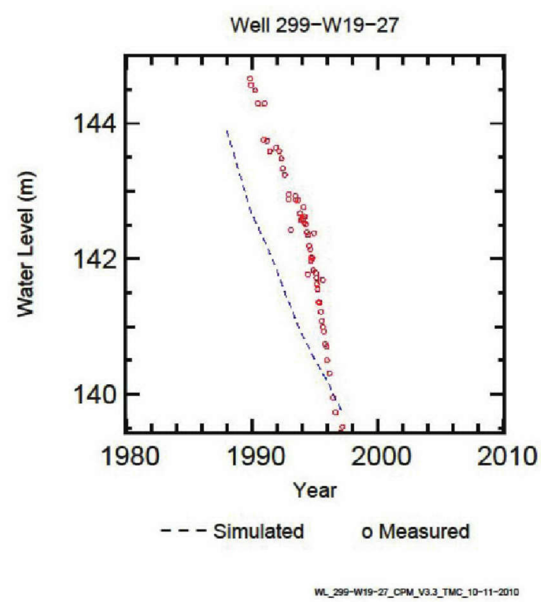
Well 299-W19-27
Water Level (m)
144
142
140
1980
1990
2000
2010
Year
- - - Simulated
o Measured
WL_299-W19-27_CPM_V3.3_TMC_10-11-2010

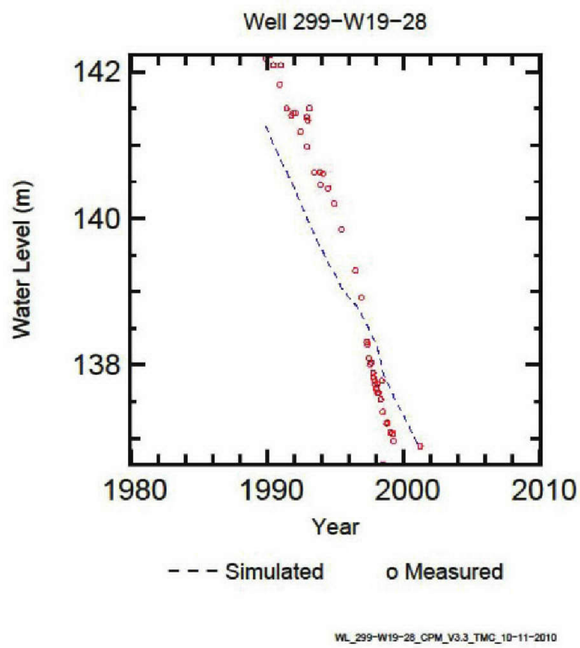
Well 299-W19-28
Water Level (m)
142
140
138
1980
1990
2000
2010
Year
Simulated
Measured
WL_299-W19-28_CPM_V3.3_TMC_10-11-2010

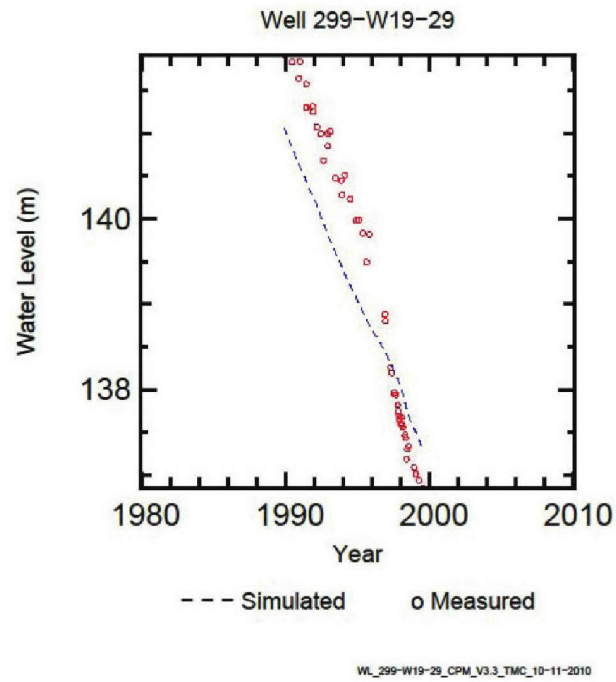
Well 299-W19-29
Water Level (m)
140
138
1980
1990
2000
2010
Year
Simulated
Measured
WL_299-W19-29_CPM_V3.3_TMC_10-11-2010

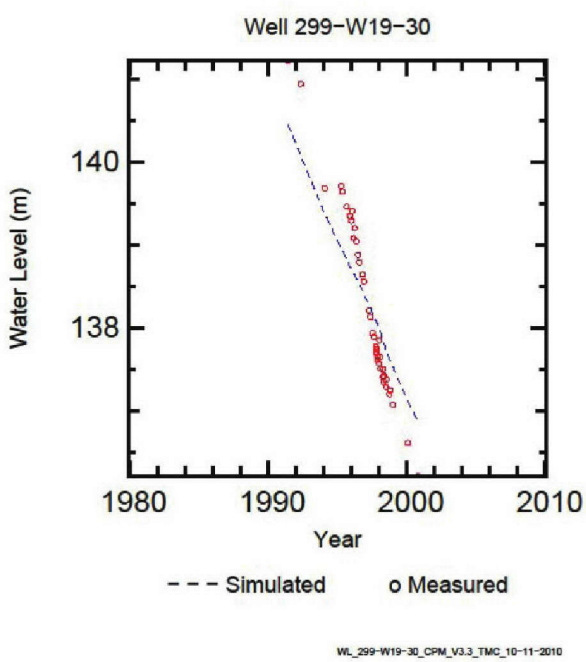
Well 299-W19-30
Water Level (m)
140
138
1980
1990
2000
2010
Year
Simulated
Measured
WL_299-W19-30_CPM_V3.3_TMC_10-11-2010

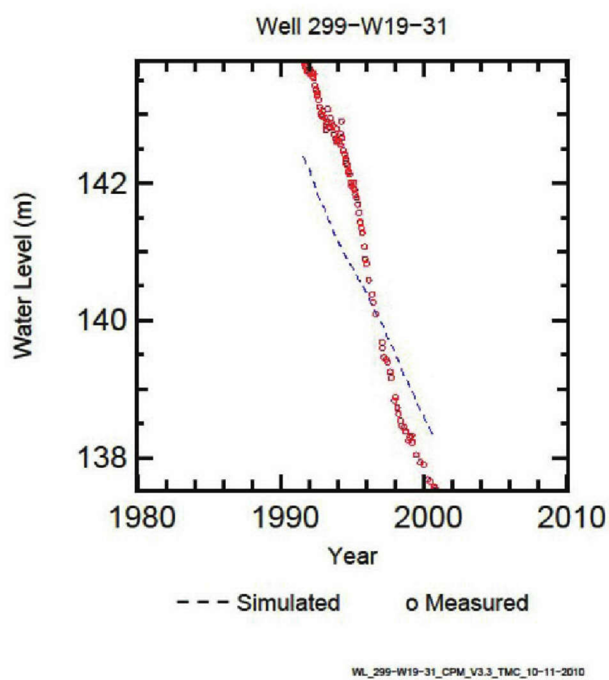
Well 299-W19-31
Water Level (m)
142
140
138
1980
1990
2000
2010
Year
Simulated
Measured
WL_299-W19-31_CPM_V3.3_TMC_10-11-2010

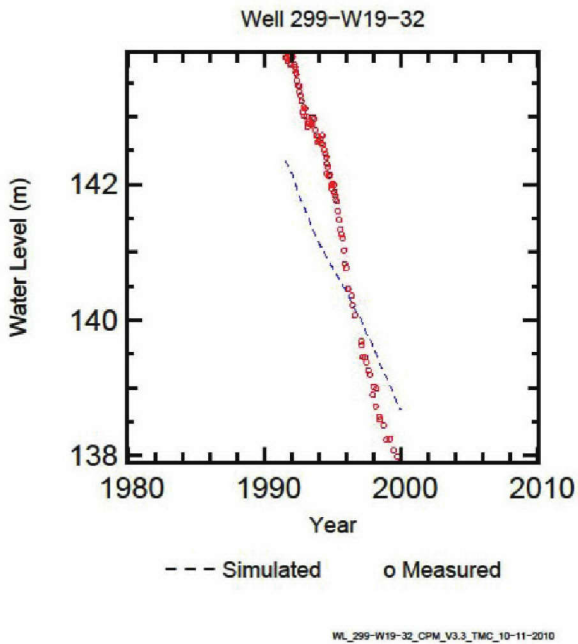
Well 299−W19−32
Water Level (m)
142
140
138
1980
1990
2000
2010
Year
- - - Simulated
o Measured
WL_299-W19-32_CPM_V3.3_TMC_10-11-2010

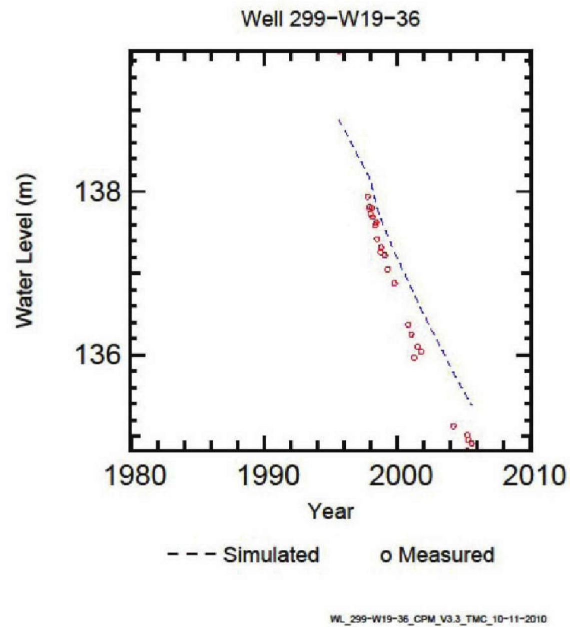
Well 299−W19−36
Water Level (m)
138
136
1980
1990
2000
2010
Year
- - - Simulated
o Measured
WL_299-W19-36_CPM_V3.3_TMC_10-11-2010

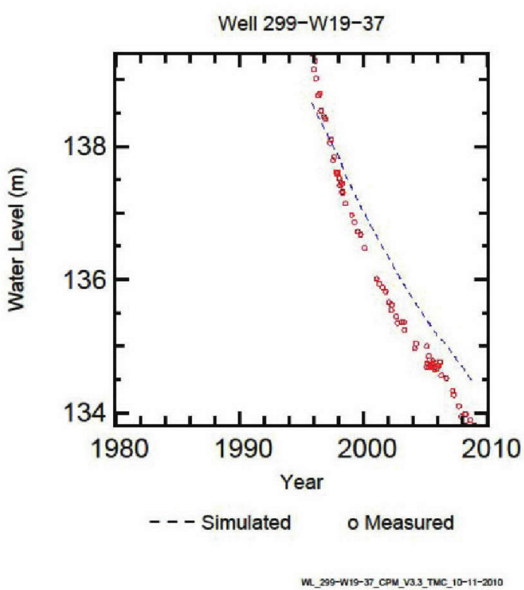
Well 299−W19−37
Water Level (m)
138
136
134
1980
1990
2000
2010
Year
- - - Simulated
o Measured
WL_299-W19-37_CPM_V3.3_TMC_10-11-2010

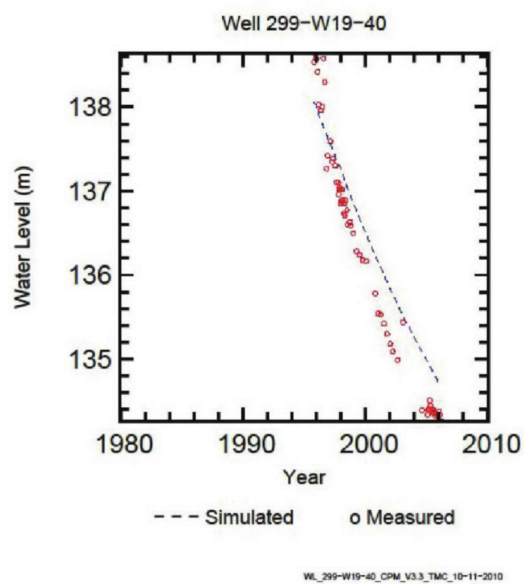
Well 299−W19−40
Water Level (m)
138
137
136
135
1980
1990
2000
2010
Year
- - - Simulated
o Measured
WL_299-W19-40_CPM_V3.3_TMC_10-11-2010

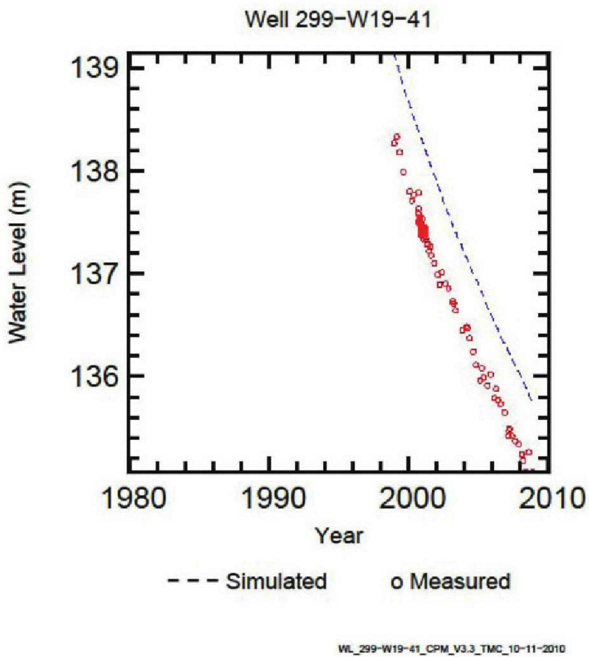
Well 299-W19-41
139
138
137
136
Water Level (m)
1980
1990
2000
2010
Year
- - - Simulated
o Measured
WL_299-W19-41_CPM_V3.3_TMC_10-11-2010

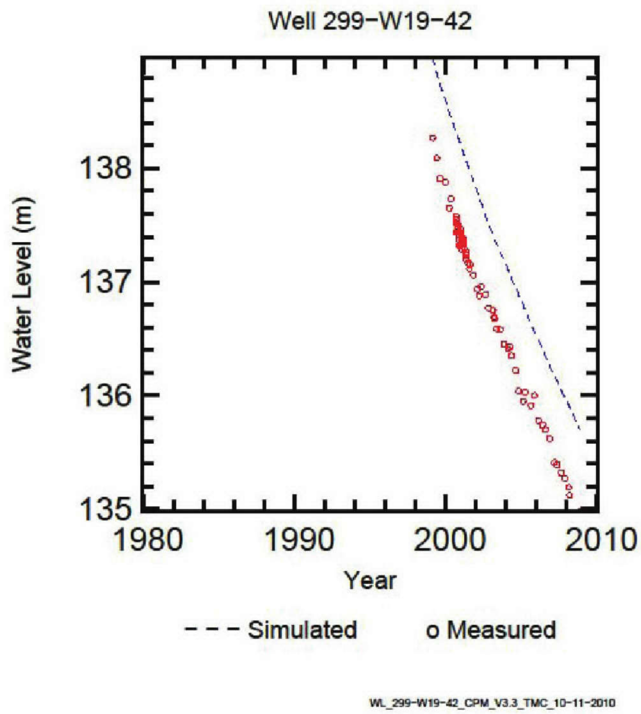
Well 299-W19-42
138
137
136
135
Water Level (m)
1980
1990
2000
2010
Year
- - - Simulated
o Measured
WL_299-W19-42_CPM_V3.3_TMC_10-11-2010

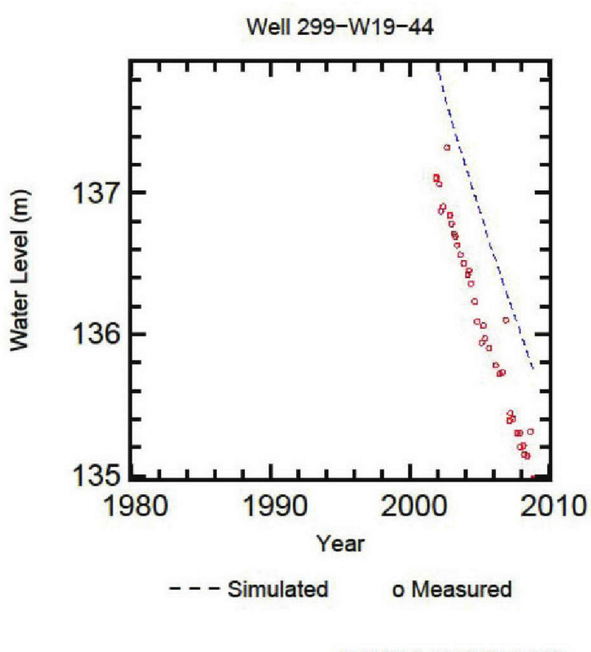
Well 299-W19-44
137
136
135
Water Level (m)
1980
1990
2000
2010
Year
- - - Simulated
o Measured
WL_299-W19-44_CPM_V3.3_TMC_10-11-2010

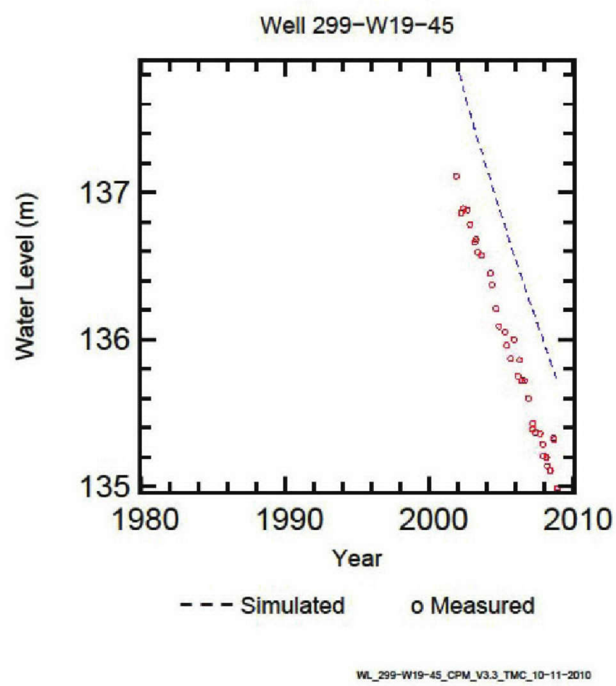
Well 299-W19-45
137
136
135
Water Level (m)
1980
1990
2000
2010
Year
- - - Simulated
o Measured
WL_299-W19-45_CPM_V3.3_TMC_10-11-2010

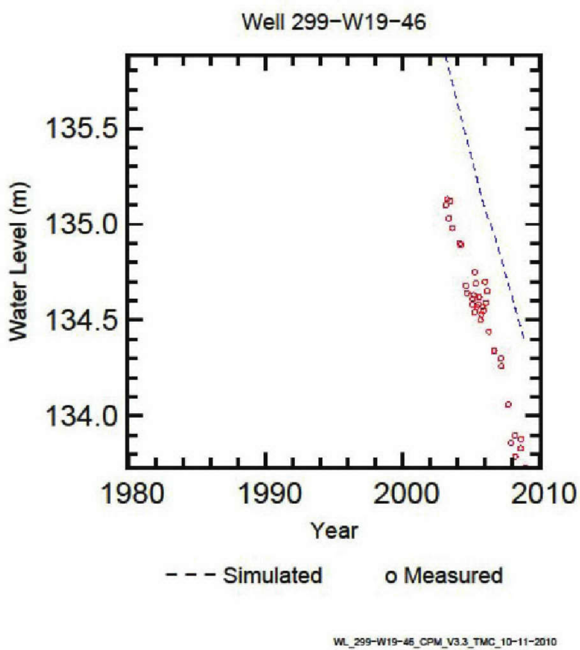
Well 299-W19-46
Water Level (m)
135.5
135.0
134.5
134.0
1980
1990
2000
2010
Year
- - - Simulated
o Measured
WL_299-W19-46_CPM_V3.3_TMC_10-11-2010

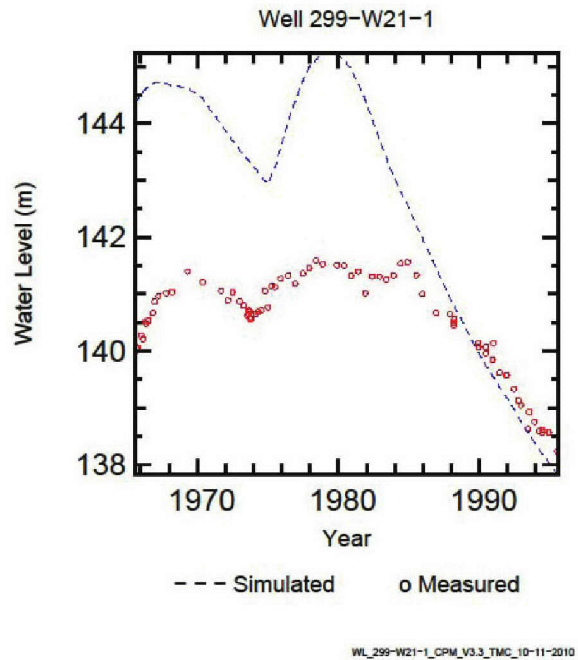
Well 299-W21-1
Water Level (m)
144
142
140
138
1970
1980
1990
Year
- - - Simulated
o Measured
WL_299-W21-1_CPM_V3.3_TMC_10-11-2010

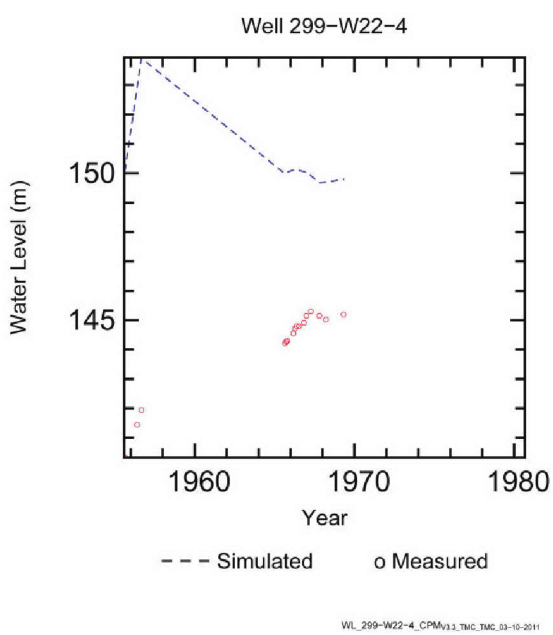
Well 299-W22-4
Water Level (m)
150
145
1960
1970
1980
Year
- - - Simulated
o Measured

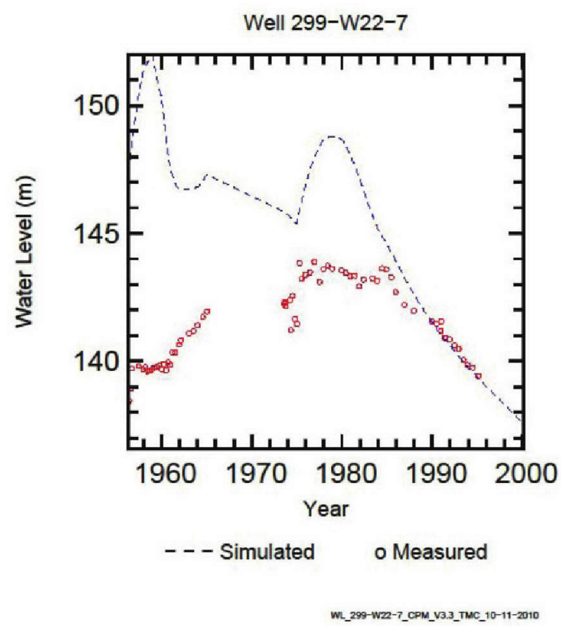
Well 299-W22-7
Water Level (m)
150
145
140
1960
1970
1980
1990
2000
Year
- - - Simulated
o Measured
WL_299-W22-7_CPM_V3.3_TMC_10-11-2010

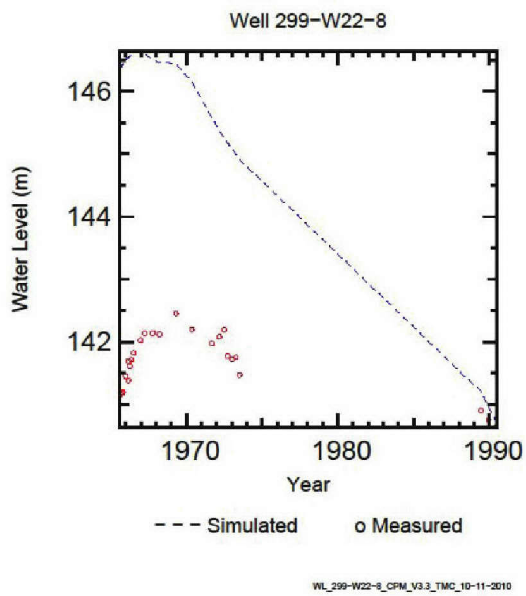
Well 299-W22-8
Water Level (m)
146
144
142
1970
1980
1990
Year
Simulated
o Measured
WL_299-W22-8_CPM_V3.3_TMC_10-11-2010

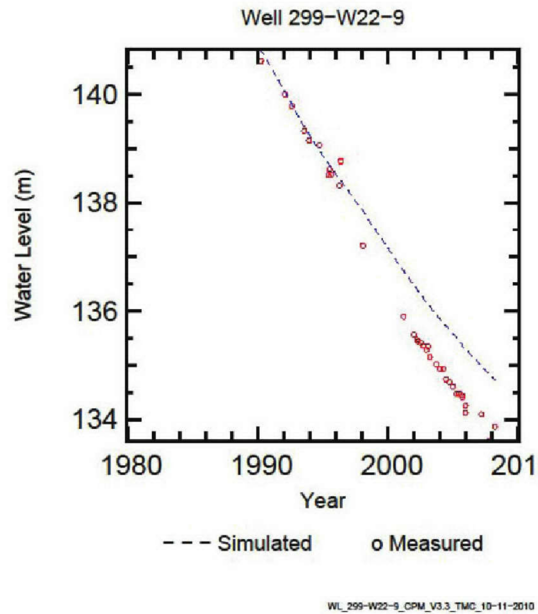
Well 299-W22-9
Water Level (m)
140
138
136
134
1980
1990
2000
2010
Year
Simulated
o Measured
WL_299-W22-9_CPM_V3.3_TMC_10-11-2010

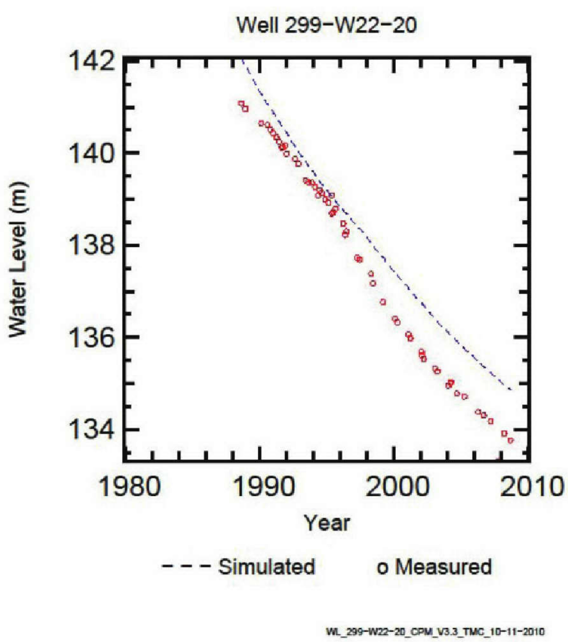
Well 299-W22-20
Water Level (m)
142
140
138
136
134
1980
1990
2000
2010
Year
Simulated
o Measured
WL_299-W22-20_CPM_V3.3_TMC_10-11-2010

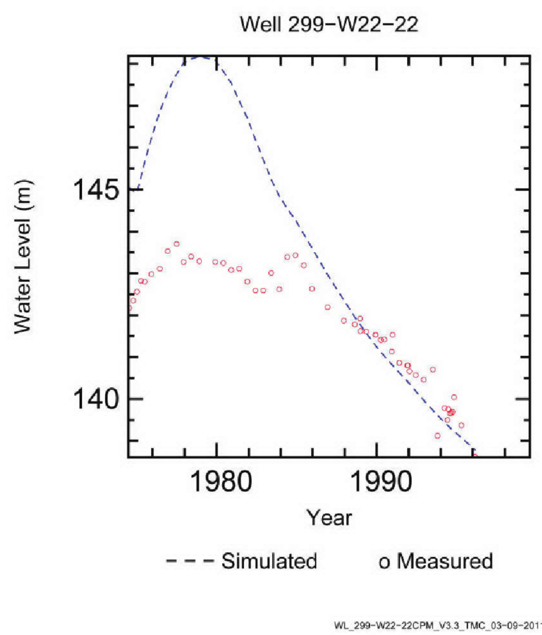
Well 299-W22-22
Water Level (m)
145
140
1980
1990
Year
Simulated
o Measured
WL_299-W22-22CPM_V3.3_TMC_03-09-2011

Well 299-W22-23

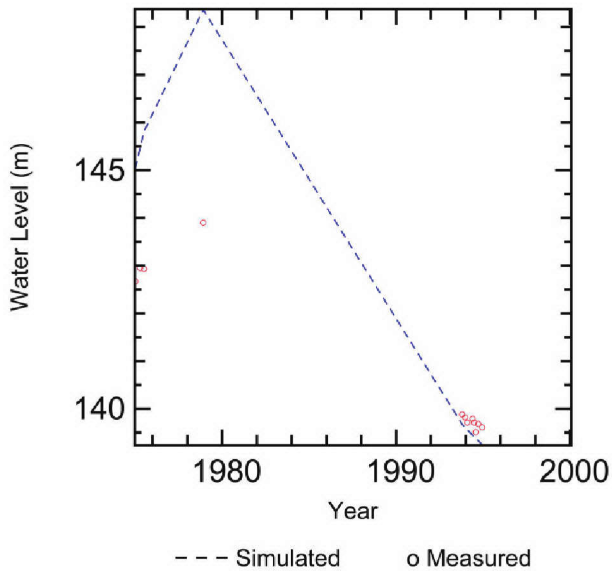

WL_299-W22-23CPM_V3.3_TMC_03-09-2011

Well 299-W22-39

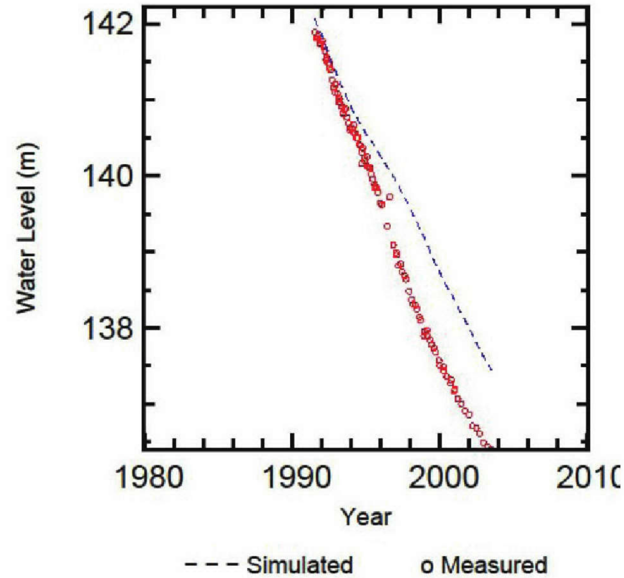

WL_299-W22-39_CPM_V3.3_TMC_10-11-2010

Well 299-W22-40

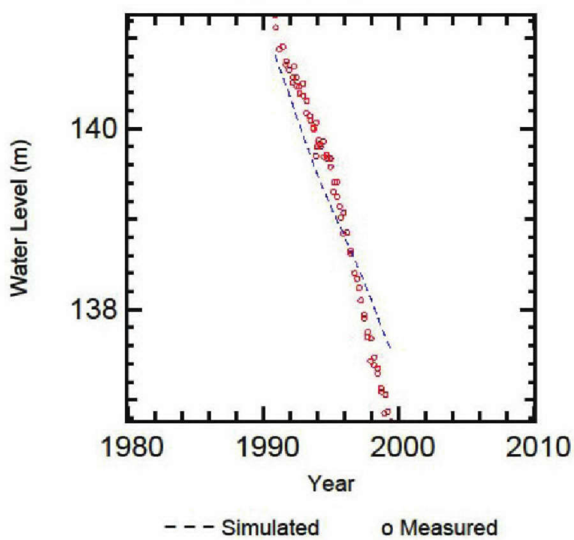

WL_299-W22-40_CPM_V3.3_TMC_10-11-2010

Well 299-W22-41

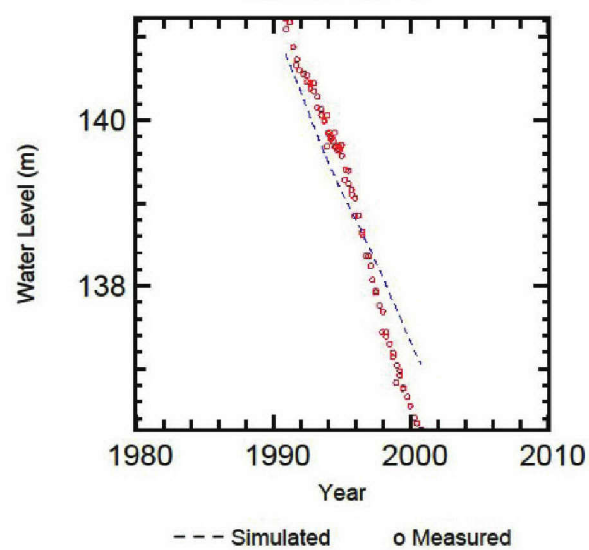

WL_299-W22-41_CPM_V3.3_TMC_10-11-2010

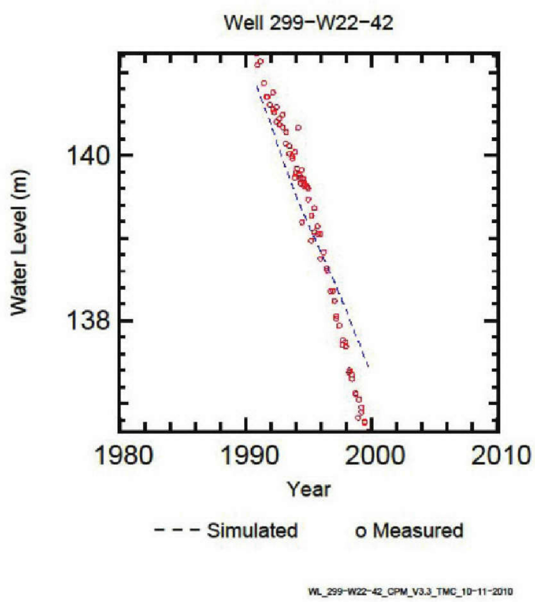
Well 299-W22-42
Water Level (m)
140
138
1980
1990
2000
2010
Year
- - - Simulated
o Measured
WL_299-W22-42_CPM_V3.3_TMC_10-11-2010

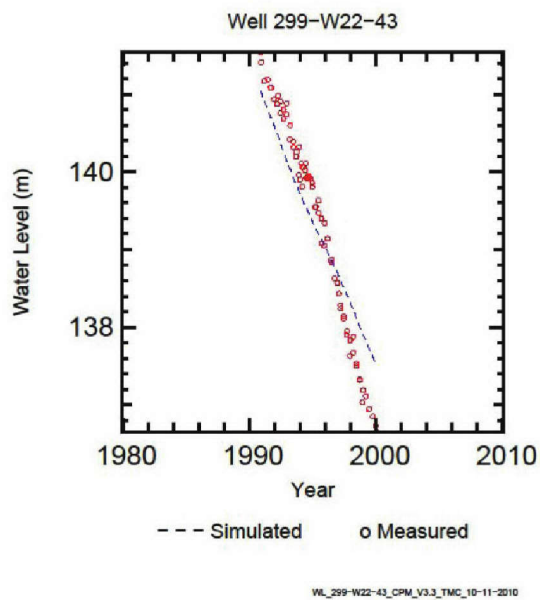
Well 299-W22-43
Water Level (m)
140
138
1980
1990
2000
2010
Year
- - - Simulated
o Measured
WL_299-W22-43_CPM_V3.3_TMC_10-11-2010

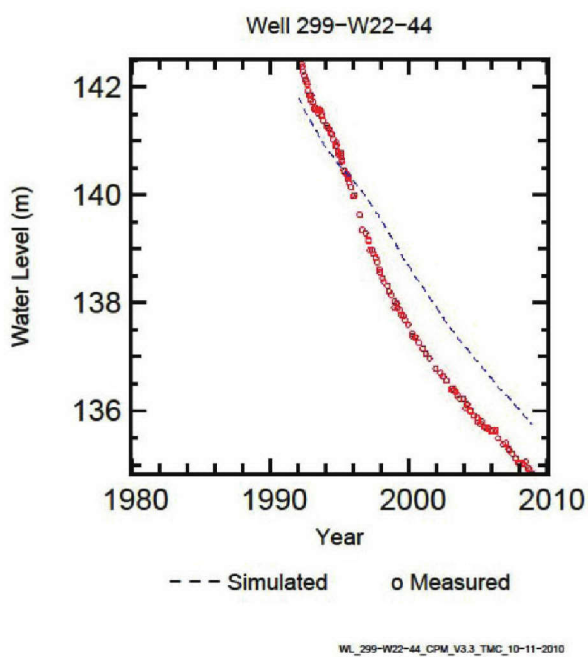
Well 299-W22-44
Water Level (m)
142
140
138
136
1980
1990
2000
2010
Year
- - - Simulated
o Measured
WL_299-W22-44_CPM_V3.3_TMC_10-11-2010

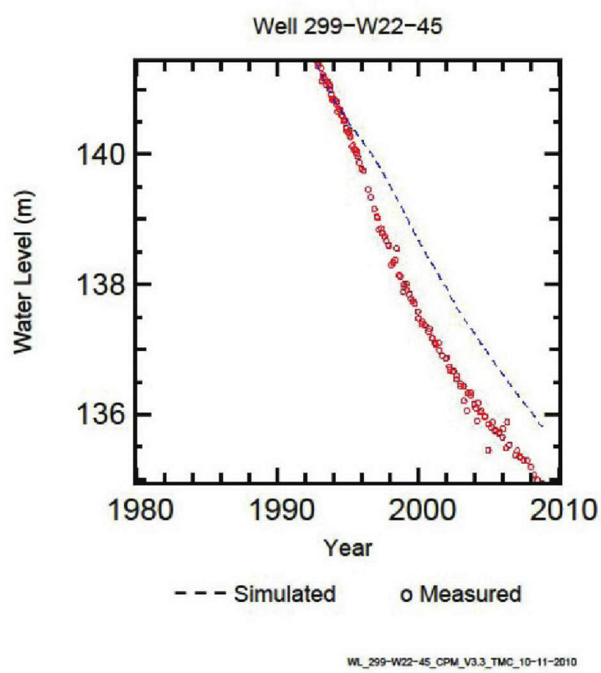
Well 299-W22-45
Water Level (m)
140
138
136
1980
1990
2000
2010
Year
- - - Simulated
o Measured
WL_299-W22-45_CPM_V3.3_TMC_10-11-2010

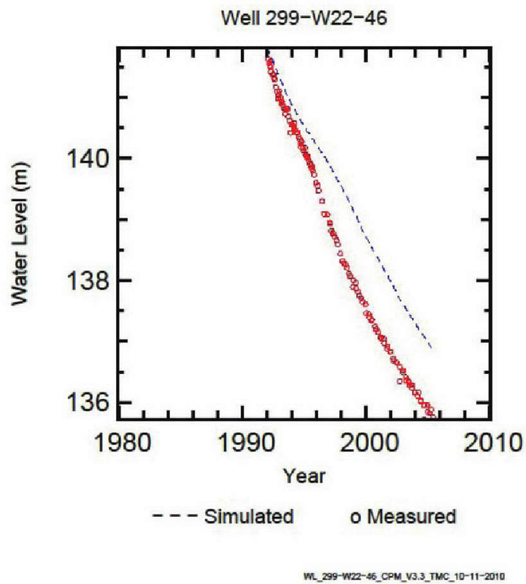
Well 299-W22-46
Water Level (m)
136
138
140
1980
1990
2000
2010
Year
Simulated
Measured
WL_299-W22-46_CPM_V3.3_TMC_10-11-2010

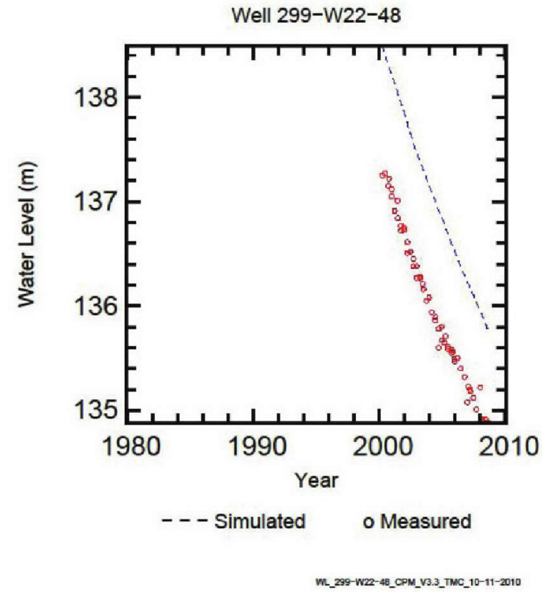
Well 299-W22-48
Water Level (m)
135
136
137
138
1980
1990
2000
2010
Year
Simulated
Measured
WL_299-W22-48_CPM_V3.3_TMC_10-11-2010

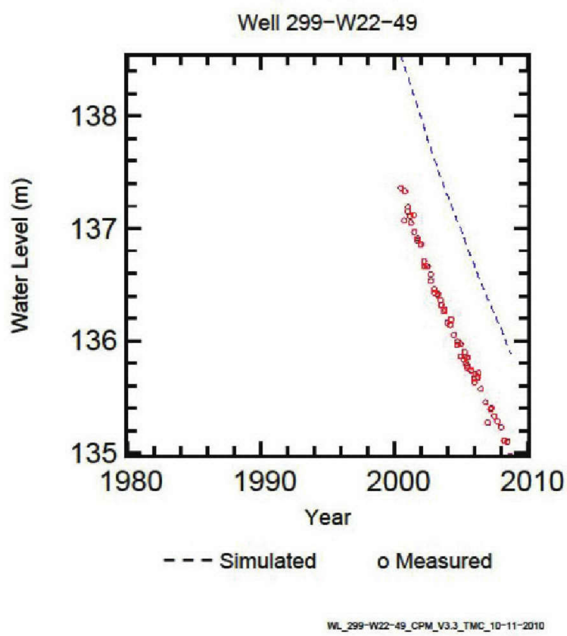
Well 299-W22-49
Water Level (m)
135
136
137
138
1980
1990
2000
2010
Year
Simulated
Measured
WL_299-W22-49_CPM_V3.3_TMC_10-11-2010

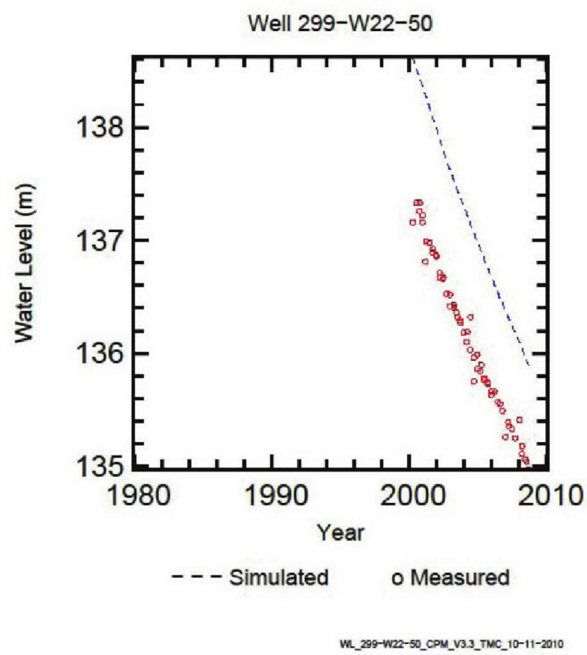
Well 299-W22-50
Water Level (m)
135
136
137
138
1980
1990
2000
2010
Year
Simulated
Measured
WL_299-W22-50_CPM_V3.3_TMC_10-11-2010

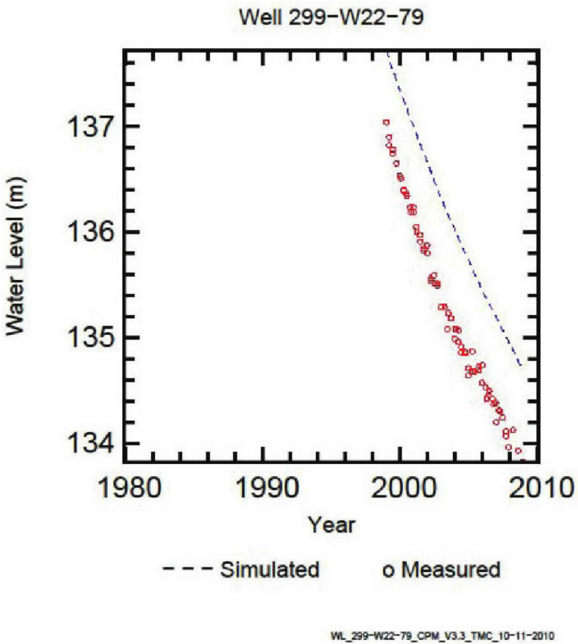
Well 299-W22-79
Water Level (m)
137
136
135
134
1980
1990
2000
2010
Year
- - - Simulated
o Measured
WL_299-W22-79_CPM_V3.3_TMC_10-11-2010

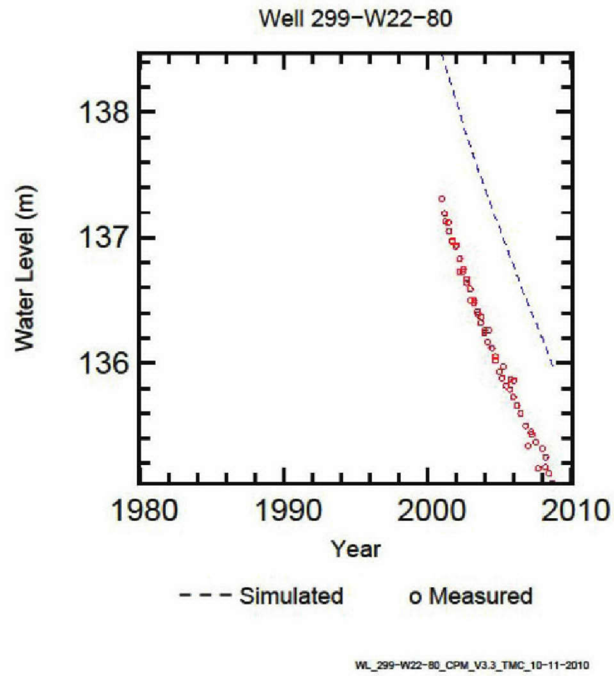
Well 299-W22-80
Water Level (m)
138
137
136
1980
1990
2000
2010
Year
- - - Simulated
o Measured
WL_299-W22-80_CPM_V3.3_TMC_10-11-2010

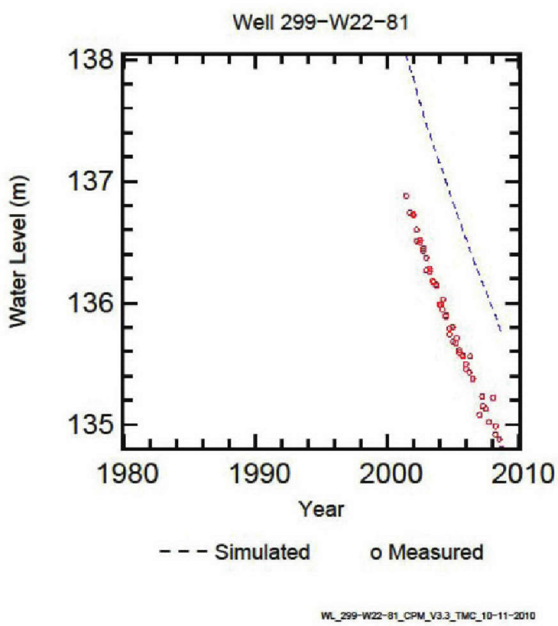
Well 299-W22-81
Water Level (m)
138
137
136
135
1980
1990
2000
2010
Year
- - - Simulated
o Measured
WL_299-W22-81_CPM_V3.3_TMC_10-11-2010

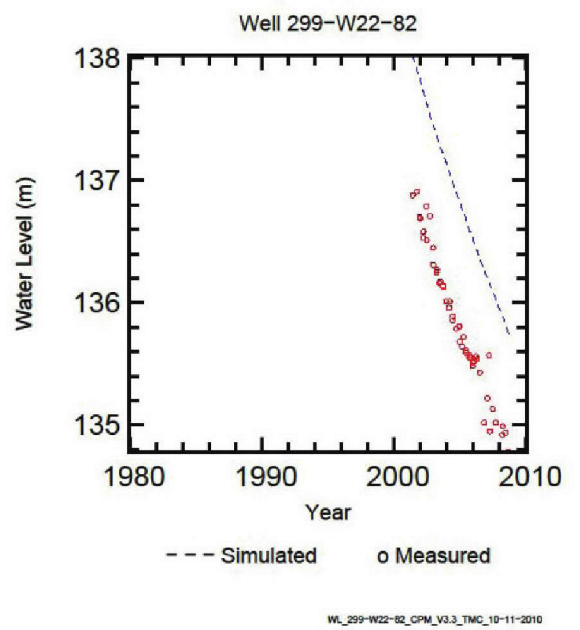
Well 299-W22-82
Water Level (m)
138
137
136
135
1980
1990
2000
2010
Year
- - - Simulated
o Measured
WL_299-W22-82_CPM_V3.3_TMC_10-11-2010

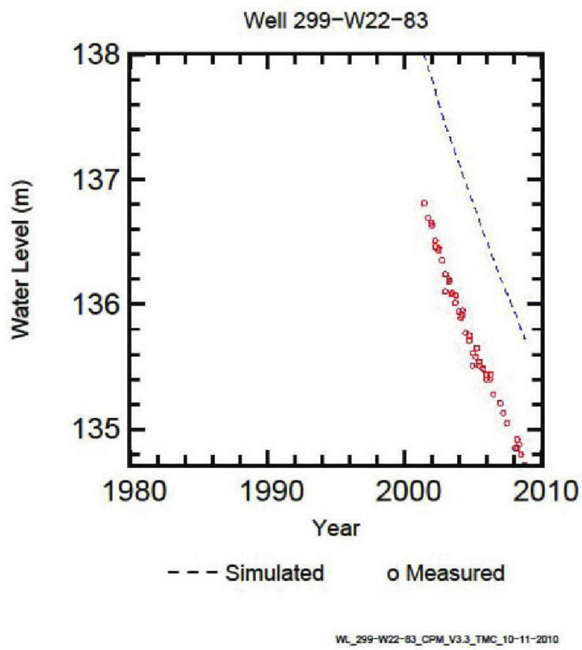
Well 299-W22-83
138
137
136
135
1980
1990
2000
2010
Year
Water Level (m)
- - - Simulated
o Measured
WL_299-W22-83_CPM_V3.3_TMC_10-11-2010

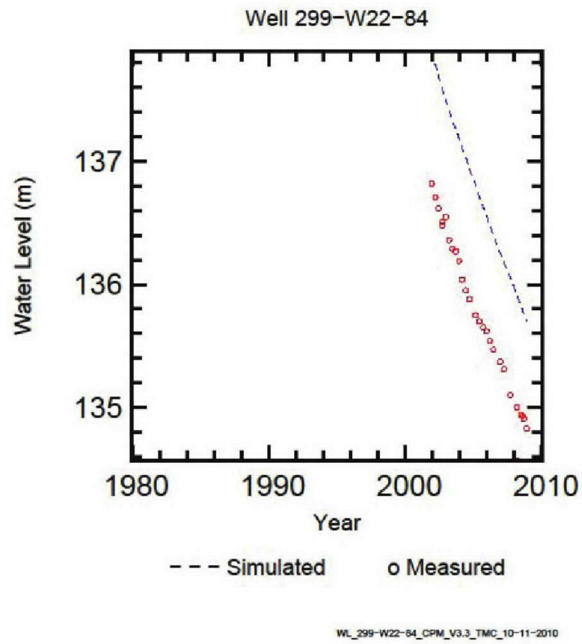
Well 299-W22-84
137
136
135
1980
1990
2000
2010
Year
Water Level (m)
- - - Simulated
o Measured
WL_299-W22-84_CPM_V3.3_TMC_10-11-2010

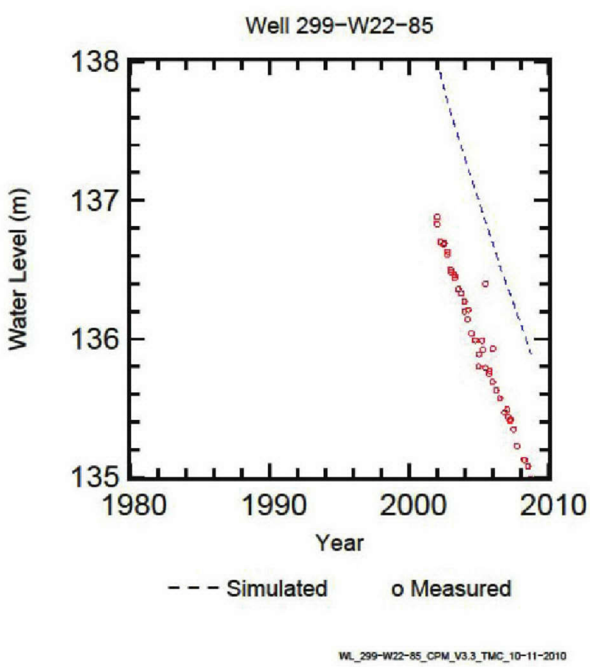
Well 299-W22-85
138
137
136
135
1980
1990
2000
2010
Year
Water Level (m)
- - - Simulated
o Measured
WL_299-W22-85_CPM_V3.3_TMC_10-11-2010

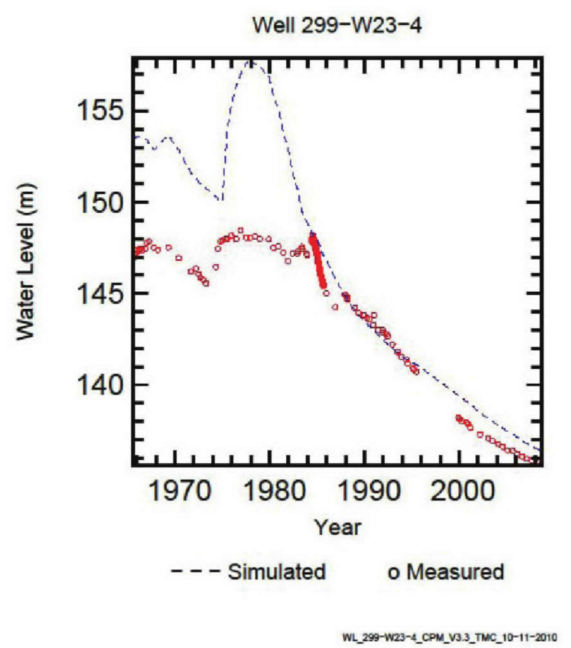
Well 299-W23-4
155
150
145
140
1970
1980
1990
2000
Year
Water Level (m)
- - - Simulated
o Measured
WL_299-W23-4_CPM_V3.3_TMC_10-11-2010

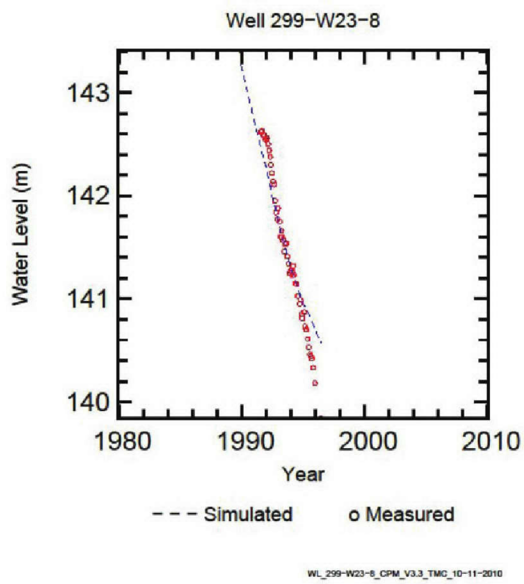
Well 299-W23-8
Water Level (m)
143
142
141
140
1980
1990
2000
2010
Year
- - - Simulated
o Measured
WL_299-W23-8_CPM_V3.3_TMC_10-11-2010

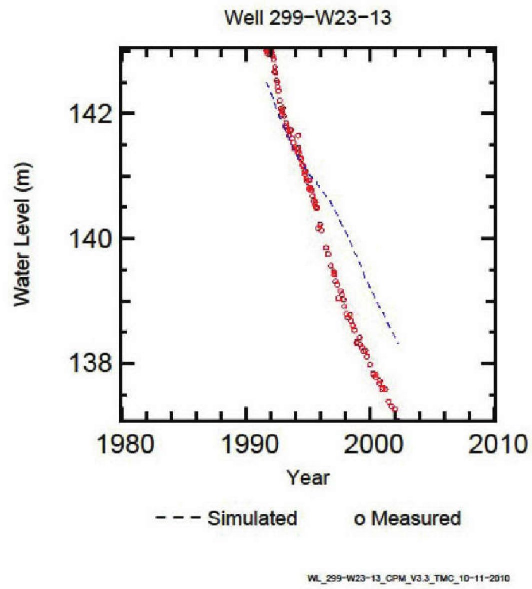
Well 299-W23-13
Water Level (m)
142
140
138
1980
1990
2000
2010
Year
- - - Simulated
o Measured
WL_299-W23-13_CPM_V3.3_TMC_10-11-2010

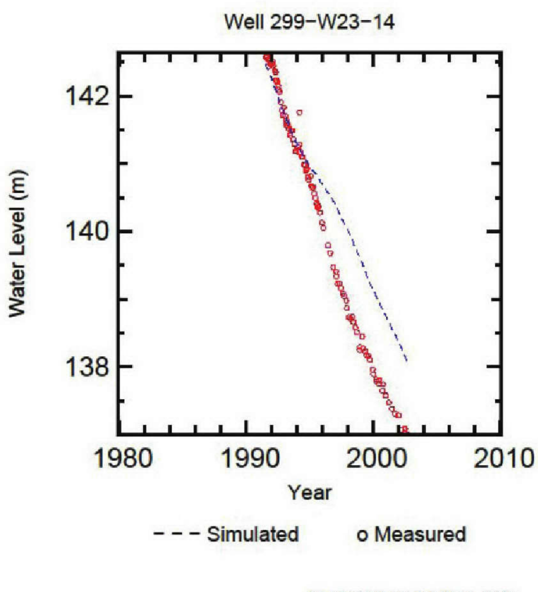
Well 299-W23-14
Water Level (m)
142
140
138
1980
1990
2000
2010
Year
- - - Simulated
o Measured
WL_299-W23-14_CPM_V3.3_TMC_10-11-2010

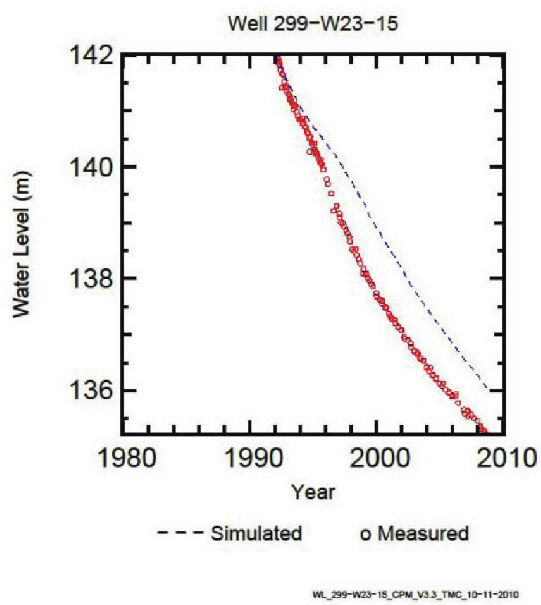
Well 299-W23-15
Water Level (m)
142
140
138
136
1980
1990
2000
2010
Year
- - - Simulated
o Measured
WL_299-W23-15_CPM_V3.3_TMC_10-11-2010

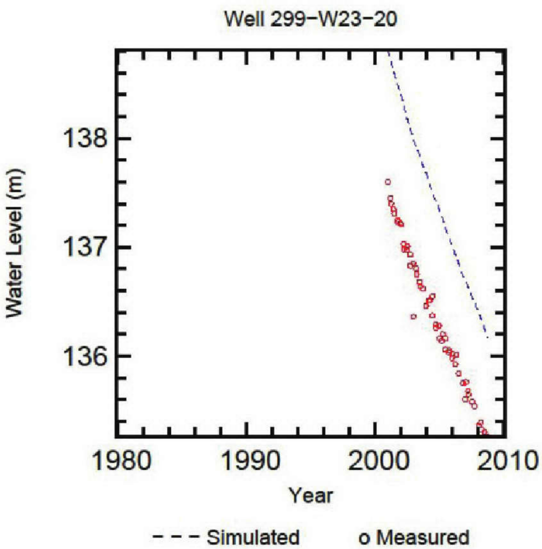

WL_299-W23-20_CPM_V3.3_TMC_10-11-2010

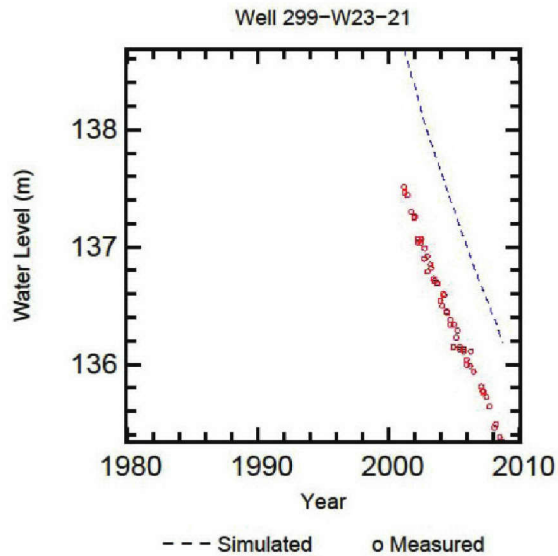

WL_299-W23-21_CPM_V3.3_TMC_10-11-2010

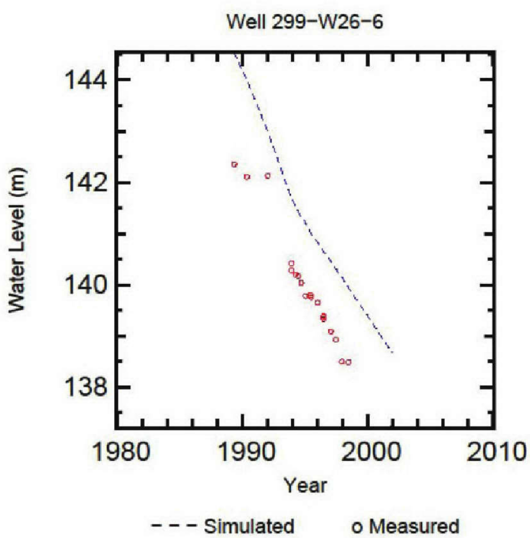

WL_299-W26-6_CPM_V3.3_TMC_10-11-2010

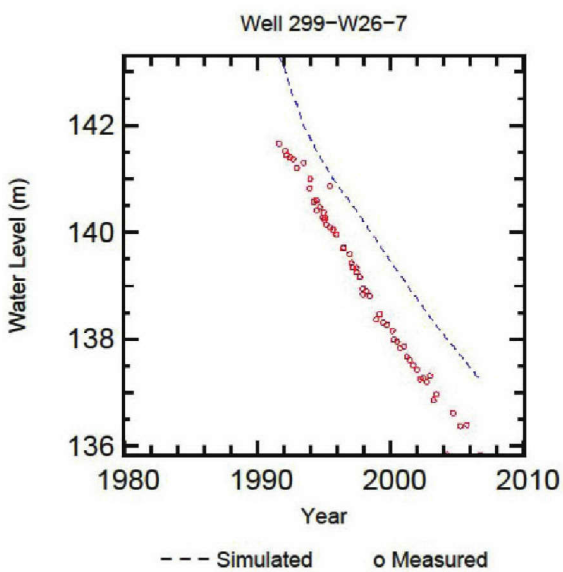

WL_299-W26-7_CPM_V3.3_TMC_10-11-2010

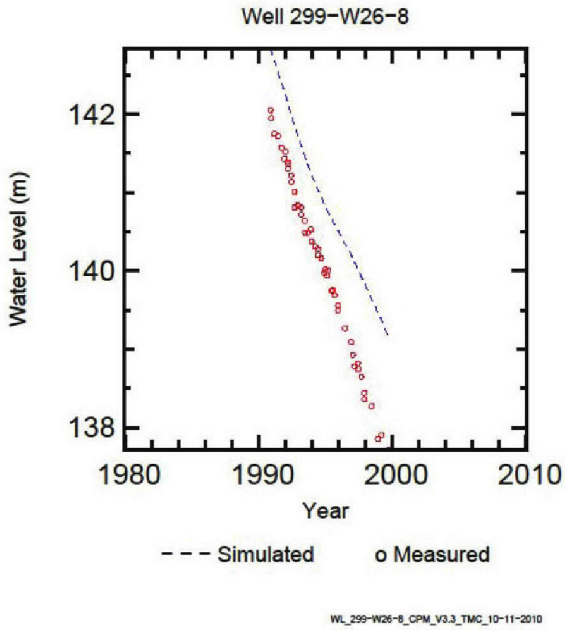
Well 299-W26-8
Water Level (m)
142
140
138
1980
1990
2000
2010
Year
- - - Simulated
o Measured
WL_299-W26-8_CPM_V3.3_TMC_10-11-2010

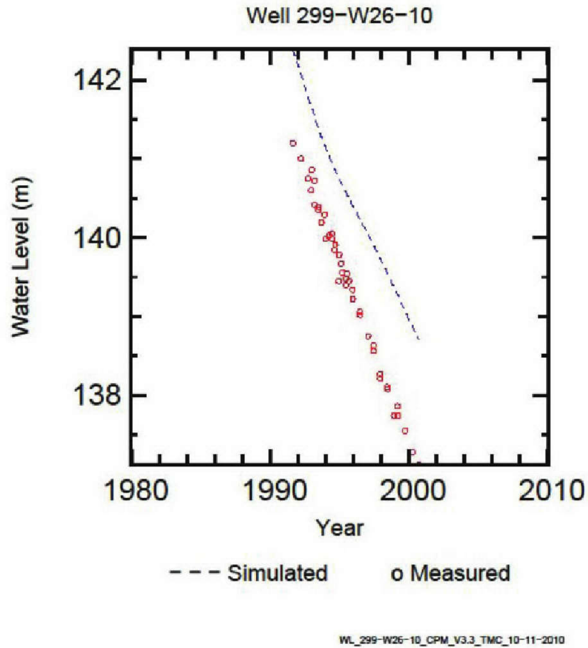
Well 299-W26-10
Water Level (m)
142
140
138
1980
1990
2000
2010
Year
- - - Simulated
o Measured
WL_299-W26-10_CPM_V3.3_TMC_10-11-2010

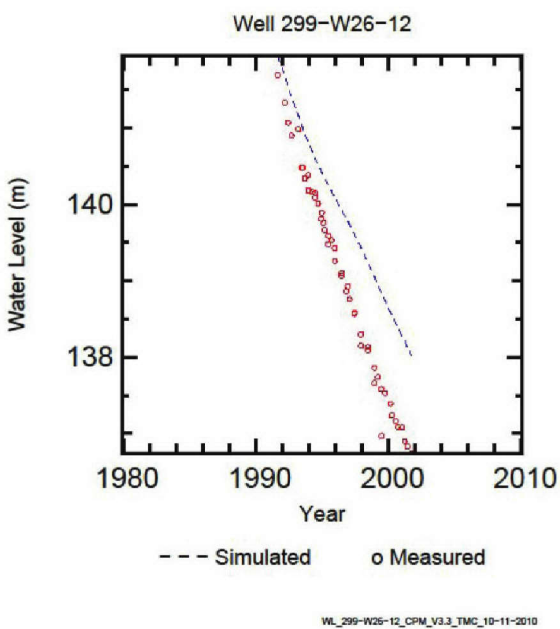
Well 299-W26-12
Water Level (m)
140
138
1980
1990
2000
2010
Year
- - - Simulated
o Measured
WL_299-W26-12_CPM_V3.3_TMC_10-11-2010

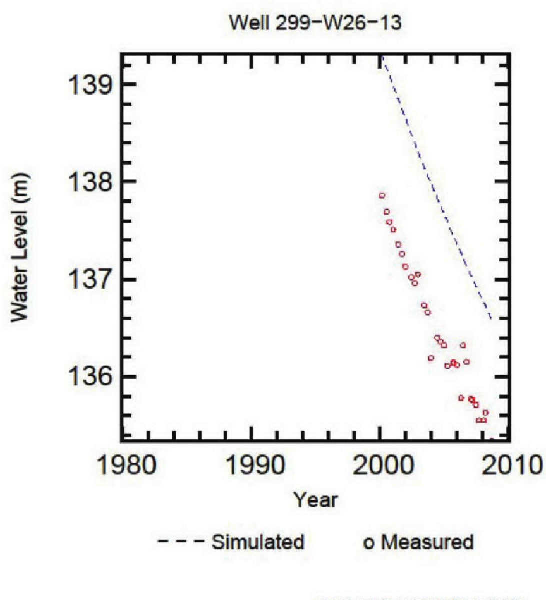
Well 299-W26-13
Water Level (m)
139
138
137
136
1980
1990
2000
2010
Year
- - - Simulated
o Measured
WL_299-W26-13_CPM_V3.3_TMC_10-11-2010

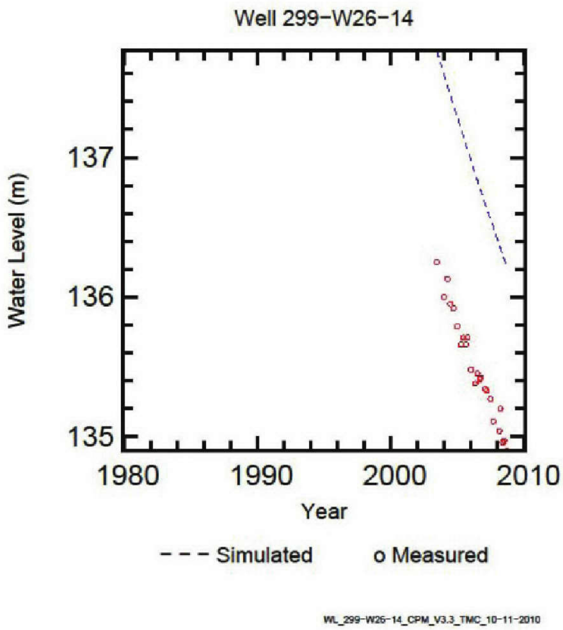
Well 299-W26-14
Water Level (m)
137
136
135
1980
1990
2000
2010
Year
- - - Simulated
o Measured
WL_299-W26-14_CPM_V3.3_TMC_10-11-2010

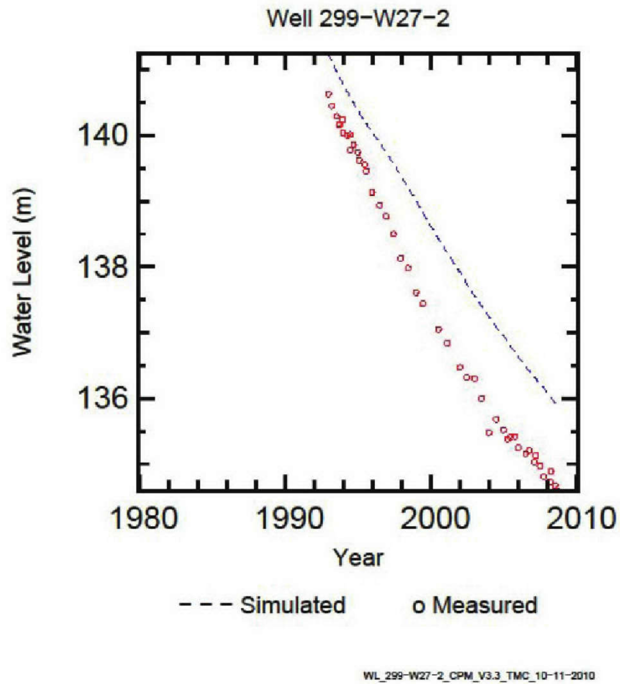
Well 299-W27-2
Water Level (m)
140
138
136
1980
1990
2000
2010
Year
- - - Simulated
o Measured
WL_299-W27-2_CPM_V3.3_TMC_10-11-2010

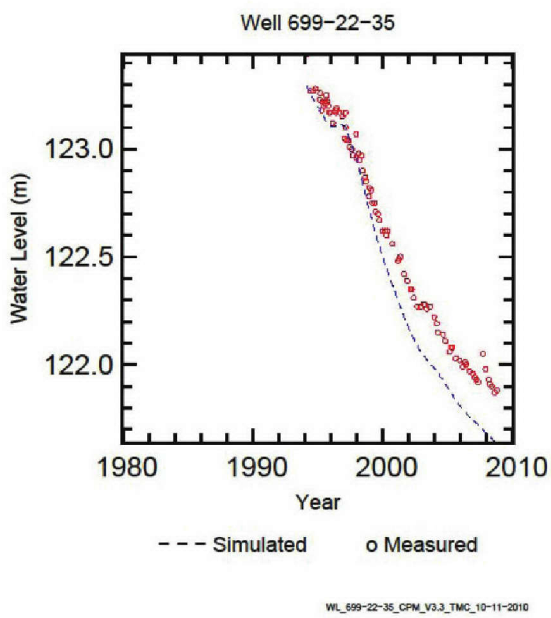
Well 699-22-35
Water Level (m)
123.0
122.5
122.0
1980
1990
2000
2010
Year
- - - Simulated
o Measured
WL_699-22-35_CPM_V3.3_TMC_10-11-2010

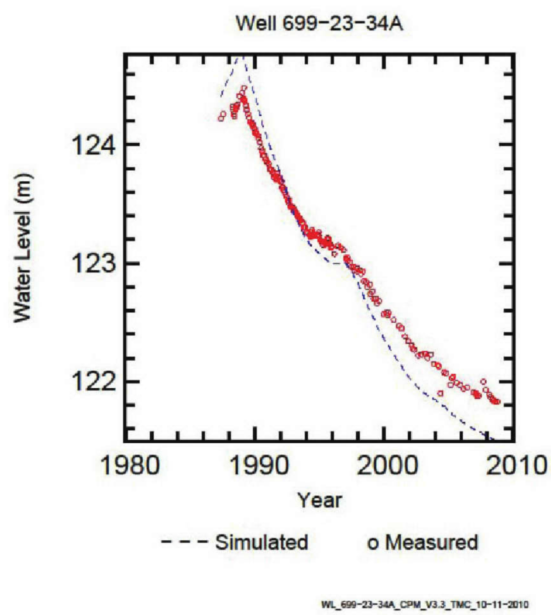
Well 699-23-34A
Water Level (m)
124
123
122
1980
1990
2000
2010
Year
- - - Simulated
o Measured
WL_699-23-34A_CPM_V3.3_TMC_10-11-2010

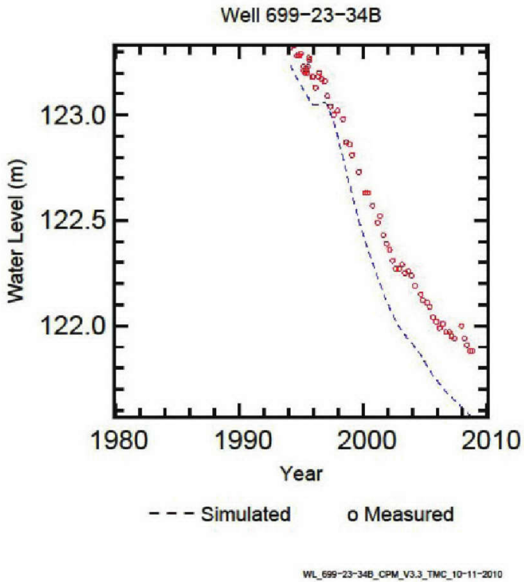
Well 699-23-34B
Water Level (m)
123.0
122.5
122.0
1980
1990
2000
2010
Year
- - - Simulated
o Measured
WL_699-23-34B_CPM_V3.3_TMC_10-11-2010

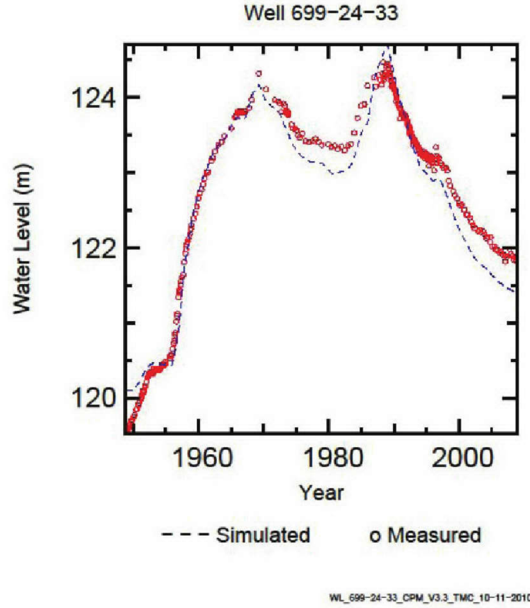
Well 699-24-33
Water Level (m)
124
122
120
1960
1980
2000
Year
- - - Simulated
o Measured
WL_699-24-33_CPM_V3.3_TMC_10-11-2010

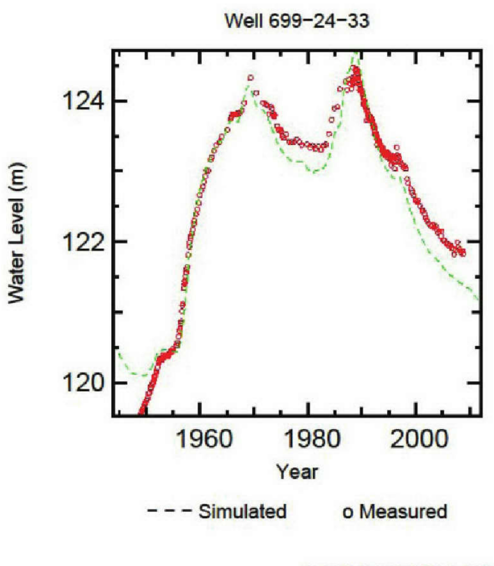
Well 699-24-33
Water Level (m)
124
122
120
1960
1980
2000
Year
- - - Simulated
o Measured
WL_699-24-33_CPM_V3.3_TMC_10-12-2010

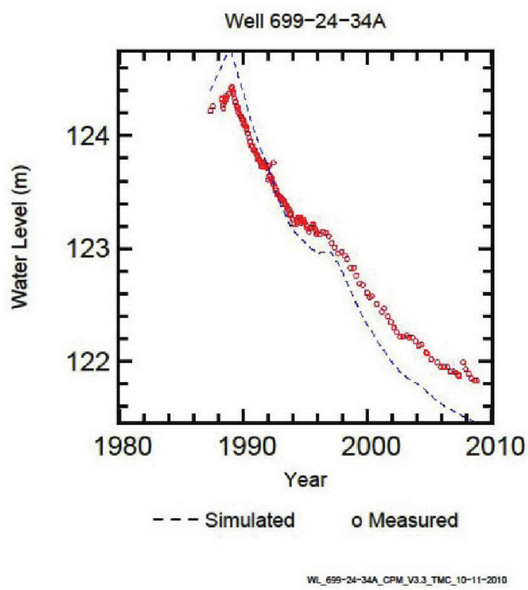
Well 699-24-34A
Water Level (m)
124
123
122
1980
1990
2000
2010
Year
- - - Simulated
o Measured
WL_699-24-34A_CPM_V3.3_TMC_10-11-2010

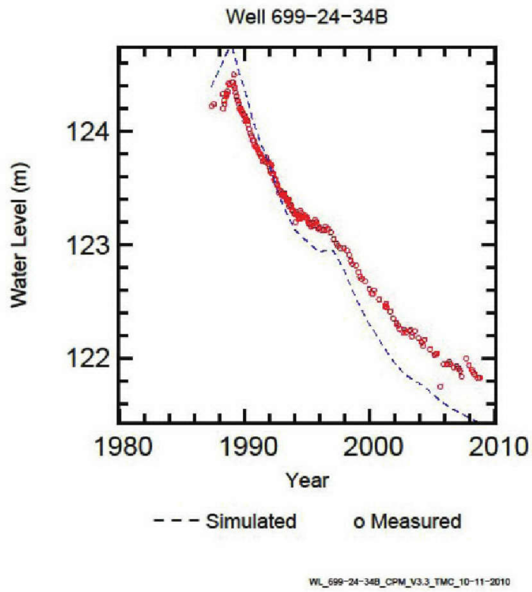
Well 699-24-34B
Water Level (m)
124
123
122
1980
1990
2000
2010
Year
Simulated
Measured
WL_699-24-34B_CPM_V3.3_TMC_10-11-2010

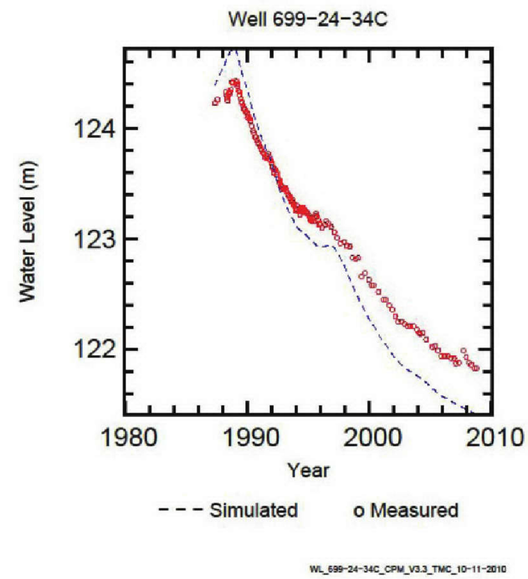
Well 699-24-34C
Water Level (m)
124
123
122
1980
1990
2000
2010
Year
Simulated
Measured
WL_699-24-34C_CPM_V3.3_TMC_10-11-2010

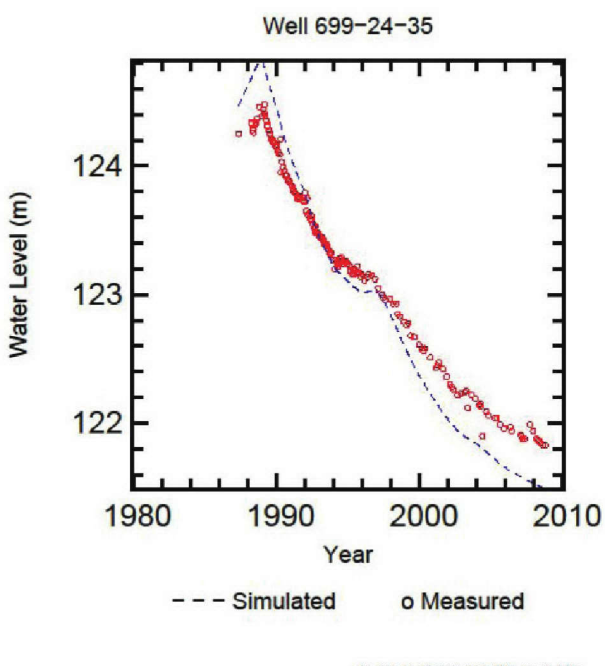
Well 699-24-35
Water Level (m)
124
123
122
1980
1990
2000
2010
Year
Simulated
Measured
WL_699-24-35_CPM_V3.3_TMC_10-11-2010

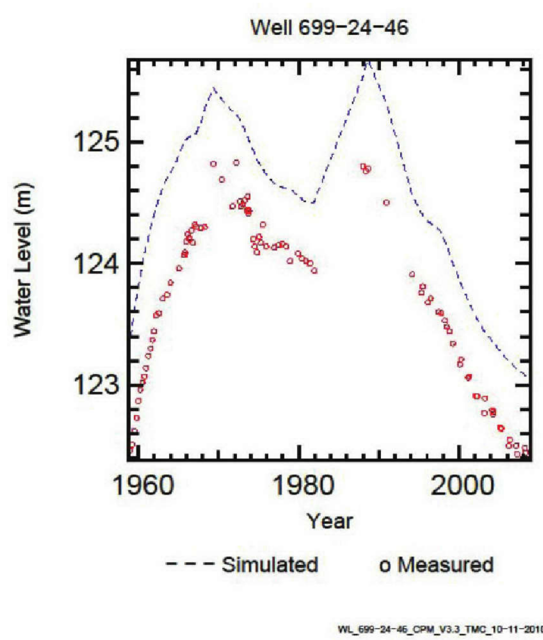
Well 699-24-46
Water Level (m)
125
124
123
1960
1980
2000
Year
Simulated
Measured
WL_699-24-46_CPM_V3.3_TMC_10-11-2010

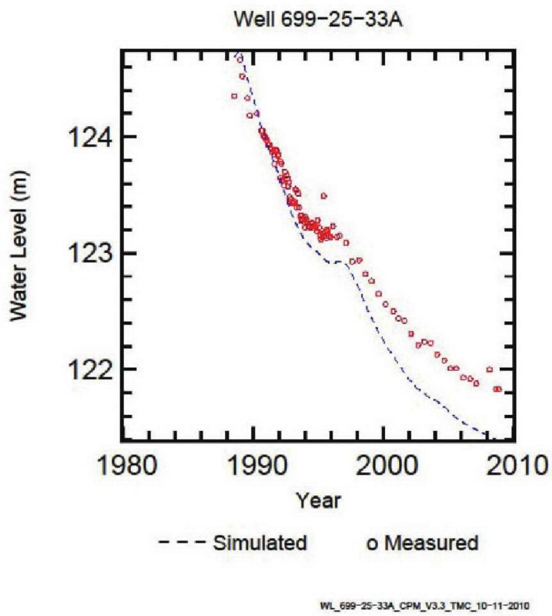
Well 699-25-33A
Water Level (m)
124
123
122
1980
1990
2000
2010
Year
- - - Simulated
o Measured
WL_699-25-33A_CPM_V3.3_TMC_10-11-2010

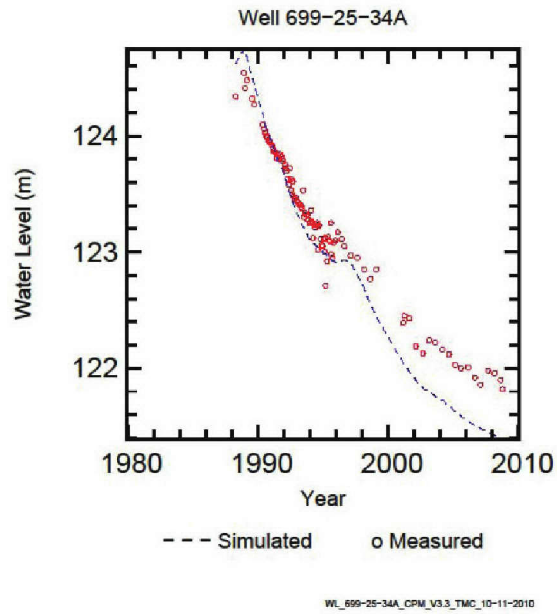
Well 699-25-34A
Water Level (m)
124
123
122
1980
1990
2000
2010
Year
- - - Simulated
o Measured
WL_699-25-34A_CPM_V3.3_TMC_10-11-2010

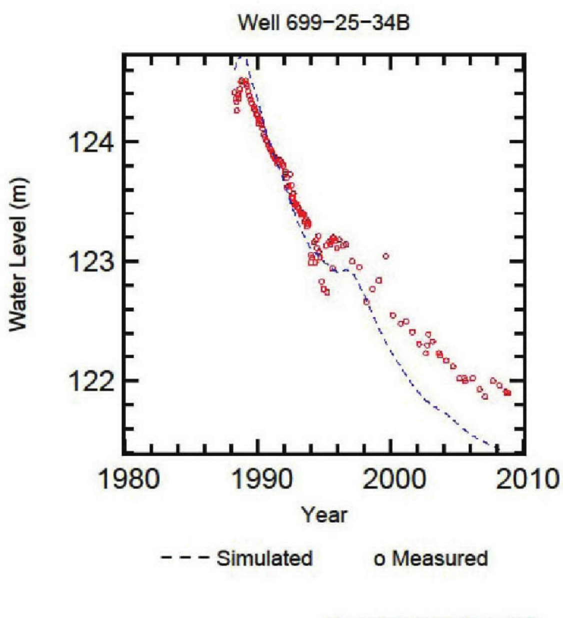
Well 699-25-34B
Water Level (m)
124
123
122
1980
1990
2000
2010
Year
- - - Simulated
o Measured
WL_699-25-34B_CPM_V3.3_TMC_10-11-2010

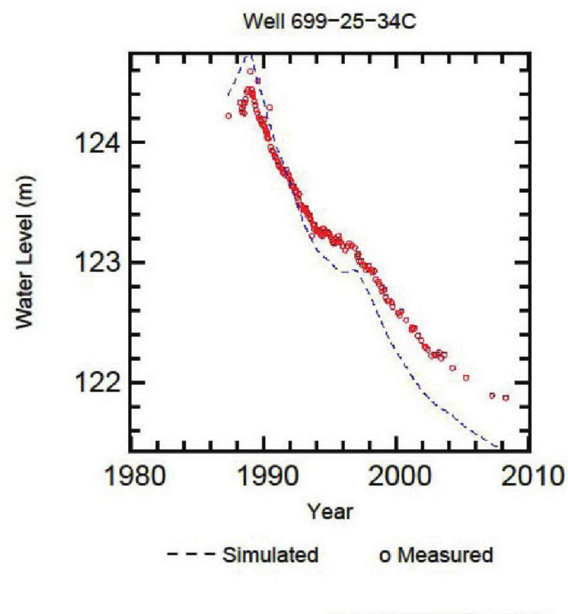
Well 699-25-34C
Water Level (m)
124
123
122
1980
1990
2000
2010
Year
- - - Simulated
o Measured
WL_699-25-34C_CPM_V3.3_TMC_10-11-2010

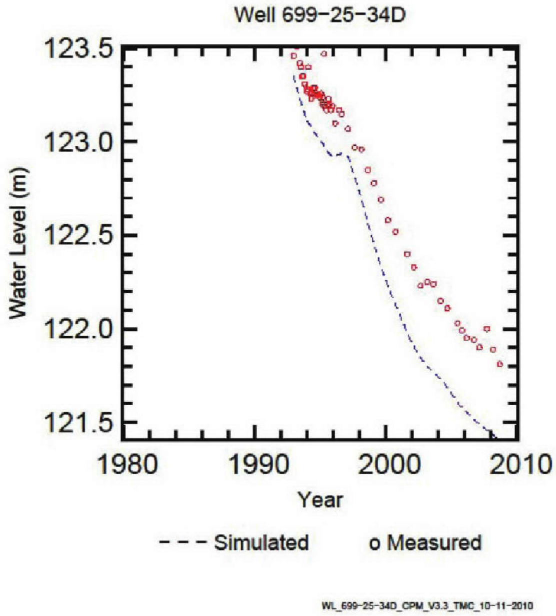
Well 699-25-34D
Water Level (m)
123.5
123.0
122.5
122.0
121.5
1980
1990
2000
2010
Year
- - - Simulated
o Measured
WL_699-25-34D_CPM_V3.3_TMC_10-11-2010

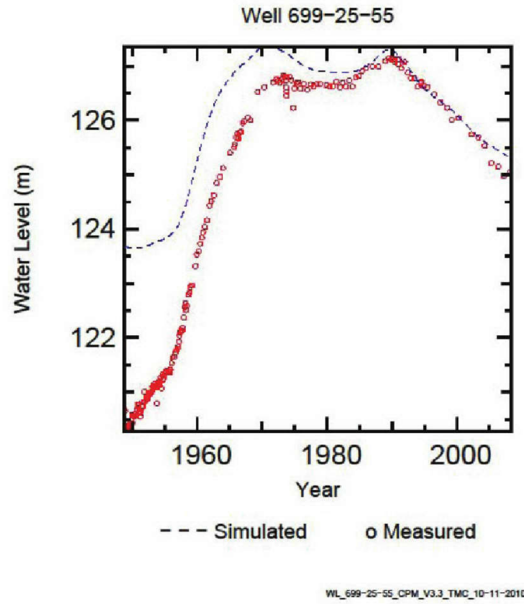
Well 699-25-55
Water Level (m)
126
124
122
1960
1980
2000
Year
- - - Simulated
o Measured
WL_699-25-55_CPM_V3.3_TMC_10-11-2010

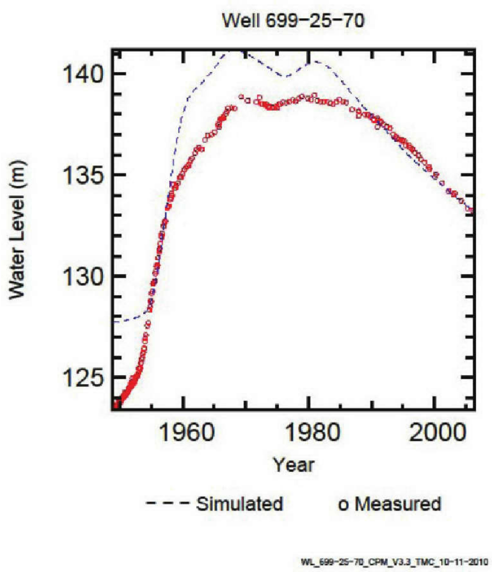
Well 699-25-70
Water Level (m)
140
135
130
125
1960
1980
2000
Year
- - - Simulated
o Measured
WL_699-25-70_CPM_V3.3_TMC_10-11-2010

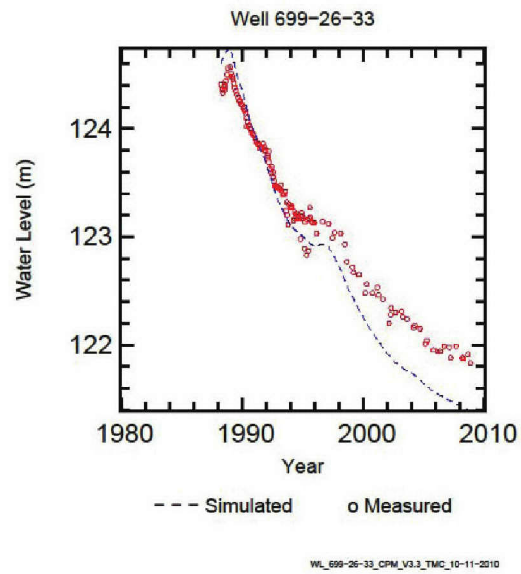
Well 699-26-33
Water Level (m)
124
123
122
1980
1990
2000
2010
Year
- - - Simulated
o Measured
WL_699-26-33_CPM_V3.3_TMC_10-11-2010

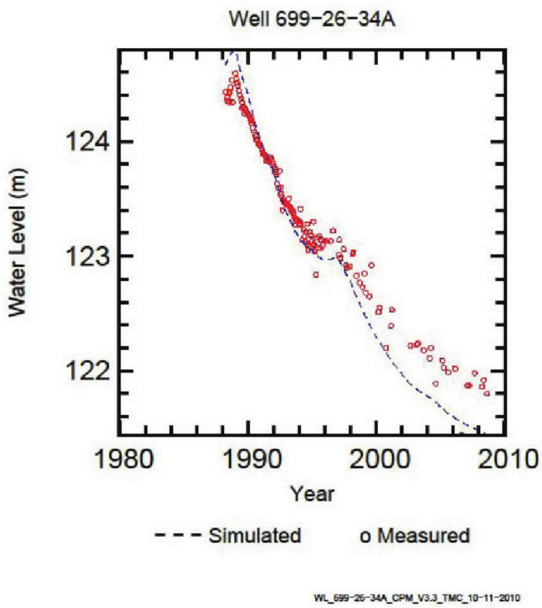
Well 699−26−34A
Water Level (m)
124
123
122
1980
1990
2000
2010
Year
− − − Simulated
o Measured
WL_699-26-34A_CPM_V3.3_TMC_10-11-2010

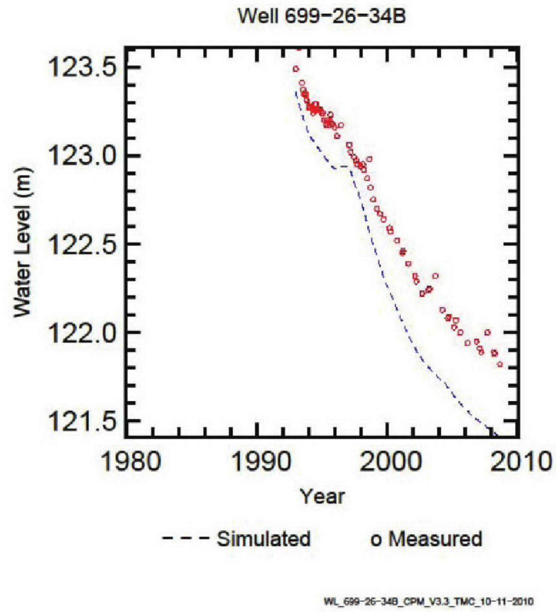
Well 699−26−34B
Water Level (m)
123.5
123.0
122.5
122.0
121.5
1980
1990
2000
2010
Year
− − − Simulated
o Measured
WL_699-26-34B_CPM_V3.3_TMC_10-11-2010

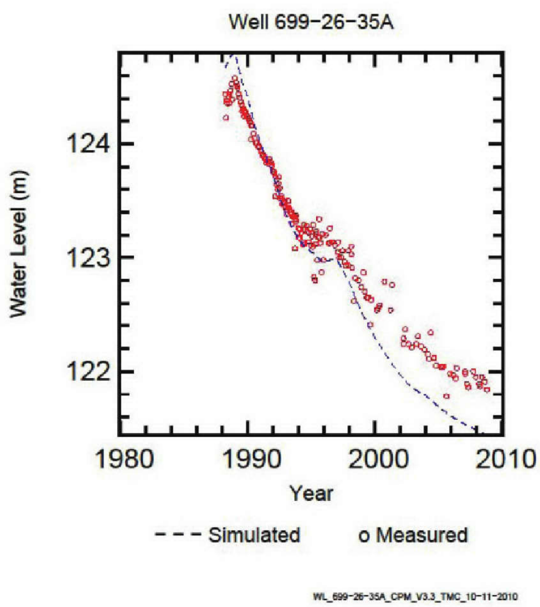
Well 699−26−35A
Water Level (m)
124
123
122
1980
1990
2000
2010
Year
− − − Simulated
o Measured
WL_699-26-35A_CPM_V3.3_TMC_10-11-2010

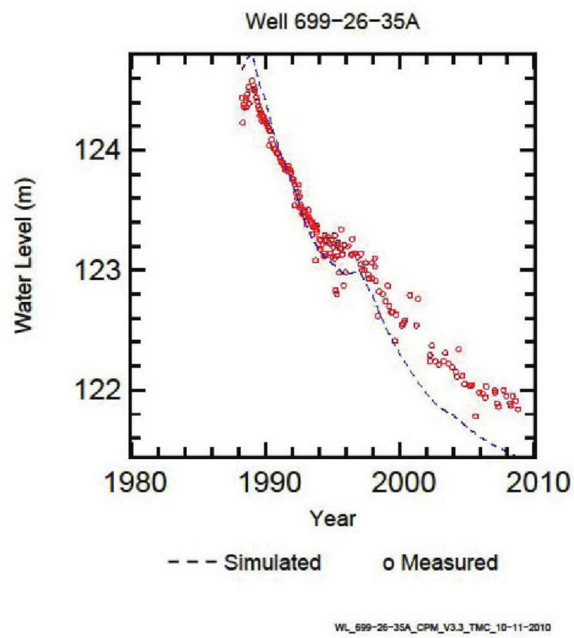
Well 699−26−35A
Water Level (m)
124
123
122
1980
1990
2000
2010
Year
− − − Simulated
o Measured
WL_699-26-35A_CPM_V3.3_TMC_10-11-2010

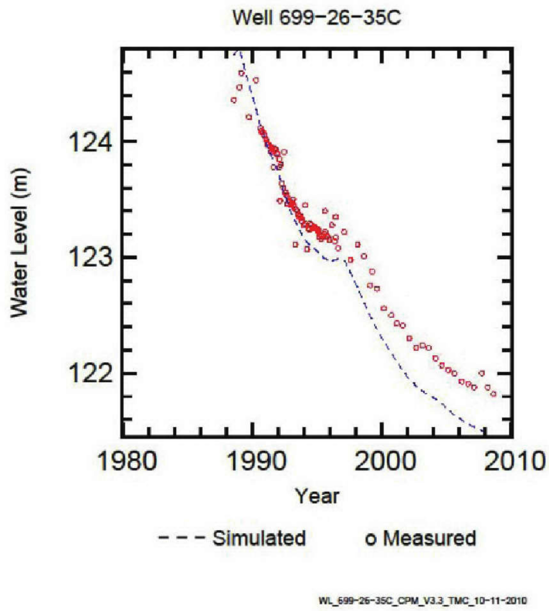
Well 699-26-35C
Water Level (m)
124
123
122
1980
1990
2000
2010
Year
- - - Simulated
o Measured
WL_699-26-35C_CPM_V3.3_TMC_10-11-2010

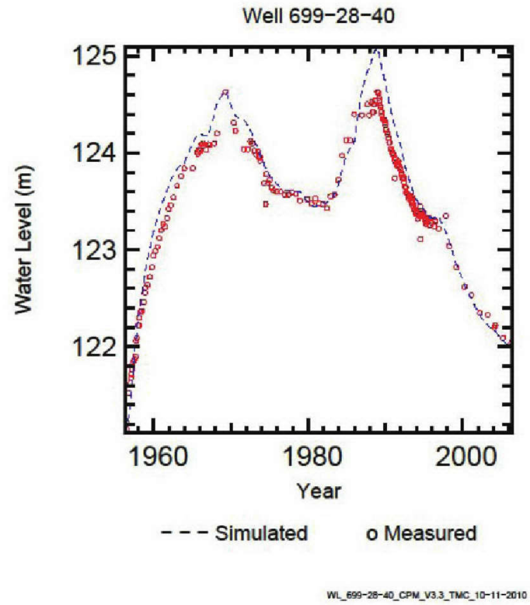
Well 699-28-40
Water Level (m)
125
124
123
122
1960
1980
2000
Year
- - - Simulated
o Measured
WL_699-28-40_CPM_V3.3_TMC_10-11-2010

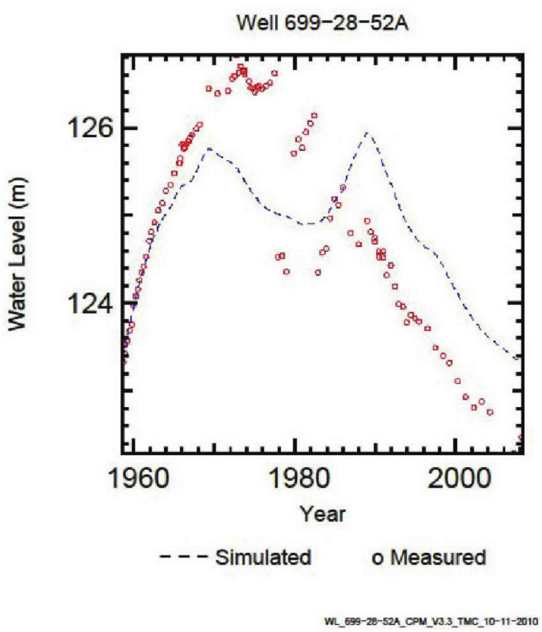
Well 699-28-52A
Water Level (m)
126
124
1960
1980
2000
Year
- - - Simulated
o Measured
WL_699-28-52A_CPM_V3.3_TMC_10-11-2010

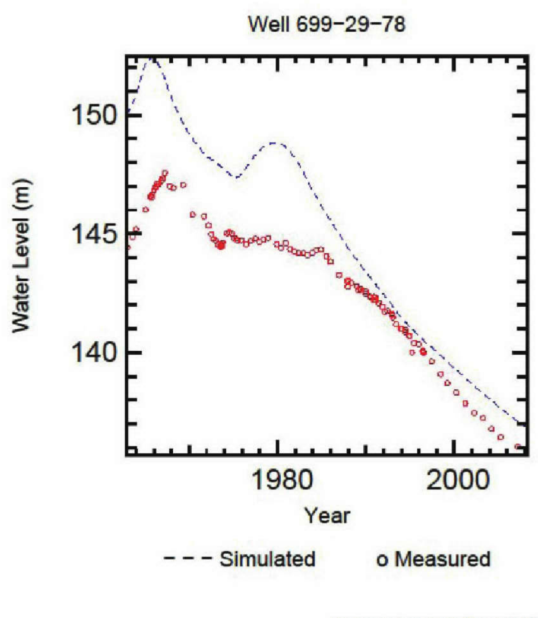
Well 699-29-78
Water Level (m)
150
145
140
1980
2000
Year
- - - Simulated
o Measured
WL_699-29-78_CPM_V3.3_TMC_10-11-2010

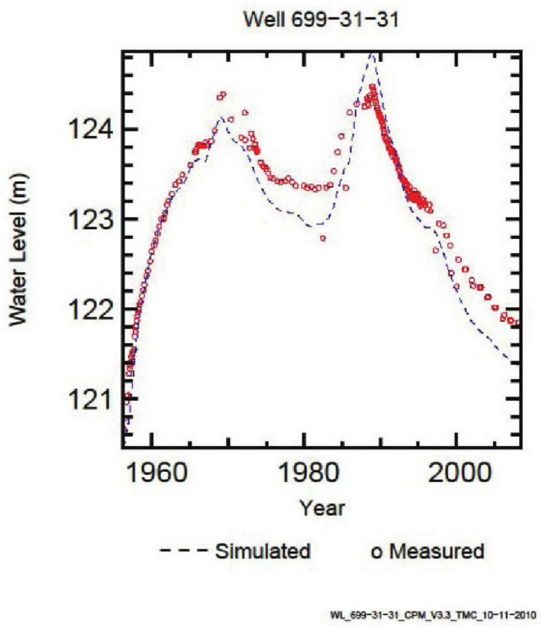
Well 699-31-31
124
123
122
121
Water Level (m)
1960
1980
2000
Year
Simulated
o Measured
WL_699-31-31_CPM_V3.3_TMC_10-11-2010

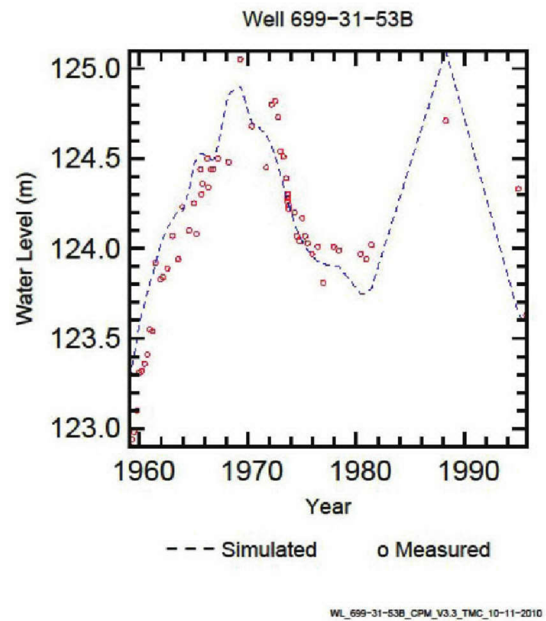
Well 699-31-53B
125.0
124.5
124.0
123.5
123.0
Water Level (m)
1960
1970
1980
1990
Year
Simulated
o Measured
WL_699-31-53B_CPM_V3.3_TMC_10-11-2010

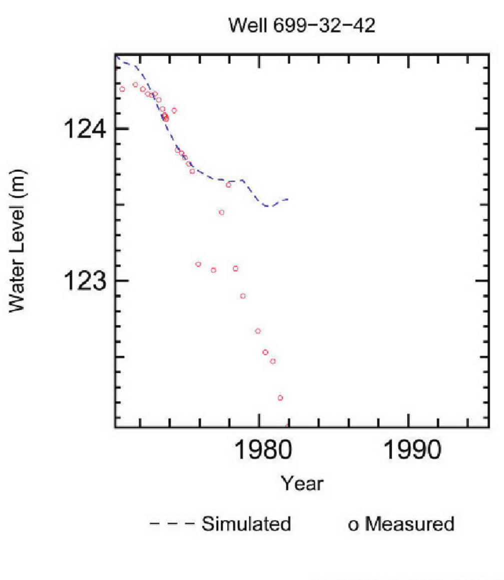
Well 699-32-42
124
123
Water Level (m)
1980
1990
Year
Simulated
o Measured
WL_699-32-42CPM_V3.3_TMC_03-09-2011

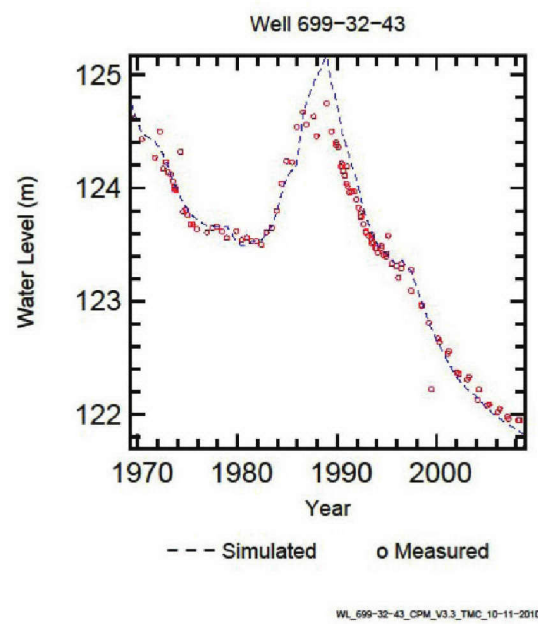
Well 699-32-43
125
124
123
122
Water Level (m)
1970
1980
1990
2000
Year
Simulated
o Measured
WL_699-32-43_CPM_V3.3_TMC_10-11-2010

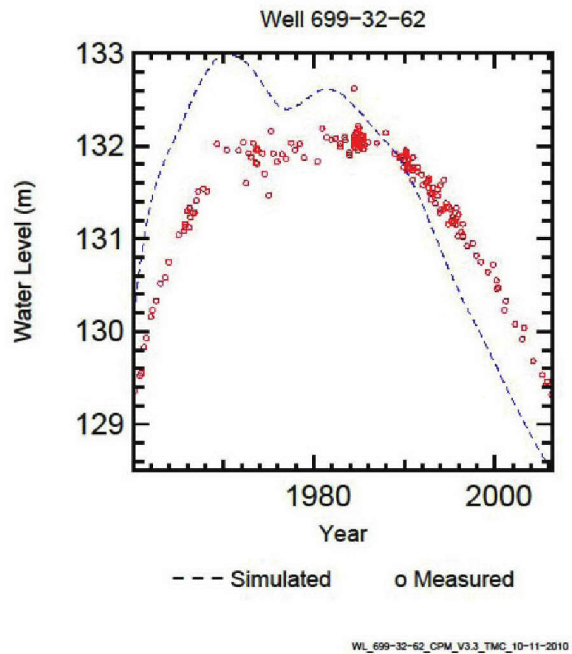
Well 699-32-62
133
132
131
130
129
Water Level (m)
1980
2000
Year
- - - Simulated
o Measured
WL_699-32-62_CPM_V3.3_TMC_10-11-2010

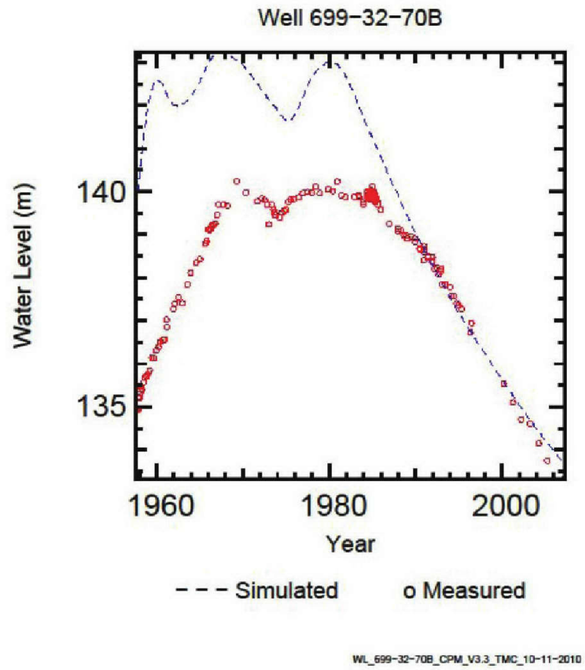
Well 699-32-70B
140
135
Water Level (m)
1960
1980
2000
Year
- - - Simulated
o Measured
WL_699-32-70B_CPM_V3.3_TMC_10-11-2010

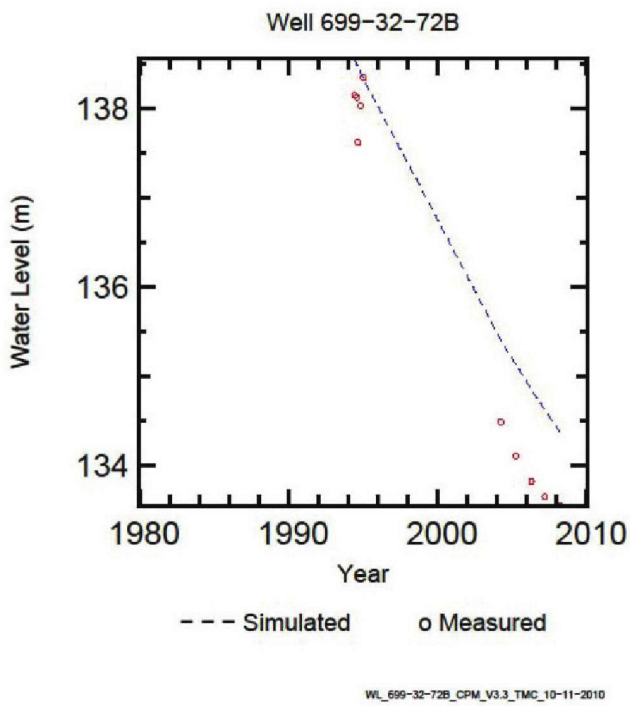
Well 699-32-72B
138
136
134
Water Level (m)
1980
1990
2000
2010
Year
- - - Simulated
o Measured
WL_699-32-72B_CPM_V3.3_TMC_10-11-2010

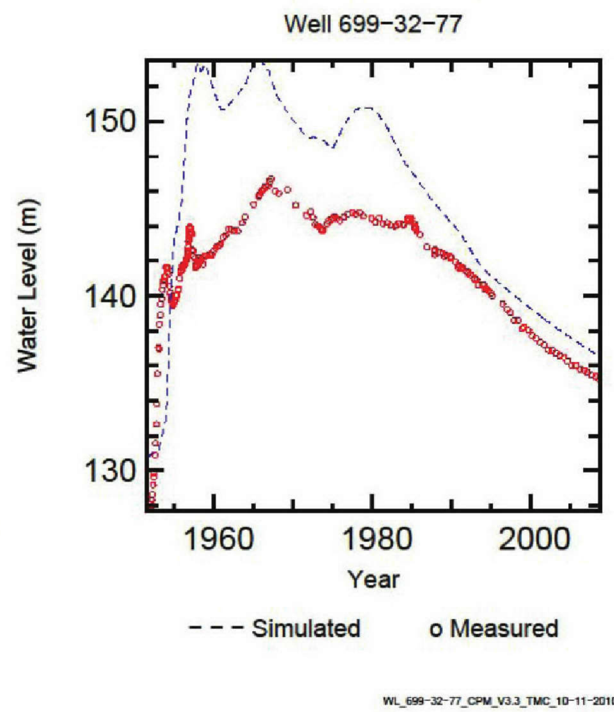
Well 699-32-77
150
140
130
Water Level (m)
1960
1980
2000
Year
- - - Simulated
o Measured
WL_699-32-77_CPM_V3.3_TMC_10-11-2010

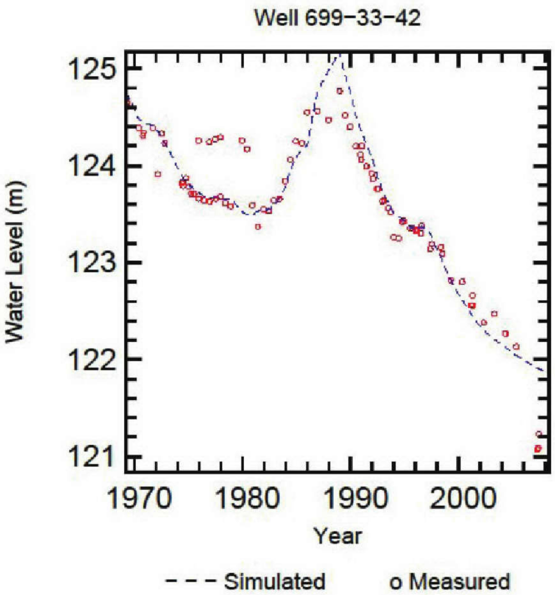

WL_699-33-42_CPM_V3.3_TMC_10-11-2010

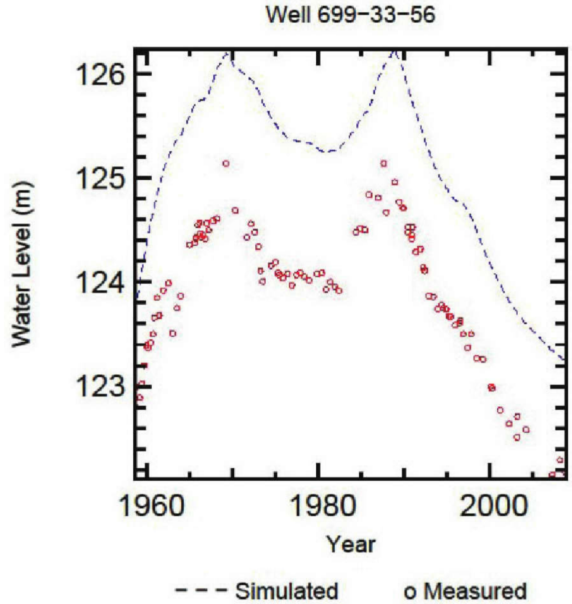

WL_699-33-56_CPM_V3.3_TMC_10-11-2010

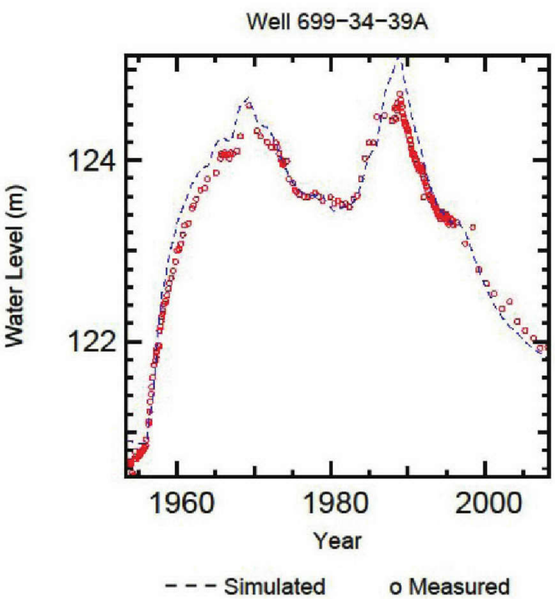

WL_699-34-39A_CPM_V3.3_TMC_10-11-2010

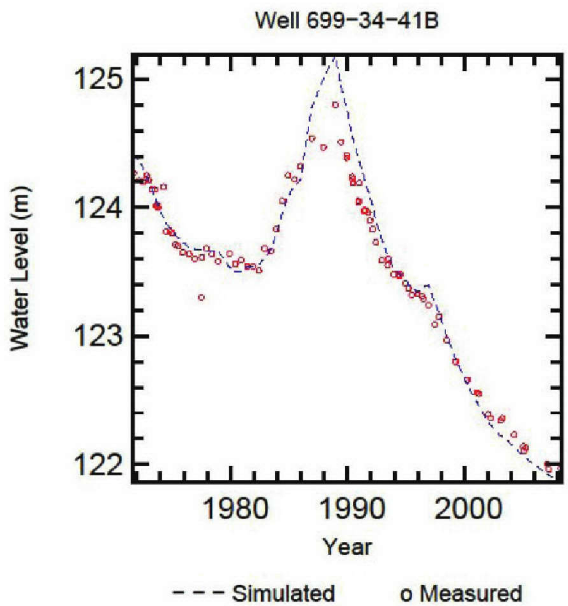

WL_699-34-41B_CPM_V3.3_TMC_10-11-2010

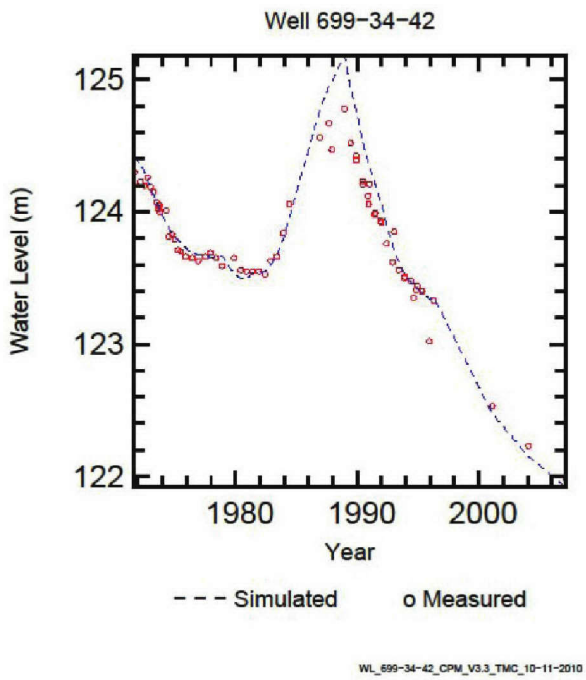
Well 699-34-42
125
124
123
122
Water Level (m)
1980
1990
2000
Year
- - - Simulated
o Measured
WL_699-34-42_CPM_V3.3_TMC_10-11-2010

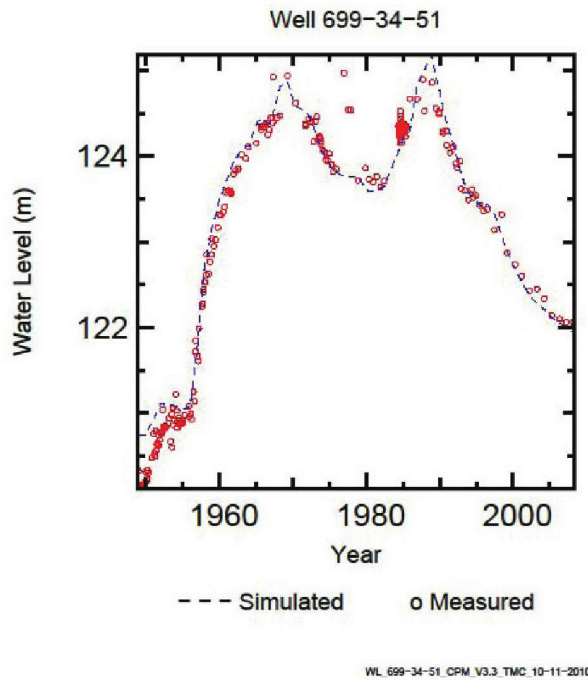
Well 699-34-51
124
122
Water Level (m)
1960
1980
2000
Year
- - - Simulated
o Measured
WL_699-34-51_CPM_V3.3_TMC_10-11-2010

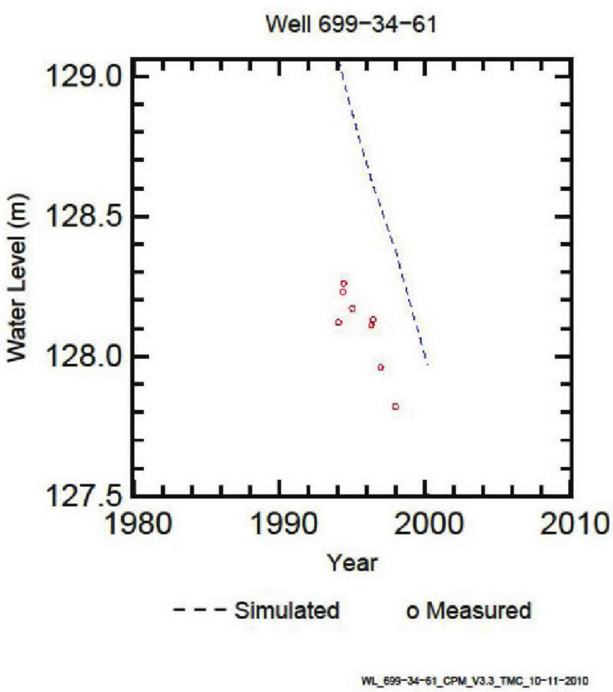
Well 699-34-61
129.0
128.5
128.0
127.5
Water Level (m)
1980
1990
2000
2010
Year
- - - Simulated
o Measured
WL_699-34-61_CPM_V3.3_TMC_10-11-2010

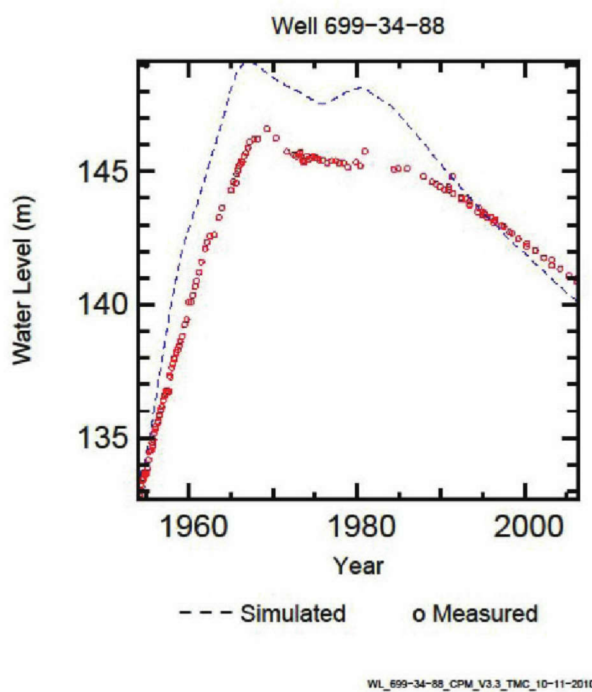
Well 699-34-88
145
140
135
Water Level (m)
1960
1980
2000
Year
- - - Simulated
o Measured
WL_699-34-88_CPM_V3.3_TMC_10-11-2010

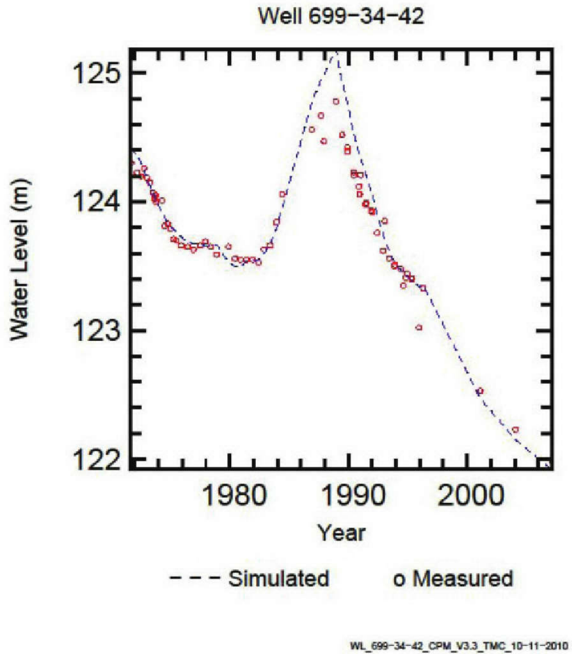
Well 699-34-42
125
124
123
122
Water Level (m)
1980
1990
2000
Year
- - - Simulated
o Measured
WL_699-34-42_CPM_V3.3_TMC_10-11-2010

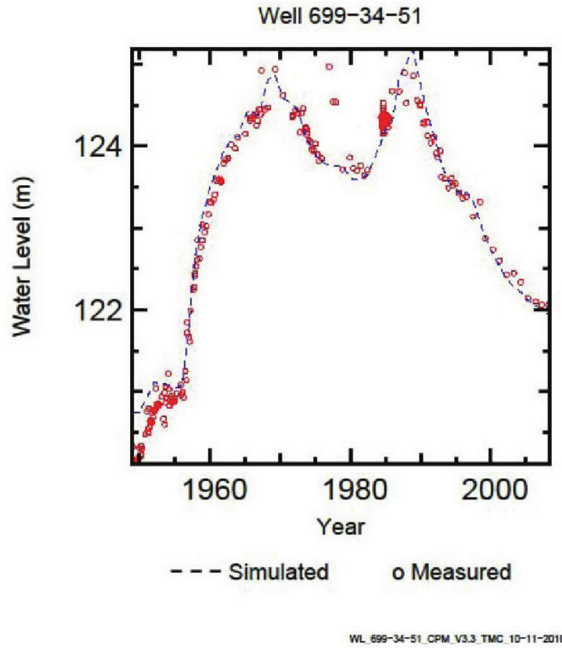
Well 699-34-51
124
122
Water Level (m)
1960
1980
2000
Year
- - - Simulated
o Measured
WL_699-34-51_CPM_V3.3_TMC_10-11-2010

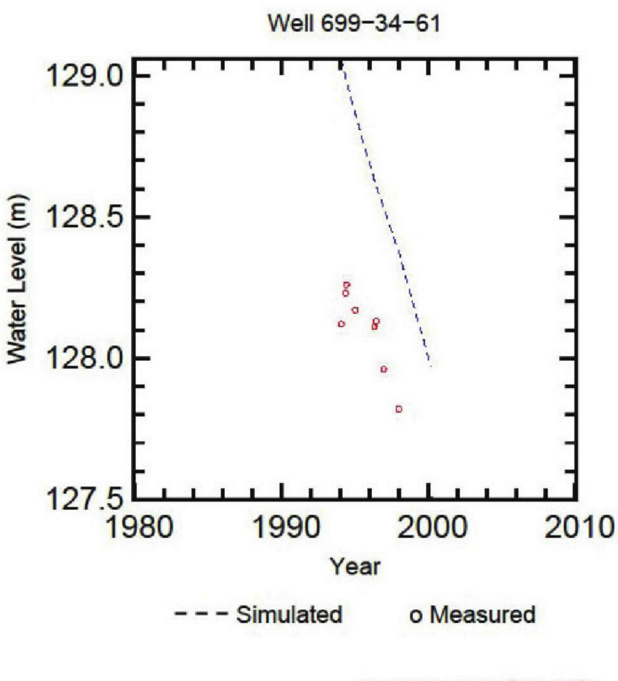
Well 699-34-61
129.0
128.5
128.0
127.5
Water Level (m)
1980
1990
2000
2010
Year
- - - Simulated
o Measured
WL_699-34-61_CPM_V3.3_TMC_10-11-2010

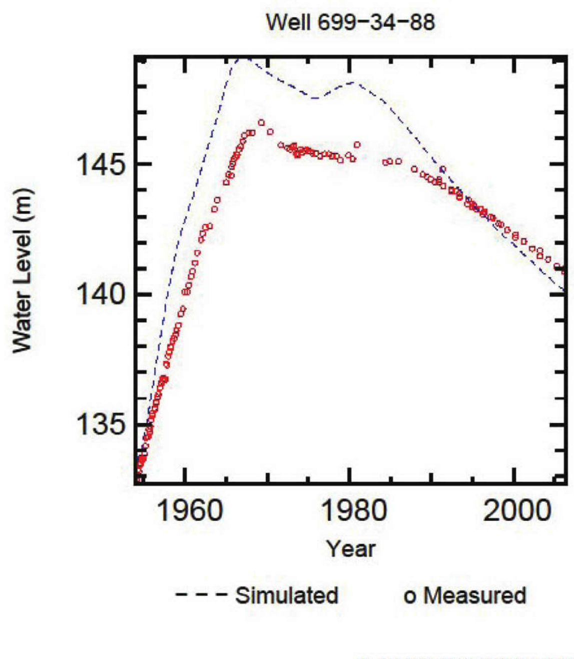
Well 699-34-88
145
140
135
Water Level (m)
1960
1980
2000
Year
- - - Simulated
o Measured
WL_699-34-88_CPM_V3.3_TMC_10-11-2010

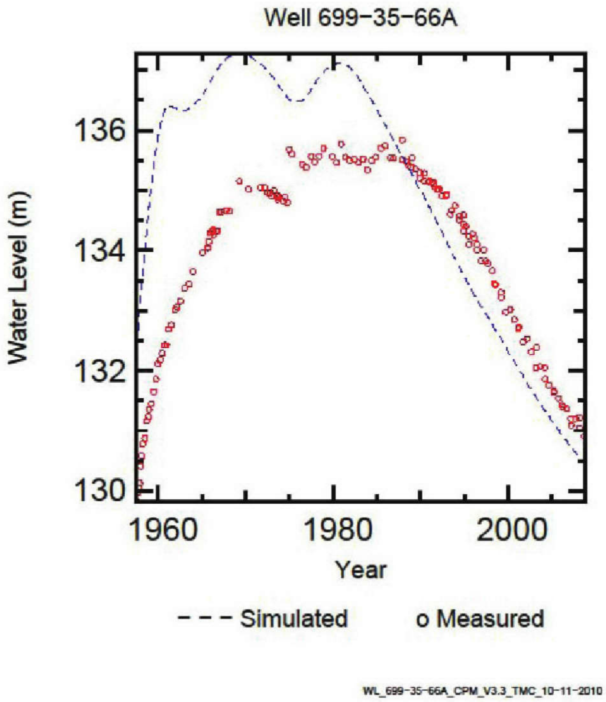
Well 699-35-66A
136
134
132
130
Water Level (m)
1960
1980
2000
Year
- - - Simulated
o Measured
WL_699-35-66A_CPM_V3.3_TMC_10-11-2010

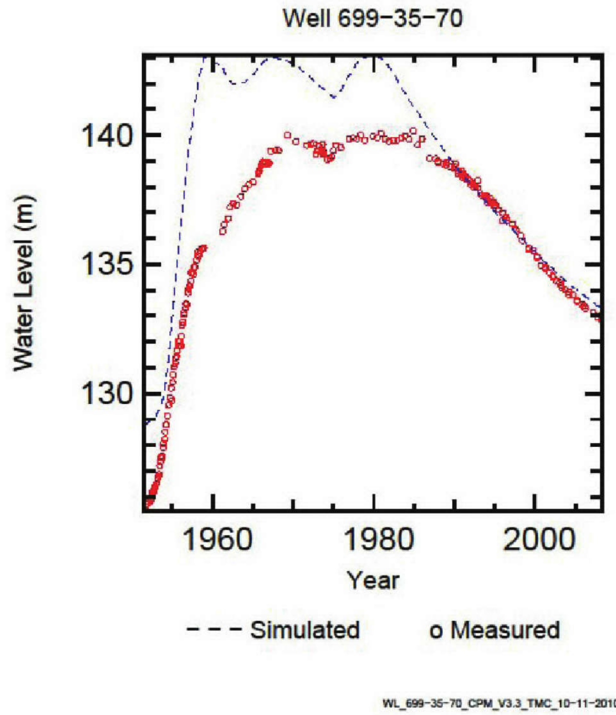
Well 699-35-70
140
135
130
Water Level (m)
1960
1980
2000
Year
- - - Simulated
o Measured
WL_699-35-70_CPM_V3.3_TMC_10-11-2010

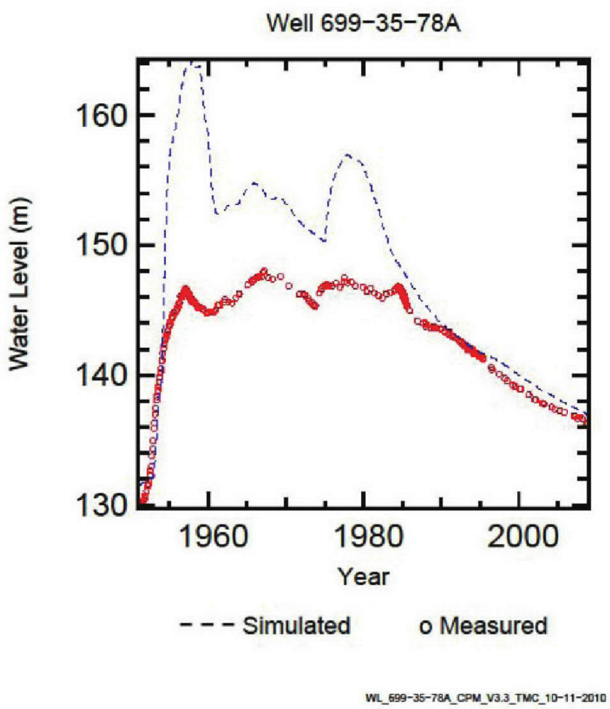
Well 699-35-78A
160
150
140
130
Water Level (m)
1960
1980
2000
Year
- - - Simulated
o Measured
WL_699-35-78A_CPM_V3.3_TMC_10-11-2010

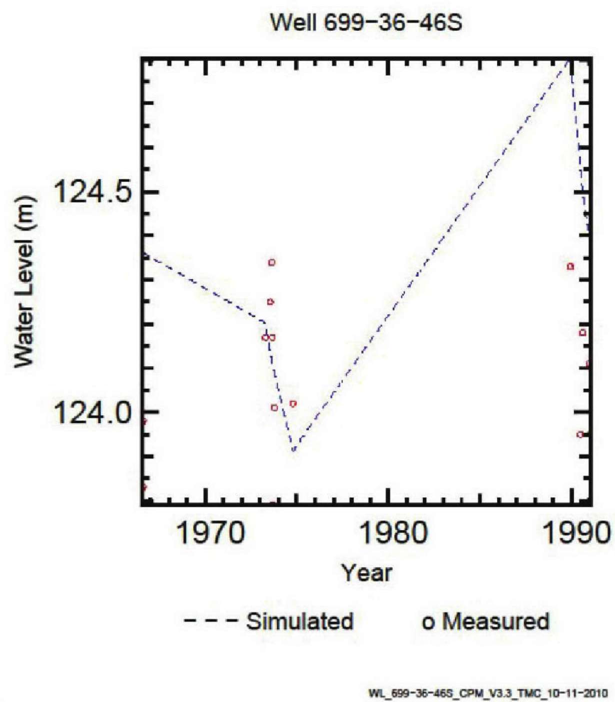
Well 699-36-46S
124.5
124.0
Water Level (m)
1970
1980
1990
Year
- - - Simulated
o Measured
WL_699-36-46S_CPM_V3.3_TMC_10-11-2010

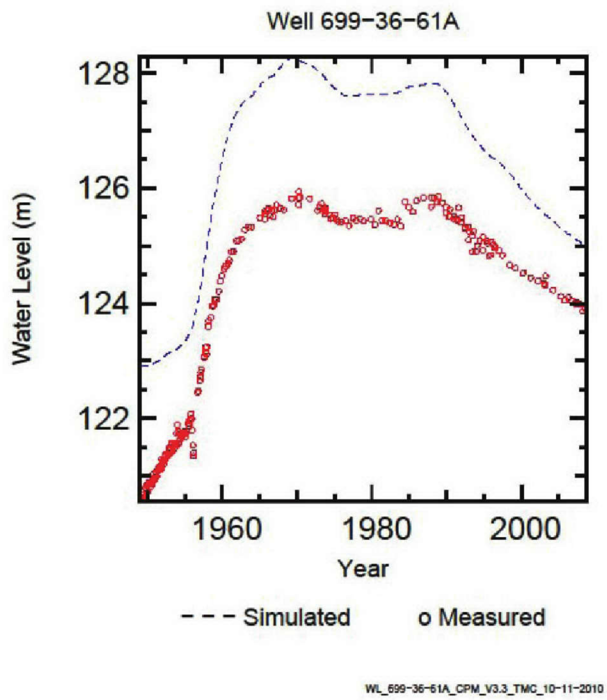
Well 699-36-61A
128
126
124
122
Water Level (m)
1960
1980
2000
Year
- - - Simulated
o Measured
WL_699-36-61A_CPM_V3.3_TMC_10-11-2010

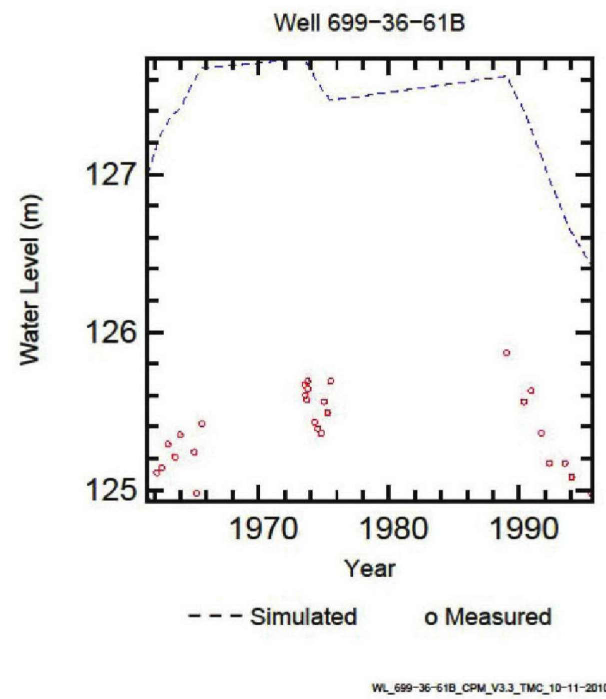
Well 699-36-61B
127
126
125
Water Level (m)
1970
1980
1990
Year
- - - Simulated
o Measured
WL_699-36-61B_CPM_V3.3_TMC_10-11-2010

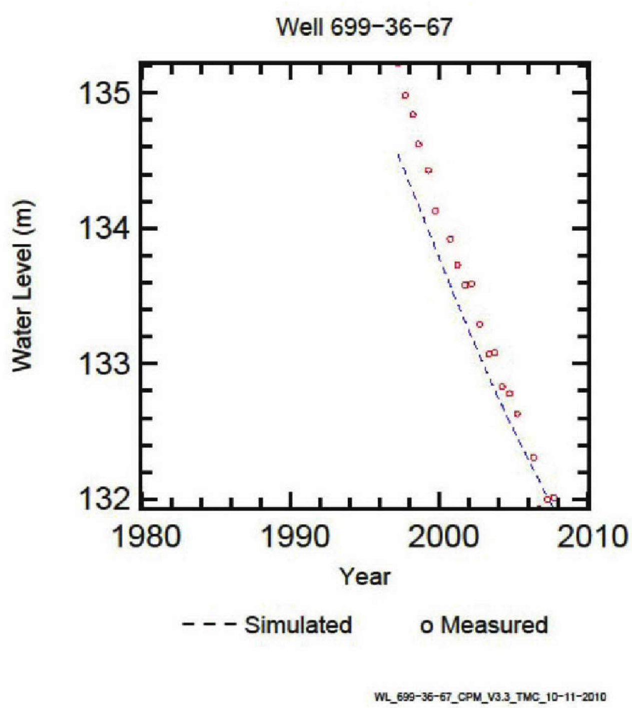
Well 699-36-67
135
134
133
132
Water Level (m)
1980
1990
2000
2010
Year
- - - Simulated
o Measured
WL_699-36-67_CPM_V3.3_TMC_10-11-2010

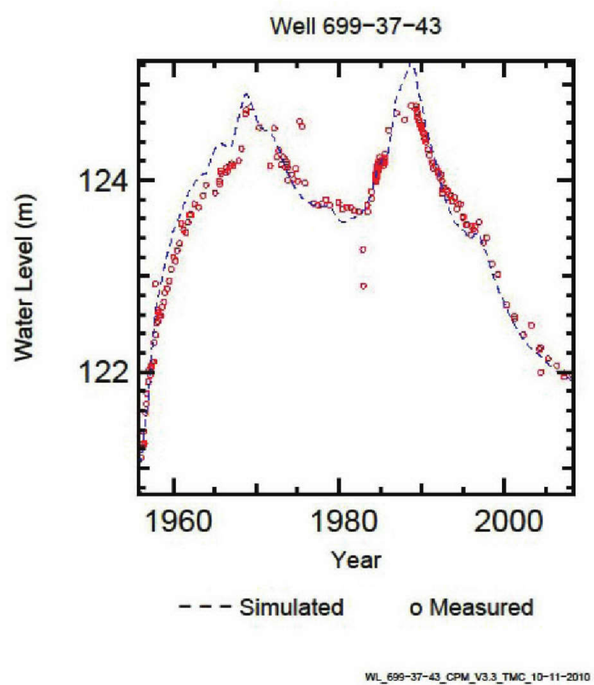
Well 699-37-43
124
122
Water Level (m)
1960
1980
2000
Year
- - - Simulated
o Measured
WL_699-37-43_CPM_V3.3_TMC_10-11-2010

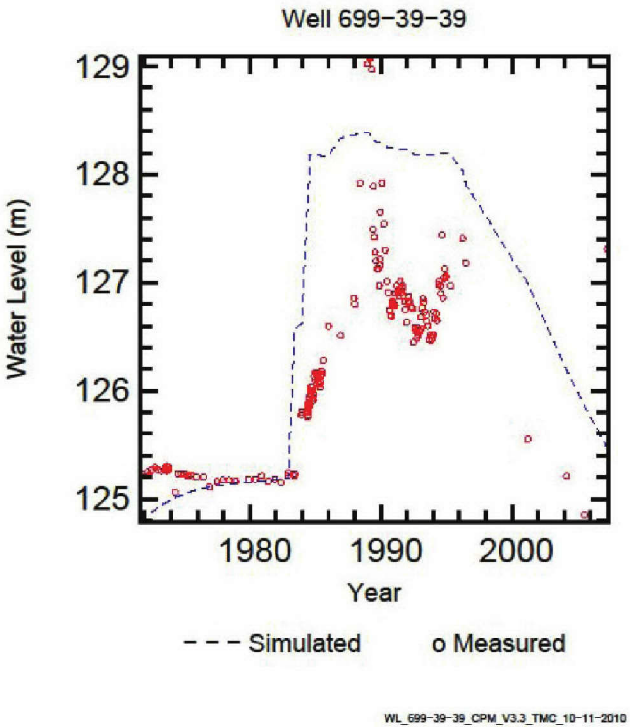
Well 699-39-39
129
128
127
126
125
Water Level (m)
1980
1990
2000
Year
- - - Simulated
o Measured
WL_699-39-39_CPM_V3.3_TMC_10-11-2010

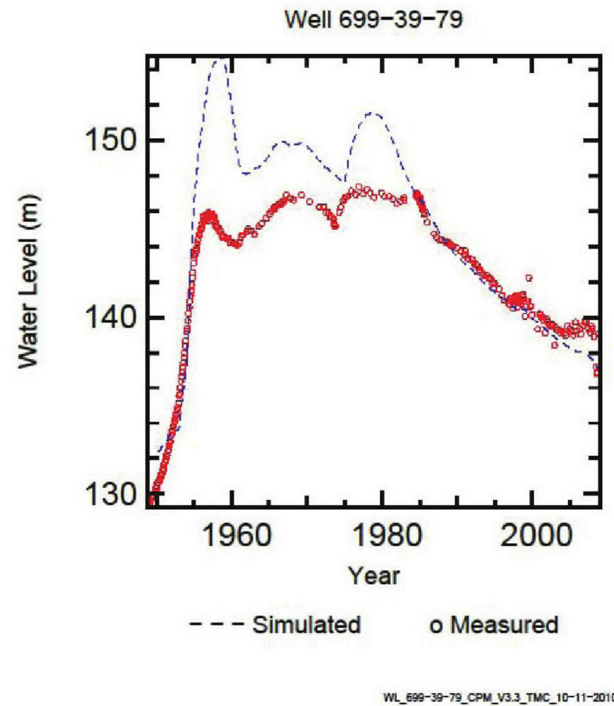
Well 699-39-79
150
140
130
Water Level (m)
1960
1980
2000
Year
- - - Simulated
o Measured
WL_699-39-79_CPM_V3.3_TMC_10-11-2010

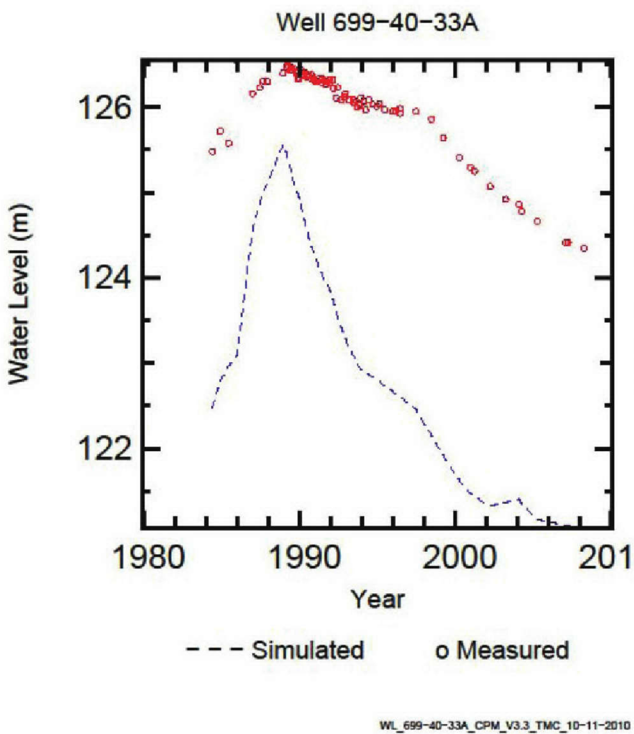
Well 699-40-33A
126
124
122
Water Level (m)
1980
1990
2000
201
Year
- - - Simulated
o Measured
WL_699-40-33A_CPM_V3.3_TMC_10-11-2010

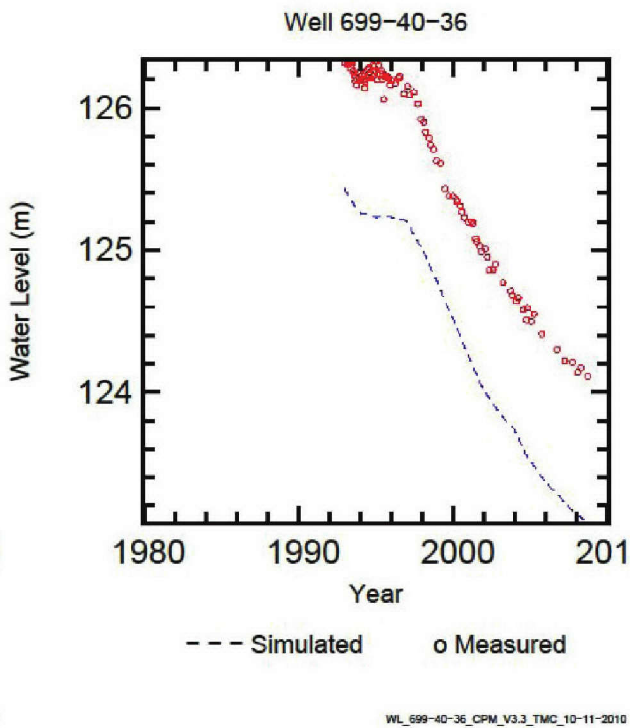
Well 699-40-36
126
125
124
Water Level (m)
1980
1990
2000
Year
- - - Simulated
o Measured
WL_699-40-36_CPM_V3.3_TMC_10-11-2010

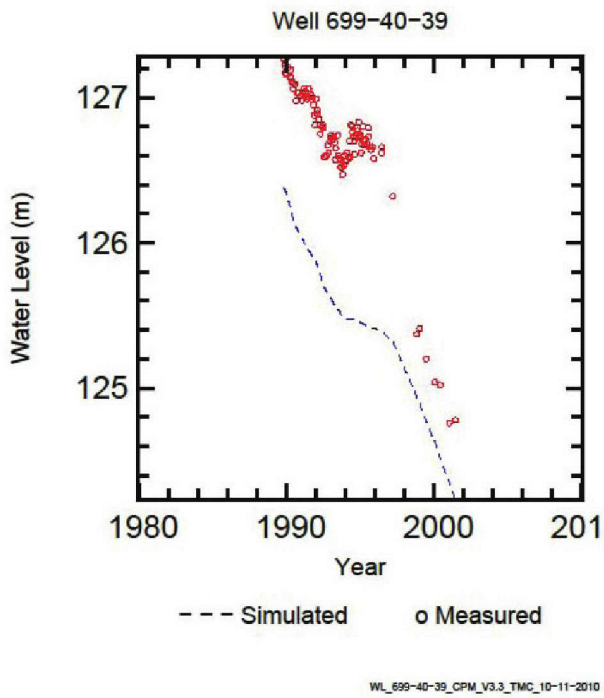
Well 699-40-39
127
126
125
Water Level (m)
1980
1990
2000
2010
Year
--- Simulated
o Measured
WL_699-40-39_CPM_V3.3_TMC_10-11-2010

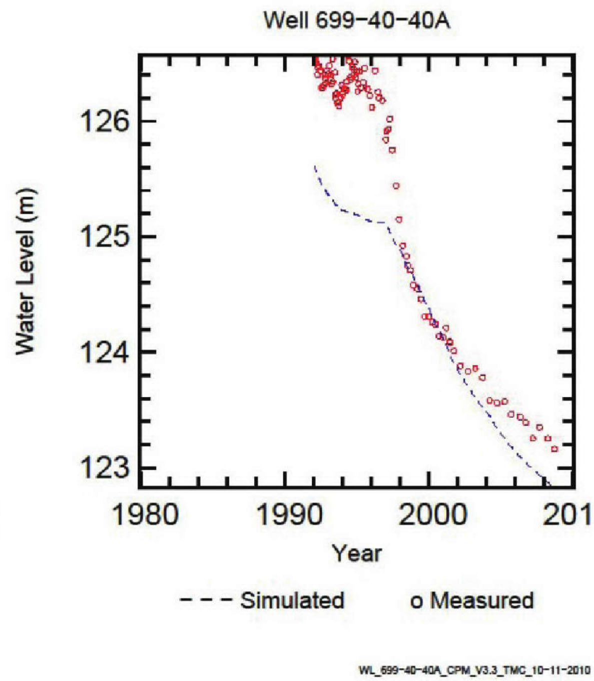
Well 699-40-40A
126
125
124
123
Water Level (m)
1980
1990
2000
201
Year
--- Simulated
o Measured
WL_699-40-40A_CPM_V3.3_TMC_10-11-2010

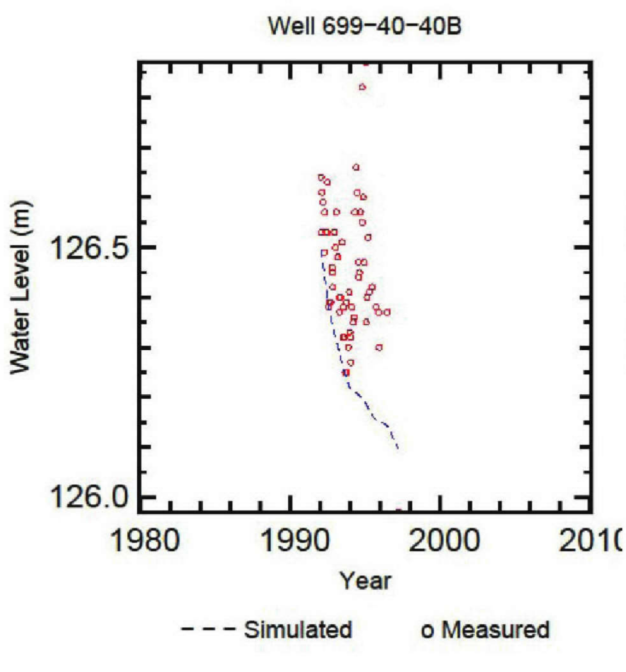
Well 699-40-40B
126.5
126.0
Water Level (m)
1980
1990
2000
2010
Year
--- Simulated
o Measured
WL_699-40-40B_CPM_V3.3_TMC_10-11-2010

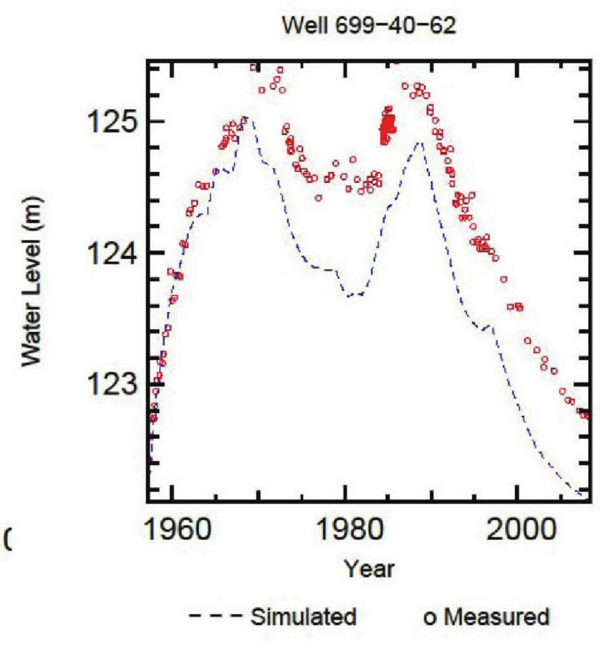
Well 699-40-62
125
124
123
Water Level (m)
1960
1980
2000
Year
--- Simulated
o Measured
WL_699-40-62_CPM_V3.3_TMC_10-11-2010

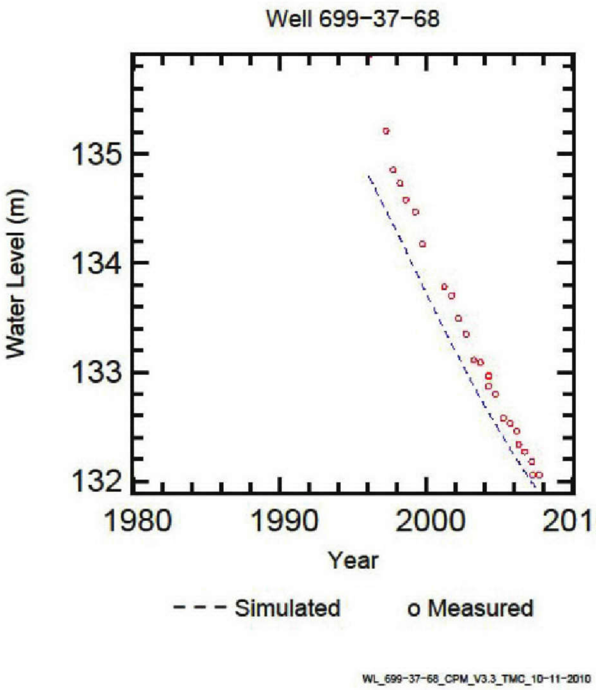
Well 699−37−68
135
134
133
132
Water Level (m)
1980
1990
2000
201
Year
− − − Simulated
o Measured
WL_699-37-68_CPM_V3.3_TMC_10-11-2010

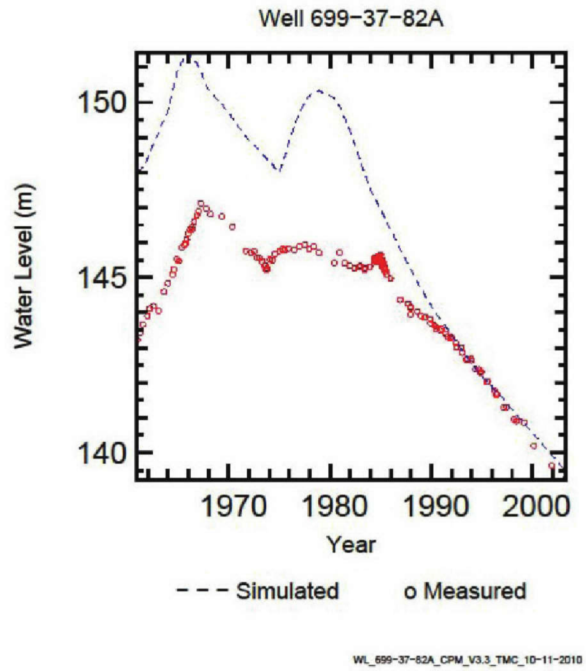
Well 699−37−82A
150
145
140
Water Level (m)
1970
1980
1990
2000
Year
− − − Simulated
o Measured
WL_699-37-82A_CPM_V3.3_TMC_10-11-2010

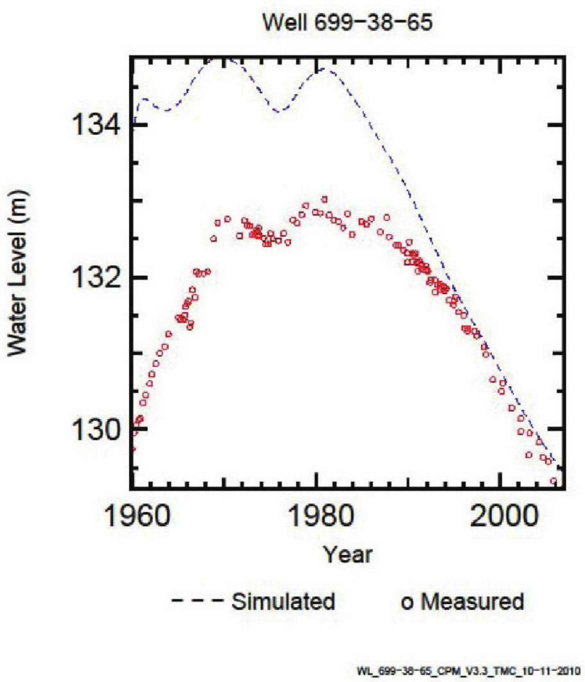
Well 699−38−65
134
132
130
Water Level (m)
1960
1980
2000
Year
− − − Simulated
o Measured
WL_699-38-65_CPM_V3.3_TMC_10-11-2010

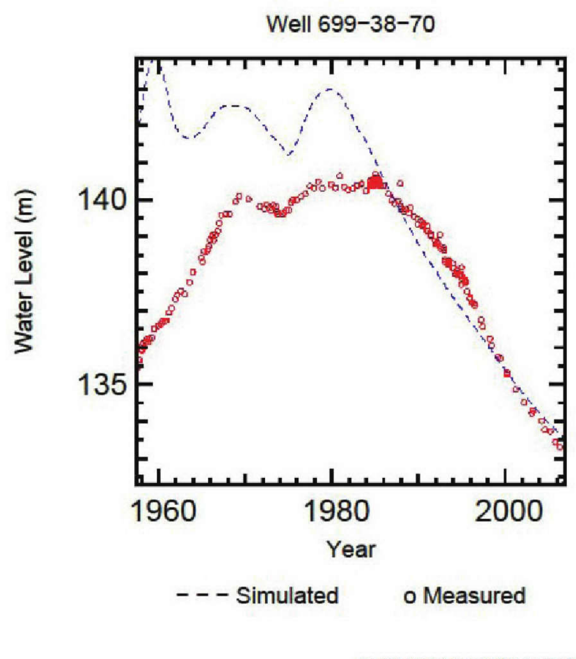
Well 699−38−70
140
135
Water Level (m)
1960
1980
2000
Year
− − − Simulated
o Measured
WL_699-38-70_CPM_V3.3_TMC_10-11-2010

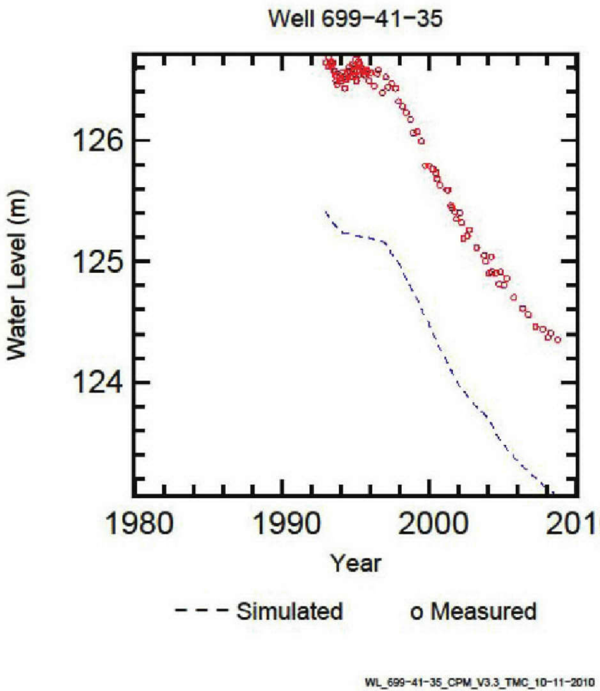
Well 699-41-35
Water Level (m)
126
125
124
1980
1990
2000
2010
Year
- - - Simulated
o Measured
WL_699-41-35_CPM_V3.3_TMC_10-11-2010

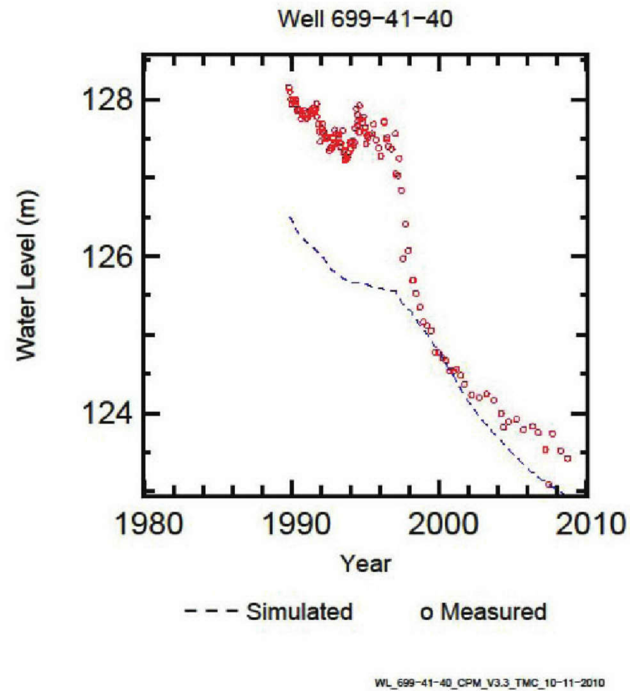
Well 699-41-40
Water Level (m)
128
126
124
1980
1990
2000
2010
Year
- - - Simulated
o Measured
WL_699-41-40_CPM_V3.3_TMC_10-11-2010

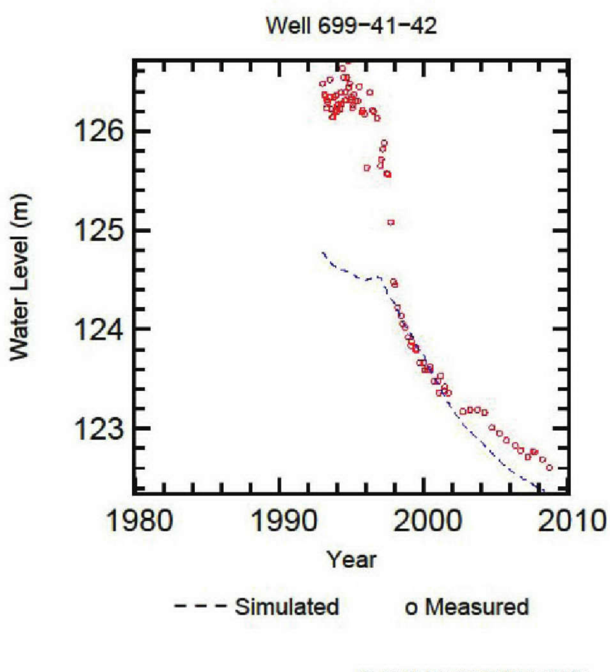
Well 699-41-42
Water Level (m)
126
125
124
123
1980
1990
2000
2010
Year
- - - Simulated
o Measured
WL_699-41-42_CPM_V3.3_TMC_10-11-2010

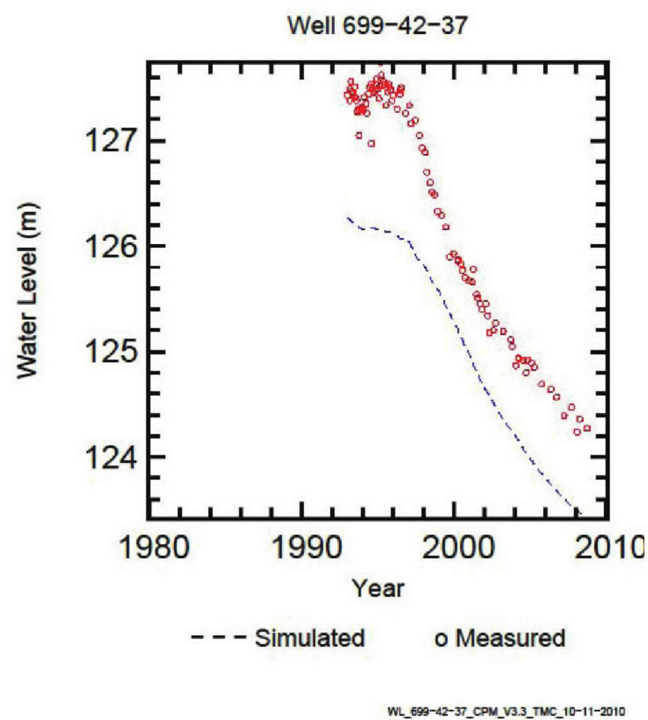
Well 699-42-37
Water Level (m)
127
126
125
124
1980
1990
2000
2010
Year
- - - Simulated
o Measured
WL_699-42-37_CPM_V3.3_TMC_10-11-2010

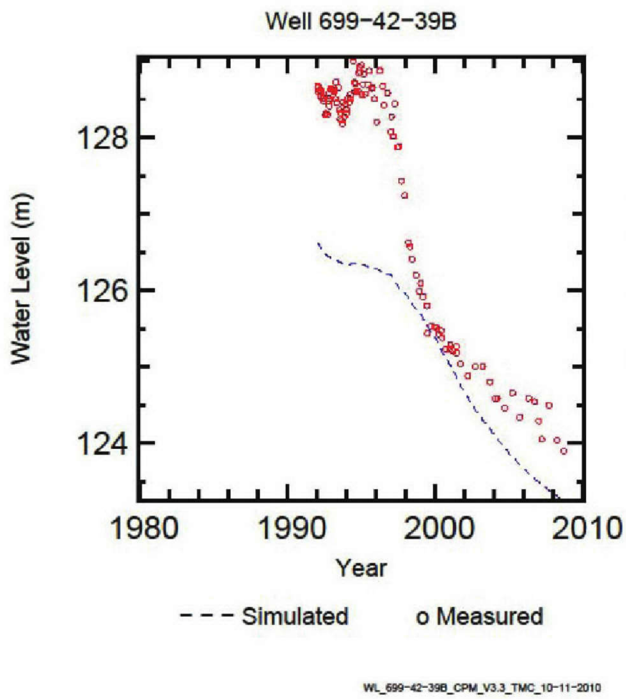
Well 699−42−39B
Water Level (m)
128
126
124
1980
1990
2000
2010
Year
Simulated
o Measured
WL_699-42-39B_CPM_V3.3_TMC_10-11-2010

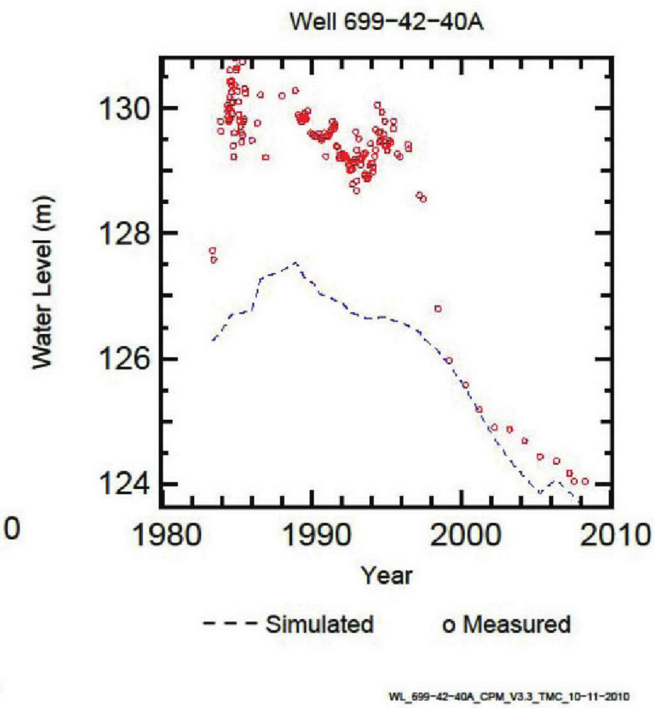
Well 699−42−40A
Water Level (m)
130
128
126
124
1980
1990
2000
2010
Year
Simulated
o Measured
WL_699-42-40A_CPM_V3.3_TMC_10-11-2010

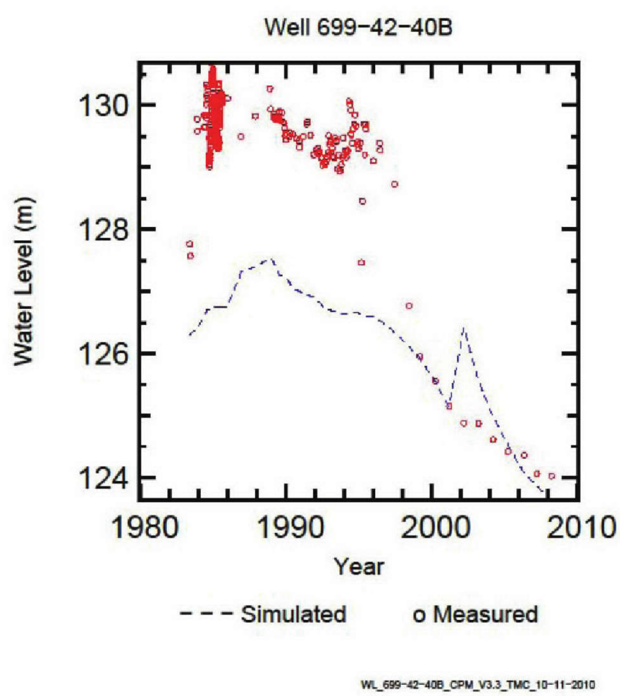
Well 699−42−40B
Water Level (m)
130
128
126
124
1980
1990
2000
2010
Year
Simulated
o Measured
WL_699-42-40B_CPM_V3.3_TMC_10-11-2010

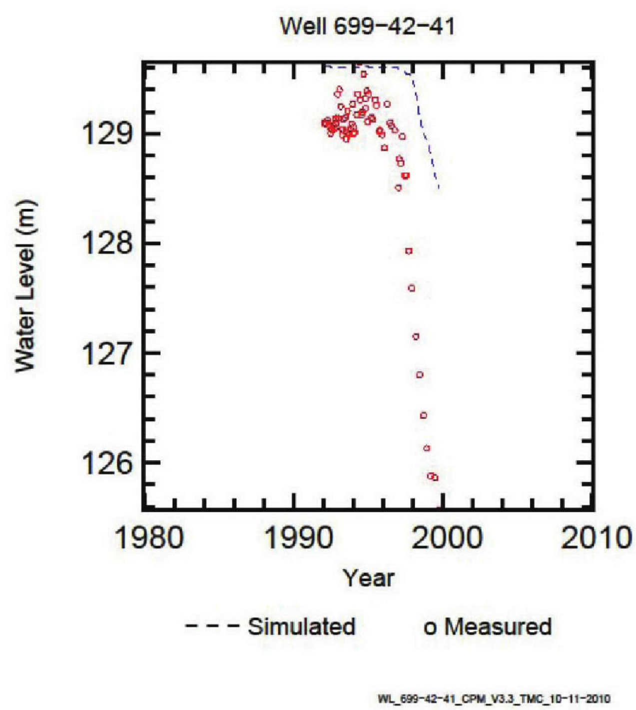
Well 699−42−41
Water Level (m)
129
128
127
126
1980
1990
2000
2010
Year
Simulated
o Measured
WL_699-42-41_CPM_V3.3_TMC_10-11-2010

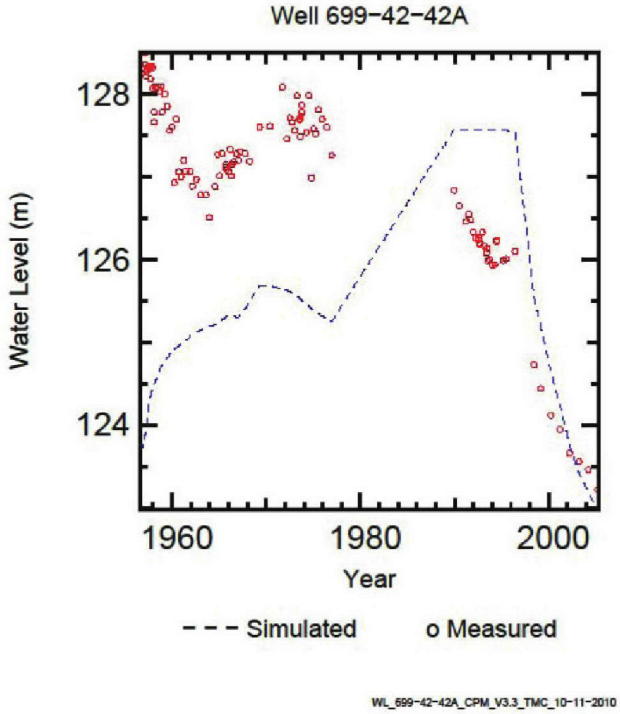
Well 699-42-42A
Water Level (m)
124
126
128
1960
1980
2000
Year
- - - Simulated
o Measured
WL_699-42-42A_CPM_V3.3_TMC_10-11-2010

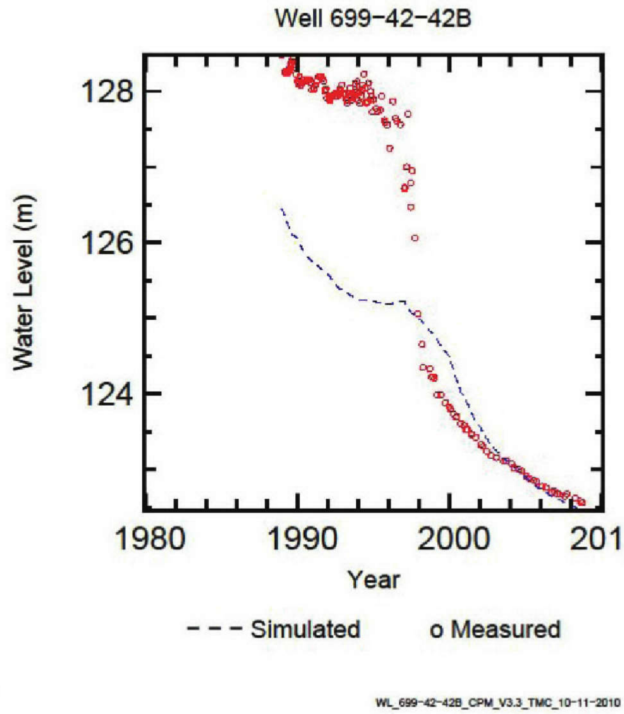
Well 699-42-42B
Water Level (m)
124
126
128
1980
1990
2000
2010
Year
- - - Simulated
o Measured
WL_699-42-42B_CPM_V3.3_TMC_10-11-2010

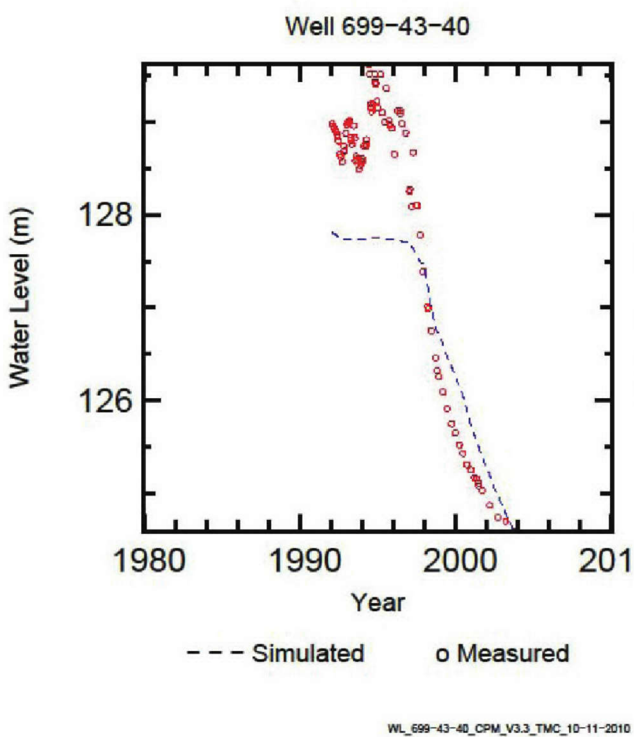
Well 699-43-40
Water Level (m)
126
128
1980
1990
2000
201
Year
- - - Simulated
o Measured
WL_699-43-40_CPM_V3.3_TMC_10-11-2010

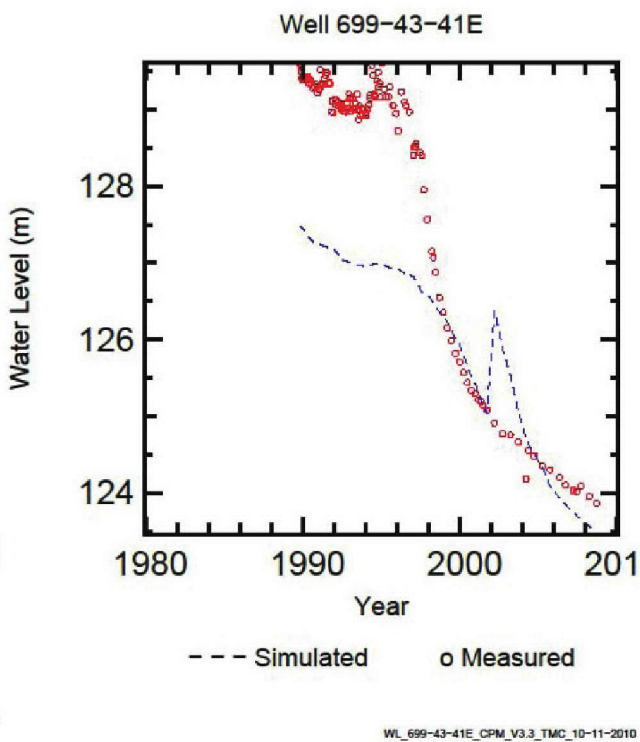
Well 699-43-41E
Water Level (m)
124
126
128
1980
1990
2000
201
Year
- - - Simulated
o Measured
WL_699-43-41E_CPM_V3.3_TMC_10-11-2010

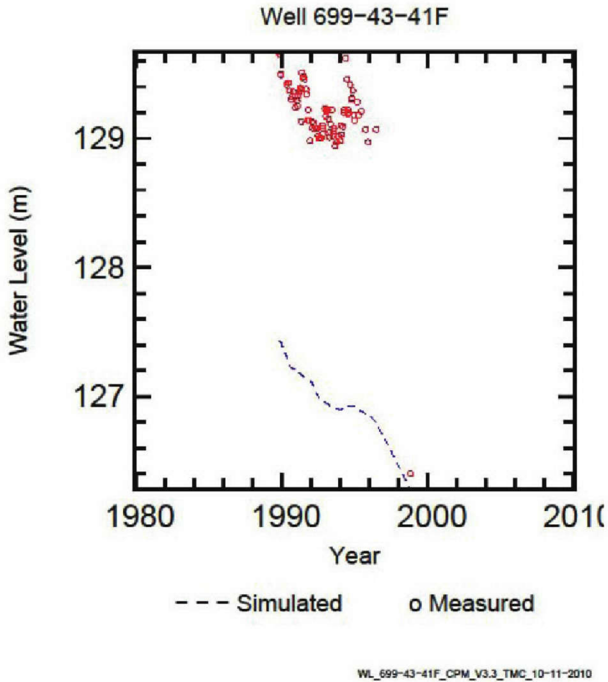
Well 699−43−41F
Water Level (m)
129
128
127
1980
1990
2000
2010
Year
- - - Simulated
o Measured
WL_699-43-41F_CPM_V3.3_TMC_10-11-2010

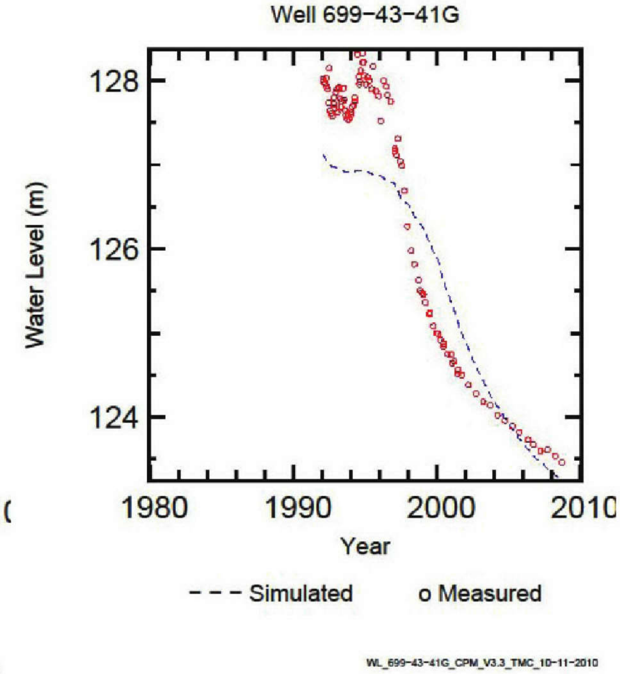
Well 699−43−41G
Water Level (m)
128
126
124
1980
1990
2000
2010
Year
- - - Simulated
o Measured
WL_699-43-41G_CPM_V3.3_TMC_10-11-2010

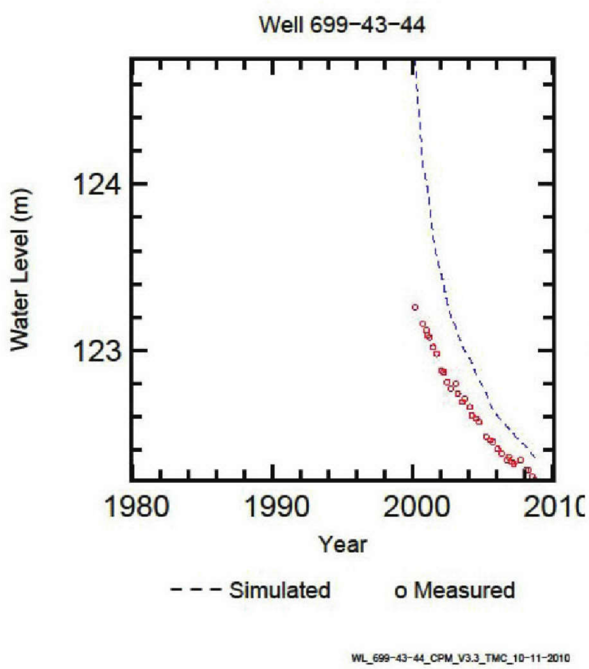
Well 699−43−44
Water Level (m)
124
123
1980
1990
2000
2010
Year
- - - Simulated
o Measured
WL_699-43-44_CPM_V3.3_TMC_10-11-2010

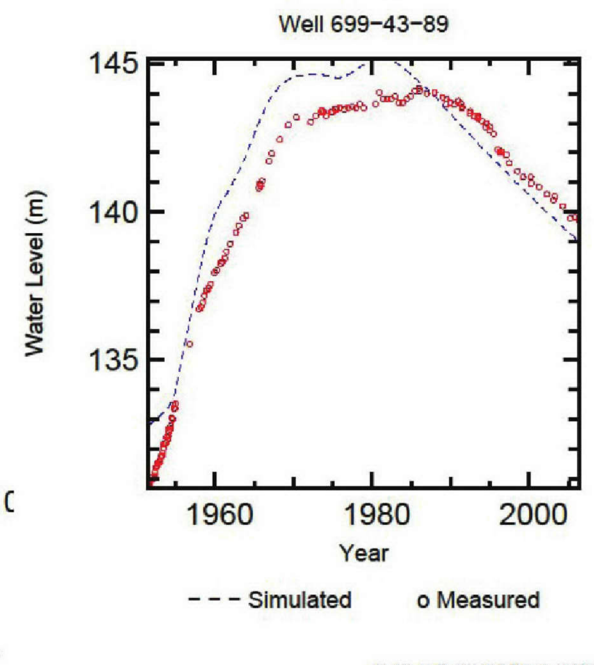
Well 699−43−89
Water Level (m)
145
140
135
1960
1980
2000
Year
- - - Simulated
o Measured
WL_699-43-89_CPM_V3.3_TMC_10-11-2010

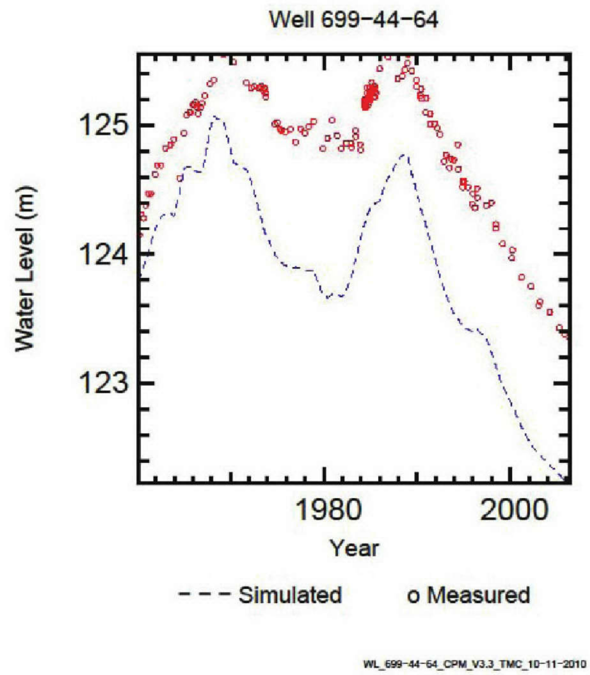
Well 699-44-64
125
124
123
Water Level (m)
1980
2000
Year
- - - Simulated
o Measured
WL_699-44-64_CPM_V3.3_TMC_10-11-2010

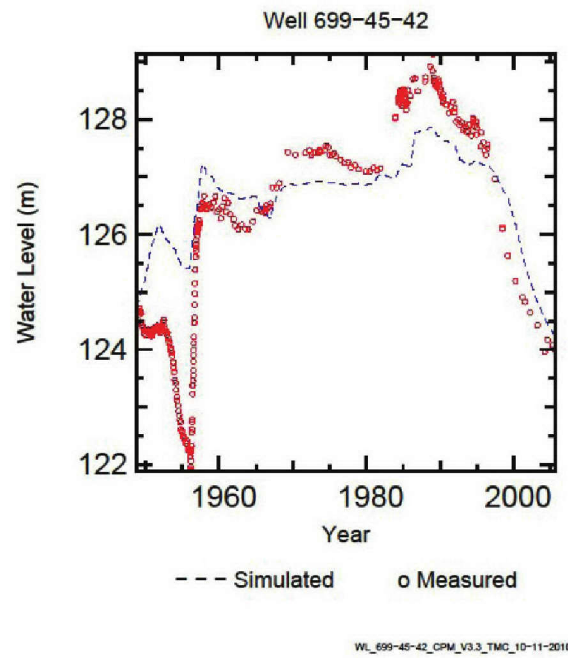
Well 699-45-42
128
126
124
122
Water Level (m)
1960
1980
2000
Year
- - - Simulated
o Measured
WL_699-45-42_CPM_V3.3_TMC_10-11-2010

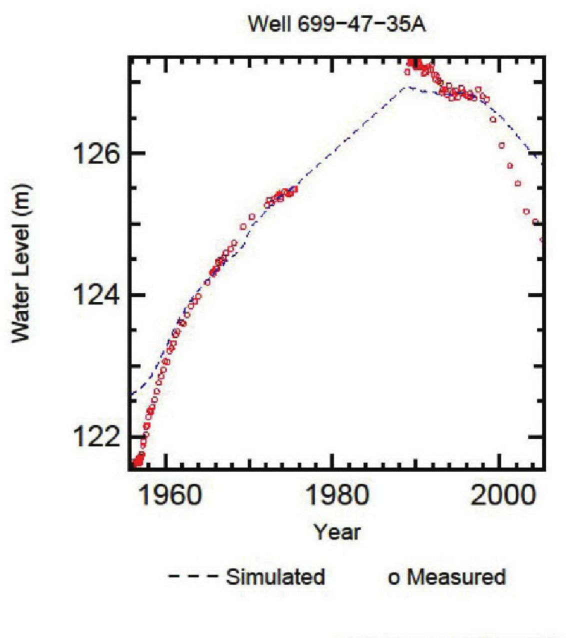
Well 699-47-35A
126
124
122
Water Level (m)
1960
1980
2000
Year
- - - Simulated
o Measured
WL_699-47-35A_CPM_V3.3_TMC_10-11-2010

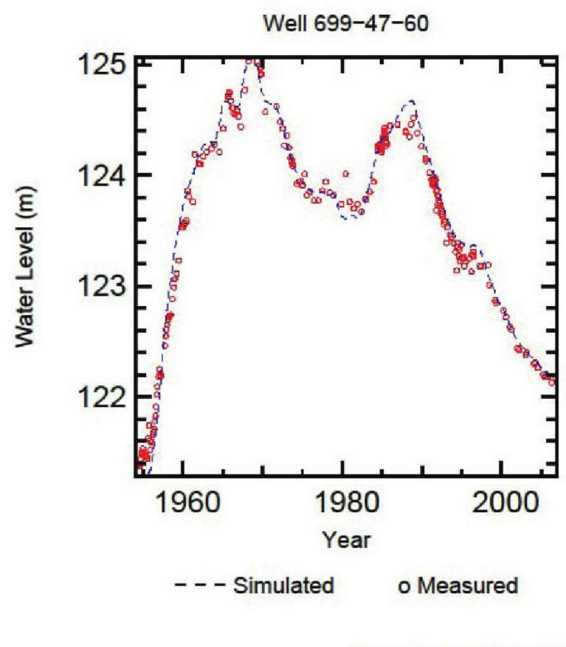
Well 699-47-60
125
124
123
122
Water Level (m)
1960
1980
2000
Year
- - - Simulated
o Measured
WL_699-47-60_CPM_V3.3_TMC_10-11-2010

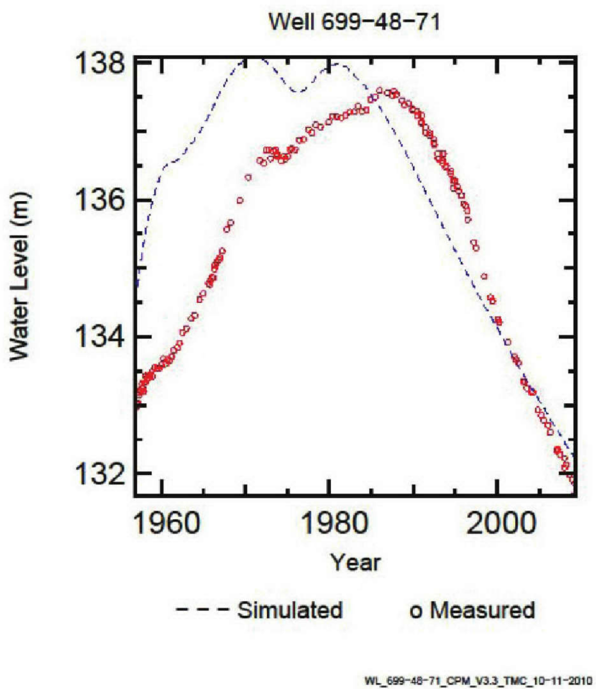
Well 699-48-71
138
136
134
132
Water Level (m)
1960
1980
2000
Year
- - - Simulated
o Measured
WL_699-48-71_CPM_V3.3_TMC_10-11-2010

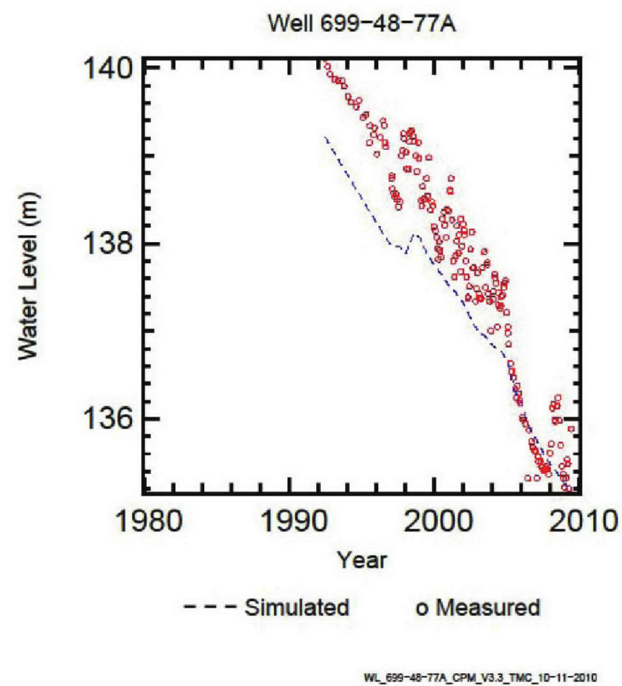
Well 699-48-77A
140
138
136
Water Level (m)
1980
1990
2000
2010
Year
- - - Simulated
o Measured
WL_699-48-77A_CPM_V3.3_TMC_10-11-2010

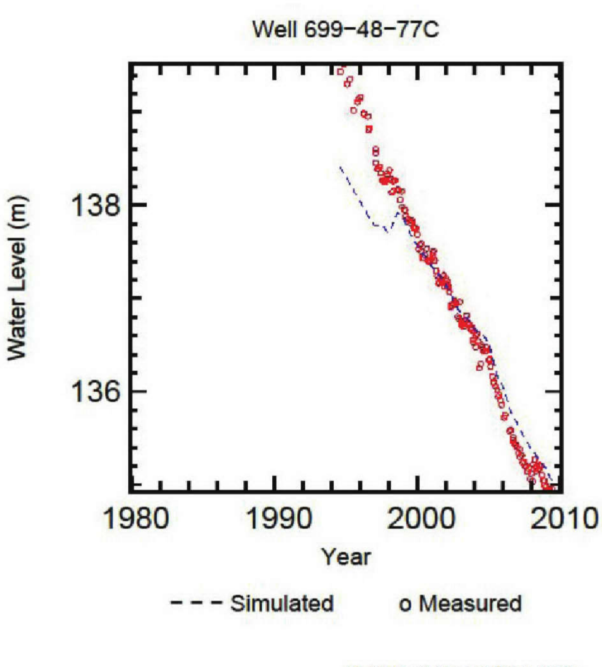
Well 699-48-77C
138
136
Water Level (m)
1980
1990
2000
2010
Year
- - - Simulated
o Measured
WL_699-48-77C_CPM_V3.3_TMC_10-11-2010

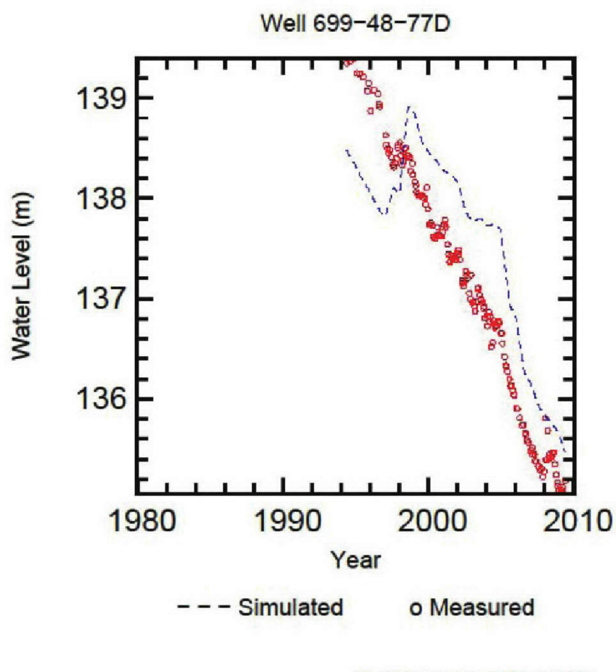
Well 699-48-77D
139
138
137
136
Water Level (m)
1980
1990
2000
2010
Year
- - - Simulated
o Measured
WL_699-48-77D_CPM_V3.3_TMC_10-11-2010

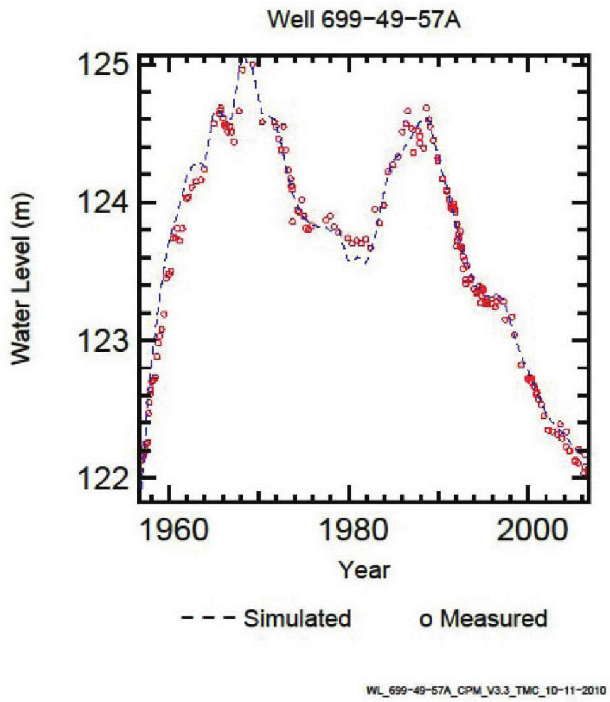
Well 699-49-57A
125
124
123
122
Water Level (m)
1960
1980
2000
Year
- - - Simulated
o Measured
WL_699-49-57A_CPM_V3.3_TMC_10-11-2010

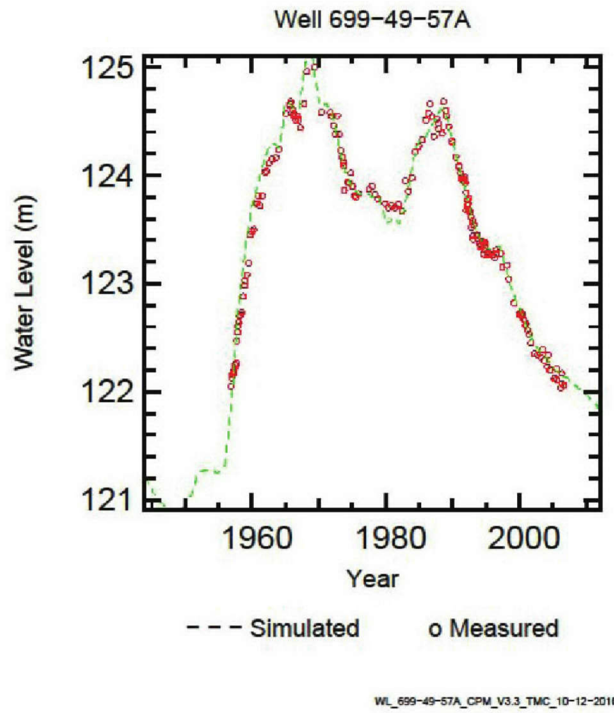
Well 699-49-57A
125
124
123
122
121
Water Level (m)
1960
1980
2000
Year
- - - Simulated
o Measured
WL_699-49-57A_CPM_V3.3_TMC_10-12-2010

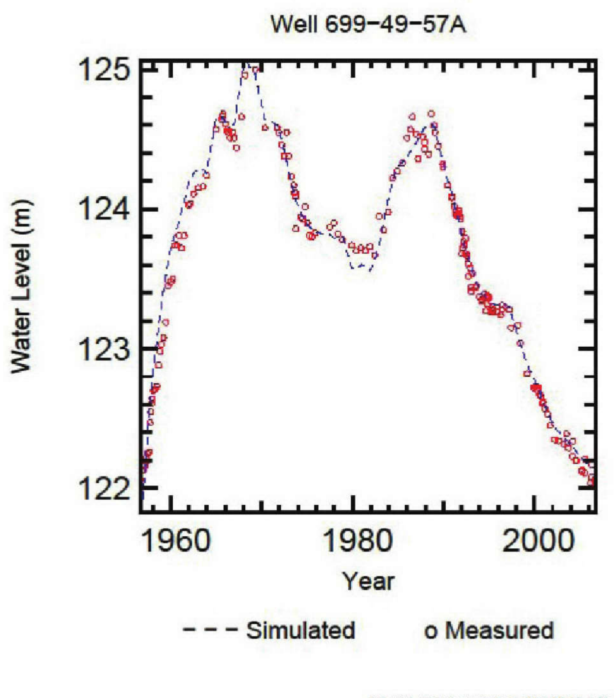
Well 699-49-57A
125
124
123
122
Water Level (m)
1960
1980
2000
Year
- - - Simulated
o Measured
WL_699-49-57A_CPM_V3.3_TMC_11-05-2010

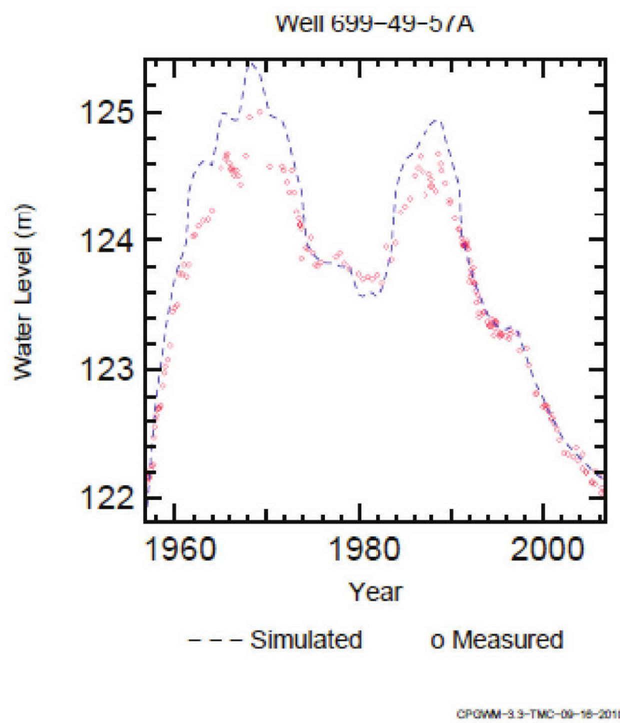
Well 699-49-57A
125
124
123
122
Water Level (m)
1960
1980
2000
Year
- - - Simulated
o Measured
CPGWM-3.3-TMC-09-16-2010

Well 699-50-42

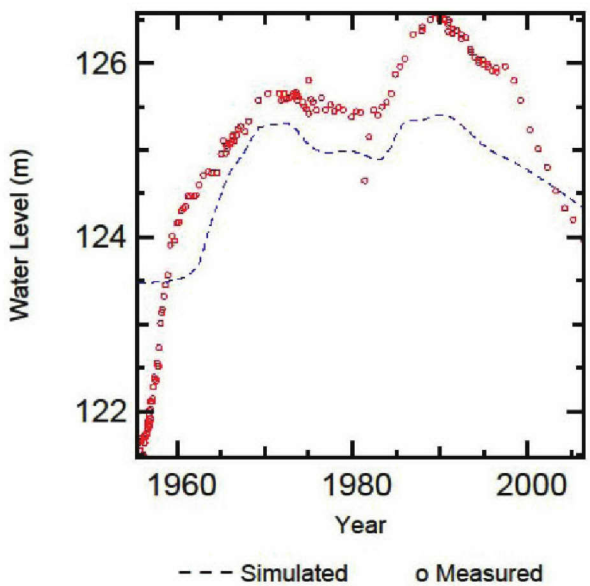

WL_699-50-42_CPM_V3.3_TMC_10-11-2010

Well 699-50-74

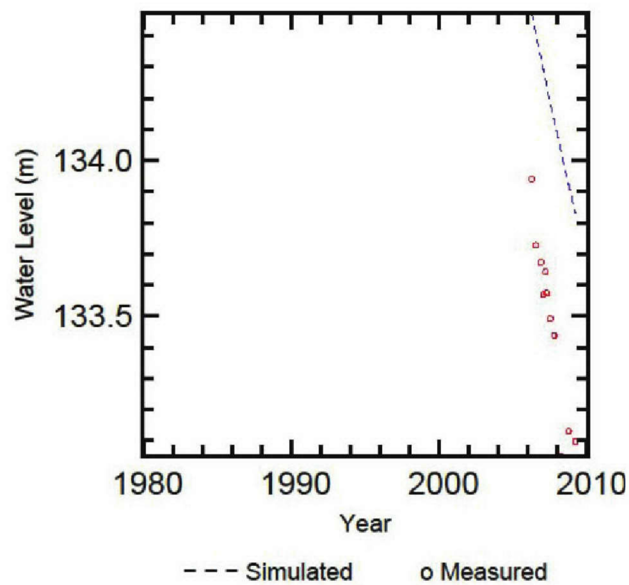

WL_699-50-74_CPM_V3.3_TMC_10-11-2010

Well 699-50-85

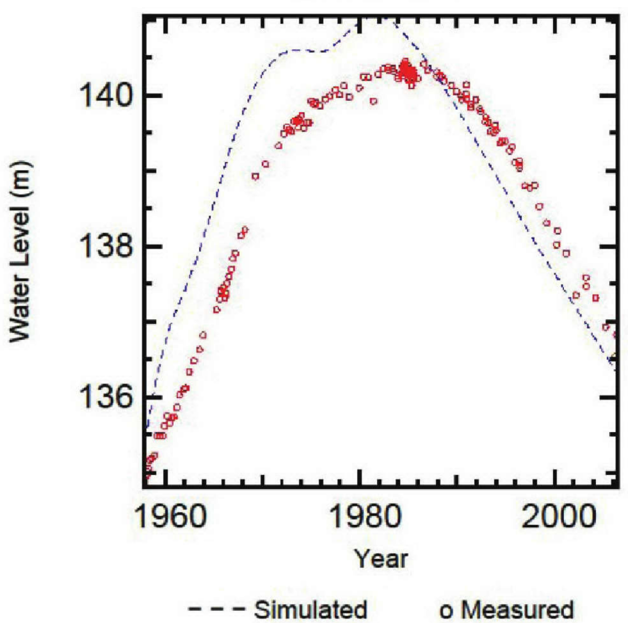

WL_699-50-85_CPM_V3.3_TMC_10-11-2010

Well 699-51-75

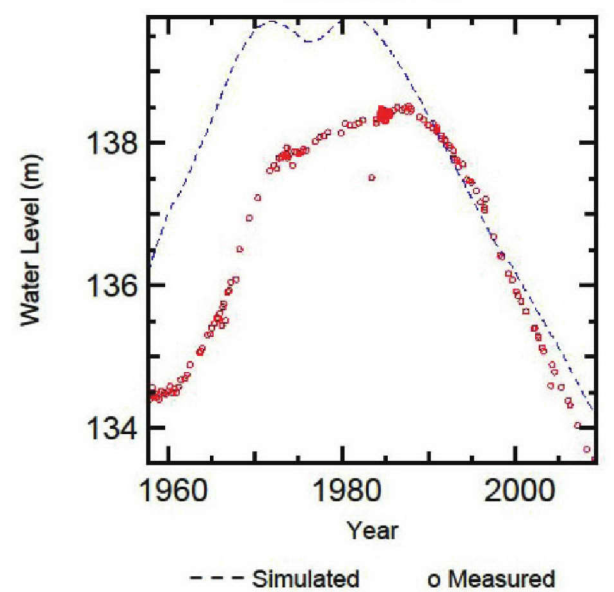

WL_699-51-75_CPM_V3.3_TMC_10-11-2010

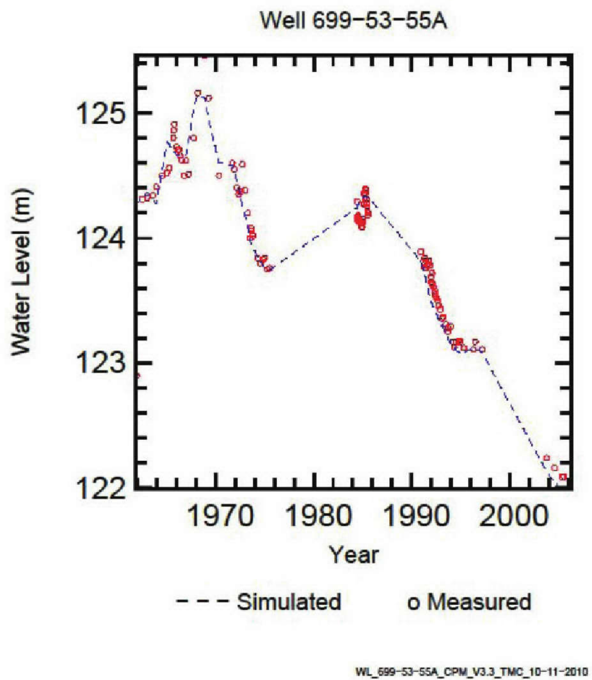
Well 699-53-55A
Water Level (m)
125
124
123
122
1970
1980
1990
2000
Year
- - - Simulated
o Measured
WL_699-53-55A_CPM_V3.3_TMC_10-11-2010

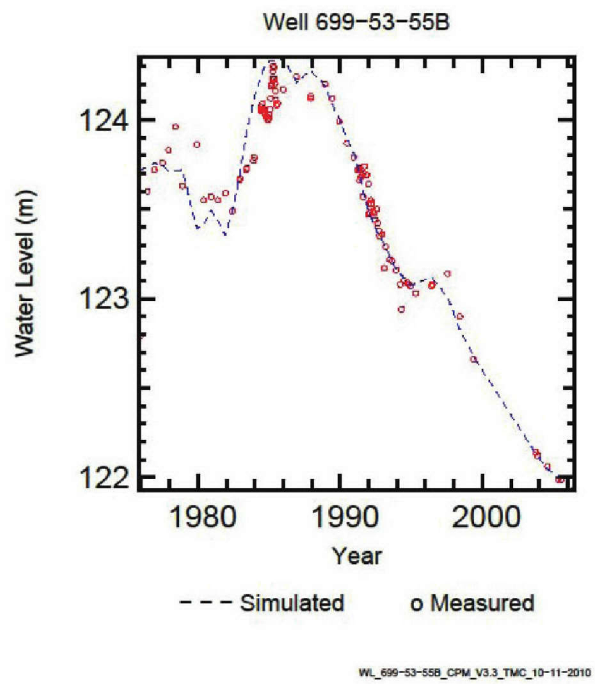
Well 699-53-55B
Water Level (m)
124
123
122
1980
1990
2000
Year
- - - Simulated
o Measured
WL_699-53-55B_CPM_V3.3_TMC_10-11-2010

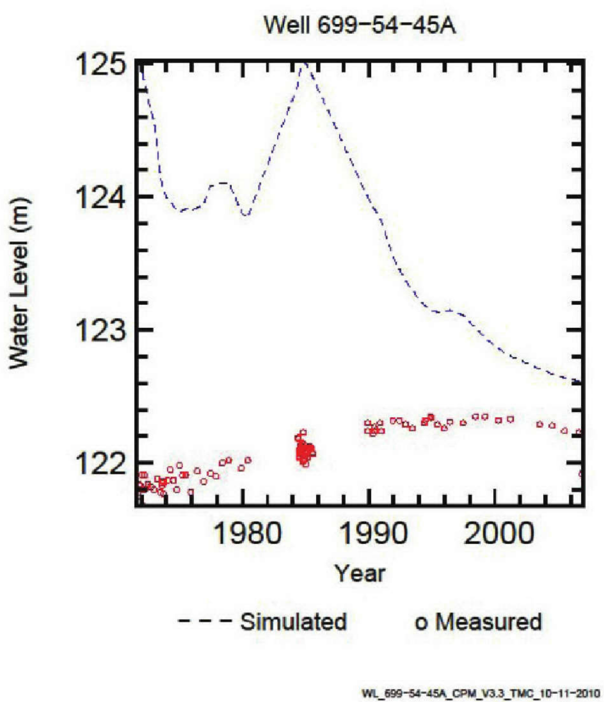
Well 699-54-45A
Water Level (m)
125
124
123
122
1980
1990
2000
Year
- - - Simulated
o Measured
WL_699-54-45A_CPM_V3.3_TMC_10-11-2010

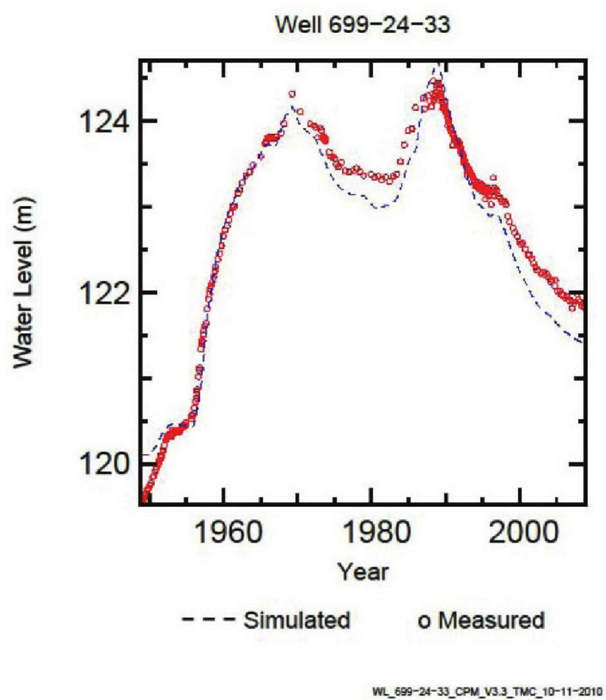
Well 699-24-33
Water Level (m)
124
122
120
1960
1980
2000
Year
- - - Simulated
o Measured
WL_699-24-33_CPM_V3.3_TMC_10-11-2010